DTIC
ELECTE
DEC 2 6 1991
S C D

AD-A243 623

LQG CONTROL OF A DEFORMABLE MIRROR ADAPTIVE
OPTICS SYSTEM WITH TIME-DELAYED MEASUREMENTS

THESIS

David J. Anderson
Captain, USAF

AFIT/GE/ENG/91D-03

91-19045

91 12 24 076

BEST

AVAILABLE

COPY

13 December 1991   Master's Thesis

LQG Control of a Deformable Mirror Adaptive
Optics System with Time-Delayed Measurements

David J. Anderson
Captain, USAF

Air Force Institute of Technology
WPAFB OH 45433-6583

AFIT/GE/ENG/91D-03

Phillips Laboratory (PL)/ARCI
KAFB NM 87117-6008

This thesis proposes a linear quadratic Gaussian (LQG) control law for a ground-based deformable mirror adaptive optics system. The incoming image wavefront is distorted, primarily in phase, due to the turbulent effects of the earth's atmosphere. The adaptive optics system attempts to compensate for the distortion with a deformable mirror. A Hartmann wavefront sensor measures the degree of distortion in the image wavefront. The measurements are input to a Kalman filter which estimates the system states. The state estimates are processed by a linear quadratic regulator which generates the appropriate control voltages to apply to the deformable mirror actuators. The dynamics model for the atmospheric phase distortion consists of 14 Zernike coefficient states; each modeled as a first-order linear time-invariant shaping filter driven by zero-mean white Gaussian noise. The dynamics of the deformable mirror are also model as 14 Zernike coefficients with first-order deterministic dynamics. A significant reduction in total wavefront phase distortion is achieved in the presence of time-delayed measurements. Wavefront sensor sampling rate is the major factor limiting system performance. The Multimode Simulation for Optimal Filter Evaluation (MSOFE) software is the performance evaluation tool of choice for this research.

Adaptive Optics, LQG Control, Time Delay Compensation, Zernike Models for the Atmosphere,   360
Shaping Filter Analysis

Unclassified   Unclassified   Unclassified   UL

GENERAL INSTRUCTIONS FOR COMPLETING SF 298

The Report Documentation Page (RDP) is used in announcing and cataloging reoprts. It is important that this information be consistent with the rest of the report, particularly the cover and title page. Instructions for filling in each block of the form follow. It is important to stay within the lines to meet optical scanning requirements.

Block 1. Agency Use Only (Leave blank).

Block 2. Report Date. Full publication date including day, month,a nd year, if available (e.g. 1 jan 88). Must cite at least the year.

Block 3. Type of Report and Dates Covered. State whether report is interim, final, etc. If applicable, enter inclusive report dates (e.g. 10 Jun 87 - 30 Jun 88).

Block 4. Title and Subtitle. A title is taken from the part of the report that provides the most meaningful and complete information. When a report is prepared in more than one volume, repeat the primary title, add volume number, and include subtitle for the specific volume. On classified documents enter the title classification in parentheses.

Block 5. Funding Numbers. To include contract and grant numbers; may include program element numbers(s), project number(s), task number(s), and work unit number(s). Use the following labels:

C	- Contract	PR	- Project
G	- Grant	TA	- Task
PE	- Program Element	WU	- Work Unit Accession No.

Block 6. Author(s). Name(s) of person(s) responsible for writing the report, performing the research, or credited with the content of the report. If editor or compiler, this should follow the name(s).

Block 7. Performing Organization Name(s) and Address(es). Self-explanatory.

Block 8. Performing Organization Report Number. Enter the unique alphanumeric report number(s) assigned by the organization performing the repor.

Block 9. Sponsoring/Monitoring Agency Names(s) and Address(es). Self-explanatory

Block 10. Sponsoring/Monitoring Agency Report Number. (If known)

Block 11. Supplementary Notes. Enter information not included elsewhere such as: Prepared in cooperation with...; Trans. of ...; To be published in... When a report is revised, include a statement whether the new report supersedes or supplements the older report.

Block 12a. Distribution/Availability Statement. Denotes public availability or limitations. Cite any availability to the public. Enter additional limitations or special markings in all capitals (e.g. NOFORN, REL, ITAR).

DOD	- See DoDD 5230.24, "Distribution Statements on Technical Documents."
DOE	- See authorities.
NASA	- See Handbook NHB 2200.2.
NTIS	- Leave blank.

Block 12b. Distribution Code.

DOD	- Leave blank.
DOE	- Enter DOE distribution categories from the Standard Distribution for Unclassified Scientific and Technical Reports.
NASA	- Leave blank.
NTIS	- Leave blank.

Block 13. Abstract. Include a brief (Maximum 200 words) factual summary of the most significant information contained in the report.

Block 14. Subject Terms. Keywords or phrases identifying major subjects in the report.

Block 15. Number of Pages. Enter the total number of pages.

Block 16. Price Code. Enter appropriate price code (NTIS only).

Blocks 17.-19. Security Classifications. Self-explanatory. Enter U.S. Security Classification in accordance with U.S. Security Regulations (I.e., UNCLASSIFIED). If form contins classified information, stamp classification on the top and bottom of the page.

Block 20. Limitation of Abstract. This block must be completed to assign a limitation to the abstract. Enter either UL (unlimited) or SAR (same as report). An entry in this block is necessary if the abstract is to be limited. If blank, the abstract is assumed to be unlimited.

LQG CONTROL OF A DEFORMABLE MIRROR ADAPTIVE OPTICS SYSTEM

WITH TIME-DELAYED MEASUREMENTS

THESIS

Presented to the Faculty of the School of Engineering

of the Air Force Institute of Technology

Air University

In Partial Fulfillment of the

Requirements for the Degree of

Master of Science in Electrical Engineering

David J. Anderson, B.S.E.E.

Captain, USAF

13 December 1991

Preface

This research effort develops a proof-of-concept linear quadratic Gaussian control law designed for a deformable mirror adaptive optics system with the purpose of compensating for optical wavefront phase aberration induced by the earth's atmosphere. The models developed for the dynamics and measurements are derived primarily from theoretical results available in the literature.

I would like to express my sincere thanks to my thesis advisor, Capt Randy Paschall. His blend of technical advise, freedom for the author, and friendly guidance along the way contributed to making this a most rewarding experience. I also wish to recognize the contributions of thesis committee members Dr. Peter Maybeck, who provided valuable stochastic modeling insights, and Capt Byron Welsh, who guided me through the intricacies of the optics. Capts Mike Roggemann and Mark Von Bokern of the Phillips Laboratory provided additional insights.

Above all, my deepest thanks go to my wife, Shelley, and my sons, Alex and Keith, whose constant love and smiling faces were a shining light at the end of some long AFIT days.

Table of Contents

List of Figures

List of Tables

List of Symbols

AFIT/GE/ENG/91D-03

Abstract

This thesis proposes a linear quadratic Gaussian (LQG) control law for a ground-based deformable mirror adaptive optics system. The incoming image wavefront is distorted, primarily in phase, due to the turbulent effects of the earth's atmosphere. The adaptive optics system attempts to compensate for the distortion with a deformable mirror. A Hartmann wavefront sensor measures the degree of distortion in the image wavefront. The measurements are input to a Kalman filter which estimates the system states. The state estimates are processed by a linear quadratic regulator which generates the appropriate control voltages to apply to the deformable mirror actuators.

The dynamics model for the atmospheric phase distortion consists of 14 Zernike coefficient states, each modeled as a first-order linear time-invariant shaping filter driven by zero-mean white Gaussian noise. The dynamics of the deformable mirror are also model as 14 Zernike coefficients with first-order deterministic dynamics. Several controller structures are presented which admit to state correlations, measurement time delay, and the truly time-varying nature of the atmosphere. The Multimode Simulation for Optimal Filter Evaluation (MSOFE) software is the performance evaluation tool of choice for this research. A significant reduction in total wavefront phase distortion is achieved in the presence of time-delayed measurements. Wavefront sensor sampling rate is the major factor limiting the performance of the system.

LQG CONTROL OF A DEFORMABLE MIRROR ADAPTIVE OPTICS SYSTEM WITH TIME-DELAYED MEASUREMENTS

1. Introduction

This thesis is an extension of previous AFIT research in which the objective is to design a Linear Quadratic Gaussian (LQG) control law for a deformable mirror adaptive optics system. LQG control is optimal in the sense of minimizing a defined cost function which assigns penalties to deviations from desired system behavior and to the amount of control energy expended. By virtue of the Kalman filter within the controller structure, LQG control also considers the effects of measurement uncertainty and the stochastic nature of the system dynamics. The reader is referred to the literature for a complete discussion of LQG control theory [1, 3, 17, 21].

1.1 Background

The Air Force has a requirement for high-resolution ground-based optical imaging of celestial and man-made bodies in space. From physics, the achievable resolution of such imaging is diffraction-limited by the receiving aperture. The resolution is a function of both the diameter of the aperture and the wavelength of light. Better resolution is achieved as the ratio of aperture diameter to wavelength increases.

A major obstacle to imaging bodies in space is the fact that the earth's atmosphere, through which the image must propagate, is by no means a benign environment. It has long been recognized that atmospheric turbulence causes severe degradation in the quality of the received

image using ground-based telescopes. When one wishes to resolve distant objects of small angular separation, it is desirable to reduce the central disk of the diffraction pattern to the greatest extent possible. This can be achieved by either increasing the diameter of the receiving aperture or by using shorter wavelength light [9:737]. Hardy [10] reports that, under average viewing conditions, atmospheric turbulence may degrade the resolution of large telescopes to two arc seconds or more; that is, in order to resolve distant objects from one another they must be separated by a minimum angular distance of two arc seconds. Two arc second resolution corresponds to diffraction-limited viewing through a six centimeter aperture at visible wavelengths. Thus, the atmosphere can effectively reduce the resolution gained by using larger telescopes to that of much smaller devices.

Adaptive optics, using deformable mirrors, provides a means for removing most of the atmospheric distortion from the incoming aberrated image. Figure 1.1 illustrates one possible approach to compensate for this distortion. The received image is reflected from a deformable mirror onto a wavefront sensor. Measurements from the wavefront sensor are input to an observer which processes an estimate of the system state vector describing the distortion in the image. Using the state estimate, a regulator generates appropriate commands to the deformable mirror actuators to negate the distortion due to atmospheric effects [30].

Many government agencies and private institutions are actively pursuing adaptive optics control techniques in order to compensate for the deleterious effects of atmospheric turbulence on optical image quality. The Phillips Laboratory (PL) at Kirtland AFB NM, is particularly interested in ground-based observation of orbiting satellites and is the sponsor of this research. As such, the controller design in this research is tailored to the specifications of an adaptive optics system configuration at the PL.
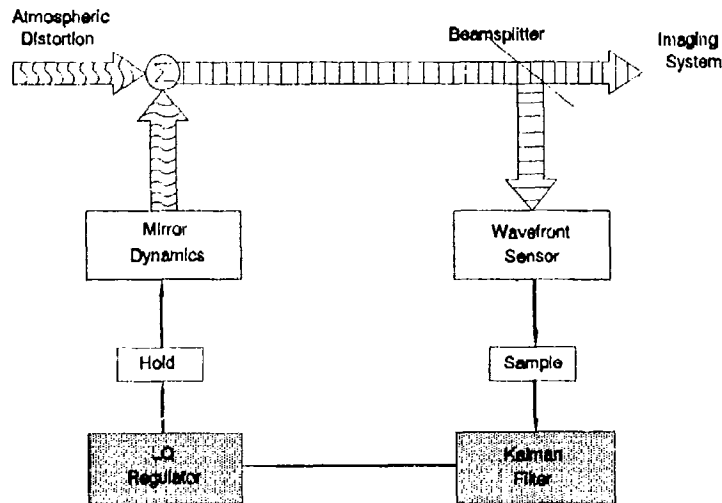
Figure 1.1. Adaptive Optics System Functional Diagram

1.2 Summary of Previous Research

The main body of previous research applicable to this thesis was conducted by Von Bokern [30]. Von Bokern developed a truth model, Kalman filter and LQG control law upon which this research builds. Additional research rele٠an٠ to this thesis is the Hartmann wavefront sensor research by Miller [22].

Von Bokern's work resulted in the mathematical models required for synthesizing the LQG regulator, that is, models for atmospheric distortion, the deformable mirror, and the wavefront sensor. He also developed the controller performance evaluation software using the Multimode Simulation for Optimal Filter Evaluation (MSOFE) computer simulation [23]. Through computer simulation of these models, Von Bokern achieved a simulated 40-60 percent reduction of the root-mean-square (rms) phase distortion in the image wavefront. In order to design a control law that was readily synthesizable, Von Bokern made a number of assumptions. Many of the assumptions were not overly restrictive and are assumed for this research, as

1-3

discussed in Section 1.4. However, several of those assumptions must be addressed before an implementable design is available. Specifically, Von Bokern assumed the individual states describing the distortive effects of the atmosphere to be uncorrelated with each other. He also assumed that measurements from the wavefront sensor are available instantaneously every 7 msecs for updating the observer state estimate. Finally, he assumed the system is time-invariant. The assumption of uncorrelated states is removed by modeling the cross-correlations through the dynamics driving noise strength matrix. The assumption of instantaneous measurement updates is also removed by modeling the wavefront sensor delay and incorporating a predictor as compensation for the delay. Finally, the time-invariance assumption is not removed, however, the impact of making this assumption is examined through a sensitivity study of the control system performance in the presence of variations in the dynamics of the atmosphere.

The important aspect of Miller's work [22], for this research, is that he quantified the system time delay resulting from the computational limitations of the wavefront sensor. Miller analyzed actual Hartmann wavefront sensor frequency response data to determine the inherent time delay and provided insights as to the characteristics of the sensor noise.

1.3 Research Objectives

The overall objective of this research is to evaluate the performance of Von Bokern's controller design in the presence of factors which were ignored during his research, but which actually exist as part of the real world system to be controlled. The ultimate goal is to modify the controller as necessary to deal with these additional factors adequately while maintaining an acceptable level of performance. The specific objectives of this research are:

1. Model the cross-covariance between the Zernike coefficients to reflect the correlated nature of the atmospheric states upon which the truth model and Kalman filter are

based. By modeling the correlatedness of the atmospheric states, a more realistic portrayal of the truth model for the atmosphere is achieved.

2. Compensate for the effects of measurement processing time delay in the wavefront sensor on Kalman filter performance. The degree to which the phase of the optical wavefront can change, from the time the wavefront is sampled to the time the measurement becomes available, can be significant and, therefore, requires compensation.

3. Investigate the sensitivity of the controller design to changing atmospheric conditions. Although assumed time-invariant for controller synthesis purposes, the true nature of the atmosphere is time-varying. Thus, it is necessary to evaluate the conditions under which the control law is valid and propose modifications to expand the range of conditions where acceptable performance can be achieved.

4. Reevaluate the initial conditions imposed on the filter covariance matrix to improve filter transient performance. The initial conditions on the filter covariance matrix were set to zero in Von Bokern's work. Since the degree of initial uncertainty as to the magnitude of the wavefront phase distortion is likely to be large, setting the initial covariances to large values will cause the filter to weight the early measurements more heavily. By so doing, the filter's transient performance may be improved.

5. Investigate the feasibility of employing a constant-gain Kalman filter in the controller. Using a constant-gain filter greatly reduces the computational burden of processing the filter algorithm.

1.4 Assumptions

This research develops a proof-of-concept LQG controller design. Although several of the assumptions made during previous research are removed for this thesis, many of the previously held assumptions are still required in order to keep the magnitude of the problem at a manageable level. The assumptions are made based on literature precedent [7,30], lack of data for developing more precise models, discussions with the sponsoring agency [28], and engineering judgment.

First, it is assumed the telescope is ground-based, with the purpose of observing orbiting satellites. It is also assumed that a separate controller is tasked with keeping the telescope pointed at the satellite. Neither of the first two assumptions are restrictive for actual applications. The telescope is assumed to use a visible point source of light in proximity to the satellite as a reference, and that anisoplanatism is negligible; that is, the light from the reference source traverses the same atmosphere as the light from the satellite. As such, deforming the mirror to compensate for the distortion in the reference image will also improve the resolution of the satellite image. Since this research deals with satellites which are stationary with respect to the observer, the reference source remains within the same isoplanatic patch [7]. Therefore, the assumption of negligible effects due to anisoplanatism is not overly restrictive and simplifies the mathematics involved.

Deforming the mirror is accomplished via 97 piezoelectric actuators arranged in evenly spaced rows and columns on the back of the mirror (Figure 2.3). Each actuator is assumed to have linear dynamics and all actuators are assumed to have identically symmetric influence functions. Actuator influence and response data [18] substantiate these assumptions. However, as the actuators are not strictly linear, symmetric, or identical in response characteristics, these

1-6

assumptions result in error contributions from each actuator to the phase front induced on the surface of the mirror. These error contributions are assumed to be small.

In actual applications, separate tilt mirrors are likely to precede the deformable mirror. The tilt mirrors remove the gross tilts of the overall wavefront distortion. The tilt mirrors are not specifically modeled as part of this research; however, it is assumed that 80 percent of the gross tilts are removed from the wavefront before it reaches the deformable mirror. As a result, this research models the residual distortion in the image reflected off the tilt mirrors.

The dynamics model describing the atmosphere is assumed to be time-invariant. This assumption is valid provided the duration of the observation is short relative to the truly time-varying nature of the atmospheric statistics. As the observation period becomes longer, the time-varying dynamics of the atmosphere will cause the performance of the controller to degrade significantly. The effects of variations in the atmosphere are evaluated in this research.

The time delay associated with light propagation through the optical components is assumed to be negligible. The time delay due to measurement processing in the wavefront sensor is not negligible and is modeled as part of this research.

1.5 Research Approach

This section provides a brief discussion of the approach taken to accomplish the objectives outlined in Section 1.3. The primary objective is to explore the limitations of the previous regulator design and seek performance improvements. The controller developed in this thesis is evaluated against the baseline design developed by Von Bokern [30] as a measure of performance improvement.

1. The assumption of a diagonal covariance matrix for the states of the atmospheric model is removed through modeling of the correlation between Zernike coefficients.

The covariances between Zernike coefficients are available in the literature [27, 32] and are incorporated into the truth and filter models through the covariance and dynamics driving noise strength matrices. Section 3.3 presents the modifications to the truth and filter models for incorporating the cross-correlation information.

2. Von Bokern's research assumed that all 138 measurements from the Hartmann wavefront sensor are available simultaneously at each sample time and can be incorporated without delay. However, by the time all measurements have been collected and are available, they are actually approximately 7 msecs [22] old. This assumption is removed and a predictor is augmented to the Kalman filter to compensate for the effects of wavefront measurement processing delay on Kalman filter performance. The resulting controller is simulated using the MSOFE computer simulation. Section 3.4 develops the models for the predictor.

3. The previous controller design was evaluated for specific atmospheric conditions. The atmosphere is typically modeled in terms of the refractive index structure constant (C_n^2) and wind velocity along the propagation path [12]. From previous research [30], C_n^2 is calculated as a function of altitude using the Hufnagel-Valley 21 model [26] and the wind velocity is also calculated as a function of altitude using the Bufton model [26]. In this research, various atmospheric conditions are independently simulated in the truth model and a performance evaluation of the nominal condition controller is conducted for each set of conditions. The filter is then retuned, separately for each set of conditions, and a new optimal controller gain matrix is computed to evaluate controller performance for the existing conditions.

Section 3.5 describes the procedures used in generating appropriate variations on the truth model in order to obtain a representative range of atmospheric conditions.

4. Time plots for the filter state covariances from Von Bokern's research reveal atypical transient performance. One typically expects to see a large covariance initially (to enhance acquisition) and a short transient to a steady-state condition for linear time-invariant systems [19]. The initially small covariance indicated in the plots suggest that the initial conditions on the covariance matrix be increased. During the simulation phase discussed in Chapter 5, a study is conducted in which the initial conditions on the covariance matrix entries are increased, and the filter's transient performance is evaluated.

5. The speed with which the filter covariance converges to a steady-state value motivates a study of employing a constant-gain filter. The appropriate steady-state Kalman filter gain is identified and the constant-gain filter structure is simulated using MSOFE [23]. The validity of the constant-gain filter is evaluated in Chapter 5 based on the degree of performance degradation exhibited in the simulation relative to the baseline filter design.

Prior to addressing the objectives outlined for this thesis, a reevaluation of the truth model was required based on discrepancies between the state covariance data presented by Von Bokern and that available in the literature. Review of the computer software used in generating Zernike coefficient autocorrelation data revealed a scale factor error. The autocorrelation data are used in the truth model development for the atmosphere via shaping filter techniques. The truth model for this research is corrected to match the atmospheric state covariance data in the literature more

closely, although the structure of the model remains the same. The truth model shaping filter analysis is presented in Appendix A.

1.6 Treatment

The subject matter of this thesis is presented in a topical manner. Chapter II establishes the foundation for this research by presenting the key concepts and results developed by Von Bokern [30]. This discussion provides background information essential to the developments of succeeding chapters. Chapter III develops the models required to address the objectives defined in Chapter I. Chapter IV describes the modifications to the baseline controller structure. Chapter V presents the results from computer simulation of the modified control law. Chapter VI discusses the significant conclusions and presents recommendations for future research.

II. Background

2.1 Optical Characteristics of the Atmosphere

Light propagating through the earth's atmosphere experiences numerous distortive effects. In particular, for imaging applications, atmospheric turbulence along the propagation path causes continuous spatial and temporal variations in the index of refraction. Such variations in index of refraction result in spatial and temporal modulation of intensity and phase of the optical image. Developments throughout the literature [12, 24, 27] strongly suggest the modulation of phase to be the dominant distortive component. This research is directed towards phase distortion compensation.

The random nature of the turbulent atmosphere prohibits a deterministic expression relating turbulent effects to optical image quality. The quality of the received image depends on such factors as the wavelength, altitude-dependent refractive index structure function constant, zenith angle to the viewed satellite, wind velocity, and wind velocity distribution as a function of altitude. The combination of these effects ultimately results in a randomly distorted wavefront. Von Bokern [30] gives a brief description of the statistics associated with a turbulent atmosphere. Further statistical details and mathematical rigor are available in the literature [12].

2.2 Zernike Function Representation of Phase Distortion

Having established the desire to compensate for the phase distortion in a received image, it becomes necessary to have a means of describing the phase distortion present in the wavefront. Assume a circular aperture is pointed at a distant point source of light. If no distortive elements exist along the optical path of the image, the phase of the wavefront at any two points within the aperture would be equal. Figure 2.1 illustrates the case of such a "planar" wavefront.
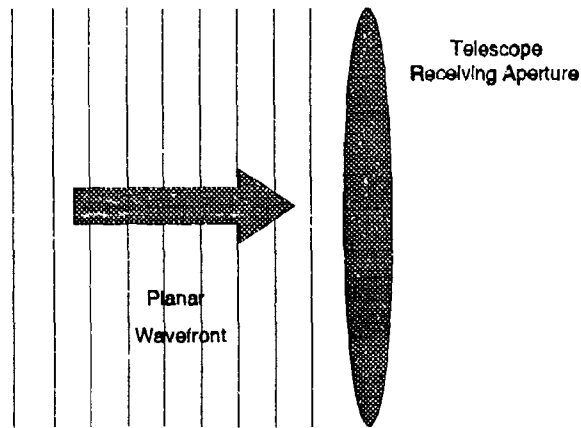
Figure 2.1. Planar Wavefront at a Circular Aperture

If the image is now allowed to propagate through a turbulent medium, the wavefront of the received image becomes distorted, that is, the phase of the image wavefront at any two points within the aperture will no longer be the same. Figure 2.2 shows the case of a distorted wavefront.
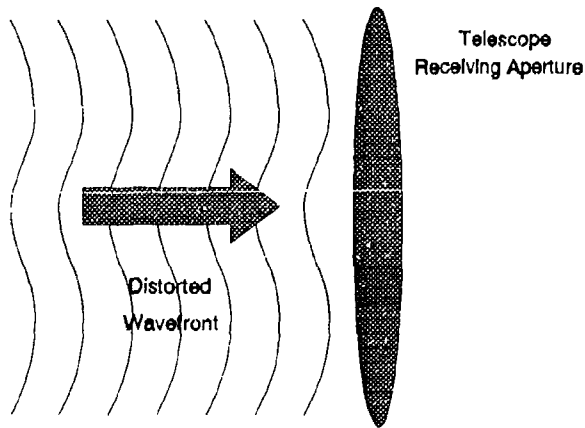
Figure 2.2. Distorted Wavefront at a Circular Aperture

A popular representation [6, 24, 29, 31, 32] for describing phase distortion is by a set of Zernike polynomials. Other functional forms are mentioned in the literature, however the Zernike function space provides an orthogonal basis set of functions corresponding to aberrations commonly studied in optics [30:2.11]. The phase distortion is, therefore, described by a linear combination of the Zernike functions:

$$\phi(r,\Theta,t) = \sum_{i=0}^{N} a_i(t)\, Z_i(r,\Theta) \tag{2.1}$$

where the $Z_i(r,\Theta)$ are the Zernike basis functions spanning the space within the aperture as functions of the radial and angular coordinates r and Θ, the $a_i(t)$ are the time-varying coefficients, and $\phi(r,\Theta,t)$ is the total phase of the wavefront as a function of time and position within the aperture. The Zernike functions are real, dimensionless, deterministic functions of position within the aperture. The Zernike coefficients are random real functions of time with units of wavelengths for this research.

In theory, an infinite number of Zernike functions are required to describe the phase of a wavefront completely [29]. Von Bokern illustrates that approximately 92 percent of the rms phase information can be modeled using the first 14 Zernike modes, excluding piston (zero[th] mode) [30:B.4]. The piston mode represents the aperture-averaged phase. It is nondistortive and unobservable by the wavefront sensor. As such, piston is removed from the summation in Equation (2.1) resulting in a functional representation for the phase deviation from aperture-averaged phase, or deviation from the "planar" wavefront. Modes beyond the first 14 could be modeled to provide a more complete portrayal of the true phase distortion; however, the amount of residual distortion modeled for each additional mode becomes very small. Further justification

for stopping at the fourteenth Zernike mode based on spatial Nyquist considerations of actuator and wavefront sensor geometry, for the problem considered in this research, is given by Von Bokern [30:B.3-B.4]. The first fifteen Zernike functions are presented in Table 2.1 along with radial order (n), azimuthal order (m), and name.

An important property of the Zernike functions is they form an orthogonal basis set of functions which satisfy the relation [29:79]:

Table 2.1. First 15 Zernike Functions

i	n	m	$Z_i(r,\Theta)$	Name
0	0	0	1	piston
1	1	1	$2(r/R)\cos(\Theta)$	y-tilt
2	1	1	$2(r/R)\sin(\Theta)$	x-tilt
3	2	0	$\sqrt{3}[2(r/R)^2-1]$	focus
4	2	2	$\sqrt{6}(r/R)^2\sin(2\Theta)$	astigmatism
5	2	2	$\sqrt{6}(r/R)^2\cos(2\Theta)$	astigmatism
6	3	1	$\sqrt{8}[3(r/R)^3-2(r/R)]\sin(\Theta)$	pure coma
7	3	1	$\sqrt{8}[3(r/R)^3-2(r/R)]\cos(\Theta)$	pure coma
8	3	3	$\sqrt{8}(r/R)^3\sin(3\Theta)$	zero curvature coma
9	3	3	$\sqrt{8}(r/R)^3\cos(3\Theta)$	zero curvature coma
10	4	0	$\sqrt{5}[6(r/R)^4-6(r/R)^2+1]$	spherical
11	4	2	$\sqrt{10}[4(r/R)^4-3(r/R)^2]\cos(2\Theta)$	5th order astigmatism
12	4	2	$\sqrt{10}[4(r/R)^4-3(r/R)^2]\sin(2\Theta)$	5th order astigmatism
13	4	4	$\sqrt{10}(r/R)^4\cos(4\Theta)$	NA
14	4	4	$\sqrt{10}(r/R)^4\sin(4\Theta)$	NA

$$\frac{1}{\pi R^2} \int\limits_0^{2\pi} d\Theta \int\limits_0^R Z_i(r,\Theta) \, Z_j(r,\Theta) \, r \, dr \, = \, \delta_{ij} \qquad (2.2)$$

where R is the radius of the aperture and δ_{ij} is the Kronecker delta function:

$$\delta_{ij} \, = \, \begin{cases} 1, & i = j \\ 0, & i \neq j \end{cases} \qquad (2.3)$$

From Equations (2.1) and (2.2), it can be shown [30:C.1-C.2] that the rms value of the phase across an aperture is simply the root-sum-square (rss) of the Zernike coefficients given by:

$$\tilde{\phi} \, = \, \sqrt{a_1^2 \, + \, a_2^2 \, + \, a_3^2 \, + \, ... \, + \, a_{14}^2} \qquad (2.4)$$

The Zernike coefficients for an arbitrary value of phase are obtained using [29:79]:

$$a_i(t) \, = \, \frac{\int d\Theta \int W(r,\Theta) \, \phi(r,\Theta,t) \, Z_i(r,\Theta) \, r \, dr}{\int d\Theta \int W(r,\Theta) \, r \, dr} \qquad (2.5)$$

where $W(r,\Theta)$ is the aperture weighting function defined for this research as [29:79]:

$$W(r,\Theta) \, = \, \begin{cases} 1, & r \leq R \\ 0, & r > R \end{cases} \qquad (2.6)$$

2.3 Deformable Mirror Dynamics

The deformable mirror considered in this research is a Low-Voltage Electrodistortive Mirror manufactured by Itek for the Phillips Laboratory (formerly the Air Force Weapons Laboratory). The mirror consists of four major components: the facesheet, base, driver electronics, and actuators. The facesheet is constructed of ultra-low expansion glass (ULE) and is bonded to 129

actuator pusher pads machined into the rear surface of the mirror. The base is also constructed of ULE in order to reduce thermal expansion effects on the actuators [18:1].

The 129 actuators are constructed of piezoelectric stacks of lead magnesium niobate (PMN). The electrorestrictive nature of PMN causes an actuator to contract whenever a positive or negative voltage is applied. Each actuator can withstand a maximum voltage magnitude of 300 volts. In order to make two-way control of the actuators possible, a bias voltage of -150 volts is applied to the piez   stack. The result of the bias is such that application of a positive voltage reduces the overall voltage magnitude, thereby allowing the piezoelectric stack to expand. Also, application of a negative voltage increases the voltage magnitude and the stack contracts further [18:4].

The mirror driver electronics convert a ±10 volts control signal to the 0-300 volt range required to dr .e the actuators. A control voltage of -10 volts corresponds to -150 volts applied to the stack for a total voltage magnitude of 300 volts. A control voltage of +10 volts results in +150 volts applied to the stack for a total voltage magnitude of 0 volts [18:15].

Although the mirror has 129 actuators available, only the central 97 are actively controlled. The remaining 32 actuators are biased to their mid-points in order to establish a fixed boundary condition [18:4]. Figure 2.3 shows the location of the 97 active actuators.

This research assumes linearity of the response of a single actuator to an applied control voltage [30:3.6] Although test data indicate the response is not strictly linear, it is assumed that a weighting matrix in the cost function associated with the LQ regulator keeps actuator responses within their respective linear regions. The linearity assumption carries with it the property of linear superposition between individual actuators. This property is exploited in the development of the mirror dynamics equation.

Y-axis (cm)

```
+5
                  68   55 — 44 — 33   22
              77  67  56  45  34  23  12
          88  78  68  57  46  35  24  14  08
      93/  87  79  69  58  47  36  25  15  07  \01
      94   88  80  70  59  48  37  26  16  08   02
  0   95 - 89 - 81 - 71 - 60 - 49 - 38 - 27 - 17 - 09 - 08
      96   90  82  72  61  50  39  28  18  10   04
      97\  91  83  73  62  51  40  29  19  11  /05
          92  84  74  63  52  41  30  20  12
              85  75  64  53  42  31  21
                  76   66   54 — 43   32
-5
   -5                    0                    +5
```

X-axis (cm)
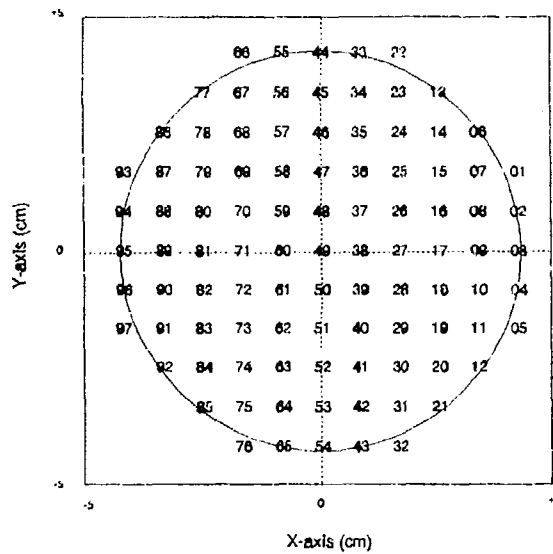
Figure 2.3. Mirror Actuator Locations

2.3.1 Steady-State Mirror Response. Upon application of a control voltage to the deformable mirror, the response is not instantaneous, and a finite period of time is required before the mirror reaches a steady-state position. This section deals with the relationship between an applied control voltage and the mirror steady-state response.

The effect of a single actuator on the shape of the mirror is mathematically described by its influence function. Each actuator's influence function is spatially limited, that is, the influence function is nonzero only in proximity to its associated actuator. This research assumes that the influence functions for each of the 97 actuators is identical. Test data show the influence functions are not quite identical, however, the data indicate this assumption is not overly restrictive [18].

Influence data were provided by Itek corresponding to two-dimensional slices of the central actuator at 90 degree (along X-axis of the mirror) and 45 degree orientations. The degree of similarity between these data are the basis for the assumption of symmetric influence functions

2-7

in all directions. The data were appropriately scaled to reflect two-way decrease in optical

pathlength. Next, the data were curve-fit to a tenth-order polynomial in X, truncated at $X=\pm 1.6739$

cm, and rotated about the actuator axis resulting in a three-dimensional influence function. The

location on the mirror at $X=\pm 1.6739$ cm represents the spatial limit of the influence function. The

resulting influence function expressed in terms of position on the mirror is given as [30:3.8]:

$$
\begin{aligned}
f(X,Y,X_A,Y_A) = &\; \{0.9673 \\
&- 2.726[(X - X_A)^2 + (Y - Y_A)^2] \\
&+ 2.943[(X - X_A)^2 + (Y - Y_A)^2]^2 \\
&- 1.573[(X - X_A)^2 + (Y - Y_A)^2]^3 \\
&+ 0.4137[(X - X_A)^2 + (Y - Y_A)^2]^4 \\
&- 0.04236[(X - X_A)^2 + (Y - Y_A)^2]^5\} \\
&\times u_{-1}([1.6739]^2 - [(X - X_A)^2 + (Y - Y_A)^2])
\end{aligned}
\tag{2.7}
$$

where

X, Y	= coordinates of a point on the mirror (cm)
X_A, Y_A	= coordinates of the actuator (cm)
$u_{-1}(\cdot)$	= unit step function
f	= two-way decrease in pathlength (wavelengths/volt)

When this concept is expanded to the case in which control voltages are applied to all 97

actuators, invoking linear superposition, a linear sum of 97 such influence functions results which

represents the contribution of the mirror to the distortion in the reflected wavefront as:

$$
\phi(X,Y) = \left[\sum_{A=1}^{97} f(X,Y,X_A,Y_A)u(A)\right] - \bar{\phi}(X,Y)
\tag{2.8}
$$

where $u(A)$ is the control voltage applied to the Ath mirror actuator and $\bar{\phi}(X,Y)$ describes the spatial

average phase which when subtracted from the total phase effectively removes the piston mode.

Since atmospheric distortion is modeled as a sum of the first 14 Zernike functions, it stands to

reason that the mirror is attempting to compensate for only those 14 modes. As such, phase

distortion imparted on the reflected wavefront by the mirror can also be modeled as a sum of 14 Zernike functions (piston removed) as given in Equation (2.1). Combining Equations (2.5) and (2.8), the Zernike coefficients, a_i, can be determined according to [30:3.12]:

$$a_i = \sum_{A=1}^{97} \left\{ \left[\frac{\int dY \int dX \ W(X,Y) \ f(X,Y,X_A,Y_A) \ Z_i(X,Y)}{\int dY \int dX \ W(X,Y)} \right] u(A) \right\} \quad (2.9)$$

An equation of the form of (2.9) can be written for each Zernike coefficient. Each of these equations can then be expressed in vector form and augmented together as [30:3.12]:

$$a = Mu \quad (2.10)$$

where a is a 14-vector of Zernike coefficients describing the steady-state mirror contribution to the distortion in the reflected wavefront, u is a 97-vector of actuator control voltages, and M is the 14 x 97 steady-state influence matrix whose individual elements are computed from the square-bracketed term in Equation (2.9). The M matrix elements are the projections of each actuator's influence function along each Zernike function direction.

2.3.2 Mirror Transient Response. As previously mentioned, the mirror does not instantaneously respond to applied control voltage. Manufacturer documentation for the mirror [18] remarks that the mirror actuators act as a high capacitive load. Thus, the actuator can be expected to respond to an applied step control voltage input in an exponential fashion to a steady-state condition.

Frequency response data provided by Itek and the PL indicate the mean bandwidth of the actuators to be 500 Hz. Assuming identical frequency response characteristics and first-order, time-invariant, deterministic dynamics for each actuator, Von Bokern derives an equation for the mirror displacement dynamics at an actuator site to be of the form [30:3.15]:

$$\dot{g}(t) = cg(t) + du(t) \tag{2.11}$$

where $g(t)$ is the two-way optical pathlength decrease at the actuator location. Using LaPlace transform techniques and the peak displacement of the described influence function, the values of c and d are found to be [30:3.16]:

$$c \approx -\frac{1}{0.00045} \ \sec^{-1}$$
$$d \approx 2150 \ \frac{wavelengths}{volt \cdot sec} \tag{2.12}$$

Combining Equations (2.11) and (2.12), the dynamic equation for a single actuator is approximately [30:3.16]:

$$\dot{g}(t) = -\frac{1}{0.00045}g(t) + 2150u(t) \tag{2.13}$$

2.4 Dynamics Modeling

The structure of the Kalman filter associated with Linear Quadratic Gaussian (LQG) control requires a linear stochastic state-space model of the dynamics of the system to be controlled. Figure 1.1 is a functional diagram of the adaptive optics system to which this research is directed. The dynamic components of the system which must be modeled are the phase distortion effects of the atmosphere, the deformable mirror, and the wavefront sensor.

For the case of a linear time-invariant system, the appropriate form for the continuous state dynamics is [19:169]:

$$\underline{\dot{x}}(t) = F\underline{x}(t) + B\underline{u}(t) + G\underline{w}(t) \tag{2.14}$$

2-10

along with sampled-data measurements of the form:

$$z(t_i) = H\underline{x}(t_i) + \underline{v}(t_i) \qquad (2.15)$$

where

$\underline{\dot{x}}(t)$	= derivative of system state vector with respect to time
$\underline{x}(t)$	= system state vector (n x 1)
F	= plant dynamics matrix (n x n)
$\underline{u}(t)$	= deterministic input vector (r x 1)
B	= input distribution matrix (n x r)
$\underline{w}(t)$	= zero-mean white Gaussian dynamics driving noise vector (s x 1)
G	= dynamics driving noise distribution matrix (n x s)
$\underline{z}(t_i)$	= sampled-data measurement vector (m x 1)
H	= discrete output matrix (m x n)
$\underline{v}(t_i)$	= zero-mean white Gaussian measurement noise (m x 1)

The appropriate strength of the zero-mean white Gaussian dynamics driving noise $\underline{w}(t)$, and

covariance kernel of the discrete-time zero-mean white Gaussian measurement corruption noise

$\underline{v}(t_i)$, are defined as [19:155,174]:

$$E\{\underline{w}(t)\ \underline{w}^T(t+\tau)\} = Q\ \delta(t-\tau) \qquad (2.16)$$

$$E\{\underline{v}(t_i)\ \underline{v}^T(t_j)\} = R\ \delta_{ij} \qquad (2.17)$$

where $E\{\cdot\}$ is the expected value operator, Q is the n x n dynamics driving noise strength matrix,

$\delta(\cdot)$ is the dirac delta, and R is the m x m measurement noise covariance matrix.

The equivalent discrete-time model for the linear system dynamics is [19:171]:

$$\underline{x}(t_{i+1}) = \Phi(t_{i+1},t_i)\underline{x}(t_i) + B_d\ \underline{u}(t_i) + \underline{w}_d(t_i) \qquad (2.18)$$

where $\Phi(t_{i+1},t_i)$ is the state transition matrix associated with the plant dynamics matrix F and the

discrete dynamics driving noise $\underline{w}_d(t_i)$ is of strength Q_d computed as [19:171]:

$$Q_d = \int_{t_i}^{t_{i+1}} \Phi(t_{i+1}, \tau) G Q G^T \Phi^T(t_{i+1}, \tau) \, d\tau \qquad (2.19)$$

The discrete input distribution matrix B_d is computed by [19:171]:

$$B_d = \int_{t_i}^{t_{i+1}} \Phi(t_{i+1}, \tau) B \, d\tau \qquad (2.20)$$

2.4.1 Stochastic Model for the Atmosphere. Using the Zernike function representation of Equation (2.1) to model the wavefront distortion in the receiving aperture, the stochastic nature of the problem resides in the random time-varying expansion coefficients. These coefficients are considered to be zero-mean Gaussian random variables [24:210]. Gaussianness is a result of the summation of the random distortive contributions from each turbulent layer of the atmosphere along the propagation path of the wavefront [30:3.1]. According to the central limit theorem [19:109], the sum of numerous independent random variables converges to a Gaussian distributed random variable as the number of individual variables grows without bound. As such, the Zernike coefficients are modeled [30] as the outputs of linear shaping filters of the form:

$$\dot{x}_a(t) = F_a x_a(t) + G_a w_a(t) \qquad (2.21)$$

where the a subscript denotes dynamics of the atmosphere.

One method for designing the appropriate shaping filters for each coefficient is to simulate autocorrelation data from analytic expressions for the autocorrelation kernels of the individual Zernike coefficients. The computer-generated autocorrelation data can then be curve-fit to standard shaping filter functions [19:180-185]. The derivation of the appropriate analytic

2-12

expressions required is mathematically rigorous and beyond the scope of this research. However, Hogge and Butts [12] derive such an expression under the assumption of Kolmogorov spectrum of turbulence [12, 5, 24, 30]:

$$E\{a_p(t)a_p(t+\tau)\} = R_p(\tau)$$

$$= 2\pi^2 k^2 L \int_0^1 dz \int_0^\infty dK\ K\ \Phi_n(K/R)$$

$$\cdot\{1 + \cos[K^2\ z\ N\ (1-z)]\}$$ (2.22)

$$\cdot \int d\rho \int d\rho'\ W(\rho;2)\ W(\rho';2)\ G_p(\rho)\ G_p(\rho')$$

$$\cdot J_0\ (K\ z\ |\rho\ \rho' + \frac{v\tau}{Rz}|)$$

where

k	= wave number = $2\pi/\lambda$ (m)$^{-1}$
L	= total propagation distance (m)
R	= radius of entrance aperture (m)
N	= $L/R^2 k$
$\Phi_n(K)$	= $0.033C_n^2 K^{-11/3}$, the Kolmogorov turbulence spectrum
$W(\rho;2)$	= aperture weighting function for unit circle
$G_p(\rho)$	= normalized p-th Zernike function
$J_0(\cdot)$	= zero order Bessel function of the first kind
$\underline{v}$	= wind velocity vector (m/sec)

Von Bokern implemented Equation (2.22) on the computer to generate autocorrelation data for each coefficient of the 14 Zernike modes included in the atmospheric model. Each set of data was plotted and curve-fit to a first order Markov process shaping filter function. Details concerning the shaping filter analysis are provided in Appendix A. The result is a 14-state model for the atmospheric phase distortion with diagonal F and Q matrices. Comparison of Zernike coefficient covariance data presented by Roddier [27:1176] and that which resulted from Von Bokern's integration of Equation (2.22) identified a scale factor error which has been corrected for this research. As such, the parameters which define the stochastic models for the atmospheric states

2-13

differ from those used by Von Bokern, although the structure remains the same. In terms of the state covariances, the resulting truth model matches the data in the literature more closely. The values used for the elements of the F and Q matrices are discussed in detail in Chapter 3.

2.4.2 Deterministic Model for Deformable Mirror. Earlier discussions concerning the dynamics at an actuator site can be extended to model the phase distortion across the entire mirror due to the actuators. Based on actuator displacement [30:3.7] and frequency response data [30:3.14], a first-order deterministic model was developed for an individual actuator. Under the assumptions of linear actuator response to applied control voltage, the property of linear superposition between actuators implies a linear model for the mirror as well. In actuality, a stochastic term could be included in the actuator model to account for noise in the control voltage as well as modeling uncertainty due to actuator nonlinearities and nonuniform bandwidth characteristics. However, due to lack of appropriate data for modeling these effects, this research assumes the deterministic actuator model is valid. We, therefore, seek a form for the dynamics equation of the mirror similar to Equation (2.14), without the driving noise term, given by:

$$\dot{x}_m(t) = F_m x_m(t) + B_m u(t) \tag{2.23}$$

where the vector $x_m(t)$ is composed of the Zernike coefficients describing the contribution of the mirror response to the overall phase distortion in the reflected wavefront.

Under the assumption of identical influence functions and frequency response characteristics for each of the 97 actuators, the entire mirror should exhibit appropriate response characteristics of a 0.00045 second time constant [30:3.16]. By defining $\phi_m(X,Y,t)$ as the contribution of the mirror to the total phase distortion in the reflected wavefront, the scalar differential equation describing the phase distortion can be written as [30:3.17]:

$$\dot{\phi}_m(X,Y,t) = -\frac{1}{\tau}\phi_m(X,Y,t) + \underline{b}_m^T(X,Y)\underline{u}(t) \tag{2.24}$$

where τ is the mirror time constant and the inner product of the vector $\underline{b}_m(X,Y)$ with the control voltage vector $\underline{u}(t)$ projects the actuator voltages onto the time rate-of-change of phase at the point (X,Y).

As previously discussed, the phase distortion contribution of the mirror can be described by a set of 14 Zernike functions similar to the atmospheric distortion. It is, therefore, desirable to express Equation (2.24) in the form of Equation (2.23). It can be shown [30:3.17-3.18] that by expressing $\phi_m(X,Y,t)$ in the equivalent rectangular coordinate form of Equation (2.1), taking its time-derivative, substituting these two expressions into Equation (2.24), and making use of the orthogonality property of Equation (2.2), an expression for each Zernike coefficient in the form of Equation (2.23) can be derived as:

$$\dot{a}_i(t) = -\frac{1}{\tau}a_i(t) + \frac{1}{\pi R^2}\mu_i^T \underline{u}(t) \tag{2.25}$$

where R is the radius of the receiving aperture, μ_i is defined such that its jth component is the projection of the jth component of $\underline{b}_m$ onto the $Z_i(X,Y)$ direction, and $i=1,2,3,...,14$. Equation (2.25) can be rewritten in state-space form as given in Equation (2.23) where F_m is a diagonal matrix with elements equal to $-1/0.00045$ and B_m is found by additional steady-state analysis [30:3.19] to be:

$$B_m = diag\left[\frac{1}{\tau}\right]M \tag{2.26}$$

where M is the steady-state influence matrix defined in Equation (2.10).

2.4.3 Augmented State-Space Dynamics Model. An overall system model which incorporates the dynamic behavior of both the atmospheric distortion and the deformable mirror is achieved through state augmentation of Equations (2.21) and (2.23). The resulting dynamics model is [30]:

$$\begin{bmatrix} \dot{x}_a(t) \\ \cdots \\ \dot{x}_m(t) \end{bmatrix} = \begin{bmatrix} F_a & \vdots & 0 \\ \cdots & & \cdots \\ 0 & \vdots & F_m \end{bmatrix} \begin{bmatrix} x_a(t) \\ \cdots \\ x_m(t) \end{bmatrix} + \begin{bmatrix} 0 \\ \cdots \\ B_m \end{bmatrix} u(t) + \begin{bmatrix} w_a(t) \\ \cdots \\ 0 \end{bmatrix}$$

(2.27)

where a subscripts denote atmospheric states and m subscripts denote mirror states. The lack of a stochastic term in the lower partition of Equation (2.27) comes from the assumption of deterministic mirror dynamics. It is important to note that, under the assumption of deterministic dynamics for the mirror, one should not include these states in an operational filter algorithm. Retension of the mirror states here is only for simulation purposes as dictated by the MSOFE software [23].

2.5 Wavefront Sensor Model

As illustrated in Figure 1.1, the wavefront reflected from the deformable mirror is sampled by a Hartmann wavefront sensor [22, 30]. The Hartmann sensor is made up of 69 square convex lenses, commonly referred to as subapertures, with dimensions of 0.06 cm on a side [22]. The function of each of the subaperture lenslets is to focus the portion of the incident light within the subaperture onto a reticon detector. The reticon uses the location of the focused spot to determine the slope or gradient of the wavefront within the particular subaperture.

The phase distortion in the reflected wavefront is modeled as the sum of the atmospheric distortion and the distortion resulting from deforming the mirror. As such, the phase distortion of the reflected wavefront can be expressed as:

$$a(t_i) = [A \vdots I] \begin{bmatrix} x_a(t_i) \\ \cdots \\ x_m(t_i) \end{bmatrix} \qquad (2.28)$$

where A is an extraction matrix for the atmospheric states. In general, multiple shaping filter states could be used to model each of the Zernike coefficients, in which case A could have off-diagonal elements. For this research, each Zernike coefficient is described by a first-order shaping filter and, therefore, A is a 14 x 14 identity matrix. As indicated in Figure 1.1, the wavefront sensor measures the phase distortion in the reflected wavefront. Sampled-data measurements for the wavefront sensor are modeled as [30:3.20]:

$$z(t_i) = Hx(t_i) + v(t_i) \qquad (2.29)$$

where the measurement matrix H is defined as:

$$H = H' [A \vdots I] \qquad (2.30)$$

and $x(t_i)$ is the augmented system state vector described in Section 2.4.3. The H' matrix is discussed in the next section.

2.5.1 *Determination of H'.* Conceptually, it is important to realize that the various modes of distortion are manifested in the wavefront sensor as a set of gradient or tilt measurements from each subaperture. Although the Hartmann sensor is normally tasked with reconstructing the image phase from the subaperture tilt measurements, this research assumes the 138 tilt measurements (69 x-tilts and 69 y-tilts) can be accessed directly for input to the Kalman filter. The Kalman filter estimates the 14 Zernike modes from the 138 tilt measurements. An expression for the noise-free measurement of x-tilt for the s-th subaperture can be derived [30] in terms of the Zernike coefficients of the reflected wavefront as:

$$z_{x_s}(t_j) = \frac{l}{A} \underline{n}_{x_s}{}^T a(t_j) \tag{2.31}$$

where l is a constant dependent upon wavelength, lenslet focal length, and output scaling, A is the area of the subaperture, and $\underline{n}_{x_s}$ is the vector of projections of the Zernike functions into the x-tilt measurement space for the sth subaperture whose elements are computed as [30:3.24]:

$$\underline{n}_{x_{s_i}} = \int_{Y_s - \frac{\sqrt{A}}{2}}^{Y_s + \frac{\sqrt{A}}{2}} dY \int_{X_s - \frac{\sqrt{A}}{2}}^{X_s + \frac{\sqrt{A}}{2}} dX \ W_\lambda(X - X_s, Y - Y_s) \frac{\partial Z_i(X,Y)}{\partial Y} \tag{2.32}$$

where X and Y are coordinates referenced to the center of the total sensor aperture and X_s and Y_s are the coordinates of the center of the sth subaperture. Equations similar to (2.32) can be derived for both x and y tilts for each of the 69 subapertures. The 138 resulting equations can be augmented together to form the following matrix relationship:

$$z(t_j) = \frac{l}{A} N a(t_j) \tag{2.33}$$

The value of l/A for this research is evaluated to be 0.19026 [30:3.25] using results of actual Hartmann sensor data collected by Miller [22]. Finally, the H' matrix of Equation (2.30) is computed by premultiplying the N matrix by l/A. The H matrix in Equation (2.29) can then be evaluated from Equation (2.30).

2.5.2 Determination of R. To this point no consideration has been given to measurement noise in the wavefront sensor. In general, the wavefront sensor puts out noise-corrupted measurements. It has been suggested in the literature [30, 25] that the noise is zero-mean, white, Gaussian, and uncorrelated between subapertures as well as uncorrelated to the phase of the wavefront. This

research treats photon shot noise as the dominant source of measurement noise. Other sources of noise include A/D quantization noise and thermal noise; however, these noises are considered small [30:3.26] compared to photon shot noise and are ignored. Photon shot noise variance is inversely proportional to the intensity of the light during the measurement. The light intensity is related to the number of photons counted during the measurement. Since the light intensity of a viewed object is expected to vary considerably from object to object, Von Bokern conducted nine studies in which the noise strength matrix R is varied between the truth and filter models. The same measurement noise studies are conducted as part of this research in order to reestablish the performance baseline using the updated truth model. R is a diagonal matrix whose elements are computed for noise strengths corresponding to 1000, 10, and 1 photons per subaperture, according to equations by Welsh and Gardner [33]. Table 2.2 gives the values of the diagonal entries of R.

2.6 Kalman Filter Design

The function of the Kalman filter of Figure 1.1 is to accept measurements from the Hartmann wavefront sensor and generate estimates of the system state vector described by Equation (2.27). The Kalman filter generates the state estimates using internal models of the dynamics of the system and the wavefront sensor to propagate the mean and covariance of the

Table 2.2. Elements of Measurement Noise Strength Matrix

Photons/Subaperture	Noise Level	$\sqrt{R_{ii}}$ (wavelengths)
1000	Low	0.01755
10	Medium	0.1755
1	High	0.555

system state vector between measurement samples. As measurements become available, the Kalman filter updates the propagated estimate with the current measurement from the wavefront sensor. The filter state estimate and covariance at time t_i conditioned on the measurements through time t_{i-1} are defined as:

$$\hat{x}(t_i^-) = E\{\underline{x}(t_i)|Z(t_{i-1})\}$$

$$P(t_i^-) = E\{[x(t_i)-\hat{x}(t_i^-)][x(t_i)-\hat{x}(t_i^-)]^T|Z(t_{i-1})\}$$

(2.34)

where $Z(t_{i-1})$ is the measurement history vector through t_{i-1}. Similarly, the updated filter state and covariance at time t_i^+ are defined as in Equation (2.34) with the conditioning on the measurements through time t_i.

Kalman filter computations can be separated into two sequential processes operating on the state estimate and covariance as defined in Equation (2.34): propagation and update. During the propagation cycle, the filter propagates the state estimates and covariances according to the internal dynamics model of the system over the ensuing sample period prior to processing the next measurement. The discrete filter propagation equations are [19]:

$$\hat{x}(t_i^-) = \Phi(t_i,t_{i-1})\hat{x}(t_{i-1}^+) + B_d u(t_{i-1})$$

(2.35)

$$P(t_i^-) = \Phi(t_i,t_{i-1})P(t_{i-1}^+)\Phi^T(t_i,t_{i-1}) + G_d Q_d G_d^T$$

(2.36)

where

$\hat{x}(t_i^-)$	= estimate of $\underline{x}$ after the propagation cycle, prior to measurement at t_i
$\hat{x}(t_{i-1}^+)$	= estimate of $\underline{x}$ at the beginning of the propagation cycle
$P(t_i^-)$	= filter covariance after the propagation cycle, prior to measurement
$P(t_{i-1}^+)$	= filter covariance at the beginning of the propagation cycle

As the next measurement becomes available, the Kalman filter processes the new information according to the update equations [19]:

$$K(t_i) \qquad {}^{r} [HP(t_i^-)H^T + R]^{-1} \qquad\qquad (2.37)$$

$$\hat{x}(t_i^+) = \hat{x}(t_i^-) + K(t_i) [z(t_i) - H\hat{x}(t_i^-)] \qquad\qquad (2.38)$$

$$P(t_i^+) = P(t_i^-) - K(t_i)HP(t_i^-) \qquad\qquad (2.39)$$

where

$K(t_i)$	=	Kalman filter gain at update
$\hat{x}(t_i^+)$	=	estimate of $\underline{x}$ after the update
$z(t_i)$	=	measurement at update time t_i
$P(t_i^+)$	=	filter covariance immediately following the update

This research implements a full-order Kalman filter, that is, the number of states in the filter is exactly equal to the number of states required to specify the truth model. The truth model, as presented in the preceding sections, consists of 28 states - 14 atmosphere and 14 mirror states. Therefore, the Kalman filter also contains 28 states with dynamics and measurement equations given by (2.14) and (2.15), respectively. In actuality, a full-order filter need not be implemented in an operational system since states 15-28 are deterministic mirror states and do not require estimation by the filter. However, all 28 states are included here for convenience during the computer simulations discussed in Chapter 5. One could, in fact, consider the 14 states for the atmosphere a reduced-order model as reality dictates an infinite number of Zernike modes to completely describe the distortion. The F and Q matrices for the continuous-time Kalman filter associated with Equation (2.14) are diagonal. The B matrix is evaluated using Equation (2.26) where the steady-state influence matrix M is given in Appendix B [30]. The G matrix is an identity matrix. The H matrix is evaluated from Equations (2.30) and (2.33) where the N matrix is given in Appendix C [30]. The measurement noise variance matrix R is a diagonal matrix whose elements are all equivalent and given in Table 2.2.

The equivalent discrete-time Kalman filter, as specified by Equations (2.35)-(2.39), requires evaluation of the state transition matrix, $\Phi(t_i, t_{i-1})$, the discrete input distribution matrix, B_d, and the discrete dynamics driving noise matrix, Q_d. Using a 0.007 second measurement sample period, corresponding to the maximum sampling rate of the Reticon chip of the Hartmann wavefront sensor [22], the state transition matrix is computed by:

$$\Phi(t_i, t_{i-1}) = e^{F(t_i - t_{i-1})}$$
$$= e^{F(0.007)} \tag{2.40}$$

The F matrix is diagonal. The elements of the state transition matrix can be computed by simply evaluating Equation (2.40) with F replaced by its individual diagonal elements. B_d is calculated using Equation (2.20) and Q_d is calculated from Equation (2.19). It is assumed for this research that tilt mirrors preceding the deformable mirror will remove 80 percent of the gross tilts in the wavefront. As such, the noise strengths for the tilt modes are reduced by 80 percent.

Initial conditions for the state vector and covariance matrix are required to get the filter algorithm started. As the Zernike coefficients are modeled as zero-mean random variables, an appropriate initial condition on the system states is a zero vector ($\underline{x}(0)=\underline{0}$). Previous research [30] assumed the Zernike coefficients to be uncorrelated, resulting in a diagonal covariance matrix. The literature [27, 32] suggests, however, that some Zernike coefficients are actually correlated. The appropriate values for the covariance matrix elements are discussed in detail in Chapter 3.

The Hartmann sensor provides measurements to the Kalman filter every 7 msecs for updating the state estimates. Previous research [30] assumed the measurements are available instantaneously for Kalman filter update processing. This research removes this assumption and incorporates a model for the inherent time delay associated with wavefront sensor measurement processing. Modeling of the time delay is presented in Section 3.4.

2-22

2.7 Linear Quadratic Regulator Design

The concept behind LQG control is to generate an optimal stochastic controller, optimal with respect to some specified performance criterion [1, 16, 17, 21]. Under the LQG assumptions, the system to be controlled is assumed to be modeled by a set of linear differential equations. The criterion for optimality is specified as a quadratic cost function, and the system is assumed to be driven by white Gaussian noise inputs.

The LQG regulator problem attempts to minimize a simple quadratic cost function which applies penalty to nonzero states and to the amount of control energy applied to drive the states to zero. The simple form of the quadratic cost function used in this research is given as [21:10]:

$$ J = E \left\{ \sum_{i=0}^{N} \frac{1}{2} [\ x^{T}(t_{i})X(t_{i})x(t_{i}) \ + \ u^{T}(t_{i})U(t_{i})u(t_{i}) \ ] \ + \ \frac{1}{2}x^{T}(t_{N+1})X_{f} \ x(t_{N+1}) \right\} \qquad (2.41) $$

where $X(t_{i})$ and $U(t_{i})$ are cost weighting matrices selected such that quadratic penalties are accrued for state deviations from zero and for requiring excessive amounts of energy to control those states over each sample period. X_{f} is the cost weighting matrix which assigns quadratic penalty to state deviations from zero at the final sample time. Assuming diagonal cost weighting matrices, the diagonal terms of each of these matrices can be chosen depending upon the relative importance of minimizing the deviation from zero of the individual states. Those states or controls for which minimization is important will have large cost matrix terms associated them.

Design of the LQ regulator requires determination of the optimal vector of control voltages, $\underline{u}^{*}(t_{i})$, to apply to the deformable mirror which minimizes the cost function defined in Equation (2.41). The minimization must be such that the phase distortion in the reflected wavefront is also

minimized. If it were possible to gain perfect knowledge of all the system states, the optimal feedback control law would be given by [21:17]:

$$u^*[x(t_i),t_i] = -G_c^*(t_i)x(t_i) \qquad (2.42)$$

where the optimal controller gain matrix, $G_c^*(t_i)$, assuming time-invariant cost matrices, is given by [21:16]:

$$G_c^*(t_i) = [U + B_d^T K_c(t_{i+1})B_d]^{-1}[B_d^T K_c(t_{i+1})\Phi(t_{i+1},t_i)] \qquad (2.43)$$

and the controller Riccati matrix, $K_c(t_i)$, satisfies the backward running Riccati difference equation [21:15]:

$$K_c(t_i) = X + \Phi^T(t_{i+1},t_i)K_c(t_{i+1})\Phi(t_{i+1},t_i)$$
$$- [\Phi^T(t_{i+1},t_i)K_c(t_{i+1})B_d] [U + B_d^T K_c(t_{i+1})B_d]^{-1} \qquad (2.44)$$
$$x [B_d^T K_c(t_{i+1})\Phi(t_{i+1},t_i)]$$

solved backwards from the terminal condition:

$$K_c(t_{N+1}) = X_f \qquad (2.45)$$

However, rarely, if ever, does one have full state access. Instead, only noise-corrupted measurements of the form of Equation (2.29) are available. In this case, a Kalman filter can be used to generate estimates of the states, given the measurements. The optimal stochastic controller is equivalent to the optimal deterministic full-state feedback controller with the state in Equation (2.42) replaced by the state estimate from the Kalman filter [21]. This result is commonly

referred to as the *certainty equivalence* property. The final form for the optimal feedback control law is:

$$u^*[\hat{x}(t_i^*),t_i] = -G_c^*(t_i)\hat{x}(t_i^*)$$

(2.46)

where the optimal controller gain matrix and controller Riccati matrix are as described by Equations (2.43) and (2.44). Therefore, the optimal feedback control law for the LQG problem is a Kalman filter cascaded with the optimal controller gain matrix corresponding to the deterministic full-state feedback control law.

For the adaptive optics system of this research, cost is assigned to phase distortion in the wavefront reflected from the deformable mirror, as it is the reflected wavefront which results from the mirror compensation. Cost is also assigned to the amount of control voltage applied to the mirror, as the actuators are restricted to maximums of ±10 volts. Von Bokern derives the appropriate cost weighting matrix for the states as [30]:

$$X = \begin{bmatrix} C & C \\ C & C \end{bmatrix}$$

(2.47)

with C defined as a 14 x 14 diagonal matrix of cost elements associated with Zernike modes of distortion in the reflected wavefront. The non-diagonal form of X results from evaluation of the quadratic involving the sum of the atmosphere and mirror states, that is, the reflected wavefront and the fact that the extraction matrix (A) is an identity matrix. The cost matrix elements can be determined, for the initial design, as the inverse of the square of the maximum allowable value for each of the states [21]. Previous research [30] assumed values of 400 for the elements of C based on maximum phase deviations of 1/20 wavelengths due to any one Zernike mode. Similar analysis applied to the control cost weighting matrix yields a 97 x 97 diagonal U matrix. The

elements of U are determined, initially, as the inverse of the square of the maximum allowable control voltage. The resulting control cost weighting matrix has diagonal elements equal 0.01 corresponding to the maximum allowable control voltage of ± 10 volts. These cost weighting matrices are available as tuning parameters for design iterations towards improved system performance.

2.8 Results of Previous Research

Von Bokern performed an extensive computer performance evaluation of the control law described in the preceding sections of this chapter using the MSOFE simulation package [23]. As part of the performance evaluation, several studies were conducted in which the measurement noise covariance matrices, K, were varied between the truth model and the Kalman filter model. The performance index for Von Bokern's research was the difference between rms phase distortion in the incident wavefront and the reflected wavefront. The key results achieved by Von Bokern are as follows.

1. Based on the truth model implemented for atmospheric distortion, the deformable mirror operated in its linear region, that is, the voltages applied to the mirror were well within the ± 10 volts saturation limits of the actuators.

2. Results from Monte Carlo analyses indicated the adaptive optics system reduced the total rms phase distortion over that in the incident wavefront for each of nine studies conducted. The nine studies involved variations of the measurement noise covariance in both the truth model and the filter model. RMS Phase distortion in the reflected wavefront was reduced to 40-60 percent of that in the incident wavefront, depending on the particular study considered. As the measurement noise covariance was increased in the truth model, filter performance degraded, even when the filter was retuned to the

2-26

appropriate noise covariance, as is anticipated since this yields a more difficult estimation (and control) problem.

3. Plots of the rms phase distortion in the incident and reflected wavefronts suggest the quality of the corrected image to be somewhat constant, even in the presence of large variations of the amount of distortion in the incident image.

4. Comparison between the residual phase distortion in the reflected wavefront and the distortion due to filter estimation error indicated state estimation error to be the limiting factor on performance of the controller.

2.9 Summary

This chapter describes the effects of atmospheric turbulence on optical image quality and a method for compensating for the resulting wavefront phase distortion. A linear quadratic Gaussian control law is proposed in which a Kalman filter estimates the leading coefficients in a summation of 14 Zernike polynomials describing the wavefront phase distortion due to atmospheric turbulence. The filter estimates are premultiplied by the optimal controller gain matrix to determine the control voltages to apply to the actuators of a deformable mirror adaptive optics system. The dynamics models for the adaptive optics system (atmospheric distortion, deformable mirror, and wavefront sensor) are presented. These models are required in order to define the Kalman filter and the optimal controller gain matrix properly. Control of the system is achieved through minimization of a quadratic cost function associated with nonzero phase distortion and nonzero control voltage magnitude. Simulated performance results achieved in previous research using this control law are also presented. Chapter 3 presents additional modeling for addressing the cross-correlation, time delay, and atmosphere variation issues.

2-27

III. Control System Modeling

3.1 Introduction

This chapter presents the mathematical models required for this research. The basic model for the control system is that developed by Von Bokern [30], as described in Chapter 2. Refinements are made to the model based on Zernike coefficient covariance data available in the literature [27, 32]. Modifications to the model structure are presented which address the objectives specified in Chapter 1. Areas requiring additional modeling include: cross-correlations between Zernike coefficients for the atmosphere, wavefront sensor measurement processing time delay, and variations in the dynamics of the atmosphere.

3.2 Baseline Control System Model

The Kalman filter used for this research is a full-order filter consisting of 28 states; 14 states describing the dynamics of the atmosphere and 14 states for the dynamics of the deformable mirror. Assuming a linear time-invariant model, the equations for the truth model continuous-time dynamics and discrete-time measurements are given in Chapter 2 and are repeated here for convenience as:

$$\dot{\underline{x}}(t) = F\underline{x}(t) + B\underline{u}(t) + G\underline{w}(t) \tag{3.1}$$

$$\underline{z}(t_i) = H\underline{x}(t_i) + \underline{v}(t_i) \tag{3.2}$$

The F matrix is a diagonal matrix whose elements are derived by curve-fitting auto-correlation data to standard first-order Markov process shaping filter functions of the form of Equation (2.21). The auto-correlation data were generated by integrating Equation (2.22). The

B matrix is computed from Equation (2.26) using the steady-state influence matrix, M, given in Appendix B. The H matrix is computed from Equations (2.30), (2.33), and the N matrix given in Appendix C. The elements of the diagonal dynamics driving noise strength matrix, Q, for the atmospheric states are computed based on the time constants associated with the individual atmospheric states and the covariances of those states as:

$$Q_{ii} = \frac{2\sigma_{ii}^2}{T} \tag{3.3}$$

where

$$\sigma_{ii}^2 = E\{a_i^2\} \tag{3.4}$$

and T is the time constant for the ith state. Expressions for the individual covariance elements of Equation (3.4), (3.5) are available throughout the literature [24, 27, 29, 32]. Roddier provides such an expression in the form [27:1175]:

$$E\{a_i\,a_j\} = \frac{K_{zz'}\,\delta_{mm'}\,\Gamma\,[(n + n' - 5/3)/2]\,(D/r_0)^{5/3}}{\Gamma\,[(n - n' + 17/3)/2]\,\Gamma\,[(n' - n + 17/3)/2]\,\Gamma\,[(n + n' + 23/3)/2]} \tag{3.5}$$

where $K_{zz'}$ is defined as:

$$K_{zz'} = \frac{\Gamma\,(14/3)\,[(24/5)\,\Gamma\,(6/5)]^{5/6}\,[\Gamma\,(11/6)]^2}{2\pi^2} \tag{3.6}$$

$$\times\,(-1)^{(n+n'-2m)/2}\sqrt{(n + 1)\,(n' + 1)}$$

and

n,n'	= radial order of the j and j' Zernike functions
m,m'	= azimuthal order of the j and j' Zernike functions
D	= diameter of the receiving aperture
r_0	= Fried's coherence length [8, 13, 24, 26, 30]
$\delta_{mm'}$	= logical Kronecker delta
$\Gamma(\cdot)$	= Gamma function

Using Equations (3.4), (3.5) and (3.6), Roddier evaluates the covariance matrix for the first 14 Zernike coefficients, normalized by the scaling factor $(D/r_0)^{5/3}$. The covariance values derived by Roddier were appropriately scaled to reflect units of wavelengths for this research. Table 3.1 shows the nonzero covariance values for the first 14 Zernike coefficients. One can observe from Table 3.1 that correlations exist between different Zernike coefficients ($i \neq j$) when i or $j > 5$. The controller design of Von Bokern assumed a diagonal Q matrix. Since this section is intended to present the updated truth model under the same assumptions made by Von Bokern, the discussion *at this point* is limited to the case of a diagonal covariance matrix so that only the diagonal covariance elements ($i = j$) are included in the model. Finally, the measurement noise covariance matrix, R, is a diagonal matrix whose elements are given in Table 2.2 for the low, medium, and high measurement noise levels studied in this research.

Table 3.2 is a summary of the state-space parameters for the baseline truth and filter models. The performance of the LQG control law based on this model will serve as the benchmark against which performance of the modified control law will be evaluated.

3.3 Zernike Coefficient Cross-Correlation

Past research has assumed that no correlations exist between the different Zernike coefficients, that is, $E\{a_i\, a_j\} = 0$ when $i \neq j$. However, as indicated in Table 3.1, several of the states are in fact correlated when either i or $j > 5$. This research removes the assumption of a diagonal covariance matrix and includes the cross-correlation information in the truth and filter

3-3

Table 3.1. Nonzero Covariance Matrix Elements

i	j	$E\{a_i\,a_j\}$ ($[D/r_0]^{5/3}$ units)	$E\{a_i\,a_j\}$ (wavelengths^2)
1	1	0.4557	3.3434
1	7	-0.0144	-0.1057
2	2	0.4557	3.3434
2	6	-0.0144	-0.1057
3	3	0.0236	0.1732
3	10	-0.0039	-0.0286
4	4	0.0236	0.1732
4	12	-0.0039	-0.0286
5	5	0.0236	0.1732
5	11	-0.0039	-0.0286
6	2	-0.0144	-0.1057
6	6	0.0063	0.0462
7	1	-0.0144	-0.1057
7	7	0.0063	0.0462
8	8	0.0063	0.0462
9	9	0.0063	0.0462
10	3	-0.0039	-0.0286
10	10	0.0025	0.0183
11	5	-0.0039	-0.0286
11	11	0.0025	0.0183
12	4	-0.0039	-0.0286
12	12	0.0025	0.0183
13	13	0.0025	0.0183
14	14	0.0025	0.0183

Table 3.2. Baseline Continuous-Time State-Space Model

j	T (sec)	F_{jj} (sec^{-1})	σ_{jj}^2 (wavelengths^2)	Q_{jj} (wavelengths^2/sec)
1	0.130	-1/0.130	3.3434	51.437
2	0.320	-1/0.320	3.3434	20.896
3	0.120	-1/0.120	0.1732	2.887
4	0.050	-1/0.050	0.1732	6.928
5	0.090	-1/0.090	0.1732	3.849
6	0.100	-1/0.100	0.0462	0.924
7	0.045	1/0.045	0.0462	2.053
8	0.050	-1/0.050	0.0462	1.848
9	0.040	-1/0.040	0.0462	2.310
10	0.250	-1/0.250	0.0183	0.146
11	0.032	-1/0.032	0.0183	1.144
12	0.025	-1/0.025	0.0183	1.464
13	0.120	-1/0.120	0.0183	0.305
14	0.025	-1/0.025	0.0183	1.464
15	0.00045	-1/0.00045	0	0
16	0.00045	-1/0.00045	0	0
17	0.00045	-1/0.00045	0	0
18	0.00045	-1/0.00045	0	0
19	0.00045	-1/0.00045	0	0
20	0.00045	-1/0.00045	0	0
21	0.00045	-1/0.00045	0	0
22	0.00045	-1/0.00045	0	0
23	0.00045	-1/0.00045	0	0
24	0.00045	-1/0.00045	0	0
25	0.00045	-1/0.00045	0	0
26	0.00045	-1/0.00045	0	0
27	0.00045	-1/0.00045	0	0
28	0.00045	-1/0.00045	0	0

models through the state covariance and dynamics driving noise strength matrices. The additional information available through the cross-correlation terms provides a more realistic portrayal of the true statistical characteristics of the atmospheric states.

If the covariance matrix, defined by the entries in Table 3.1, is to be used in the mathematical truth and filter models, consideration must be given as to the appropriate dynamics driving noise strength matrix to incorporate into the modified model as well. The choice of Q must satisfy the covariance propagation differential equation for the stochastic process described by Equation (3.1) given as [19:219]:

$$\dot{P}(t) = F(t)P(t) + P(t)F^T(t) + G(t)Q(t)G^T(t) \tag{3.7}$$

Under the assumptions of a linear time-invariant system model with $G(t)$ as an identity matrix, Equation (3.7) can be rewritten:

$$\dot{P}(t) = FP(t) + P(t)F^T + Q(t) \tag{3.8}$$

Also, assuming stationary statistics for the dynamics driving noise, appropriate for time-invariant system models, one can allow $P(t)$ to go to steady-state by setting the initial condition at $t=-\infty$ (thus allowing $\dot{P}(t){\rightarrow}0$) and solve for the desired Q matrix:

$$Q = -[FP + PF^T] \tag{3.9}$$

The Q matrix computed using Equation (3.9) will no longer be diagonal due to the off-diagonal terms in the P matrix. The F matrix remains diagonal, as the states represent the expansion coefficients (magnitudes) of an orthogonal set of functions.

3-6

3.4 Wavefront Sensor Processing Delay

The measurement processing limitations of the Hartmann wavefront sensor preclude the availability of instantaneous samples of the optical wavefront. The time delay associated with processing of the measurement data is significant, relative to the shortest time constant associated with the plant dynamics, and must be addressed in the adaptive mirror control law design. Past research has assumed the measurements to be available to the Kalman filter for updating the state estimate immediately following a sampling of the wavefront, thus ignoring the time delay. This research recognizes the time delay issue and proposes a predictor model augmented with the existing Kalman filter to compensate for the delay.

3.4.1 Wavefront Sensor Operation. Figure 3.1 illustrates the principle behind the Hartmann technique for sampling an observed wavefront. The Hartmann wavefront sensor consists of four major components: a monolithic lenslet array, a front end detector (FRED), a digitizer, and a programmable microcoded processor (PMP). As shown in Figure 3.1, the mirror aperture is subdivided by the lenslet array into 69 subapertures. Each lenslet focuses the light within its respective subaperture onto an optical detector array. The wavefront sensor measures the slope or gradient of the wavefront within the subaperture from the location of the focused "spot" of light in both the x and y directions, commonly referred to as x-tilt and y-tilt. X-tilt is defined to be wavefront tilt about the x-axis.

Each lenslet actually focuses a diffraction pattern on the FRED rather than a well-defined spot of light. The FRED senses the light intensity in the 69 diffraction patterns with a Reticon RA0100A optical sensing chip. The Reticon chip contains a 10,000 pixel array (100 rows x 100 columns) of photodiode pixels which provide analog output of the intensity sensed during the latest wavefront sample. Each subaperture lenslet is centered over a 25 pixel array (5 rows x 5
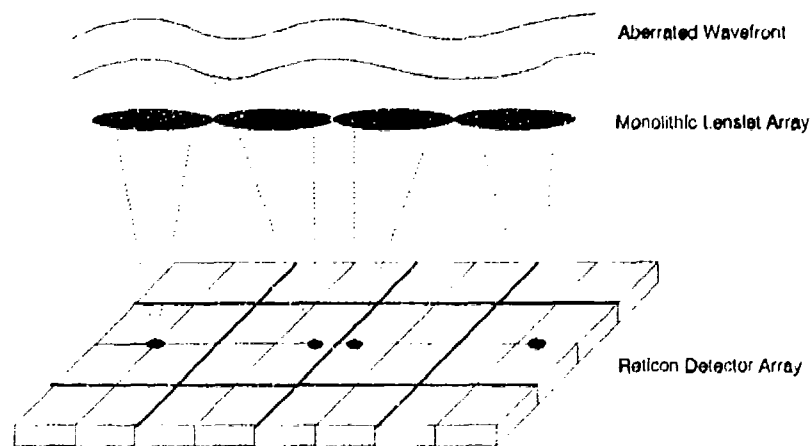
Figure 3.1. Wavefront Sensor Sampling

columns). The analog output of each pixel is converted to a digital word by the digitizer for processing by the PMP. The PMP performs a number of functions, the most important of which, for this research, is to compute the wavefront gradients about the x and y axes for each subaperture. The PMP employs a centroid algorithm known as weighted pixel averaging to determine the centroid of the diffraction pattern from the 25 pixel values within the individual subapertures. The reader is referred to Miller [22] for a complete discussion of the weighted pixel averaging technique. Determining the "spot" location is accomplished in the tilt processor module of the PMP whose output consists of 69 vector pairs of x and y tilt measurements. These 138 tilt measurements are assumed to be accessible as output and are applied as measurements to the Kalman filter for this research. Normally, the PMP processes the tilt data and reconstructs the

3-8

phase of the wavefront as the final output. However, the phase reconstruction requires additional computation time and is therefore not used here.

The wavefront sensor requires approximately 7 msecs in order to record and process the outputs from all of the 10,000 photodiode pixels [22:16]. The resultant sampling rate of the wavefront sensor is approximately 140 Hz. Miller's analysis of frequency response plots of the Hartmann wavefront sensor revealed the system time delay associated with processing of the sensor data corresponds to the sampling rate of the Reticon chip, that is, the output from the wavefront sensor experiences a 7 msec time delay.

3.4.2 Time Delay Compensation. In any control system, one desires the most accurate and up-to-date measurements possible in order to generate the appropriate control commands to apply to the system. Using the control law developed to this point, if one removes the assumption of instantaneous wavefront sampling and admits to the fact that the measurements are "old" when they become available, control at the current time would be applied based on estimates of the wavefront distortion at the previous sample time. Control of the system under such conditions is obviously undesirable and, therefore, some means of compensation for the measurement time delay is required.

Kleinman and Baron consider the problem of controlling linear systems whose output is a time-delayed combination of the system states with additive corruptive noise [16, 2]. According to Kleinman, the optimal control law for problems of this type consists of a feedback loop with a Kalman filter in cascade with a least mean-square predictor. Figure 3.2 shows the functional diagram for this type of control law. The wavefront sensor provides time-delayed measurements to the Kalman filter. The Kalman filter produces time-delayed estimates of the system states. The delayed state estimates are then input to the predictor which propagates the delayed state vector

3-9
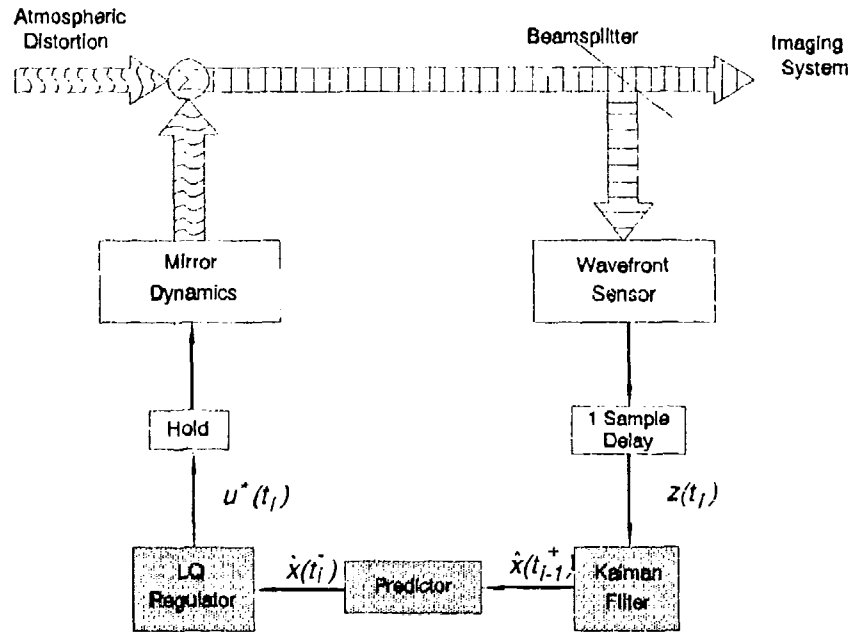
Figure 3.2. Predictor Modified Adaptive Optics System Functional Diagram

forward to the current time. Finally, the predictor output is used by the regulator to generate the correct control voltages to apply to the mirror actuators.

The system described by Equation (3.1) can be represented in terms of its equivalent discrete-time system model given by [19:275]:

$$x(t_{i+1}) = \Phi(t_{i+1},t_i)x(t_i) + B_d\,u(t_i) + \underline{w}_d(t_i) \tag{3.10}$$

For the system model of Equation (3.10), the Kalman filter requires measurements of the form of Equation (3.2). However, since the wavefront sensor outputs measurements with a one sample period delay, the actual available measurements take on the form:

$$z(t_i) = Hx(t_{i-1}) + \underline{v}(t_i) \tag{3.11}$$

where $\underline{x}(t_{i-1})$ is the state vector at the previous sample time. In order achieve a measurement equation of the form of Equation (3.2), define the "previous" value of the state at the current time to be:

$$\underline{x}_p(t_i) = \underline{x}(t_{i-1}) \tag{3.12}$$

where p is used to denote the state vector at the "previous" sample time. Using the definition in Equation (3.12), an augmented state variable is defined as:

$$\underline{x}_{ap}(t_i) = \begin{bmatrix} \underline{x}(t_i) \\ \cdots\cdots \\ \underline{x}_p(t_i) \end{bmatrix} \tag{3.13}$$

where the ap subscript stands for "augmented with previous value". Having defined the augmented state vector in Equation (3.13), and given a full sample period delay before measurements are available from the wavefront sensor, the measurement equation can be written in terms of the augmented state variable as:

$$\underline{z}(t_i) = [\ 0\ \vdots\ H\ ] \begin{bmatrix} \underline{x}(t_i) \\ \cdots\cdots \\ \underline{x}_p(t_i) \end{bmatrix} + \underline{v}(t_i) \tag{3.14}$$

or

$$\underline{z}(t_i) = H_{ap}\underline{x}_{ap}(t_i) + \underline{v}(t_i) \tag{3.15}$$

3-11

which is of the same form as Equation (3.2). Substitution of Equation (3.13) into Equation (3.10) yields the following augmented system model:

$$\begin{bmatrix} x(t_i) \\ \cdots \\ x_p(t_i) \end{bmatrix} = \begin{bmatrix} \Phi(t_i,t_{i-1}) & \vdots & 0 \\ \cdots & & \cdots \\ I & \vdots & 0 \end{bmatrix} \begin{bmatrix} x(t_{i-1}) \\ \cdots \\ x_p(t_{i-1}) \end{bmatrix} + \begin{bmatrix} B_d \\ \cdots \\ 0 \end{bmatrix} \underline{u}(t_{i-1}) + \begin{bmatrix} I \\ \cdots \\ 0 \end{bmatrix} w_d(t_{i-1}) \qquad (3.16)$$

or expressed in the augmented system notation:

$$\underline{x}_{ap}(t_i) = \Phi_{ap}(t_i,t_{i-1})\underline{x}_{ap}(t_{i-1}) + B_{ap}u(t_{i-1}) + G_{ap}w_d(t_{i-1}) \qquad (3.17)$$

Equation (3.17) is of the same form as Equation (3.10). As such, standard Kalman filter propagation and update equations can be implemented based on the model of Equation (3.16) to perform both the filter and predictor functions. The output of such a Kalman filter is the augmented state estimate defined as:

$$\underline{\hat{x}}_{ap}(t_i) = \begin{bmatrix} \hat{x}(t_i) \\ \cdots \\ \hat{x}_p(t_i) \end{bmatrix} \qquad (3.18)$$

where the lower partition of Equation (3.18) is the filter time-delayed estimate of the system state or, in other words, the filter estimate of the system state at the previous sample time. Using this system model, the filter propagation equations become:

$$\underline{\hat{x}}_{ap}(t_i^-) = \Phi_{ap}(t_i,t_{i-1})\underline{\hat{x}}_{ap}(t_{i-1}^+) + B_{ap}u(t_{i-1}) \qquad (3.19)$$

3-12

$$P_{ap}(t_i^-) = \Phi_{ap}(t_i,t_{i-1})P_{ap}(t_{i-1}^+)\Phi_{ap}^T(t_i,t_{i-1}) + G_{ap}Q_d G_{ap}^T \qquad (3.20)$$

Similarly, the augmented system Kalman filter update equations are:

$$K_{ap}(t_i) = P_{ap}(t_i^-)H_{ap}^T [H_{ap}P_{ap}(t_i^-)H_{ap}^T + R]^{-1} \qquad (3.21)$$

$$\hat{x}_{ap}(t_i^+) = \hat{x}_{ap}(t_i^-) + K_{ap}(t_i) [z(t_i) - H_{ap}\hat{x}_{ap}(t_i^-)] \qquad (3.22)$$

$$P_{ap}(t_i^+) = P_{ap}(t_i^-) - K_{ap}(t_i)H_{ap}P_{ap}(t_i^-) \qquad (3.23)$$

The upper partition of Equation (3.18) represents the time-delayed estimate of the system state vector propagated to the current time. The upper partition of Equation (3.22), $\hat{x}_{ap}(t_i^+)$, is then multiplied by the regulator gain matrix to generate the required actuator control voltages. The modified control law, in terms of the augmented system model, is:

$$u^*[\hat{x}_{ap}(t_i^+),t_i] = [-G_c^* \vdots 0] \begin{bmatrix} \hat{x}(t_i^+) \\ \cdots \\ \hat{x}_p(t_i^+) \end{bmatrix} \qquad (3.24)$$

or

$$u^*[\hat{x}_{ap}(t_i^+),t_i] = -G_{c\ ap}^* \hat{x}_{ap}(t_i^+) \qquad (3.25)$$

where G_c^* is the steady-state controller gain matrix. Since this system is never expected to reach the terminal condition, t_{N+1}, the steady-state controller gain is appropriate and is found by solving Equation (2.43) using the steady-state solution to the backward Riccati Equation (2.44) for K_c for

all time. The steady-state optimal controller gain matrix is computed in $MATRIX_X$ using the DREGULATOR option. The resulting gain matrix is provided in Appendix D.

3.5 Variation of the Dynamics of the Atmosphere

To this point, the control law is designed to compensate for the optical wavefront phase distortion resulting from propagation of the image through a turbulent atmosphere. However, this design considers the effects only under specific atmospheric conditions; that is, a time-invariant model for the atmosphere has been assumed. The assumed conditions for this design in terms of the coherence length, r_0, and the average wind velocity long the propagation path, according to the Hufnagel-Valley turbulence model [26], are 5 cm and 21 m/sec, respectively. The time-invariant assumption for the atmospheric dynamics may be valid for short period observations under the design conditions. However, as the observation period increases, the truly time-varying nature of the atmospheric statistics will cause the performance of this controller to degrade significantly. It, therefore, becomes necessary to investigate the sensitivity of the controller to variations in the dynamics of the atmosphere states. Specifically, controller stability, along with the degree to which performance is degraded over the anticipated range of atmospheric conditions, is evaluated.

The approach taken for the sensitivity study is to develop several new dynamics models for the adaptive optics system which are representative of various atmospheric conditions. To accomplish this task, additional autocorrelation data are generated in the same manner as described in Chapter 2 for each atmospheric condition selected. These data sets are then curve-fit to first-order shaping filter functions providing a new state-space model for each condition. The free parameters available for modeling changes in the dynamics, based on the equations used in generating the shaping filter data, are the average wind velocity along the propagation path and

3-14

the zenith angle to the source. As such, parameter studies on both the average wind velocity and the zenith angle are conducted for the sensitivity study. Variations in the average wind velocity directly affect the refractive index structure constant (C_n^2) which can be computed as a function of altitude as [26]:

$$C_n^2(h) = 5.94x10^{-53} \left(\frac{w}{27}\right)^2 h^{10} e^{\left(-\frac{h}{1000}\right)} + 2.7x10^{-16} e^{\left(-\frac{h}{1500}\right)} + 1.7x10^{-14} e^{\left(-\frac{h}{100}\right)} \quad (3.26)$$

where h is altitude and w is the average wind velocity. Equation (3.26) can then be integrated over altitude to find the corresponding coherence length for the specified wind conditions as [26]:

$$r_0 = 0.185 \left[\frac{\lambda^2}{\sec(\zeta) \int C_n^2(h)dh}\right]^{\frac{3}{5}} \quad (3.27)$$

where λ is the wavelength of light and ζ is the zenith angle to the source. As previously mentioned, the nominal controller model is based on an average wind velocity of 21 m/sec and an r_0 of 5 cm. The zenith angle for the nominal controller is assumed to be $0°$. During the sensitivity study, six models are developed, corresponding to wind velocities of 5, 15, 35, 45, 55, and 65 m/sec and four additional models, corresponding to zenith angles of $15°$, $30°$, $45°$, and $60°$. By implementing each of the new models in the truth model of MSOFE, the filter, still implementing the nominal model, is evaluated for stability and performance in the presence of the truth model variation from the filter model dynamics. It should be noted from Equations (3.26) and (3.27) that variations in either the wind velocity or the zenith angle result in a corresponding variation in the coherence length.

3.6 Summary

This chapter presents the additional models required to address the objectives of this research as described in Chapter 1. Modifications to the original truth model are made based on recently published covariance data [27] concerning Zernike function representations for optical wavefront phase distortion. The modified truth model serves as the performance baseline for further controller modifications. Covariance data is presented for incorporating cross-correlations between the atmosphere states into the truth and filter models. A predictor model is proposed to compensate for the undesirable processing delay associated with the Hartmann wavefront sensor. Finally, additional dynamics models which represent various atmospheric conditions are described in order to conduct the sensitivity analysis of the controller. Chapter 4 provides values for the specific model parameters for each of the control system modifications.

IV. Control Law Design

4.1 Introduction

This chapter presents the control law designs associated with each of the state-space model modifications described in Chapter 3. The final controller design evolves from the baseline controller associated with the state-space description summarized in Table 3.2. First, the baseline controller is modified to account for the cross-correlations between the Zernike coefficient states. Next, a steady-state Kalman filter implementation is proposed. Then, a least mean-square predictor model is augmented to the controller to compensate for the inherent time delay associated with measurement processing in the actual wavefront sensor. Lastly, several additional state-space models are developed to provide a representative sampling of the variations in the atmospheric dynamics which are likely to be encountered during an observation period. The model for each atmospheric condition is implemented in the MSOFE truth models for the sensitivity study.

4.2 Controller with Correlated States

This section presents the modified dynamics model for the adaptive optics system to include the added information available from the correlations between the atmosphere states. As indicated in Table 3.1, accurate modeling of distortive modes beyond mode five (astigmatism) involves correlations between some of the modes. The additional information provided through these correlations contributes to developing a more accurate statistical representation of the dynamic behavior of the atmosphere. Accurate mathematical models of the system to be controlled are essential to any control system design effort, regardless of the technique involved. In the case of LQG control, it is desirable to provide the Kalman filter with the most accurate

model of the system possible. It is equally, if not more, important to have the most accurate system truth model available in order to evaluate the performance of the controller design adequately. Incorporating the correlations into the model is accomplished by solving the steady-state covariance differential equation given by Equation (3.7) for the appropriate noise strength matrix $Q(t)$, where the elements of $P(t)$ are given in Table 3.1 and the elements of F are given in Table 3.2. The resulting fully-populated Q matrix and modified continuous-time state-space model are given in Table 4.1.

Any on-line implementation of an optimal control algorithm such as that described herein will, in all likelihood, be accomplished on a digital computer. Thus, an equivalent discrete-time system model is required that generates system state values identical to those generated by the continuous-time model evaluated at the discrete sample times. The desired equivalent discrete-time model has the form given in Equation (2.18) where the state transition matrix $\Phi(t_{i+1},t_i)$ is computed from Equation (2.40), the discrete input distribution matrix B_d is computed from Equation (2.20), and the discrete dynamics noise covariance matrix Q_d is computed according to Equation (2.19).

Using the 7 msec Hartmann sensor sampling period and the fact that the modified controller plant matrix F retains its diagonal characteristic, the state transition matrix is computed term-by-term replacing F in Equation (2.40) with its individual diagonal elements. With the noise distribution matrix G equal to a 28 x 28 identity matrix, Equation (2.19) simplifies to:

$$Q_d = \int_{t_i}^{t_{i+1}} \Phi(t_{i+1},\tau) \; Q \; \Phi^T(t_{i+1},\tau)d\tau \tag{4.1}$$

Equation (4.1) can be approximated, with diagonal F given in Table 4.1, as [19:358]:

4-2

Table 4.1. Continuous-Time State-Space with Correlated States

i	j	F_{ij} (sec^{-1})	$E\{a_i\ a_j\}$ (wavelengths^2)	Q_{ij} (wavelengths^2/sec)
1	1	-7.6923	3.3434	51.4349
1	7	0.000	-0.1057	-3.1619
2	2	-3.1250	3.3434	20.8962
2	6	0.000	-0.1057	-1.3873
3	3	-8.3333	0.1732	2.8866
3	10	0.000	-0.0286	-0.3527
4	4	-20.0000	0.1732	6.9280
4	12	0.000	-0.0286	-1.7160
5	5	-11.1111	0.1732	3.8489
5	11	0.000	-0.0286	-1.2115
6	2	0.000	-0.1057	-1.3873
6	6	-10.0000	0.0462	0.9240
7	1	0.000	-0.1057	-3.1619
7	7	-22.2222	0.0462	2.0533
8	8	-20.0000	0.0462	1.8480
9	9	-25.0000	0.0462	2.3100
10	3	0.000	-0.0286	-0.3527
10	10	-4.0000	0.0183	0.1464
11	5	0.000	-0.0286	-1.2115
11	11	-31.2500	0.0183	1.1438
12	4	0.000	-0.0286	-1.7160
12	12	-40.0000	0.0183	1.4640
13	13	-8.3333	0.0183	0.3050
14	14	-40.0000	0.0183	1.4640
15-28	15-28	-2222.2222	0.0000	0.0000

$$Q_d = \frac{1}{2} \left[\Phi(t_{i+1},t_i)\, G\, Q\, G^T\, \Phi^T(t_{i+1},t_i) + G\, Q\, G^T \right] \cdot \Delta t$$

$$= \frac{1}{2} \left[e^{F(\Delta t)}\, Q\, e^{F(\Delta t)} + Q \right] \cdot \Delta t$$

$$= \frac{1}{2} \left[e^{F(0.007)}\, Q\, e^{F(0.007)} + Q \right] \cdot (0.007) \tag{4.2}$$

The nonzero elements of $\Phi(t_{i+1},t_i)$ and Q_d are provided in Table 4.2. The Q_d entries associated with the two tilt modes reflect 80 percent attenuation due to the assumption of tilt mirrors preceeding the deformable mirror. The individual elements of the B_m and B_d matrices are not tabulated here due to the dimensionalities involved. However, the steady-state influence matrix M, from which both B_m and B_d are derived, is available in Appendix B.

As discussed in Chapter 2, the Kalman filter algorithm requires initial conditions for the state vector and covariance matrix in order to get the algorithm started. As before, the initial condition for the states is a zero vector ($\underline{x}(0)-\underline{0}$) owing to modeling of the Zernike coefficients as zero-mean random variables. Unless the controller designer has a priori information about the initial statistics of the states, the elements of $P(0)$ are set to large values reflecting the high degree of initial uncertainty. The steady-state covariance values presented in the literature [27, 32] provide such a priori statistics for the atmosphere states. As such, the initial conditions for the upper left 14 x 14 block of P are set to the covariance values indicated in Table 4.1. The covariance values for the deterministic mirror states are zero for all time.

4.3 Steady-State Kalman Filter

The results to be presented in Chapter 5 along with those from previous research [30] indicate the Kalman filter covariance converges to its steady-state values very quickly. These results motivate a constant-gain filter implementation provided the performance degradation using

4-4

Table 4.2. Equivalent Discrete-Time State-Space with Correlated States

i	j	$\Phi_{ij}(t_i, t_{j-1})$	$Q_{d_{ij}}$ (wavelengths^2)
1	1	0.9475799180	0.0170832482
1	7	0.0000000000	-0.0044795554
2	2	0.9783625227	0.0071571451
2	6	0.0000000000	-0.002075208
3	3	0.943337 9	0.0190878074
3	10	0.0000000000	-0.002368091
4	4	0.8693582353	0.0425618094
4	12	0.0000000000	-0.009956982
5	5	0.9251707162	0.0249940334
5	11	0.0000000000	-0.007596117
6	2	0.0000000000	-0.002075208
6	6	0.9323938199	0.0056483950
7	1	0.0000000000	-0.0044795555
7	7	0.8559408541	0.01245
8	8	0.8692 82354	0.011
9	9	0.8394570208	0.01
10	3	0.0000000000	-0.002
10	10	0.9723883668	0.0009991876
11	5	0.0000000000	-0.007396117
11	11	0.8035225737	0.0006602917
12	4	0.0000000000	-0.009
12	12	0.7557837414	. 98
13	13	0.9433376498	. 0135
14	14	0.7557837415	0.0080693962
15-28	15-28	0.0000001758	0.0000000000

the constant-gain filter is acceptable. The advantage of the constant-gain Kalman filter lies in the precomputability of the gain matrix K. Off-line precomputation and storage of the filter gains greatly reduces the computational burden of processing the filter algorithm. As presented later in Chapter 5, simulation results of the controller with a constant-gain Kalman filter indicate very little performance degradation. Therefore, the control system structures presented in the remainder of this chapter are based on a constant-gain Kalman filter. The appropriate constant K matrix is is found by outputting the Kalman filter gain matrix values from the MSOFE simulation once the system has reached its steady-state condition. An analytic solution for the steady-state filter gain was found using MATRIX$_x$; however, the analytic solution provided poor results and was abandoned. Further details concerning steady-state gain selection are given in Chapter 5. The steady-state K matrix is listed in Appendix E.

4.4 Predictor Design

The wavefront sensor associated with the adaptive optics control system of Figure 1.1 produces measurements of the gradient of the wavefront which are delayed by one full sample period (7 msecs). As the measurement delay simulation presented in Chapter 5 will show, this time delay causes severe degradation in the performance of the Kalman filter and, consequently, the entire control system. According to Kleinman [10], optimal control of systems whose output is a time-delayed combination of the system states plus additive noise is achieved by cascading a least mean-square predictor with the Kalman filter in the feedback loop.

The model for incorporating the dynamics of the predictor is achieved through simple state augmentation. The augmented system Φ matrix, as presented in Chapter 3, is found by augmenting the state transition matrix defined in Table 4.2 with a 28 x 28 identity matrix in the lower left partition and a 28 x 28 zero matrix in the upper and lower right partitions. Similarly,

the augmented system B_d and G_d matrices are augmented with 28 x 97 and 28 x 28 blocks of zeros, respectively. The resulting augmented system dynamics equation is repeated here as:

$$\begin{bmatrix} x(t_i) \\ \hline x_p(t_i) \end{bmatrix} = \begin{bmatrix} \Phi(t_i,t_{i-1}) & \vdots & 0 \\ \hline I & \vdots & 0 \end{bmatrix} \begin{bmatrix} x(t_{i-1}) \\ \hline x_p(t_{i-1}) \end{bmatrix} + \begin{bmatrix} B_d \\ \hline 0 \end{bmatrix} u(t_{i-1}) + \begin{bmatrix} I \\ \hline 0 \end{bmatrix} w_d(t_{i-1})$$

(4.3)

with sampled-data measurements of the form:

$$z(t_i) = \begin{bmatrix} 0 & \vdots & H \end{bmatrix} \begin{bmatrix} x(t_i) \\ \hline x_p(t_i) \end{bmatrix} + v(t_i)$$

(4.4)

where $x_p(t_i)$ is the state vector from the previous sample time. With a Kalman filter based on the dynamics model of Equation (4.3), the optimal control voltage vector for the augmented system is given as:

$$u^*[\hat{x}_{ap}(t_i^-),t_i] = \begin{bmatrix} G_c^* & \vdots & 0 \end{bmatrix} \begin{bmatrix} \hat{x}(t_i^-) \\ \hline \hat{x}_p(t_i^-) \end{bmatrix}$$

(4.5)

The steady-state Kalman filter has been identified for the controller model assuming no measurement delays. This gain matrix is appropriate for updating the "previous" state values. One must now identify the appropriate augmented system steady-state filter gain which updates the augmented system state vector, including the current and "previous" states. The augmented system steady-state filter gain is found by using Equation (3.21) which is repeated here as:

$$K_{ap}(t_i) = P_{ap}(t_i)H_{ap}^T [H_{ap}P_{ap}(t_i)H_{ap}^T + R]^{-1}$$

(4.6)

where the covariance matrix prior to update can be expressed as:

4-7

$$P_{ap}(t_i) = \begin{bmatrix} P_{11}(t_i^-) & \vdots & P_{12}(t_i^-) \\ \cdots & & \cdots \\ P_{21}(t_i^-) & \vdots & P_{22}(t_i^-) \end{bmatrix} \quad \backslash \qquad (4.7)$$

Substituting Equation (4.7), (4.10) along with the augmented measurement matrix H_{ap} into Equation (4.6), (4.9), the augmented system Kalman filter gain is evaluated as:

$$K_{ap}(t_i) = \begin{bmatrix} P_{11}(t_i^-) & \vdots & P_{12}(t_i^-) \\ \cdots & & \cdots \\ P_{21}(t_i^-) & \vdots & P_{22}(t_i^-) \end{bmatrix}\begin{bmatrix} 0 \\ \cdots \\ H^T \end{bmatrix} \left(\begin{bmatrix} 0 & \vdots & H \end{bmatrix}\begin{bmatrix} P_{11}(t_i^-) & \vdots & P_{12}(t_i^-) \\ \cdots & & \cdots \\ P_{21}(t_i^-) & \vdots & P_{22}(t_i^-) \end{bmatrix}\begin{bmatrix} 0 \\ \cdots \\ H^T \end{bmatrix} + R \right)^{-1}$$

$$= \begin{bmatrix} P_{12}(t_i^-)\, H^T \\ \cdots \\ P_{22}(t_i^-)\, H^T \end{bmatrix}\begin{bmatrix} HP_{22}(t_i^-)H^T + R \end{bmatrix}^{-1} \qquad (4.8)$$

Expressions for the partitions of $P_{ap}(t_i)$ can be found by solving the discrete-time covariance propagation difference equation given by Equation (3.20). Substitution of Equation (4.7) and an equivalent expression for $P_{ap}(t_{i-1})$ into Equation (3.20) yields:

$$\begin{bmatrix} P_{11}(t_i^-) & \vdots & P_{12}(t_i^-) \\ \cdots & & \cdots \\ P_{21}(t_i^-) & \vdots & P_{22}(t_i^-) \end{bmatrix} = \begin{bmatrix} \Phi & \vdots & 0 \\ \cdots & & \cdots \\ I & \vdots & 0 \end{bmatrix}\begin{bmatrix} P_{11}(t_{i-1}) & \vdots & P_{12}(t_{i-1}) \\ \cdots & & \cdots \\ P_{21}(t_{i-1}) & \vdots & P_{22}(t_{i-1}) \end{bmatrix}\begin{bmatrix} \Phi^T & \vdots & I \\ \cdots & & \cdots \\ 0 & \vdots & 0 \end{bmatrix}$$

$$\cdot \begin{bmatrix} I \\ \cdots \\ 0 \end{bmatrix} Q_d \begin{bmatrix} I \\ \cdots \\ 0 \end{bmatrix}^T$$

$$= \begin{bmatrix} \Phi P_{11}(t_{i-1})\Phi^T & \vdots & \Phi P_{11}(t_{i-1}) \\ \cdots & & \cdots \\ P_{11}(t_{i-1})\Phi^T & \vdots & P_{11}(t_{i-1}) \end{bmatrix} + \begin{bmatrix} Q_d & \vdots & 0 \\ \cdots & & \cdots \\ 0 & \vdots & 0 \end{bmatrix} \qquad (4.9)$$

Now, equating partitions on the left-hand side of Equation (4.9) to those of the right-hand side, one makes the identifications:

$$P_{12}(t_i^-) = \Phi P_{11}(t_{i-1}^-)$$

(4.10)

$$P_{22}(t_i^-) = P_{11}(t_{i-1}^-)$$

(4.11)

Substitution of Equation (4.11) into Equation (4.10) yields:

$$P_{12}(t_i^-) = \Phi P_{22}(t_i^-)$$

(4.12)

Equation (4.12) can now be substituted back into Equation (4.8) to get:

$$
K_{ap}(t_i) = \begin{bmatrix} P_{12}(t_i^-)\ H^T \\ \cdots \\ P_{22}(t_i^-)\ H^T \end{bmatrix} \begin{bmatrix} H P_{22}(t_i^-) H^T + R \end{bmatrix}^{-1}
$$

$$
= \begin{bmatrix} \Phi P_{22}(t_i^-) H^T \\ \cdots \\ P_{22}(t_i^-) H^T \end{bmatrix} \begin{bmatrix} H P_{22}(t_i^-) H^T + R \end{bmatrix}^{-1}
$$

$$
= \begin{bmatrix} \Phi K(t_i) \\ \cdots \\ K(t_i) \end{bmatrix}
$$

(4.13)

where $K(t_i)$ is the steady-state Kalman filter gain for the unaugmented system. Equation (4.13) shows that the augmented system steady-state Kalman filter gain is formed by premultiplying the steady-state gain for the original system by the state transition matrix and augmenting the result

Table 4.3. Dimensionality of Adaptive Optics Kalman Filter

Matrix/Vector	Dimensions
$\Phi_{ap}(t_{i+1},t_i)$	56 x 56
$\underline{x}_{ap}(t_i)$	56 x 1
$\boldsymbol{B}_{ap}$	56 x 97
$\underline{u}(t_i)$	97 x 1
$\boldsymbol{G}_{ap}$	56 x 28
$\underline{w}_d(t_i)$	28 x 1
$\boldsymbol{Q}_d$	28 x 28
$\underline{z}(t_i)$	138 x 1
$\boldsymbol{H}_{ap}$	138 x 56
$\underline{v}(t_i)$	138 x 1
$\boldsymbol{R}$	138 x 138

with the original steady-state gain matrix. The dimensions of each of the matrices and vectors in the discrete-time state-space model for the adaptive optics system are summarized in Table 4.3. Once again, one should note that 28 of 56 states shown in Table 4.3 are deterministic and, therefore, need not (and should not) be included in an operational filter.

4.5 Models for Variations of Atmosphere Dynamics

This section provides the truth model parameter values for each of the models developed for the sensitivity study. Parameter studies were conducted for variations in the average wind velocity along the propagation path (w) and zenith angle to the source (ζ). Table 4.4 shows the parameter values evaluated, along with the resultant coherence length (r_0) corresponding to the specific atmospheric condition. The values for r_0 are computed from Equation (3.27), where the

Table 4.4. Atmospheric Conditions for Sensitivity Study

Parameter		r_0 (cm)
w (m/sec)	ζ (deg)	
5	0	5.186
15	0	5.105
21 (nominal)	0	5.021
35	0	4.745
45	0	4.501
55	0	4.238
65	0	3.972
21	15	4.918
21	30	4.606
21	45	4 078
21	60	3.313

refractive index structure constant (C_n^2) is found by integrating Equation (3.26) over altitude. Since C_n^2 appears in Equation (2.22), from which the autocorrelation data are derived, changes in the average wind velocity directly affect the plant dynamics and noise strength matrices. Changes in the zenith angle, however, only affect the strengths of the noises, as ζ does not appear in Equation (2.22). The specific values of the plant and noise strength matrix entries associated with each of the atmospheric conditions in Table 4.4 are presented in Tables 4.5 through 4.11. Table 4.11 alone contains all the data for the variations in zenith angle since only the noise strength matrix values change.

When the Kalman filter is retuned to model the changes in the atmosphere resulting from wind velocity variations, the optimal controller gain matrix must be recomputed based on the new

Table 4.5. Continuous State-Space Model for Average Winds of 5 meters/sec

i	j	F_{ij} (sec^{-1})	$E\{a_i a_j\}$ (wavelengths^2)	Q_{ij} (wavelengths^2/sec)
1	1	-7.1429	3.1459	44.9420
1	7	0.0000	-0.0994	-2.9194
2	2	-2.6316	3.1459	16.5600
2	6	0.0000	-0.0994	-1.2558
3	3	-8.3333	0.1629	2.7153
3	10	0.0000	-0.0269	-0.3205
4	4	-14.2857	0.1629	4.6550
4	12	0.0000	-0.0269	-1.2821
5	5	-11.1111	0.1629	3.6205
5	11	0.0000	-0.0269	-1.1405
6	2	0.0000	-0.0994	-1.2558
6	6	-10.0000	0.0435	0.8698
7	1	0.0000	-0.0994	-2.9194
7	7	-22.2222	0.0435	1.9330
8	8	-20.0000	0.0435	1.7397
9	9	-25.0000	0.0435	2.1746
10	3	0.0000	-0.0269	-0.3205
10	10	-3.5714	0.0173	0.1233
11	5	0.0000	-0.0269	-1.1405
11	11	-31.2500	0.0173	1.0787
12	4	0.0000	-0.0269	-1.2821
12	12	-33.3333	0.0173	1.1506
13	13	-8.3333	0.0173	0.2876
14	14	-33.3333	0.0173	1.1506
15-28	15-28	-2222.2222	0.0000	0.0000

Table 4.6. Continuous State-Space Model for Average Winds of 15 meters/sec

i	j	F_{ij} (sec^{-1})	$E\{a_i\,a_j\}$ (wavelengths^2)	Q_{ij} (wavelengths^2/sec)
1	1	-7.4074	3.2296	47.8420
1	7	0.0000	-0.1021	-3.0236
2	2	-2.7778	3.2296	17.9440
2	6	0.0000	-0.1021	-1.3041
3	3	-8.3333	0.1673	2.7875
3	10	0.0000	-0.0276	-0.3327
4	4	-16.6667	0.1673	5.5753
4	12	0.0000	-0.0276	-1.3820
5	5	-11.1111	0.1673	3.7167
5	11	0.0000	-0.0276	-1.1708
6	2	0.0000	-0.1021	-1.3041
6	6	-10.0000	0.0446	0.8930
7	1	0.0000	-0.1021	-3.0236
7	7	-22.2222	0.0446	1.9844
8	8	-20.0000	0.0446	1.7859
9	9	-25.0000	0.0446	2.2324
10	3	0.0000	-0.0276	-0.3327
10	10	-3.7037	0.0177	0.1313
11	5	0.0000	-0.0276	-1.1708
11	11	-31.2500	0.0177	1.1074
12	4	0.0000	-0.0276	-1.3820
12	12	-33.3333	0.0177	1.1812
13	13	-8.3333	0.0177	0.2953
14	14	-33.3333	0.0177	1.1812
15-28	15-28	-2222.2222	0.0000	0.0000

Table 4.7. Continuous State-Space Model for Average Winds of 35 meter/sec

i	j	F_{ij} (sec^{-1})	$E\{a_i\ a_j\}$ (wavelengths^2)	Q_{ij} (wavelengths^2/sec)
1	1	-9.0909	3.6487	66.3400
1	7	0.0000	-0.1153	-4.8916
2	2	-3.5714	3.6487	26.0600
2	6	0.0000	-0.1153	-2.0590
3	3	-12.5000	0.1890	4.7240
3	10	0.0000	-0.0312	-0.5740
4	4	-22.2222	0.1890	8.3982
4	12	0.0000	-0.0312	-2.0516
5	5	-15.3846	0.1890	5.8143
5	11	0.0000	-0.0312	-1.7295
6	2	0.0000	-0.1153	-2.0590
6	6	-14.2857	0.0504	1.4413
7	1	0.0000	-0.1153	-4.8916
7	7	-33.3333	0.0504	3.3628
8	8	-25.0000	0.0504	2.5221
9	9	-31.2500	0.0504	3.1527
10	3	0.0000	-0.0312	-0.5740
10	10	-5.8824	0.0200	0.2355
11	5	0.0000	-0.0312	-1.7295
11	11	-40.0000	0.0200	1.6014
12	4	0.0000	-0.0312	-2.0516
12	12	-43.4783	0.0200	1.7406
13	13	-13.3333	0.0200	0.5338
14	14	-43.4783	0.0200	1.7406
15-28	15-28	-2222.2222	0.0000	0.0000

Table 4.8. Continuous State-Space Model for Average Winds of 45 meters/sec

i	j	F_{ij} (sec^{-1})	$E\{a_i\ a_j\}$ (wavelengths^2)	Q_{ij} (wavelengths^2/sec)
1	1	-10.5263	3.9842	83.8710
1	7	0.0000	-0.1259	-5.9882
2	2	-4.0000	3.9842	31.8740
2	6	0.0000	-0.1259	-2.4114
3	3	-12.5000	0.2063	5.1584
3	10	0.0000	-0.0341	-0.6698
4	4	-25.0000	0.2063	10.3167
4	12	0.0000	-0.0341	-2.4761
5	5	-17.5439	0.2063	7.2398
5	11	0.0000	-0.0341	-2.0807
6	2	0.0000	-0.1259	-2.4114
6	6	-15.1515	0.0551	1.6692
7	1	0.0000	-0.1259	-5.9882
7	7	-37.0370	0.0551	4.0800
8	8	-27.7778	0.0551	3.0601
9	9	-35.7143	0.0551	3.9343
10	3	0.0000	-0.0341	-0.6698
10	10	-7.1429	0.0219	0.3123
11	5	0.0000	-0.0341	-2.0807
11	11	-43.4783	0.0219	1.9006
12	4	0.0000	-0.0341	-2.4761
12	12	-47.6190	0.0219	2.0817
13	13	-14.7059	0.0219	0.6429
14	14	-47.6190	0.0219	2.0817
15-28	15-28	-2222.2222	0.0000	0.0000

Table 4.9. Continuous State-Space Model for Average Winds of 55 meters/sec

i	j	F_{ij} (sec^{-1})	$E\{a_i\, a_j\}$ (wavelengths^2)	Q_{ij} (wavelengths^2/sec)
1	1	-12.5000	4.4042	110.1060
1	7	0.0000	-0.1392	-7.7905
2	2	-5.0000	4.4042	44.0420
2	6	0.0000	-0.1392	-3.0156
3	3	-14.2857	0.2281	6.5169
3	10	0.0000	-0.0377	-0.8526
4	4	-28.5714	0.2281	13.0334
4	12	0.0000	-0.0377	-3.1710
5	5	-19.2308	0.2281	8.7727
5	11	0.0000	-0.0377	-2.4382
6	2	0.0000	-0.1392	-3.0156
6	6	-16.6667	0.0609	2.0296
7	1	0.0000	-0.1392	-7.7905
7	7	-43.4783	0.0609	5.2946
8	8	-30.3030	0.0609	3.6902
9	9	-40.0000	0.0609	4.8710
10	3	0.0000	-0.0377	-0.8526
10	10	-8.3333	0.0242	0.4027
11	5	0.0000	-0.0377	-2.4282
11	11	-45.4545	0.0242	2.1966
12	4	0.0000	-0.0377	-3.1710
12	12	-55.5556	0.0242	2.6847
13	13	-22.2222	0.0242	1.0739
14	14	-55.5556	0.0242	2.6847
15-28	15-28	-2222.2222	0.0000	0.0000

Table 4.10. Continuous State-Space Model for Average Winds of 65 meters/sec

i	j	F_{ij} (sec^{-1})	$E\{a_i a_j\}$ (wavelengths^2)	Q_{ij} (wavelengths^2/sec)
1	1	-15.3846	4.9067	150.9800
1	7	0.0000	-0.1551	-9.7689
2	2	-5.5556	4.9067	54.5240
2	6	0.0000	-0.1551	-3.6806
3	3	-16.6667	0.2541	8.4705
3	10	0.0000	-0.0420	-1.1198
4	4	-33.3333	0.2541	16.9405
4	12	0.0000	-0.0420	-4.1993
5	5	-20.8333	0.2541	10.5878
5	11	0.0000	-0.0420	-2.9745
6	2	0.0000	-0.1551	-3.6806
6	6	-18.1818	0.0678	2.4667
7	1	0.0000	-0.1551	-9.7689
7	7	-47.6190	0.0678	6.4604
8	8	-33.3333	0.0678	4.5223
9	9	-45.4545	0.0678	6.1668
10	3	0.0000	-0.0420	-1.1198
10	10	-10.0000	0.0269	0.5384
11	5	0.0000	-0.0420	-2.9745
11	11	-50.0000	0.0269	2.6918
12	4	0.0000	-0.0420	-4.1993
12	12	-66.6667	0.0269	3.5891
13	13	-28.5714	0.0269	1.5382
14	14	-66.6667	0.0269	3.5891
15-28	15-28	-2222.2222	0.0000	0.0000

Table 4.11. Continuous State-Space Models for Various Zenith Angles (ζ)

i	j	F_{ij} (sec^{-1})	Q_{ij} (wavelengths^2/sec)			
			ζ=15°	ζ=30°	ζ=45°	ζ=60°
1	1	-7.6923	52.8720	58.9740	72.2420	102.1340
1	7	0.0000	-3.2486	-3.6238	-4.4390	-6.2757
2	2	-3.1250	21.4800	23.9600	29.3500	41.4940
2	6	0.0000	-1.4253	-1.5898	-1.9476	-2.7535
3	3	-8.3333	2.9663	3.3087	4.0531	5.7302
3	10	0.0000	-0.3628	-0.4046	-0.4957	-0.7007
4	4	-20.0000	7.1195	7.9413	9.7279	13.7529
4	12	0.0000	-1.7648	-1.9685	-2.4114	-3.4091
5	5	-11.1111	3.9552	4.4118	5.4043	7.6404
5	11	0.0000	-1.2460	-1.3898	-1.7025	-2.4069
6	2	0.0000	-1.4253	-1.5898	-1.9476	-2.7535
6	6	-10.0000	0.9503	1.0600	1.2984	1.8357
7	1	0.0000	-3.2486	-3.6238	-4.4390	-6.2757
7	7	-22.2222	2.1117	2.3554	2.8854	4.0792
8	8	-20.0000	1.9005	2.1199	2.5969	3.6713
9	9	-25.0000	2.3757	2.6499	3.2461	4.5892
10	3	0.0000	-0.3628	-0.4046	-0.4967	-0.7007
10	10	-4.0000	0.1508	0.1682	0.2061	0.2914
11	5	0.0000	-1.2460	-1.3898	-1.7025	-2.4069
11	11	-31.2500	1.1784	1.3144	1.6102	2.2764
12	4	0.0000	-1.7648	-1.9685	-2.4114	-3.4091
12	12	-40.0000	1.5084	1.6825	2.0610	2.9138
13	13	-8.3333	0.3142	0.3505	0.4294	0.6070
14	14	-40.0000	1.5084	1.6825	2.0610	2.9138
15 -28	15 - 28	-2222.2222	0.0000	0.0000	0.0000	0.0000

plant matrix. No such recomputation of the optimal controller gain is required when modeling changes in the zenith angle in the filter. This occurs due to the fact that zenith angle changes affect only the dynamics noise strength matrix and that G_c^* is unaffected by the stochastic nature of the problem.

4.6 Summary

This chapter provides the specific parameter values needed for the adaptive optics control system model as a result of the modifications discussed in Chapter 3. First, the off-diagonal covariance and dynamics noise strength values are added. Next, the steady-state Kalman filter gain matrix is identified and listed in Appendix E. Then, the augmented system for the predictor is described along with the appropriate augmented system steady-state Kalman filter gain. Finally, numerous dynamics models are presented corresponding to various atmospheric wind conditions and zenith angle locations of the satellite. Chapter 5 presents the results from simulation of these models using the MSOFE computer software.

V. Simulation Results

5.1 Introduction

A critical phase in any control system design effort is the computer simulation of the proposed design. It is here that performance of the control law can be evaluated against a complete mathematical representation of the real world and inadequacies identified prior to reaching operational test. For the adaptive optics system of this research, the Multi-mode Simulation for Optimal Filter Evaluation (MSOFE) [23] computer software tool was chosen for the LQG control law performance evaluation. The state-space models developed in previous chapters for the atmosphere, mirror, and wavefront sensor serve as the system truth model from which sampled-data Hartmann wavefront sensor measurements are simulated. These simulated measurements are input to a Kalman filter which produces estimates of the system state vector. The state estimates are then multiplied by the optimal LQ (Linear system, Quadratic cost) regulator gain matrix to generate the appropriate control voltages to apply to the mirror actuators. Both the Kalman filter and LQ regulator functions are embedded in the simulation.

The performance evaluation consists of ten Monte Carlo simulation runs from which single sample realizations and ensemble statistics of the states are generated. Post-processing of the simulation data using $MATRIX_x$ [14] provides time histories of the rms phase distortion incident on the mirror, the residual rms phase distortion after correction, and the actuator control voltage envelope. Initially, the measurement noise studies conducted by Von Bokern [30] are reaccomplished to establish a new performance baseline as a result of the updated model for the atmosphere. Additional simulations are conducted following each modification to the baseline control system.

5.2 Baseline Controller Performance Evaluation

As discussed in Chapter 2, the light intensity of the viewed object, and consequently the variance of the measurement noise, are expected to vary considerably from object to object in a real adaptive optics system. In order to investigate the effect of variations in the measurement noise covariance matrix R, Von Bokern conducted nine studies [30] in which the measurement noise covariance was varied between the truth model and the filter model. Table 5.1 lists the studies conducted and the corresponding truth and filter model noise levels. As the dynamics model for the atmosphere has been altered from that used by Von Bokern, it becomes necessary to repeat the measurement noise studies for the new dynamics model in order to evaluate the sensitivity of the controller to variations in R. The results of the noise studies, particularly study 1, serve as the performance baseline against which controller performance following each modification is evaluated.

Table 5.1. Measurement Noise Covariance Studies

Noise Study	Truth Level	Filter Level
1	Low	Low
2	Low	Medium
3	Low	High
4	Medium	Low
5	Medium	Medium
6	Medium	High
7	High	Low
8	High	Medium
9	High	High

Although all nine studies are accomplished, the focus of this section is on the results of study 1, in which the measurement noise level in the truth model is low and is correctly modeled in the filter as such. Study 1 represents the most optimistic condition of all the studies from a performance standpoint. Tabulated data for the remaining eight studies are provided here and the corresponding plots are given in Appendix F. States 15-28 which model the dynamics of the deformable mirror are assumed to be deterministic in both the truth and filter models. As such the filter estimates of these states are identical to the truth states so that little is gained from evaluating filter performance for these states. In fact, states 15-28 need only be included in the system truth model for the purpose of generating the simulated wavefront sensor measurements and could be eliminated from the filter model in an operational system.

The purpose of the Kalman filter in the LQG controller is to provide accurate estimates of the 14 Zernike coefficients describing the degree of atmospheric distortion present in the incident wavefront. Assuming that tilt mirrors preceding the deformable mirror remove 80 percent of the gross tilts from the wavefront, it follows that the filter must estimate the residual tilt mode distortion along with the remaining 12 distortive modes. The degree to which the filter can accurately estimate each of the modes of distortion directly affects overall performance of the controller. A sample realization from a single Monte Carlo run of the true y-tilt Zernike coefficient a_1 (state x_1) is plotted in Figure 5.1 along with the filter's estimate of y-tilt ($\hat{x}_1$). From the plots one can get a feel for the capability of the filter to track the x_1 state. However, Figure 5.1 offers no statistical information about the estimation error committed by the filter. Filter estimation error is defined as the difference between the truth model state and the filter's estimate of that state. Figure 5.2 shows a plot of the filter estimation error for x_1 along with the
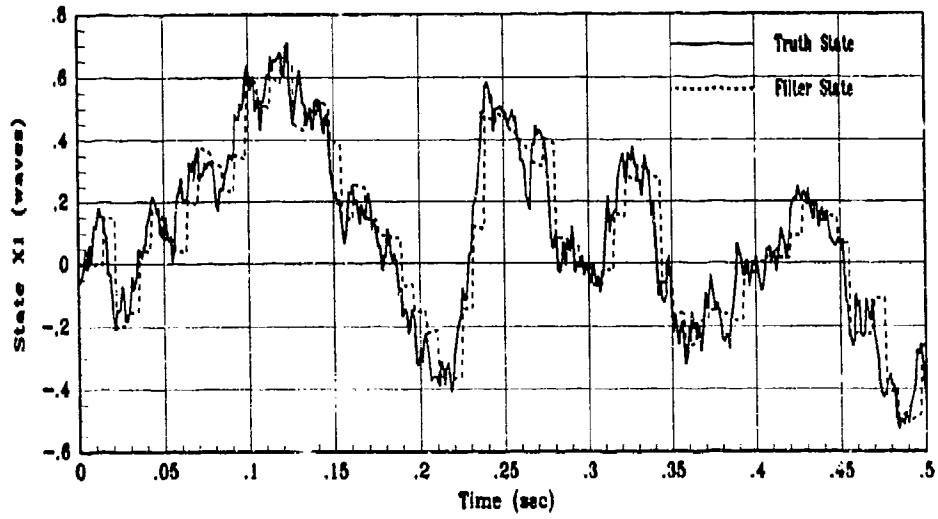
Figure 5.1. Y-tilt Truth Model and Filter States
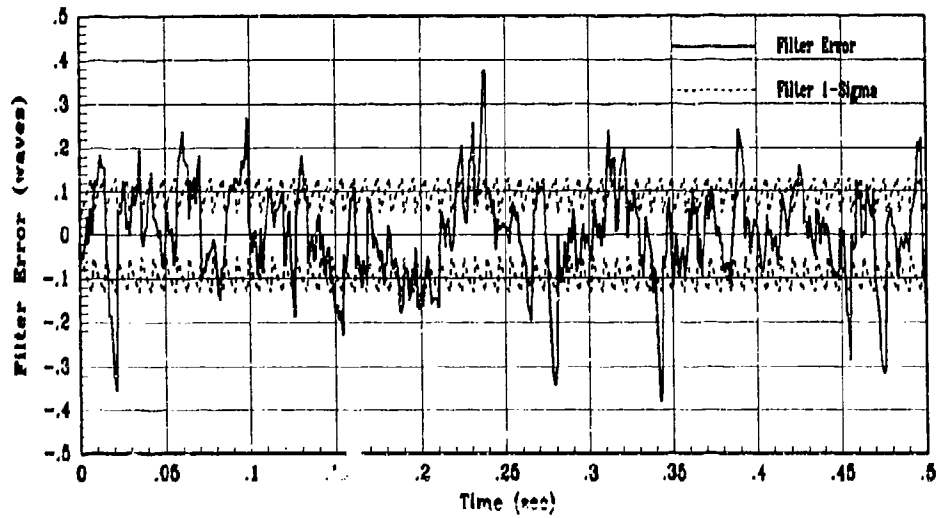
Figure 5.2. Y-tilt i .ter Estimation Error for 1 Monte Carlo Run

5-4

filter-computed 1-σ bounds. The 1-σ bounds for state 1 are determined as the square root of the (1,1) entry of the filter covariance matrix P. The filter covariance matrix is the filter's internally computed measure of uncertainty in its own estimates. Inspection of Figure 5.2 reveals that the filter error is approximately zero-mean and that the filter-computed 1-σ bound appears to be a reasonable characterization of the variance of the error, that is, the error is bounded by the filter-computed standard deviation approximately 68 percent of the time. Although the single run error appears to be zero-mean and having a standard deviation well represented by the square root of the filter variance, one requires multiple Monte Carlo runs in order to establish the true statistics of the random process x_j. Theoretically, an infinite number of runs is required to find the true mean and covariance. Obviously, only a finite number of runs are possible; for this research ten Monte Carlo runs are used. For any scalar variable of interest x, the equations used to describe the mean and covariance of the error in estimating x over ten Monte Carlo runs are:

$$\mu_e(t) \approx \frac{1}{10} \sum_{k=1}^{10} e_k(t) \tag{5.1}$$

$$\sigma_e^2(t) \approx \frac{1}{10-1} \sum_{k=1}^{10} \left[e_k^2(t) - \mu_e^2(t) \right] \tag{5.2}$$

where

$e_k(t)$	$= x(t) - \hat{x}(t)$ (truth state minus filter estimate at time t of run k)
k	$=$ Monte Carlo run number
$\mu_e(t)$	$=$ mean of the error process over k runs
$\sigma_e^2(t)$	$=$ variance of the error process over k runs

Following completion of the ten Monte Carlo runs, the truth and filter model state time histories are processed according to Equations (5.1) and (5.2). The results for y-tilt are plotted in Figure 5.3, where the true mean and 1-σ bounds on the filter estimation error support the data from the single sample realization, that is, the error is approximately zero-mean with a standard

5-5
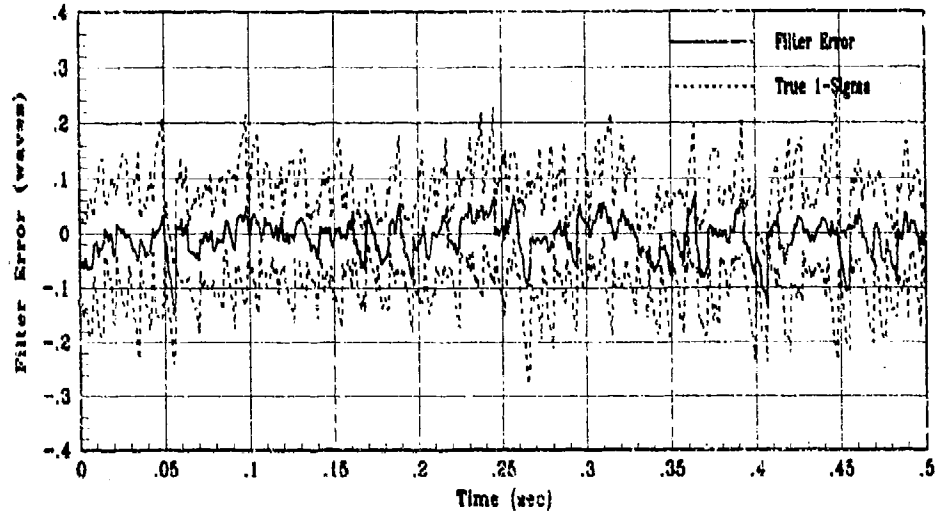
Figure 5.3. Y-tilt True Filter Estimation Error (Mean ± 1-σ) for 10 Monte Carlo Runs

deviation of approximately 0.1 wavelengths. Comparison of Figures 5.2 and 5.3 shows that the

filter-computed statistics are a good representation of the true statistics of the y-tilt process. This

result is emphasized in Figure 5.4 where the filter-computed standard deviation of y-tilt is plotted

along with the true standard deviation.

Although not shown here, similar analysis was accomplished for the remaining 13 states.

The complete set of plots which correspond to Figures 5.1, 5.2, and 5.3 for all the states are

provided in Appendix F, Figures F.1 through F.14.

The performance index for the overall LQG controller is the difference between the rms

phase distortion in the incident wavefront and the rms phase distortion in the corrected wavefront.

Post-processing of the MSOFE state time histories using Equation (2.4) results in the rms phase

distortion for the incident wavefront, $\tilde{\phi}_{Inc}(t)$, as:
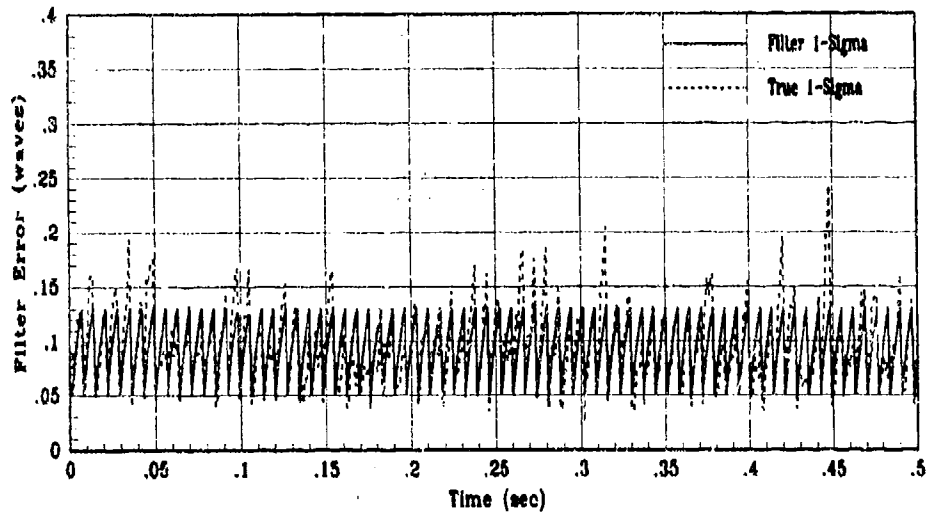
Figure 5.4. Filter-Computed 1-σ vs True 1-σ for Y-tilt Estimation Error

$$\phi_{inc}(t) = \sqrt{\sum_{i=1}^{14} x_i^2(t)} \tag{5.3}$$

Since reflection off the deformable mirror is modeled as the sum of the distortion due to the atmosphere and the counterdistortion imparted on the wavefront by the mirror, the phase distortion in the reflected wavefront, $\phi_{cor}(t)$, is found by manipulating Equation (2.1):

$$
\begin{aligned}
\phi_{cor}(r,\theta) &= \sum_{i=1}^{14} a_i(t)\ Z_i(r,\theta) + \sum_{i=1}^{14} a_{i+14}(t)\ Z_i(r,\theta) \\
&= \left[\sum_{i=1}^{14} a_i(t) + \sum_{i=1}^{14} a_{i+14}(t) \right] Z_i(r,\theta) \\
&= \sum_{i=1}^{14} \left[a_i(t) + a_{i+14}(t) \right] Z_i(r,\theta)
\end{aligned}
\tag{5.4}
$$

5-7

One sees from Equation (5.4) that the Zernike coefficients associated with modes of distortion in the reflected wavefront are equal to the sum of the atmosphere and mirror coefficients for equivalent modes. Again invoking Equation (2.4), the rms phase distortion in the corrected wavefront, $\tilde{\phi}_{cor}(t)$, is given by:

$$\tilde{\phi}_{cor}(t) = \sqrt{\sum_{i=1}^{14}[a_i(t) + a_{i+14}(t)]^2}$$

$$= \sqrt{\sum_{i=1}^{14}[x_i(t) + x_{i+14}(t)]^2}$$

(5.5)

Single sample realization time histories for the incident and reflected rms phase distortion are generated by Equations (5.3) and (5.5). The mean and variance of the incident and reflected rms phase distortion over the ten Monte Carlo runs are determined from Equations (5.1) and (5.2) with the filter error replaced by the rms phase distortion. One may find it strange to think of a mean and variance for rms phase distortion, as "rms" generally implies ensemble averaging has already been done. However the rms phase distortion, as defined by Equation (2.4), does not include ensemble averaging over the ten Monte Carlo runs and is therefore different from the generally accepted "rms" definition. The results are shown in Figure 5.5. The upper three plots represent the mean of the incident rms phase distortion ± the 1-σ value. The lower three plots show the mean ± 1-σ value for the reflected rms phase distortion resulting from deforming the mirror. From Figure 5.5 one can see that the rms phase distortion in the incident wavefront is approximately 1 wavelength in steady-state. Similarly, the rms phase distortion for the corrected wavefront is about 0.3 wavelengths. As noted by Von Bokern [30:5.7], an interesting aspect of Figure 5.5 is that the rms distortion in the corrected wavefront seems to be more tightly bounded by its 1-σ value than is that of the incident wavefront. This suggests that the rms phase distortion
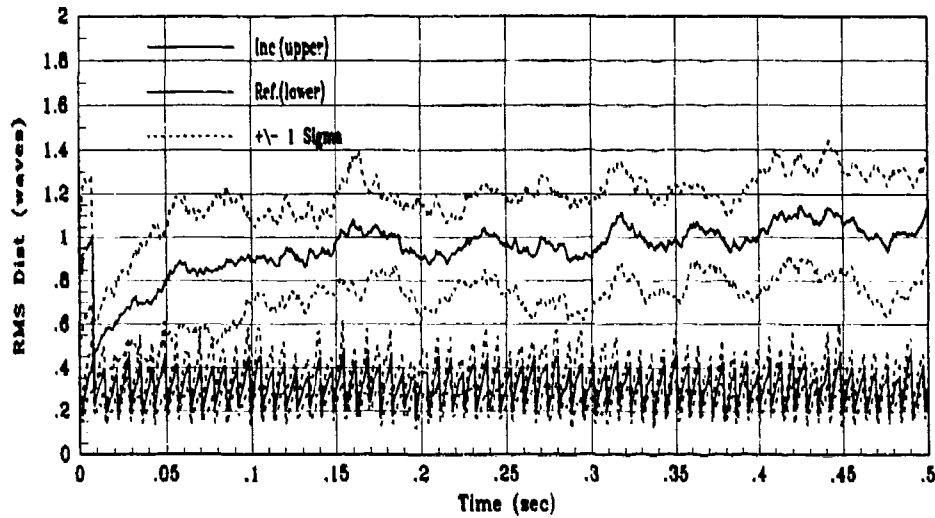
Figure 5.5. Incident and Reflected RMS Distortion (Mean $\pm$ 1-σ) for 10 Monte Carlo Runs

in the corrected wavefront tends toward a constant value, even in the presence of wide variation

in the distortion of the incident wavefront. The question remaining is, what is limiting the

performance of the controller? The most obvious source is filter estimation error. Since the filter

is limited in the accuracy with which it can estimate the system states, the control applied to the

mirror, as given by Equation (2.46), must also be in error as a direct result of filter estimation

error. The contribution to the rms phase distortion in tne reflected wavefront due solely to filter

estimation error, $\phi_{fil}(t)$, assuming the mirror can perfectly implement the filter estimate, is

computed as:

$$\tilde{\phi}_{fil}(t) = \sqrt{\sum_{i=1}^{14} [\ x_i(t) - \hat{x}_i(t)\ ]^2} \qquad (5.6)$$

5-9

The mean and standard deviation for the filter's contribution to rms phase error are computed using Equations (5.1) and (5.2). The resulting time histories are plotted in Figure 5.6. Inspection of Figure 5.6 reveals that the rms filter estimation error is also approximately 0.3 wavelengths; indicating filter estimation error to be the dominant source of error limiting controller performance. This result is consistent with Von Bokern's results [30]. Another possible error source could be saturation of the mirror actuators such that they no longer operate in their linear region. This possibility is discounted immediately based on the commanded control voltage envelope shown in Figure 5.7. Figure 5.7 shows the minimum and maximum of the control voltages applied to any actuator at each sample time over the ten Monte Carlo runs. Since the magnitude of the commanded control voltage never exceeded ± 5 volts, and with actuator saturation occurring when control voltage exceeds ± 10 volts, actuator saturation did not occur at any time during the 10 Monte Carlo runs. The final candidate error source is the selection of the cost weighting matrices in the LQ regulator. This error source was not investigated during this
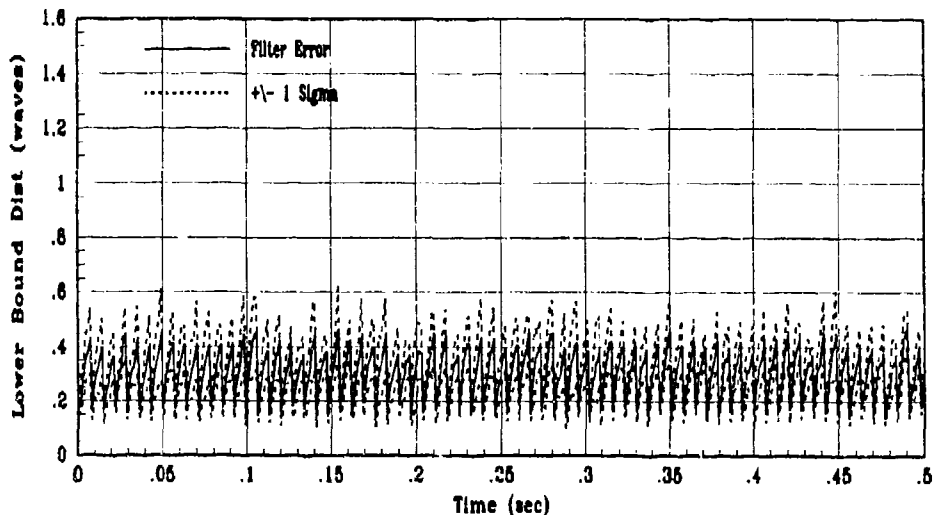
Figure 5.6. RMS Filter Error (Mean ± 1-σ) for 10 Monte Carlo Runs

5-10
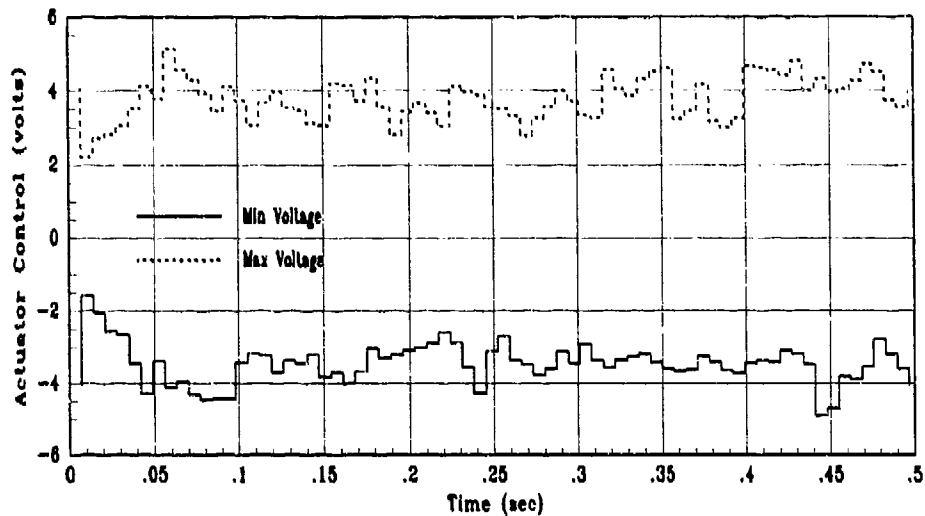
Figure 5.7. Actuator Control Voltage Envelope for 10 Monte Carlo Runs

research. However, Von Bokern [30] conducted some limited tuning on the cost weighting matrices, ran the simulations again based on the new G_c^*, and saw no improvement in performance. The cost weighting matrices should not be discounted at this time as a possible error contributor as Von Bokern's tuning was limited and it is possible that further tuning may result in some performance improvement.

The analysis to this point has dealt only with results for measurement noise study 1. Although not presented here in detail, the same analysis was accomplished for the remaining eight noise studies of Table 5.1 as well. Plots for all nine noise studies are provided in Appendix F, Figures F.1 through F.47. For comparison purposes between noise studies, the time histories for the incident rms phase distortion, the reflected rms phase distortion, and the rms filter estimation error were compressed through temporal averaging to establish a set of performance parameters for each study. Table 5.2 gives the adaptive optics control system performance parameters for the

5-11

measurement noise studies. The values in the "Percent Reduction" column were determined as one minus the ratio of the temporal average of rms phase distortion in the reflected wavefront to the temporal average of the rms phase distortion of the incident wavefront (expressed in percent). As one might expect, the best performance was achieved for the case in which low measurement noise in the truth model was correctly modeled in the filter (study 1). As the level of noise modeled in the filter increased, controller performance degraded. Performance also degraded as the level of noise increased in the truth model, even when the filter was retuned to the correct noise levels. The poorest performance occurred in the case of high measurement noise incorrectly modeled in the filter as low (study 7), as might be anticipated. In this case, the filter inappropriately weighted the measurements too heavily while disregarding its internal model of the dynamics, thereby accepting poor measurements as good. The end result was rms phase distortion after correction by the mirror of 0.461 wavelengths.

Table 5.2. Baseline Control System Performance for Measurement Noise Studies

Measurement Noise Study	RMS Phase Distortion (wavelengths)			Percent Reduction
	Incident	Reflected	Filter Error	
1	0.941	0.323	0.307	65.70
2	0.941	0.326	0.309	65.32
3	0.941	0.361	0.340	61.61
4	0.941	0.340	0.327	63.88
5	0.941	0.340	0.325	63.89
6	0.941	0.368	0.348	60.93
7	0.941	0.461	0.462	51.03
8	0.941	0.438	0.436	53.44
9	0.941	0.418	0.406	55.63

Although the trends in the data of Table 5.2 match those resulting from Von Bokern's simulations [30:5.11], one important difference has emerged as a result of updating the shaping filters for the atmosphere dynamics. The dynamics driving noise strength matrix Q resulting from the shaping filter analysis contains significantly larger entries than that of Von Bokern. As a consequence, the eigenvalues of Q are now much larger than the eigenvalues of Q from Von Bokern's work. This implies the eigenvalues of Q are now larger relative to the eigenvalues of R; viewed in the scalar case, the Q/R ratio has become larger. As such, the Kalman filter gain increases so that the measurements are weighted more heavily and the dynamics model less so.

One might wonder, when the estimation problem becomes more difficult, as in the case in which the truth model measurement noise statistics change without retuning the filter, if estimation of the higher order Zernike modes becomes more difficult than estimating the lower order modes, where most of the energy is concentrated. However, if one examines the relative change in filter estimation performance for modes 1, 6, and 14, a representative sampling of the states in terms of spatial frequency content, there is nothing in the data to suggest that the ability of the filter to estimate state 14 deteriorates any more than its ability to estimate state 1 as the truth model measurement noise changes. The plots describing filter estimation performance for states 1, 6, and 14 are provided in Appendix F for the nine measurement noise studies conducted.

5.3 Controller Performance with Correlated States

The critical component for reliably evaluating the performance of a control system through computer simulation is the truth model representation of the real world. In the interest of compiling the most accurate mathematical representation for the dynamics of the atmosphere, this research admits correlations between the Zernike coefficients as presented by Roddier [27]. Not only do these correlations provide better atmospheric statistics for the truth model, they are also

incorporated into the filter model of the controller, giving the filter a better model of the dynamics of the system. The state correlations are incorporated into the dynamics model as indicated in Table 4.1. The correlations are manifested in the dynamics through the off-diagonal terms in the Q matrix. Table 5.3 shows the simulation results for the dynamics model with correlated states in both the truth and filter models. All nine noise studies were conducted once more. Again, the data in Table 5.3 are compressed through the temporal averaging process. Comparison of the data in Table 5.3 with the data for the original controller (Table 5.2) shows that modeling of the state correlations results in slightly degraded performance for the studies involving high measurement noise in the filter. This result is not unexpected since modeling of the correlations has caused the eigenvalues of Q change. Table 5.4 shows the eigenvalues of Q with and without state correlations. As indicated in the previous section, the incoming measurements are heavily weighted under the condition of low noise in the filter, so that small changes in Q have little

Table 5.3. Performance Summary for Controller with State Correlations

Measurement Noise Study	RMS Phase Distortion (wavelengths)			Percent Reduction
	Incident	Reflected	Filter Error	
1	0.941	0.323	0.307	65.70
2	0.941	0.327	0.309	65.28
3	0.941	0.364	0.342	61.30
4	0.941	0.340	0.327	63.88
5	0.941	0.340	0.325	63.84
6	0.941	0.371	0.350	60.61
7	0.941	0.461	0.462	51.03
8	0.941	0.438	0.436	53.42
9	0.941	0.421	0.409	55.24

Table 5.4. Eigenvalue Comparison of Q With/Without State Correlations

Eigenvalue	Dynamics Noise Strength Q	
	Without Correlations	With Correlations
1	6.928	7.422
2	3.849	4.312
3	2.887	3.066
4	2.572	2.931
5	2.310	2.310
6	2.053	1.848
7	1.848	1.560
8	1.464	1.464
9	1.464	1.300
10	1.144	0.970
11	1.045	0.681
12	0.924	0.668
13	0.305	0.305
14	0.146	0.102
15 - 28	0.000	0.000

effect on the filter gains. However, when large noises are present in the filter model, small changes in Q can affect the filter gains. Plots corresponding to measurement noise study 1 with state correlations are provided in Appendix G.

In previous research, Von Bokern [30] set the initial conditions on the state covariance matrix P to zero. As a result, the performance evaluation plots indicated undesirable transient performance. One typically expects to see a large initial covariance (to enhance acquisition), due to the initial uncertainty of the state values, followed by a short transient to a steady-state

condition for linear time-invariant system models. This characteristic was not evident in Von Bokern's data. Therefore, the initial conditions were arbitrarily set to large values in an attempt to improve transient performance. Performance plots are provided in Appendix G, Figures G.1 through G.14, for a modified noise study 1 in which the states are correlated and the initial conditions for P are arbitrarily large. Comparison of the plots in Appendix G with correponding plots in Appendix F, in which the the initial conditions on P are set to zero, shows no transient performance improvement is achieved with arbitrarily large initial conditions for P. This is another result of the relative magnitudes of the eigenvalues of Q and R and the corresponding effect on the filter gains. When the eigenvalues of Q are large with respect to the eigenvalues of R, steady-state is reached quickly; in this instance steady-state is essentially reached after one sample period. Since R is a diagonal matrix, the eigenvalues of R are located along the diagonal and are given in Table 2.2.

The final stage of simulating this filter structure was to investigate the relative merits of implementing a steady-state constant-gain Kalman filter. If the performance of a constant-gain filter is not significantly degraded over that achievable with time-varying gains, then the constant-gain implementation may be desirable in order to relieve some of the computational burden associated with processing of filter algorithm. Two methods are used to identify the appropriate steady-state Kalman filter gain for the simulation. Method one involves loading the state-space formulation for the adaptive optics problem into MATRIX$_x$ and using the DESTIMATOR option to compute the filter gain. As other researchers at AFIT have experienced accuracy problems with some of the stochastic options in MATRIX$_x$, confirmation that the correct gain matrix had been identified was desired. Method two involves allowing a single MSOFE run to reach steady-state and then writing the elements of the Kalman filter gain to an external file. Comparison of the two

5-16

sets of filter gains revealed markedly different solutions. Separate simulations were conducted using each solution to determine which resulted in the best performance. As suspected, the solution from MATRIX$_x$ yielded significantly poorer performance and was abandoned. Finally, a ten-run Monte Carlo analysis for noise study 1 was conducted using the steady-state Kalman filter gain computed from MSOFE. Post-processing of the performance data shows that no significant performance degradation occurs using the steady-state filter. In fact, the difference in performance is not even detectable from the plots for the steady-state filter (see Figures G.1 through G.19) and, as indicated in Table 5.5, only shows up in the fifth decimal place of reflected rms phase distortion. It should be noted that six significant figure accuracy for this simulation is unrealistic and is only shown here to point out that the performance degradation associated with the steady-state filter is negligible.

In view of the results presented thus far, the controller incorporating the constant-gain Kalman filter and state correlations is considered as the baseline control system for the purposes of evaluating the effects of the remaining issues, that is, measurement delays and dynamics variations. The fact that the state correlations provide a more accurate depiction of the atmospheric dynamics and that the constant-gain filter performs essentially as well as the time-varying filter substantiates this decision.

Table 5.5. Performance Comparison for Time-varying vs. Steady-state Filter Gain

Kalman Filter Gain	RMS Phase Distortion (wavelengths)			Percent Reduction
	Incident	Reflected	Filter Error	
Time-varying	0.940913	0.322729	0.306888	65.7011
Steady-state	0.940933	0.322730	0.306889	65.7010

5.4 Control System Performance with Time-Delayed Measurements

One very restrictive assumption made in the development of the controller to this point is that the measurements from the Hartmann wavefront sensor are instantaneously available to the Kalman filter for updating of the state estimate. In reality, there is a full sample period delay involved with the wavefront sensor before the measurement vector becomes available for filter processing. Specifically, the wavefront sensor requires 7 msecs in order to sample the analog outputs from all 10,000 pixels of the reticon array. Considering the time constants associated with the atmospheric states, as described in Chapters 3 and 4, 7 msecs is a considerable delay. It therefore becomes necessary to investigate the impact of such a delay on the performance of the overall control system.

A study is conducted in which the controller based on the time-varying filter gain implementation of the model in Table 4.1 is simulated using MSOFE with the measurements delayed by one sample period. The measurement noises correspond to study 1 (low truth model noise/low filter model noise). Figure 5.8 shows that the filter's ability to track the Y-tilt mode of distortion is severely degraded in the presence of the measurement delay. Although the filter does not become unstable under these conditions, the performance is clearly unacceptable. Figure 5.9 shows the error between the filter estimate and the true state along with the filter-computed 1-σ bounds for the error. It is apparent from Figure 5.8 that the filter is overly optimistic as to the quality of its estimate. This condition is extremely undesirable from a filter performance evaluation standpoint. When the filter underestimates its own errors, one must be on the lookout for filter divergence problems. Normally, one thinks of filter divergence arising from mistuned noise parameters causing the filter to deweight the measurements. However, in this case, it has already been established that the filter essentially disregards the dynamics model in lieu of the

5-18
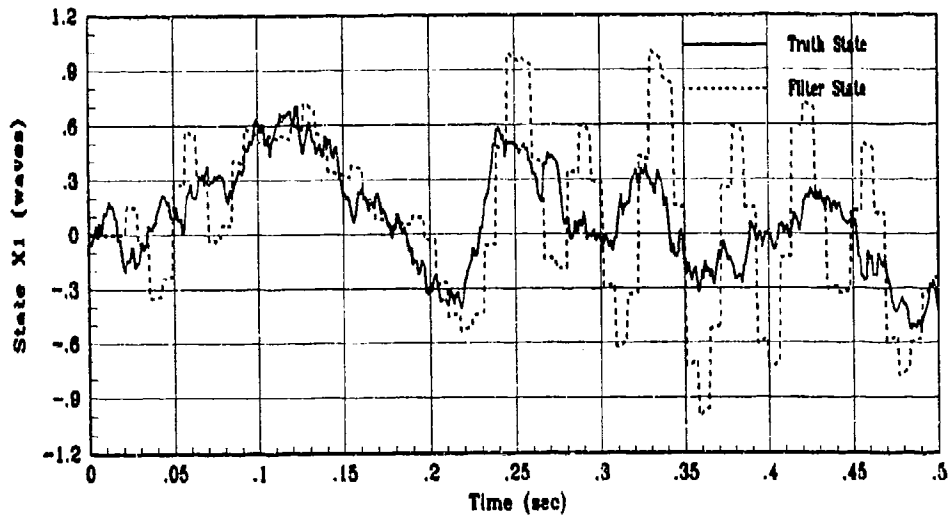
Figure 5.8. Y-tilt Truth Model and Filter States with Measurement Delay
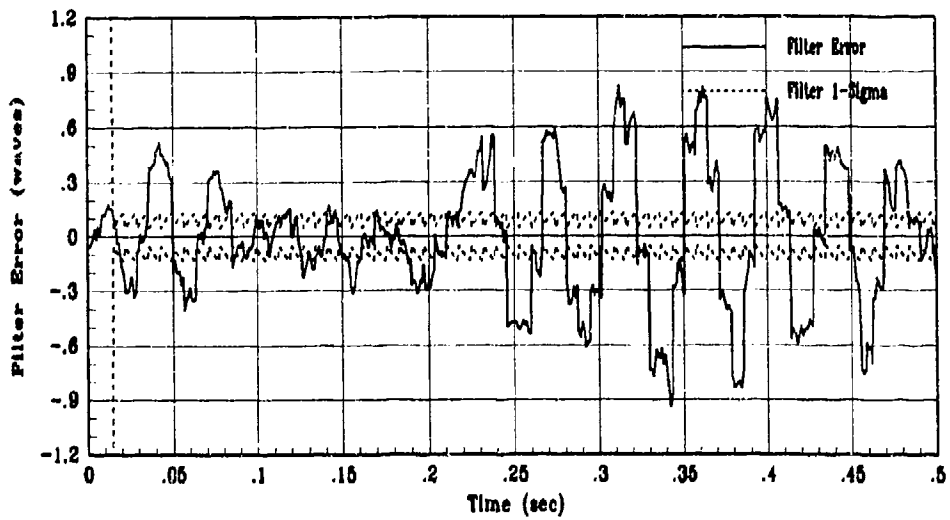
Figure 5.9. Y-tilt Filter Estimation Error with Measurement Delay (1 Run)

5-19

measurement for noise study 1. The result is that, although the filter believes it is performing well, by relying so heavily on the delayed measurements, which it assumes to be delay-free, large errors are introduced into the filter estimates. A combination of effects are responsible for these large estimation errors. First of all, since the filter weights the measurement so heavily, the filter estimates tend to track the delayed measurement. In addition, the poor filter estimates are fed back to the mirror as compensation for the distortion. Although the atmosphere states have no feedback applied, the inappropriate control couples back into the filter estimates of these states through the measurement which is modeled as the sum of the atmosphere and mirror states. Although this controller remains stable during the simulation, feedback control based on delayed measurements can induce instabilities into the system. Figure 5.10 gives the true filter estimation error (mean $\pm$ 1-σ) for 10 Monte Carlo runs of the Y-tilt mode. From Figure 5.10 one sees that the error is still approximately zero mean; however, the standard deviation of the error has increased to 0.6 wavelengths. This represents an increase in standard deviation of the Y-tilt mode
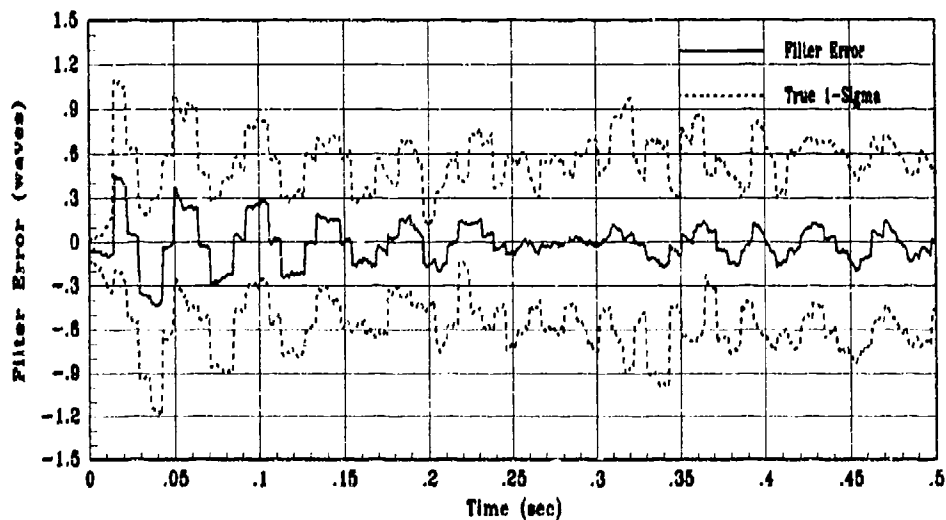
Figure 5.10. Y-tilt Filter Estimation Error (Mean $\pm$ 1-σ) with Measurement Delay (10 Runs)

5-20

error of approximately one half wavelength due solely to the measurement delay. Similar effects occur for the remaining 13 states, as indicated in Figures H.2 through H.14 of Appendix H.

As one might expect, overall control system performance is severely degraded when subjected to delayed measurements. The rms phase distortion in the corrected wavefront degrades from 0.323 wavelengths under the assumption of no delays to 1.184 wavelengths with a 7 msec measurement delay. In fact, as indicated by Figure 5.11, the rms phase distortion in the reflected wavefront is greater than that in the incident wavefront. This suggests that attempting to compensate for atmospheric distortion with this controller, in the presence of time-delayed measurements, actually makes matters worse than if no compensation were applied at all. Clearly, additional compensation is required to deal specifically with the measurement delay. The absence of 1-σ bounds in Figure 5.11 is to avoid confusion due to the proximity of the mean plots.

5.5 Controller Performance with Predictor Compensation

According to Kleinman and Baron [15, 16], among others, time-delay compensation can be accomplished by inserting a least mean-square predictor in series with the Kalman filter in the
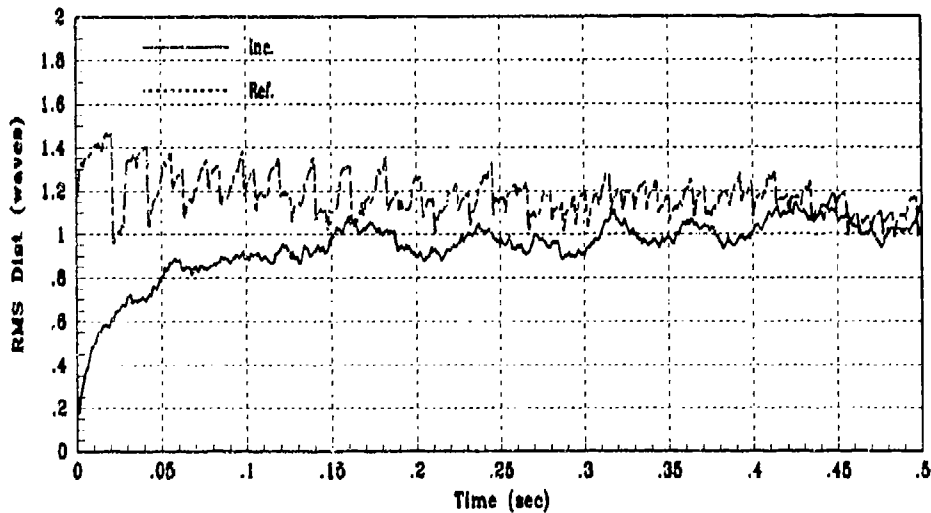
Figure 5.11. Incident and Reflected RMS Phase Distortion (Mean) with Measurement Delay

feedback loop. The time-delayed measurements are input to the Kalman filter, which in turn generates time-delayed estimates of the system states. The time-delayed estimates are fed to the predictor which propagates the filter estimates forward to the current time. The output of the predictor is premultiplied by the optimal controller gain to produce the control voltages for the mirror actuators.

An important question is; what kind of performance can be expected with predictor compensation? Examination of figure 5.12 reveals the best performance one could hope to achieve from the predictor model is performance equivalent to that of a suboptimal controller, assuming no measurement delay, in which the filter estimate prior to processing the available measurement, $\hat{x}(t_i)$, is used to generate the appropriate control vector. Under the assumption of no measurement delay, standard LQG regulator control propagates the state estimate from t_0 to
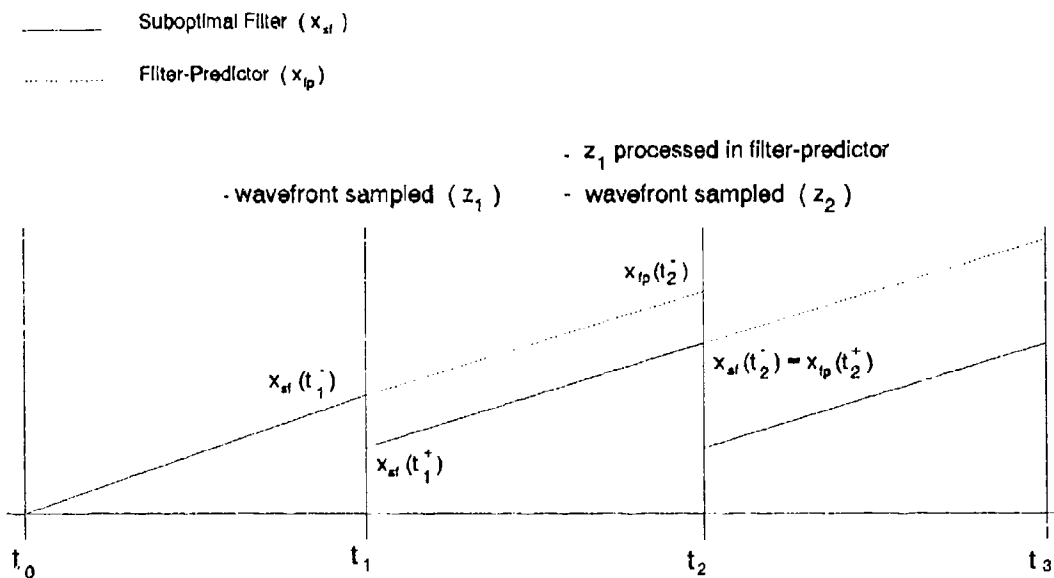
Figure 5.12. Suboptimal Filter vs Predictor-Filter Timeline

t_i, accepts the measurement at t_i, updates the state estimate at t_i^+, and premultiplies this result by the regulator gain matrix $G_c^*(t_i)$. The suboptimal control implementation, using $\hat{x}(t_i^-)$ rather than $\hat{x}(t_i^+)$ to compute the control at t_i, is generally used to avoid any destabilizing computational delay associated generating the control signal. In this case, the state estimates at the end of the propagation cycle, and consequently the suboptimal control, are computed somewhere in the interval $t_0 < t < t_1^-$. Although some reduction in performance results from the suboptimal implementation, because $\hat{x}(t_i^+)$ is a better estimate than $\hat{x}(t_i^-)$, the benefit of eliminating the additional computations associated with processing the measurement first may be worthwhile. One should note that the states do not actually ramp as shown in Figure 5.12; this feature is only to illustrate the concept in a simplistic manner.

Suboptimal control is very much akin to the predictor model described by Kleinman and Baron. The difficulty arises in the predictor implementation; that is, similar destabilizing computational delays occur if one is required to wait for the delayed measurement to arrive at time t_2 (which is actually the measurement from t_1), process the update to $\hat{x}(t_1^-)$, propagate $\hat{x}(t_1^+)$ to $\hat{x}(t_2^-)$, and generate the control, all at time t_2. A Kalman filter based on the models given in Equations (3.14) and (3.16) provides the means by which suboptimal controller performance is achieved while avoiding the situation just described. The appropriate update to the current state values is achieved through correlations between the states at times t_1 and t_2. The correlations result in a fully populated covariance matrix P_{ap} for the filter-predictor. The off-diagonal elements of P_{ap} lead to the appropriate filter gains for updating the current state values according to Equation (4.10). In the end, if the filter-predictor performs correctly, overall system performance is equivalent to that of a suboptimal controller without a delay.

Simulation of the predictor model was conducted for noise study 1 using a constant-gain Kalman filter. The simulation presented some difficulty in that the MSOFE software requires a continuous state-space representation of the system, while the predictor model presented in Chapter 3 is inherently discrete. Normally, one anticipates discretizing a continuous model in order to simulate the model on a digital computer. However, reversing the process presents a problem in that there is no unique solution. In order to make MSOFE simulate the discrete-time process in Equation (3.16), the previous values of the states were maintained in the dynamics model by setting $\underline{x}_p(t_i) = \underline{x}(t_i)$ and propagating it without dynamics over the next cycle. The steady-state discrete-time Kalman filter gain matrix K is computed as the steady-state solution to Equations (2.36) and (2.39) for the baseline 28-state model and augmented as described in Equation (4.10).

Filter-predictor performance plots for estimating Y-tilt are given in Figures 5.13 through 5.15. The plots indicate the filter does much better in tracking the true state, while no longer underestimating the magnitude of its own errors, compared to the performance of the controller prior to predictor compensation. Inspection of Figure 5.14 indicates the filter-computed 1-σ value to be somewhat conservative. This effect is a direct result of forcing MSOFE to simulate the discrete predictor model. The method previously described to force MSOFE to simulate the predictor results in a continuous plant matrix F, required for the MSOFE simulation, which has nonzero entries only in the upper left 28 x 28 partition. Discretization of this F matrix yields a state transition matrix with a 28 x 28 identity matrix in the lower right block instead of the lower left block, as required in Equation (4.3). As such, this ad hoc method for simulating the discrete-time model fails to simulate the discrete-time covariance propagation and update cycle completely. This shortfall has no adverse effect on updating the state estimate, as the steady-state filter gain
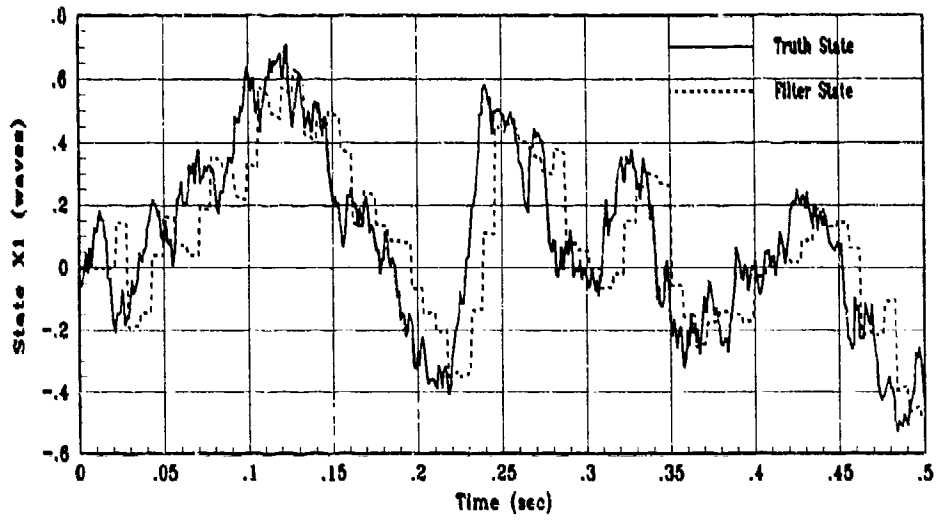
Figure 5.13. Y-tilt Truth and Filter States with Predictor Model
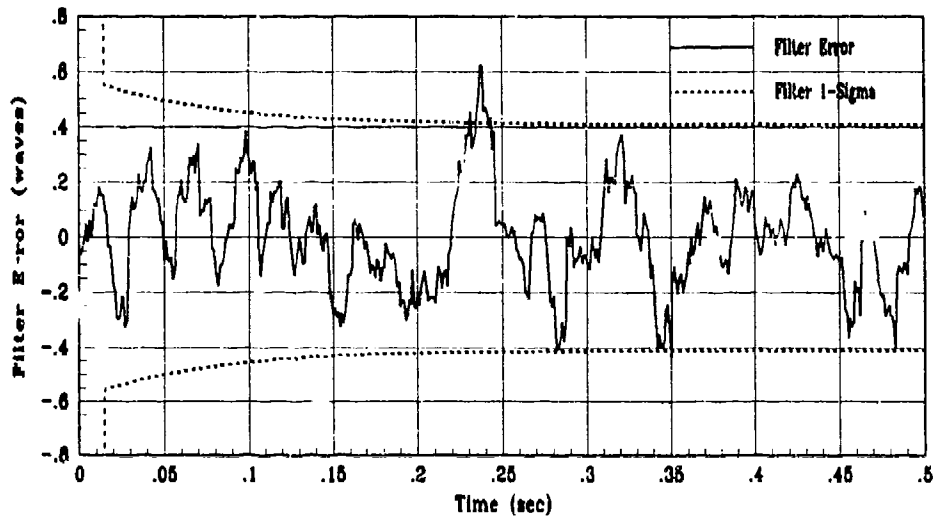
Figure 5.14. Y-tilt Filter Estimation Error with Predictor Model (1 Run)
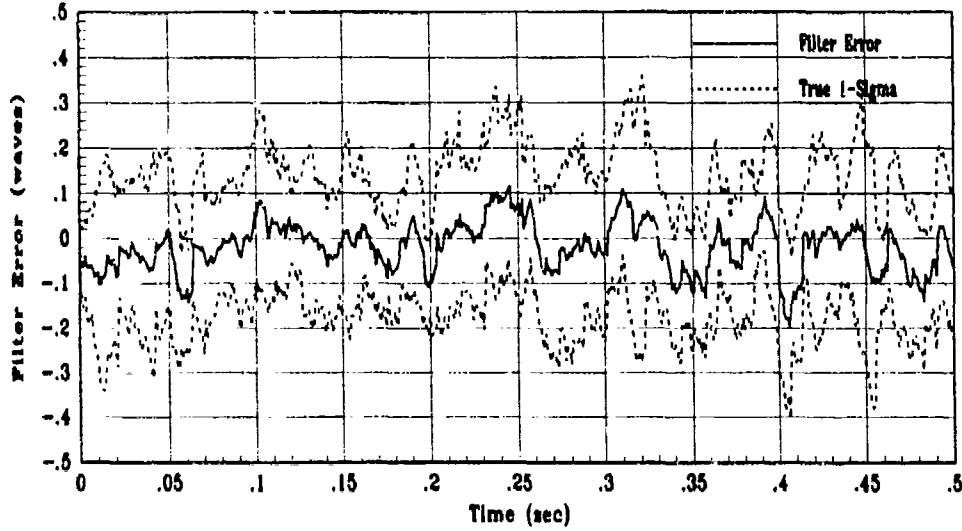
Figure 5.15. Y-tilt Filter Estimation Error (Mean ± 1-σ) with Predictor Model (10 Runs)

alleviates any real need for computing the filter covariance. Figure 5.15 shows that the true filter

estimation error over ten Monte Carlo runs is reduced from approximately 0.6 wavelengths 1-σ

to approximately 0.15 wavelengths 1-σ. A complete set of plots for states 1-14 is provided in

Appendix I, Figures I.1 through I.14.

Finally, overall control system performance is shown in Figure 5.16, where the rms phase

distortion in the reflected wavefront is reduced from 1.184 wavelengths without predictor

compensation to 0.513 wavelengths with compensation. Two questions remain:

(1) Does this controller, in fact, provide performance equivalent to the suboptimal

controller without delays?

(2) If so, is this level of performance acceptable?

The answer to the first question was found by conducting a simple test. The original 28-

state system without delays was simulated over ten Monte Carlo runs while outputting the filter

5-26

RMS Dist (waves)

1.8
1.6
1.4
1.2
1
.8
.6
.4
.2
0

Inc.(upper)
Ref.(lower)
+\- 1 Sigma

0   .05   .1   .15   .2   .25   .3   .35   .4   .45   .5

Time (sec)
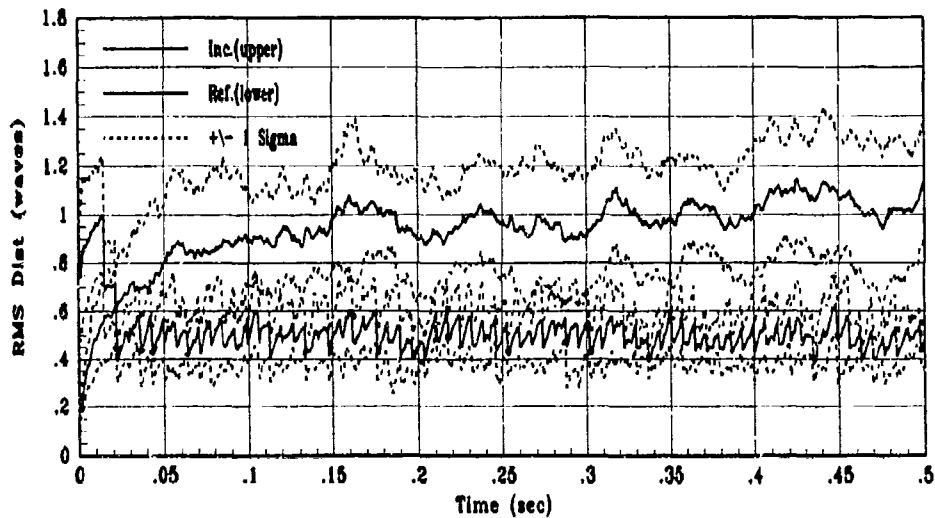
Figure 5.16. Incident and Reflected RMS Phase Distortion (Mean ± 1-σ) with Predictor Model

estimates at t_i. The estimates of states 1-14 at t_i, assuming no delay, were compared to the filter-

predictor estimates of the same states at t_i'. The results for Y-tilt are plotted in Figure 5.17.

From the figure, one can see that the performance of the filter-predictor is virtually the same as

the suboptimal filter. Also, as part of the same simulation, the suboptimal control law was applied

as [21:190]:

$$\underline{u}(t_i) = -G_c^* \, \hat{\underline{x}}(t_i^-)$$
(5.7)

The overall control system, based on the suboptimal control of Equation (5.7), yields rms phase

distortion in the reflected wavefront of 0.511 wavelengths. Clearly the control system using

predictor compensation performs essentially as well as the suboptimal controller without

measurement delays.
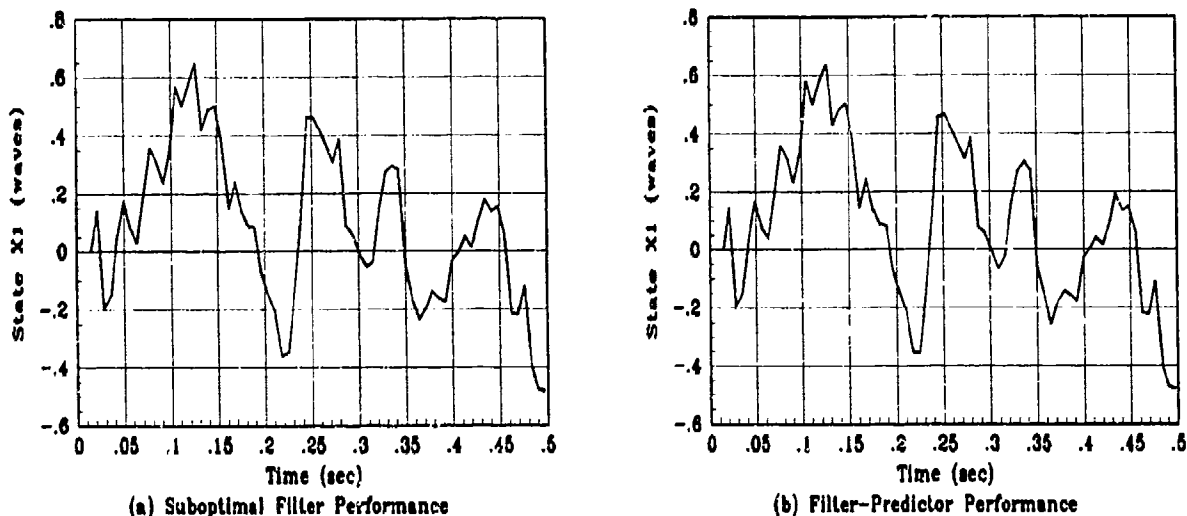
Figure 5.17. Suboptimal Filter vs Filter-Predictor Estimation Performance

Is such performance acceptable for the adaptive optics system of this research? If it is assumed that the performance exhibited by the optimal controller with no delays is only marginally acceptable, the answer is no. Although the predictor reduces the rms phase distortion in the reflected wavefront by as much as 57 percent over that when no compensation is applied, the reduction in rms phase distortion over that in the incident wavefront is only 46 percent, as compared to 65 percent reduction under the assumption of no delays. More than half the total rms phase distortion in the incident wavefront remains after correction by the deformable mirror. Due to the significant effect on performance as a result of the delay, it is apparent that the sampling rate of the wavefront sensor is the dominant limiting factor for this system. One might wonder, at this point, what wavefront sensor sampling rate would result in acceptable performance in the presence of a full sample period delay. In order to answer this question, a simulation of the predictor model was conducted in which the sample period was arbitrarily decreased to 3 msecs.

5-28

Figure 5.18 shows the resulting rms phase distortion for the incident and reflected wavefronts. As before, the time histories are compressed through temporal averaging. The rms phase distortion in the reflected wavefront is 0.363 wavelengths. Comparison of this result with the data in Table 5.3 indicates that this controller, using a wavefront sensor with a 3 msec sample period, can nearly recover the performance of the original system without delays. It appears a sample period slightly shorter than 3 msec could duplicate the baseline performance. Additional performance plots for the predictor with a 3 msec sample rate are provided in Appendix I, Figures I.17 through I.20.

5.6 Sensitivity Study

The controller developed and simulated thus far assumes time-invariance for the dynamics of the atmosphere. In reality, the dynamics of the atmosphere can be expected to vary with time unless the observation period is very short. It, therefore, becomes necessary to investigate the
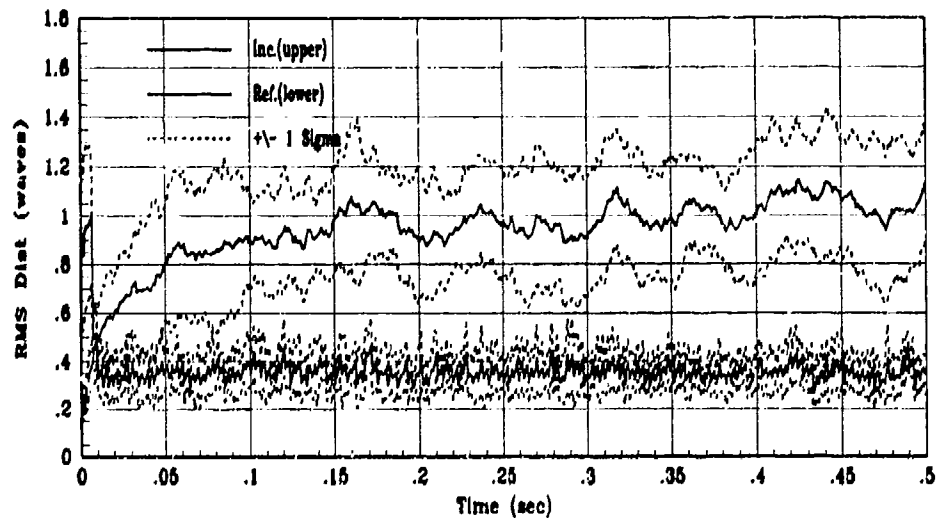

Figure 5.18. RMS Distortion (Mean ± 1-σ) with Predictor Model and 3 msec Sample Rate

5-29

effects on controller performance when such changes occur. Several studies are conducted in which the average wind velocity along the propagation path and the zenith angle to the viewed object are varied. During these studies the truth model is changed, according to the models presented in Chapter 4, to simulate new atmospheric conditions. The nominal controller is simulated against each condition and the resulting performance is evaluated. In consideration of the possibility of using a multiple-model adaptive estimation algorithm [20] to address the variations in the atmosphere dynamics, the models for each atmospheric condition are then simulated in both the truth and filter models. The results provide insights as to whether or not a multiple-model approach is worthwhile for this system.

The first series of studies addresses variation in the average wind velocity along the propagation path of the wavefront. Separate dynamics models are generated according to the procedures of Appendix A for wind velocities of 5, 15, 35, 45, 55, and 65 m/sec. Table 5.6 presents the performance results for the case in which the truth model simulates the new condition

Table 5.6. Predictor Controller Performance for Wind Velocity Studies

Average Wind Velocity w (m/sec)	RMS Phase Distortion (wavelengths)			Percent Reduction
	Incident	Reflected	Filter Error	
5	0.904	0.481	0.464	46.81
15	0.919	0.493	0.477	46.34
21 (nominal)	0.941	0.513	0.497	45.53
35	1.007	0.589	0.575	41.55
45	1.062	0.639	0.626	39.80
55	1.128	0.707	0.696	37.31
65	1.201	0.786	0.776	34.57

while the filter model is "unaware" of the changes. Examination of the results reveals that the filter performs better as the average winds decrease. This is to be expected since decreasing the winds along the propagation path slows down the dynamics of the system; thus the estimation problem becomes easier. Similarly, as the winds increase, performance is degraded as the dynamics become faster and the estimation problem becomes more difficult. The most important result from this phase of the sensitivity study is that, although the performance degrades gracefully with the severity of the atmospheric conditions, the system remains stable over the entire range of conditions investigated. The standard complement of filter and controller performance plots substantiate the stability claims and are provided in Appendix J, Figures J.1 through J.24.

The next series of studies investigated the effect of changes in the zenith angle to the viewed object. Table 5.7 shows results of the truth model simulating the true condition while the filter is again "unaware" of the mismatch. As indicated in Table 5.7, the controller performance degrades as the zenith angle to the source increases, or as the object is located lower

Table 5.7. Predictor Controller Performance for Zenith Angle Studies

Zenith Angle ζ (deg)	RMS Phase Distortion (wavelengths)			Percent Reduction
	Incident	Reflected	Filter Error	
0 (nominal)	0.940918	0.512455	0.496628	45.53
15	0.954068	0.519645	0.503597	45.53
30	1.007627	0.548811	0.531862	45.53
45	1.115228	0.607407	0.588649	45.53
60	1.326025	0.722206	0.699902	45.53

on the horizon. This result is consistent with intuition since viewing an object lower on the horizon requires viewing through more of the atmosphere, resulting in a greater degree of distortion in the wavefront. Again, the system remains stable over the range of conditions evaluated. It is not surprising that the percent reduction in the rms phase distortion for the zenith angle study is the same, regardless of the location of the source. This occurs due to the fact that the atmosphere dynamics have not changed as a result of changing zenith angle (only the dynamics driving noise strength changes) and the filter uses the same constant gain in all cases. The result is that the measurement residual increases as the dynamics driving noise strength of the truth model increases, however the residual is weighted identically in each case, thereby providing the same degree of reduction in the distortion. Performance plots are provided in Appendix J, Figures J.25 through J.40. The need for the additional accuracy shown for the zenith angle study becomes evident later as the filter is made "aware" of the changes in the dynamics.

Once again, upon inspection of the plots of states 1, 6, and 14 of Appendix J for the various dynamics variations, there is nothing in the data to suggest that the relative difficulty for the filter to estimate the higher order states is any greater that of the lower order states as a result of the changing dynamics.

The results presented can also be interpreted in terms of the optical characteristics of the system. The coherence length, r_0, is widely viewed in the optics community as the critical parameter characterizing the quality of the viewing. The coherence length defines the spatial dimension of an aperture wherein a unique phase error can be measured and corrected [26]. It has also been described [28, 30] as the diameter of an aperture across which the rms phase distortion is one radian. Table 4.4 shows the corresponding values of r_0 for the specific atmospheric conditions evaluated, as computed from Equations (3.26) and (3.27). The
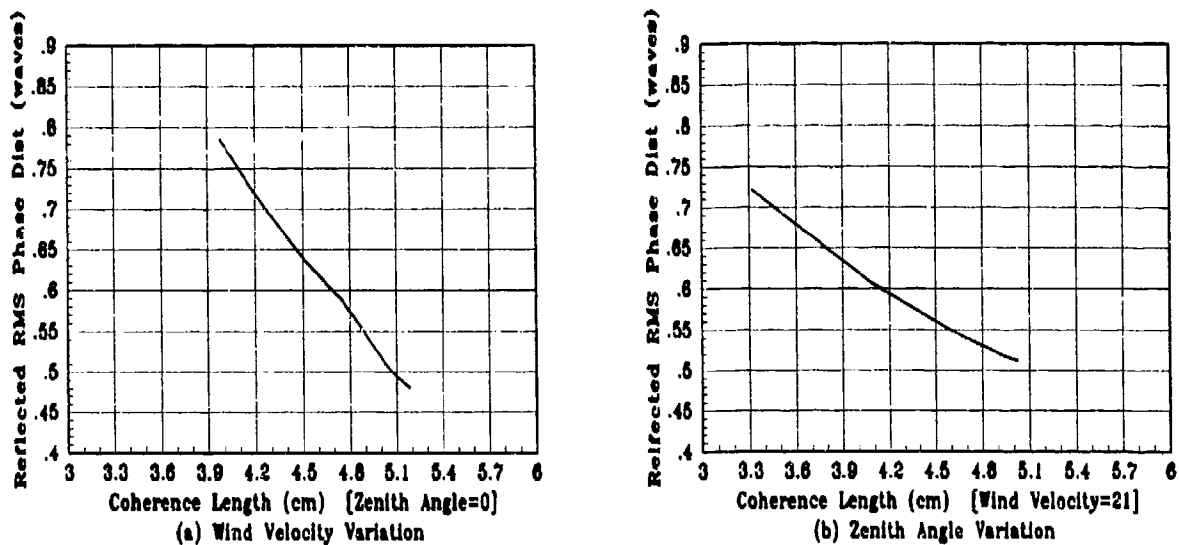
Figure 5.19. Controller Performance vs Coherence Length

performance of the controller for variations in the wind velocity and zenith angle is shown in

Figures 5.19(a) and 5.19(b), respectively, as a function of increasing r_0. From Figures 5.19(a) and

(b), one sees that the overall performance of the controller degrades significantly as the coherence

length becomes smaller. Also evident from the plots is that, although specific changes in either

wind velocity or zenith angle can result in the same r_0 value, controller performance seems to

degrade more rapidly with changes in the average wind velocity. This result is due to the fact that

wind velocity changes couple directly into the plant dynamics through the refractive index

structure constant, C_n^2, and the integration of Equation (2.22). As a consequence, the dynamics

model undergoes changes in both the plant dynamics matrix F and the dynamics noise strength

matrix Q. On the other hand, changes in the zenith angle, for a given wind velocity, have no

effect on the plant dynamics and only effect the dynamics driving noise strength matrix through

a change in the covariance matrix as indicated by Equations (3.5) and (3.9).

5-33

The final phase of the sensitivity study is to reaccomplish the simulations for each atmospheric condition with the new dynamics in both the truth and filter models. Here the filter is "informed" of the variation of the important parameters. The additional simulations are conducted to investigate the possible merits of a multiple-model adaptive estimation approach to deal with the degrading effects of real-world and filter model mismatches, allowing the parameters to be estimated. These studies thus yield the best performance attainable from such an adaptive algorithm. The results are shown in Tables 5.8 and 5.9. Comparison of the data in Tables 5.6 and 5.8 reveals that very little performance improvement is realized by retuning the filter model to match the truth model when the wind velocity is varied. This result can be attributed to the relationship between the eigenvalues of Q and R. The eigenvalues of Q are so much larger than

Table 5.8. Retuned Controller Performance for Wind Velocity Studies

Average Wind Velocity w (m/sec)	RMS Phase Distortion (wavelengths)			Percent Reduction
	Incident	Reflected	Filter Error	
5	0.904	0.479	0.464	46.95
15	0.919	0.492	0.477	46.45
21 (nominal)	0.941	0.513	0.497	45.53
35	1.007	0.588	0.573	41.58
45	1.062	0.638	0.623	39.86
55	1.128	0.705	0.689	37.50
65	1.201	0.781	0.765	34.97

Table 5.9. Retuned Controller for Zenith Angle Studies

Zenith Angle ζ (deg)	RMS Phase Distortion (wavelengths)			Percent Reduction
	Incident	Reflected	Filter Error	
0 (nominal)	0.940918	0.512455	0.496628	45.53
15	0.954068	0.519644	0.503597	45.53
30	1.007627	0.548810	0.531862	45.53
45	1.115228	0.607405	0.588650	45.54
60	1.326025	0.722201	0.699904	45.54

the eigenvalues of R that the filter already weights the measurements heavily prior to retuning the filter. When the filter is retuned to the correct conditions, the change in the eigenvalues of Q does not significantly affect the relative size of the eigenvalues of Q and R. Heuristically, one can think of the Q/R ratio (for the scalar case) as being so large that a modest change in Q has no significant affect on the ratio, that is, the filter is past the point of diminishing returns in sensitivity to further variation in the Q/R ratio. The same effect is apparent from the data in Tables 5.7 and 5.9 for the zenith angle variations. In fact, for these studies, retuning has even less affect on the overall performance of the controller. The performance improvement occurs in the sixth decimal place and is negligible. Again, six decimal accuracy is not very realistic for this simulation and is shown only to illustrate the insignificance of the change in performance. The consequence of these results is that the improvement in performance achieved by adjusting the filter model to the current atmospheric conditions does not warrant a multiple-model adaptive estimation approach for this system, under the conditions of noise study 1.

5.7 Summary

This chapter presents the results of computer simulation of the various controller structures developed during this research. The MSOFE software [23] is used to simulate the behavior of the real world, the performance of the Kalman filter, and the overall performance of the LQG controller. First, nine separate measurement noise studies are conducted with varying levels of measurement noise in both the truth and filter models. Then, both cross-correlations between the states and new initial conditions for the state covariances are simulated and a new performance baseline is established. Next, the results using a steady-state Kalman filter in the controller are shown. Then, the performance of the controller is simulated in the presence of measurement delays. The predictor model is then simulated to show the effect of compensating for the wavefront sensor processing delay. Lastly, several models are simulated to show the effects of changing atmospheric conditions on the performance of the nominal and retuned filter models. The data from the simulations are tabulated and analyzed in detail.

VI. Conclusions and Recommendations

6.1 Summary

This research proposes a linear quadratic Gaussian (LQG) approach to designing a control law for a deformable mirror adaptive optics system. Optical image quality is distorted in phase, intensity distortion is neglected, as a result of propagation through the earth's turbulent atmosphere. Compensation of the image wavefront is accomplished by estimating the degree of distortion in the incident wavefront and deforming the mirror to counterdistort the wavefront, ideally canceling the phase distortion in the wavefront. Estimates of the system states describing the distortion are generated by a Kalman filter based on Hartmann wavefront sensor measurements of the gradient of the wavefront within the 69 subapertures of the mirror. The filter estimates are processed by a linear quadratic regulator which determines the appropriate control voltages to apply to the mirror actuators in order to minimize the phase distortion in the reflected wavefront.

The dynamics of the atmospheric distortion are modeled as a set of 14 time-varying Zernike coefficients, each represented as a first-order Markov process. The deformable mirror dynamics are also modeled as 14 Zernike coefficients; however, the mirror dynamics are modeled as deterministic first-order lag states. Tilt mirrors preceding the deformable mirror are assumed to remove 80 percent of the gross tilts in the image wavefront. The model for the Hartmann wavefront sensor includes a full sample period time delay associated with processing the measurements. Time delay compensation, in the form of a least mean-square predictor, requires tracking of the state values from the previous sample time within the dynamics model. State augmentation results in a 56-state dynamics model which is embedded in the Kalman filter algorithm in order to generate the state estimates. The deterministic mirror states are only included in the filter model to satisfy constraints imposed by the MSOFE software. In a final

implementation, the mirror states should be removed from the filter and processed outside the filter algorithm with an auxiliary set of equations.

Variations in the atmospheric dynamics model are considered for discrete changes in the average wind velocity along the propagation path and the zenith angle to the light source. New dynamics models, specifically plant and noise strength matrices, are determined for each atmospheric condition evaluated. The overall control system is simulated with the MSOFE software.

6.2 Conclusions

This section presents the significant findings resulting from the extensive simulation phase of this research as described in Chapter 5. As anticipated, the results from simulating the updated truth model, under the same assumptions made by Von Bokern [30], are consistent with Von Bokern's measurement noise study results. The significant conclusions are as follows:

1. Under the assumption of no measurement processing delay, the adaptive optics system reduced the rms phase distortion in the reflected wavefront by 55-65 percent, depending on the levels of noise in the truth and filter models. This performance was achieved over variations of four orders of magnitude in the covariance of the measurement noise.

2. The performance plots indicated that the rms phase distortion in the reflected wavefront was somewhat constant, even in the presence of wide variation of the distortion in the incident wavefront. This is likely the result of the mirror actuators operating well within the saturation limits at all times. Also, filter estimation error seems to be the most significant contributor to the residual phase error in the reflected wavefront.

3. Evaluation of the performance of the constant-gain Kalman filter showed negligible performance degradation over that achievable with time-varying gains. As a result, the constant-gain implementation is recommended in order to reduce computational loading.

4. Simulation of the controller without predictor compensation, when subjected to time delayed measurements, revealed severely degraded performance. In fact, under these conditions, this controller induces more phase distortion into the reflected wavefront than that in the incident wavefront. The requirement for time delay compensation was clearly demonstrated.

5. Simulation of the suboptimal control law, assuming no measurement delay, revealed that the filter-predictor model performs virtually the same as the suboptimal controller. Although this represents a significant improvement over the case of no delay compensation, the residual distortion in the reflected wavefront may well be unacceptable.

6. Based on simulation of the predictor-compensated controller using a 3 msec wavefront sampling period, and assuming the performance of the controller without delays (the baseline) is acceptable, the controller with predictor compensation, in the presence of time-delayed measurements, could recover the performance of the baseline system provided a wavefront sensor with a sample period slightly less than 3 msecs were available.

7. The sensitivity studies of the predictor-compensated control law show the performance of this controller degrades gracefully over the evaluated range of variations in the dynamics of the atmosphere. Also, the performance degrades more quickly due to changes in the wind velocity as opposed to changes in the zenith angle. This occurs as

a result of the coupling of the wind velocity directly into the plant dynamics matrix, whereas zenith angle changes only affect the strengths of the dynamics driving noise. Finally, the controller remains stable over the range of wind velocity and zenith angle variations investigated.

8.   Based on the results from   sensitivity studies, there does not appear to be any justification, in the way of performance improvement, for implementing a multiple-model adaptive estimation structure to estimate the changing parameters of the atmosphere under the condition of low measurement noise. That is not to say that there will be no improvement when the measurement noise is increased. Under these conditions, retuning the Q matrix will affect the filter gains to some degree, particularly when high measurement noises are modeled.

9.   One underlying characteristic of the models for the atmosphere dynamics and the Hartmann sensor, which greatly impacts the performance of the controller, is the relationship between the eigenvalues of the dynamics driving noise strength matrix and the measurement noise covariance matrix. The fact that the eigenvalues of Q are much larger than the eigenvalues of R causes the filter to weight the measurements heavily in lieu of the dynamics model. This has two notable effects. First, as the filter weights the measurements heavily, the system converges to steady-state very quickly; thus a constant-gain filter is attractive. Second, as the dynamics model changes, the strengths of the white noises driving the states increase or decrease according to conditions. However, the relationship between the eigenvalues of Q and R does not change significantly enough, under the condition of low measurement noise, when the filter is

retuned to the specific atmospheric conditions, to warrant the added complexity of a multiple-model structure.

6.3 Recommendations

This section presents recommendations based on the results of Chapter 5 and the conclusions drawn in Section 6.2. The specific recommendations are as follows:

1. The truth model developed in this thesis carries with it no claims of being complete. It is, in fact, a reduced-order model; reduced from an infinite number of Zernike modes to only 14 modes. More research is needed in developing the best truth model possible before a controller of this type can be fielded. Although first-order curve-fits were used to generate models for the Zernike states, higher-order effects were evident in the autocorrelation data. This suggests that higher-order shaping filters might produce a better fit to the data. Also, even as the mirror may have difficulty compensating for modes with spatial frequencies higher than that of Zernike mode 14, inclusion of higher-order modes in the truth model (not necessarily the filter model) would provide a more accurate evaluation of the true capabilities of the controller. One must always bear in mind that the LQG controller is only as good as the truth model upon which it is based.

2. The deformable mirror is modeled as deterministic for this research. The deterministic model resulted from several assumptions including identically symmetric influence functions for all 97 actuators and interactuator linearity of the responses. However, one might consider the uncertainty left out of the problem under these assumptions by adding pseudonoise to the mirror dynamics. Also, additional pseudonoise could account for any random variations in the voltages applied to the actuators resulting from power supply fluctuations.

3. Under the assumption of deterministic mirror dynamics, the Kalman filter need not estimate the mirror states. Elimination of the mirror states from the filter would greatly reduce the computational requirements for processing the filter algorithm by reducing the total number of states from 56 to 28, without sacrificing performance. In this case, the solution to the mirror state equation could be computed separately from the filter algorithm. In fact, inclusion of deterministic states could induce numerical precision problems associated with all the zero eigenvalues of the augmented covariance matrix.

4. The data presented in Chapter 5 seem to indicate that the Kalman filter statistics accurately depict the true statistics of the atmosphere states. However, no observability test has been performed on this system. Therefore, it is possible that the Kalman filter model contains unobservable states, although there is nothing in the data to suggest such. It might be worthwhile to conduct some limited filter tuning runs to investigate the possibility of better filter performance if, in fact, some of the states are unobservable.

5. The intent during this research was to account for 95 percent reduction of x and y tilts in the truth model due to tilt mirror preprocessing of the wavefront. However, a mathematical oversight early on resulted in only accounting for approximately 80 percent reduction in the gross tilts. It would be interesting to rerun the simulations based on 95 percent attenuation of x and y tilts and observe the changes in controller performance. By so doing, the eigenvalues of Q will be reduced somewhat. This may impact the performance improvement gained by retuning the filter to changing atmospheric conditions. It should be noted that Von Bokern's results also reflect 80 percent tilt mode attenuation rather than 95 percent.

6. The predictor model used for compensating for the measurement time delay is inherently a discrete-time model. This presented some difficulty when trying to simulate the augmented system model with MSOFE, as MSOFE requires a continuous state-space representation of the dynamics. Although a work-around was found which forced MSOFE to simulate the discrete model, it would be effort well spent to develop either new software or a modification to MSOFE which would allow future control system designers to simulate the discrete-time model directly.

Appendix A. Dynamics Model Shaping Filter Analysis

This appendix gives the details of the shaping filter analysis used to model the effects of atmospheric turbulence on optical image quality. The general procedure is:

1. Analytically determine the autocorrelation kernel for each of the Zernike coefficients.

2. Evaluate the autocorrelation kernel for various values of τ and plot the resulting data.

3. Curve-fit an appropriate shaping filter function to the autocorrelation data.

4. Determine the parameters for the shaping filter from the functional curve-fit.

The covariance function as defined by Hogge and Butts [12:145] for the pth Zernike coefficient is given by:

$$R_p(\tau) = E\left\{ \left[a_p(t) - E\left\{a_p(t)\right\}\right]\left[a_p(t+\tau) - E\left\{a_p(t+\tau)\right\}\right] \right\} \qquad (A.1)$$

When the Zernike coefficients are modeled as zero-mean Gaussian random variables, Equation (A.1) reduces to the autocorrelation kernel:

$$R_p(\tau) = E\left\{ a_p(t)a_p(t+\tau) \right\} \qquad (A.2)$$

Hogge and Butts derived an expression for the right-hand side of Equation (A.2) by viewing the atmosphere as being comprised of many thin layers of turbulence; each layer having an associated average velocity and refractive index structure constant. The combined effects of all the layers, assuming a Kolmogorov spectrum [5, 12, 23] of turbulence for each layer, are realized by integrating over the altitude. The mathematical details of the derivation are beyond the scope of this research, however, the resulting expression given in Equation (2.22) determines the autocorrelation kernel for the pth Zernike coefficient.

A-1

Equation (2.22) is integrated on a computer to generate the autocorrelation data for the shaping filter analysis. For this research, C_n^2 is computed from the Hufnagel-Valley 21 model [26] given in Equation (3.26). The wind velocity profile is determined from the Bufton model [26] as:

$$v(h) = v_g + 30 \, e^{-\left(\frac{h - 9400}{4800}\right)^2}$$

(A.3)

where v_g is the ground wind speed assumed to have a nominal value of 5 m/sec and $v(h)$ is assumed to be directed along the positive x-axis of the aperture. Additional parameter values and assumptions required to evaluate Equation (2.22) are:

1. The wavelength of light from the source is 0.514 µm.

2. The entrance aperture radius of the telescope is 0.75 m.

3. The satellite altitude is 100 km.

4. The satellite is assumed to be in geosynchronous orbit so that it remains stationary with respect to the observer.

Equation (2.22) is integrated using a set of 14 FORTRAN programs, one for each Zernike function, called ACOVAR#.f, where # indicates the Zernike coefficient whose autocorrelation kernel is desired. It is important to note that Hogge and Butts do not adhere to the Zernike Function definitions presented in Chapter 2. Although closely related to the functions defined for this research, their definitions differ slightly. It therefore becomes necessary to establish the appropriate conversion between the Hogge and Butts function definitions and those used in this research. As alluded to in Chapters 1 and 2, the conversion factor used in previous research [30] was found to be in error. In order to determine the correct scale factor one can force equivalence

A-2

between any one of the functions listed in Table 2.1 and its counterpart Hogge and Butts definition. By so doing, one finds the two sets of functions related as:

$$Z_p(\rho) = \sqrt{\pi} \; G_p(\rho) \tag{A.4}$$

Now, the G_p product under the integral of Equation (2.22) is converted to the Z_p product consistent with this research as:

$$Z_p(\rho) \; Z_p(\rho') = \pi \; G_p(\rho) \; G_p(\rho') \tag{A.5}$$

Combining Equation (2.22) with the result in Equation (A.5) and converting units from radians to wavelengths yields the autocorrelation kernel for the Zernike function definitions of this research as:

$$
\begin{aligned}
\tilde{R}_p(\tau) &= \pi \cdot \frac{1}{4\pi^2} \; R_p(\tau) \\
&= \frac{1}{4\pi} \; R_p(\tau)
\end{aligned}
\tag{A.6}
$$

Following integration of Equation (2.22) and subsequent scaling according to Equation (A.6), the resulting data points are plotted and curve-fit to standard first-order Markov process (output of a first-order lag driven by white Gaussian noise) shaping filter functions. As an example, consider the autocorrelation data for Zernike coefficient a_1 (y-tilt) which is plotted in Figure A.1. According to Maybeck [19], one approach to generating shaping filter models from such data, the approach taken in this research, is to assume an a priori functional form for the autocorrelation kernel associated with the process a_1 and then curve-fit the data to that form. This research assumes an a priori form of a first-order Gauss-Markov process for all 14 Zernike coefficients. The autocorrelation kernel for a first-order Gauss-Markov process is characterized by:
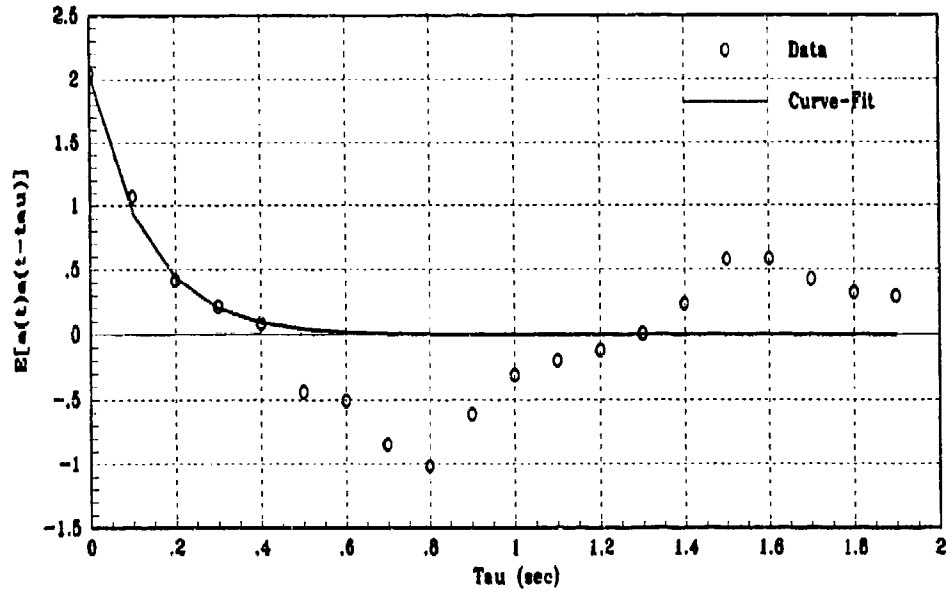
Figure A.1. Autocorrelation Data for Zernike Coefficient a_i

$$E \{ x(t)x(t+\tau) \} = \sigma^2 e^{-\frac{|\tau|}{T}}$$ (A.7)

where T is the correlation time and σ^2 is the mean squared value. The state-space model of a first-order Gauss-Markov process is a first-order lag driven by white Gaussian noise of strength Q given by:

$$\dot{x}(t) = -\frac{1}{T} x(t) + w(t)$$ (A.8)

where the strength of the white Gaussian noise is determined by:

$$Q = \frac{2\sigma^2}{T}$$ (A.9)

A-4

The curve-fit for the data shown in Figure A.1 results in the shaping filter parameters σ^2=2.0433 wavelengths^2 and T=0.13 seconds for Zernike coefficient a_1. The solid line of Figure A.1 is the plot of Equation (A.7) using the aforementioned parameter values. From Equation (A.8), the state-space model for a_1 is:

$$\dot{a}_1(t) = -\frac{1}{0.13} a_1(t) + w(t) \tag{A.10}$$

and

$$Q = 51.437 \frac{wavelengths^2}{sec} \tag{A.11}$$

Similar analysis is used to generate shaping filters for the remaining 13 Zernike coefficients, each state modeled as a first-order Gauss-Markov process. It should be noted that, for nine of the Zernike coefficients, the autocorrelation data for τ=0 agrees quite well with the covariance data available in the literature [27, 32], as expected. The data for the remaining five coefficients, including a_1, provide a somewhat poorer covariance match. However, the data generated after the scale factor correction is generally in much better agreement with the literature than the data used in previous research. The state-space models for all 14 states are developed as described above, with the exception that the white noise strengths are calculated using the covariance values found in the literature. The autocorrelation data and the curve-fit for the remaining 13 atmosphere states are shown in Figures A.2 throught A.14.
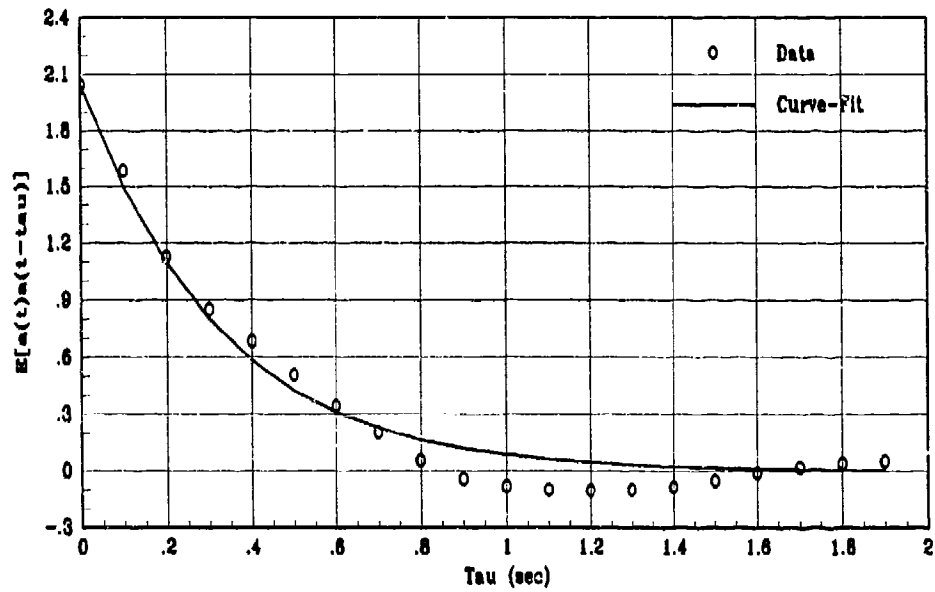
Figure A.2. Autocorrelation Data for Zernike Coefficient a_2
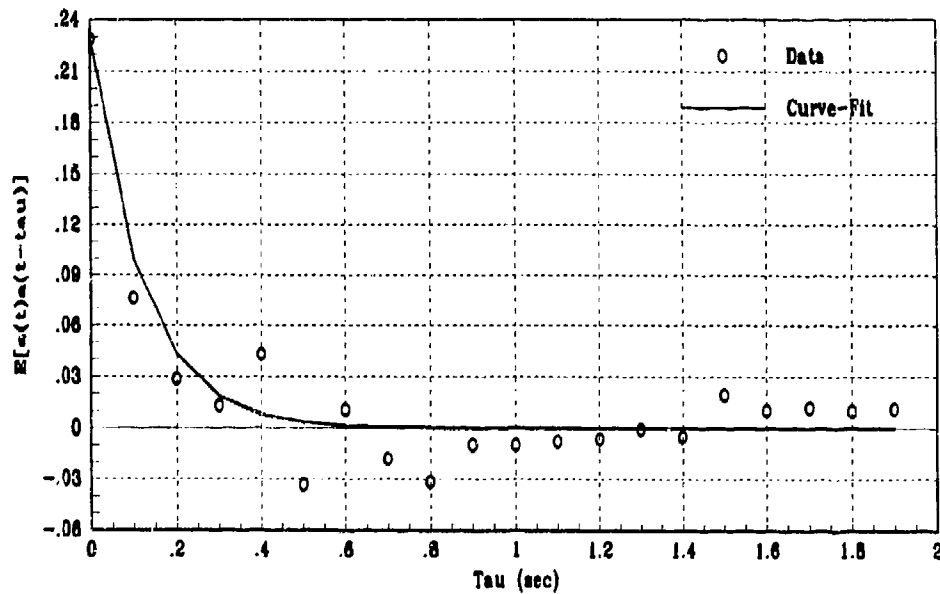
Figure A.3. Autocorrelation Data for Zernike Coefficient a_3

A-6
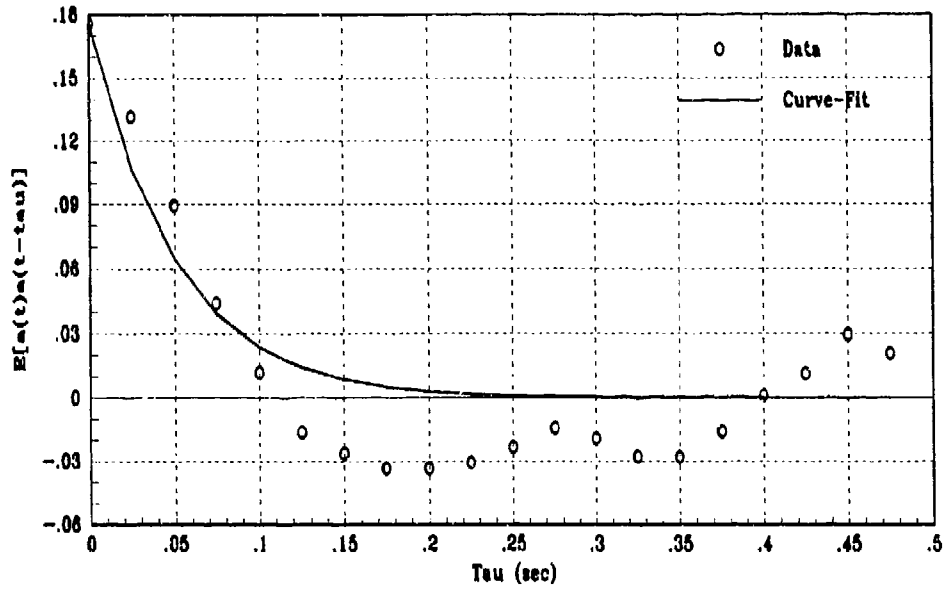
Figure A.4. Autocorrelation Data for Zernike Coefficient a_4
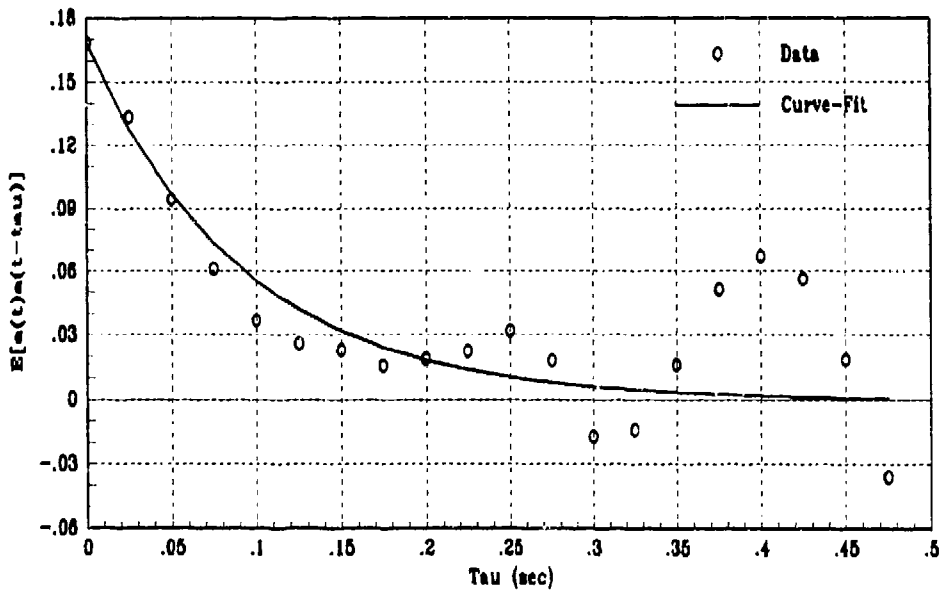
Figure A.5. Autocorrelation Data for Zernike Coefficient a_5
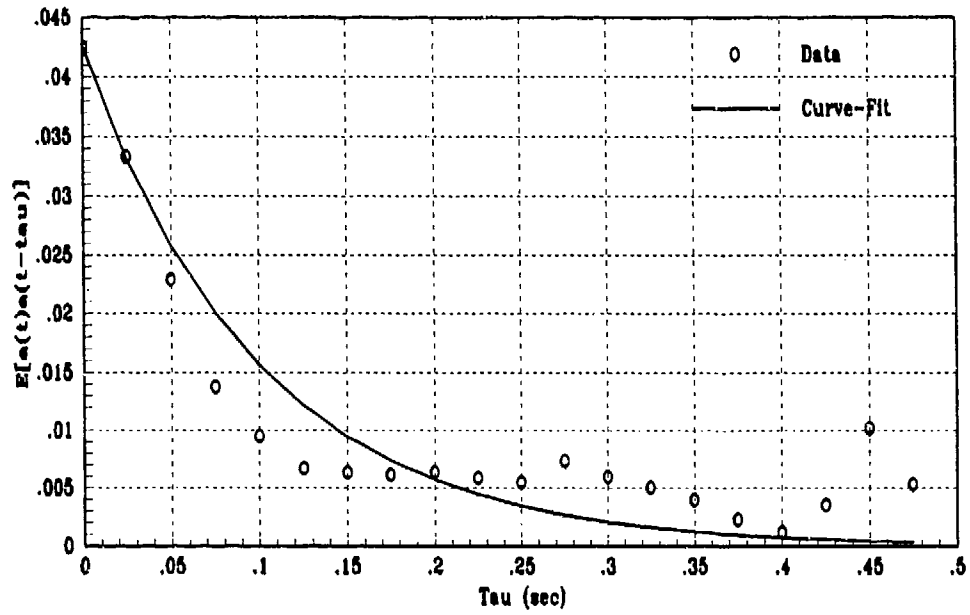
Figure A.6. Autocorrelation Data for Zernike Coefficient a_6
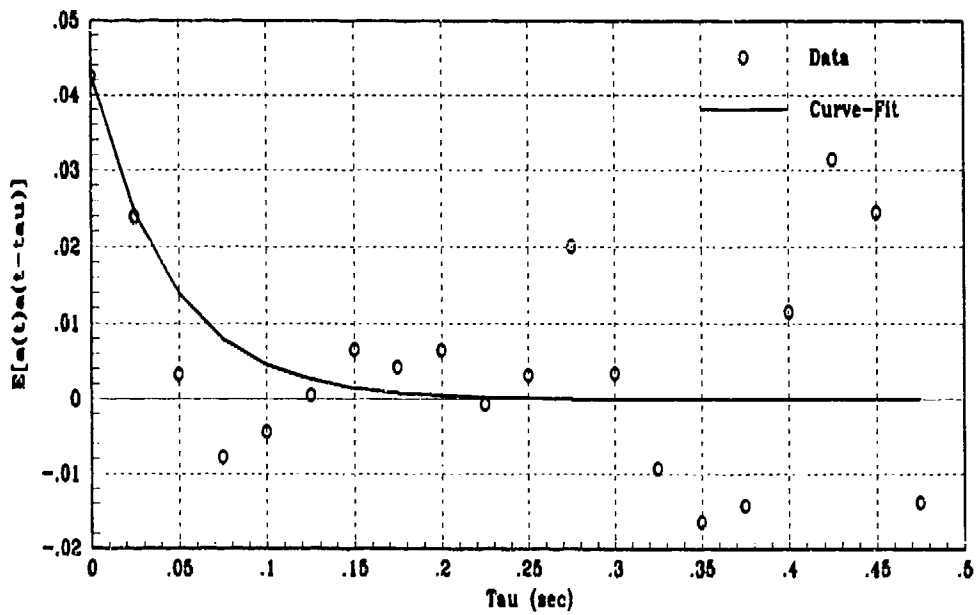
Figure A.7. Autocorrelation Data for Zernike Coefficient a_7

A-8
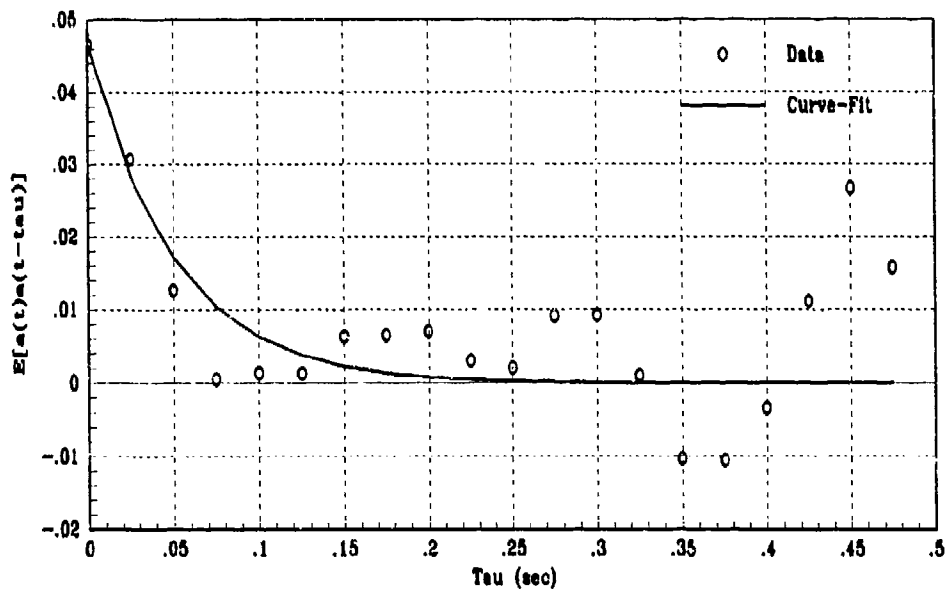
Figure A.8. Autocorrelation Data for Zernike Coefficient a_8
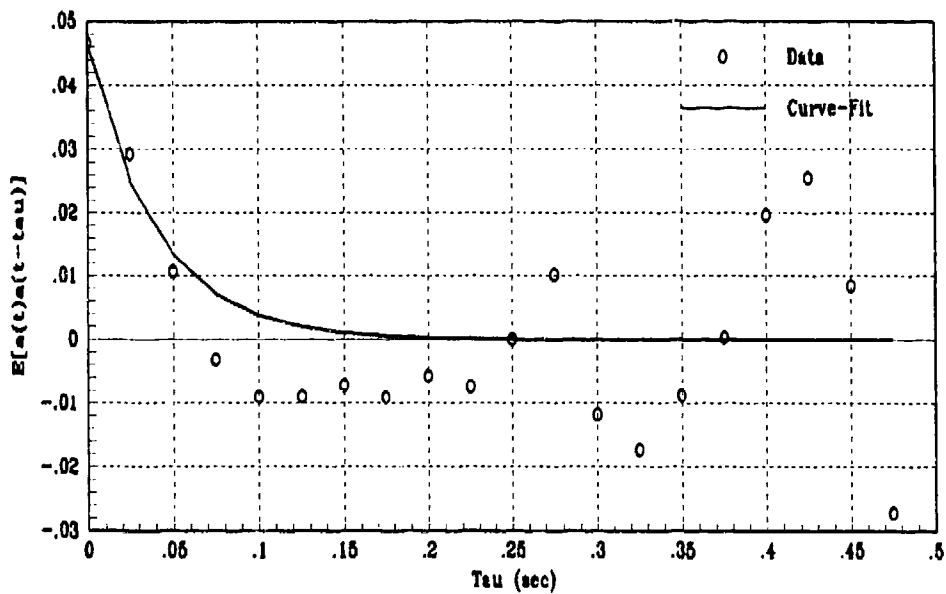
Figure A.9. Autocorrelation Data for Zernike Coefficient a_9

A-9
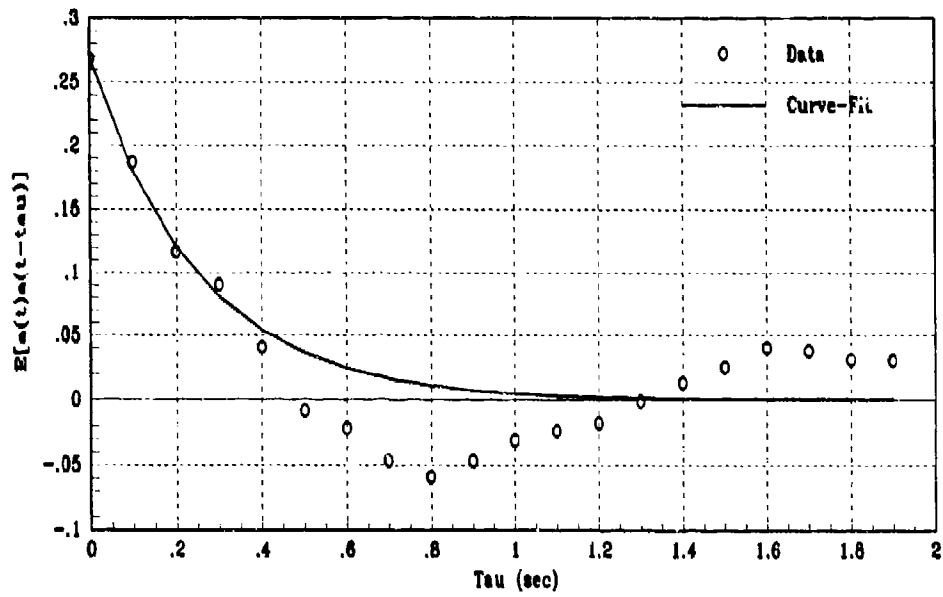
Figure A.10. Autocorrelation Data for Zernike Coefficient a_{10}
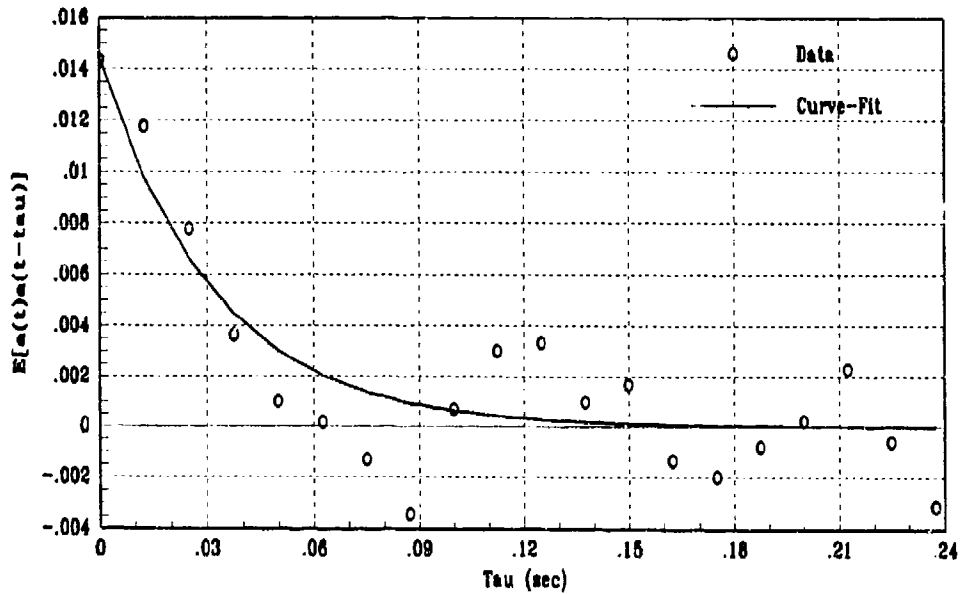
Figure A.11. Autocorrelation Data for Zernike Coefficient a_{11}

A-10
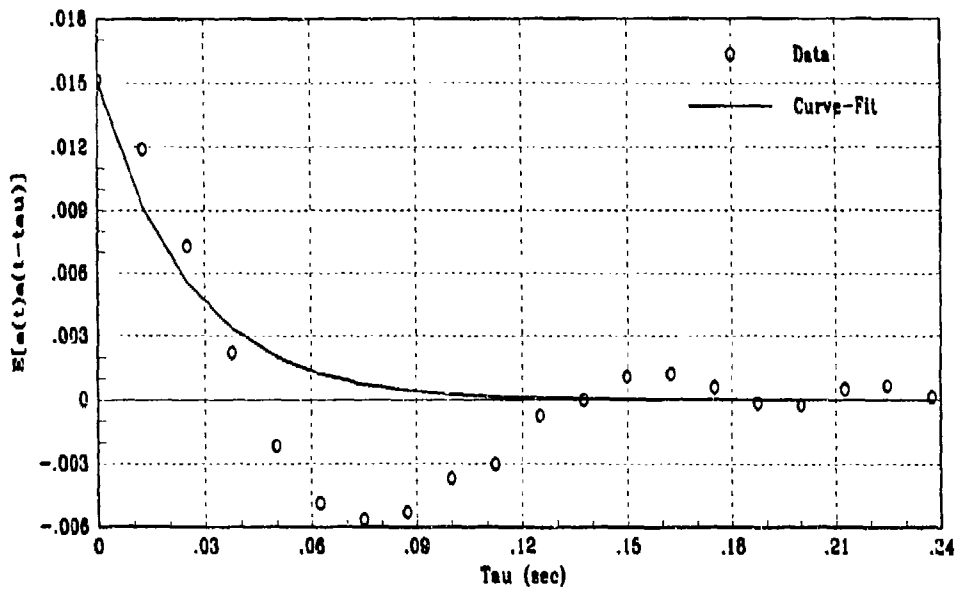
Figure A.12. Autocorrelation Data for Zernike Coefficient a_{12}
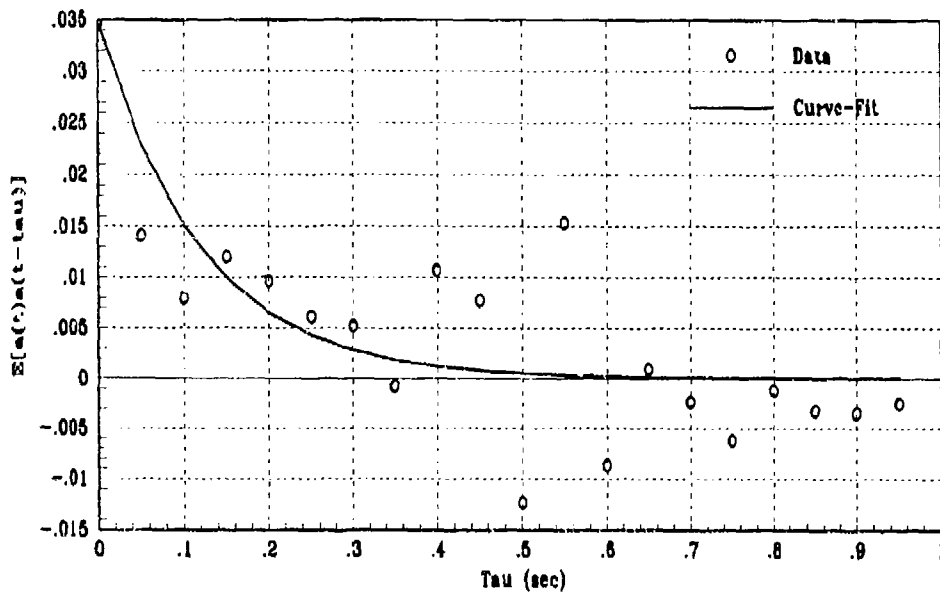
Figure A.13. Autocorrelation Data for Zernike Coefficient a_{13}

A-11
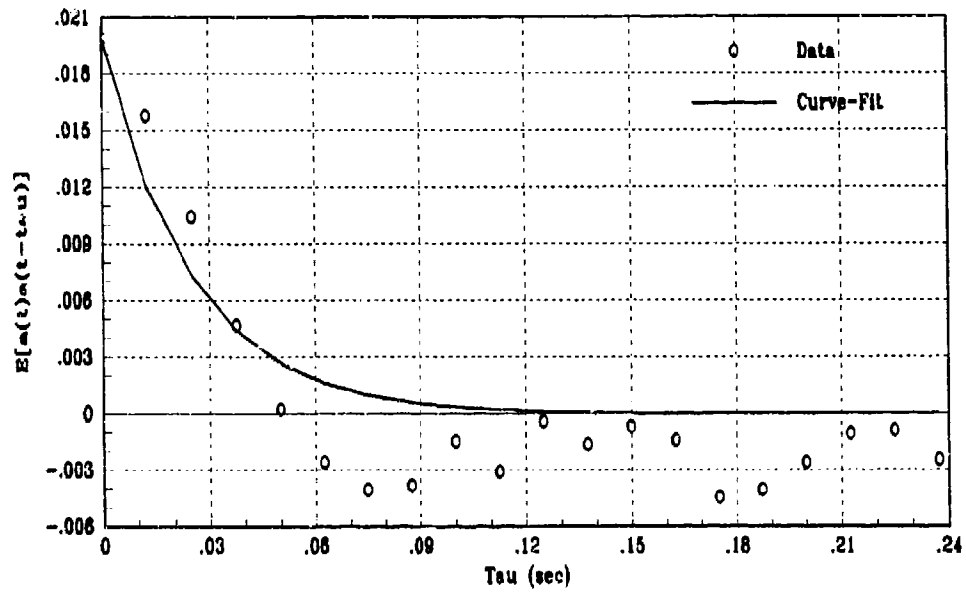
Figure A.14. Autocorrelation Data for Zernike Coefficient a_{14}

Appendix B. Steady-State Influence Matrix

This appendix is a listing of the elements of the steady-state influence matrix, *M*, used in this research. The elements of *M* are the projections of each actuator's influence function along each Zernike function direction. *M* has dimensions 14 x 97.

$$M \quad =$$

Columns   1 thru   4

0.002911721304727	0.008981676165652	0.011195052500622	0.008981676165652
0.001164141143822	0.001799016835620	0.000000000000000	-0.001799016835620
0.002826131020464	0.007148205728924	0.008384317407948	0.007148205728924
0.002721880988100	0.004187350229244	0.000000000000000	-0.004187350229244
0.002859713828053	0.010033338120027	0.013100302093135	0.010033338120027
0.001713688683701	0.002017892987421	0.000000000000000	-0.002017892987421
0.004286231010559	0.010070717272325	0.011527663661071	0.010070717272325
0.004237433142768	0.006771947305613	0.000000000000000	-0.006771947305613
0.001941806029709	0.010047797271526	0.014390793714810	0.010047797271526
0.003399382934574	0.006237863616008	0.006418736589525	0.006237863616008
0.003613045429789	0.009083751139173	0.010513091254295	0.009083751139173
0.003438747844868	0.003793530386194	0.000000000000000	-0.003793530386194
0.000260477623347	0.009148020072048	0.015222267311141	0.009148020072048
0.005282776028768	0.009245538663069	0.000000000000000	-0.009245538663069

Columns   5 thru   8

0.002908859711674	0.009328843598495	0.019054038929399	0.021374910318742
-0.001161994949031	0.007003957769305	0.009527571412212	0.005339012135326
0.002823033255114	0.008791007243634	0.012548382283186	0.009371418955018
-0.002717675322401	0.013130712733319	0.018695681017103	0.010667767407415
0.002858487175557	0.003814949142037	0.014020030981531	0.020025020163886
-0.001710653505921	0.007320087997640	0.005686684510538	0.001011069953242
0.004282184106852	0.009746133619187	0.011371912695841	0.004070700896766
-0.004232698265432	0.014076327823767	0.023742958779147	0.014787113998714
0.001943586667340	-0.005319654784218	0.004313963613427	0.016386473326402
0.003395383736704	0.006939582598671	0.002448509856498	-0.005585362155632
0.003611461828226	0.003131304335798	0.004405804471588	-0.003244878707508
-0.003433318353797	0.010802649564836	0.005877146381255	-0.001746213836076
0.000265246526338	-0.013467740084741	-0.006744303958088	0.011616112298937
-0.005279735513768	0.008544558070343	0.023100472516452	0.017272706364118

Columns   9 thru   12

0.0213869100007502	0.0213749108187742	0.019054038929399	0.009328843598495
0.000000000000000	-0.005339012135326	-0.009527571412212	-0.007003957769305
0.007514511701974	0.009371418955018	0.012548382283186	0.008791007243634
0.000000000000000	-0.010667767407415	-0.018695681017103	-0.013130712733319
0.021403188847963	0.020025020163886	0.014020030981531	0.003814949142037
0.000000000000000	-0.001011069953242	-0.005686684510538	-0.007320087997640
0.000379224918694	0.004070700896766	0.011371912695840	0.009746133619187
0.000000000000000	-0.014787113998714	-0.023742958779147	-0.014076327823767
0.020257427230268	0.016386473326402	0.004313963613427	-0.005319654784218
-0.008340190247034	-0.005585362155632	0.002448509856498	0.006939582598671
-0.007931923190416	-0.003244878707508	0.004405804471588	0.003131304335798
0.000000000000000	0.001746213836076	-0.005877146381255	-0.010802649564836
0.018615095488063	0.011616112298937	-0.006744303958088	-0.013467740084741
0.000000000000000	-0.017272706364118	-0.023104472516452	-0.008544558070343

Columns   13 thru   16

0.007003957769305	0.015778529623438	0.015420325599217	0.014858668418439
0.009328843598495	0.015778529623438	0.010278017830203	0.004952881449524
0.008791007243634	0.010917137450154	0.001330775531165	-0.004461129988376
0.013130712733319	0.023554625233884	0.015320554084289	0.007274662172351
-0.003814949142037	0.000000000000000	0.006388308342816	0.009699583972614
0.009746133619187	0.005444809723699	-0.005857572666400	-0.005766612503066
0.007320087997640	0.005444809723699	-0.008781686738004	-0.017299782615144
0.005319654784218	0.016588155572821	0.013820086544237	0.007273086646469
-0.014076327823767	-0.016588155572821	-0.002696498748243	0.005035261679375
0.006939582598671	-0.002690061769481	-0.013659962686529	-0.012814230975196
-0.003131304335798	0.000000000000000	-0.007032019807939	-0.018117056066695
0.010802649564836	0.000504752591274	-0.016891575595796	-0.013587850212685
-0.013467740084741	-0.022620426591332	-0.008180615925508	0.001748954222112
-0.008544558070343	0.000000000000000	0.008263960469042	0.005996195123123

Columns   17 thru   20

0.014874647080535	0.014858668418439	0.015420325599217	0.015778529623438
0.000000000000000	-0.004952881449524	-0.010278017830203	-0.015778529623438
-0.006163177311510	-0.004461129988376	0.001330775531165	0.010917137450154
0.000000000000000	-0.007274662172351	-0.015320554084289	-0.023554625233884
0.010930588635373	0.009699583972614	0.006388308342816	0.000000000000000
0.000000000000000	0.005766612503066	0.005857572666400	-0.005444809723699
-0.019798841739957	-0.017299782615144	-0.008781686738004	0.005444809723699
0.000000000000000	-0.007273086646469	-0.013820086544237	-0.016588155572821
0.007572933949260	0.005035261679375	-0.002696498748243	-0.016588155572821
-0.011100617319337	-0.012814230975196	-0.013659962686529	-0.002690061769481
-0.022611761413843	-0.018117056066695	-0.007032019807939	0.000000000000000
0.000000000000000	0.013587850212685	0.016891575595796	-0.000504752591274
0.005080075790243	0.001748954222112	-0.008180615925508	-0.022620426591332
0.000000000000000	-0.005996195123123	-0.008263960469042	0.000000000000000

Columns   21 thru   24

```
 0.007003957769305    0.001164141143822    0.009275571412212    0.010278017830203
-0.009328843598495    0.002911721304727    0.019054038929399    0.015420325599217
 0.008791007243634    0.002826131020464    0.012548382283186    0.001330775531165
-0.013130712733319    0.002721880988100    0.018956681017103    0.015320554084289
-0.003814949142037   -0.002859713828053   -0.014020030981531   -0.006388308342816
-0.009746133619187    0.004286231010559    0.011371912695841   -0.008781686738004
 0.007320087997640    0.001713688683701    0.005686684510538   -0.005857572666400
-0.005319654784218   -0.001941806029709   -0.004313963613427    0.002696498748243
-0.014076327823767   -0.004237433142768   -0.023742958779147   -0.013820086544237
 0.006939582598671    0.003399382934574    0.002448509856498   -0.013659962686529
-0.003131304335798   -0.003613045429789   -0.004405804471588    0.007032019807939
-0.010802649564836    0.003438747844868    0.005877146381255   -0.016891575595796
-0.013467740084741    0.000260477623347   -0.006744303958088   -0.008180615925508
 0.008544558070343   -0.005282776028768   -0.023104472516452   -0.008263960469042
```

Columns   25 thru   28

```
 0.009916431387023    0.009916431387023    0.009916431387023    0.009916431387023
 0.009916431387023    0.004958215693512    0.000000000000000   -0.004958215693512
-0.007880753610721   -0.013033482508352   -0.014751058807563   -0.013033482508353
 0.009716078786998    0.004858039393499    0.000000000000000   -0.004858039393499
 0.000000000000000    0.003643529545124    0.004858039393499    0.003643529545124
-0.014882102037585   -0.009965362335212    0.000000000000000    0.009965362335212
-0.014882102037585   -0.019930724670425   -0.021613598881372   -0.019930724670425
 0.004487664562525    0.003085269386736    0.000000000000000   -0.003085269386736
-0.004487664562524    0.000560958070316    0.002243832281262    0.000560958070316
-0.008877950682030    0.000983078543178    0.005334431389343    0.000983078543178
 0.000000000000000   -0.010547670711218   -0.015067033250492   -0.010547670711218
-0.022106288083374   -0.014063560948291    0.000000000000000    0.014063560948291
-0.004013891948456   -0.000439021871864    0.001003469562550   -0.000439021871864
 0.000000000000000    0.001505208453304    0.000000000000000   -0.001505208453304
```

Columns   29 thru   32

```
 0.009916431387023    0.010278017830203    0.009275571412212    0.001164141143822
-0.009916431387023   -0.015420325599217   -0.019054038929399   -0.002911721304728
-0.007880753610721    0.001330775531165    0.012548382283186    0.002826131020464
-0.009716078786998   -0.015320554084289   -0.018956681017103   -0.002721880988100
 0.000000000000000   -0.006388308342816   -0.014020030981531   -0.002859713828053
 0.014882102037585    0.008781686738004   -0.011371912695841   -0.004286231010559
-0.014882102037585   -0.005857572666400    0.005686684510538    0.001713688683701
-0.004487664562525   -0.002696498748243    0.004313963613427    0.001941806029710
-0.004487664562524   -0.013820086544237   -0.023742958779147   -0.004237433142769
-0.008877950682030   -0.013659962686529    0.002448509856498    0.003399382934574
 0.000000000000000    0.007032019807939   -0.004405804471588   -0.003613045429789
 0.022106288083374    0.016891575595796   -0.005877146381255   -0.003438747844868
-0.004013891948456   -0.008180615925508   -0.006744303958088    0.000260477623347
 0.000000000000000    0.008263960469042    0.023104472516452    0.005282776028769
```

B-3

Columns   33 thru   36
0.001799016835620   0.005339012135326   0.004952881449524   0.004958215693512
0.008981676165652   0.021374910818742   0.014858668418439   0.009916431387023
0.007148205728924   0.009371418955018   -0.004461129988376   -0.013033482508352
0.004187350229244   0.010667767407415   0.007274662172351   0.004858039393499
-0.010033338120027   -0.020025020163886   -0.009699583972614   -0.003643529545124
0.010070717272325   0.004070700896766   -0.017299782615144   -0.019930724670425
0.002017892987421   0.001011069953242   -0.005766612503066   -0.009965362335212
-0.010047797271526   -0.016386473326402   -0.005035261679375   -0.000560958070316
-0.006771947305613   -0.014787113998714   -0.007273086646469   -0.003085269386736
0.006237863616008   -0.005585362155632   -0.012814230975196   0.000983078543178
-0.009083751139173   0.003244878707508   0.018117056066695   0.010547670711218
0.003793530386194   -0.001746213836076   -0.013587850212685   -0.014063560948291
0.009148020072048   0.011616112298937   0.001748954222111   -0.000439021871864
-0.009245538663069   -0.017272706364118   -0.005996195123123   -0.001505208453304

Columns   37 thru   40
0.004958215693512   0.004958215693512   0.004958215693512   0.004958215693512
0.004958215693512   0.000000000000000   -0.004958215693512   -0.009916431387023
-0.018186211405984   -0.019903787705195   -0.018186211405984   -0.013033482508352
0.002429019696749   0.000000000000000   -0.002429019696749   -0.004858039393499
0.000000000000000   0.001214509848375   0.000000000000000   -0.003643529545124
-0.012489673651633   0.000000000000000   0.012489673651633   0.019930724670425
-0.012489673651632   -0.013331110757106   -0.012489673651633   -0.009965362335212
0.000560958070316   0.000000000000000   -0.000560958070316   0.000560958070316
-0.000560958070316   0.000280479035158   -0.000560958070316   -0.003085269386736
0.015633651738315   0.021581519241123   0.015633651738315   0.000983078543178
0.000000000000000   -0.004519362539274   0.000000000000000   0.010547670711218
-0.008536988927447   0.000000000000000   0.008536988927448   0.014063560948291
-0.000250870815201   0.000062714279236   -0.000250870815201   -0.000439021871864
0.000000000000000   0.000000000000000   0.000000000000000   0.001505208453304

Columns   41 thru   44
0.004952881449524   0.005339012135326   0.001799016835620   0.000000000000000
-0.014858668418439   -0.021374910818742   -0.008981676165652   0.011195052500622
-0.004461129988376   0.009371418955018   0.007148205728924   0.008384317407948
-0.007274662172351   -0.010667767407415   -0.004187350229245   0.000000000000000
-0.009699583972614   -0.020025020163886   -0.010033338120028   -0.013100302093135
0.017299782615144   -0.004070700896766   -0.010070717272326   0.011527663661071
-0.005766612503066   0.001011069953242   0.002017892987421   0.000000000000000
0.005035261679375   0.016386473326402   0.010047797271526   -0.014390793714810
-0.007273086646469   -0.014787113998714   -0.006771947305613   0.000000000000000
-0.012814230975196   -0.005585362155632   0.006237863616008   0.006418736589525
0.018117056066695   0.003244878707508   -0.009083751139173   -0.010513091254295
0.013587850212685   0.001746213836076   -0.003793530386194   0.000000000000000
0.001748954222111   0.011616112298937   0.009148020072049   0.015222267311141
0.005996195123123   0.017272706364118   0.009245538663069   0.000000000000000

B-4

Columns   45 thru   48

0.000000000000000	0.000000000000000	0.000000000000000	0.000000000000000
0.021386910007502	0.014874647080535	0.009916431387023	0.004958215693512
0.007514511701974	-0.006163177311510	-0.014751058807563	-0.019903787705195
0.000000000000000	0.000000000000000	0.000000000000000	0.000000000000000
-0.021403188847963	-0.010930588635373	-0.004858039393499	-0.001214509848375
0.000379224918694	-0.019798841739957	-0.021613598881372	-0.013331110757106
0.000000000000000	0.000000000000000	0.000000000000000	0.000000000000000
-0.020257427230268	-0.007572933949260	-0.002243832281262	-0.000280479035158
0.000000000000000	0.000000000000000	0.000000000000000	0.000000000000000
-0.008340190247034	-0.011100617319337	0.005334431389343	0.021581519241123
0.007931923190416	0.022611761413843	0.015067033250492	0.004519362539274
0.000000000000000	0.000000000000000	0.000000000000000	0.000000000000000
0.018615095488063	0.005080075790243	0.001003469562550	0.000062714279236
0.000000000000000	0.000000000000000	0.000000000000000	0.000000000000000

Columns   49 thru   52

0.000000000000000	0.000000000000000	0.000000000000000	0.000000000000000
0.000000000000000	-0.004958215693512	-0.009916431387023	-0.014874647080535
-0.021621364004405	-0.019903787705195	-0.014751058807563	-0.006163177311510
0.000000000000000	0.000000000000000	0.000000000000000	0.000000000000000
0.000000000000000	-0.001214509848375	-0.004858039393499	-0.010930588635373
0.000000000000000	0.013331110757106	0.021613598881372	0.019798841739957
0.000000000000000	0.000000000000000	0.000000000000000	0.000000000000000
0.000000000000000	0.000280479035158	0.002243832281262	0.007572933949260
0.000000000000000	0.000000000000000	0.000000000000000	0.000000000000000
0.028061558296145	0.021581519241123	0.005334431389343	-0.011100617319337
0.000000000000000	0.004519362539274	0.015067033250492	0.022611761413843
0.000000000000000	0.000000000000000	0.000000000000000	0.000000000000000
-0.000000002739651	0.000062714279236	0.001003469562550	0.005080075790243
0.000000000000000	0.000000000000000	0.000000000000000	0.000000000000000

Columns   53 thru   56

0.000000000000000	0.000000000000000	-0.001799016835620	-0.005339012135326
-0.021386910007502	-0.011195052500623	0.008981676165652	0.021374910818742
0.007514511701974	0.008384317407949	0.007148205728924	0.009371418955018
0.000000000000000	0.000000000000000	-0.004187350229244	-0.010667767407415
-0.021403188847963	-0.013100302093136	-0.010033338120027	-0.020025020163886
-0.000379224918694	-0.011527663661072	0.010070717272325	0.004070700896766
0.000000000000000	0.000000000000000	-0.002017892987421	-0.001011069953242
0.020257427230268	0.014390793714810	-0.010047797271526	-0.016386473326402
0.000000000000000	0.000000000000000	0.006771947305613	0.014787113998714
-0.008340190247034	0.006418736589525	0.006237863616008	-0.005585362155632
0.007931923190416	-0.010513091254296	-0.009083751139173	0.003244878707508
0.000000000000000	0.000000000000000	-0.003793530386194	0.001746213836076
0.018615095488063	0.015222267311142	0.009148020072048	0.011616112298937
0.000000000000000	0.000000000000000	0.009245538663069	0.017272706364118

Columns   57 thru   60

-0.004952881449524	-0.004958215693512	-0.004958215693512	-0.004958215693512
0.014858668418439	0.009916431387023	0.004958215693512	0.000000000000000
-0.004461129988376	-0.013033482508352	-0.018186211405984	-0.019903787705195
-0.007274662172351	-0.004858039393499	-0.002429019696749	0.000000000000000
-0.009699583972614	-0.003643529545124	0.000000000000000	0.001214509848375
-0.017299782615144	-0.019930724670425	-0.012489673651633	0.000000000000000
0.005766612503066	0.009965362335212	0.012489673651633	0.013331110757106
-0.005035261679375	-0.000560958070316	0.000560958070316	0.000000000000000
0.007273086646469	0.003085269386736	0.000560958070316	-0.000280479035158
-0.012814230975196	0.000983078543178	0.015633651738315	0.021581519241123
0.018117056066695	0.010547670711218	0.000000000000000	-0.004519362539274
0.013587850212685	0.014063560948291	0.008536988927448	0.000000000000000
0.001748954222112	-0.000439021871864	-0.000250870815201	0.000062714279236
0.005996195123123	0.001505208453304	0.000000000000000	0.000000000000000

Columns   61 thru   64

-0.004958215693512	-0.004958215693512	-0.004952881449524	-0.005339012135326
-0.004958215693512	-0.009916431387023	-0.014858668418439	-0.021374910818742
-0.018186211405984	-0.013033482508353	-0.004461129988376	0.009371418955018
0.002429019696749	0.004858039393499	0.007274662172351	0.010667767407415
0.000000000000000	-0.003643529545124	-0.009699583972614	-0.020025020163886
0.012489673651632	0.019930724670425	0.017299782615144	-0.004070700896766
0.012489673651633	0.009965362335212	0.005766612503066	-0.001011069953242
-0.000560958070316	0.000560958070316	0.005035261679375	0.016386473326402
0.000560958070316	0.003085269386736	0.007273086646469	0.014787113998714
0.015633651738315	0.000983078543178	-0.012814230975196	-0.005585362155632
0.000000000000000	0.010547670711218	0.018117056066695	0.003244878707508
-0.008536988927448	-0.014063560948291	-0.013587850212685	-0.001746213836076
-0.000250870815201	-0.000439021871864	0.001748954222112	0.011616112298937
0.000000000000000	-0.001505208453304	-0.005996195123123	-0.017272706364118

Columns   65 thru   68

-0.001799016835620	-0.001161994949031	-0.009527571412212	-0.010278017830203
-0.008981676165652	0.002908859711674	0.019054038929399	0.015420325599217
0.007148205728924	0.002823033255114	0.012548382283186	0.001330775531165
0.004187350229245	-0.002717675322401	-0.018695681017103	-0.015320554084289
-0.010033338120028	-0.002858487175557	-0.014020030981531	-0.006388308342816
-0.0100707172723256	0.004282184106852	0.011371912695840	-0.008781686738004
-0.002017892987421	-0.001710653505921	-0.005686684510538	0.005857572666400
0.010047797271526	-0.001943586667340	-0.004313963613427	0.002696498748243
0.006771947305613	0.004232698265432	0.023742958779147	0.013820086544237
0.006237863616008	0.003395383736704	0.002448509856498	-0.013659962686529
-0.009083751139173	-0.003611461828226	-0.004405804471588	0.007032019807939
0.003793530386194	-0.003433318353797	-0.005877146381255	0.016891575595796
0.009148020072049	0.000265246526338	-0.006744303958088	-0.008180613925508
-0.009245538663069	0.005279735513768	0.023104472516452	0.008263960469042

Columns   69 thru   72

```
-0.009916431387023  -0.009916431387023  -0.009916431387023  -0.009916431387023
 0.009916431387023   0.004958215693512   0.000000000000000  -0.004958215693512
-0.007880753610721  -0.013033482508352  -0.014751058807563  -0.013033482508352
-0.009716078786998  -0.004858039393499   0.000000000000000   0.004858039393499
 0.000000000000000   0.003643529545124   0.004858039393499   0.003643529545124
-0.014882102037585  -0.009965362335212   0.000000000000000   0.009965362335212
 0.014882102037585   0.019930724670425   0.021613598881372   0.019930724670425
 0.004487664562524   0.003085269386736   0.000000000000000  -0.003085269386736
 0.004487664562525  -0.000560958070316  -0.002243832281262  -0.000560958070316
-0.008877950682030   0.000983078543178   0.005334431389343   0.000983078543178
 0.000000000000000  -0.010547670711218  -0.015067033250492  -0.010547670711218
 0.022106288083374   0.014063560948291   0.000000000000000  -0.014063560948291
-0.004013891948456  -0.000439021871864   0.001003469562550  -0.000439021871864
 0.000000000000000  -0.001505208453304   0.000000000000000   0.001505208453304
```

Columns   73 thru   76

```
-0.009916431387023  -0.010275871635413  -0.009527571412212  -0.001164141143822
-0.009916431387023  -0.015417464006163  -0.019054038929399  -0.002911721304728
-0.007880753610721   0.001327677765816   0.012548382283186   0.002826131020464
 0.009716078786998   0.015316348418589   0.018695681017103   0.002721880988100
 0.000000000000000  -0.006387081690321  -0.014020030981531  -0.002859713828053
 0.014882102037585   0.008785733641711  -0.011371912695841  -0.004286231010559
 0.014882102037585   0.005860607844180  -0.005686684510538  -0.001713688683701
-0.004487664562524  -0.002694718110613   0.004313963613427   0.001941806029710
 0.004487664562525   0.013815351666900   0.023742958779147   0.004237433142769
-0.008877950682030  -0.013663961884399   0.002448509856498   0.003399382934574
 0.000000000000000   0.007033603409501  -0.004405804471588  -0.003613045429789
-0.022106288083374  -0.016897005086867   0.005877146381255   0.003438747844868
-0.004013891948456  -0.008175847022517  -0.006744303958088   0.000260477623347
 0.000000000000000  -0.008260919954042  -0.023104472516452  -0.005282776028769
```

Columns   77 thru   80

```
-0.007003957769305  -0.015778529623438  -0.015420325599217  -0.014858668418439
 0.009328843598495   0.015778529623438   0.010278017830203   0.004952881449524
 0.008791007243634   0.010917137450154   0.001330775531165  -0.004461129988376
-0.013130712733319  -0.023554625233884  -0.015320554084289  -0.007274662172351
-0.003814949142037   0.000000000000000   0.006388308342816   0.009699583972614
 0.009746133619187   0.005444809723699  -0.005857572666400  -0.005766612503066
-0.007320087997640  -0.005444809723699   0.008781686738004   0.017299782615144
 0.005319654784218   0.016588155572821   0.013820086544237   0.007273086646469
 0.014076327823767   0.016588155572821   0.002696498748243  -0.005035261679375
 0.006939582598671  -0.002690061769481  -0.013659962686529  -0.012814230975196
-0.003131304335798   0.000000000000000  -0.007032019807939  -0.018117056066695
-0.010802649564836  -0.000504752591274   0.016891575595796   0.013587850212685
-0.013467740084741  -0.022620426591332  -0.008180615925508   0.001748954222112
 0.008544558070343   0.000000000000000  -0.008263960469042  -0.005996195123123
```

Columns   81 thru   84

-0.014874647080535 -0.014858668418439 -0.015417464006163 -0.015784819039899
 0.000000000000000 -0.004952881449524 -0.010275871635413 -0.015784819039899
-0.006163177311510 -0.004461129988376   0.001327677765816   0.010924918585055
 0.000000000000000   0.007274662172351   0.015316348418589   0.023565189252930
 0.010930588635373   0.009699583972614   0.006387081690321   0.000000000000000
 0.000000000000000   0.005766612503066   0.005860607844180 -0.005453704301758
 0.019798841739957   0.017299782615144   0.008785733641711 -0.005453704301758
 0.000000000000000 -0.007273086646469 -0.013815351666900 -0.016596338584635
-0.007572933949260 -0.005035261679375   0.002694718110613   0.016596338584635
-0.011100617319337 -0.012814230975196 -0.013663961884398 -0.002680016367519
-0.022611761413843 -0.018117056066695 -0.007033603409501   0.000000000000000
 0.000000000000000 -0.013587850212685 -0.016897005086867   0.000518390681219
 0.005080075790243   0.001748954222112 -0.008175847022517 -0.022632405380334
 0.000000000000000   0.005996195123123   0.008260919954042   0.000000000000000

Columns   85 thru   88

-0.007003957769305 -0.009328843598495 -0.019054038929399 -0.021374910818742
-0.009328843598495   0.007003957769305   0.009527571412212   0.005339012135326
 0.008791007243634   0.008791007243634   0.012548382283186   0.009371418955018
 0.013130712733319 -0.013130712733319 -0.018695681017103 -0.010667767407415
-0.003814949142037   0.003814949142037   0.014020030981531   0.020025020163886
-0.009746133619187   0.007320087997640   0.005686684510538   0.001011069953242
-0.007320087997640 -0.009746133619187 -0.011371912695841 -0.004070700896766
-0.005319654784218   0.014076327823767   0.023742958779147   0.014787113998714
 0.014076327823767   0.005319654784218 -0.004313963613427 -0.016386473326402
 0.006939582598671   0.006939582598671   0.002448509856498 -0.005585362155632
-0.003131304335798   0.003131304335798   0.004405804471588 -0.003244878707508
 0.010802649564836 -0.010802649564836 -0.005877146381255   0.001746213836076
-0.013467740084741 -0.013467740084741 -0.006744303958088   0.011616112298937
-0.008544558070343 -0.008544558070343 -0.023104472516452 -0.017272706364118

Columns   89 thru   92

-0.021386910007502 -0.021374910818742 -0.019054038929399 -0.009328843598495
 0.000000000000000 -0.005339012135326 -0.009527571412212 -0.007003957769305
 0.007514511701974   0.009371418955018   0.012548382283186   0.008791007243634
 0.000000000000000   0.010667767407415   0.018695681017103   0.013130712733319
 0.021403188847963   0.020025020163886   0.014020030981531   0.003814949142037
 0.000000000000000 -0.001011069953242 -0.005686684510538 -0.007320087997640
-0.000379224918694 -0.004070700896766 -0.011371912695841 -0.009746133619187
 0.000000000000000 -0.014787113998714 -0.023742958779147 -0.014076327823767
-0.020257427230268 -0.016386473326402 -0.004313963613427   0.005319654784218
-0.008340190247034 -0.005585362155632   0.002448509856498   0.006939582598671
-0.007931923190416 -0.003244878707508   0.004405804471588   0.003131304335798
 0.000000000000000 -0.001746213836076   0.005877146381255   0.010802649564836
 0.018615095488063   0.011616112298937 -0.006744303958088 -0.013467740084741
 0.000000000000000   0.017272706364118   0.023104472516452   0.008544558070343

B-8

Columns   93 thru   96

-0.002911721304728	-0.008981676165652	-0.011195052500623	-0.008981676165652
0.001164141143822	0.001799016835620	0.000000000000000	-0.001799016835620
0.002826131020464	0.007148205728924	0.008384317407949	0.007148205728924
-0.002721880988100	-0.004187350229245	0.000000000000000	0.004187350229245
0.002859713828053	0.010033338120028	0.013100302093136	0.010033338120028
0.001713688683701	0.002017892987421	0.000000000000000	-0.002017892987421
-0.004286231010559	-0.010070717272326	-0.011527663661072	-0.010070717272326
0.004237433142769	0.006771947305613	0.000000000000000	-0.006771947305613
-0.001941806029710	-0.010047797271526	-0.014390793714810	-0.010047797271526
0.003399382934574	0.006237863616008	0.006418736589525	0.006237863616008
0.003613045429789	0.009083751139173	0.010513091254296	0.009083751139173
-0.003438747844868	-0.003793530386194	0.000000000000000	0.003793530386194
0.000260477623347	0.009148020072049	0.015222267311142	0.009148020072049
-0.005282776028769	-0.009245538663069	0.000000000000000	0.009245538663069

Column 97

-0.002911721304728
-0.001164141143822
0.002826131020464
0.002721880988100
0.002859713828053
-0.001713688683701
-0.004286231010559
-0.004237433142769
-0.001941806029710
0.003399382934574
0.003613045429789
0.003438747844868
0.000260477623347
0.005282776028769

Appendix C. Hartmann Sensor Gain Matrix

This appendix provides the elements of the Hartmann wavefront sensor gain matrix, N, used in this research. The N matrix represents the projections of the Zernike functions into the x-tilt and y-tilt measurement space for each of the 69 subaperture measurement pairs. The N matrix has dimensions 138 x 14.

$N \quad = $

Columns   1 thru   4

0.000000000000000	2.041935721855007	2.748145661847014	3.886464869153949
0.000000000000000	2.041935721855007	1.374072829933366	3.886464869153949
0.000000000000000	2.041935721855007	-0.000000001980357	3.886464869153949
0.000000000000000	2.041935721855007	-1.374072833894063	3.886464869153949
0.000000000000000	2.041935721855007	-2.748145665807738	3.886464869153949
0.000000000000000	2.041935721855007	4.122218493760689	2.914848651865464
0.000000000000000	2.041935721855007	2.748145661847014	2.914848651865464
0.000000000000000	2.041935721855007	1.374072829933366	2.914848651865464
0.000000000000000	2.041935721855007	-0.000000001980357	2.914848651865464
0.000000000000000	2.041935721855007	-1.374072833894063	2.914848651865464
0.000000000000000	2.041935721855007	-2.748145665807738	2.914848651865464
0.000000000000000	2.041935721855007	-4.122218497721480	2.914848651865464
0.000000000000000	2.041935721855007	5.496291325674279	1.943232434576978
0.000000000000000	2.041935721855007	4.122218493760689	1.943232434576978
0.000000000000000	2.041935721855007	2.748145661847014	1.943232434576978
0.000000000000000	2.041935721855007	1.374072829933366	1.943232434576978
0.000000000000000	2.041935721855007	-0.000000001980357	1.943232434576978
0.000000000000000	2.041935721855007	-1.374072833894063	1.943232434576978
0.000000000000000	2.041935721855007	-2.748145665807738	1.943232434576978
0.000000000000000	2.041935721855007	-4.122218497721480	1.943232434576978
0.000000000000000	2.041935721855007	-5.496291329635093	1.943232434576978
0.000000000000000	2.041935721855007	5.496291325674279	0.971616217288498
0.000000000000000	2.041935721855007	4.122218493760689	0.971616217288498
0.000000000000000	2.041935721855007	2.748145661847014	0.971616217288498
0.000000000000000	2.041935721855007	1.374072829933366	0.971616217288498
0.000000000000000	2.041935721855007	-0.000000001980357	0.971616217288498
0.000000000000000	2.041935721855007	-1.374072833894063	0.971616217288498
0.000000000000000	2.041935721855007	-2.748145665807738	0.971616217288498
0.000000000000000	2.041935721855007	-4.122218497721480	0.971616217288498
0.000000000000000	2.041935721855007	-5.496291329635093	0.971616217288498
0.000000000000000	2.041935721855007	5.496291325674279	0.000000000000000
0.000000000000000	2.041935721855007	4.122218493760689	0.000000000000000
0.000000000000000	2.041935721855007	2.748145661847014	0.000000000000000
0.000000000000000	2.041935721855007	1.374072829933366	0.000000000000000

0.000000000000000	2.041935721855007	-0.000000001980357	0.000000000000000
0.000000000000000	2.041935721855007	-1.374072833894063	0.000000000000000
0.000000000000000	2.041935721855007	-2.748145665807738	0.000000000000000
0.000000000000000	2.041935721855007	-4.122218497721480	0.000000000000000
0.000000000000000	2.041935721855007	-5.496291329635093	0.000000000000000
0.000000000000000	2.041935721855007	5.496291325674279	-0.971616217288490
0.000000000000000	2.041935721855007	4.122218493760689	-0.971616217288490
0.000000000000000	2.041935721855007	2.748145661847014	-0.971616217288490
0.000000000000000	2.041935721855007	1.374072829933366	-0.971616217288490
0.000000000000000	2.041935721855007	-0.000000001980357	-0.971616217288490
0.000000000000000	2.041935721855007	-1.374072833894063	-0.971616217288490
0.000000000000000	2.041935721855007	-2.748145665807738	-0.971616217288490
0.000000000000000	2.041935721855007	-4.122218497721480	-0.971616217288490
0.000000000000000	2.041935721855007	-5.496291329635093	-0.971616217288490
0.000000000000000	2.041935721855007	5.496291325674279	-1.943232434576981
0.000000000000000	2.041935721855007	4.122218493760689	-1.943232434576981
0.000000000000000	2.041935721855007	2.748145661847014	-1.943232434576981
0.000000000000000	2.041935721855007	1.374072829933366	-1.943232434576981
0.000000000000000	2.041935721855007	-0.000000001980357	-1.943232434576981
0.000000000000000	2.041935721855007	-1.374072833894063	-1.943232434576981
0.000000000000000	2.041935721855007	-2.748145665807738	-1.943232434576981
0.000000000000000	2.041935721855007	-4.122218497721480	-1.943232434576981
0.000000000000000	2.041935721855007	-5.496291329635093	-1.943232434576981
0.000000000000000	2.041935721855007	4.122218493760689	-2.914848651865490
0.000000000000000	2.041935721855007	2.748145661847014	-2.914848651865490
0.000000000000000	2.041935721855007	1.374072829933366	-2.914848651865490
0.000000000000000	2.041935721855007	-0.000000001980357	-2.914848651865490
0.000000000000000	2.041935721855007	-1.374072833894063	-2.914848651865490
0.000000000000000	2.041935721855007	-2.748145665807738	-2.914848651865490
0.000000000000000	2.041935721855007	-4.122218497721480	-2.914848651865490
0.000000000000000	2.041935721855007	2.748145661847014	-3.886464869153971
0.000000000000000	2.041935721855007	1.374072829933366	-3.886464869153971
0.000000000000000	2.041935721855007	-0.000000001980357	-3.886464869153971
0.000000000000000	2.041935721855007	-1.374072833894063	-3.886464869153971
0.000000000000000	2.041935721855007	-2.748145665807738	-3.886464869153971
2.041935721855051	0.000000000000000	5.496291325674293	1.943232434576980
2.041935721855051	0.000000000000000	5.496291325674293	0.971616217288494
2.041935721855051	0.000000000000000	5.496291325674293	0.000000000000000
2.041935721855051	0.000000000000000	5.496291325674293	-0.971616217288488
2.041935721855051	0.000000000000000	5.496291325674293	-1.943232434576989
2.041935721855051	0.000000000000000	4.122218493760798	2.914848651865470
2.041935721855051	0.000000000000000	4.122218493760798	1.943232434576980
2.041935721855051	0.000000000000000	4.122218493760798	0.971616217288494
2.041935721855051	0.000000000000000	4.122218493760798	0.000000000000000
2.041935721855051	0.000000000000000	4.122218493760798	-0.971616217288488
2.041935721855051	0.000000000000000	4.122218493760798	-1.943232434576989
2.041935721855051	0.000000000000000	4.122218493760798	-2.914848651865490
2.041935721855051	0.000000000000000	2.748145661847000	3.886464869153960
2.041935721855051	0.000000000000000	2.748145661847000	2.914848651865470

2.041935721855051	0.000000000000000	2.748145661847000	1.943232434576980
2.041935721855051	0.000000000000000	2.748145661847000	0.971616217288494
2.041935721855051	0.000000000000000	2.748145661847000	0.000000000000000
2.041935721855051	0.000000000000000	2.748145661847000	-0.971616217288488
2.041935721855051	0.000000000000000	2.748145661847000	-1.943232434576989
2.041935721855051	0.000000000000000	2.748145661847000	-2.914848651865490
2.041935721855051	0.000000000000000	2.748145661847000	-3.886464869153968
2.041935721855051	0.000000000000000	1.374072829933361	3.886464869153960
2.041935721855051	0.000000000000000	1.374072829933361	2.914848651865470
2.041935721855051	0.000000000000000	1.374072829933361	1.943232434576980
2.041935721855051	0.000000000000000	1.374072829933361	0.971616217288494
2.041935721855051	0.000000000000000	1.374072829933361	0.000000000000000
2.041935721855051	0.000000000000000	1.374072829933361	-0.971616217288488
2.041935721855051	0.000000000000000	1.374072829933361	-1.943232434576989
2.041935721855051	0.000000000000000	1.374072829933361	-2.914848651865490
2.041935721855051	0.000000000000000	1.374072829933361	-3.886464869153968
2.041935721855051	0.000000000000000	-0.000000001980354	3.886464869153960
2.041935721855051	0.000000000000000	-0.000000001980354	2.914848651865470
2.041935721855051	0.000000000000000	-0.000000001980354	1.943232434576980
2.041935721855051	0.000000000000000	-0.000000001980354	0.971616217288494
2.041935721855051	0.000000000000000	-0.000000001980354	0.000000000000000
2.041935721855051	0.000000000000000	-0.000000001980354	-0.971616217288488
2.041935721855051	0.000000000000000	-0.000000001980354	-1.943232434576989
2.041935721855051	0.000000000000000	-0.000000001980354	-2.914848651865490
2.041935721855051	0.000000000000000	-0.000000001980354	-3.886464869153968
2.041935721855051	0.000000000000000	-1.374072833894098	3.886464869153960
2.041935721855051	0.000000000000000	-1.374072833894098	2.914848651865470
2.041935721855051	0.000000000000000	-1.374072833894098	1.943232434576980
2.041935721855051	0.000000000000000	-1.374072833894098	0.971616217288494
2.041935721855051	0.000000000000000	-1.374072833894098	0.000000000000000
2.041935721855051	0.000000000000000	-1.374072833894098	-0.971616217288488
2.041935721855051	0.000000000000000	-1.374072833894098	-1.943232434576989
2.041935721855051	0.000000000000000	-1.374072833894098	-2.914848651865490
2.041935721855051	0.000000000000000	-1.374072833894098	-3.886464869153968
2.041935721855051	0.000000000000000	-2.748145665807706	3.886464869153960
2.041935721855051	0.000000000000000	-2.748145665807706	2.914848651865470
2.041935721855051	0.000000000000000	-2.748145665807706	1.943232434576980
2.041935721855051	0.000000000000000	-2.748145665807706	0.971616217288494
2.041935721855051	0.000000000000000	-2.748145665807706	0.000000000000000
2.041935721855051	0.000000000000000	-2.748145665807706	-0.971616217288488
2.041935721855051	0.000000000000000	-2.748145665807706	-1.943232434576989
2.041935721855051	0.000000000000000	-2.748145665807706	-2.914848651865490
2.041935721855051	0.000000000000000	-2.748145665807706	-3.886464869153968
2.041935721855051	0.000000000000000	-4.122218497721514	2.914848651865470
2.041935721855051	0.000000000000000	-4.122218497721514	1.943232434576980
2.041935721855051	0.000000000000000	-4.122218497721514	0.971616217288494
2.041935721855051	0.000000000000000	-4.122218497721514	0.000000000000000
2.041935721855051	0.000000000000000	-4.122218497721514	-0.971616217288488
2.041935721855051	0.000000000000000	-4.122218497721514	-1.943232434576989

2.041935721855051	0.000000000000000	-4.122218497721514	-2.914848651865490
2.041935721855051	0.000000000000000	-5.496291329634936	1.943232434576980
2.041935721855051	0.000000000000000	-5.496291329634936	0.971616217288494
2.041935721855051	0.000000000000000	-5.496291329634936	0.000000000000000
2.041935721855051	0.000000000000000	-5.496291329634936	-0.971616217288488
2.041935721855051	0.000000000000000	-5.496291329634936	-1.943232434576989

Columns   5 thru   8

-1.943232433176658	3.446836257059080	5.230611059786413	3.936367260396866
-0.971616215888176	0.504617536635955	2.615305528008590	4.917106833871241
0.000000001400324	-0.476122034953794	-0.000000003769260	5.244020024401139
0.971616218688818	0.504617542289836	-2.615305535547089	4.917106831986613
1.943232435977297	3.446836268366883	-5.230611067324960	3.936367256627601
-2.914848650465113	6.062141786009939	5.884437443673175	0.013408963672443
-1.943232433176658	1.158443916753478	3.922958294839821	1.647974920091261
-0.971616215888176	-1.783774803669663	1.961479146006446	2.628714493565631
0.000000001400324	-2.764514375259397	-0.000000002826945	2.955627684095551
0.971616218688818	-1.783774798015790	-1.961479151660318	2.628714491681012
1.943232435977297	1.158443928061275	-3.922958300493710	1.647974916321993
2.914848653265834	6.062141802971724	-5.884437449327113	0.013408958018519
-3.886464867753603	11.292752846738686	5.230611061671043	-3.909549333305198
-2.914848650465113	4.427575828648788	3.922958295782119	-1.621156993688691
-1.943232433176658	-0.476122040607658	2.615305529893222	0.013408962730129
-0.971616215888176	-3.418340761030794	1.307652764004300	0.994148536204503
0.000000001400324	-4.399080332620521	-0.000000001884630	1.321061726734423
0.971616218688818	-3.418340755376923	-1.307652767773548	0.994148534319876
1.943232435977297	-0.476122029299858	-2.615305533662487	0.013408958960863
2.914848653265834	4.427575845610566	-3.922958299551403	-1.621156999342614
3.886464870554231	11.292752869354363	-5.230611065440326	-3.909549340590578
-3.886464867753603	10.312013272322064	2.615305530835529	-4.890288907468674
-2.914848650465113	3.446836254232097	1.961479147891062	-2.601896568105388
-1.943232433176658	-1.456861615024353	1.307652764946615	-0.967330611686566
-0.971616215888176	-4.399080335447478	0.653826382002150	0.013408961787815
0.000000001400324	-5.379819907037209	-0.000000000942315	0.340322152317733
0.971616218688818	-4.399080329793531	-0.653826383886776	0.013408959903188
1.943232435977297	-1.456861603716554	-1.307652766831243	-0.967330615455827
2.914848653265834	3.446836271193874	-1.961479149775709	-2.601896573759316
3.886464870554231	10.312013294937739	-2.615305532720172	-4.890288915007243
-3.886464867753603	9.985100080849746	0.000000000000000	-5.217202098940906
-2.914848650465113	3.119923062759871	0.000000000000000	-2.928809759577606
-1.943232433176658	-1.783774806496584	0.000000000000000	-1.294243803158798
-0.971616215888176	-4.725993526919694	0.000000000000000	-0.313504229684418
0.000000001400324	-5.706733098509479	0.000000000000000	0.013408960845499
0.971616218688818	-4.725993521265811	0.000000000000000	-0.313504231569044
1.943232435977297	-1.783774795188783	0.000000000000000	-1.294243806928062
2.914848653265834	3.119923079721642	0.000000000000001	-2.928809765231549
3.886464870554231	9.985100103465458	0.000000000000001	-5.217202106479481
-3.886464867753603	10.312013272321952	-2.615305530835524	-4.890288907468678
-2.914848650465113	3.446836254232103	-1.961479147891068	-2.601896568105386

-1.943232433176658	-1.456861615024350	-1.307652764946609	-0.967330611686566
-0.971616215888176	-4.399080335447479	-0.653826382002149	0.013408961787811
0.000000001400324	-5.379819907037211	0.000000000942315	0.340322152317727
0.971616218688818	-4.399080329793612	0.653826383886773	0.013408959903184
1.943232435977297	-1.456861603716556	1.307652766831237	-0.967330615455834
2.914848653265834	3.446836271193875	1.961479149775700	-2.601896573759307
3.886464870554231	10.312013294937655	2.615305532720154	-4.890288915007245
-3.886464867753603	11.292752846738674	-5.230611061671080	-3.909549333051972
-2.914848650465113	4.427575828648767	-3.922958295782125	-1.621156993688682
-1.943232433176658	-0.476122040607653	-2.615305529893211	0.013408962730134
-0.971616215888176	-3.418340761030785	-1.307652764004310	0.994148536204514
0.000000001400324	-4.399080332620537	0.000000001884630	1.321061726734422
0.971616218688818	-3.418340755376907	1.307652767773549	0.994148534319878
1.943232435977297	-0.476122029299855	2.615305533662480	0.013408958960868
2.914848653265834	4.427575845610568	3.922958299551413	-1.621156999342610
3.886464870554231	11.292752869354430	5.230611065440360	-3.909549340590535
-2.914848650465113	6.062141786009926	-5.884437443673161	0.013408963672478
-1.943232433176658	1.158443916753512	-3.922958294839823	1.647974920091302
-0.971616215888176	-1.783774803669619	-1.961479146006444	2.628714493565659
0.000000001400324	-2.764514375259351	0.000000002826945	2.955627684095602
0.971616218688818	-1.783774798015739	1.961479151660327	2.628714491681043
1.943232435977297	1.158443928061310	3.922958300493755	1.647974916322028
2.914848653265834	6.062141802971710	5.884437449327119	0.013408958018552
-1.943232433176658	3.446836257059134	-5.230611059786441	3.936367260396930
-0.971616215888176	0.504617536635999	-2.615305528008587	4.917106833871282
0.000000001400324	-0.476122034953750	0.000000003769260	5.244020024401181
0.971616218688818	0.504617542289881	2.615305535547109	4.917106831986660
1.943232435977297	3.446836268366932	5.230611067324918	3.936367256627656
3.886464867753692	5.230611061671070	11.292752846738665	5.230611061671070
3.886464867753692	2.615305530835540	10.312013272322048	2.615305530835540
3.886464867753692	0.000000000000000	9.985100080849772	0.000000000000000
3.886464867753692	-2.615305530835524	10.312013272322039	-2.615305530835524
3.886464867753692	-5.230611061671079	11.292752846738670	-5.230611061671079
2.914848650465005	5.884437443673153	6.062141786009920	5.884437443673153
2.914848650465005	3.922958295782113	4.427575828648789	3.922958295782113
2.914848650465005	1.961479147891067	3.446836254 88	1.961479147891067
2.914848650465005	0.000000000000000	3.1199230u2...875	0.000000000000000
2.914848650465005	-1.961479147891056	3.446836254232083	-1.961479147891056
2.914848650465005	-3.922958295782125	4.427575828648798	-3.922958295782125
2.914848650465005	-5.884437443673186	6.062141786009962	-5.884437443673186
1.943232433176696	5.230611059786439	3.446836257059100	5.230611059786439
1.943232433176696	3.922958294839821	1.158443916753477	3.922958294839821
1.943232433176696	2.615305529893205	-0.476122040607659	2.615305529893205
1.943232433176696	1.307652764946614	-1.456861615024353	1.307652764946614
1.943232433176696	0.000000000000000	-1.783774806496563	0.000000000000000
1.943232433176696	-1.307652764946606	-1.456861615024356	-1.307652764946606
1.943232433176696	-2.615305529893207	-0.476122040607653	-2.615305529893207
1.943232433176696	-3.922958294839844	1.158443916753513	-3.922958294839844

1.943232433176696	-5.230611059786466	3.446836257059148	-5.230611059786466
0.971616215888129	2.615305528008586	0.504617536635953	2.615305528008586
0.971616215888129	1.961479146006445	-1.783774803669651	1.961479146006445
0.971616215888129	1.307652764004303	-3.418340761030787	1.307652764004303
0.971616215888129	0.653826382002148	-4.399080335447494	0.653826382002148
0.971616215888129	0.000000000000000	-4.725993526919694	0.000000000000000
0.971616215888129	-0.653826382002144	-4.399080335447495	-0.653826382002144
0.971616215888129	-1.307652764004305	-3.418340761030784	-1.307652764004305
0.971616215888129	-1.961479146006456	-1.783774803669615	-1.961479146006456
0.971616215888129	-2.615305528008599	0.504617536635999	-2.615305528008599
-0.000000001400324	-0.000000003769260	-0.476122034953796	-0.000000003769260
-0.000000001400324	-0.000000002826945	-2.764514375259396	-0.000000002826945
-0.000000001400324	-0.000000001884630	-4.399080332620539	-0.000000001884630
-0.000000001400324	-0.000000000942315	-5.379819907037206	-0.000000000942315
-0.000000001400324	0.000000000000000	-5.706733098509472	0.000000000000000
-0.000000001400324	0.000000000942315	-5.379819907037209	0.000000000942315
-0.000000001400324	0.000000001884630	-4.399080332620529	0.000000001884630
-0.000000001400324	0.000000002826945	-2.764514375259359	0.000000002826945
-0.000000001400324	0.000000003769260	-0.476122034953751	0.000000003769260
-0.971616218688831	-2.615305535547096	0.504617542289835	-2.615305535547096
-0.971616218688831	-1.961479151660315	-1.783774798015779	-1.961479151660315
-0.971616218688831	-1.307652767773544	-3.418340755376923	-1.307652767773544
-0.971616218688831	-0.653826383886777	-4.399080329793624	-0.653826383886777
-0.971616218688831	0.000000000000000	-4.725993521265830	0.000000000000000
-0.971616218688831	0.653826383886773	-4.399080329793628	0.653826383886773
-0.971616218688831	1.307652767773546	-3.418340755376918	1.307652767773546
-0.971616218688831	1.961479151660328	-1.783774798015743	1.961479151660328
-0.971616218688831	2.615305535547105	0.504617542289879	2.615305535547105
-1.943232435977316	-5.230611067324944	3.446836268366874	-5.230611067324944
-1.943232435977316	-3.922958300493710	1.158443928061273	-3.922958300493710
-1.943232435977316	-2.615305533662479	-0.476122029299860	-2.615305533662479
-1.943232435977316	-1.307652766831245	-1.456861603716554	-1.307652766831245
-1.943232435977316	0.000000000000000	-1.783774795188774	0.000000000000000
-1.943232435977316	1.307652766831237	-1.456861603716558	1.307652766831237
-1.943232435977316	2.615305533662482	-0.476122029299854	2.615305533662482
-1.943232435977316	3.922958300493731	1.158443928061310	3.922958300493731
-1.943232435977316	5.230611067324962	3.446836268366915	5.230611067324962
-2.914848653265941	-5.884437449327087	6.062141802971684	-5.884437449327087
-2.914848653265941	-3.922958299551405	4.427575845610580	-3.922958299551405
-2.914848653265941	-1.961479149775707	3.446836271193888	-1.961479149775707
-2.914848653265941	0.000000000000000	3.119923079721656	0.000000000000000
-2.914848653265941	1.961479149775691	3.446836271193888	1.961479149775691
-2.914848653265941	3.922958299551415	4.427575845610582	3.922958299551415
-2.914848653265941	5.884437449327118	6.062141802971720	5.884437449327118
-3.886464870554244	-5.230611065440353	11.292752869354432	-5.230611065440353
-3.886464870554244	-2.615305532720168	10.312013294937698	-2.615305532720168
-3.886464870554244	0.000000000000000	9.985100103465401	0.000000000000000
-3.886464870554244	2.615305532720153	10.312013294937689	2.615305532720153

-3.886464870554244 5.230611065440357 11.292752869354445 5.230611065440357

-5.230611059786413	5.591061857732818	4.400605111548550	6.438863177073491
-2.615305528008590	1.590603866868249	3.336318680788719	-0.377233592457184
0.000000003769260	-0.000000001675601	-0.000000005389958	-2.649265844601393
2.615305535547089	-1.590603873692596	-3.336318688294167	-0.377233579359113
5.230611067324960	-5.591061874976676	-4.400605109230389	6.438863203269694
-5.884437443673175	5.976738660485351	0.920827028196673	9.373211895279704
-3.922958294839821	-0.031931098400853	4.400605111548550	0.853090930091952
-1.961479146006446	-1.220892609172569	3.336318680788719	-4.258981647056023
0.000000002826945	0.000000002376416	-0.000000005389958	-5.963005836164207
1.961479151660318	1.220892610452249	-3.336318688294167	-4.258981637232498
3.922958300493710	0.031931089261040	-4.400605109230389	0.853090949739127
5.884437449327113	-5.976738686991079	-0.920827009505755	9.373211924750601
-5.230611061671043	11.182123710194826	-9.375047827960390	12.307560616760611
-3.922958295782119	-0.047896651104931	0.920827028196673	4.355447714608811
-2.615305529893222	-4.048354638496280	4.400605111548550	-1.324632928849707
-1.307652764004300	-3.229104377773150	3.336318680788719	-4.732681313615056
0.000000001884630	0.000000005270714	-0.000000005389958	-5.868697439687165
1.307652767773548	3.229104384841409	-3.336318688294167	-4.732681307066015
2.615305533662487	4.048354635145064	-4.400605109230389	-1.324632915751588
3.922958299551403	0.047896630387819	-0.920827009505755	4.355447734256078
5.230611065440326	-11.182123755224223	9.375047869573013	12.307560642956958
-2.615305530835529	6.362415460343713	-9.375047827960390	5.585772243707031
-1.961479147891062	-3.662677838059136	0.920827028196673	1.609715792631099
-1.307652764946615	-6.458208762553568	4.400605111548550	-1.230324529098167
-0.653826382002150	-4.434031438933495	3.336318680788719	-2.934348721480840
0.000000000942315	0.000000007007293	-0.000000005389958	-3.502356784516900
0.653826383886776	4.434031449474911	-3.336318688294167	-2.934348718206315
1.307652766831243	6.458208762675530	-4.400605109230389	-1.230324522549108
1.961479149775709	3.662677820815198	-0.920827009505755	1.609715802454730
2.615305532720172	-6.362415501899911	9.375047869573013	5.585772256805193
0.000000000000000	4.755846043726650	-9.375047827960390	0.000000000000000
0.000000000000000	-4.867604900377219	0.920827028196673	0.000000000000000
0.000000000000000	-7.261493470572672	4.400605111548550	0.000000000000000
0.000000000000000	-4.835673792653617	3.336318680788719	0.000000000000000
0.000000000000000	0.000000007586152	-0.000000005389958	0.000000000000001
0.000000000000000	4.835673804352725	-3.336318688294167	0.000000000000000
0.000000000000000	7.261493471852331	-4.400605109230389	0.000000000000000
-0.000000000000001	4.867604884290994	-0.920827009505755	0.000000000000000
-0.000000000000001	-4.755846084125126	9.375047869573013	0.000000000000000
2.615305530835524	6.362415460343690	-9.375047827960390	-5.585772243706958
1.961479147891068	-3.662677838059147	0.920827028196673	-1.609715792631084
1.307652764946609	-6.458208762553562	4.400605111548550	1.230324529098167
0.653826382002149	-4.434031438933516	3.336318680788719	2.934348721480817
-0.000000000942315	0.000000007007293	-0.000000005389958	3.502356784516916
-0.653826383886773	4.434031449474923	-3.336318688294167	2.934348718206305
-1.307652766831237	6.458208762675532	-4.400605109230389	1.230324522549104

C-7

-1.961479149775700	3.662677820815214	-0.920827009505755	-1.609715802454724
-2.615305532720154	-6.362415501899849	9.375047869573013	-5.585772256805173
5.230611061671080	11.182123710194871	-9.375047827960390	-12.307560616760650
3.922958295782125	-0.047896651104911	0.920827028196673	-4.355447714608834
2.615305529893211	-4.048354638496264	4.400605111548550	1.324632928849702
1.307652764004310	-3.229104377773146	3.336318680788719	4.732681313615061
-0.000000001884630	0.000000005270714	-0.000000005389958	5.868697439687149
-1.307652767773549	3.229104384841387	-3.336318688294167	4.732681307066032
-2.615305533662480	4.048354635145056	-4.400605109230389	1.324632915751589
-3.922958299551413	0.047896630387801	-0.920827009505755	-4.355447734256090
-5.230611065440360	-11.182123755224255	9.375047869573013	-12.307560642956988
5.884437443673161	5.976738660485495	0.920827028196673	-9.373211895279818
3.922958294839823	-0.031931098400766	4.400605111548550	-0.853090930092020
1.961479146006444	-1.220892609172530	3.336318680788719	4.258981647055990
-0.000000002826945	0.000000002376416	-0.000000005389958	5.963005836164176
-1.961479151660327	1.220892610452204	-3.336318688294167	4.258981637232458
-3.922958300493755	0.031931089260955	-4.400605109230389	-0.853090949739189
-5.884437449327119	-5.976738686991194	-0.920827009505755	-9.373211924750715
5.230611059786441	5.591061857732927	4.400605111548550	-6.438863177073618
2.615305528008587	1.590603866868294	3.336318680788719	0.377233592457081
-0.000000003769260	-0.000000001675601	-0.000000005389958	2.649265844601290
-2.615305535547109	-1.590603873692648	-3.336318688294167	0.377233579359009
-5.230611067324918	-5.591061874976747	-4.400605109230369	-6.438863203269836
3.909549333051991	11.182123710194903	9.375047827960220	12.307560616760611
4.890288907468671	6.362415460343731	9.375047827960220	5.585772243707000
5.217202098940930	4.755846043726661	9.375047827960220	0.000000000000000
4.890288907468674	6.362415460343710	9.375047827960220	-5.585772243706966
3.909549333051983	11.182123710194938	9.375047827960220	-12.307560616760655
-0.013408963672444	5.976738660485350	-0.920827028196690	9.373211895279697
1.621156993688683	-0.047896651104934	-0.920827028196690	4.355447714608801
2.601896568105386	-3.662677838059122	-0.920827028196690	1.609715792631100
2.928809759577604	-4.867604900377210	-0.920827028196690	0.000000000000000
2.601896568105390	-3.662677838059138	-0.920827028196690	-1.609715792631087
1.621156993688678	-0.047896651104912	-0.920827028196690	-4.355447714608816
-0.013408963672478	5.976738660485478	-0.920827028196690	-9.373211895279809
-3.936367260396866	5.591061857732820	-4.400605111548589	6.438863177073475
-1.647974920091264	-0.031931098400854	-4.400605111548589	0.853090930091954
-0.013408962730128	-4.048354638496292	-4.400605111548589	-1.324632928849709
0.967330611686562	-6.458208762553580	-4.400605111548589	-1.230324529098170
1.294243803158804	-7.261493470572697	-4.400605111548589	0.000000000000000
0.967330611686566	-6.458208762553590	-4.400605111548589	1.230324529098167
-0.013408962730133	-4.048354638496280	-4.400605111548589	1.324632928849706
-1.647974920091299	-0.031931098400769	-4.400605111548589	-0.853090930092019
-3.936367260396912	5.591061857732930	-4.400605111548589	-6.438863177073619
-4.917106833871242	1.590603866868251	-3.336318680788636	-0.377233592457186
-2.628714493565631	-1.220892609172574	-3.336318680788636	-4.258981647056038
-0.994148536204504	-3.229104377773160	-3.336318680788636	-4.732681313615068
-0.013408961787815	-4.434031438933489	-3.336318680788636	-2.934348721480847

0.313504229684419	-4.835673792653603	-3.336318680788636	0.000000000000000
-0.013408961787811	-4.434031438933494	-3.336318680788636	2.934348721480833
-0.994148536204511	-3.229104377773156	-3.336318680788636	4.732681313615073
-2.628714493565663	-1.220892609172533	-3.336318680788636	4.258981647056000
-4.917106833871282	1.590603866868302	-3.336318680788636	0.377233592457081
-5.244020024401139	-0.000000001675601	0.000000005389956	-2.649265844601388
-2.955627684095545	0.000000002376416	0.000000005389956	-5.963005836164180
-1.321061726734421	0.000000005270714	0.000000005389956	-5.868697439687161
-0.340322152317733	0.000000007007293	0.000000005389956	-3.502356784516897
-0.013408960845499	0.000000007586152	0.000000005389956	0.000000000000000
-0.340322152317730	0.000000007007292	0.000000005389956	3.502356784516881
-1.321061726734427	0.000000005270714	0.000000005389956	5.868697439687167
-2.955627684095581	0.000000002376417	0.000000005389956	5.963005836164152
-5.244020024401188	-0.000000001675601	0.000000005389956	2.649265844601293
-4.917106831986613	-1.590603873692591	3.336318688294047	-0.377233579359116
-2.628714491681017	1.220892610452241	3.336318688294047	-4.258981637232488
-0.994148534319880	3.229104384841399	3.336318688294047	-4.732681307066017
-0.013408959903188	4.434031449474892	3.336318688294047	-2.934348718206321
0.313504231569045	4.835673804352727	3.336318688294047	0.000000000000000
-0.013408959903184	4.434031449474892	3.336318688294047	2.934348718206309
-0.994148534319884	3.229104384841393	3.336318688294047	4.732681307066017
-2.628714491681044	1.220892610452199	3.336318688294047	4.258981637232447
-4.917106831986660	-1.590603873692647	3.336318688294047	0.377233579359009
-3.936367256627580	-5.591061874976657	4.400605109230395	6.438863203269701
-1.647974916321992	0.031931089261044	4.400605109230395	0.853090949739123
-0.013408958960862	4.048354635145078	4.400605109230395	-1.324632915751590
0.967330615455827	6.458208762675508	4.400605109230395	-1.230324522549111
1.294243806928048	7.261493471852331	4.400605109230395	0.000000000000000
0.967330615455830	6.458208762675518	4.400605109230395	1.230324522549106
-0.013408958960868	4.048354635145064	4.400605109230395	1.324632915751586
-1.647974916322025	0.031931089260960	4.400605109230395	-0.853090949739184
-3.936367256627627	-5.591061874976771	4.400605109230395	-6.438863203269841
-0.013408958018520	-5.976738686991073	0.920827009505755	9.373211924750606
1.621156999342617	0.047896630387815	0.920827009505755	4.355447734256055
2.601896573759300	3.662677820815193	0.920827009505755	1.609715802454732
2.928809765231547	4.867604884290992	0.920827009505755	0.000000000000000
2.601896573759302	3.662677820815207	0.920827009505755	-1.609715802454719
1.621156999342612	0.047896630387796	0.920827009505755	-4.355447734256073
-0.013408958018553	-5.976738686991204	0.920827009505755	-9.373211924750720
3.909549340590552	-11.182123755224215	-9.375047869572718	12.307560642956972
4.890288915007244	-6.362415501899870	-9.375047869572718	5.585772256805186
5.217202106479486	-4.755846084125112	-9.375047869572718	0.000000000000000
4.890288915007245	-6.362415501899845	-9.375047869572718	-5.585772256805152
3.909549340590547	-11.182123755224239	-9.375047869572718	-12.307560642956993

Columns   13 thru   14

-8.354082865199837	1.561284022178192
-4.461045461240316	4.969332406948914
0.000000006574786	6.105348533022815
4.461045473571248	4.969332400399862
8.354082875074887	1.561284009080078
-5.147019464415578	-5.077125692326685
-4.378026415345557	-0.817065209726076
-2.473017237745784	1.738971078851965
0.000000003709578	2.590983173407394
2.473017244346303	1.738971073940186
4.378026419490211	-0.817065219549665
5.147019464467047	-5.077125707062106
1.468092324413839	-8.307487020423677
-0.886958981405641	-4.331430569341459
-1.537986094021138	-1.491390247607720
-1.052997078106861	0.212633944777643
0.000000001663000	0.780642007814595
1.052997080614222	0.212633941503125
1.537986094072612	-1.491390254156780
0.886958977363938	-4.331430579165100
-1.468092334186006	-8.307487033521861
4.876140711231139	-4.437747542548953
1.669077308400342	-2.449719317007844
0.166038098773543	-1.029699156140968
-0.200984982323491	-0.177687059948282
0.000000000435054	0.106316971570193
0.200984982374967	-0.177687061585542
-0.166038101177963	-1.029699159415500
-1.669077314897954	-2.449719321919666
-4.876140723459206	-4.437747549098058
6.012156840170259	0.000000000000000
2.521089405002346	0.000000000000000
0.734046163038441	0.000000000000000
0.083019049604301	0.000000000000000
0.000000000025738	0.000000000000000
-0.083019050371454	0.000000000000000
-0.734046166261493	0.000000000000000
-2.521089412318601	0.000000000000000
-6.012156853216944	0.000000000000000
4.876140711231161	4.437747542548929
1.669077308400350	2.449719317007834
0.166038098773550	1.029699156140964
-0.200984982323487	0.177687059948283
0.000000000435054	-0.106316971570192
0.200984982374963	0.177687061585542
-0.166038101177971	1.029699159415490

```
-1.669077314897962    2.449719321919642
-4.876140723459220    4.437747549098033
 1.468092324413828    8.307487020423691
-0.886958981405654    4.331430569341463
-1.537986094021138    1.491390247607715
-1.052997078106857   -0.212633944777647
 0.000000001663000   -0.780642007814596
 1.052997080614226   -0.212633941503129
 1.537986094072624    1.491390254156779
 0.886958977363946    4.331430579165094
-1.468092334185980    8.307487033521852
-5.147019464415663    5.077125692326695
-4.378026415345641    0.817065209726050
-2.473017237745829   -1.738971078852007
 0.000000003709578   -2.590983173407424
 2.473017244346341   -1.738971073940227
 4.378026419490284    0.817065219549638
 5.147019464467132    5.077125707062133
-8.354082865199921   -1.561284022178250
-4.461045461240332   -4.969332406948987
 0.000000006574786   -6.105348533022861
 4.461045473571272   -4.969332400399948
 8.354082875074990   -1.561284009080143
 1.468092324413839    8.307487020423682
 4.876140711231124    4.437747542548951
 6.012156840170239    0.000000000000000
 4.876140711231141   -4.437747542548929
 1.468092324413821   -8.307487020423693
-5.147019464415581    5.077125692326697
-0.886958981405641    4.331430569341466
 1.669077308400342    2.449719317007846
 2.521089405002347    0.000000000000000
 1.669077308400350   -2.449719317007833
-0.886958981405655   -4.331430569341475
-5.147019464415669   -5.077125692326693
-8.354082865199828   -1.561284022178192
-4.378026415345587    0.817065209726074
-1.537986094021125    1.491390247607714
 0.166038098773544    1.029699156140970
 0.734046163038439    0.000000000000000
 0.166038098773551   -1.029699156140967
-1.537986094021134   -1.491390247607714
-4.378026415345643   -0.817065209726050
-8.354082865199929    1.561284022178249
-4.461045461240309   -4.969332406948899
-2.473017237745789   -1.738971078851964
-1.052997078106856   -0.212633944777643
-0.200984982323491    0.177687059948282
```

0.083019049604301	0.000000000000000
-0.200984982323488	-0.177687059948282
-1.052997078106861	0.212633944777647
-2.473017237745818	1.738971078852005
·4.461045461240350	4.969332406948968
0.000000006574786	-6.105348533022778
0.000000003709577	-2.590983173407376
0.000000001663000	-0.780642007814596
0.000000000435054	-0.106316971570193
0.000000000025738	0.000000000000000
0.000000000435054	0.106316971570192
0.000000001663000	0.780642007814600
0.000000003709578	2.590983173407425
0.000000006574786	6.105348533022863
4.461045473571221	-4.969332400399865
2.473017244346305	-1.738971073940184
1.052997080614221	-0.212633941503124
0.200984982374966	0.177687061585542
-0.083019050371454	0.000000000000000
0.200984982374963	-0.177687061585542
1.052997080614226	0.212633941503128
2.473017244346337	1.738971073940227
4.461045473571267	4.969332400399932
8.354082875074887	-1.561284009080079
4.378026419490227	0.817065219549660
1.537986094072614	1.491390254156775
-0.166038101177964	1.029699159415493
-0.734046166261493	0.000000000000000
-0.166038101177971	-1.029699159415494
1.537986094072624	-1.491390254156774
4.378026419490286	-0.817065219549637
8.354082875074967	1.561284009080139
5.147019464467027	5.077125707062133
0.886958977363937	4.331430579165083
-1.669077314897952	2.449719321919660
-2.521089412318598	0.000000000000000
-1.669077314897960	-2.449719321919645
0.886958977363952	-4.331430579165087
5.147019464467117	-5.077125707062132
-1.468092334186004	8.307487033521820
-4.876140723459240	4.437747549098026
-6.012156853216958	0.000000000000000
-4.876140723459253	-4.437747549098004
-1.468092334185987	-8.307487033521829

Appendix D. Optimal Controller Gain Matrix

This appendix provides the elements of the optimal controller steady-state gain matrix, G_c^*, used in this research. G_c^* premultiplies the Kalman filter state estimate to generate the optimal control voltage to apply to the deformable mirror actuators. G_c^* has dimensions 97 x 28.

$$G_c^* \quad = $$

Columns 1 thru 4

0.339258247919758	0.130244421813319	0.370583390863166	0.314474151321678
0.999960664585836	0.189619794128763	0.909575854870053	0.451280708081004
1.232289787422465	-0.000032549855010	1.061588016203898	0.000019672507300
0.999972007829858	-0.189660239277984	0.909606990563429	-0.451273580395381
0.338937472555964	-0.130002399249115	0.370219076330197	-0.314007681003168
0.996521655546898	0.752823260269258	0.995911150616209	1.391288591641871
1.917253597983644	0.939189973733048	1.274064345297248	1.774436408918833
2.023192606177944	0.484715519455123	0.822534917180600	0.901717186320969
1.968113833031372	-0.000047661529629	0.594980381648395	0.000067095393288
2.023245674240074	-0.484790899899605	0.822529647847116	-0.901634781705149
1.917303593457313	-0.939200768898203	1.274127888606638	-1.774495117897197
0.996520665426280	-0.752788458673974	0.996010410200767	-1.391402898053652
0.729136886044108	1.028894156937397	0.995911150616202	1.391288591641527
1.481158025364800	1.529274180159296	0.909569853293850	2.085620601573523
1.230471165637522	0.823185765904822	-0.268525985327608	0.982332943092106
1.048078041875218	0.343186225281348	-0.775302931555626	0.345468599319955
1.011359316062551	-0.000005725339577	-0.883333778995705	0.000037452457279
1.048134971249576	-0.343203847405432	-0.775389280112075	-0.345391701603417
1.230549261115302	-0.823207451393587	-0.268621338296578	-0.982280700863035
1.481177893357645	-1.529256251562521	0.909620102120099	-2.085688007469848
0.729102587471884	-1.028860724969281	0.996016887194381	-1.391376514225568
0.126146490362058	0.350279220763050	0.370583390862662	0.314474151321442
0.909639870327800	1.979536534256512	1.274064345297307	1.774436408919401
0.797285548501973	1.270443633165433	-0.268525985327516	0.982332943092218
0.627201416018589	0.647576365820464	-1.030964405261619	0.375339144916594
0.549937599768340	0.277321619971590	-1.259964359774148	0.122221819164016
0.524198018612319	0.000022292565717	-1.306795426827538	-0.000015068524321
0.549970721000512	-0.277296441430972	-1.260038569926717	-0.122222176905982
0.627250014312483	-0.647598002480591	-1.031075435902693	-0.375269765069312
0.797310283090181	-1.270501505793439	-0.268588747845387	-0.982221515924218
0.909592291977047	-1.979561849773617	1.274152746492531	-1.774406138637332
0.126131646808892	-0.350275951860706	0.370611221404271	-0.314482629108538
0.183653711994539	1.032444883896145	0.909575854869943	0.451280708081440
0.469464724491668	2.088917023797523	0.822534917180347	0.901717186320315
0.332388422145502	1.082125378100562	-0.775302931555585	0.345468599319946

D-1

0.268596140809759	0.567802596087029	-1.259964359774181	0.122221819163956
0.229974175819561	0.237445001247098	-1.374875518008038	0.028353424616996
0.217100230452356	0.000030992101424	-1.383653233193210	-0.000047076611708
0.229970427103577	-0.237407974492965	-1.374892994284507	-0.028404746217842
0.268587559645854	-0.567829037183226	-1.259991317356199	-0.122164246107551
0.332372906066985	-1.082219615390883	-0.775323510126011	-0.345294803767021
0.469434301011418	-2.089016079267397	0.822556341555813	-0.901536509797992
0.183642076085002	-1.032459710673198	0.909592559596987	-0.451250860241505
-0.000031525725767	1.272321333788876	1.061588016204173	0.000019672507380
-0.000046161936581	2.032048989322500	0.594980381648505	0.000067095393389
-0.000005545201828	1.044213826224591	-0.883333778995802	0.000037452457299
0.000021591165449	0.541226851839984	-1.306795426827506	-0.000015068524353
0.000030016984597	0.224152839363874	-1.383653233193283	-0.000047076611695
0.000017550702044	0.000018120845264	-1.379717358399179	-0.000038510670761
-0.000011375987431	-0.224139443929528	-1.383598622046661	0.000011090173423
-0.000045718117864	-0.541270590633853	-1.306707604185751	0.000082586499167
-0.000067817448666	-1.044314773617413	-0.883255544196038	0.000137238591412
-0.000046571415842	-2.032138831876334	0.594969839107561	0.000102504116100
0.000002959748384	-1.272323852076924	1.061534509229493	-0.000003649885048
-0.183692884601172	1.032456595632342	0.909606990563455	-0.451273580396200
-0.469537733211258	2.088971815802730	0.822529647847017	-0.901634781704980
-0.332405489819264	1.082184156853773	-0.775389280112073	-0.345391701603393
-0.268571754472410	0.567836793277904	-1.260038569926814	-0.122222176906070
-0.229938314052793	0.237441130751548	-1.374892994284505	-0.028404746217869
-0.217087256483459	-0.000011745541980	-1.383598622046694	0.000011090173433
-0.230005840720726	-0.237477694797706	-1.374780336798526	0.028451315618942
-0.268674770726880	-0.567901171699044	-1.259864049265320	0.122322313238191
-0.332480196184952	-1.082257120619768	-0.775254065606369	0.345516187828225
-0.469456676685459	-2.088947499372331	0.822424513113941	0.901606949682281
-0.183610841861463	-1.032405507089655	0.909486549924083	0.451195188068814
-0.125912082648130	0.349948024851724	0.370219076330255	-0.314007681003513
-0.909650325840932	1.979588153860965	1.274127888606599	-1.774495117896941
-0.797306551692227	1.270524265613316	-0.268621338296514	-0.982280700863021
-0.627222371915801	0.647626542852836	-1.031075435902659	-0.375269765069334
-0.549963208937392	0.277312760043143	-1.259991317356149	-0.122164246107558
-0.524240381234456	-0.000047203293338	-1.306707604185533	0.000082586499185
-0.550033073857475	-0.277402804218950	-1.259864049265353	0.122322313238183
-0.627313504266851	-0.647692095309536	-1.030901088685571	0.375386914379231
-0.797070311787122	-1.270160824317585	-0.268977303244165	0.981747952475765
-0.909437250709204	-1.979376629236132	1.273819953830245	1.774139281513326
-0.126095011738471	-0.350233670574856	0.370531220540692	0.314414693968178
-0.729103179425135	1.028893134655140	0.996010410200545	-1.391402898053682
-1.481140660862826	1.529294693575316	0.909620102120127	-2.085688007469812
-1.230527217396081	0.823211304007648	-0.268588747845415	-0.982215159924273
-1.048169314139251	0.343170205153960	-0.775323510126053	-0.345294803766905
-1.011457087306163	-0.000070020531867	-0.883255544196091	0.000137238591400
-1.048205639327663	-0.343280980644143	-0.775254065606535	0.345516187828131
-1.230197254916766	-0.822963537116936	-0.268977303244344	0.981747952475729

-1.481644132287273	-1.529776078507216	0.910291302390653	2.086499124326871
-0.728912275493536	-1.028679347302836	0.995707432829698	1.391033290629153
-0.996489275461531	0.752787847492683	0.996016887194317	-1.391376514225516
-1.917278116988975	0.939140849775398	1.274152746492680	-1.774406138637470
-2.023288545025977	0.484684107652152	0.822556341555824	-0.901536509797963
-1.968200848832830	-0.000048084312655	0.594969839107498	0.000102504116052
-2.023222122887610	-0.484707210213403	0.822424513113835	0.901606949682319
-1.917098724117968	-0.938980771915973	1.273819953830546	1.774139281513476
-0.996313604551249	-0.752591353134774	0.995707432829725	1.391033290629162
-0.339255081868596	0.130229096060472	0.370611221404263	-0.314482629108522
-0.999975024862247	0.189607780221487	0.909592559596926	-0.451250860241574
-1.232292226477108	0.000003055895881	1.061534509229551	-0.000003649885110
-0.999922526707279	-0.189575531340817	0.909486549924101	0.451195188068794
-0.339214130895313	-0.130191270882144	0.370531220540786	0.314414693968221

Columns   5 thru   8

0.392674428395098	0.181689482723812	0.445782934443492	0.379219291989418
1.270437274810795	0.216730914257002	1.093142468532478	0.607793316420320
1.618556502980760	-0.000048089799547	1.272079588612113	-0.000037289278403
1.270445669658173	-0.216790530002738	1.093152111399541	-0.607844075878943
0.392510778748874	-0.181361910105178	0.445368508883415	-0.378807716534256
0.473422230396328	0.820497465851682	1.033521373501817	1.250527910191491
1.527797600799846	0.674708440805888	1.356816247847528	2.128648868848440
1.897406337999417	0.155331313309422	0.745656611657904	1.332576082478851
1.894720909737190	-0.000070061388153	0.413554084747666	-0.000045726206220
1.897423111274789	-0.155442369048966	0.745722161486370	-1.332655039389444
1.527829632689093	-0.674724014328523	1.356871836597938	-2.128680930908232
0.473446522767382	-0.820444794650838	1.033511747109098	-1.250515124799040
-0.473422230395929	1.125835899488472	0.753219601762129	0.444831664234859
-0.000000000000319	0.773959753195507	0.710497815460950	1.467942123415542
0.426251870616875	-0.450101491395121	-0.578140899581154	1.252004462303234
0.425050671590548	-0.514793248060297	-1.356392890492311	0.665895016416246
0.413446898395366	-0.000007768161520	-1.581256327417492	0.000001984814809
0.425055162744116	0.514767124586931	-1.356312010303667	-0.665899125018196
0.426265951763673	0.450066626051993	-0.578030763796296	-1.252022347856223
0.000031605172913	-0.773934944182912	0.710524507831155	-1.467944376403298
-0.473401259844410	-1.125784617023821	0.753171603667317	-0.444817959246932
-0.392674428394805	0.485600437342902	0.166791593536604	-0.191508370095188
-1.527797600799843	1.478007596170653	0.619384756492823	-0.451626806108037
-0.426251870616755	-0.629780666746446	-0.413194775383528	0.238637772798850
0.000000000000057	-1.341483673986137	-1.231486800081915	0.425174920941875
0.047930801622824	-0.926923739866534	-1.686483899274075	0.294943895995406
0.033945230867114	0.000033955041162	-1.838127462457112	0.000026436570708
0.047927691651356	0.926960914268058	-1.686433789825605	-0.294909130105789
-0.000003191646003	1.341446989608428	-1.231412009219657	-0.425185048971646
-0.426247670810597	0.629687970047701	-0.413151917609267	-0.238689169145976
-1.527779474985068	-1.478044804144494	0.619324793929892	0.451589067808268

-0.392670607436973	-0.485594068098986	0.166771673630640	0.191507607495916
-1.270437274810658	1.190782373624827	0.198959752736308	-0.952364519670182
-1.897406337999772	0.812258946576983	0.142594699948434	-1.536255301834562
-0.425050671590395	-1.477546424355588	-0.472582038866004	-0.443505259005540
-0.047930801622747	-1.837121288809020	-0.850193011l6149	-0.022046827302043
-0.000000000000055	-1.174726632674371	-1.078403241049088	0.071341946496632
-0.013987136895087	0.0000047241979932	-1.154230070331721	0.000030005203923
-0.000008011119391	1.174781913706608	-1.078405609664129	-0.071303428947552
-0.047944201013822	1.837077309208128	-0.850926287574681	0.022030294037194
-0.425064231465815	1.477398112844155	-0.472598052368114	0.443428389494022
-1.897410161732496	-0.812407499736397	0.142556063160700	1.536167225754191
-1.270435142617161	-1.190800077941301	0.198943691845945	0.952348622633847
-1.618556502980845	1.385702225988507	-0.000044146607649	-1.354412593437994
-1.894720909737359	0.450492894426980	-0.000064316604017	-1.879617277248085
-0.413446898395299	-1.722494749820717	-0.000007131199888	0.668397859749593
-0.033945230866977	-2.002309713291116	0.000031170849050	-0.171098282532854
0.013987136895054	-1.257326343467762	0.000043368306225	-0.003187925148811
-0.000000000000042	0.000028662248971	0.000026312046860	0.000013999312270
0.013977356909453	1.257347647463065	-0.000014071143521	0.003197631103250
-0.033962573446151	2.002241303995592	-0.000062778537040	0.171062538278103
-0.413467368779192	1.722337979067200	-0.000095731459790	0.668317791131018
-1.894737365457102	-0.450625788130129	-0.000071072483797	1.879551569327561
-1.618560154138322	-1.385699020748606	-0.000000762063604	1.354416091611660
-1.270445669657686	1.190792877795803	-0.199014480203390	-0.952381372505776
-1.897423111274925	0.812330351342281	-0.142696649513380	-1.536239447553934
-0.425055162744033	-1.477458319917793	0.472558057424392	-0.443438680637902
-0.047927691651298	-1.837066703565357	0.850953427349652	-0.021994325358445
0.000008011119230	-1.1747292l2854659	1.07845398923·333	0.071349746348461
-0.013977356909569	-0.000015327983299	1.154249627475390	-0.000015762818953
-0.000000000000076	1.174677368559422	1.078358016415817	-0.071389778626852
-0.047941901947709	1.836969642456133	0.850805590006446	0.021938200937276
-0.425071952967385	1.477346675724878	0.47244619984053·5	0.443386919071563
-1.897436240384151	-0.812287249477035	-0.142597530223681	1.536288078393620
-1.270448518340752	-1.190709053940363	-0.1·8906888715417	0.952438184703034
-0.392510778748655	0.485148995132470	-0.166490880703394	-0.1·1672248424820
-1.527829632688907	1.478068150130546	-0.619399053041469	-0.451649322042273
-0.426265951763635	-0.629660693590710	0.413162768874335	0.238718617597745
0.000003191646082	-1.341402202775005	1.231453123692610	0.425254721103758
0.047944201013858	-0.926931350357877	1.686443525843608	0.294954967004205
0.033962573446155	-0.000063385939932	1.838064662479950	-0.000048953194729
0.047941901947820	0.926799872036794	1.686344687380709	-0.295045008179177
0.000000000000u64	1.341304953267616	1.231322733824615	-0.425311738688602
-0.426096741309639	0.6301577240l3819	0.413459773756031	-0.238526236097188
-1.527823954014648	-1.477740820717424	-0.619111259700105	0.451871217573740
-0.392679242583213	-0.485524735039061	-0.166721736330203	0.191573581057983
-0.473446522767558	1.125825413262928	-0.753171249412825	0.444778104501451
-0.000031605173130	0.773988829738908	-0.710475040698802	1.467931073974167
0.426247670810669	-0.450054805547736	0.578055803681092	1.252054772381855

0.425064231465794	-0.514810691894435	1.356256739995378	0.665900384527881
0.413467368779016	-0.000104282230404	1.581112411306572	-0.000070734104918
0.425071952967412	0.514645275841066	1.356209520536194	-0.666011183318799
0.426096741309825	0.450390159524216	0.578487039498429	-1.251630753914165
-0.000000000000004	-0.774600741338373	-0.711086244863531	-1.468403954424745
-0.473430155450606	-1.125499434148806	-0.752901858149583	-0.444569254047077
0.473401259844205	0.820445180548336	-1.033474296016326	1.250467893767728
1.527779474985092	0.674643122364580	-1.356850404899831	2.128598682868911
1.897410161732730	0.155289225468996	-0.745792983988368	1.332554686708402
1.894737365456804	-0.000077420705465	-0.413676081641542	-0.000057192483221
1.897436240383990	-0.155334396386229	-0.745682593821316	-1.332598450083113
1.527823954014760	-0.674410515175446	-1.356571347029142	-2.128462584936687
0.473430155450540	-0.820513341257369	-1.033212497119263	-1.250286239367583
0.392670607436985	0.181667783564503	-0.445777087454856	0.379201780645799
1.270435142617247	0.216713418801736	-1.093158721158330	0.607780197497646
1.618560154138468	-0.000000830131608	-1.272076646190624	-0.000007094800315
1.270448518340631	-0.216673328401819	-1.093075160800813	-0.607765239259898
0.392679242583174	-0.181613385845328	-0.445713439458465	-0.379170817738438

Columns   9 thru   12

0.184921519419597	0.474430507466180	0.434087886172966	0.354344374962234
0.919608338432117	0.965582586892291	1.165105266467606	0.413310713513985
1.307828136052588	1.049356215568620	1.387037167156926	0.000022008117665
0.919624611620920	0.965621037552962	1.165123704251418	-0.413302923314786
0.185079761222358	0.473936946770073	0.433909890781873	-0.353811416562881
-0.429531864303997	0.985916778478126	0.410864490562499	1.199678807974202
0.436093290098859	0.599124530671337	0.802452916227604	0.871009174398685
1.483416440184622	-0.336082630488516	0.196006158536205	0.047840599602014
1.814968623376377	-0.674649846805381	-0.235159742921086	0.000075331423300
1.483401131205287	-0.336086494749731	0.196040110280886	-0.047748272047495
0.436115031606131	0.599204841318688	0.802508062147355	-0.871075730007002
-0.429480146733935	0.986038436943413	0.410897374189008	-1.199807741522667
-1.207516523245584	0.985916778476791	-0.410864490562427	1.199678807973885
-1.417452865103743	-0.118108659011708	-0.000000000000088	0.489558623659999
-0.230429925935206	-1.589964325757181	-0.534886088793323	-1.198394349090567
0.428251080228670	-1.604687268933233	-1.553222865493305	-1.059412002068327
0.645408593580726	-1.436776961035555	-1.969165791758215	0.000042116887911
0.428186791796483	-1.604789548802772	-1.553314938110762	1.059498453500952
-0.230507990110773	-1.590076095837996	-0.534867610912401	1.198452959704788
-1.417442195703241	-0.118044802857865	0.000028968252489	-0.489634792866226
-1.207458571062338	0.986045200811840	-0.410851864873834	-1.199777907836219
-0.366176202289836	0.474430507466239	-0.434087886173053	0.354344374962006
-2.055434877042756	0.599124530671475	-0.802452916227670	0.871009174398821
-1.208942289962142	-1.589964325757386	0.534886088793276	-1.198394349090649
-0.410551206512406	-1.268496971863047	-0.000000000000050	-1.763680858459055
0.021288535854260	-0.247350321803572	-0.956291930281158	-1.147044535402773
0.165213428324322	0.217924544865026	-1.375024570846104	-0.000016905811048

0.021237839693151	-0.247438653239715	-0.956296986525433	1.147044224862487
-0.410628261981018	-1.268628958099847	0.000008445730284	1.763758997263914
-1.208990869646646	-1.590038168828743	0.534878393066345	1.198519758447342
-2.055386417189208	0.599231555340151	-0.802454890644114	-0.870975123628505
-0.366159293241161	0.474463891942692	-0.434087918901953	-0.354353909971544
-0.586888518292319	0.965582586892811	-1.165105266467577	0.413310713514062
-1.286742682799380	-0.336082630488792	-0.196006158536314	0.047840599602115
-0.642991834501478	-1.604687268933479	1.553322865493508	-1.059412002068273
-0.284799423461089	-0.247350321803538	0.956291930281113	-1.147044535432795
-0.068888169942199	1.314731432666902	-0.000000000 0009	-0.706162046563287
0.003078277790560	1.960346196452692	-0.418735089259308	-0.000052377657397
-0.068895701521397	1.314710798527265	-0.000011608010561	0.706104485069113
-0.284810113687235	-0.247382188721816	0.956271969667909	1.147109501755699
-0.642997017979235	-1.604711721002284	1.553301058617548	1.059607742866865
-1.286722022927443	-0.336057606425371	-0.196018486467974	-0.047637110093289
-0.586875850589748	0.965601971169944	-1.165104806445140	-0.413277053722718
0.000036006729601	1.049356215568639	-1.387037167156665	0.000022008117546
0.000044153472397	-0.674649846805226	0.235169742920767	0.000075331423242
-0.000001916547883	-1.436776961035192	1.969165791758559	0.000042116887793
-0.000025527295834	0.217924544865076	1.375024570845882	-0.000016905811017
-0.000028973187424	1.960346196452613	0.418735089259194	-0.000052877657329
-0.000013517811717	2.666109154373783	-0.000000000000071	-0.000043214124499
0.000015220663364	1.960411919668156	0.418721826875662	0.000012615614722
0.000047269469933	0.218030117469360	1.375002890127573	0.0000930
0.000068301234810	-1.436683286737311	1.969145780810163	0.000154
0.000055225371527	-0.674663873173910	0.235168259227142	0.00011
0.000006850777677	1.049290849984381	-1.387027081699394	-0.00000
0.586937531900203	0.965621037552480	-1.165123704250834	-0.413302
1.286818924019715	-0.336086494749615	-0.196040110280842	-0.047748
0.642995801789887	-1.604789548802794	1.553314938110861	1.059498453500918
0.284765853329805	-0.247438653239707	0.956296986525405	1.147044224862332
0.068850977188215	1.314710798527128	0.000011608010510	0.706104485069139
-0.003087649912840	1.960411919668083	-0.418721826875772	0.000012615614772
0.068934356006203	1.314846263959053	-0.000000000000060	-0.706051835735833
0.284897057933411	-0.247228871434738	0.956280203202179	-1.146931 26399
0.643194005891800	-1.604627244764308	1.553305788386096	-1 3585 207
1.286764281079219	-0.336213648254880	-0.196015977882437	0.047 9734
0.586861406834496	0.965475722141651	-1.165103728155024	132, 6007475
0.365773782800456	0.473936946769953	-0.433909890781794	-0.353811416562965
2.055465836341582	0.599204841318478	-0.802508062148392	-0.871075730007015
1.208995960348930	-1.590070095638281	0.534867610912579	1.198452959704655
0.410560980192819	-1.268628958099900	0.000008445730224	1.763758997263882
-0.021272571244246	-0.247382188721800	-0.956271969667789	1.147109501755929
-0.165178913478367	0.218030117469385	-1.375002890127431	0.000093088646866
-0.021183045648125	-0.247228871434743	-0.956280203202100	-1.146931374886340
0.410683318662852	-1.268418747812110	0.000000000000057	-1.763627075320221
1.208581435117424	-1.590559232058899	0.535066888873187	-1.199050774358777
2.055235000268519	0.598837151676660	-0.802461266171302	0.870674807909100

0.366129395290101	0.474368496221076	-0.434088344749395	0.354277475364280
1.207504177601753	0.986038436943718	-0.410897374188401	-1.199807741522354
1.417455040600865	-0.118044802857951	-0.000028968252359	-0.489634792866330
0.230479554526383	-1.590038168828740	-0.534878393066380	1.198519758447256
-0.428176854611955	-1.604711721002380	-1.553301058617748	1.059607742866948
-0.645331278888810	-1.436683286737402	-1.969145380810251	0.000154628320393
-0.428136810547501	-1.604627244764308	-1.553305788386182	-1.059358324329191
0.230322225491835	-1.590559232058639	-0.535066888873293	-1.199060774358817
1.417898811627725	-0.117093222660910	0.000000000000001	0.490567425577672
1.207283164589509	0.985676010976111	-0.410867121103299	1.199391402055059
0.429518630692256	0.986045200811871	0.410851864873839	-1.199777907836278
-0.436056849791459	0.599231555340282	0.802454890644131	-0.870975123628497
-1.483331393444629	-0.336057606425252	0.196018486467839	-0.047637110093242
-1.814905175452793	-0.674663873173925	-0.235168259227166	0.000115646355428
-1.483448089407726	-0.336213648254937	0.196015977882396	0.047716809709736
-0.436329295133208	0.598835715676557	0.802461266171321	0.870674807909059
0.429278479604175	0.985676010976131	0.410867121103262	1.199391402055239
-0.184920783049761	0.474463891942705	0.434087918901942	-0.354353909971535
-0.919592988167356	0.965601971170091	1.165104806445047	-0.413277053722710
-1.307831513907768	1.049290849984500	1.387027081699409	-0.000003930339307
-0.919679469786567	0.965475722141696	1.165103728155034	0.413214626007453
-0.184984487478656	0.474368496221042	0.434088344749386	0.354277475364322

Columns   13 thru   16

0.055695269997836	0.442327720974760	0.000000062935863	0.000000023401460
1.054725415986520	0.774124291943072	0.000000185502897	0.000000034069636
1.722308561382118	-0.000019407837835	0.000000228602318	-0.000000000005848
1.054696889841608	-0.774156650010080	0.000000185505001	-0.000000034076903
0.056155703248249	-0.442085167094905	0.000000062876356	-0.000000023357975
-1.398552504401856	0.715440029567162	0.000000184864926	0.000000135262325
-0.671114736241579	1.934549324989554	0.000000355670087	0.000000168747469
1.278764180025200	1.446250787266384	0.000000375322853	0.000000087090492
2.020797851955622	-0.000009489273042	0.000000365105179	-0.000000000008564
1.278787564753628	-1.446277776206415	0.000000375332698	-0.000000087104036
-0.671159754995129	-1.934587167804681	0.000000355679362	-0.000000168749409
-1.398649218378172	-0.715462631210536	0.000000184864742	-0.000000135256072
-1.398552504401352	-0.715440029567734	0.000000135262325	0.000000184864926
-2.430680728566875	0.000000000000221	0.000000274769913	0.000000274769913
-0.948005594634044	0.691951847859579	0.000000228264945	0.000000147904097
0.113301266613878	0.502077392262042	0.000000194429161	0.000000061661441
0.476933360231944	0.000014469671036	0.000000187617463	-0.000000000001029
0.113409358432311	-0.502055272708493	0.000000194439722	-0.000000061664607
-0.947878152294329	-0.691949584523814	0.000000228279432	-0.000000147968493
-2.430713731461110	-0.000018700759559	0.000000274773599	-0.000000274766692
-1.398662270644685	0.715430456895194	0.000000135255963	-0.000000184858919
0.055695269997754	-0.442327720974273	0.000000023401460	0.000000062935863
-0.671114736241691	-1.934549324989491	0.000000168747469	0.000000355670087

-0.948005594633954	-0.691951847859585	0.000000147904597	0.000000228264945
-0.510696678173708	-0.000000000000073	0.000000116352257	0.000000116352257
-0.097683556218927	0.126040925492532	0.000000102019031	0.000000049827322
0.072213484424467	0.000014848073086	0.000000097244076	0.000000000004005
-0.097596866741951	-0.126017409440742	0.000000102025175	-0.000000049822798
-0.510565876229792	0.000007964302010	0.000000116361272	-0.000000116356144
-0.947927056251830	0.691943471714727	0.000000147909185	-0.000000228275343
-0.671206964862184	1.934541138573620	0.000000168738643	-0.000000355674636
0.055664712500980	0.442328765113882	0.000000023398706	-0.000000062935276
1.054725415986540	-0.774124291943245	0.000000034069636	0.000000185502897
1.278764180025399	-1.446250787266423	0.000000087090492	0.000000375322853
0.113301266613954	-0.502077392262158	0.000000061661441	0.000000194429161
-0.097683556218849	-0.126040925492638	0.000000049827322	0.000000102019031
-0.031695975782164	-0.000000000000040	0.000000042662554	0.000000042662554
0.022496072986069	0.000007436070730	0.000000040274306	0.000000000005568
-0.031681159046267	0.000009405224823	0.000000042661859	-0.000000042655901
-0.097661416969956	0.126036918486573	0.000000049825730	-0.000000102023782
0.113315881320799	0.502060981904651	0.000000061658562	-0.000000194446093
1.278736523332663	1.446240937163558	0.000000087084848	-0.000000375340651
1.054707643283774	0.774128969533544	0.000000034067477	-0.000000185505561
1.722308561382240	0.000019407837799	-0.000000000005848	0.000000228602318
2.020797851955562	0.000009489273158	-0.000000000008564	0.000000365105179
0.476933360231993	-0.000014469671114	-0.000000000001029	0.000000187617463
0.072213484424441	-0.000014848073155	0.000000000004005	0.000000097244076
0.022496072986053	-0.000007436070751	0.000000000005568	0.000000040274306
0.038084815153159	0.000000000000016	0.000000000003256	0.000000000003256
0.027423473734669	0.000002682327763	-0.000000000002110	-0.000000040271899
0.072095874396291	-0.000001178377796	-0.000000000008481	-0.000000097251935
0.476825916420533	-0.000010382890527	-0.000000000012581	-0.000000187635601
2.020802135699542	-0.000022073253308	-0.000000000008639	-0.000000365121322
1.722372663740620	-0.000011853918696	0.000000000000549	-0.000000228602770
1.054696889841275	0.774156650009603	-0.000000034076903	0.000000185505001
1.278787564752374	1.446277776206351	-0.000000087104036	0.000000375332698
0.113409358432278	0.502055272708476	-0.000000061664607	0.000000194439722
-0.097596866741891	0.126017409440699	-0.000000049822798	0.000000102025175
-0.031681159046267	-0.000009405224826	-0.000000042655901	0.000000042661859
0.022423473734635	-0.000002682327734	-0.000000040271899	-0.000000000002110
-0.031827054822486	-0.000000003000004	-0.000000042668428	-0.000000042668428
-0.097815147074866	-0.126035947850539	-0.000000049841909	-0.000000102036742
0.113238102122592	-0.502079101683621	-0.000000061678466	-0.000000194452832
1.278911058733216	-1.446283181626264	-0.000000087088999	-0.000000375328329
1.054842840966423	-0.774147707812960	-0.000000034061683	-0.000000185495822
0.056155703248174	0.442085167095147	-0.000000023357975	0.000000062875356
-0.671159751995108	1.934587167804781	-0.000000168749409	0.000000355679362
-0.947878152294355	0.691949584523820	-0.000000147908493	0.000000228279432
-0.510565876229830	-0.000007964302086	-0.000000116356144	0.000000116361272
-0.097661416969920	-0.126036918486620	-0.000000102023782	0.000000049825730
0.072095874396315	0.000001178377743	-0.000000097251935	-0.000000000008481

D-8

-0.097815147074759	0.126035947850508	-0.000000102036742	-0.000000049841909
-0.510775582484897	-0.000000000000058	-0.000000116373050	-0.000000116373050
-0.947429671096340	-0.691703355964984	-0.000000147864668	-0.000000228214132
-0.670778775922084	-1.934576404055079	-0.000000168709881	-0.000000355641357
0.055765964652504	-0.442334855758409	-0.000000023391910	-0.000000062927679
-1.398649218377215	0.715462631210438	-0.000000135256072	0.000000184864742
-2.430713736146323	0.000018700759278	-0.000000274766692	0.000000274773599
-0.947927056251928	-0.691943471714740	-0.000000228275343	0.000000147909185
0.113315881320801	-0.502060981904681	-0.000000194446093	0.000000061658562
0.476825916420583	0.000010382890462	-0.000000187635601	-0.000000000012581
0.113238102122620	0.502079101683572	-0.000000194452832	-0.000000061678466
-0.947429671096230	0.691703355964971	-0.000000228214132	-0.000000147864668
-2.431537457020776	-0.000000000000098	-0.000000274860091	-0.000000274860091
-1.398271056635136	-0.715448520430300	-0.000000135220658	-0.000000184826330
-1.398662270644793	-0.715430456895114	-0.000000184858919	0.000000135255963
-0.671206964862211	-1.934541138573725	-0.000000355674636	0.000000168738643
1.278736523332616	-1.446240937163663	-0.000000375340651	0.000000087084848
2.020802135699540	0.000022073253276	-0.000000365121322	-0.000000000008639
1.278911058733225	1.446283181626308	-0.000000375328329	-0.000000087088999
-0.670778775922133	1.934576404055068	-0.000000355641357	-0.000000168709881
-1.398271056635268	0.715448520430267	-0.000000184826330	-0.000000135220658
0.055664712501009	-0.442328765113883	-0.000000062935276	0.000000023398706
1.054707643283812	-0.774128969533567	-0.000000185505561	0.000000034067477
1.722372663740719	0.000011853918704	-0.000000228602770	0.000000000000549
1.054842840966318	0.774147707885948	-0.000000185495822	-0.000000034061683
0.055765964652509	0.442334855758396	-0.000000062927679	-0.000000023391910

Columns   17 thru   20

0.000000069056158	0.000000063587216	0.000000074609541	0.000000034254216
0.000000169494412	0.000000091249738	0.000000241387612	0.000000040860634
0.000000197821034	0.000000000003978	0.000000307531506	-0.000000000009066
0.000000169500213	-0.000000091248296	0.000000241389207	-0.000000040871874
0.000000068988270	-0.000000063492895	0.000000074578447	-0.000000034192458
0.000000185582515	0.000000281320953	0.000000089951912	0.000000154689732
0.000000237414818	0.000000358794102	0.000000290286991	0.000000127203888
0.000000153274816	0.000000182328770	0.000000360513969	0.000000029284867
0.000000110871291	0.000000000013567	0.000000360003728	-0.000000000013209
0.000000153273824	-0.000000182312108	0.000000360517156	-0.000000029305805
0.000000237426659	-0.000000358805973	0.000000290293077	-0.000000127206824
0.000000185601011	-0.000000281344066	0.000000089956527	-0.000000154679801
0.000000185582515	0.000000281320953	-0.000000089951912	0.000000212255687
0.000000169493293	0.000000421716083	0.000000000000000	0.000000145915900
-0.000000050038327	0.000000198629415	0.000000080989375	-0.000000084858372
-0.000000144473398	0.000000069854347	0.000000080761143	-0.000000097054815
-0.000000164604346	0.000000000007573	0.000000078556385	-0.000000000001465
-0.000000144489488	-0.000000069838798	0.000000080761996	0.000000097049889
-0.000000050056095	-0.000000198618852	0.000000080992051	0.000000084851798

0.000000169502657	-0.000000421729712	0.000000000006005	-0.000000145911223
0.000000185602218	-0.000000281338731	-0.000000089947927	-0.000000212246018
0.000000069056158	0.000000063587216	-0.000000074609541	0.000000091551046
0.000000237414818	0.000000358794102	-0.000000290286991	0.000000278651194
-0.000000050038327	0.000000198629415	-0.000000080989375	-0.000000118733581
-0.000000192114494	0.000000075894223	0.000000000000000	-0.000000252912115
-0.000000234787364	0.000000024713463	0.000000009107023	-0.000000174754451
-0.000000243514074	-0.000000000003047	0.000000006449715	0.000000000006402
-0.000000234801193	-0.000000024713535	0.000000009106432	0.000000174761460
-0.000000192135184	-0.000000075880194	-0.000000000000606	0.000000252905199
-0.000000050050022	-0.000000198606885	-0.000000080988577	0.000000118716105
0.000000237431292	-0.000000358787982	-0.000000290283547	-0.000000278658209
0.000000069061344	-0.000000063588930	-0.000000074608815	-0.000000091549845
0.000000169494412	0.000000091249738	-0.000000241387612	0.000000224500152
0.000000153274816	0.000000182328770	-0.000000360513969	0.000000153136510
-0.000000144473398	0.000000069854347	-0.000000080761143	-0.000000278564248
-0.000000234787364	0.000000024713463	-0.000000009107023	-0.000000346355487
-0.000000256200421	0.000000005733111	0.000000000000000	-0.000000221473137
-0.000000257836099	-0.000000000009519	-0.000000002657606	0.000000000008907
-0.000000256203678	-0.000000005743489	-0.000000000001522	0.000000221483559
-0.000000234792388	-0.000000024701821	-0.000000009109569	0.000000346347195
-0.000000144477232	-0.000000069819205	-0.000000080763720	0.000000278536287
0.000000153278808	-0.000000182292237	-0.000000360514696	-0.000000153164517
0.000000169497524	-0.000000091243702	-0.000000241387207	-0.000000224503490
0.000000197821034	0.000000000003978	-0.000000307531506	0.000000261248711
0.000000110871291	0.000000000013567	-0.000000360003728	0.000000084932164
-0.000000164604346	0.000000000007573	-0.000000078556385	-0.000000324744758
-0.000000243514074	-0.000000000003047	-0.000000006449715	-0.000000377498731
-0.000000257836099	-0.000000000009519	0.000000002657606	-0.000000237045796
-0.000000257102671	-0.000000000007787	0.000000000000000	0.000000000005404
-0.000000257825923	0.000000000002242	0.000000002655748	0.000000237049812
-0.000000243497709	0.000000000016699	-0.000000006453010	0.000000377485834
-0.000000164589768	0.000000000027750	-0.000000078560274	0.000000324715201
0.000000110869327	0.000000000020727	-0.000000360006855	-0.000000084957218
0.000000197811063	-0.000000000000738	-0.000000307532200	-0.000000261248107
0.000000169500213	-0.000000091248296	-0.000000241389207	0.000000224502132
0.000000153273834	-0.000000182312108	-0.000000360517156	0.000000153149972
-0.000000144489488	-0.000000069838798	-0.000000080761996	-0.000000278547638
-0.000000234801193	-0.000000024713535	-0.000000009106432	-0.000000346345196
-0.000000256203678	-0.000000005743489	0.000000000001522	-0.000000221473623
-0.000000257825923	0.000000000002242	-0.000000002655748	-0.000000000002890
-0.000000256182684	0.000000005752905	0.000000000000000	0.000000221463849
-0.000000234768672	0.000000024733783	-0.000000009109132	0.000000346326897
-0.000000144464292	0.000000069863969	-0.000000080765187	0.000000278526589
0.000000153254243	0.000000182306480	-0.000000360519651	-0.000000153141846
0.000000169477770	0.000000091232445	-0.000000241389748	-0.000000224486329
0.000000068988270	-0.000000063492895	-0.000000074578447	0.000000091465935
0.000000237426659	-0.000000358805973	-0.000000290293077	0.000000278662610

-0.000000050056095   -0.000000198618852   -0.000000080992051   -0.000000118710962
-0.000000192135184   -0.000000075880194   0.000000000000606   -0.000000252896755
-0.000000234792388   -0.000000024701821   0.000000009109569   -0.000000174755886
-0.000000243497709   0.000000000016699   0.000000006453010   -0.000000000012893
-0.000000234768672   0.000000024733783   0.000000009109132   0.000000174731098
-0.000000192102695   0.000000075903882   0.000000000000000   0.000000252878421
-0.000000050122427   0.000000198511129   -0.000000080959900   0.000000118804668
 0.000000237369277   0.000000358734023   -0.000000290291998   -0.000000278600898
 0.000000069046436   0.000000063575193   -0.000000074610456   -0.000000091536774
 0.000000185601011   -0.000000281344066   -0.000000089956527   0.000000212253710
 0.000000169502657   -0.000000421729712   -0.000000000006005   0.000000145921382
-0.000000050050022   -0.000000198606885   0.000000080988577   -0.000000084849570
-0.000000144477232   -0.000000069819205   0.000000080763720   -0.000000097058103
-0.000000164589768   0.000000000027750   0.000000078560274   -0.000000000019660
-0.000000144464292   0.000000069863969   0.000000080765187   0.000000097026917
-0.000000050122427   0.000000198511129   0.000000080959900   0.000000084912795
 0.000000169627731   0.000000421893722   0.000000000000000   -0.000000146036747
 0.000000185544553   0.000000281269331   -0.000000089953417   -0.000000212192252
 0.000000185602218   -0.000000281338731   0.000000089947927   0.000000154679874
 0.000000237431292   -0.000000358787982   0.000000290283547   0.000000127191573
 0.000000153278808   -0.000000182292237   0.000000360514696   0.000000029276932
 0.000000110869327   0.000000000020727   0.000000360006855   -0.000000000014596
 0.000000153254243   0.000000182306480   0.000000360519651   -0.000000029285448
 0.000000237369277   0.000000358734023   0.000000290291998   -0.000000127147719
 0.000000185544553   0.000000281269331   0.000000089953417   -0.000000154624476
 0.000000069061344   -0.000000063588930   0.000000074608815   0.000000034250125
 0.000000169497524   -0.000000091243702   0.000000241387207   0.000000040857336
 0.000000197811063   -0.000000000000738   0.000000307532200   -0.000000000000157
 0.000000169477770   0.000000091232445   0.000000241389748   -0.000000040849778
 0.000000069046436   0.000000063575193   0.000000074610456   -0.000000034239869

Columns   21 thru   24
 0.000000091551046   0.000000076678795   0.000000038723323   0.000000085766262
 0.000000224500152   0.000000122896857   0.000000192569748   0.000000174555404
 0.000000261248711   -0.000000000007540   0.000000273864562   0.000000189699774
 0.000000224502132   -0.000000122907121   0.000000192573156   0.000000174562355
 0.000000091465935   -0.000000076595574   0.000000038756459   0.000000085677037
 0.000000212255687   0.000000252858900   -0.000000089945730   0.000000178231364
 0.000000278651194   0.000000430416473   0.000000091319719   0.000000108308110
 0.000000153136510   0.000000269449182   0.000000310633472   -0.000000060756107
 0.000000084932164   -0.000000000009246   0.000000380061855   -0.000000121961372
 0.000000153149972   -0.000000269465147   0.000000310630266   -0.000000060756806
 0.000000278662610   -0.000000430422956   0.000000091324272   0.000000108322628
 0.000000212253710   -0.000000252856315   -0.000000089934900   0.000000178253357
 0.000000154689732   0.000000089945730   -0.000000252858900   0.000000178231364
 0.000000145915900   0.000000296820429   -0.000000296820429   -0.000000021351363
-0.000000118733581   0.000000253157462   -0.000000048252969   -0.000000287429443

-0.000000278564248	0.000000134645121	0.000000089677528	-0.000000290091017
-0.000000324744758	0.000000000000401	0.000000135151200	-0.000000259736647
-0.000000278547638	-0.000000134645952	0.000000089664066	-0.000000290109507
-0.000000118710962	-0.000000253161078	-0.000000048269316	-0.000000287449649
0.000000145921382	-0.000000296820885	-0.000000296818195	-0.000000021339820
0.000000154679874	-0.000000089942959	-0.000000252846765	0.000000178254580
0.000000034254216	-0.000000038723323	-0.000000076678795	0.000000085766262
0.000000127203888	-0.000000091319719	-0.000000430416473	0.000000108308110
-0.000000084858372	0.000000048252969	-0.000000253157462	-0.000000287429443
-0.000000252912115	0.000000085971102	-0.000000085971102	-0.000000229315446
-0.000000346355487	0.000000059638164	0.000000004457907	-0.000000044715321
-0.000000377498731	0.000000000005346	0.000000034596368	0.000000039395809
-0.000000346345196	-0.000000059631135	0.000000004447291	-0.000000044731289
-0.000000252896755	-0.000000085973150	-0.000000085987238	-0.000000229339306
-0.000000084849570	-0.000000048263362	-0.000000253167634	-0.000000287442793
0.000000127191573	0.000000091312088	-0.000000430406325	0.000000108327457
0.000000034250125	0.000000038723169	-0.000000076675254	0.000000085772297
0.000000040860634	-0.000000192569748	-0.000000122896857	0.000000174555404
0.000000029284867	-0.000000310633472	-0.000000269449182	-0.000000060756107
-0.000000097054815	-0.000000089677528	-0.000000134645121	-0.000000290091017
-0.000000174754451	-0.000000004457907	-0.000000059638164	-0.000000044715321
-0.000000221473137	0.000000014425465	-0.000000014425465	0.000000237673587
-0.000000237045796	0.000000000006067	0.000000000644604	0.000000354386075
-0.000000221473623	-0.000000014417676	-0.000000014427042	0.000000237669856
-0.000000174755886	0.000000004454563	-0.000000059640403	-0.000000044721082
-0.000000097058103	0.000000089661985	-0.000000134646206	-0.000000290095438
0.000000029276932	0.000000310615663	-0.000000269444856	-0.000000060751584
0.000000040857336	0.000000192566534	-0.000000122894204	0.000000174558908
-0.000000000009066	-0.000000273864562	0.000000000007540	0.000000189699774
-0.000000000013209	-0.000000380061855	0.000000000009246	-0.000000121961372
-0.000000000001465	-0.000000135151200	-0.000000000000401	-0.000000259736647
0.000000000006402	-0.000000034596368	-0.000000000005346	0.000000039395809
0.000000000008907	-0.000000000644604	-0.000000000006067	0.000000354386075
0.000000000005404	0.000000000002831	-0.000000000002831	0.000000481971990
-0.000000000002890	0.000000000646567	0.000000000003187	0.000000354397956
-0.000000000012893	0.000000034589140	0.000000000009898	0.000000039414894
-0.000000000019660	0.000000135135010	0.000000000014303	-0.000000259719712
-0.000000000014596	0.000000380048569	0.000000000011564	-0.000000121963907
-0.000000000000157	0.000000273865270	0.000000000001435	0.000000189687957
-0.000000040871874	-0.000000192573156	0.000000122907121	0.000000174562355
-0.000000029305805	-0.000000310630266	0.000000269465147	-0.000000060756806
0.000000097049889	-0.000000089664066	0.000000134645952	-0.000000290109507
0.000000174761460	-0.000000004447291	0.000000059631135	-0.000000044731289
0.000000221483559	0.000000014427042	0.000000014417676	0.000000237669856
0.000000237049812	-0.000000000003187	-0.000000000646567	0.000000354397956
0.000000221463849	-0.000000014435136	0.000000014435136	0.000000237694346
0.000000174731098	0.000000004435942	0.000000059658610	-0.000000044693366
0.000000097026917	0.000000089653600	0.000000134668610	-0.000000290080166

-0.000000029285448   0.000000310640099   0.000000269453705 -0.000000060779793
-0.000000040849778   0.000000192584644   0.000000122891180   0.000000174536085
-0.000000034192458 -0.000000038756459   0.000000076595574   0.000000085677037
-0.000000127206824 -0.000000091324272   0.000000430422956   0.000000108322628
 0.000000084851798   0.000000048269316   0.000000253161078 -0.000000287449649
 0.000000252905199   0.000000085987238   0.000000085973150 -0.000000229339306
 0.000000346347195   0.000000059640403 -0.000000004454563 -0.000000044721082
 0.000000377485834 -0.000000000009898 -0.000000034589140   0.000000039414894
 0.000000346326897 -0.000000059658610 -0.000000004435942 -0.000000044693366
 0.000000252878421 -0.000000085998767   0.000000085998767 -0.000000229301305
 0.000000084912795 -0.000000048230416   0.000000253081897 -0.000000287536989
-0.000000127147719   0.000000091369140   0.000000430378806   0.000000108255898
-0.000000034239869   0.000000038736509   0.000000076668993   0.000000085755052
-0.000000154679801   0.000000089934900   0.000000252856315   0.000000178253357
-0.000000145911223   0.000000296818195   0.000000296820885 -0.000000021339820
 0.000000118716105   0.000000253167634   0.000000048263362 -0.000000287442793
 0.000000278536287   0.000000134646206 -0.000000089661985 -0.000000290095438
 0.000000324715201 -0.000000000014303 -0.000000135135010 -0.000000259719712
 0.000000278526589 -0.000000134668610 -0.000000089653600 -0.000000290080166
 0.000000118804668 -0.000000253081897   0.000000048230416 -0.000000287536989
-0.000000146036747 -0.000000296913812   0.000000296913812 -0.000000021167796
-0.000000154624476 -0.000000089892670   0.000000252810034   0.000000178187839
-0.000000212246018   0.000000252846765   0.000000089942959   0.000000178254580
-0.000000278658209   0.000000430406325 -0.000000091312088   0.000000108327457
-0.000000153164517   0.000000269444856 -0.000000310615663 -0.000000060751584
-0.000000084957218 -0.000000000011564 -0.000000380048569 -0.000000121963907
-0.000000153141846 -0.000000269453705 -0.000000310640099 -0.000000060779793
-0.000000278600898 -0.000000430378806 -0.000000091369140   0.000000108255898
-0.000000212192252 -0.000000252810034   0.000000089892670   0.000000178187839
-0.000000091549845   0.000000076675254 -0.000000038723169   0.000000085772297
-0.000000224503490   0.000000122894204 -0.000000192566534   0.000000174558908
-0.000000261248107 -0.000000000001435 -0.000000273865270   0.000000189687957
-0.000000224486329 -0.000000122891180 -0.000000192584644   0.000000174536085
-0.000000091536774 -0.000000076668993 -0.000000038736509   0.000000085755052

Columns   25 thru   28
0.000000094964921   0.000000082416018   0.000000010378504   0.000000102879831
0.000000254888776   0.000000096130842   0.000000196542227   0.000000180051515
0.000000303440569   0.000000000005119   0.000000320942640 -0.000000000004514
0.000000254892809 -0.000000096129030   0.000000196536911 -0.000000180059041
0.000000094925981 -0.000000082292058   0.000000010464304 -0.000000102823416
0.000000089884365   0.000000279030110 -0.000000260612496   0.000000166402298
0.000000175551727   0.000000202585712 -0.000000125058506   0.000000449951693
0.000000042880048   0.000000011127118   0.000000238290607   0.000000336379632
-0.000000051447822   0.000000000017521   0.000000376564462 -0.000000000002207
0.000000042887476 -0.000000011105644   0.000000238294964 -0.000000336385910
0.000000175563791 -0.000000202601192 -0.000000125066895 -0.000000449960495

0.000000089891559	-0.000000279060098	-0.000000260630518	-0.000000166407555
-0.000000089884365	0.000000279030110	-0.000000260612496	-0.000000166402298
0.000000000000000	0.000000113865141	-0.000000452943861	0.000000000000000
-0.000000117016431	-0.000000278731361	-0.000000176655580	0.000000160939244
-0.000000339818706	-0.000000246405826	0.000000021113062	0.000000116776848
-0.000000430792198	0.000000000009796	0.000000088873884	0.000000000003365
-0.000000339816971	0.000000246425933	0.000000021133204	-0.000000116771703
-0.000000117012389	0.000000278744993	-0.000000176631832	-0.000000160938717
0.000000000006337	-0.000000113882857	-0.000000452950012	-0.000000000004350
-0.000000089881603	-0.000000279053159	-0.000000260632950	0.000000166400071
-0.000000094964921	0.000000082416018	0.000000010378504	-0.000000102879831
-0.000000175551727	0.000000202585712	-0.000000125058506	-0.000000449951 6′
0.000000117016431	-0.000000278731361	-0.000000176655580	-0.00000016093924
0.000000000000000	-0.000000410209850	-0.000000095165491	0.000000000000000
-0.000000209206916	-0.000000266788044	-0.000000018202788	0.000000029315524
-0.000000300812587	-0.000000000003932	0.000000013456582	0.000000000003453
-0.000000209208022	0.000000266787972	-0.000000018186634	-0.000000029310055
-0.000000000001848	0.000000410228024	-0.000000095141117	0.000000000001852
0.000000117014748	0.000000278760530	-0.000000176640945	0.000000160937296
-0.000000175552159	-0.000000202577792	-0.000000125075692	0.000000449949789
-0.000000094964928	-0.000000082418235	0.000000010372810	0.000000102880074
-0.000000254888776	0.000000096130842	0.000000196542227	-0.000000180051515
-0.000000042880048	0.000000011127118	0.000000238290607	-0.000000336379632
0.000000339818706	-0.000000246405826	0.000000021113062	-0.000000116776848
0.000000209206916	-0.000000266788044	-0.000000018202788	-0.000000029315524
0.000000000000000	-0.000000164244356	-0.000000005906369	0.000000000000000
-0.000000091606207	-0.000000000012299	0.000000004192018	0.000000000001730
-0.000000000002539	0.000000164230968	-0.000000005903608	0.000000000002188
0.000000209202549	0.000000266803155	-0.000000018198663	0.000000029314592
0.000000339813935	0.000000246451353	0.000000021115785	0.000000116773031
-0.000000042882745	-0.000000011079789	0.000000238285453	0.000000336377341
-0.000000254888675	-0.000000096123013	0.000000196538915	0.000000180052603
-0.000000303440569	0.000000000005119	0.000000320942640	0.000000000004514
0.000000051447822	0.000000000017521	0.000000376564462	0.000000000002207
0.000000430792198	0.000000000009796	0.000000088873884	-0.000000000003365
0.000000300812587	-0.000000000003932	0.000000013456582	-0.000000000003453
0.000000091606207	-0.000000000012299	0.000000004192018	-0.000000000001730
0.000000000000000	-0.000000000010051	0.000000007096894	0.000000000000000
0.000000091603306	0.000000000002934	0.000000004178490	0.000000000000624
0.000000300807844	0.000000000021651	0.000000013434666	-0.000000000000274
0.000000430787732	0.000000000035965	0.000000088853863	-0.000000000002415
0.000000051447497	0.000000000026898	0.000000376565261	-0.000000000005134
-0.000000303438363	-0.000000000000914	0.000000320954585	-0.000000000002757
-0.000000254892809	-0.000000096129030	0.000000196536911	0.000000180059041
-0.000000042887476	-0.000000011105644	0.000000238294964	0.000000336385910
0.000000339816971	0.000000246425933	0.000000021133204	0.000000116771703
0.000000209208022	0.000000266787972	-0.000000018186634	0.000000029310055
0.000000000002539	0.000000164230968	-0.000000005903608	-0.000000000002188

-0.000000091603306	0.000000000002934	0.000000004178490	-0.000000000000624
0.000000000000000	-0.000000164218723	-0.000000005929785	0.000000000000000
0.000000209204350	-0.000000266761725	-0.000000018227310	-0.000000029314367
0.000000339814970	-0.000000246393341	0.000000021101292	-0.000000116777246
-0.000000042882196	0.000000011098326	0.000000238317977	-0.000000336387167
-0.000000254888439	0.000000096108493	0.000000196564108	-0.000000180056961
-0.000000094925981	-0.000000082292058	0.000000010464304	0.000000102823416
-0.000000175563791	-0.000000202601192	-0.000000125066895	0.000000449960495
0.000000117012389	0.000000278744993	-0.000000176631832	0.000000160938717
0.000000000001848	0.000000410228024	-0.000000095141117	-0.000000000001852
-0.000000209202549	0.000000266803155	-0.000000018198663	-0.000000029314592
-0.000000300807844	0.000000000021651	0.000000013434666	0.000000000000274
-0.000000209204350	-0.000000266761725	-0.000000018227310	0.000000029314367
0.000000000000000	-0.000000410197341	-0.000000095180195	0.000000000000000
0.000000117055985	-0.000000278886363	-0.000000176548260	-0.000000160881448
-0.000000175553554	0.000000202507943	-0.000000124995901	-0.000000449957992
-0.000000094965022	0.000000082400458	0.000000010391678	-0.000000102881490
-0.000000089891559	-0.000000279060098	-0.000000260630518	0.000000166407555
-0.000000000006337	-0.000000113882857	-0.000000452950012	0.000000000004350
-0.000000117014748	0.000000278760530	-0.000000176640945	-0.000000160937296
-0.000000339813935	0.000000246451353	0.000000021115785	-0.000000116773031
-0.000000430787732	0.000000000035965	0.000000088853863	0.000000000002415
-0.000000339814970	-0.000000246393341	0.000000021101292	0.000000116777246
-0.000000117055985	-0.000000278886363	-0.000000176548260	0.000000160881448
0.000000000000000	0.000000114099776	-0.000000453103508	0.000000000000000
-0.000000089884851	0.000000278963263	-0.000000260560050	-0.000000166404273
0.000000089881603	-0.000000279053159	-0.000000260632950	-0.000000166400071
0.000000175552159	-0.000000202577792	-0.000000125075692	-0.000000449949789
0.000000042882745	-0.000000011079789	0.000000238285453	-0.000000336377341
-0.000000051447497	0.000000000026898	0.000000376565261	0.000000000005134
0.000000042882196	0.000000011098326	0.000000238317977	0.000000336387167
0.000000175553554	0.000000202507943	-0.000000124995901	0.000000449957992
0.000000089884851	0.000000278963263	-0.000000260560050	0.000000166404273
0.000000094964928	-0.000000082418235	0.000000010372810	-0.000000102880074
0.000000254888675	-0.000000096123013	0.000000196538915	-0.000000180052603
0.000000303438363	-0.000000000000914	0.000000320954585	0.000000000002757
0.000000254888439	0.000000096108493	0.000000196564108	0.000000180056961
0.000000094965022	0.000000082400458	0.000000010391678	0.000000102881490

Appendix E. Steady-State Kalman Filter Gain Matrix

This appendix lists the elements of the steady-state Kalman filter gain matrix, *K*, for the 28 state filter model with correlated states. The *K* matrix was generated as output from MSOFE after the system had reached steady-state. *K* has dimensions 28 x 138.

K   =

Columns   1 thru   4
```
-0.059943348169327    0.036650460213423    0.083679191768169    0.128526076674461
 0.019283980131149    0.073402099311352    0.057799868285656    0.016275893896818
 0.100572660565376   -0.036880090832710   -0.336197853088370   -0.129910886287689
 0.259788483381271    0.855362594127655    0.837016940116882    0.316500037908554
-0.207298308610916    0.054775301367044    0.861950099468231    0.193780660629272
 0.042516980320215   -0.107836194336414    0.245319142937660    0.232317194342613
 0.165758341550827   -0.101347669959068   -0.231393888592720   -0.355406761169434
 0.113991886377335    0.217648208141327    0.436197042465210    0.253728240728378
-0.183141902089119    0.111976265907288    0.255661070346832    0.392679244279861
-0.002394271548837   -0.008902597241104    0.085813738405704   -0.030975667759776
 0.109832778573036   -0.003532463219017   -0.659467041492462   -0.013885100372136
 0.031838972121477   -0.427666515111923    0.335355520248413    0.426667988300323
-0.043286655098200    0.021511206403375    0.099847115576267    0.075552277266979
 0.031441416591406    0.264602810144424    0.030887544155121   -0.079028293490410
 0.000000000000000    0.000000000000000    0.000000000000000    0.000000000000000
 0.000000000000000    0.000000000000000    0.000000000000000    0.000000000000000
 0.000000000000000    0.000000000000000    0.000000000000000    0.000000000000000
 0.000000000000000    0.000000000000000    0.000000000000000    0.000000000000000
 0.000000000000000    0.000000000000000    0.000000000000000    0.000000000000000
 0.000000000000000    0.000000000000000    0.000000000000000    0.000000000000000
 0.000000000000000    0.000000000000000    0.000000000000000    0.000000000000000
 0.000000000000000    0.000000000000000    0.000000000000000    0.000000000000000
 0.000000000000000    0.000000000000000    0.000000000000000    0.000000000000000
 0.000000000000000    0.000000000000000    0.000000000000000    0.000000000000000
 0.000000000000000    0.000000000000000    0.000000000000000    0.000000000000000
 0.000000000000000    0.000000000000000    0.000000000000000    0.000000000000000
 0.000000000000000    0.000000000000000    0.000000000000000    0.000000000000000
 0.000000000000000    0.000000000000000    0.000000000000000    0.000000000000000
```

Columns   5 thru   8
```
 0.148104652762413   -0.034875307232141    0.108128763735294    0.001906691584736
-0.000641763501335    0.080314584076405    0.296803027391434    0.427406609058380
 0.058290030807257    0.553611814975739    0.204882711172104   -0.903635799884796
 0.052979201078415    0.835386991500854    0.936599314212799    1.071691632270813
```

E-1

```
-0.384910017251968   -0.071806930005550   -0.534099578857422    0.347911506891251
 0.123073972761631    0.123826980590820   -0.373319000005722   -0.644633114337921
-0.409546375274658    0.096438929438591   -0.299003064632416   -0.005272442940623
 0.096033990383148   -0.293364107608795   -0.100267767906189   -0.017645852640271
 0.452496409416199   -0.106552809476852    0.330360800027847    0.005825454834849
-0.123299390077591   -0.086819574236870   -0.140162155032158    0.190819323062897
 0.521650016307831   -0.205270484089851    0.571102857589722    0.040917377918959
 0.252309232950211   -0.291535228490829   -0.257840931415558   -0.265725702047348
 0.045187201350927    0.142540797591209    0.039903394877911   -0.226822569966316
-0.067947573959827   -0.437117725610733   -0.707887649536133   -0.902477562427521
 0.000000000000000    0.000000000000000    0.000000000000000    0.000000000000000
 0.000000000000000    0.000000000000000    0.000000000000000    0.000000000000000
 0.000000000000000    0.000000000000000    0.000000000000000    0.000000000000000
 0.000000000000000    0.000000000000000    0.000000000000000    0.000000000000000
 0.000000000000000    0.000000000000000    0.000000000000000    0.000000000000000
 0.000000000000000    0.000000000000000    0.000000000000000    0.000000000000000
 0.000000000000000    0.000000000000000    0.000000000000000    0.000000000000000
 0.000000000000000    0.000000000000000    0.000000000000000    0.000000000000000
 0.000000000000000    0.000000000000000    0.000000000000000    0.000000000000000
 0.000000000000000    0.000000000000000    0.000000000000000    0.000000000000000
 0.000000000000000    0.000000000000000    0.000000000000000    0.000000000000000
 0.000000000000000    0.000000000000000    0.000000000000000    0.000000000000000
 0.000000000000000    0.000000000000000    0.000000000000000    0.000000000000000
```

Columns   9 thru   12
```
-0.057783313095570   -0.028320169076324    0.051033440977335    0.063230849802494
 0.303228735923767    0.058082934468985   -0.163352265954018   -0.137169763445854
-1.270150303840637   -1.165383100509644   -1.073284745216370   -0.393444120883942
 0.943836271762848    0.794638037681580    0.844267129898071    0.395260334014893
 0.742558181285858    0.577750384807587    0.208731055259705   -0.110177688300610
-0.386440068483353    0.163151398301125    0.730831444263458    0.492493510246277
 0.159785315394402    0.078312359750271   -0.141120254993439   -0.174849063158035
-0.096472315490246   -0.299306154251099   -0.566881000995636   -0.332513660192490
-0.176542997360229   -0.086525827646255    0.155920103192329    0.193186357617378
 0.322182923555374    0.273564308881760    0.183114573359489    0.027386520057917
-0.265730828046799   -0.111779727041721    0.309323042631149    0.351416885852814
-0.258453816175461   -0.283427745103836   -0.376255005598068   -0.196410536766052
-0.312402874231339   -0.289256453514099   -0.274583280086517   -0.105382815003395
-0.717711031436920   -0.396502941846848   -0.184172526001930   -0.022285683080554
 0.000000000000000    0.000000000000000    0.000000000000000    0.000000000000000
 0.000000000000000    0.000000000000000    0.000000000000000    0.000000000000000
 0.000000000000000    0.000000000000000    0.000000000000000    0.000000000000000
 0.000000000000000    0.000000000000000    0.000000000000000    0.000000000000000
 0.000000000000000    0.000000000000000    0.000000000000000    0.000000000000000
 0.000000000000000    0.000000000000000    0.000000000000000    0.000000000000000
```

0.000000000000000   0.000000000000000   0.000000000000000   0.000000000000000

0.000000000000000	0.000000000000000	0.000000000000000	0.000000000000000
0.000000000000000	0.000000000000000	0.000000000000000	0.000000000000000
0.000000000000000	0.000000000000000	0.000000000000000	0.000000000000000
0.000000000000000	0.000000000000000	0.000000000000000	0.000000000000000
0.000000000000000	0.000000000000000	0.000000000000000	0.000000000000000
0.000000000000000	0.000000000000000	0.000000000000000	0.000000000000000
0.000000000000000	0.000000000000000	0.000000000000000	0.000000000000000
0.000000000000000	0.000000000000000	0.000000000000000	0.000000000000000

Columns   13 thru   16

0.028429495170712	0.137737929821014	0.088154487311840	0.020338043570518
-0.036476179957390	0.530923962593079	0.708198904991150	0.895513653755188
0.249380111694336	0.735867857933044	0.493956625461578	0.179965853691101
0.279238462448120	0.250472187995911	0.105642728507519	0.034244339913130
-0.128043532371521	-0.670823037624359	-0.426880359649658	-0.091433495283127
0.431872069835663	-0.199142530560493	-0.587921202182770	-0.883560001850128
-0.078614711761475	-0.380879878997803	-0.243769139051437	-0.056239724159241
-0.494461238384247	-0.729645609855652	-0.553575634956360	-0.517499387264252
0.086859315633774	0.420824915170670	0.269333779811859	0.062137674540281
0.007680253125727	-0.090190932154655	-0.051522787660360	0.005915968678892
-0.093837112188339	0.189412429928780	0.089879713952541	-0.069261305034161
-0.186764165759087	0.131629720330238	0.312544137239456	0.454765111207962
-0.017076525837183	0.001478445134126	-0.003152766497806	-0.012494925409555
0.244834423065186	0.318924129009247	0.219840541481972	0.188599780201912
0.000000000000000	0.000000000000000	0.000000000000000	0.000000000000000
0.000000000000000	0.000000000000000	0.000000000000000	0.000000000000000
0.000000000000000	0.000000000000000	0.000000000000000	0.000000000000000
0.000000000000000	0.000000000000000	0.000000000000000	0.000000000000000
0.000000000000000	0.000000000000000	0.000000000000000	0.000000000000000
0.000000000000000	0.000000000000000	0.000000000000000	0.000000000000000
0.000000000000000	0.000000000000000	0.000000000000000	0.000000000000000
0.000000000000000	0.000000000000000	0.000000000000000	0.000000000000000
0.000000000000000	0.000000000000000	0.000000000000000	0.000000000000000
0.000000000000000	0.000000000000000	0.000000000000000	0.000000000000000
0.000000000000000	0.000000000000000	0.000000000000000	0.000000000000000
0.000000000000000	0.000000000000000	0.000000000000000	0.000000000000000
0.000000000000000	0.000000000000000	0.000000000000000	0.000000000000000
0.000000000000000	0.000000000000000	0.000000000000000	0.000000000000000

Columns   17 thru   20

-0.042400766164064	-0.084010906517506	-0.111505411565304	-0.078213796019554
0.855304777622223	0.061634624004364	0.477368116378784	0.204989209771156
-0.153559103608131	-0.440279722213745	-0.712362706661224	-0.600098848342896
0.051359992474318	0.161861211061478	0.369736224412918	0.405945956707001
0.214298620820045	0.410069346427917	0.530600786209106	0.361452490091324
-0.317574620240887	-0.460160434246003	0.024831090122461	0.359346717596054

0.117248773574829	0.232311189174652	0.308340370655060	0.216280713677406
-0.528530478477478	-0.633214831352234	-0.921554088592529	-0.849805355072021
-0.129544660449028	-0.256673723459244	-0.340676605701447	-0.238962396979332
0.047444257885218	0.057315919548273	0.041552908718586	0.002061530947685
-0.157796993851662	-0.127184554934502	0.005703560076654	0.140924200415611
0.423163503408432	0.254126876592636	0.031705297529697	-0.134567558765411
-0.013463676907122	-0.002425661077723	0.019598521292210	0.031650546938181
0.196915820240974	0.262221843004227	0.416802525520325	0.401391893625259
0.000000000000000	0.000000000000000	0.000000000000000	0.000000000000000
0.000000000000000	0.000000000000000	0.000000000000000	0.000000000000000
0.000000000000000	0.000000000000000	0.000000000000000	0.000000000000000
0.000000000000000	0.000000000000000	0.000000000000000	0.000000000000000
0.000000000000000	0.000000000000000	0.000000000000000	0.000000000000000
0.000000000000000	0.000000000000000	0.000000000000000	0.000000000000000
0.000000000000000	0.000000000000000	0.000000000000000	0.000000000000000
0.000000000000000	0.000000000000000	0.000000000000000	0.000000000000000
0.000000000000000	0.000000000000000	0.000000000000000	0.000000000000000
0.000000000000000	0.000000000000000	0.000000000000000	0.000000000000000
0.000000000000000	0.000000000000000	0.000000000000000	0.000000000000000
0.000000000000000	0.000000000000000	0.000000000000000	0.000000000000000
0.000000000000000	0.000000000000000	0.000000000000000	0.000000000000000

Columns   21 thru   24

-0.015890166163445	0.175430089235306	0.144304528832436	0.071474097669125
0.004424632526934	0.226383343338966	0.620495319366455	0.697833776473999
-0.194897741079330	0.518125295639038	0.456124514341354	0.230538889765739
0.194535419344902	0.029659651219845	-0.135030671954155	-0.178520053625107
0.065637834370136	-0.666866302490234	-0.576781094074249	-0.290041923522949
0.269821852445602	0.141806587576866	-0.300286859273911	-0.422620594501495
0.043940283358097	-0.485108137130737	-0.399038136005402	-0.197643667459488
-0.359619081020355	-0.379928737878799	-0.417710810899734	-0.392919093370438
-0.048548668622971	0.535982370376587	0.440885990858078	0.218370527029037
-0.019265225157142	0.086799323558807	0.036889377981424	0.012941746041179
0.128137171268463	0.029192043468356	0.089217826724052	0.054259955883026
-0.114276096224785	-0.045095648616552	0.260898113250732	0.340801209211349
0.019441101700068	-0.229005306959152	-0.152360200881958	-0.069901868700981
0.175824254751205	0.287977308034897	0.307975083589554	0.287041813135147
0.000000000000000	0.000000000000000	0.000000000000000	0.000000000000000
0.000000000000000	0.000000000000000	0.000000000000000	0.000000000000000
0.000000000000000	0.000000000000000	0.000000000000000	0.000000000000000
0.000000000000000	0.000000000000000	0.000000000000000	0.000000000000000
0.000000000000000	0.000000000000000	0.000000000000000	0.000000000000000
0.000000000000000	0.000000000000000	0.000000000000000	0.000000000000000
0.000000000000000	0.000000000000000	0.000000000000000	0.000000000000000
0.000000000000000	0.000000000000000	0.000000000000000	0.000000000000000

0.000000000000000	0.000000000000000	0.000000000000000	0.000000000000000
0.000000000000000	0.000000000000000	0.000000000000000	0.000000000000000
0.000000000000000	0.000000000000000	0.000000000000000	0.000000000000000
0.000000000000000	0.000000000000000	0.000000000000000	0.000000000000000
0.000000000000000	0.000000000000000	0.000000000000000	0.000000000000000
0.000000000000000	0.000000000000000	0.000000000000000	0.000000000000000

Columns   25 thru   28

-0.000358588324161	-0.066946528851986	-0.121833451092243	-0.163099780678749
0.714997291564941	0.692187309265137	0.596725404262543	0.458890974521637
-0.002638861304149	-0.217745393514633	-0.386674702167511	-0.500729024410248
-0.180397495627403	-0.156108334660530	-0.106120027601719	-0.044716380536556
0.002853065729141	0.273375242948532	0.488455593585968	0.637940347194672
-0.425010412931442	-0.352422356605530	-0.213180720806122	-0.046444904059172
0.000991625129245	0.185123935341835	0.336899995803833	0.451011657714844
-0.409828782081604	-0.450186222791672	-0.470142900943756	-0.467900991439819
-0.001095912186429	-0.204538509249687	-0.372231751680374	-0.498310625553131
0.001643848489039	-0.010036038234830	-0.029324725270271	-0.058764934539795
-0.003500863676891	-0.054764401167631	-0.078764118254185	-0.068583324551582
0.344716101884842	0.300775498151779	0.208710879087448	0.094930082559586
-0.001432399963960	0.063297107815742	0.126735284924507	0.190019726753235
0.299694210290909	0.331373751163483	0.348996609449387	0.350470960140228
0.000000000000000	0.000000000000000	0.000000000000000	0.000000000000000
0.000000000000000	0.000000000000000	0.000000000000000	0.000000000000000
0.000000000000000	0.000000000000000	0.000000000000000	0.000000000000000
0.000000000000000	0.000000000000000	0.000000000000000	0.000000000000000
0.000000000000000	0.000000000000000	0.000000000000000	0.000000000000000
0.000000000000000	0.000000000000000	0.000000000000000	0.000000000000000
0.000000000000000	0.000000000000000	0.000000000000000	0.000000000000000
0.000000000000000	0.000000000000000	0.000000000000000	0.000000000000000
0.000000000000000	0.000000000000000	0.000000000000000	0.000000000000000
0.000000000000000	0.000000000000000	0.000000000000000	0.000000000000000
0.000000000000000	0.000000000000000	0.000000000000000	0.000000000000000
0.000000000000000	0.000000000000000	0.000000000000000	0.000000000000000
0.000000000000000	0.000000000000000	0.000000000000000	0.000000000000000

Columns   29 thru   32

-0.174351975321770	-0.122346013784409	0.146971493959427	0.093235105276108
0.288224965333939	0.101976461708546	0.266284942626953	0.495136260986328
-0.513648390769958	-0.341438561677933	0.310720652341843	0.208116650581360
0.012516547925770	0.038976501673460	-0.253823101520538	-0.437512069940567
0.661548674106598	0.446296691894531	-0.544442892074585	-0.361551821231842
0.100140444934368	0.145461529493332	0.111729025840759	-0.039046261459589
0.482126832008362	0.338317334651947	-0.406413018703461	-0.257818400859833
-0.410935461521149	-0.244990170001984	0.030786709859967	0.081233970820904

-0.532689929008484 -0.373797804117203   0.449034869670868   0.284856349229813
-0.087757296860218 -0.083488307893276   0.110505439341068   0.051490567624569
-0.026193792000413   0.023012768477201   0.037865202873945   0.063994728028774
-0.012542417272925 -0.065844245254993 -0.045933712273836   0.094733148813248
 0.229155376553535   0.183664724230766 -0.245755806565285 -0.137299761176109
 0.310471236705780   0.186720043420792   0.078545816242695   0.077226802706718
 0.000000000000000   0.000000000000000   0.000000000000000   0.000000000000000
 0.000000000000000   0.000000000000000   0.000000000000000   0.000000000000000
 0.000000000000000   0.000000000000000   0.000000000000000   0.000000000000000
 0.000000000000000   0.000000000000000   0.000000000000000   0.000000000000000
 0.000000000000000   0.000000000000000   0.000000000000000   0.000000000000000
 0.000000000000000   0.000000000000000   0.000000000000000   0.000000000000000
 0.000000000000000   0.000000000000000   0.000000000000000   0.000000000000000
 0.000000000000000   0.000000000000000   0.000000000000000   0.000000000000000
 0.000000000000000   0.000000000000000   0.000000000000000   0.000000000000000
 0.000000000000000   0.000000000000000   0.000000000000000   0.000000000000000
 0.000000000000000   0.000000000000000   0.000000000000000   0.000000000000000
 0.000000000000000   0.000000000000000   0.000000000000000   0.000000000000000
 0.000000000000000   0.000000000000000   0.000000000000000   0.000000000000000
 0.000000000000000   0.000000000000000   0.000000000000000   0.000000000000000

    Columns   33 thru   36
 0.045474074780941   0.003589177737013 -0.034477304667234 -0.069714389741421
 0.577420771121979   0.596641600131989   0.599313378334045   0.575464248657227
 0.104801803827286   0.008741054683924 -0.079296842217445 -0.157825455069542
-0.502643167972565 -0.519310653209686 -0.526375055313110 -0.513688564300537
-0.181188806891441 -0.014992028474808   0.137135013937950   0.273594796657562
-0.099812239408493 -0.103594556450844 -0.070111930370331 -0.008150532841682
-0.125747174024582 -0.009924964979291   0.095338366925716   0.192777708172798
 0.100009463727474   0.103383116424084   0.100546590983868   0.090794041752815
 0.138934388756752   0.010965651832521 -0.105336762964725 -0.212994709610939
 0.019537022337317   0.000747335725464 -0.015085997991264 -0.034759346395731
 0.043191067874432   0.005116064101458 -0.032159231603146 -0.055887822061777
 0.150094479322433   0.155426383018494   0.131344065070152   0.082926809787750
-0.061391647905111 -0.004051017574966   0.046818848699331   0.098922424018383
 0.074924886226654   0.077290780842304   0.087103337049484   0.100137904286385
 0.000000000000000   0.000000000000000   0.000000000000000   0.000000000000000
 0.000000000000000   0.000000000000000   0.000000000000000   0.000000000000000
 0.000000000000000   0.000000000000000   0.000000000000000   0.000000000000000
 0.000000000000000   0.000000000000000   0.000000000000000   0.000000000000000
 0.000000000000000   0.000000000000000   0.000000000000000   0.000000000000000
 0.000000000000000   0.000000000000000   0.000000000000000   0.000000000000000
 0.000000000000000   0.000000000000000   0.000000000000000   0.000000000000000
 0.000000000000000   0.000000000000000   0.000000000000000   0.000000000000000
 0.000000000000000   0.000000000000000   0.000000000000000   0.000000000000000
 0.000000000000000   0.000000000000000   0.000000000000000   0.000000000000000

0.000000000000000	0.000000000000000	0.000000000000000	0.000000000000000
0.000000000000000	0.000000000000000	0.000000000000000	0.000000000000000
0.000000000000000	0.000000000000000	0.000000000000000	0.000000000000000
0.000000000000000	0.000000000000000	0.000000000000000	0.000000000000000

Columns   37 thru   40

-0.099029645323753	-0.108785964548588	-0.080974653363228	0.072150170803070
0.515261411666870	0.391444772481918	0.199282690882683	0.462740123271942
-0.217903718352318	-0.230563536286354	-0.163031533360481	0.100124306976795
-0.470489084720612	-0.368058562278748	-0.195652469992638	-0.627463519573212
0.379400044679642	0.403828352689743	0.287969172000885	-0.268129318952560
0.068208314478397	0.127947375178337	0.124419368803501	0.184573799371719
0.273841679096222	0.300820380449295	0.223915174603462	-0.199513286352158
0.073956675827503	0.048785053193569	0.019074164330959	0.405157268047333
-0.302560001611710	-0.332368016242981	-0.247397616505623	0.220436796545982
-0.060012333095074	-0.080825649201870	-0.074687629938126	0.075480908155441
-0.056542675942183	-0.030107432976365	0.008787570521235	0.020878979936242
0.019137626513839	-0.041029725223780	-0.064159311354160	-0.104109011590481
0.151151239871979	0.180936306121979	0.149197503924370	-0.151526704430580
0.110717654228210	0.105342306196690	0.070160843431950	-0.108321256935596
0.000000000000000	0.000000000000000	0.000000000000000	0.000000000000000
0.000000000000000	0.000000000000000	0.000000000000000	0.000000000000000
0.000000000000000	0.000000000000000	0.000000000000000	0.000000000000000
0.000000000000000	0.000000000000000	0.000000000000000	0.000000000000000
0.000000000000000	0.000000000000000	0.000000000000000	0.000000000000000
0.000000000000000	0.000000000000000	0.000000000000000	0.000000000000000
0.000000000000000	0.000000000000000	0.000000000000000	0.000000000000000
0.000000000000000	0.000000000000000	0.000000000000000	0.000000000000000
0.000000000000000	0.000000000000000	0.000000000000000	0.000000000000000
0.000000000000000	0.000000000000000	0.000000000000000	0.000000000000000
0.000000000000000	0.000000000000000	0.000000000000000	0.000000000000000
0.000000000000000	0.000000000000000	0.000000000000000	0.000000000000000
0.000000000000000	0.000000000000000	0.000000000000000	0.000000000000000

Columns   41 thru   44

0.039294119924307	0.014173669740558	-0.006910344585776	-0.025316398590803
0.612048268318176	0.667402982711792	0.661850452423096	0.641715407371521
0.058502778410912	0.022968932986259	-0.009037911891937	-0.037495601922274
-0.803819298744202	-0.867560088634491	-0.858979105949402	-0.836781203746796
-0.157778963446617	-0.062435463070869	0.024048734456301	0.101073004305363
0.144108489155769	0.122166229707813	0.116705591926575	0.128100156784058
-0.108658075332642	-0.039193749427795	0.019108818843961	0.070006161928177
0.507833719253540	0.544135868549347	0.538143694400787	0.526000320911407
0.120053425431252	0.043304432183504	-0.021113066002727	-0.077348150312901
0.029269885271788	0.004994845949113	-0.008873509243131	-0.019443348050117

0.040433567017317   0.028241675347090   0.002036384306848   -0.024613553658128
-0.044544868171215 -0.016603892669082 -0.011600011959672 -0.025288397446275
-0.071424581110477 -0.020547755062580   0.016054304316640   0.046566255390644
-0.144336372613907 -0.157755404710770 -0.156498521566391 -0.151577010750771
0.000000000000000   0.000000000000000   0.000000000000000   0.000000000000000
0.000000000000000   0.000000000000000   0.000000000000000   0.000000000000000
0.000000000000000   0.000000000000000   0.000000000000000   0.000000000000000
0.000000000000000   0.000000000000000   0.000000000000000   0.000000000000000
0.000000000000000   0.000000000000000   0.000000000000000   0.000000000000000
0.000000000000000   0.000000000000000   0.000000000000000   0.000000000000000
0.000000000000000   0.000000000000000   0.000000000000000   0.000000000000000
0.000000000000000   0.000000000000000   0.000000000000000   0.000000000000000
0.000000000000000   0.000000000000000   0.000000000000000   0.000000000000000
0.000000000000000   0.000000000000000   0.000000000000000   0.000000000000000
0.000000000000000   0.000000000000000   0.000000000000000   0.000000000000000
0.000000000000000   0.000000000000000   0.000000000000000   0.000000000000000
0.000000000000000   0.000000000000000   0.000000000000000   0.000000000000000

Columns   45 thru   48
-0.041431147605181 -0.053661826997995 -0.056175384670496 -0.041781675070524
0.606055378913879   0.543643355369568   0.425473958253860   0.238090291619301
-0.061573948711157 -0.078072585165501 -0.078652262687683 -0.054994259029627
-0.798391461372375 -0.727092266082764 -0.580467820167542 -0.334175199270248
0.166033715009689   0.210082739591599   0.210815861821175   0.146436557173729
0.152058273553848   0.178241893649101   0.183259889483452   0.138386249542236
0.114567466080189   0.148388370871544   0.155338972806931   0.115536764264107
0.505486488342285   0.465166568756104   0.376328974962234   0.220640137791634
-0.126582816243172 -0.163950920104980 -0.171630054712296 -0.127654120326042
-0.031190739944577 -0.045399609953165 -0.056698203086853 -0.052611295133829
-0.041825104504824 -0.041894003748894 -0.021338770166039   0.009759375825524
-0.052827082574368 -0.086358144879341 -0.108345307409763 -0.094056629420280
0.075617462396622   0.102629400789738   0.116036199033260   0.096092984080315
-0.142823368310928 -0.127670288085938 -0.099453695118427 -0.055271942168474
0.000000000000000   0.000000000000000   0.000000000000000   0.000000000000000
0.000000000000000   0.000000000000000   0.000000000000000   0.000000000000000
0.000000000000000   0.000000000000000   0.000000000000000   0.000000000000000
0.000000000000000   0.000000000000000   0.000000000000000   0.000000000000000
0.000000000000000   0.000000000000000   0.000000000000000   0.000000000000000
0.000000000000000   0.000000000000000   0.000000000000000   0.000000000000000
0.000000000000000   0.000000000000000   0.000000000000000   0.000000000000000
0.000000000000000   0.000000000000000   0.000000000000000   0.000000000000000
0.000000000000000   0.000000000000000   0.000000000000000   0.000000000000000
0.000000000000000   0.000000000000000   0.000000000000000   0.000000000000000
0.000000000000000   0.000000000000000   0.000000000000000   0.000000000000000
0.000000000000000   0.000000000000000   0.000000000000000   0.000000000000000

0.000000000000000 0.000000000000000 0.000000000000000 0.000000000000000
0.000000000000000 0.000000000000000 0.000000000000000 0.000000000000000

Columns   49 thru   52
0.028954178094864   0.012954813428223   0.000959501543548 -0.008821797557175
0.386750340461731   0.427263200283051   0.428836852312088   0.398561447858810
0.014164083637297   0.008358211256564   0.002100343583152 -0.004158598370850
-0.601229786872864 -0.652679562568665 -0.650316357612610 -0.603241264820099
-0.111783541738987 -0.059082794934511 -0.011025194078684   0.033354576677084
0.190484464168549   0.163451939821243   0.144627526402473   0.129675716161728
-0.080065555870533 -0.035823296755552 -0.002653271658346   0.024394461885095
0.498267978429794   0.527172625064850   0.519485056400299   0.480459898710251
0.088463097810745   0.039580270648003   0.002930985763669 -0.026952799409628
0.043307978659868   0.010898220352829 -0.005409801844507 -0.013853058218956
0.008285525254905   0.025737006217241   0.016058689311147 -0.000814865110442
-0.143066465854645 -0.101840913295746 -0.078975111246109 -0.067727327346802
-0.080081045627594 -0.028150035068393   0.003546317340806   0.024995068088174
-0.221359759569168 -0.235613435506821 -0.232787385582924 -0.215451315045357
0.000000000000000   0.000000000000000   0.000000000000000   0.000000000000000
0.000000000000000   0.000000000000000   0.000000000000000   0.000000000000000
0.000000000000000   0.000000000000000   0.000000000000000   0.000000000000000
0.000000000000000   0.000000000000000   0.000000000000000   0.000000000000000
0.000000000000000   0.000000000000000   0.000000000000000   0.000000000000000
0.000000000000000   0.000000000000000   0.000000000000000   0.000000000000000
0.000000000000000   0.000000000000000   0.000000000000000   0.000000000000000
0.000000000000000   0.000000000000000   0.000000000000000   0.000000000000000
0.000000000000000   0.000000000000000   0.000000000000000   0.000000000000000
0.000000000000000   0.000000000000000   0.000000000000000   0.000000000000000
0.000000000000000   0.000000000000000   0.000000000000000   0.000000000000000
0.000000000000000   0.000000000000000   0.000000000000000   0.000000000000000
0.000000000000000   0.000000000000000   0.000000000000000   0.000000000000000
0.000000000000000   0.000000000000000   0.000000000000000   0.000000000000000

Columns   53 thru   56
-0.017031196504831 -0.023663954809308 -0.027966998517513 -0.027711821720004
0.360707700252533   0.316839307546616   0.263915985822678   0.193471267819405
-0.009742504917085 -0.013935587368906 -0.015842702239752 -0.014176896773279
-0.547397196292877 -0.484471827745438 -0.408936202526093 -0.306036800146103
0.072087578475475   0.101952195167542   0.117675505578518   0.109768033027649
0.123266041278839   0.123139381408691   0.124528288841248   0.116775691509247
0.047095503658056   0.065436743199825   0.077335722744465   0.076630108058453
0.437755346298218   0.391884684562683   0.337309956550598   0.259907931089401
-0.052034657448530 -0.072299025952816 -0.085446096956730 -0.084665738046169
-0.019551344715870 -0.025491412729025 -0.032758962363005 -0.038847364485264
-0.020262300030815 -0.032503012567759 -0.031574320048094 -0.014690148644149
-0.068360905409   -0.077830478549004 -0.091099023818970 -0.097273789346218

0.041739728301764	0.056478593498468	0.069132968783379	0.074287496507168
-0.196111664175987	-0.175087466835976	-0.150016799569130	-0.114820316433907
0.000000000000000	0.000000000000000	0.000000000000000	0.000000000000000
0.000000000000000	0.000000000000000	0.000000000000000	0.000000000000000
0.000000000000000	0.000000000000000	0.000000000000000	0.000000000000000
0.000000000000000	0.000000000000000	0.000000000000000	0.000000000000000
0.000000000000000	0.000000000000000	0.000000000000000	0.000000000000000
0.000000000000000	0.000000000000000	0.000000000000000	0.000000000000000
0.000000000000000	0.000000000000000	0.000000000000000	0.000000000000000
0.000000000000000	0.000000000000000	0.000000000000000	0.000000000000000
0.000000000000000	0.000000000000000	0.000000000000000	0.000000000000000
0.000000000000000	0.000000000000000	0.000000000000000	0.000000000000000
0.000000000000000	0.000000000000000	0.000000000000000	0.000000000000000
0.000000000000000	0.000000000000000	0.000000000000000	0.000000000000000
0.000000000000000	0.000000000000000	0.000000000000000	0.000000000000000
0.000000000000000	0.000000000000000	0.000000000000000	0.000000000000000

Columns   57 thru   60

-0.020128441974521	0.012444825842977	0.003507371991873	-0.003012405941263
0.102620966732502	0.187571495771408	0.161674678325653	0.146926492452621
-0.008289655670524	-0.010273084975779	-0.001714645652100	0.003058528294787
-0.168184310197830	-0.331904828548431	-0.281734198331833	-0.254109561443329
0.070728309452534	-0.058436863124371	-0.019993178546429	0.012439396232367
0.085805438458920	0.118853501975536	0.083164267241955	0.067041777074337
0.055660173296923	-0.034413054585457	-0.009698767215014	0.008330047130585
0.149689704179764	0.344793736934662	0.280129551887512	0.247022137045860
-0.061498031020164	0.038022838532925	0.010716436430812	-0.009204637259245
-0.036635845899582	0.024261066690087	0.003218021476641	-0.007625794503838
0.011203501373529	0.015028023160994	0.013086281716824	0.000648693356197
-0.080147273838520	-0.119497813284397	-0.071801036596298	-0.051438190042973
0.061584692448378	-0.045694917440414	-0.009469393640757	0.012712674215436
-0.065440781414509	-0.216901540756226	-0.174147680401802	-0.152591109275818
0.000000000000000	0.000000000000000	0.000000000000000	0.000000000000000
0.000000000000000	0.000000000000000	0.000000000000000	0.000000000000000
0.000000000000000	0.000000000000000	0.000000000000000	0.000000000000000
0.000000000000000	0.000000000000000	0.000000000000000	0.000000000000000
0.000000000000000	0.000000000000000	0.000000000000000	0.000000000000000
0.000000000000000	0.000000000000000	0.000000000000000	0.000000000000000
0.000000000000000	0.000000000000000	0.000000000000000	0.000000000000000
0.000000000000000	0.000000000000000	0.000000000000000	0.000000000000000
0.000000000000000	0.000000000000000	0.000000000000000	0.000000000000000
0.000000000000000	0.000000000000000	0.000000000000000	0.000000000000000
0.000000000000000	0.000000000000000	0.000000000000000	0.000000000000000
0.000000000000000	0.000000000000000	0.000000000000000	0.000000000000000
0.000000000000000	0.000000000000000	0.000000000000000	0.000000000000000

Columns   61 thru   64

```
-0.007976754568517  -0.011446966789663  -0.013246333226562  -0.012639661319554
 0.129562452435493   0.108227431774139   0.082853414118290   0.052611876279116
 0.005958141759038   0.008016247302294   0.009810903109610   0.011036994867027
-0.224129021167755  -0.188816979527473  -0.147411376237869  -0.097430415451527
 0.039328269660473   0.058029942214489   0.065555535256863   0.057548262178898
 0.059343039989471   0.056646954268217   0.056063087314701   0.052563607692719
 0.022057712078094   0.031653720885515   0.036629412323236   0.034951817244291
 0.218027204275131   0.188386142253876   0.154551869630810   0.113724455237389
-0.024372033774853  -0.034974910318851  -0.040472447872162  -0.038618981838226
-0.013628607615829  -0.017921445891261  -0.022377768531442  -0.026492759585381
-0.014332835562527  -0.024568684399128  -0.024421842768788  -0.010735079646111
-0.045722220093012  -0.049643315374851  -0.058552082628012  -0.064629882574081
 0.027478959411383   0.037892606109381   0.045393038541079   0.048155322670937
-0.134706676006317  -0.117225088179111  -0.098176807165146  -0.073610775172710
 0.000000000000000   0.000000000000000   0.000000000000000   0.000000000000000
 0.000000000000000   0.000000000000000   0.000000000000000   0.000000000000000
 0.000000000000000   0.000000000000000   0.000000000000000   0.000000000000000
 0.000000000000000   0.000000000000000   0.000000000000000   0.000000000000000
 0.000000000000000   0.000000000000000   0.000000000000000   0.000000000000000
 0.000000000000000   0.000000000000000   0.000000000000000   0.000000000000000
 0.000000000000000   0.000000000000000   0.000000000000000   0.000000000000000
 0.000000000000000   0.000000000000000   0.000000000000000   0.000000000000000
 0.000000000000000   0.000000000000000   0.000000000000000   0.000000000000000
 0.000000000000000   0.000000000000000   0.000000000000000   0.000000000000000
 0.000000000000000   0.000000000000000   0.000000000000000   0.000000000000000
 0.000000000000000   0.000000000000000   0.000000000000000   0.000000000000000
 0.000000000000000   0.000000000000000   0.000000000000000   0.000000000000000
 0.000000000000000   0.000000000000000   0.000000000000000   0.000000000000000
```

Columns   65 thru   68

```
 0.005962720606476   0.000448337610578  -0.003638325026259  -0.006507182028145
 0.051450692117214   0.044564709067345   0.038842946290970   0.029903363436460
-0.014689327217638  -0.000729451770894   0.008837470784783   0.015552558004856
-0.108977548778057  -0.092631980776787  -0.080363795161247  -0.062619693577290
-0.034153532236814  -0.003632759908214   0.021199099719524   0.038630798459053
 0.055816050618887   0.036907766014338   0.029732819646597   0.027771919965744
-0.016488416120410  -0.001239768345840   0.010060873813927   0.017993975430727
 0.159691095352173   0.124475225806236   0.105544969439507   0.087162792682648
 0.018218709155917   0.001370591926388  -0.011116929352283  -0.019882509484887
 0.016802249476314   0.000152333188453  -0.009878551587462  -0.016918916255236
 0.010683540254831   0.003495875047520  -0.007425640709698  -0.015094240196049
-0.083913251757622  -0.049165658652782  -0.037844136357307  -0.039171960204840
-0.030734248459339  -0.001258620410226   0.018398866057396   0.032197274267673
-0.149330362677574  -0.115318372845650  -0.097524851560593  -0.081066466867924
 0.000000000000000   0.000000000000000   0.000000000000000   0.000000000000000
```

0.000000000000000   0.000000000000000   0.000000000000000   0.000000000000000
0.000000000000000   0.000000000000000   0.000000000000000   0.000000000000000
0.000000000000000   0.000000000000000   0.000000000000000   0.000000000000000
0.000000000000000   0.000000000000000   0.000000000000000   0.000000000000000
0.000000000000000   0.000000000000000   0.000000000000000   0.000000000000000
0.000000000000000   0.000000000000000   0.000000000000000   0.000000000000000
0.000000000000000   0.000000000000000   0.000000000000000   0.000000000000000
0.000000000000000   0.000000000000000   0.000000000000000   0.000000000000000
0.000000000000000   0.000000000000000   0.000000000000000   0.000000000000000
0.000000000000000   0.000000000000000   0.000000000000000   0.000000000000000
0.000000000000000   0.000000000000000   0.000000000000000   0.000000000000000
0.000000000000000   0.000000000000000   0.000000000000000   0.000000000000000
0.000000000000000   0.000000000000000   0.000000000000000   0.000000000000000

Columns   69 thru   72
-0.007754317950457   -0.005812264978886   -0.003019649069756   -0.002203237498179
 0.017630355432630   -0.000139011142892   0.007578123826534   0.011977496556938
 0.019186316058040   0.127090066671371   0.088015586137772   0.065668620169163
-0.038634542375803   -0.000120961245557   0.007000952493399   0.010117438621819
 0.044184796512127   0.179659366607666   0.119574435055256   0.088964812457561
 0.027519334107637   0.000196733686607   -0.010724524036050   -0.016950502991676
 0.021442618221045   0.235727429389954   0.147151514887810   0.108967103064060
 0.064878679811954   0.000399298529373   -0.021767076104879   -0.034403651952744
-0.023694809526205   0.235623449087143   0.150882884860039   0.111947119235992
-0.022095220163465   0.009367801249027   -0.000642007798888   -0.000845768023282
-0.013304563239217   0.013321916572750   0.009167045354843   0.006837501190603
-0.046010602265596   0.000590992684010   -0.033056113868952   -0.050291776657104
 0.040201153606176   0.013286629691720   0.018604805693030   0.014366707764566
-0.061462506651878   0.000865232839715   -0.047213204205036   -0.074514143168926
 0.000000000000000   0.000000000000000   0.000000000000000   0.000000000000000
 0.000000000000000   0.000000000000000   0.000000000000000   0.000000000000000
 0.000000000000000   0.000000000000000   0.000000000000000   0.000000000000000
 0.000000000000000   0.000000000000000   0.000000000000000   0.000000000000000
 0.000000000000000   0.000000000000000   0.000000000000000   0.000000000000000
 0.000000000000000   0.000000000000000   0.000000000000000   0.000000000000000
 0.000000000000000   0.000000000000000   0.000000000000000   0.000000000000000
 0.000000000000000   0.000000000000000   0.000000000000000   0.000000000000000
 0.000000000000000   0.000000000000000   0.000000000000000   0.000000000000000
 0.000000000000000   0.000000000000000   0.000000000000000   0.000000000000000
 0.000000000000000   0.000000000000000   0.000000000000000   0.000000000000000
 0.000000000000000   0.000000000000000   0.000000000000000   0.000000000000000
 0.000000000000000   0.000000000000000   0.000000000000000   0.000000000000000
 0.000000000000000   0.000000000000000   0.000000000000000   0.000000000000000

Columns   73 thru   76
-0.002034915843979 -0.002173969754949   0.407519131898880   0.222715541720390
 0.012841389514506   0.011270420625806 -0.000690010201652   0.002906289184466
 0.040503341704607   0.016379265114665   0.595113217830658   0.332054674625397
 0.010538135655224   0.010047932155430   0.000616236706264 -0.001443513319828
 0.058136221021414   0.030033268034458   0.841890096664429   0.463388919830322
-0.018173076212406 -0.015949847176671   0.000976492709015 -0.004112984053791
 0.078043960034847   0.053217958658934 -0.187735617160797 -0.108002118766308
-0.036885056644678 -0.032372668385506   0.001981952693313 -0.008347930386662
 0.077321082353592   0.047807652503252 -0.188132956624031 -0.101506382226944
 0.004278365522623   0.011323893442750 -0.169137850403786 -0.100636050105095
 0.004256261512637   0.001800393336453 -0.240569040179253 -0.129930287599564
-0.053281836211681 -0.048411224037409   0.000770635320805 -0.005717949941754
 0.002529074437916 -0.011630697175860 -0.240632325410843 -0.117571584880352
-0.079853370785713 -0.070175446569920   0.001032185275108 -0.003611200256273
 0.000000000000000   0.000000000000000   0.000000000000000   0.000000000000000
 0.000000000000000   0.000000000000000   0.000000000000000   0.000000000000000
 0.000000000000000   0.000000000000000   0.000000000000000   0.000000000000000
 0.000000000000000   0.000000000000000   0.000000000000000   0.000000000000000
 0.000000000000000   0.000000000000000   0.000000000000000   0.000000000000000
 0.000000000000000   0.000000000000000   0.000000000000000   0.000000000000000
 0.000000000000000   0.000000000000000   0.000000000000000   0.000000000000000
 0.000000000000000   0.000000000000000   0.000000000000000   0.000000000000000
 0.000000000000000   0.000000000000000   0.000000000000000   0.000000000000000
 0.000000000000000   0.000000000000000   0.000000000000000   0.000000000000000
 0.000000000000000   0.000000000000000   0.000000000000000   0.000000000000000
 0.000000000000000   0.000000000000000   0.000000000000000   0.000000000000000
 0.000000000000000   0.000000000000000   0.000000000000000   0.000000000000000

Columns   77 thru   80
 0.156517714262009   0.120120353996754   0.096956133842468   0.079310268163681
 0.006200120784342   0.009184882976115   0.011789949610829   0.013561623170972
 0.237892344594002   0.183457568287849   0.145110741257668   0.112164191901684
-0.005139631219208 -0.009259076789021 -0.012661595828831 -0.013957137241960
 0.327338063240051   0.252028077840805   0.201994895935059   0.162088990211487
-0.008774411864579 -0.012998445890844 -0.016685139387846 -0.019192405045033
-0.079495549201965 -0.061710827052593 -0.047459516674280 -0.033636707812548
-0.017809018492699 -0.026382349431515 -0.033865056931973 -0.038953937590122
-0.070463187992573 -0.053906641900539 -0.044082004576921 -0.037317100912333
-0.076179906725883 -0.059530355036259 -0.044480778276920 -0.028517808765173
-0.090282186865807 -0.069087281823158 -0.056435294449329 -0.047650247812271
-0.007778003811836 -0.007992259226739 -0.008593133650720 -0.011187074705958
-0.073349289596081 -0.054481741040945 -0.050040323287249 -0.054314546287060
-0.009020734578371 -0.014414939098060 -0.018999656662345 -0.021466668695211
 0.000000000000000   0.000000000000000   0.000000000000000   0.000000000000000

0.000000000000000 0.000000000000000 0.000000000000000 0.000000000000000
0.000000000000000 0.000000000000000 0.000000000000000 0.000000000000000
0.000000000000000 0.000000000000000 0.000000000000000 0.000000000000000
0.000000000000000 0.000000000000000 0.000000000000000 0.000000000000000
0.000000000000000 0.000000000000000 0.000000000000000 0.000000000000000
0.000000000000000 0.000000000000000 0.000000000000000 0.000000000000000
0.000000000000000 0.000000000000000 0.000000000000000 0.000000000000000
0.000000000000000 0.000000000000000 0.000000000000000 0.000000000000000
0.000000000000000 0.000000000000000 0.000000000000000 0.000000000000000
0.000000000000000 0.000000000000000 0.000000000000000 0.000000000000000
0.000000000000000 0.000000000000000 0.000000000000000 0.000000000000000
0.000000000000000 0.000000000000000 0.000000000000000 0.000000000000000
0.000000000000000 0.000000000000000 0.000000000000000 0.000000000000000

Columns   81 thru   84
0.060681208968163   1.969767928123474   1.300133466720581   0.994962155818939
0.013383945450187   -0.007462786044925   -0.002144439611584   0.001920530106872
0.076704494655132   0.306871116161346   0.209030911326408   0.164805412292480
-0.011453973129392   0.016232386231422   0.006882980465889   -0.002285791328177
0.119626432657242   0.438656955957413   0.292464494705200   0.226005598902702
-0.018940955400467   0.010561346076429   0.003034812398255   -0.002717941766605
-0.018512971699238   -0.926856577396393   -0.618224084377289   -0.477933436632156
-0.038443587720394   0.021435873582959   0.006159610114992   -0.005516493227333
-0.030304461717606   -0.935511887073517   -0.613375186920166   -0.466340333223343
-0.010856171138585   0.252901256084442   0.158947035670280   0.115684106945992
-0.038522999733686   0.348265916109085   0.231478795409203   0.178345739841461
-0.016019124537706   -0.003840614808723   -0.006509527564049   -0.003620741888881
-0.060192480683327   0.337350189685822   0.236432358622551   0.191210404038429
-0.019702311605215   -0.011759574525058   0.000283096364001   0.006148749496788
0.000000000000000   0.000000000000000   0.000000000000000   0.000000000000000
0.000000000000000   0.000000000000000   0.000000000000000   0.000000000000000
0.000000000000000   0.000000000000000   0.000000000000000   0.000000000000000
0.000000000000000   0.000000000000000   0.000000000000000   0.000000000000000
0.000000000000000   0.000000000000000   0.000000000000000   0.000000000000000
0.000000000000000   0.000000000000000   0.000000000000000   0.000000000000000
0.000000000000000   0.000000000000000   0.000000000000000   0.000000000000000
0.000000000000000   0.000000000000000   0.000000000000000   0.000000000000000
0.000000000000000   0.000000000000000   0.000000000000000   0.000000000000000
0.000000000000000   0.000000000000000   0.000000000000000   0.000000000000000
0.000000000000000   0.000000000000000   0.000000000000000   0.000000000000000
0.000000000000000   0.000000000000000   0.000000000000000   0.000000000000000
0.000000000000000   0.000000000000000   0.000000000000000   0.000000000000000
0.000000000000000   0.000000000000000   0.000000000000000   0.000000000000000

Columns   85 thru   88

0.804303646087646	0.671635687351227	0.573604345321655	0.495281726121902
0.005544428247958	0.008845058269799	0.011790878139436	0.014213825576007
0.135871514678001	0.113879814743996	0.095481887459755	0.078556805849075
-0.011853702366352	-0.021116273477674	-0.029190639033914	-0.034966662526131
0.183894440531731	0.153751507401466	0.130506321787834	0.110927931964397
-0.007846488617361	-0.012517547234893	-0.016686476767063	-0.020115435123444
-0.388986706733704	-0.325242757797241	-0.276001065969467	-0.234441623091698
-0.015925671905279	-0.025406306609511	-0.033867791295052	-0.040827386081219
-0.375302791595459	-0.313131749629974	-0.268550753593445	-0.234341979026794
0.090258516371250	0.074853748083115	0.066113501787186	0.061870459467173
0.144826933741570	0.121042288839817	0.102934435009956	0.087914951145649
0.002351252594963	0.009126202203333	0.014703797176480	0.017183294519782
0.160190612077713	0.134659379720688	0.111233726143837	0.087790273129940
0.009076911956072	0.010839019902050	0.012729468755424	0.015712475404143
0.000000000000000	0.000000000000000	0.000000000000000	0.000000000000000
0.000000000000000	0.000000000000000	0.000000000000000	0.000000000000000
0.000000000000000	0.000000000000000	0.000000000000000	0.000000000000000
0.000000000000000	0.000000000000000	0.000000000000000	0.000000000000000
0.000000000000000	0.000000000000000	0.000000000000000	0.000000000000000
0.000000000000000	0.000000000000000	0.000000000000000	0.000000000000000
0.000000000000000	0.000000000000000	0.000000000000000	0.000000000000000
0.000000000000000	0.000000000000000	0.000000000000000	0.000000000000000
0.000000000000000	0.000000000000000	0.000000000000000	0.000000000000000
0.000000000000000	0.000000000000000	0.000000000000000	0.000000000000000
0.000000000000000	0.000000000000000	0.000000000000000	0.000000000000000
0.000000000000000	0.000000000000000	0.000000000000000	0.000000000000000
0.000000000000000	0.000000000000000	0.000000000000000	0.000000000000000

Columns   89 thru   92

0.421105951070786	0.329193681478500	1.326097249984741	0.906724572181702
0.015644349157810	0.015017755329609	-0.006164656952024	-0.002510329708457
0.061022732406855	0.040601834654808	-0.118333235383034	-0.076723918318748
-0.036729402840137	-0.031801421195269	0.026081960648298	0.011887371540070
0.091705925762653	0.068477191030979	-0.166387811303139	-0.110339559614658
-0.022139914333820	-0.021253155544400	0.008724247105420	0.003552627516910
-0.193583309650421	-0.144255876541138	-0.314265578985214	-0.220809891819954
-0.044936385005713	-0.043136563152075	0.017707206308842	0.007210600655526
-0.202898055315018	-0.163106873631477	-0.322404861450195	-0.215613916516304
0.059705216437578	0.055413451045752	0.136640265583992	0.090321853756905
0.073317423462868	0.055553209036589	0.191623926162720	0.131781786680222
0.014632937498391	0.005623692646623	-0.013151098042727	-0.010182447731495
0.062391169369221	0.033693633973598	0.189036920666695	0.134870216250420
0.020193096250296	0.025090513750911	-0.024060234427452	-0.004769217222929
0.000000000000000	0.000000000000000	0.000000000000000	0.000000000000000

0.000000000000000	0.000000000000000	0.000000000000000	0.000000000000000
0.000000000000000	0.000000000000000	0.000000000000000	0.000000000000000
0.000000000000000	0.000000000000000	0.000000000000000	0.000000000000000
0.000000000000000	0.000000000000000	0.000000000000000	0.000000000000000
0.000000000000000	0.000000000000000	0.000000000000000	0.000000000000000
0.000000000000000	0.000000000000000	0.000000000000000	0.000000000000000
0.000000000000000	0.000000000000000	0.000000000000000	0.000000000000000
0.000000000000000	0.000000000000000	0.000000000000000	0.000000000000000
0.000000000000000	0.000000000000000	0.000000000000000	0.000000000000000
0.000000000000000	0.000000000000000	0.000000000000000	0.000000000000000
0.000000000000000	0.000000000000000	0.000000000000000	0.000000000000000
0.000000000000000	0.000000000000000	0.000000000000000	0.000000000000000
0.000000000000000	0.000000000000000	0.000000000000000	0.000000000000000

Columns   93 thru   96

0.709636569023132	0.596034884452820	0.518160045146942	0.453546553850174
0.000362335558748	0.002966203726828	0.005290918517858	0.007169664371759
-0.056874047964811	-0.046022035181522	-0.039785530418158	-0.036047145724297
-0.000397099764086	-0.012308993376791	-0.023289678618312	-0.032152667641640
-0.083757445216179	-0.068918265402317	-0.059730723500252	-0.053283780813217
-0.000512780155987	-0.004197784699500	-0.007487729191780	-0.010146536864340
-0.177307695150375	-0.151398137211800	-0.131933838129044	-0.113750189542770
-0.001040773466229	-0.008520060218871	-0.015197510831058	-0.020593969151378
-0.165085926651955	-0.136641651391983	-0.118530526757240	-0.105161383748055
0.068335101008415	0.056099213659763	0.048603609204292	0.043450213968754
0.103711925446987	0.087425671517849	0.076043523848057	0.066339664161205
-0.003556548152119	0.005410465411842	0.014734324999154	0.022226888686419
0.109810046851635	0.094574779272079	0.082518011331558	0.070588096976280
0.005924230441451	0.012532517313957	0.017059214413166	0.020761912688613
0.000000000000000	0.000000000000000	0.000000000000000	0.000000000000000
0.000000000000000	0.000000000000000	0.000000000000000	0.000000000000000
0.000000000000000	0.000000000000000	0.000000000000000	0.000000000000000
0.000000000000000	0.000000000000000	0.000000000000000	0.000000000000000
0.000000000000000	0.000000000000000	0.000000000000000	0.000000000000000
0.000000000000000	0.000000000000000	0.000000000000000	0.000000000000000
0.000000000000000	0.000000000000000	0.000000000000000	0.000000000000000
0.000000000000000	0.000000000000000	0.000000000000000	0.000000000000000
0.000000000000000	0.000000000000000	0.000000000000000	0.000000000000000
0.000000000000000	0.000000000000000	0.000000000000000	0.000000000000000
0.000000000000000	0.000000000000000	0.000000000000000	0.000000000000000
0.000000000000000	0.000000000000000	0.000000000000000	0.000000000000000
0.000000000000000	0.000000000000000	0.000000000000000	0.000000000000000

Columns   97 thru   100

0.394293308258057	0.339617192745209	0.285204410552979	1.488296151161194
0.008467270992696	0.009142669849098	0.009044424630702	-0.001084392428480
-0.033879879862070	-0.032946385443211	-0.032502349466085	-0.556867957115173
-0.037911783903837	-0.040078166872263	-0.037788502871990	0.030060518532991
-0.048404384404421	-0.044774957001209	-0.041560385376215	-0.787680447101593
-0.011982914991677	-0.012938742525876	-0.012799708172679	0.001535360701382
-0.095289260149002	-0.076744168996811	-0.057601649314165	0.215142384171486
-0.024321183562279	-0.026261182501912	-0.025978989899158	0.003116262378171
-0.094356313347816	-0.085617259144783	-0.077479183673859	0.200990691781044
0.039659827947617	0.036953762173653	0.034620210528374	0.002413998357952
0.057212453335524	0.048597313463688	0.039935745298862	0.004155062139034
0.026020716875792	0.024827228859067	0.017474802210927	-0.011747978627682
0.057956691831350	0.044870603829622	0.031197385862470	0.004959001205862
0.024757983162999	0.030138175934553	0.037195395678282	-0.022807067260146
0.000000000000000	0.000000000000000	0.000000000000000	0.000000000000000
0.000000000000000	0.000000000000000	0.000000000000000	0.000000000000000
0.000000000000000	0.000000000000000	0.000000000000000	0.000000000000000
0.000000000000000	0.000000000000000	0.000000000000000	0.000000000000000
0.000000000000000	0.000000000000000	0.000000000000000	0.000000000000000
0.000000000000000	0.000000000000000	0.000000000000000	0.000000000000000
0.000000000000000	0.000000000000000	0.000000000000000	0.000000000000000
0.000000000000000	0.000000000000000	0.000000000000000	0.000000000000000
0.000000000000000	0.000000000000000	0.000000000000000	0.000000000000000
0.000000000000000	0.000000000000000	0.000000000000000	0.000000000000000
0.000000000000000	0.000000000000000	0.000000000000000	0.000000000000000
0.000000000000000	0.000000000000000	0.000000000000000	0.000000000000000
0.000000000000000	0.000000000000000	0.000000000000000	0.000000000000000
0.000000000000000	0.000000000000000	0.000000000000000	0.000000000000000

Columns   101 thru   104

1.103705167770386	0.901536762714386	0.779535531997681	0.692856371402740
-0.000805996998679	-0.000349612440914	0.000221366906771	0.000809793651570
-0.412183493375778	-0.336100041866302	-0.290288537740707	-0.257951319217682
0.015834974125028	0.003585356986150	-0.008004620671272	-0.018705574795604
-0.582424044609070	-0.474467724561691	-0.409542858600616	-0.363875508308411
0.001140656531788	0.000494773150422	-0.000313283671858	-0.001146031194367
0.154786050319672	0.122895158827305	0.104269631206989	0.092317230999470
0.002315143821761	0.001004219637252	-0.000635858858004	-0.002326049143448
0.157281816005707	0.134587302803993	0.119821324944496	0.107117041945457
0.002626425353810	0.002765778925434	0.002742694690824	0.002500668168068
0.003016667440534	0.002416063798591	0.002062059706077	0.001827948843129
-0.010897212661803	-0.005822964478284	0.001772477175109	0.010015049017966
0.002435689326376	0.001066709985025	0.000402189820306	0.000264085916569
-0.005956446751952	0.002968231216073	0.007817354053259	0.010712484829128
0.000000000000000	0.000000000000000	0.000000000000000	0.000000000000000

0.000000000000000	0.000000000000000	0.000000000000000	0.000000000000000
0.000000000000000	0.000000000000000	0.000000000000000	0.000000000000000
0.000000000000000	0.000000000000000	0.000000000000000	0.000000000000000
0.000000000000000	0.000000000000000	0.000000000000000	0.000000000000000
0.000000000000000	0.000000000000000	0.000000000000000	0.000000000000000
0.000000000000000	0.000000000000000	0.000000000000000	0.000000000000000
0.000000000000000	0.000000000000000	0.000000000000000	0.000000000000000
0.000000000000000	0.000000000000000	0.000000000000000	0.000000000000000
0.000000000000000	0.000000000000000	0.000000000000000	0.000000000000000
0.000000000000000	0.000000000000000	0.000000000000000	0.000000000000000
0.000000000000000	0.000000000000000	0.000000000000000	0.000000000000000
0.000000000000000	0.000000000000000	0.000000000000000	0.000000000000000
0.000000000000000	0.000000000000000	0.000000000000000	0.000000000000000

Columns   105 thru   108

0.616425931453705	0.541458725929260	0.469195365905762	0.396767616271973
0.001299732364714	0.001587360398844	0.001603312441148	0.001282415003516
-0.229695409536362	-0.202199637889862	-0.175882473587990	-0.149616643786430
-0.027634136378765	-0.033978477120399	-0.037413481622934	-0.037347704172134
-0.324170619249344	-0.285704225301743	-0.249033361673355	-0.212521910667419
-0.001839397242293	-0.002246452728286	-0.002269031479955	-0.001814899733290
0.083343394100666	0.075871869921684	0.069804951548576	0.064400121569633
-0.003733343211934	-0.004559525754303	-0.004605353344232	-0.003683626651764
0.093209654092789	0.077269352972507	0.059941977262497	0.041406556963921
0.002012327080593	0.001299633411691	0.000413294212194	-0.000059373548720
0.001642745570280	0.001479093218222	0.001336782937869	0.001203420106322
0.016871774569154	0.020529024302959	0.019702546298504	0.013281164690852
0.000550515775103	0.001178383361548	0.002079703845084	0.003159496234730
0.013154647313058	0.016452912241220	0.021849302574992	0.030027221888304
0.000000000000000	0.000000000000000	0.000000000000000	0.000000000000000
0.000000000000000	0.000000000000000	0.000000000000000	0.000000000000000
0.000000000000000	0.000000000000000	0.000000000000000	0.000000000000000
0.000000000000000	0.000000000000000	0.000000000000000	0.000000000000000
0.000000000000000	0.000000000000000	0.000000000000000	0.000000000000000
0.000000000000000	0.000000000000000	0.000000000000000	0.000000000000000
0.000000000000000	0.000000000000000	0.000000000000000	0.000000000000000
0.000000000000000	0.000000000000000	0.000000000000000	0.000000000000000
0.000000000000000	0.000000000000000	0.000000000000000	0.000000000000000
0.000000000000000	0.000000000000000	0.000000000000000	0.000000000000000
0.000000000000000	0.000000000000000	0.000000000000000	0.000000000000000
0.000000000000000	0.000000000000000	0.000000000000000	0.000000000000000
0.000000000000000	0.000000000000000	0.000000000000000	0.000000000000000

Columns   109 thru   112

1.6069815515884399	1.1218514442443851	0.8746924996376041	0.7203146219253541
0.0047037727199491	0.0013900855556131	-0.0006849614437671	-0.0021913661621511
-0.7706171274185181	-0.5390800833702091	-0.4211482703685761	-0.3473060429096221
0.0244736615568401	0.0104695493355391	-0.0006506493082271	-0.0107503645122051
-1.0923244953155521	-0.7606897950172421	-0.5916825532913211	-0.4864260256290441
-0.0066567752510311	-0.0019672473426911	0.0009693576721471	0.0031012201216071
0.4954532980918881	0.3408696949481961	0.2619815766811371	0.2135286778211591
-0.0135109350085261	-0.0039928257465361	0.0019674641080201	0.0062944064848121
0.4812582433223721	0.3443583846092221	0.2748338282108311	0.2300336509943011
-0.0895118117332461	-0.0574907660484311	-0.0410448834300041	-0.0315918177366261
-0.1209938077911873	-0.0845002904534341	-0.0659088417887691	-0.0542910099029541
-0.0007967927958821	-0.0051906853914261	-0.0043435706757011	-0.0006258042994891
-0.1148471385240551	-0.0869126170873641	-0.0728589370846751	-0.0629768297076231
-0.0068317735567691	0.0016157602658501	0.0042660161852841	0.0039140428416431
0.0000000000000000	0.0000000000000000	0.0000000000000000	0.0000000000000000
0.0000000000000000	0.0000000000000000	0.0000000000000000	0.0000000000000000
0.0000000000000000	0.0000000000000000	0.0000000000000000	0.0000000000000000
0.0000000000000000	0.0000000000000000	0.0000000000000000	0.0000000000000000
0.0000000000000000	0.0000000000000000	0.0000000000000000	0.0000000000000000
0.0000000000000000	0.0000000000000000	0.0000000000000000	0.0000000000000000
0.0000000000000000	0.0000000000000000	0.0000000000000000	0.0000000000000000
0.0000000000000000	0.0000000000000000	0.0000000000000000	0.0000000000000000
0.0000000000000000	0.0000000000000000	0.0000000000000000	0.0000000000000000
0.0000000000000000	0.0000000000000000	0.0000000000000000	0.0000000000000000
0.0000000000000000	0.0000000000000000	0.0000000000000000	0.0000000000000000
0.0000000000000000	0.0000000000000000	0.0000000000000000	0.0000000000000000
0.0000000000000000	0.0000000000000000	0.0000000000000000	0.0000000000000000
0.0000000000000000	0.0000000000000000	0.0000000000000000	0.0000000000000000

Columns   113 thru   116

0.6129416227340701	0.5309244394302371	0.4636423587799071	0.4042236804962161
-0.0034115796443071	-0.0045066636876613	-0.0055927098728721	-0.0067355982027951
-0.2956524789333341	-0.2558347284793851	-0.2227894365787511	-0.1932601630687711
-0.0200189799070361	-0.0281517300754791	-0.0347091257572171	-0.0390926226973531
-0.4137183129787451	-0.3587948679924011	-0.3143835980367661	-0.2757547199726101
0.0048280656337741	0.0063777896575631	0.0079147974029181	0.0095322141423821
0.1811664886474601	0.1580904722213751	0.1408907920122151	0.1272722333669661
0.0097993062809111	0.0129447067156431	0.0160643067210911	0.0193470977246761
0.1966350823640821	0.1683730483055111	0.1422923058271411	0.1166308447718621
-0.0263514686375861	-0.0239878781139851	-0.0237730168889761	-0.0251538064330821
-0.0462016947567461	-0.0400117821991441	-0.0349224545061591	-0.0304175354540351
0.0040506836958231	0.0079640178009871	0.0095358034595851	0.0073368111162531
-0.0543050803244111	-0.0454718843102461	-0.0358992628753191	-0.0253338180482391
0.0024076108820741	0.0012636330211541	0.0018230613786731	0.0052380021661521
0.0000000000000000	0.0000000000000000	0.0000000000000000	0.0000000000000000

0.000000000000000   0.000000000000000   0.000000000000000   0.000000000000000
0.000000000000000   0.000000000000000   0.000000000000000   0.000000000000000
0.000000000000000   0.000000000000000   0.000000000000000   0.000000000000000
0.000000000000000   0.000000000000000   0.000000000000000   0.000000000000000
0.000000000000000   0.000000000000000   0.000000000000000   0.000000000000000
0.000000000000000   0.000000000000000   0.000000000000000   0.000000000000000
0.000000000000000   0.000000000000000   0.000000000000000   0.000000000000000
0.000000000000000   0.000000000000000   0.000000000000000   0.000000000000000
0.000000000000000   0.000000000000000   0.000000000000000   0.000000000000000
0.000000000000000   0.000000000000000   0.000000000000000   0.000000000000000
0.000000000000000   0.000000000000000   0.000000000000000   0.000000000000000
0.000000000000000   0.000000000000000   0.000000000000000   0.000000000000000
0.000000000000000   0.000000000000000   0.000000000000000   0.000000000000000

Columns   117 thru   120

0.339716762304306   0.733792483806610   0.518910944461823   0.413616597652435
-0.007762315217406   0.009023640304804   0.002505518030375   -0.001740897307172
-0.161140441894531   -0.396411240100861   -0.282885223627090   -0.227324306964874
-0.039672523736954   0.021722964942455   0.008215680718422   -0.002280563581735
-0.233920127153397   -0.565520942211151   -0.397912889719009   -0.315729767084122
 0.010985221713781   -0.012770269066095   -0.003545812098309   0.002463720738888
 0.112767845392227   0.311374127864838   0.215131863951683   0.167837396264076
 0.022296197712421   -0.025919226929545   -0.007196770515293   0.005000504665077
 0.088302686810493   0.299779295921326   0.219793051481247   0.180806562304497
-0.026930302381516   -0.081559024751186   -0.049380172044039   -0.033391352742910
-0.025524985045195   -0.105039529502392   -0.074167102575302   -0.059036266058683
 0.000220814268687   0.009952254593372   -0.001466841204092   -0.005620156414807
-0.013486732728779   -0.094626188278198   -0.077770277857780   -0.069799646735191
 0.012076490558684   0.008337860926986   0.006393956951797   0.001959122484550
 0.000000000000000   0.000000000000000   0.000000000000000   0.000000000000000
 0.000000000000000   0.000000000000000   0.000000000000000   0.000000000000000
 0.000000000000000   0.000000000000000   0.000000000000000   0.000000000000000
 0.000000000000000   0.000000000000000   0.000000000000000   0.000000000000000
 0.000000000000000   0.000000000000000   0.000000000000000   0.000000000000000
 0.000000000000000   0.000000000000000   0.000000000000000   0.000000000000000
 0.000000000000000   0.000000000000000   0.000000000000000   0.000000000000000
 0.000000000000000   0.000000000000000   0.000000000000000   0.000000000000000
 0.000000000000000   0.000000000000000   0.000000000000000   0.000000000000000
 0.000000000000000   0.000000000000000   0.000000000000000   0.000000000000000
 0.000000000000000   0.000000000000000   0.000000000000000   0.000000000000000
 0.000000000000000   0.000000000000000   0.000000000000000   0.000000000000000
 0.000000000000000   0.000000000000000   0.000000000000000   0.000000000000000
 0.000000000000000   0.000000000000000   0.000000000000000   0.000000000000000

Columns 121 thru 124

0.342020899057388	0.288984864950180	0.248467445373535	0.215249776840210
-0.004962712060660	-0.007643529213965	-0.010067387484014	-0.012309622950852
-0.188962638378143	-0.159810721874237	-0.136725679039955	-0.116961658000946
-0.011630089022219	-0.020068466663361	-0.027502037584782	-0.033394727855921
-0.260304868221283	-0.219822928309441	-0.189533710479736	-0.165357694029808
0.007023237645626	0.010817134752870	0.014247382059693	0.017420595511794
0.136831775307655	0.115317240357399	0.100491598248482	0.089995034039021
0.014254746027291	0.021955044940114	0.028917264193296	0.035357791930437
0.152520731091499	0.129326879978180	0.109125055372715	0.090007126331329
-0.024409085512161	-0.020138001069427	-0.019515302032232	-0.021722773090005
-0.048773668706417	-0.041203889995813	-0.035456821322441	-0.030782185494900
-0.006087097804993	-0.005199640057981	-0.004776826128364	-0.006291306577623
-0.061907667666674	-0.052943840622902	-0.042641170322895	-0.030638299882412
-0.003993857186288	-0.010177571326494	-0.015402572229505	-0.018398612737656
0.000000000000000	0.000000000000000	0.000000000000000	0.000000000000000
0.000000000000000	0.000000000000000	0.000000000000000	0.000000000000000
0.000000000000000	0.000000000000000	0.000000000000000	0.000000000000000
0.000000000000000	0.000000000000000	0.000000000000000	0.000000000000000
0.000000000000000	0.000000000000000	0.000000000000000	0.000000000000000
0.000000000000000	0.000000000000000	0.000000000000000	0.000000000000000
0.000000000000000	0.000000000000000	0.000000000000000	0.000000000000000
0.000000000000000	0.000000000000000	0.000000000000000	0.000000000000000
0.000000000000000	0.000000000000000	0.000000000000000	0.000000000000000
0.000000000000000	0.000000000000000	0.000000000000000	0.000000000000000
0.000000000000000	0.000000000000000	0.000000000000000	0.000000000000000
0.000000000000000	0.000000000000000	0.000000000000000	0.000000000000000
0.000000000000000	0.000000000000000	0.000000000000000	0.000000000000000
0.000000000000000	0.000000000000000	0.000000000000000	0.000000000000000

Columns 125 thru 128

0.182217806577682	0.139827638864517	0.221666574478149	0.165019035339355
-0.014048168435693	-0.014285837300122	0.009083637036383	0.002152012428269
-0.096814356744289	-0.071602217853069	-0.137249127030373	-0.104578904807568
-0.036294706165791	-0.033497605472803	0.013477741740644	0.004196172114462
-0.141703382134438	-0.110844202339649	-0.196544706821442	-0.144603803753853
0.019880982115865	0.020217331126332	-0.012855186127126	-0.003045531455427
0.080533921718597	0.067120298743248	0.133117094635963	0.095217153429985
0.040351528674364	0.041034199297428	-0.026091586798429	-0.006181378383189
0.069490410387516	0.045122042298317	0.130797296762466	0.101569421589375
-0.025519115850329	-0.028305646032095	-0.047765504568815	-0.027641892433167
-0.026155479252338	-0.020189596340060	-0.062481697648764	-0.045888293534517
-0.010698161087930	-0.017486056312919	0.014015490189195	0.001287825638428
-0.016607403755188	-0.001330020953901	-0.057310033589602	-0.052018940448761
-0.017604690045118	-0.011531985364854	0.021241841837764	0.007114490028471
0.000000000000000	0.000000000000000	0.000000000000000	0.000000000000000

```
0.000000000000000        0.000000000000000        0.000000000000000        0.000000000000000
0.000000000000000        0.000000000000000        0.000000000000000        0.000000000000000
0.000000000000000        0.000000000000000        0.000000000000000        0.000000000000000
0.000000000000000        0.000000000000000        0.000000000000000        0.000000000000000
0.000000000000000        0.000000000000000        0.000000000000000        0.000000000000000
0.000000000000000        0.000000000000000        0.000000000000000        0.000000000000000
0.000000000000000        0.000000000000000        0.000000000000000        0.000000000000000
0.000000000000000        0.000000000000000        0.000000000000000        0.000000000000000
0.000000000000000        0.000000000000000        0.000000000000000        0.000000000000000
0.000000000000000        0.000000000000000        0.000000000000000        0.000000000000000
0.000000000000000        0.000000000000000        0.000000000000000        0.000000000000000
0.000000000000000        0.000000000000000        0.000000000000000        0.000000000000000
0.000000000000000        0.000000000000000        0.000000000000000        0.000000000000000
```

Columns   129 thru   132
```
 0.136764779686928        0.116144694387913        0.098489135503769        0.081160083413124
-0.002685654442757       -0.006433743052185       -0.009352056309581       -0.011368140578270
-0.088029935956001       -0.074977718293667       -0.062738500535488       -0.049908015877008
-0.003471923293546       -0.010075635276735       -0.015195251442492       -0.018042145296931
-0.118878044188023       -0.100797891616821       -0.086075015366077       -0.072207108139992
 0.003800745587796        0.009105049073696        0.013235052116215        0.016088219359517
 0.076723650097847        0.064800672233105        0.056308794766665        0.049293994903564
 0.007714203093201        0.018480105325580        0.026862582191825        0.032653525471687
 0.086547970771790        0.073883384466171        0.061182707548141        0.047289300709963
-0.018440965563059       -0.014935850165784       -0.015436738729477       -0.018620802089572
-0.037678074091673       -0.031940028071404       -0.027303855866194       -0.022966323420405
-0.005183017347008       -0.008853700943291       -0.011756571941078       -0.015159952454269
-0.048391852527857       -0.041952162981033       -0.032300282269716       -0.019645530730486
-0.005215829238296       -0.016144441440701       -0.024607686325908       -0.029022434726357
 0.000000000000000        0.000000000000000        0.000000000000000        0.000000000000000
 0.000000000000000        0.000000000000000        0.000000000000000        0.000000000000000
 0.000000000000000        0.000000000000000        0.000000000000000        0.000000000000000
 0.000000000000000        0.000000000000000        0.000000000000000        0.000000000000000
 0.000000000000000        0.000000000000000        0.000000000000000        0.000000000000000
 0.000000000000000        0.000000000000000        0.000000000000000        0.000000000000000
 0.000000000000000        0.000000000000000        0.000000000000000        0.000000000000000
 0.000000000000000        0.000000000000000        0.000000000000000        0.000000000000000
 0.000000000000000        0.000000000000000        0.000000000000000        0.000000000000000
 0.000000000000000        0.000000000000000        0.000000000000000        0.000000000000000
 0.000000000000000        0.000000000000000        0.000000000000000        0.000000000000000
 0.000000000000000        0.000000000000000        0.000000000000000        0.000000000000000
 0.000000000000000        0.000000000000000        0.000000000000000        0.000000000000000
 0.000000000000000        0.000000000000000        0.000000000000000        0.000000000000000
```

Columns   133 thru   136
0.061413474380970	0.056393094360828	0.043542593717575	0.036373812705278
-0.011985959485173	0.005774934776127	0.000373997143470	-0.003612515050918
-0.035207178443670	-0.041369613260031	-0.033853873610497	-0.028783293440938
-0.017433380708098	0.003992991521955	0.000562907429412	-0.002600301522762
-0.056461788713932	-0.060778174549341	-0.045784171670675	-0.037945184856653
0.016962554305792	-0.008172707632184	-0.000529281678610	0.005112444516271
0.041430357843637	0.056002765893936	0.040686454623938	0.033315487205982
0.034428127110004	-0.016587769612670	-0.001074259984307	0.010376495309174
0.031317293643951	0.054158128798008	0.043841857463121	0.037156771868467
-0.022513803094625	-0.030708035454154	-0.017571296542883	-0.013062535785139
-0.018044598400593	-0.038753725588322	-0.029193162918091	-0.024194821715355
-0.019204074516892	0.012959190644324	0.000215470179683	-0.007896557450294
-0.004912527743727	-0.034111827611923	-0.033119395375252	-0.029451398178935
-0.027301071211696	0.020069703459740	0.001953481929377	-0.012774786911905
0.000000000000000	0.000000000000000	0.000000000000000	0.000000000000000
0.000000000000000	0.000000000000000	0.000000000000000	0.000000000000000
0.000000000000000	0.000000000000000	0.000000000000000	0.000000000000000
0.000000000000000	0.000000000000000	0.000000000000000	0.000000000000000
0.000000000000000	0.000000000000000	0.000000000000000	0.000000000000000
0.000000000000000	0.000000000000000	0.000000000000000	0.000000000000000
0.000000000000000	0.000000000000000	0.000000000000000	0.000000000000000
0.000000000000000	0.000000000000000	0.000000000000000	0.000000000000000
0.000000000000000	0.000000000000000	0.000000000000000	0.000000000000000
0.000000000000000	0.000000000000000	0.000000000000000	0.000000000000000
0.000000000000000	0.000000000000000	0.000000000000000	0.000000000000000
0.000000000000000	0.000000000000000	0.000000000000000	0.000000000000000
0.000000000000000	0.000000000000000	0.000000000000000	0.000000000000000
0.000000000000000	0.000000000000000	0.000000000000000	0.000000000000000

Columns   137 thru   138
0.029406102374196	0.021314786747098
-0.006510867271572	-0.008051437325776
-0.022396450862288	-0.014185924082994
-0.004901506006718	-0.005512909963727
-0.031199220567942	-0.023840608075261
0.009214201010764	0.011394418776035
0.028100755065680	0.023106062784791
0.018701648339629	0.023126738145947
0.029114006087184	0.018933344632387
-0.013364939950407	-0.016265647485852
-0.019893420860171	-0.015201377682388
-0.013791400007904	-0.018178712576628
-0.020712001249194	-0.007747321389616
-0.023485885933042	-0.027864985167980
0.000000000000000	0.000000000000000

E-23

```
0.000000000000000    0.000000000000000
0.000000000000000    0.000000000000000
0.000000000000000    0.000000000000000
0.000000000000000    0.000000000000000
0.000000000000000    0.000000000000000
0.000000000000000    0.000000000000000
0.000000000000000    0.000000000000000
0.000000000000000    0.000000000000000
0.000000000000000    0.000000000000000
0.000000000000000    0.000000000000000
0.000000000000000    0.000000000000000
0.000000000000000    0.000000000000000
0.000000000000000    0.000000000000000
```

Appendix F. Performance Plots for Baseline Controller

The plots on the ensuing pages show the results of computer simulation of the baseline LQG controller based on the updated truth model described in Chapters 3 and 4 and Appendix A. Plots are provided to demonstrate the performance of the Kalman filter in estimating the 14 Zernike coefficient states. The Zernike coefficients describe the phase distortion in the optical wavefront resulting from propagation through the turbulent atmosphere. Each state is modeled with a first-order Markov process shaping filter. Plots are also provided which show the overall performance of the LQG controller in generating the appropriate control to apply to the deformable mirror as compensation for the atmospheric phase distortion. Each section contains the plots corresponding to specified levels of measurement noise as described in Chapter 5.

Section F.1 contains the performance plots corresponding to measurement noise study 1, in which low noise is simulated in both the truth and filter models. Filter estimation performance is shown in the form of 3-plot sets for each of the atmosphere states. These plots correspond to Figures 5.1, 5.2, and 5.3. The first plot in each set demonstrates the tracking capability of the filter. The filter-computed statistics of its own estimation error for a single realization are shown in the second plot. Finally, the true error statistics over 10 Monte Carlo runs, as computed from Equations 5.1 and 5.2, are shown in the third plot of the set. Control system performance is shown in a set of plots corresponding to Figures 5.4, 5.5, and 5.6. Detailed analysis of the results contained in the plots are presented in Chapter 5.

Sections F.2 through F.9 show identical sets of plots for the remaining eight noise studies. In order to keep the abundance of plots to a minimum, only the plots for states 1, 6, and 14 and the control system performance plots are provided for these studies.
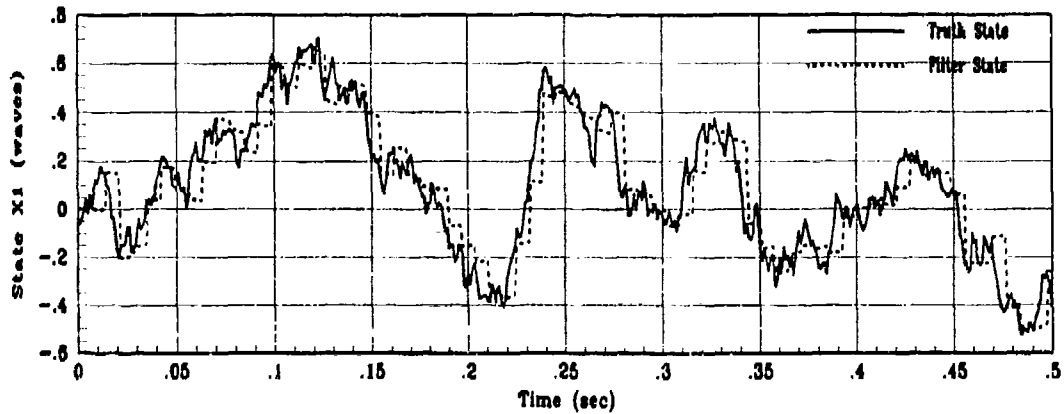
(a) Truth and Filter States: XS1, XF1
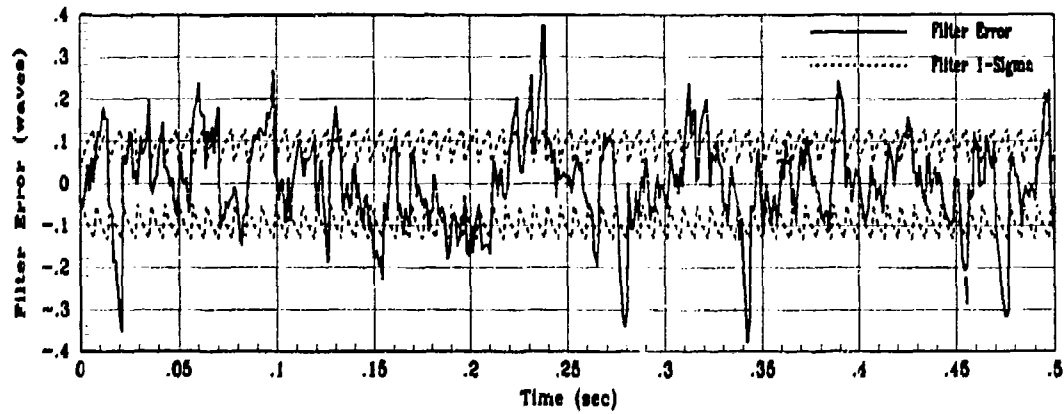
(b) X1 Filter Error for 1 MC Run
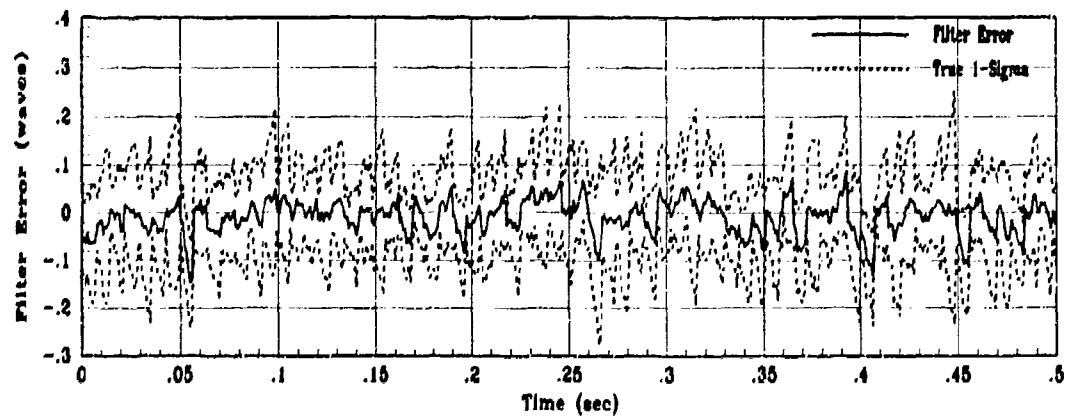
(o) X1 True Filter Error for 10 MC Runs

Figure F.1. Baseline State 1 Filter Estimation Error for Study 1
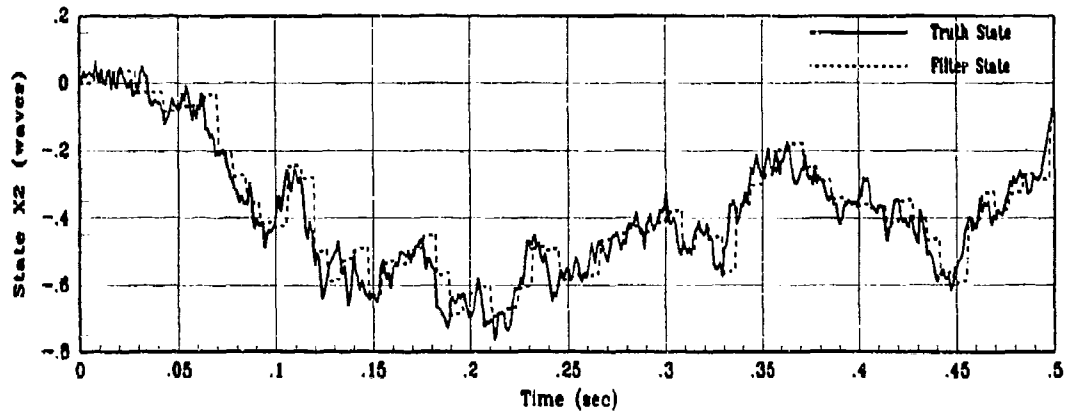
(a) Truth and Filter States: XS2, XF2
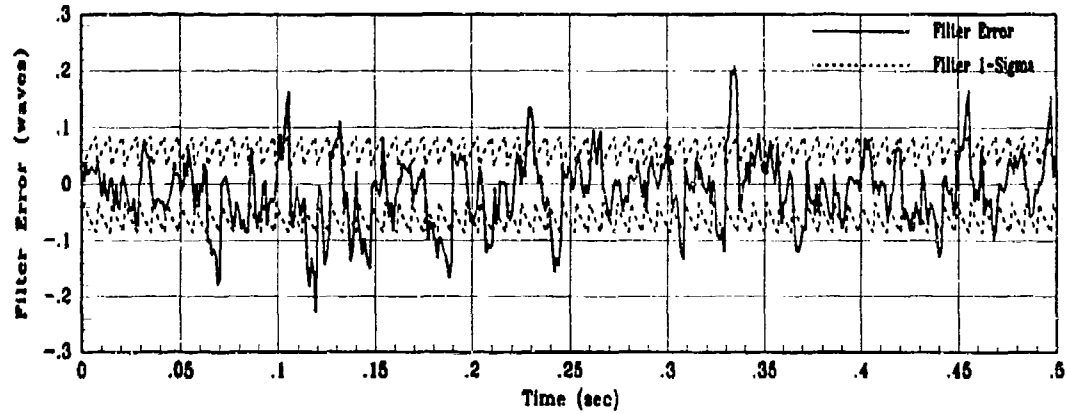
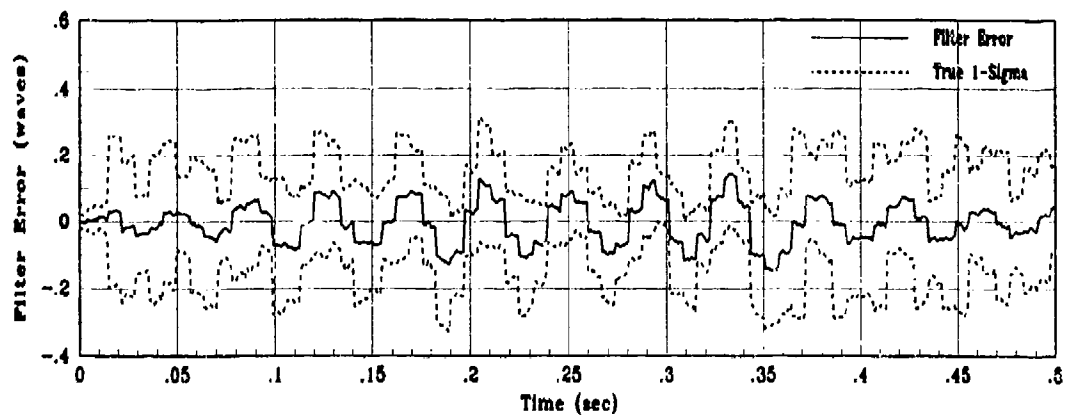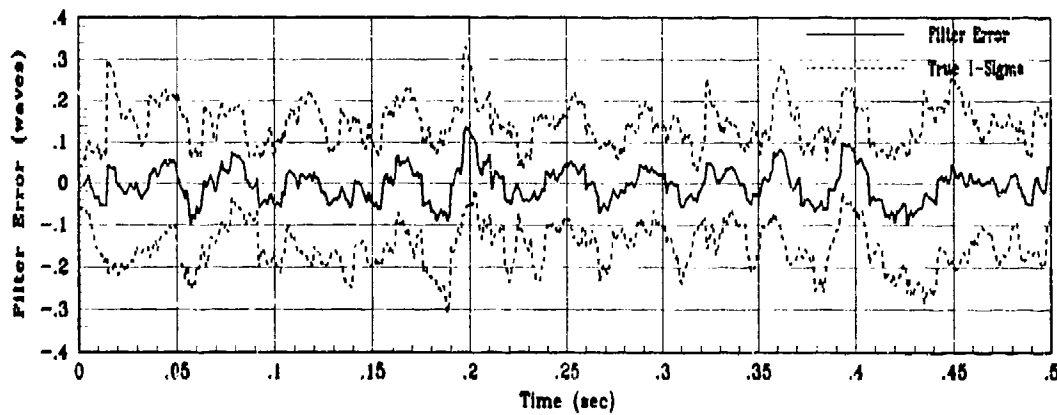(b) X2 Filter Error for 1 MC Run
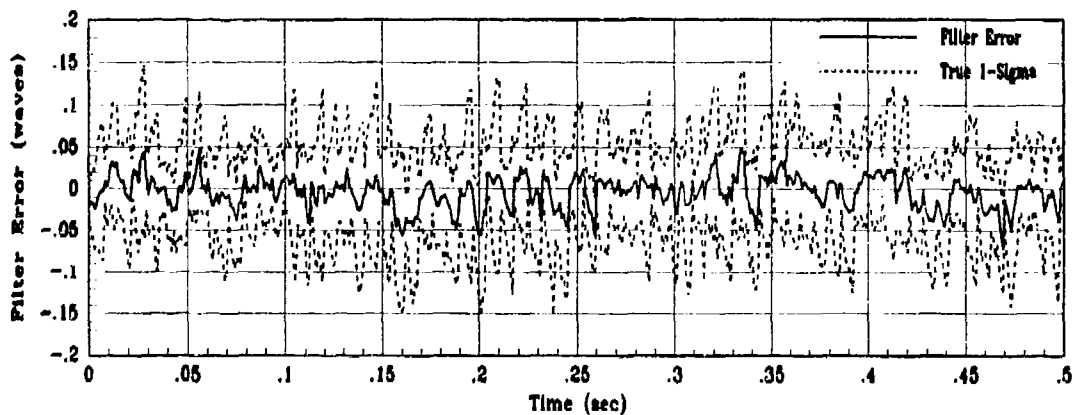
(c) X2 True Filter Error for 10 MC runs

Figure F.2. Baseline State 2 Filter Estimation Error for Study 1
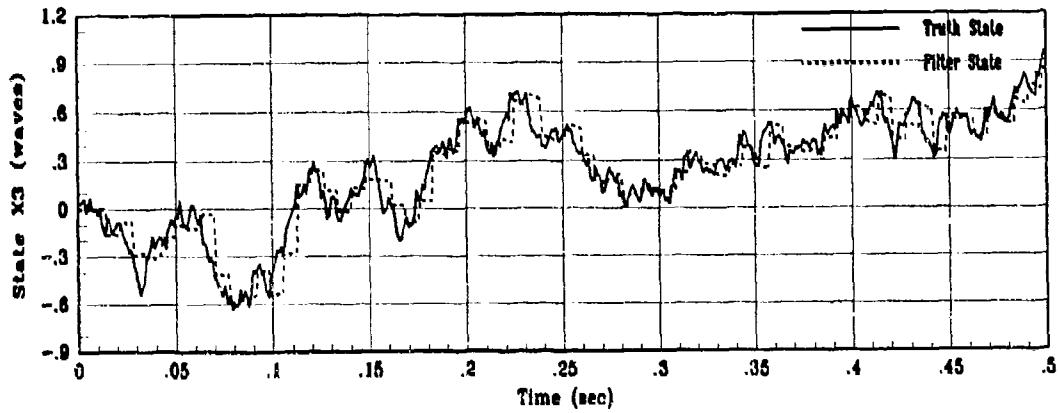
F-3

(a) Truth and Filter States: XS3, XF3
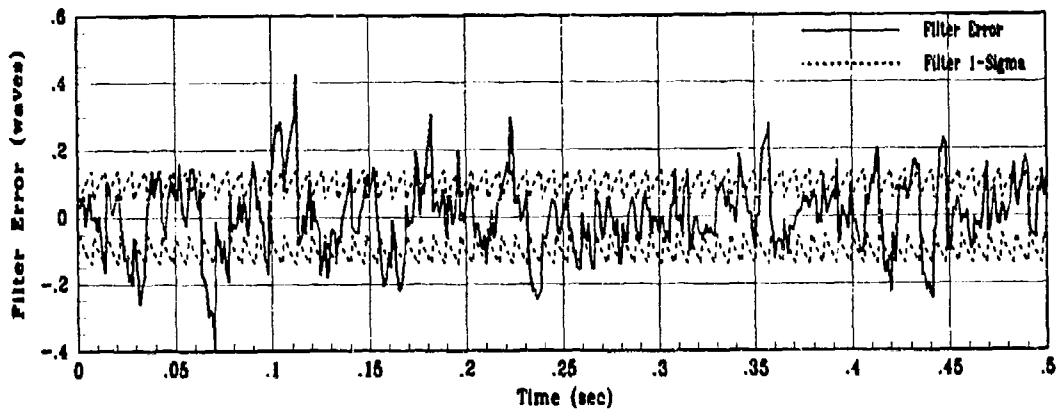
(b) X3 Filter Error for 1 MC Run
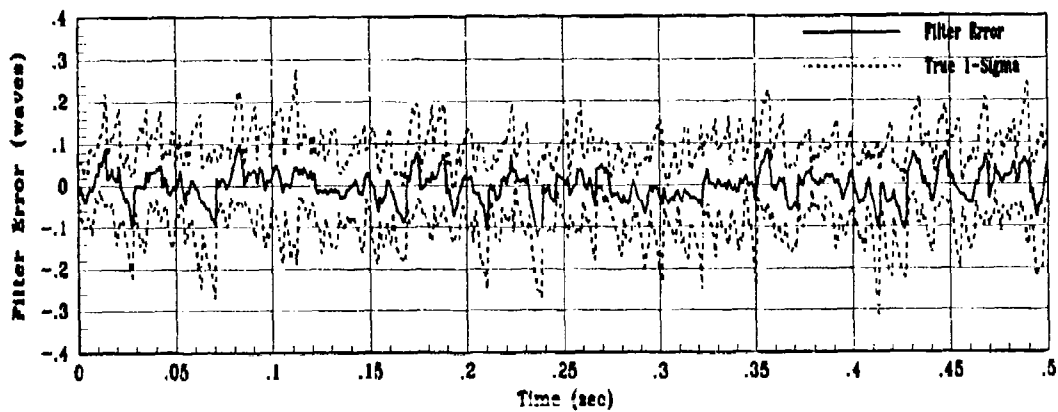
(c) X3 True Filter Error for 10 MC runs

Figure F.3. Baseline State 3 Filter Estimation Error for Study 1
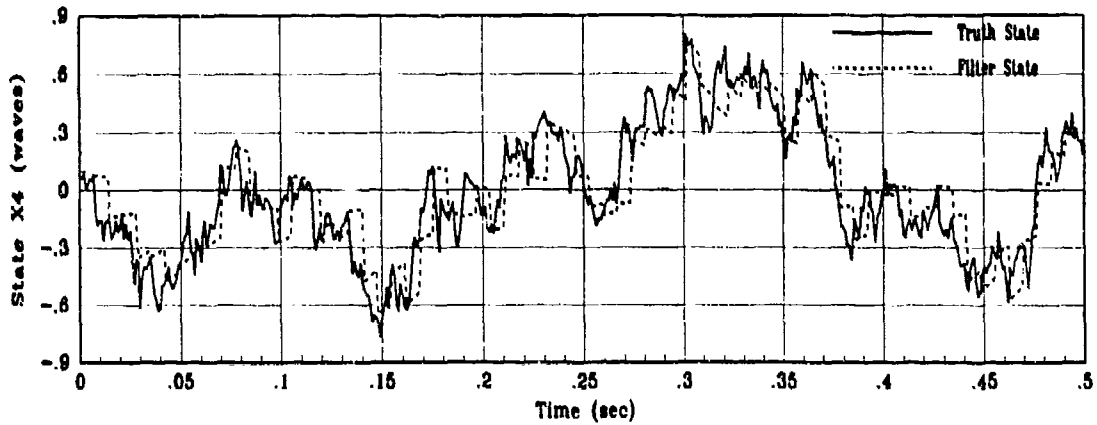
(a) Truth and Filter States: XS4, XF4
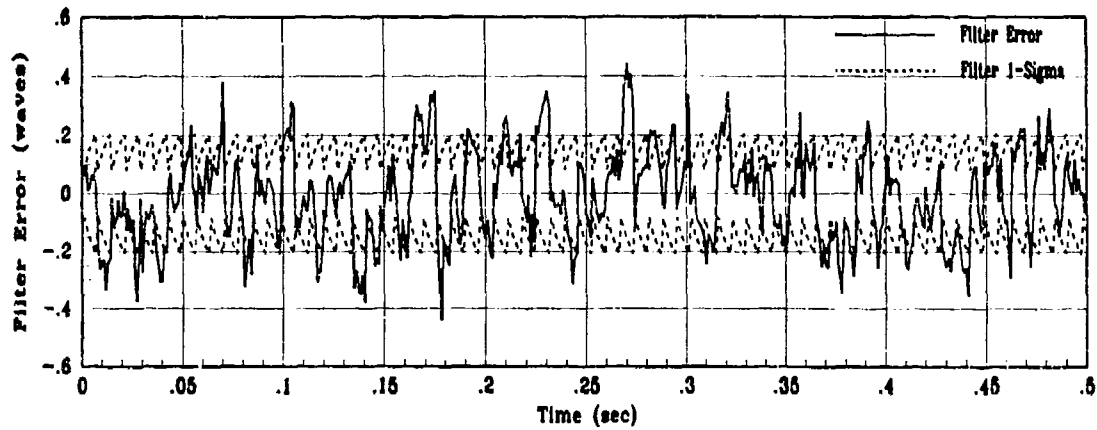
(b) X4 Filter Error for 1 MC Run
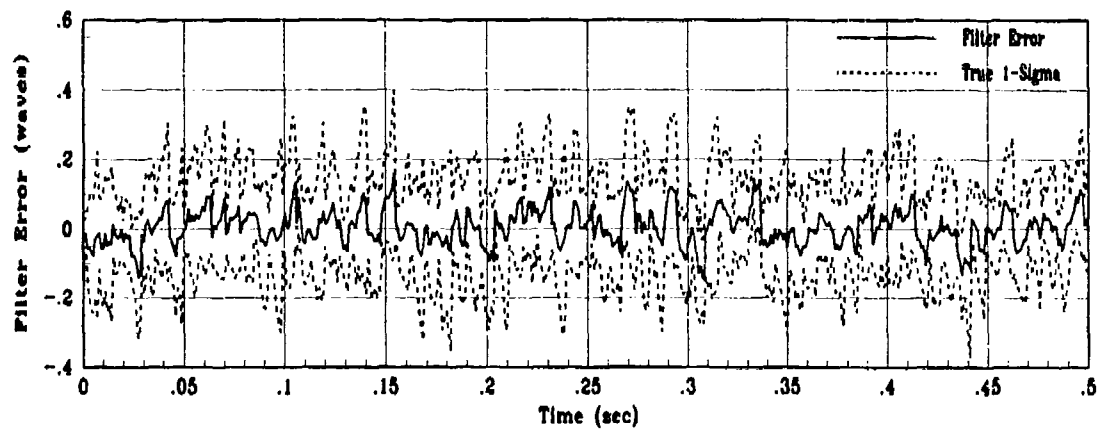
(c) X4 True Filter Error for 10 MC runs

Figure F.4. Baseline State 4 Filter Estimation Error for Study 1
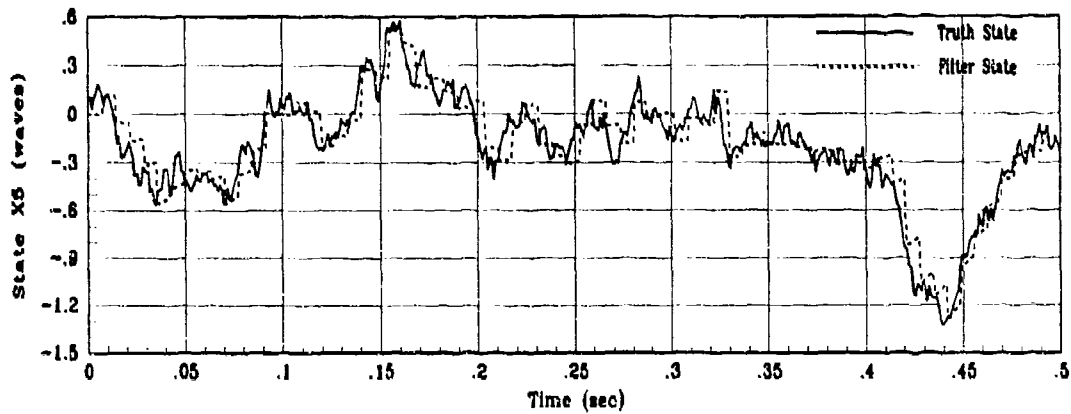
(a) Truth and Filter States: XS5, XF5
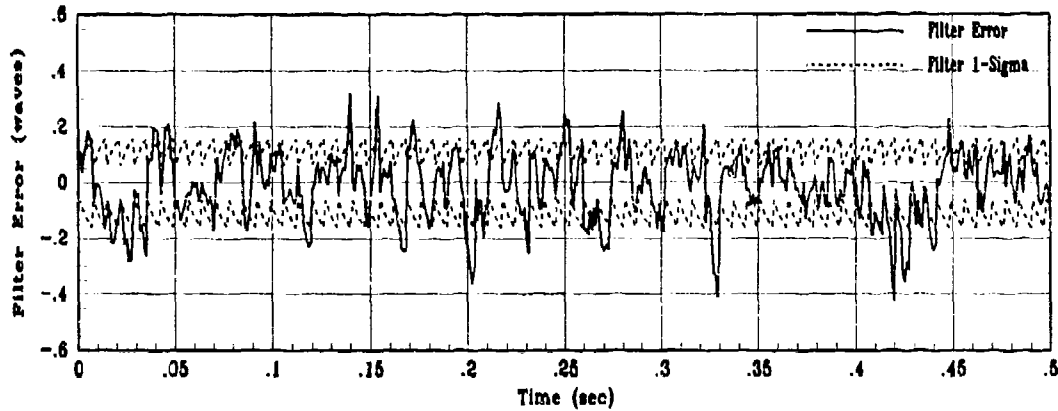
(b) X5 Filter Error for 1 MC Run
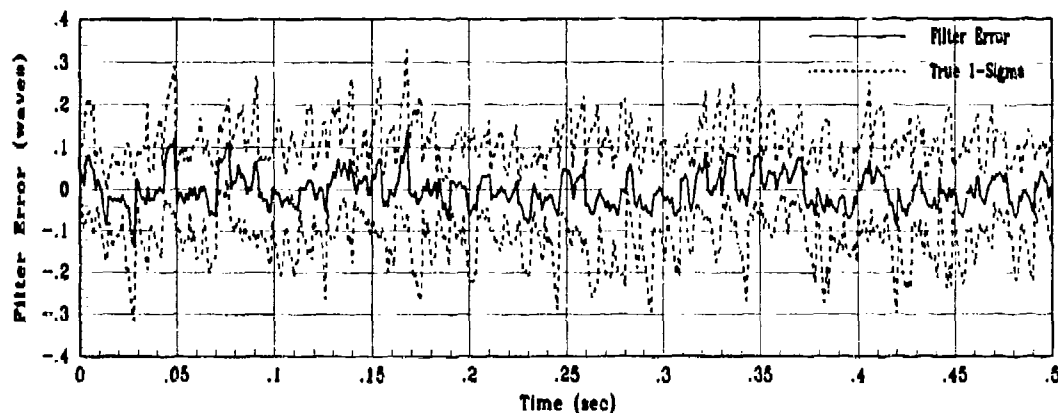
(c) X5 True Filter Error for 10 MC runs

Figure F.5. Baseline State 5 Filter Estimation Error for Study 1
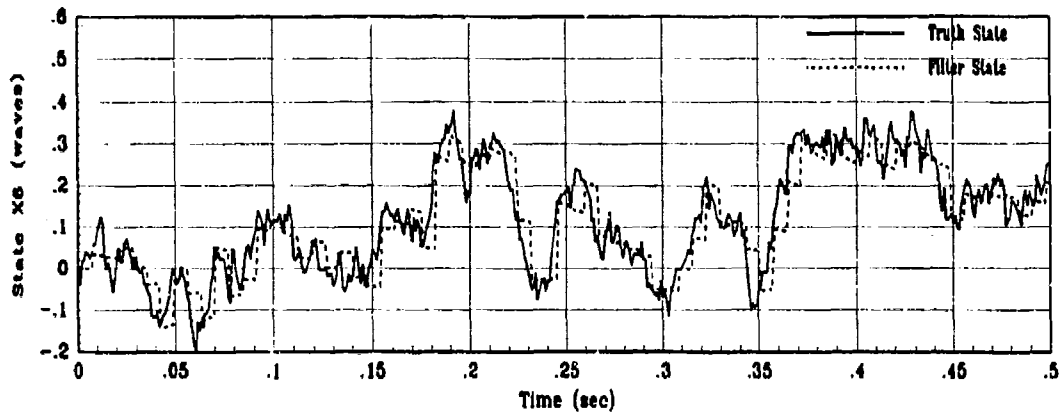
(a) Truth and Filter States: XS6, XF6
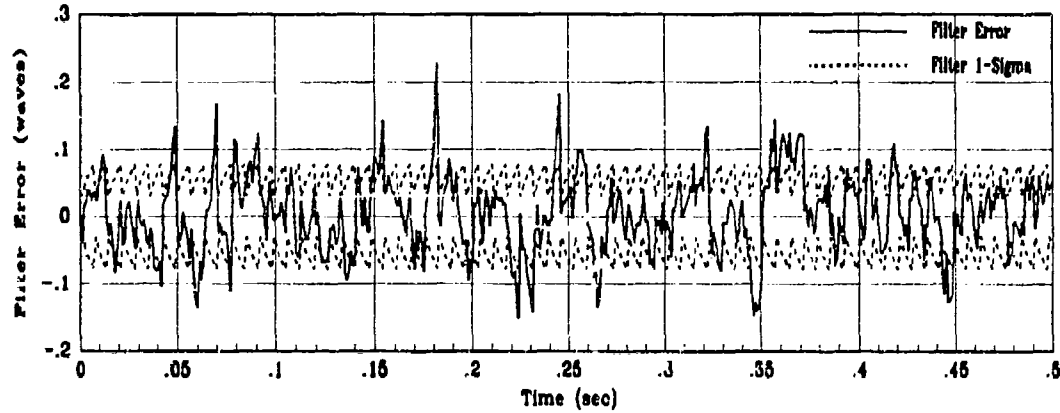
(b) X6 Filter Error for 1 MC Run
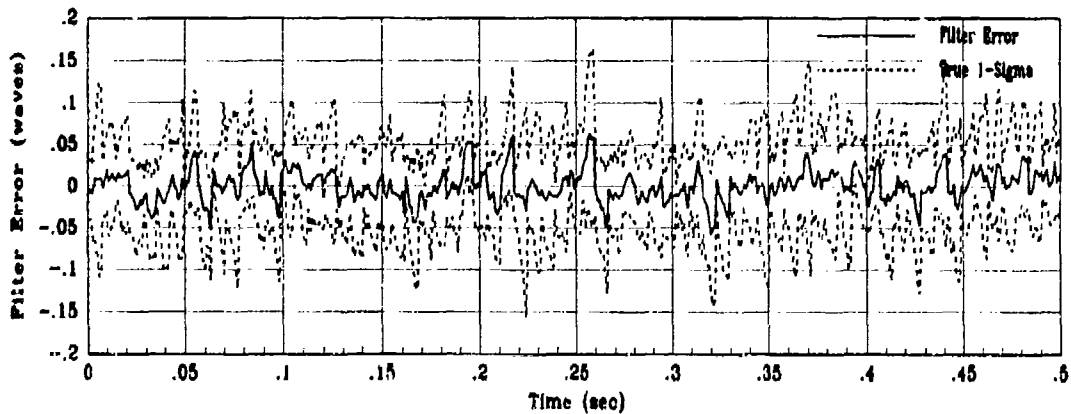
(c) X6 True Filter Error for 10 MC runs

Figure F.6. Baseline State 6 Filter Estimation Error for Study 1
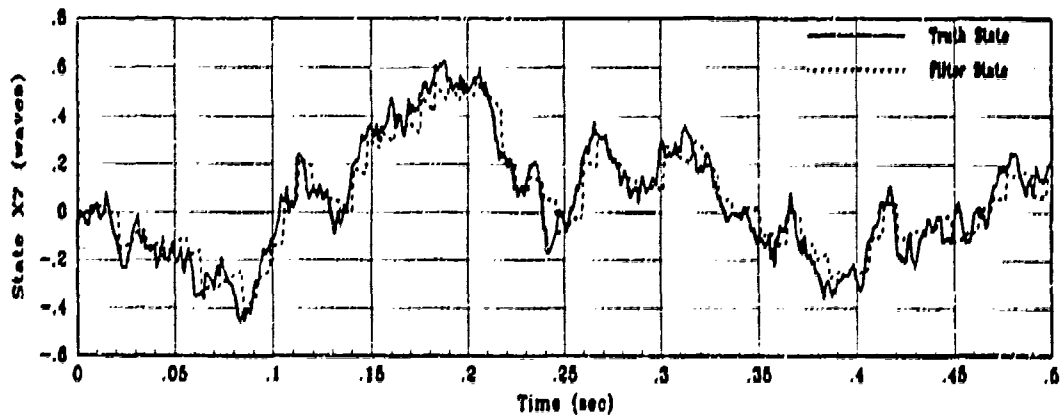
(a) Truth and Filter States: XS7, XF7
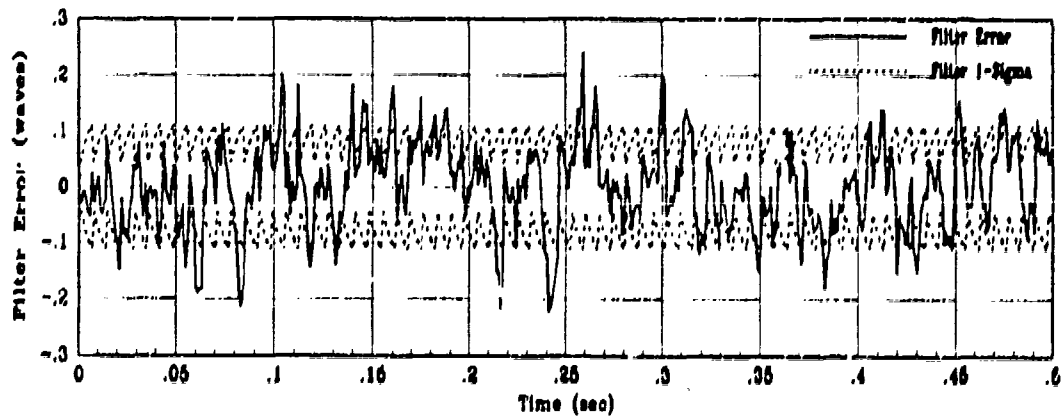
(b) X7 Filter Error for 1 MC Run
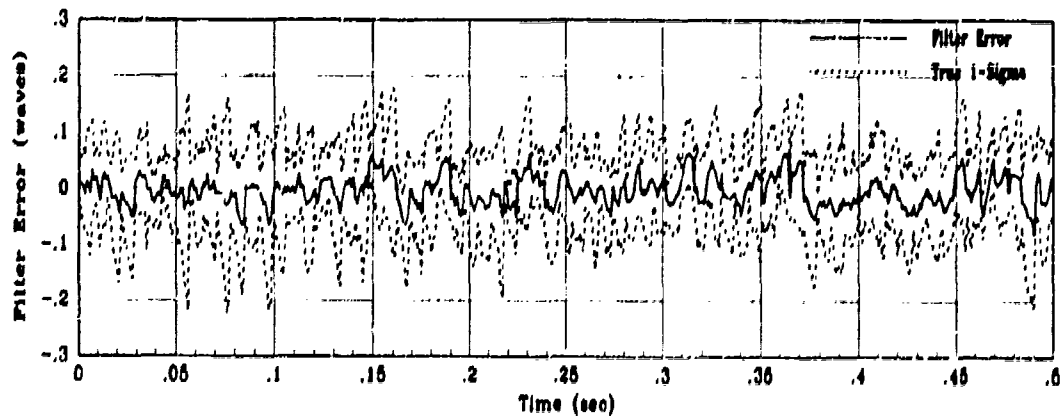
(c) X7 True Filter Error for 10 MC runs

Figure F.7. Baseline State 7 Filter Estimation Error for Study 1
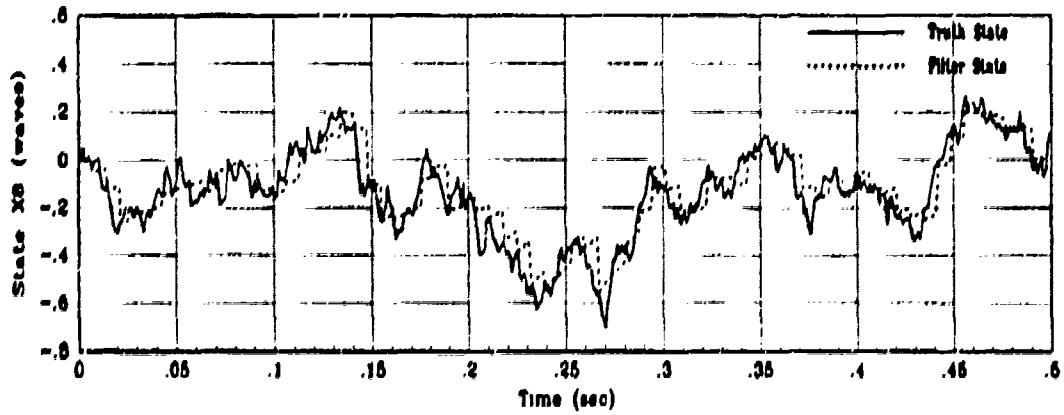
(a) Truth and Filter States: X88, XF8
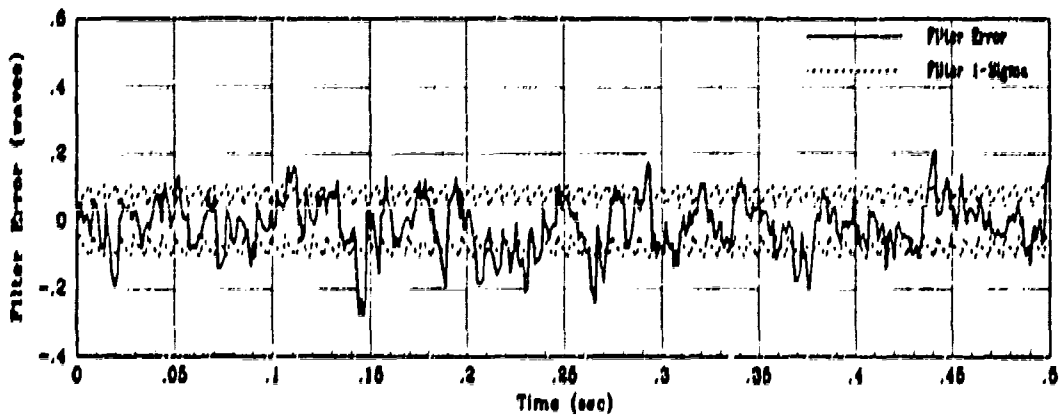
(b) X8 Filter Error for 1 MC Run
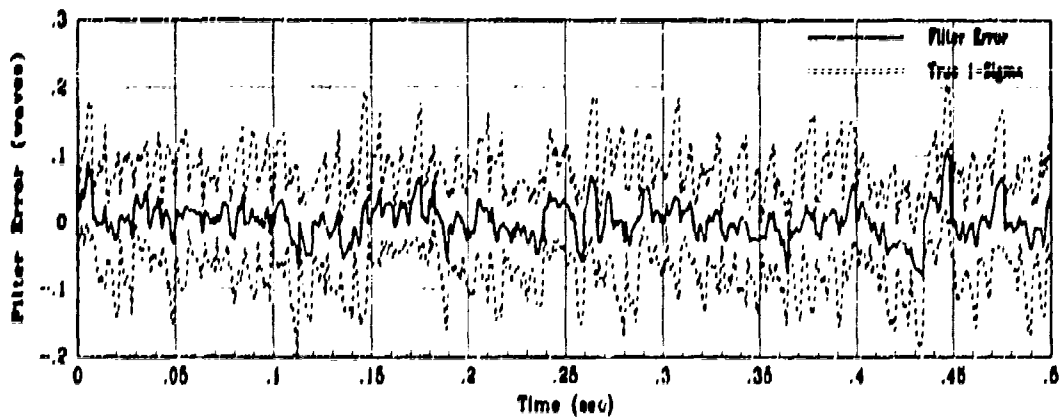
(c) X8 True Filter Error for 10 MC runs

Figure E.8. Baseline State 8 Filter Estimation Error for Study 1
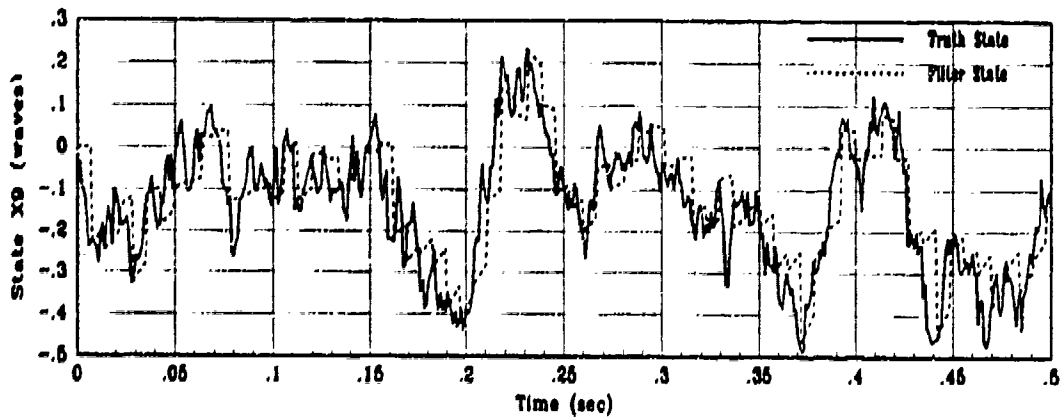
(a) Truth and Filter States: XS9, XF9
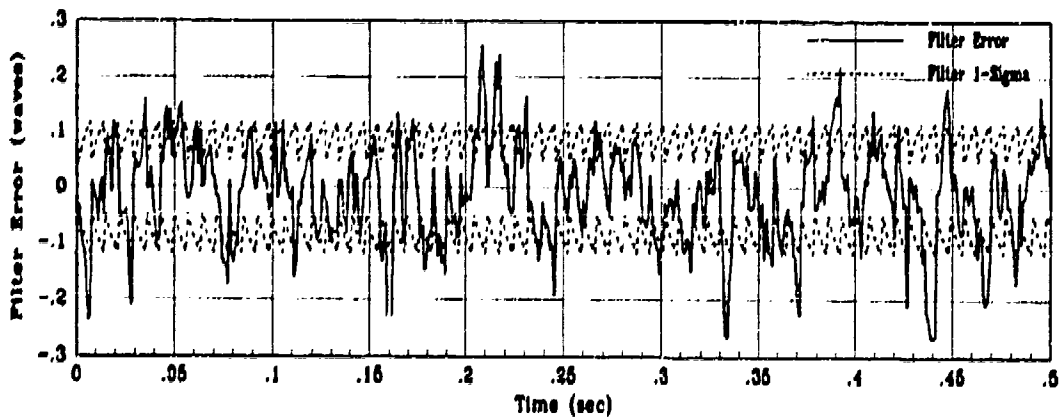
(b) X9 Filter Error for 1 MC Run
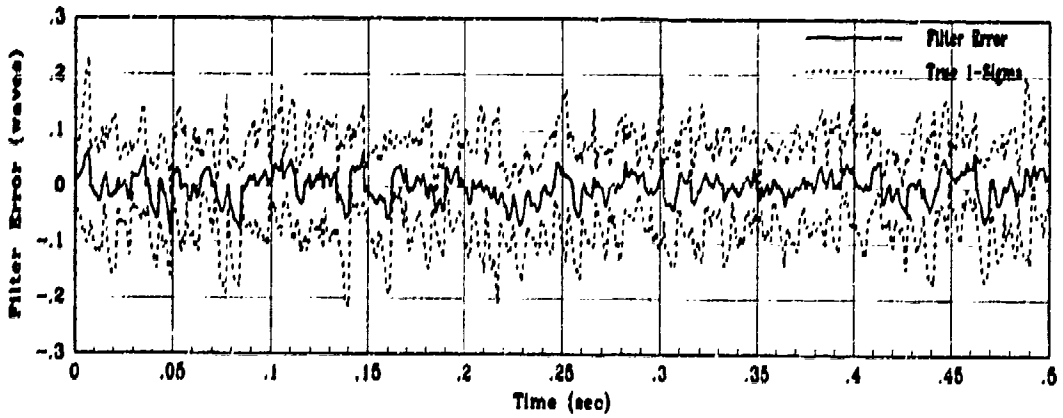
(c) X9 True Filter Error for 10 MC runs

Figure F.9. Baseline State 9 Filter Estimation Error for Study 1
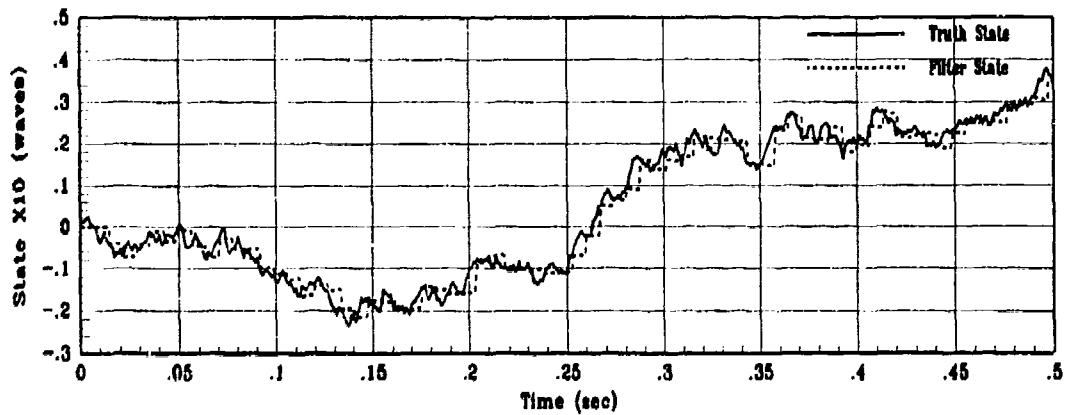
(a) Truth and Filter States: XS10, XF10
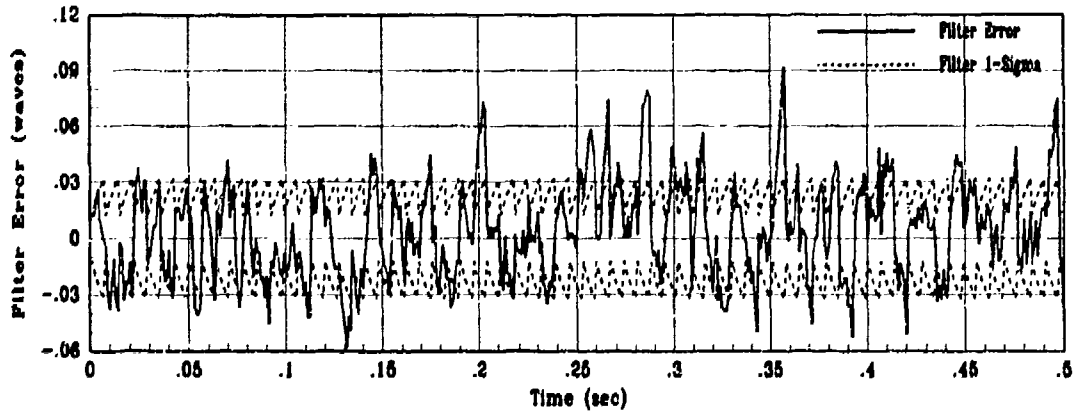
(b) X10 Filter Error for 1 MC Run
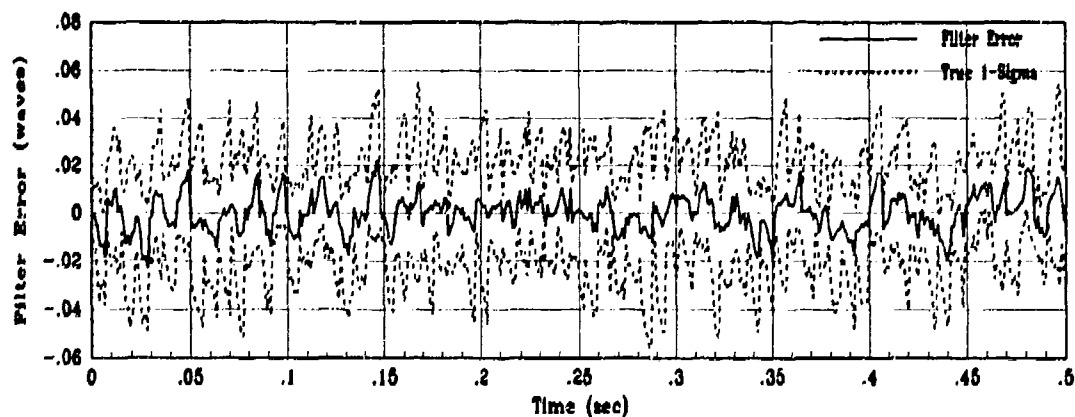
(c) X10 True Filter Error for 10 MC runs

Figure F.10. Baseline State 10 Filter Estimation Error for Study 1
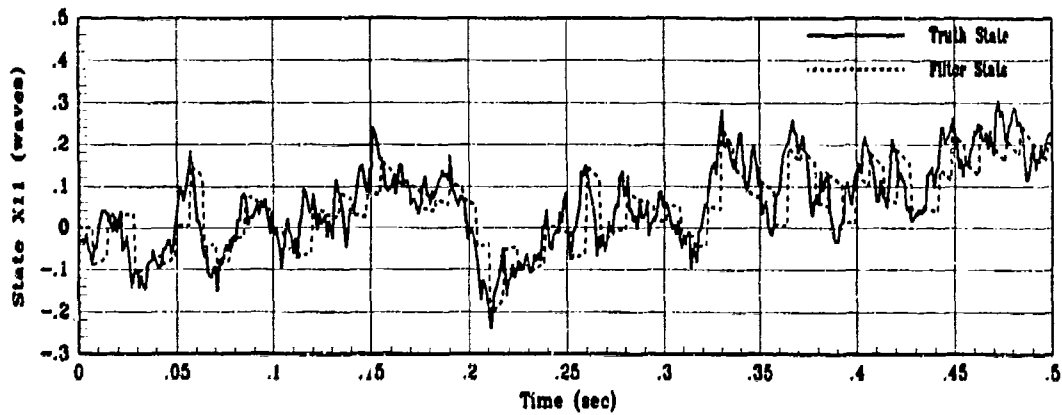
(a) Truth and Filter States: XS11, XF11
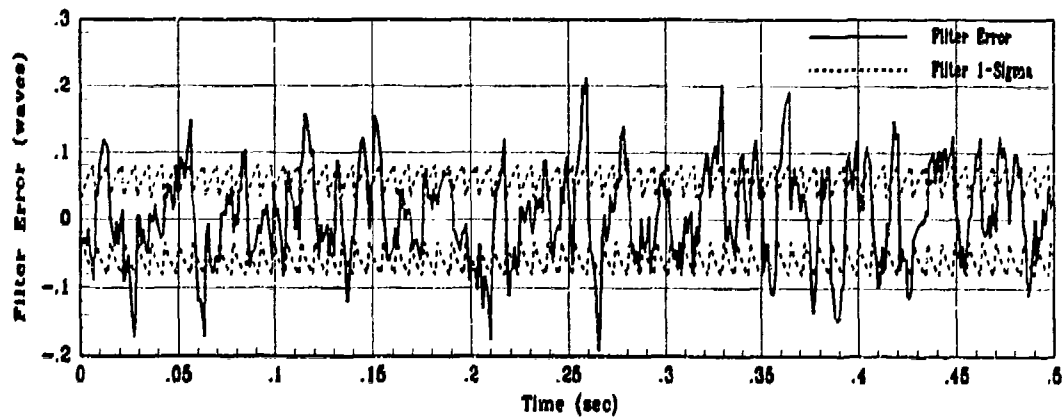
(b) X11 Filter Error for 1 MC Run
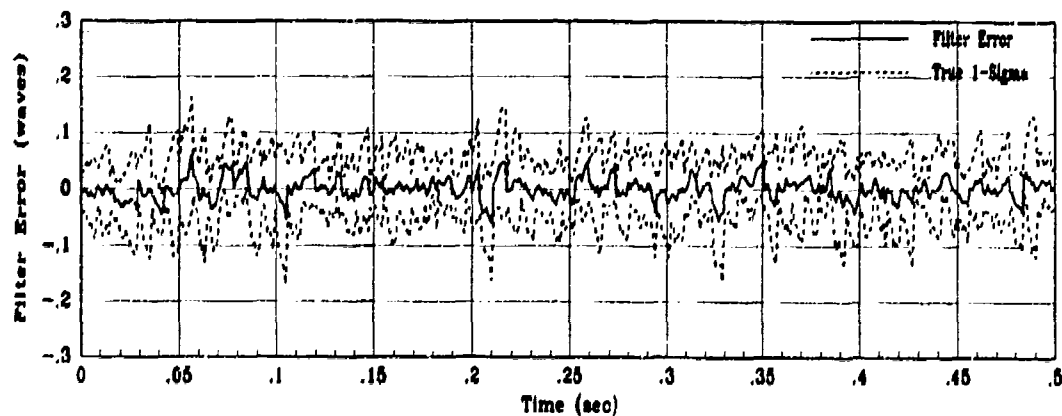
(c) X11 True Filter Error for 10 MC runs

Figure F.11. Baseline State 11 Filter Estimation Error for Study 1
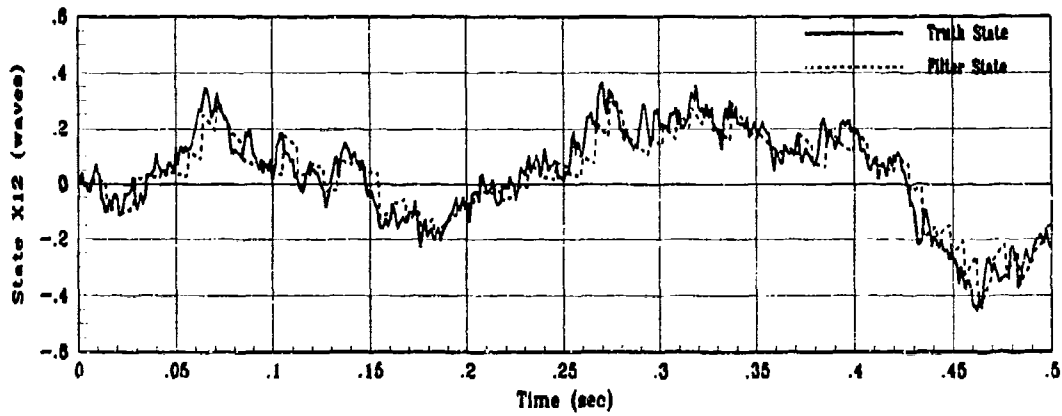
(a) Truth and Filter States: XS12, XF12
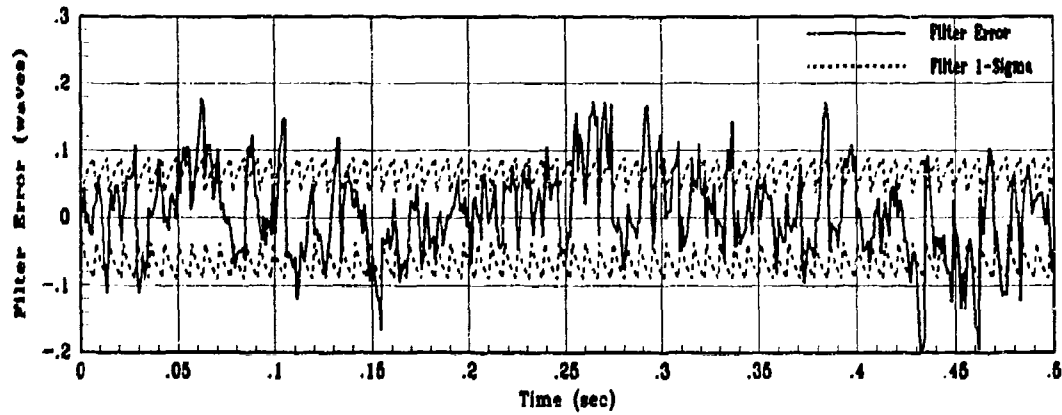
(b) X12 Filter Error for 1 MC Run
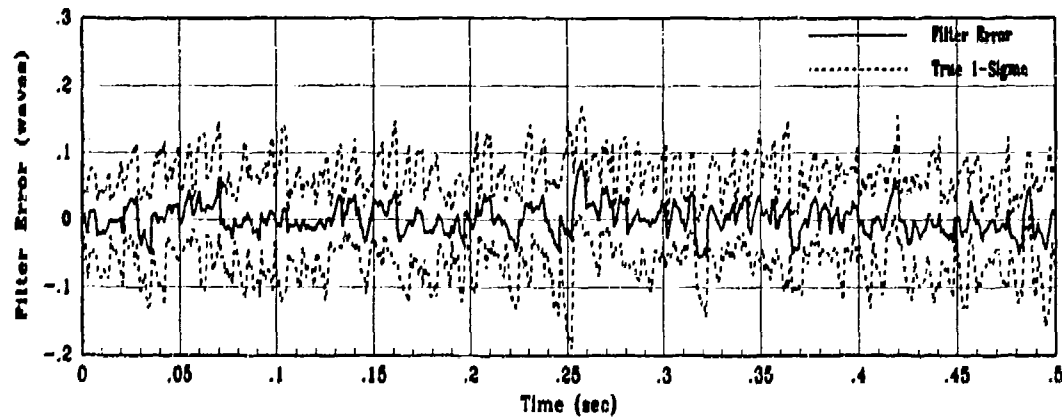
(c) X12 True Filter Error for 10 MC runs

Figure F.12. Baseline State 12 Filter Estimation Error for Study 1
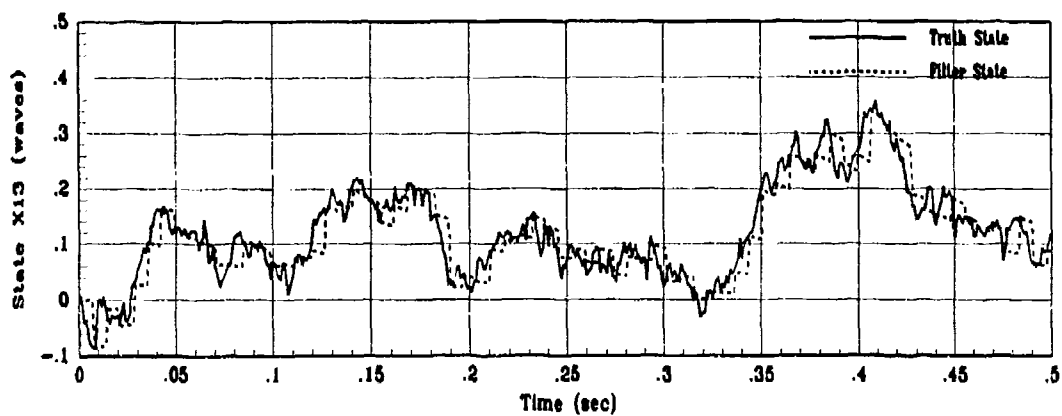
(a) Truth and Filter States: XS13, XF13
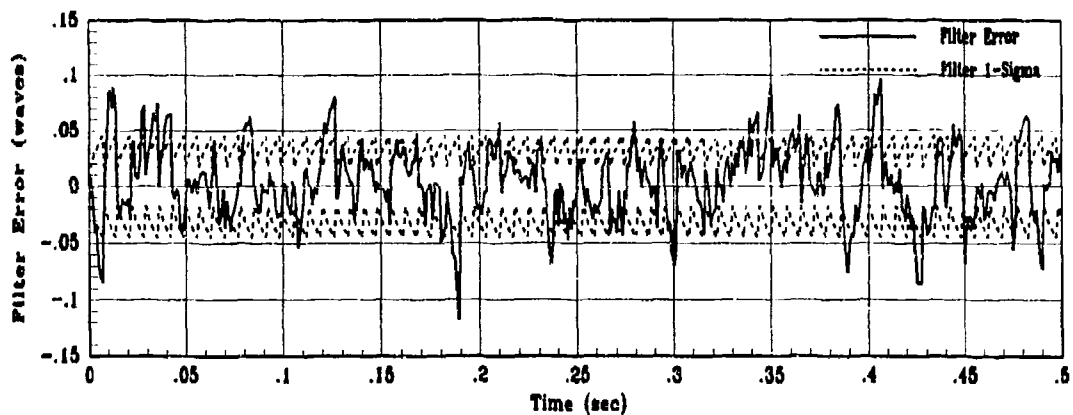
(b) X13 Filter Error for 1 MC Run
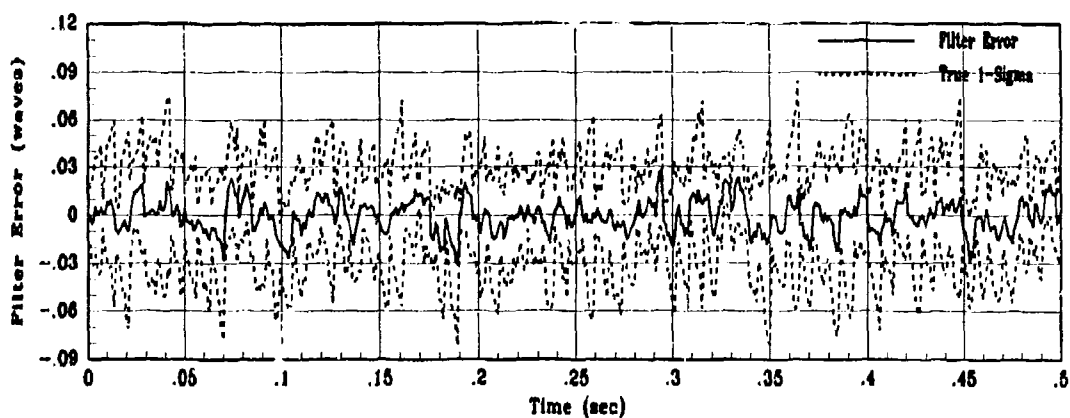
(c) X13 True Filter Error for 10 MC runs

Figure F.13. Baseline State 13 Filter Estimation Error for Study 1
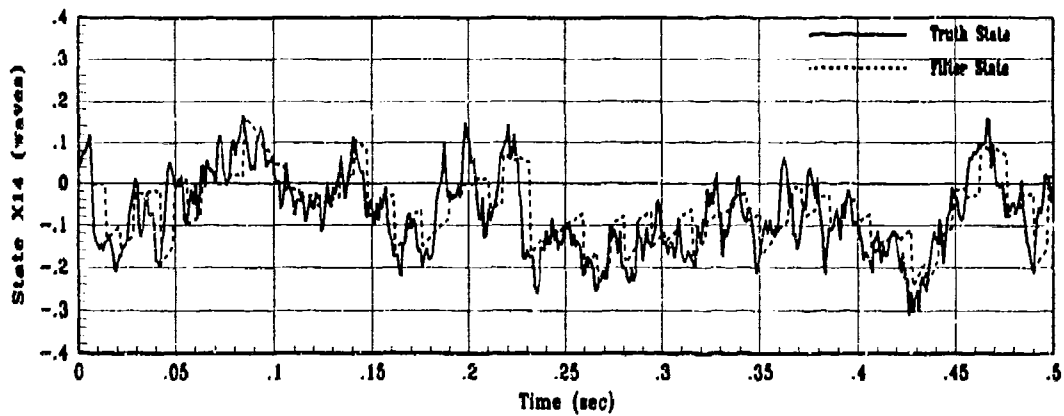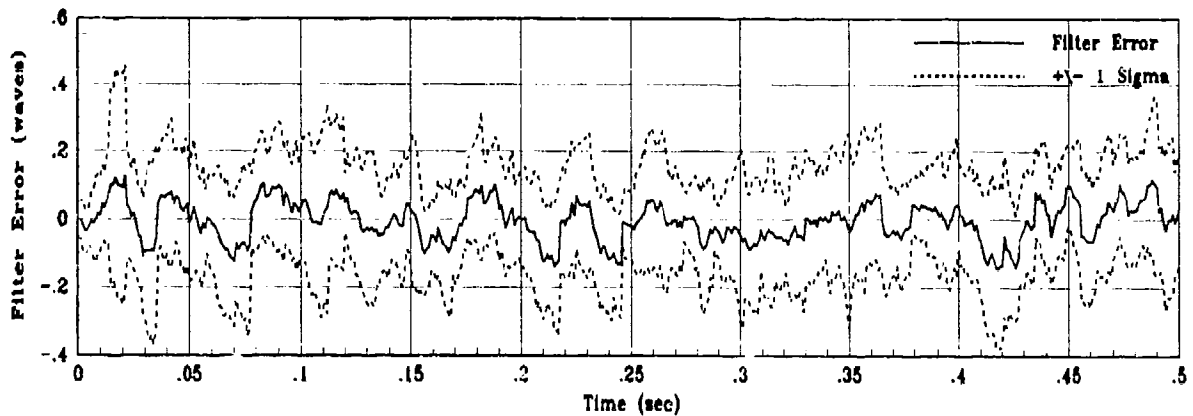
(a) Truth and Filter States: XS14, XF14
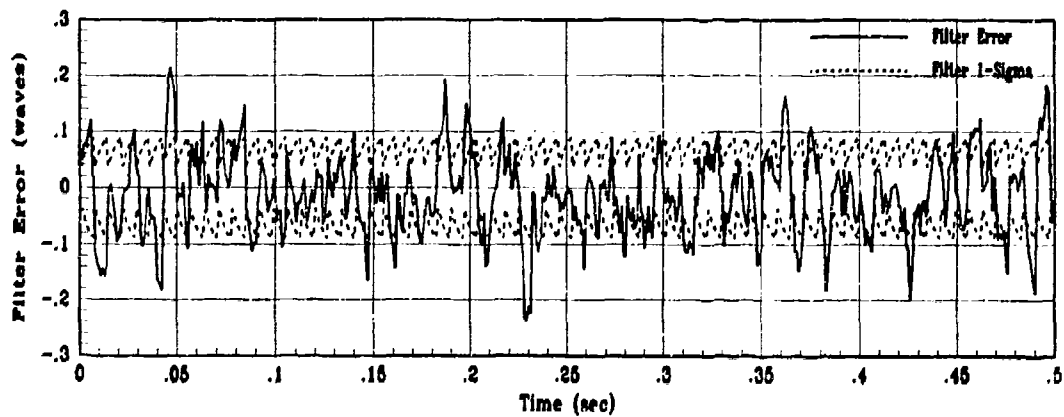
(b) X14 Filter Error for 1 MC Run
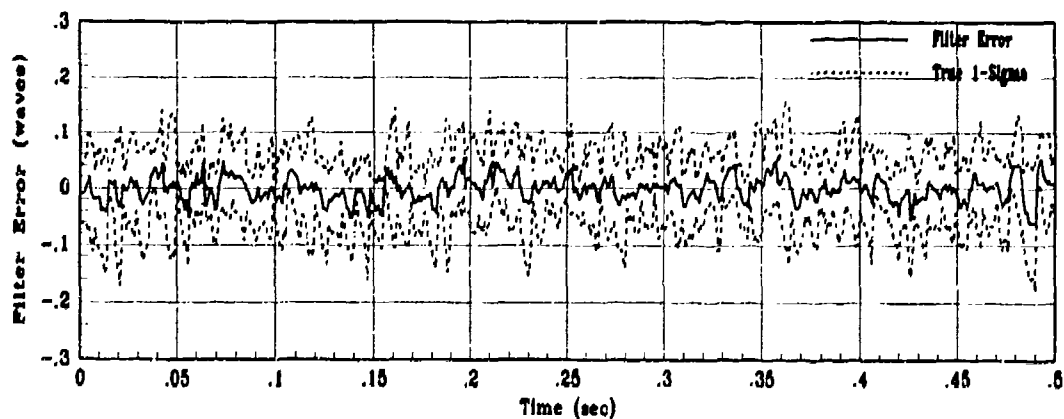
(c) X14 True Filter Error for 10 MC runs

Figure F.14. Baseline State 14 Filter Estimation Error for Study 1
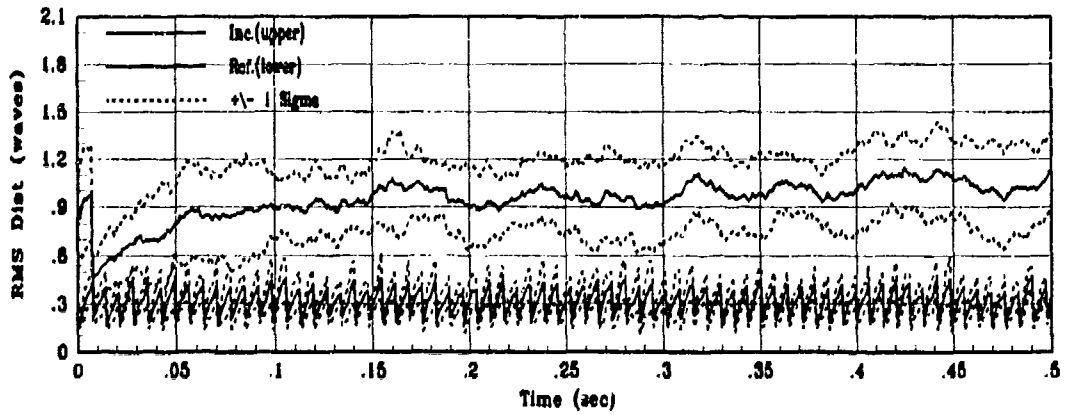
(a) Incident and Reflected RMS Phase Distortion for 10 MC Runs
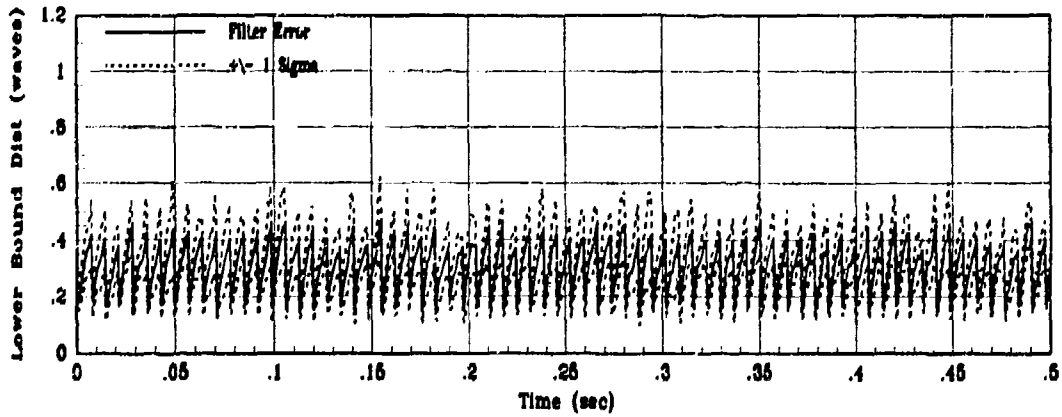
(b) RMS Filter Error for 10 MC Runs
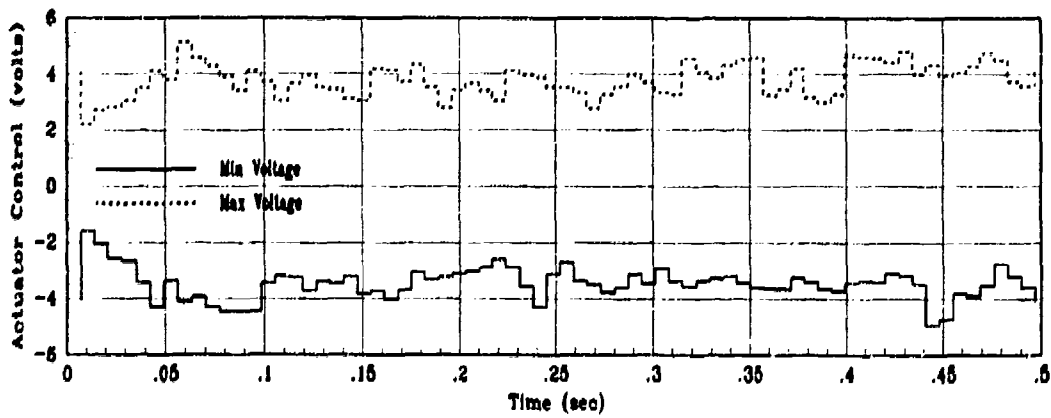
(c) Actuator Control Voltage Envelope

Figure F.15. Baseline Control System Performance for Study 1
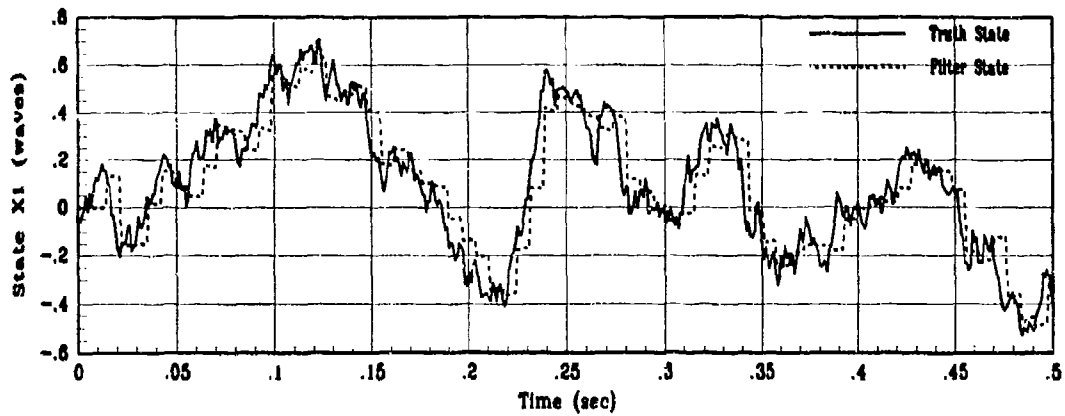
(a) Truth and Filter States: XS1, XF1
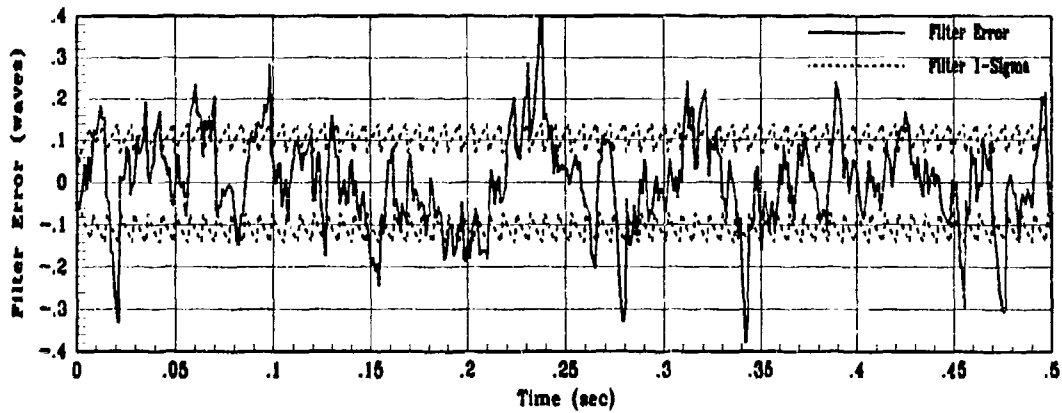
(b) X1 Filter Error for 1 MC Run
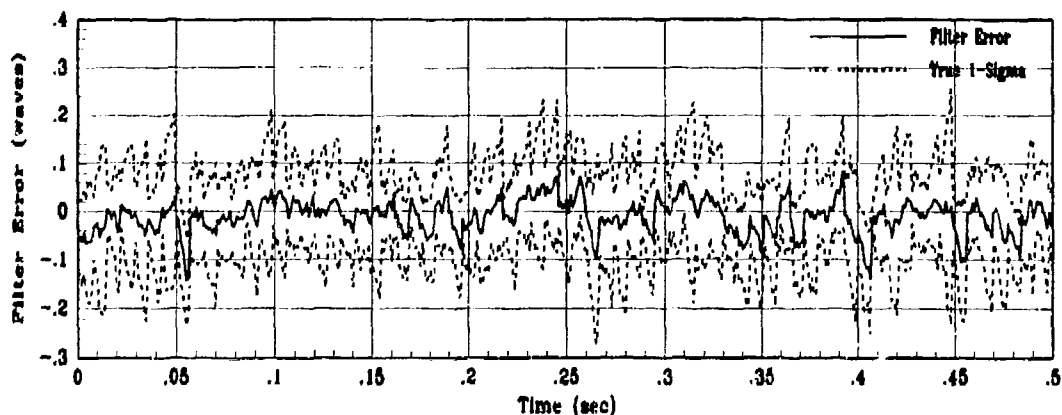
(c) X1 True Filter Error for 10 MC Runs

Figure F.16. Baseline State 1 Filter Estimation Error for Study 2
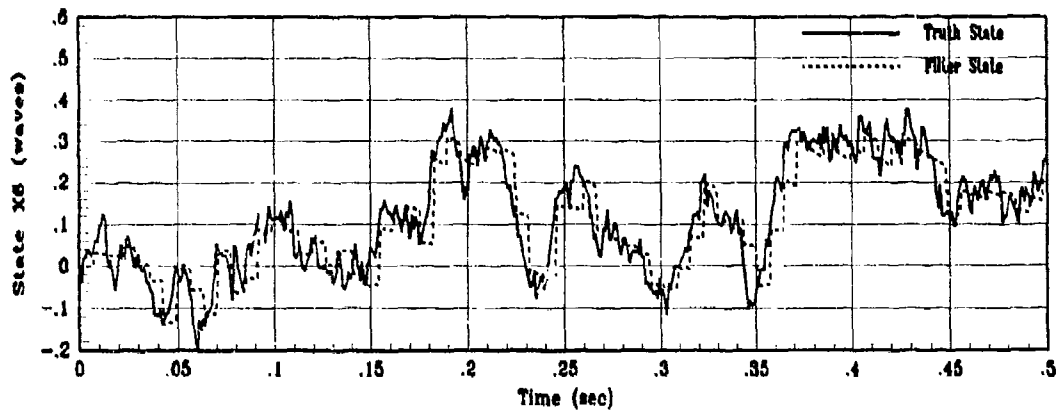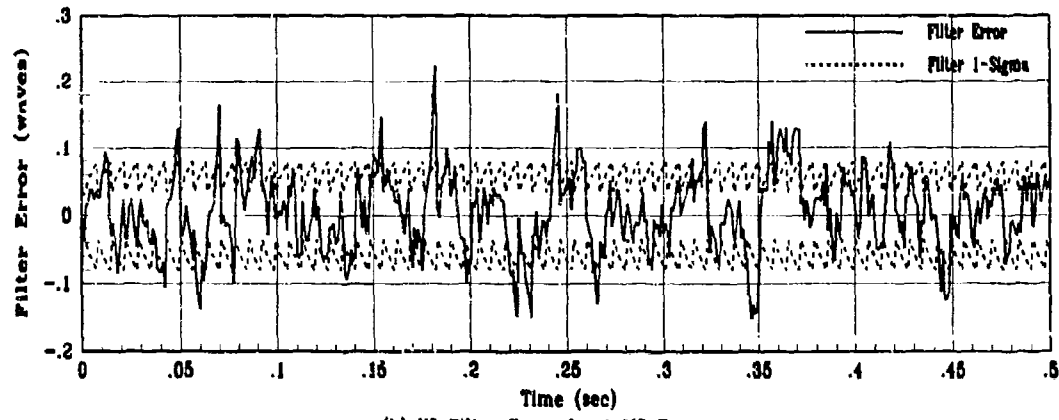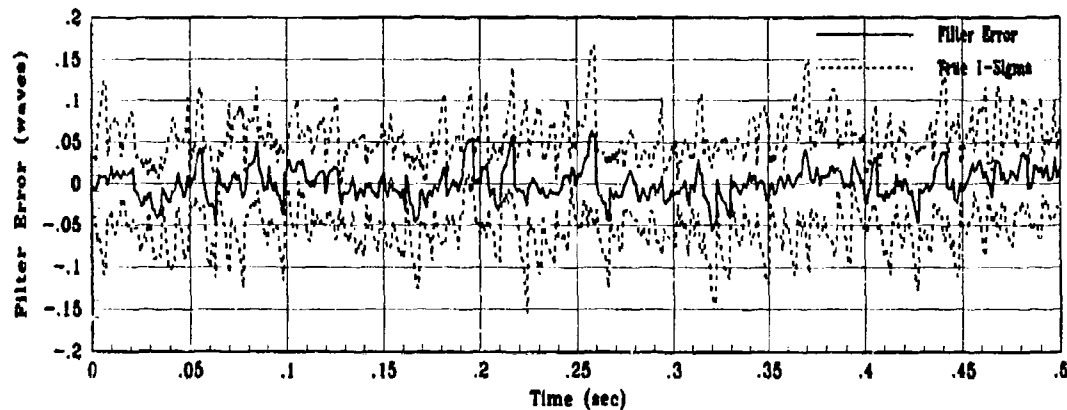
Figure F.17. Baseline State 6 Filter Estimation Error for Study 2
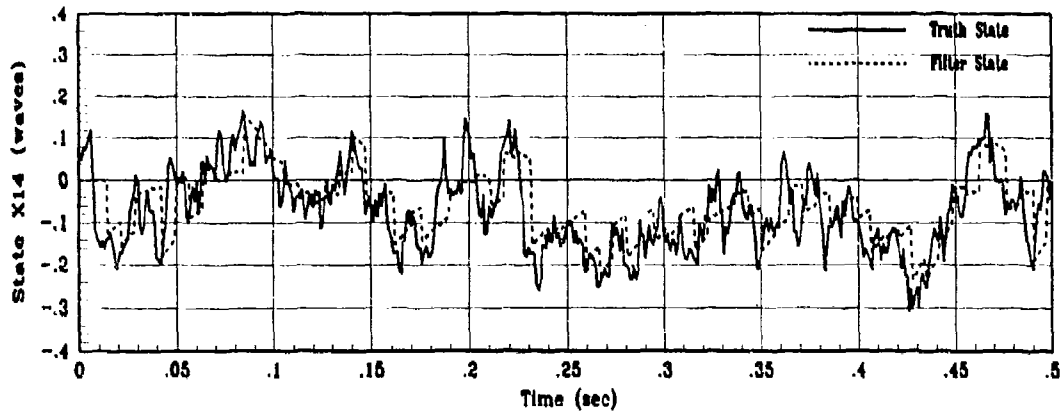
(a) Truth and Filter States: XS14, XF14
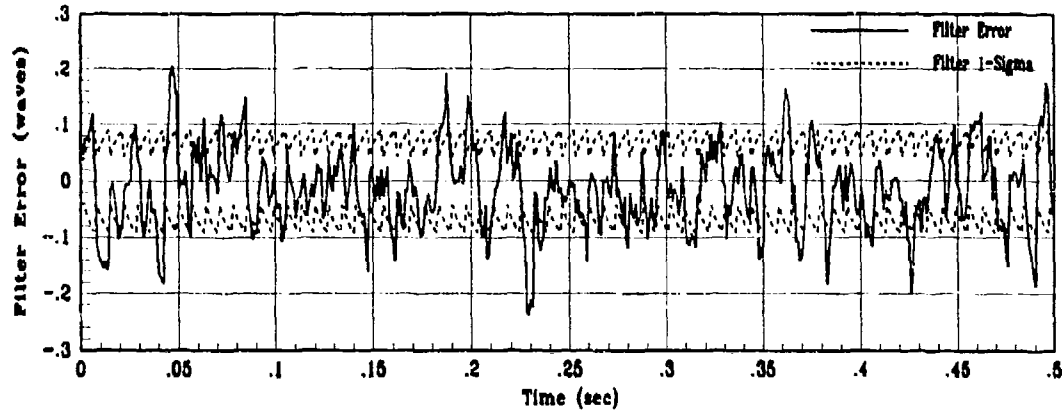
(b) X14 Filter Error for 1 MC Run
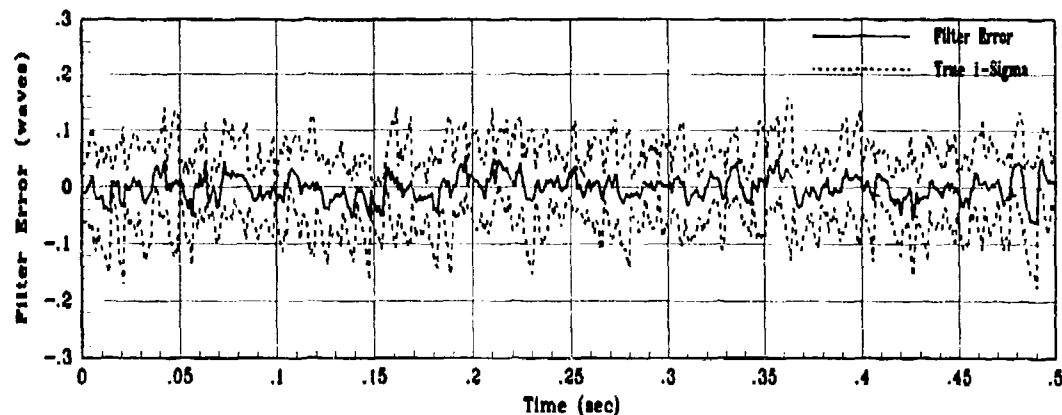
(c) X14 True Filter Error for 10 MC runs

Figure F.18. Baseline State 14 Filter Estimation Error for Study 2
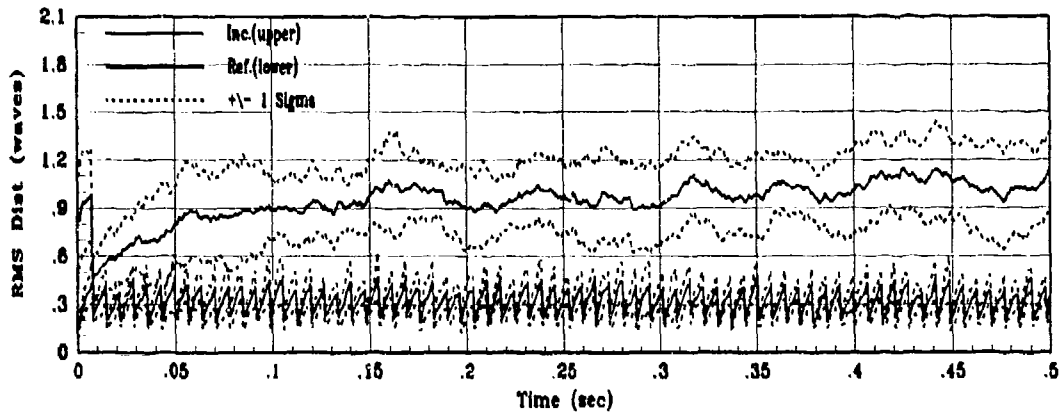
(a) Incident and Reflected RMS Phase Distortion for 10 MC Runs
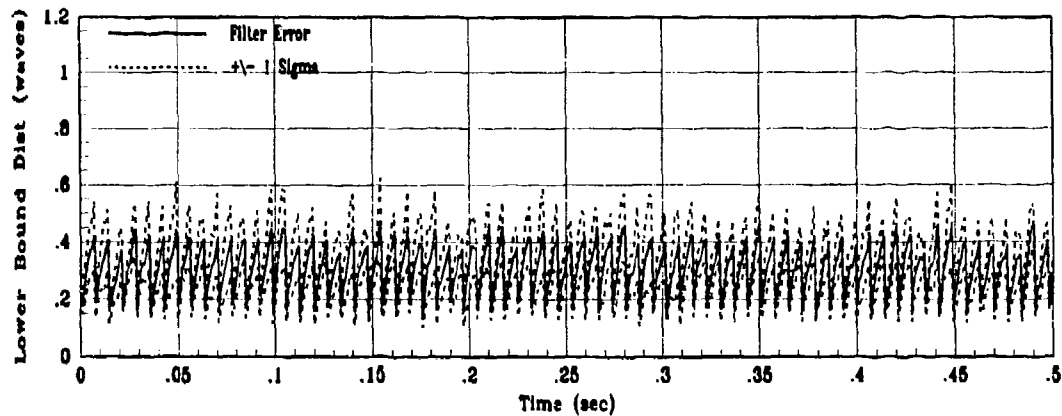
(b) RMS Filter Error for 10 MC Runs
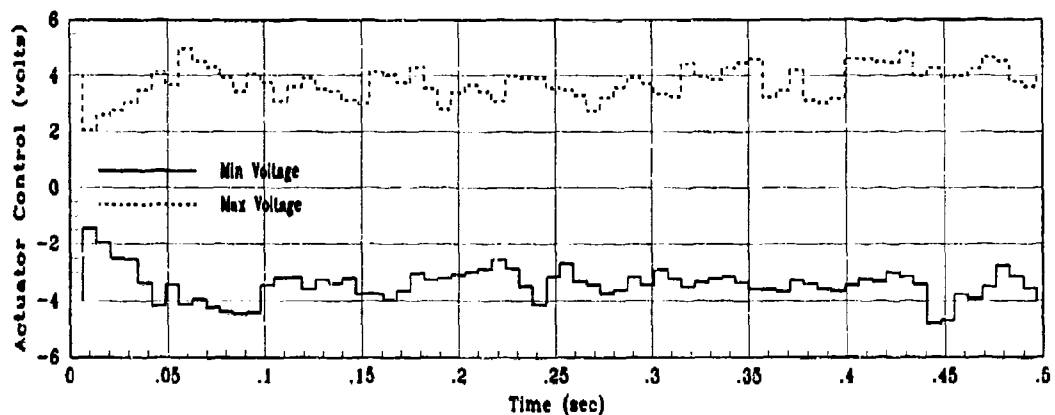
(c) Actuator Control Voltage Envelope

Figure F.19.   Baseline Control System Performance for Study 2
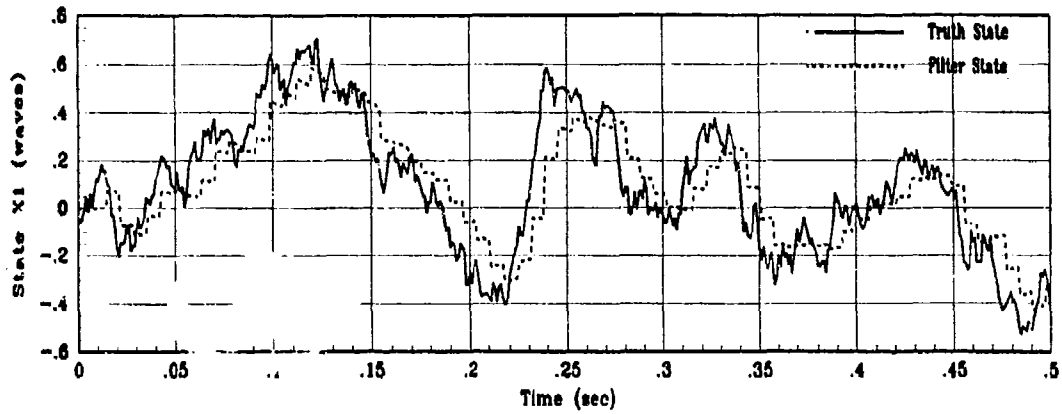
(a) Truth and Filter States: XS1, XF1
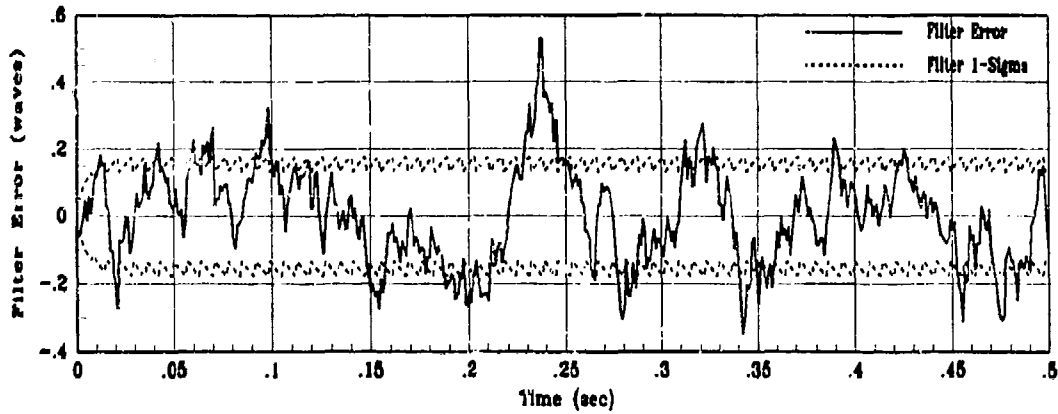
(b) X1 Filter Error for 1 MC Run
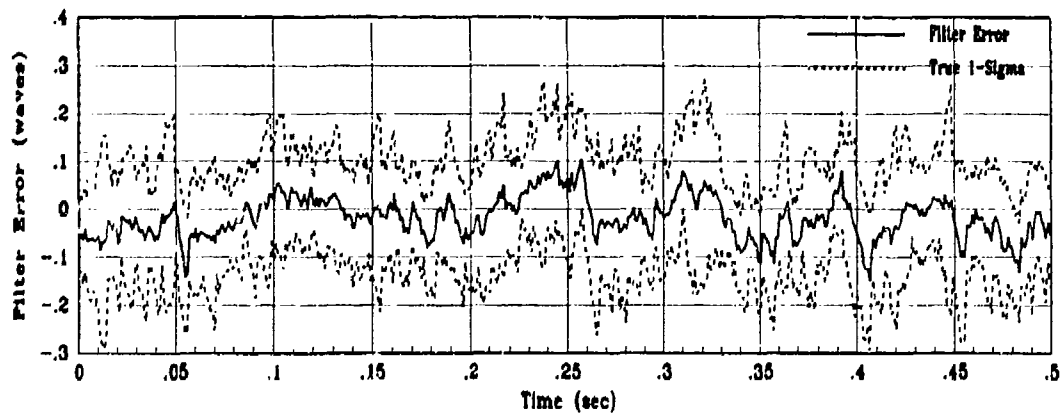
(c) X1 True Filter Error for 10 MC Runs

Figure F.20. Baseline State 1 Filter Estimation Error for Study 3
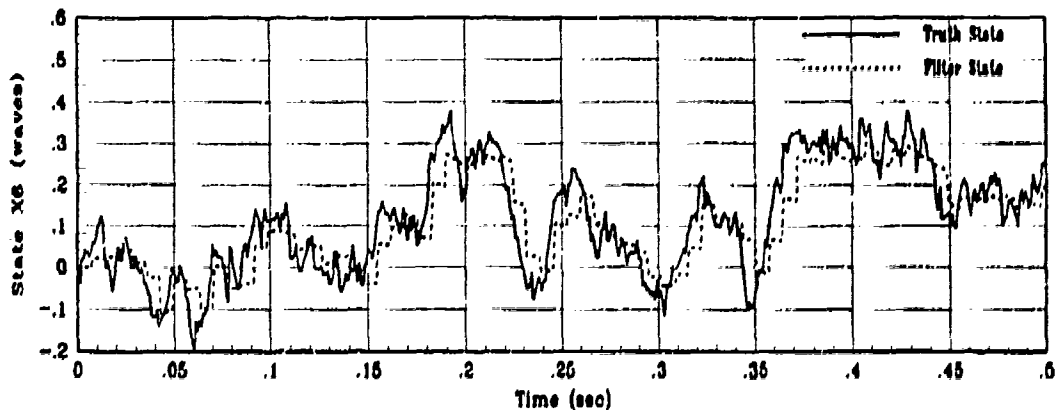
(a) Truth and Filter States: XS6, XF6
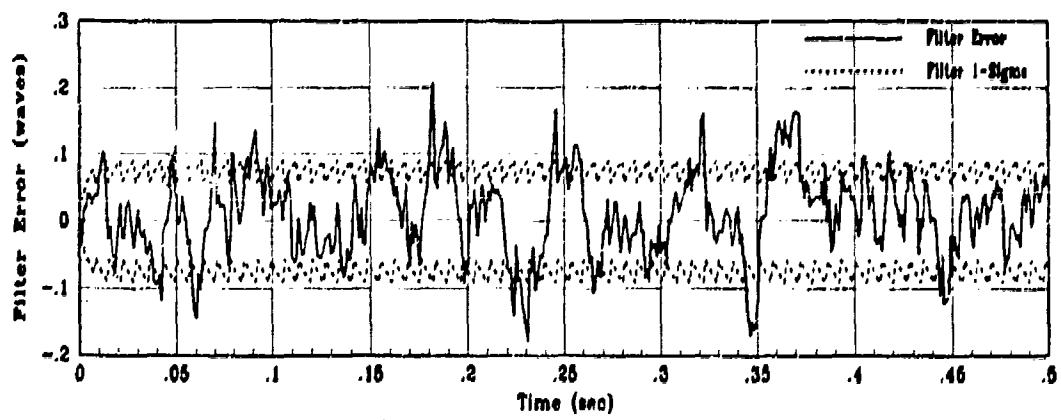
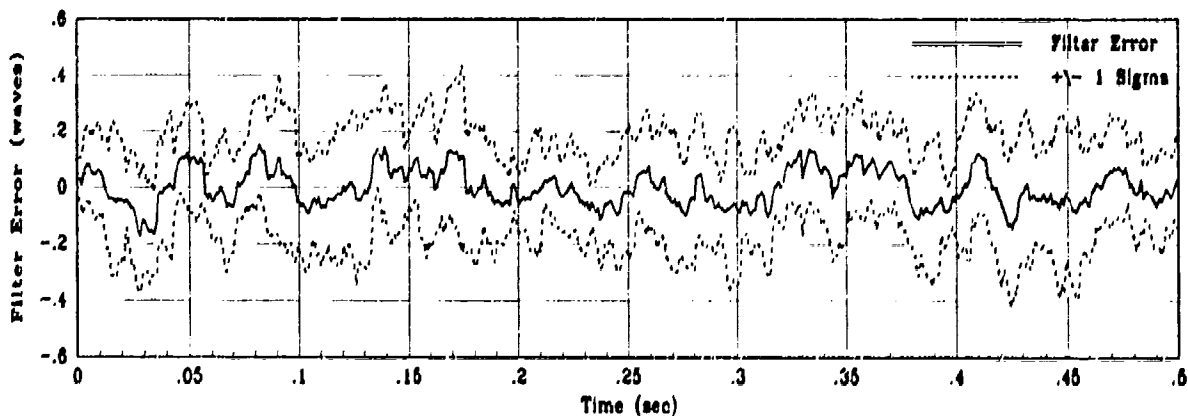(b) X6 Filter Error for 1 MC Run
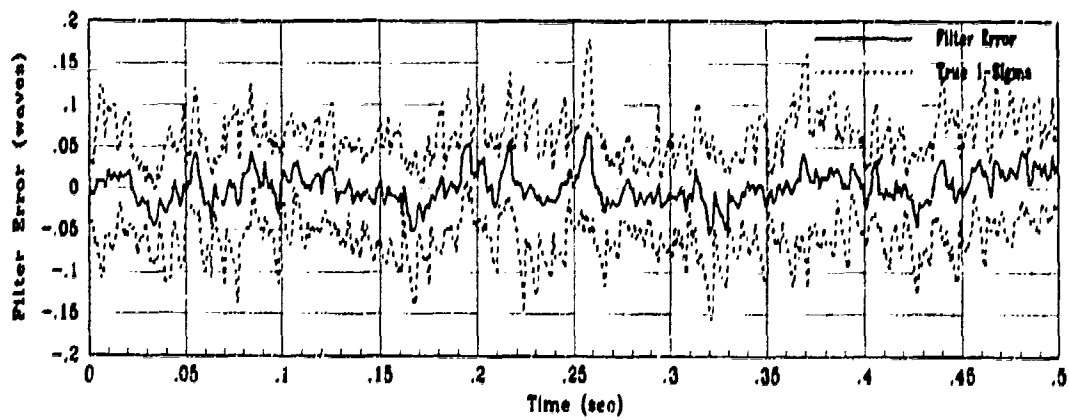
(c) X6 True Filter Error for 10 MC runs

Figure F.21. Baseline State 6 Filter Estimation Error for Study 3
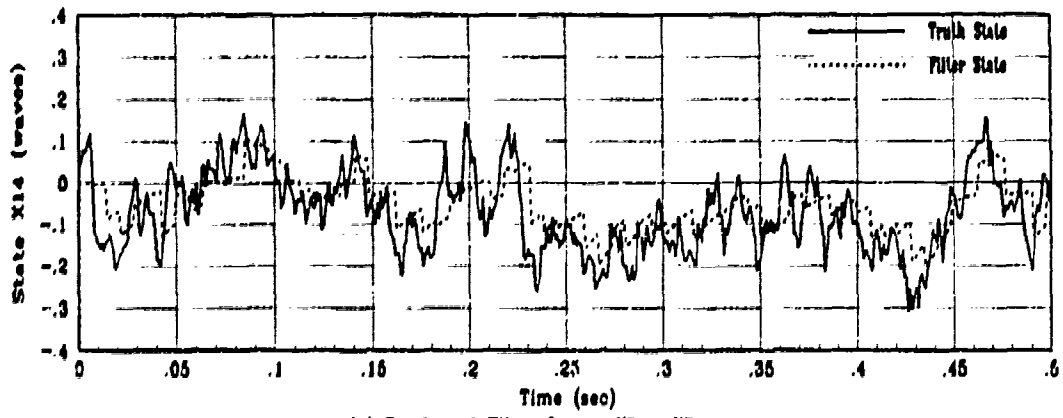
(a) Truth and Filter States: XS14, XF14
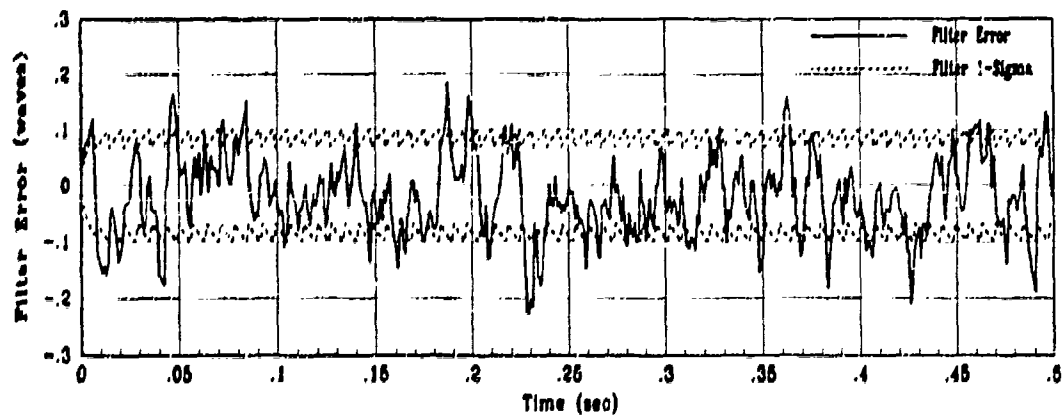
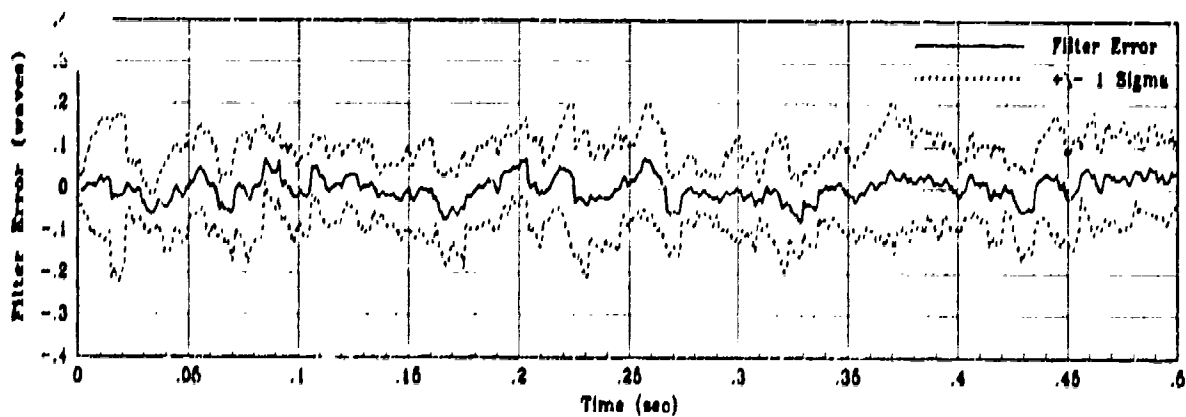(b) X14 Filter Error for 1 MC Run
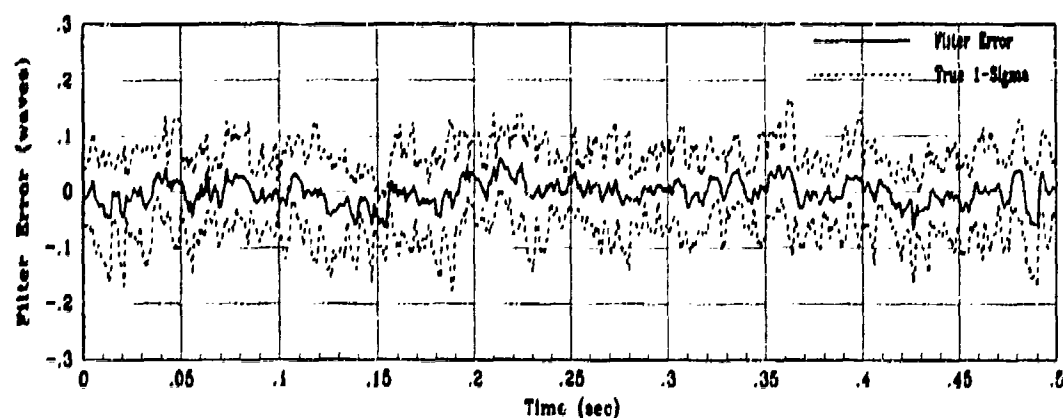
(c) X14 True Filter Error for 10 MC runs

Figure F.22. Baseline State 14 Filter Estimation Error for Study 3
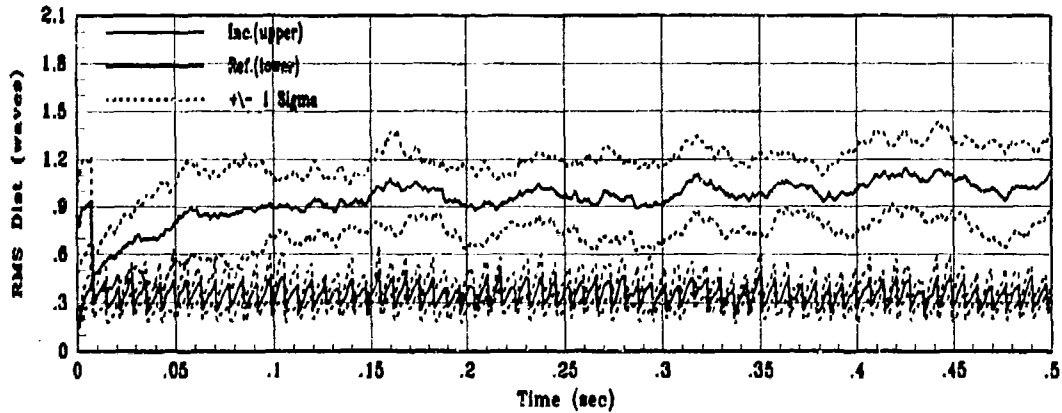
F-23

(a) Incident and Reflected RMS Phase Distortion for 10 MC Runs
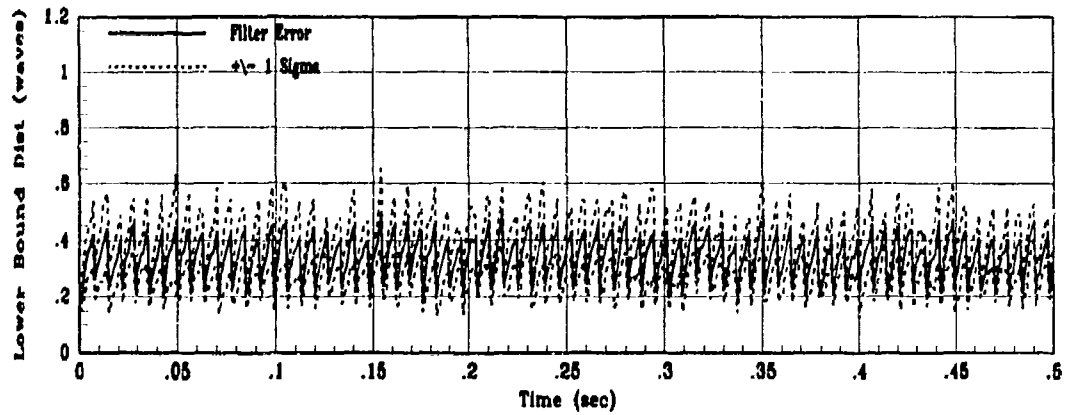
(b) RMS Filter Error for 10 MC Runs
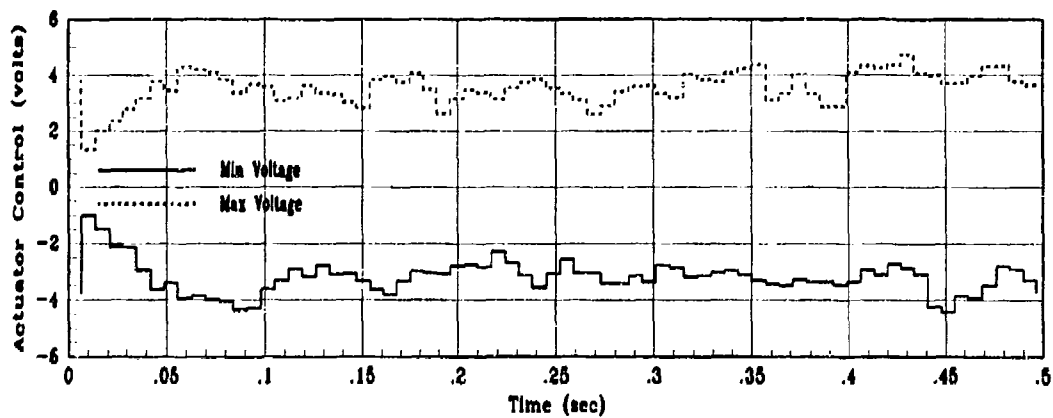
(c) Actuator Control Voltage Envelope

Figure F.23. Baseline Control System Performance for Study 3
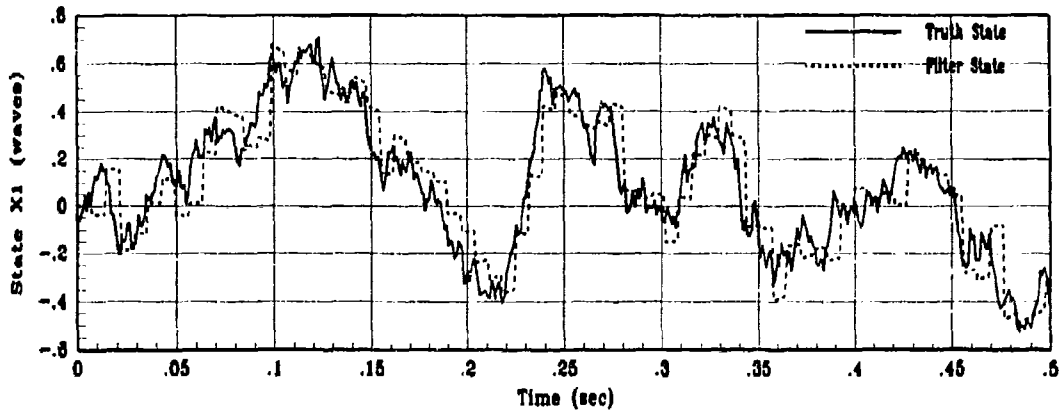
(a) Truth and Filter States: XS1, XF1
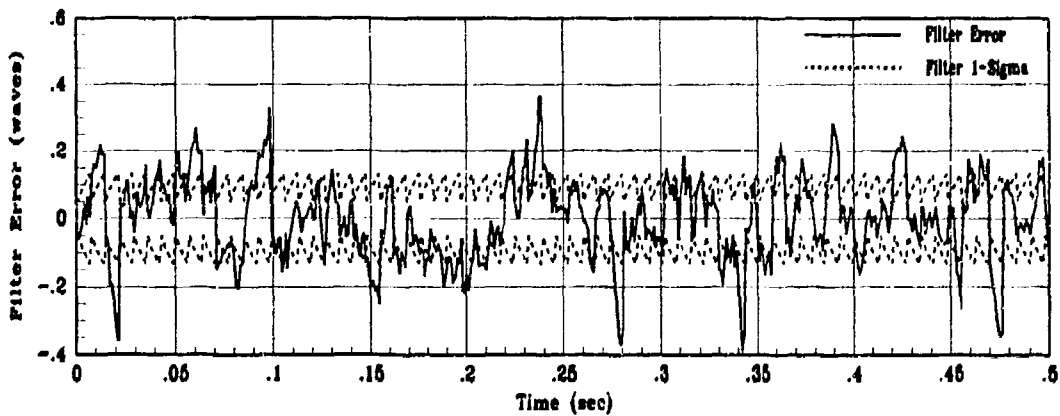
(b) X1 Filter Error for 1 MC Run
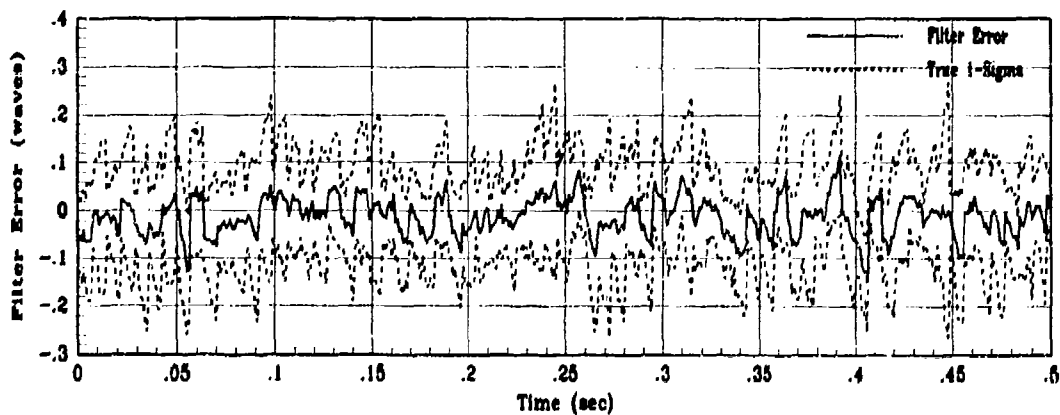
(c) X1 True Filter Error for 10 MC Runs

Figure F.24. Baseline State 1 Filter Estimation Error for Study 4
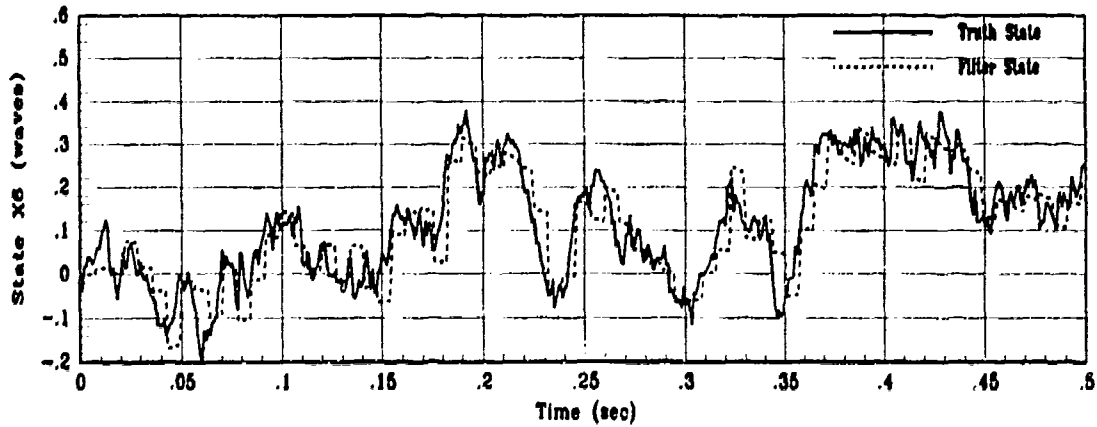
(a) Truth and Filter States: XS6, XF6
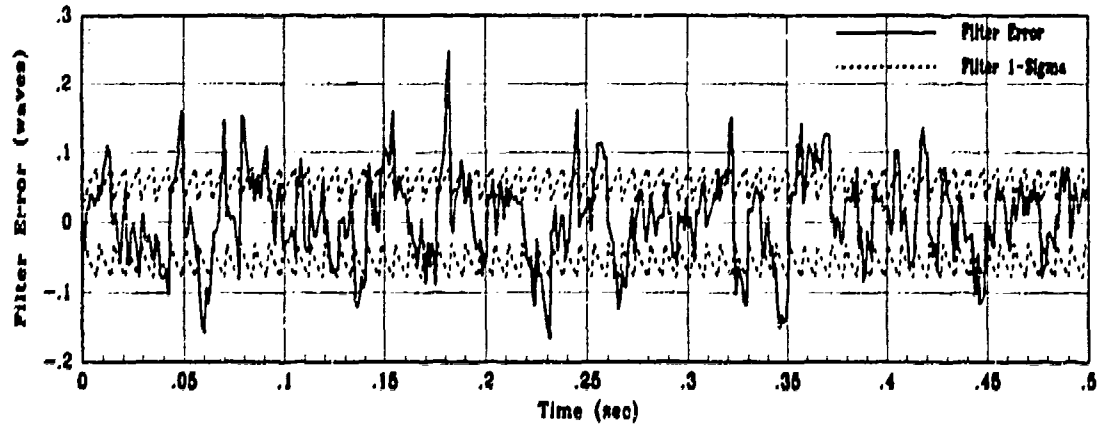
(b) X6 Filter Error for 1 MC Run
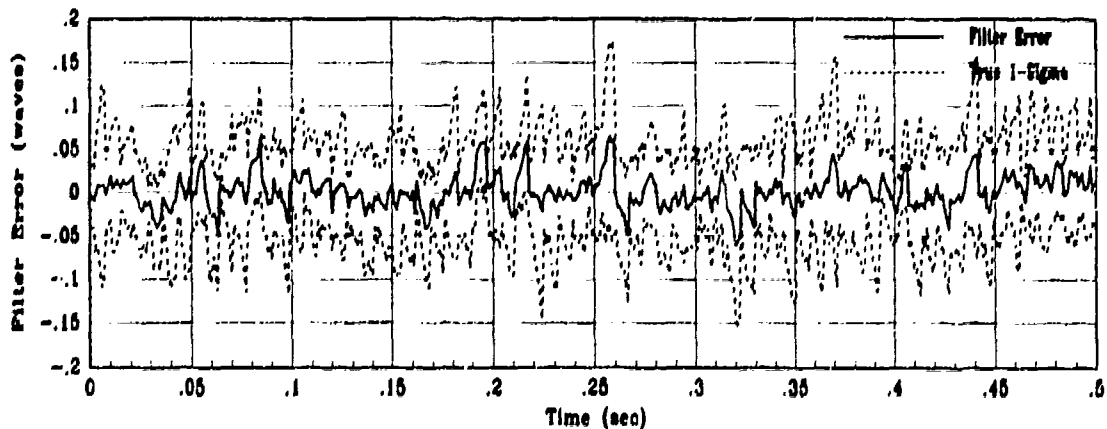
(c) X6 True Filter Error for 10 MC runs

Figure F.25. Baseline State 6 Filter Estimation Error for Study 4
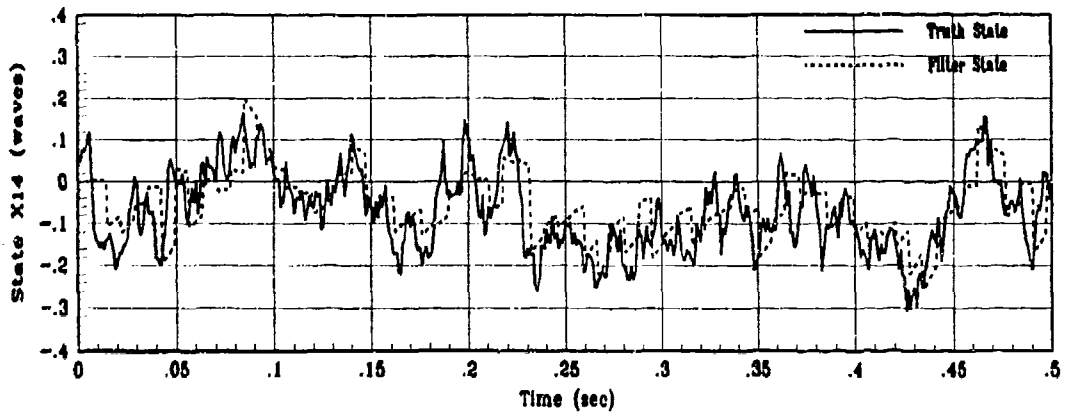
(a) Truth and Filter States: XS14, XF14
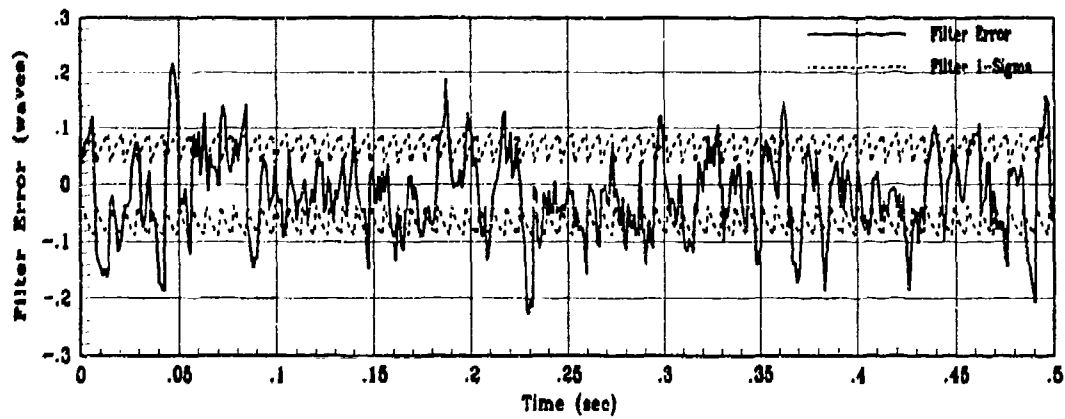
(b) X14 Filter Error for 1 MC Run
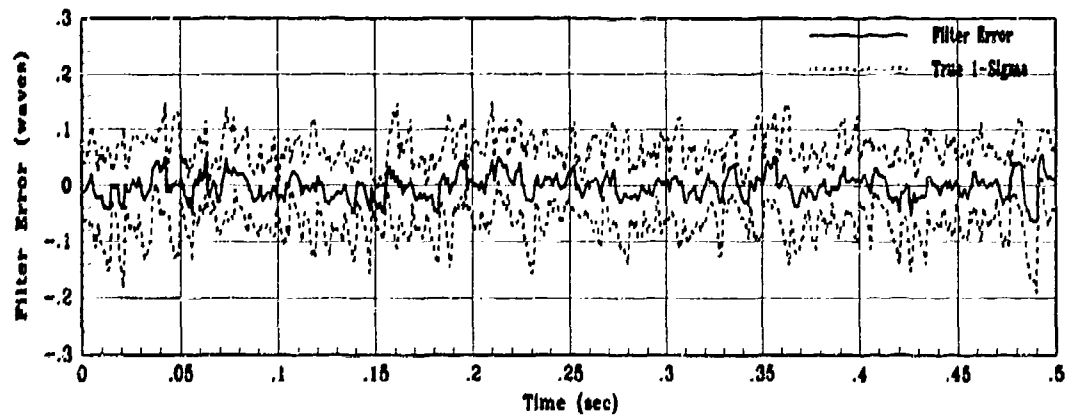
(c) X14 True Filter Error for 10 MC runs

Figure F.26. Baseline State 14 Filter Estimation Error for Study 4
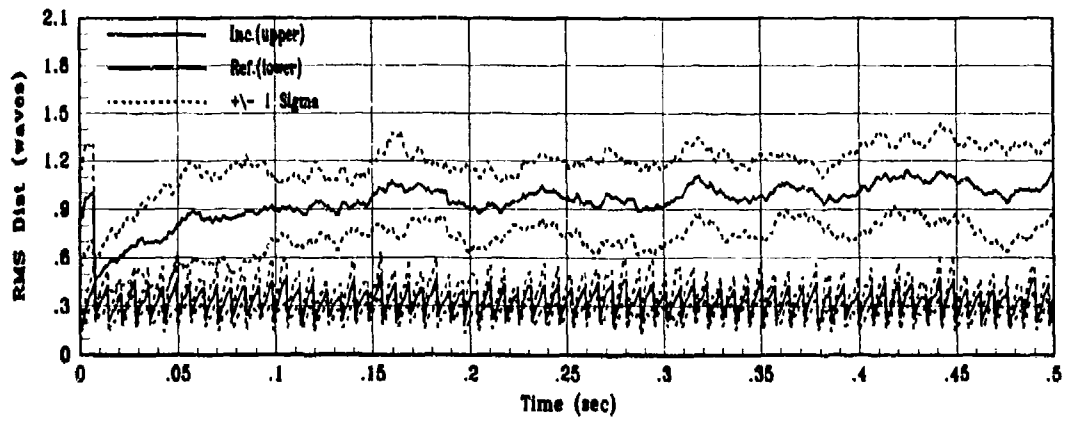
F-27

(a) Incident and Reflected RMS Phase Distortion for 10 MC Runs
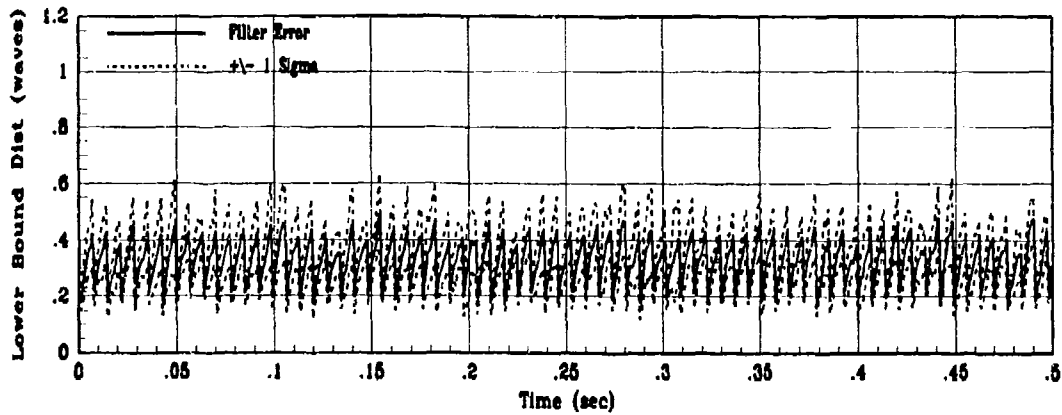
(b) RMS Filter Error for 10 MC Runs
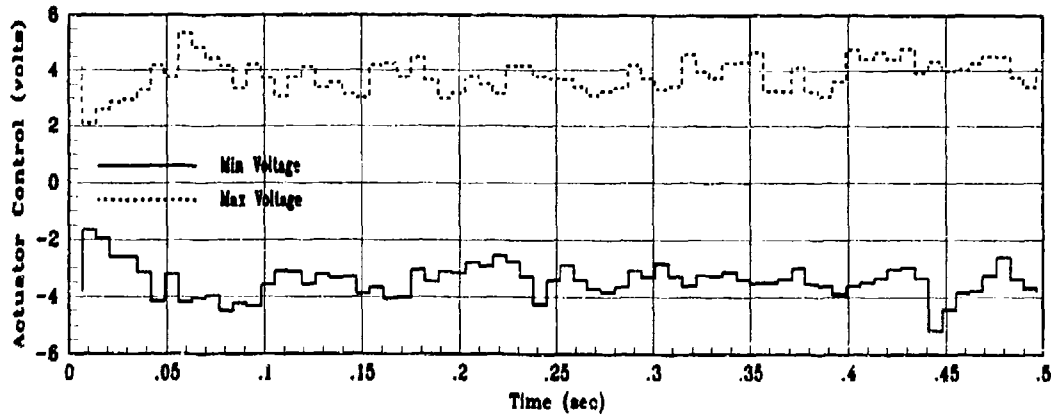
(c) Actuator Control Voltage Envelope

Figure F.27. Baseline Control System Performance for Study 4
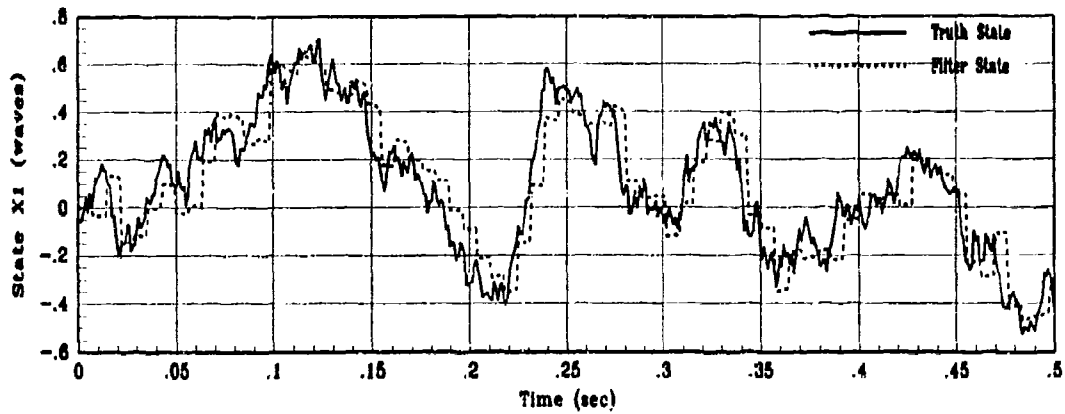
(a) Truth and Filter States: XS1, XF1
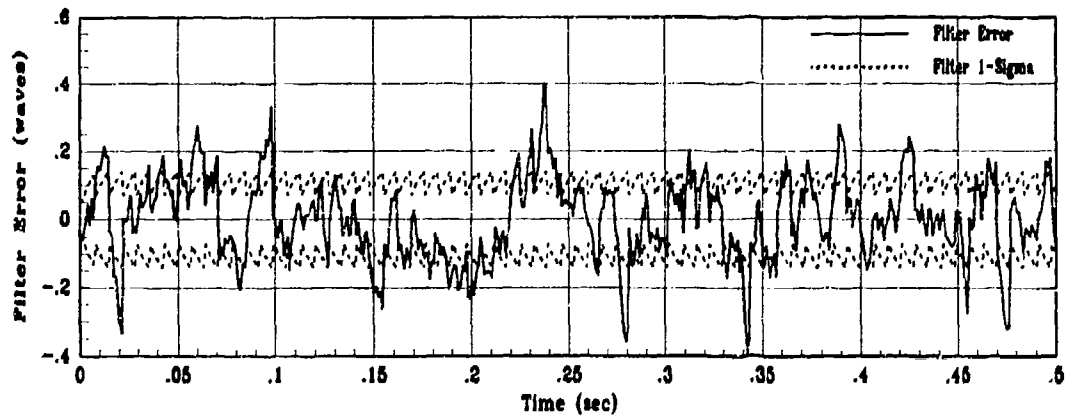
(b) X1 Filter Error for 1 MC Run
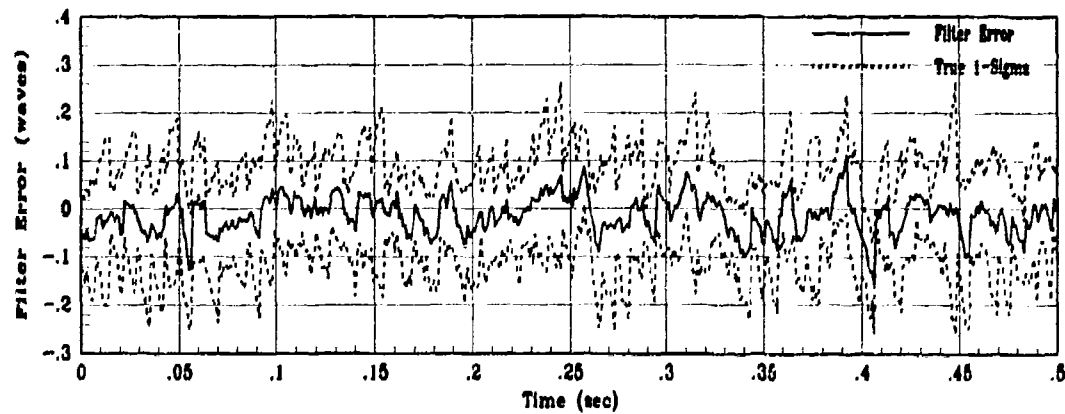
(c) X1 True Filter Error for 10 MC Runs

Figure F.28. Baseline State 1 Filter Estimation Error for Study 5
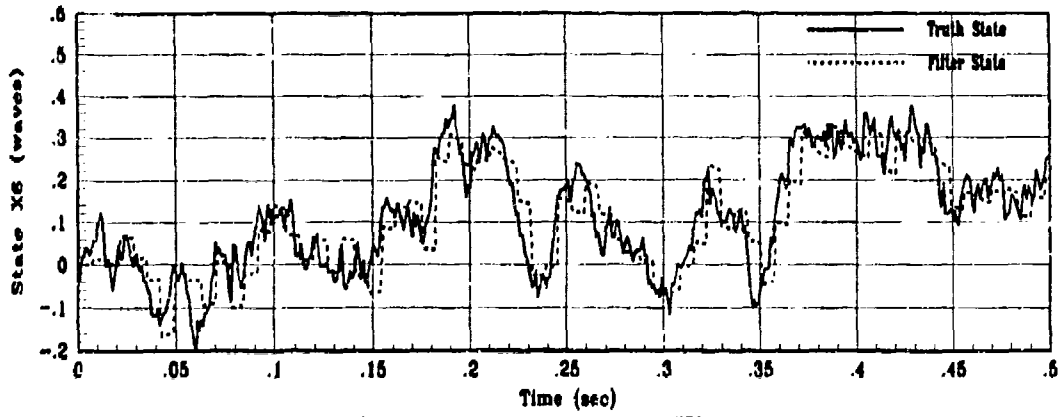
(a) Truth and Filter States. XS6, XF6
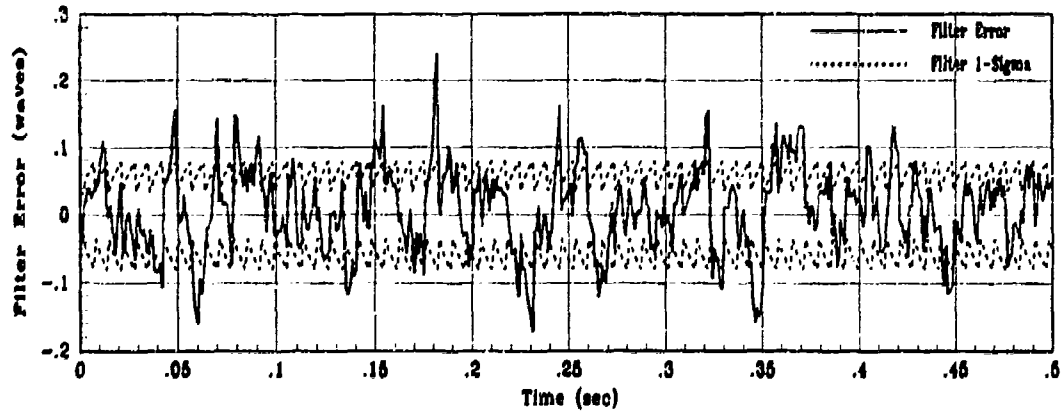
(b) X6 Filter Error for 1 MC Run
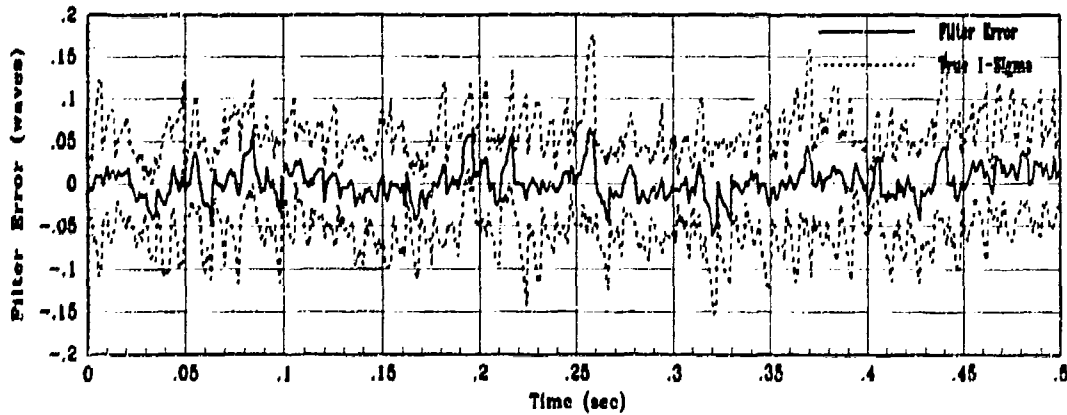
(c) X6 True Filter Error for 10 MC runs

Figure F.29. Baseline State 6 Filter Estimation Error for Study 5
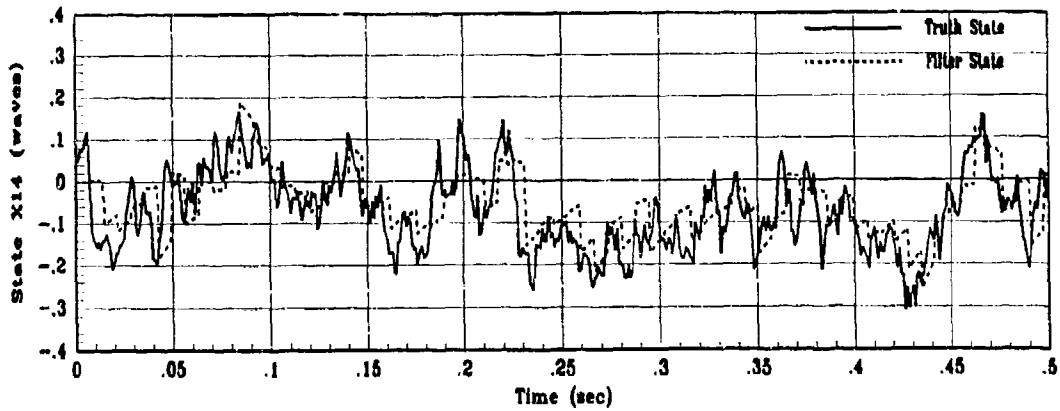
(a) Truth and Filter States: XS14, XF14
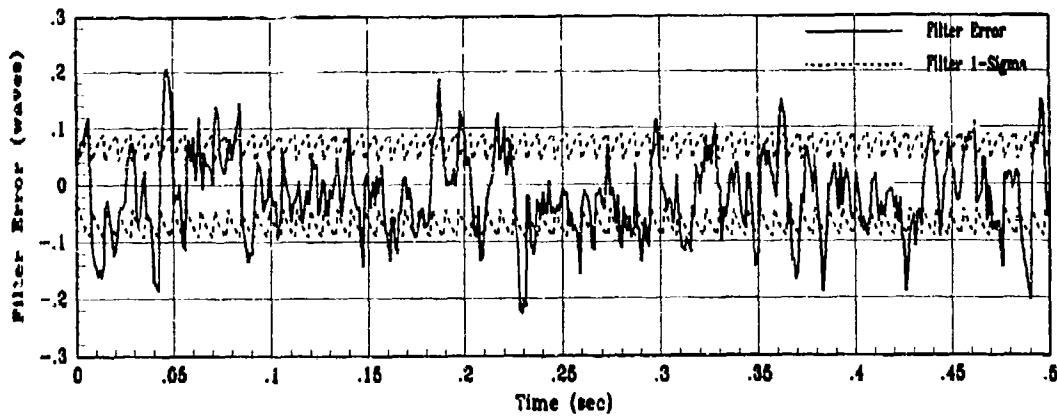
(b) X14 Filter Error for 1 MC Run
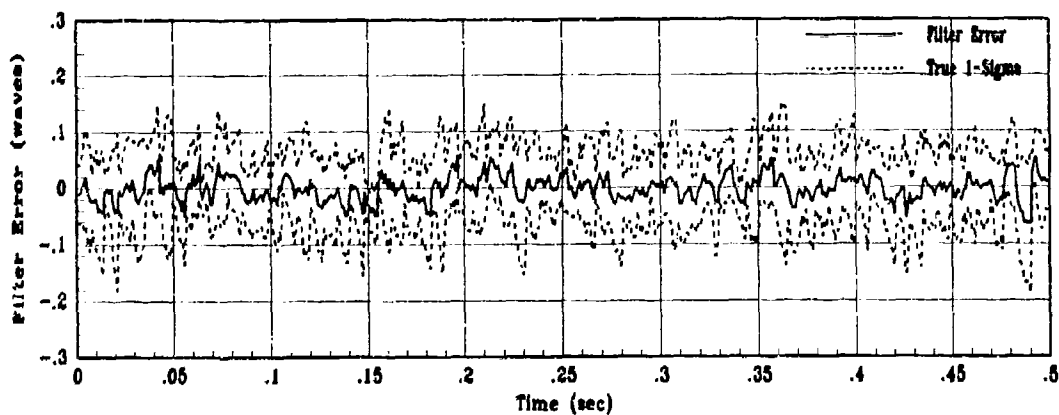
(c) X14 True Filter Error for 10 MC runs

Figure F.30. Baseline State 14 Filter Estimation Error for Study 5
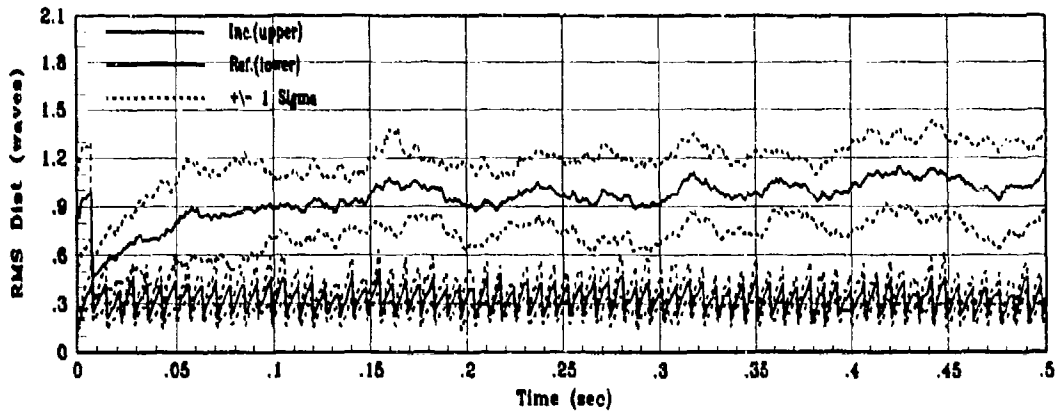
(a) Incident and Reflected RMS Phase Distortion for 10 MC Runs
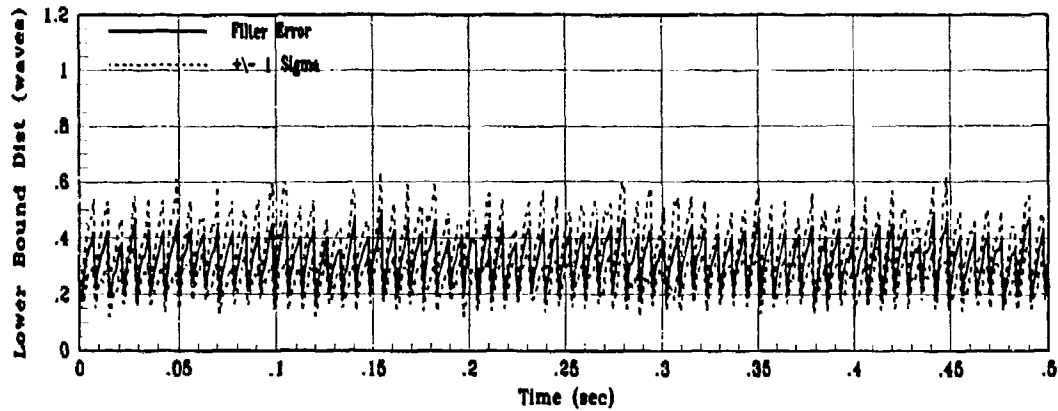
(b) RMS Filter Error for 10 MC Runs
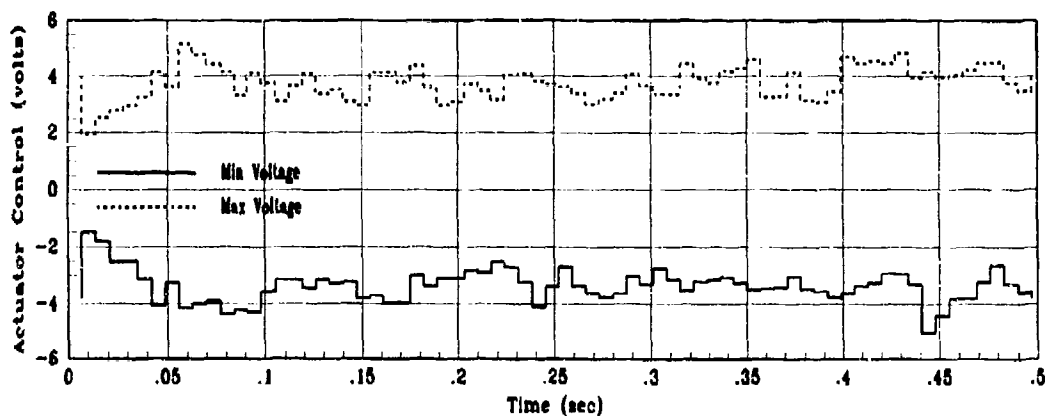
(c) Actuator Control Voltage Envelope

Figure F.31. Baseline Control System Performance for Study 5
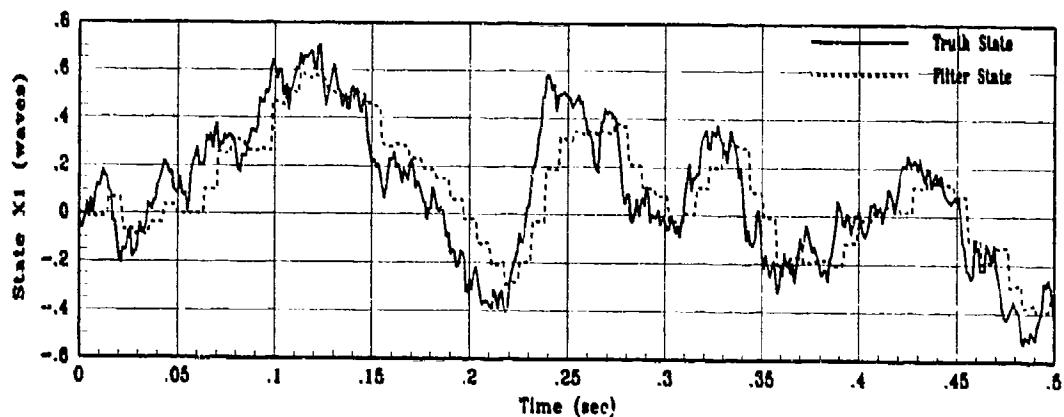
(a) Truth and Filter States: XS1, XF1
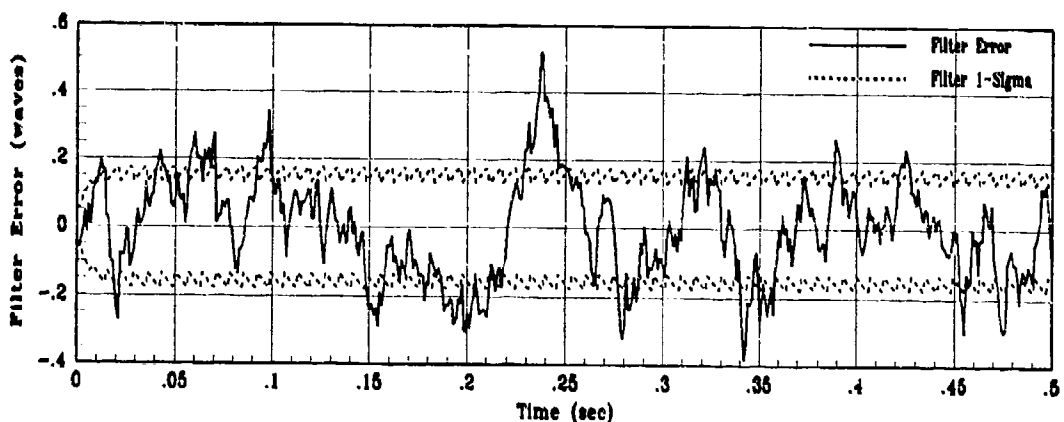
(b) X1 Filter Error for 1 MC Run
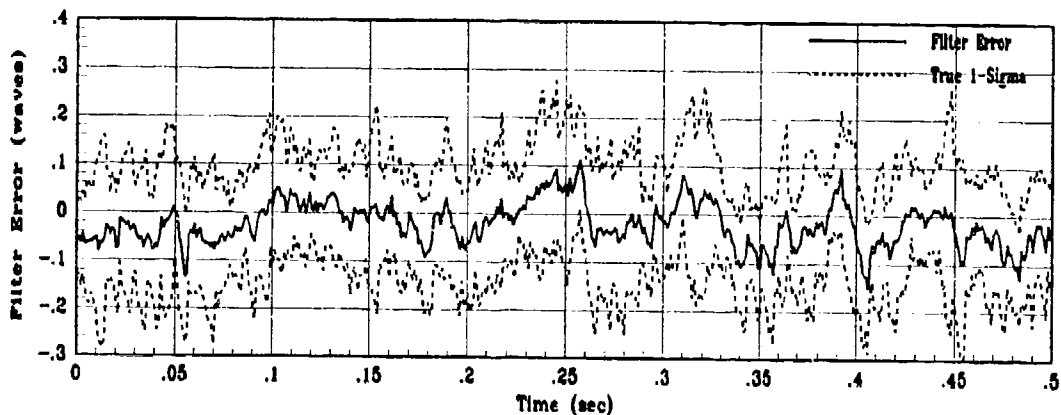
(c) X1 True Filter Error for 10 MC Runs

Figure F.32. Baseline State 1 Filter Estimation Error for Study 6
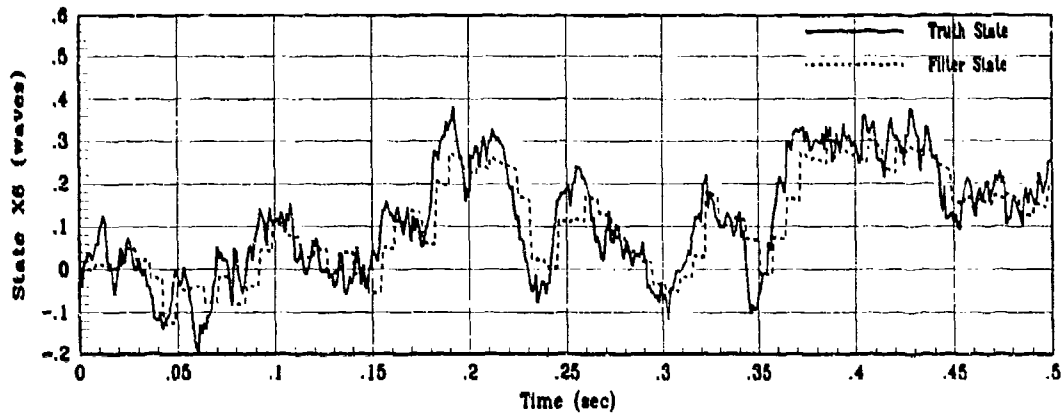
(a) Truth and Filter States: XS6, XF6
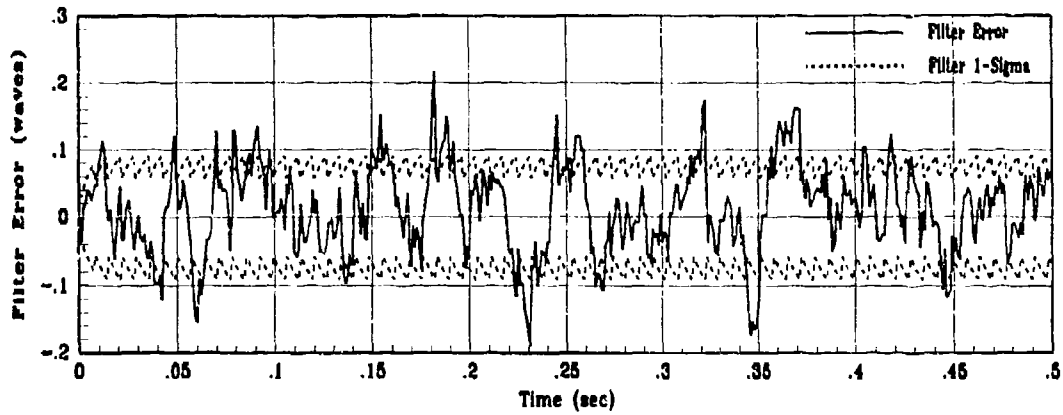
(b) X6 Filter Error for 1 MC Run
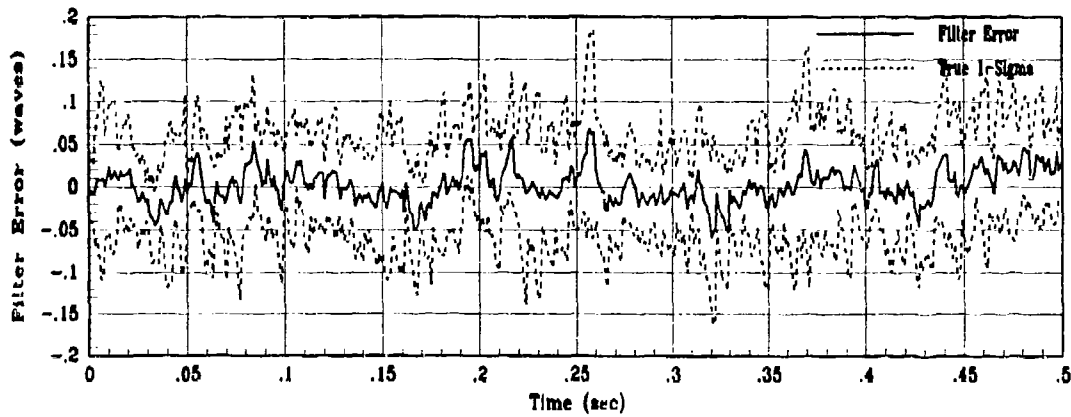
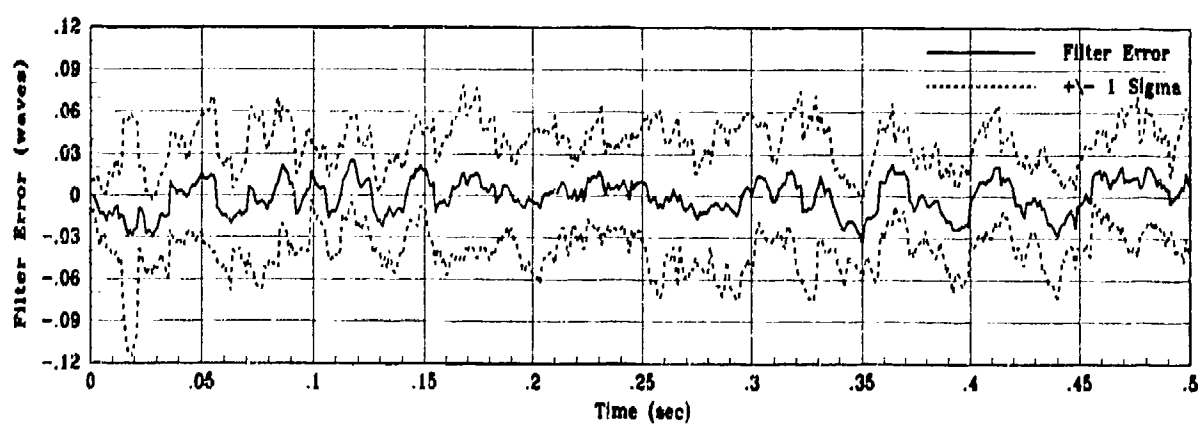(c) X6 True Filter Error for 10 MC runs

Figure F.33. Baseline State 6 Filter Estimation Error for Study 6
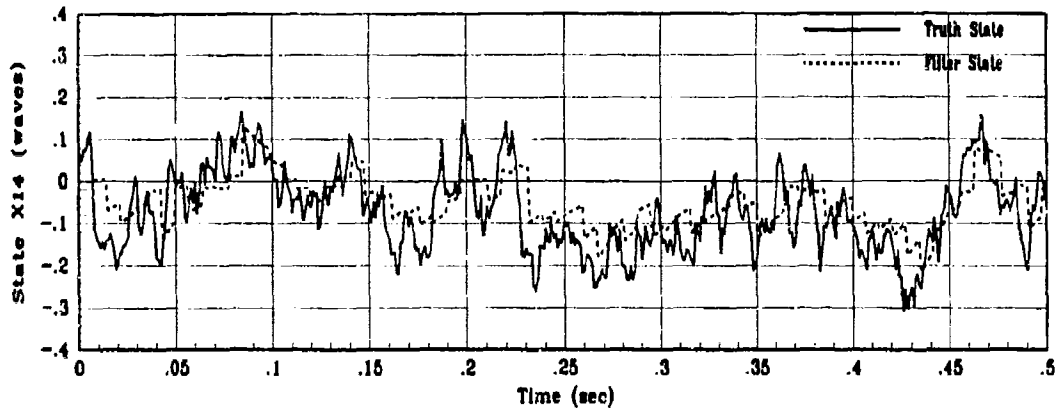
(a) Truth and Filter States: XS14, XF14
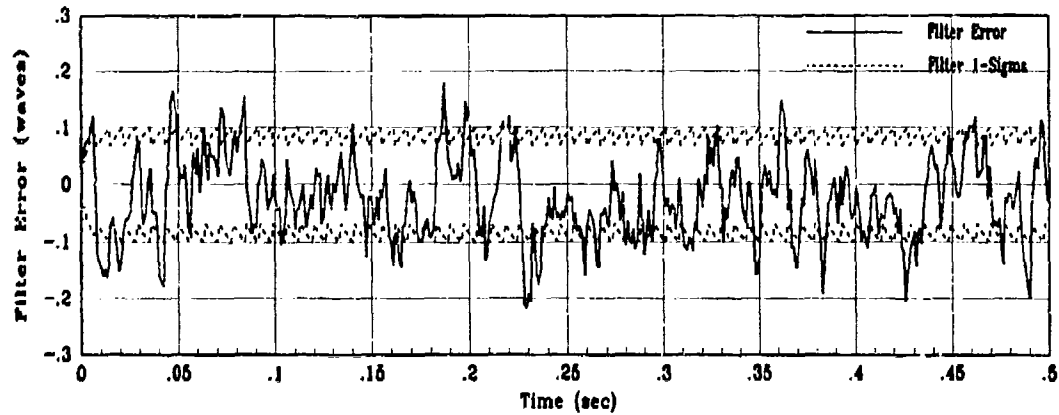
(b) X14 Filter Error for 1 MC Run
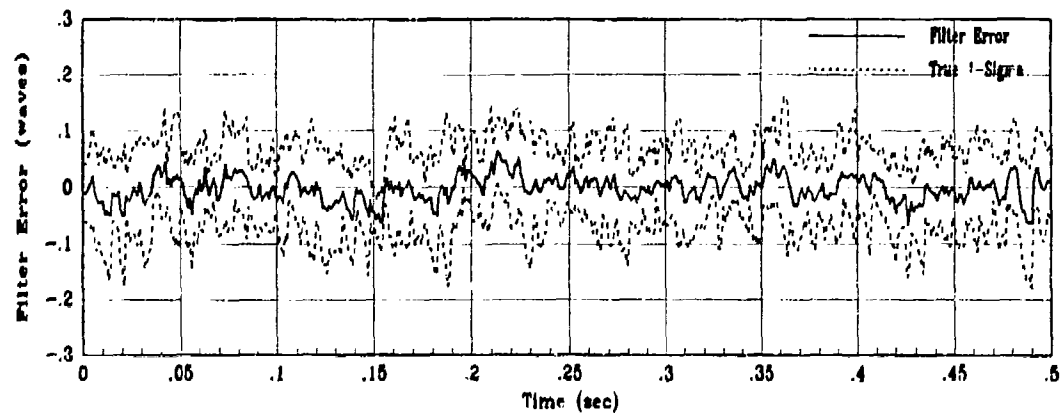
(c) X14 True Filter Error for 10 MC runs

Figure F.34. Baseline State 14 Filter Estimation Error for Study 6
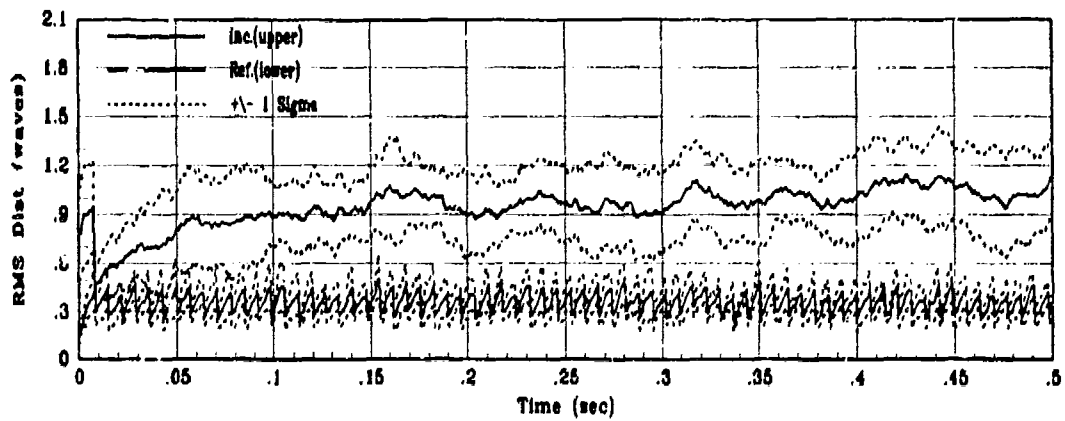
(a) Incident and Reflected RMS Phase Distortion for 10 MC Runs
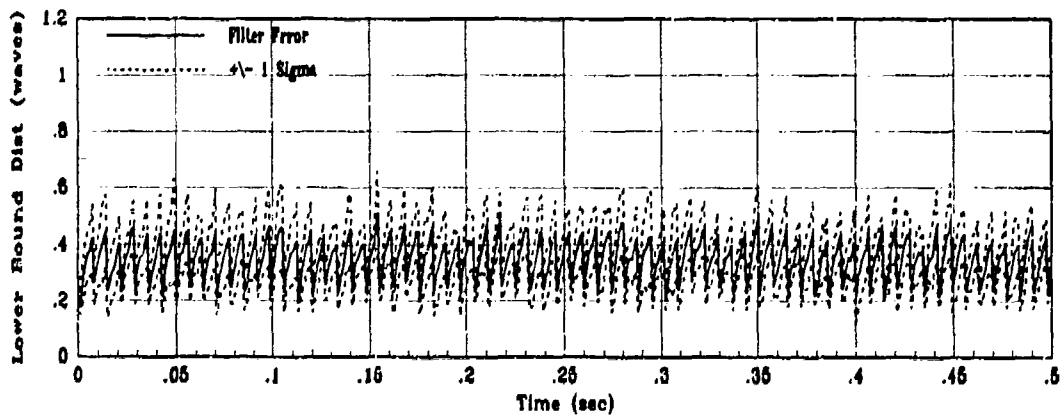
(b) RMS Filter Error for 10 MC Runs
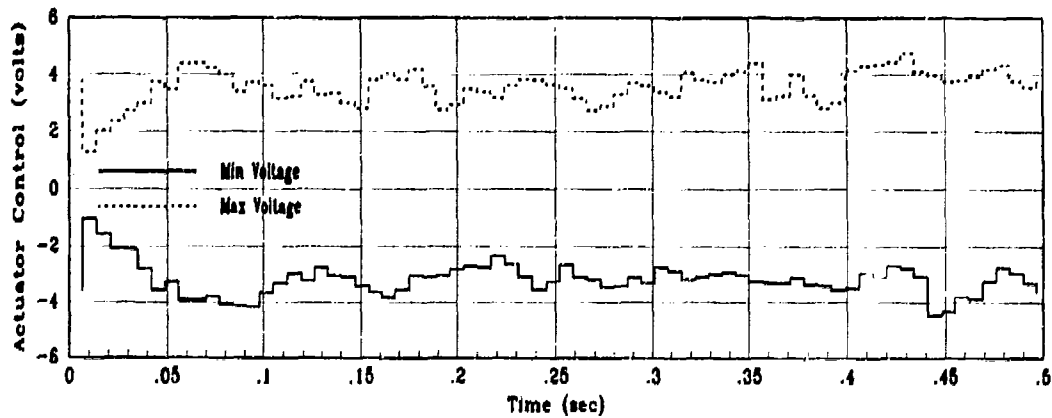
(c) Actuator Control Voltage Envelope

Figure F.35. Baseline Control System Performance for Study 6
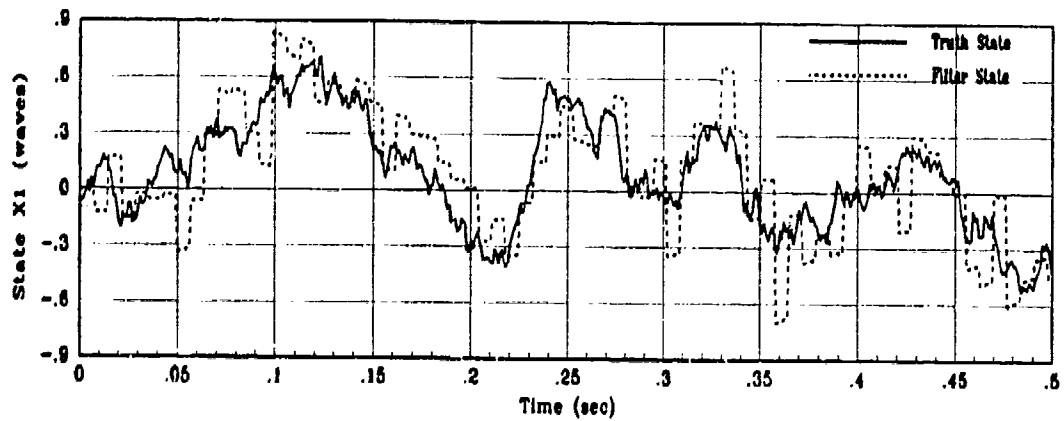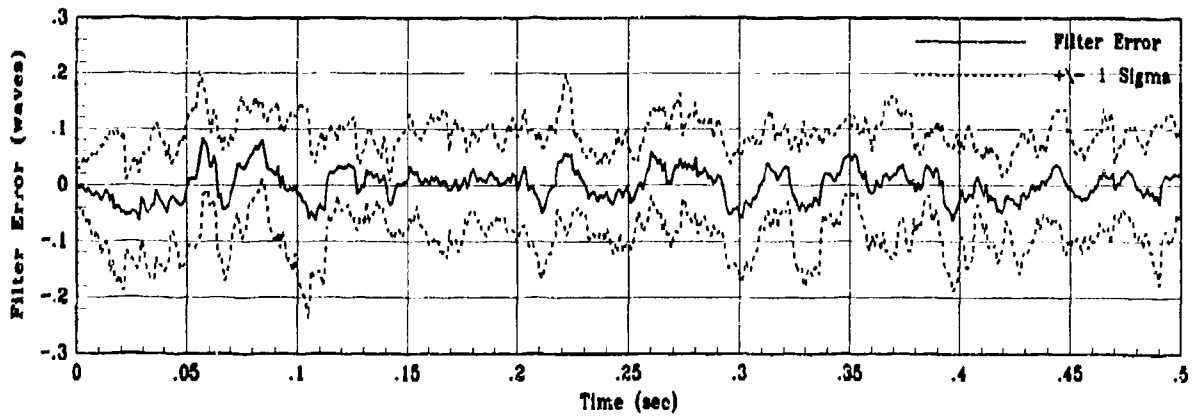
(a) Truth and Filter States: XS1, XF1
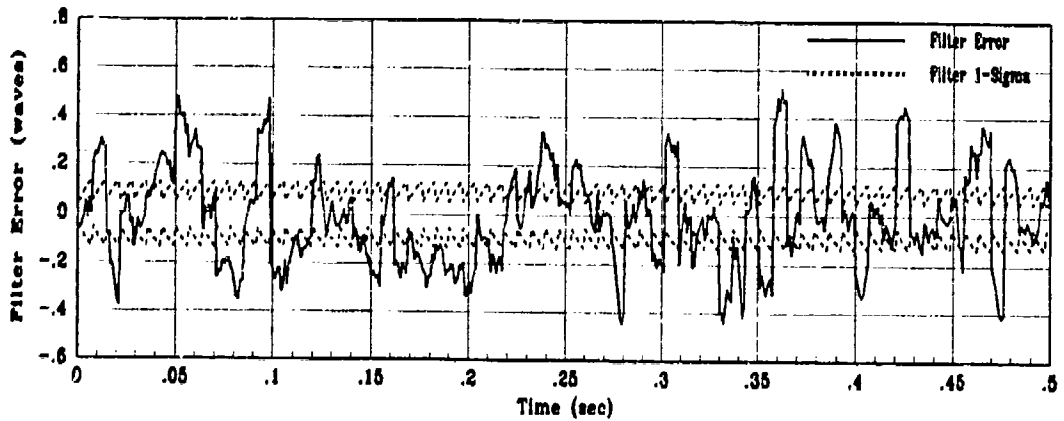
(b) X1 Filter Error for 1 MC Run
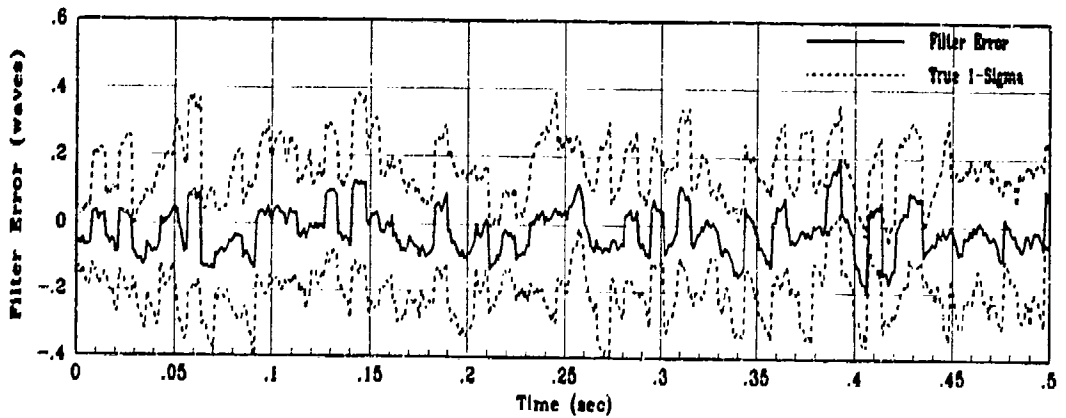
(c) X1 True Filter Error for 10 MC Runs

Figure F.36. Baseline State 1 Filter Estimation Error for Study 7
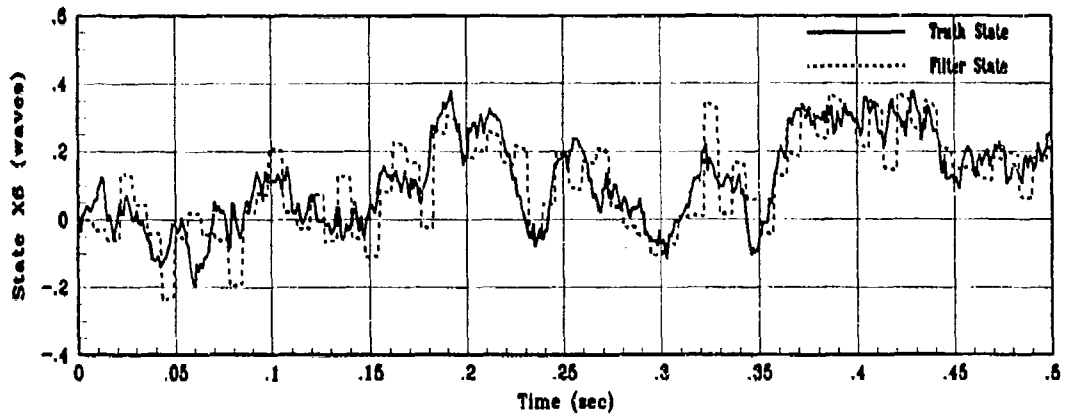
(a) Truth and Filter States: XS6, XF6
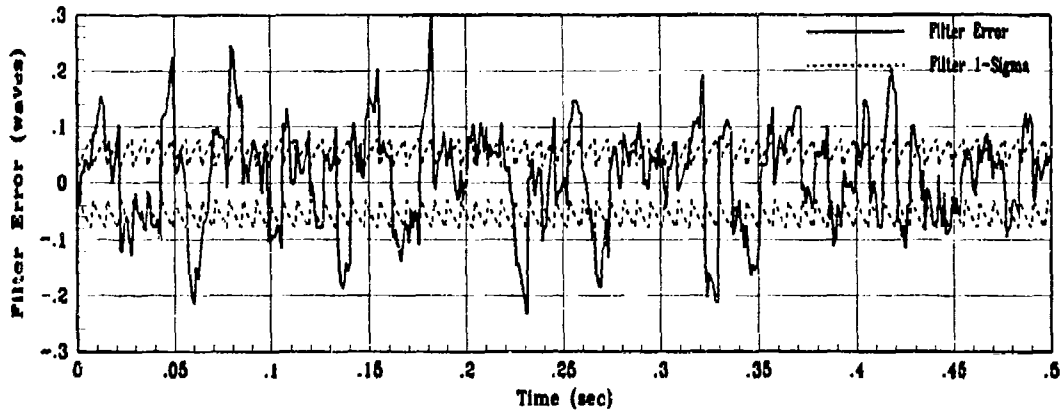
(b) X6 Filter Error for 1 MC Run
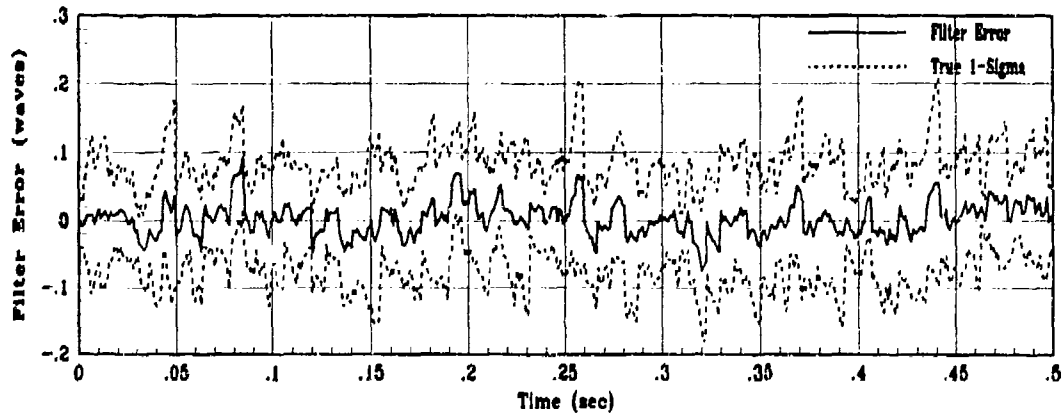
(c) X6 True Filter Error for 10 MC runs

Figure F.37. Baseline State 6 Filter Estimation Error for Study 7
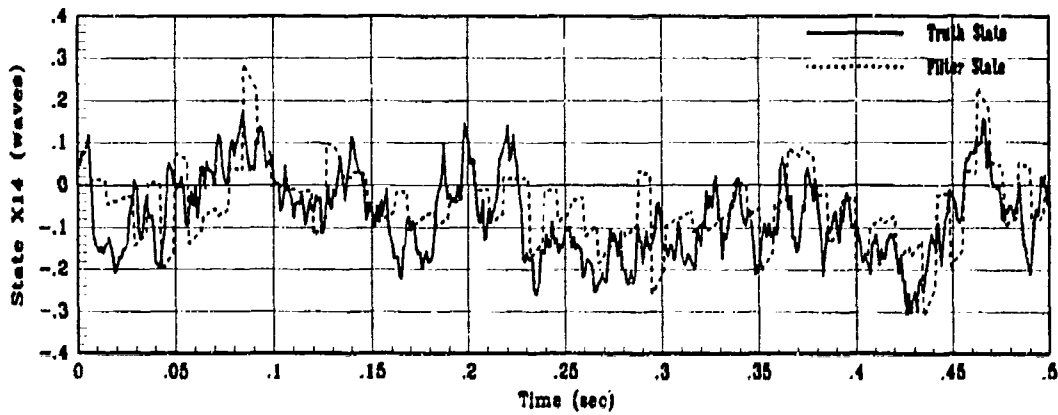
(a) Truth and Filter States: XS14, XF14
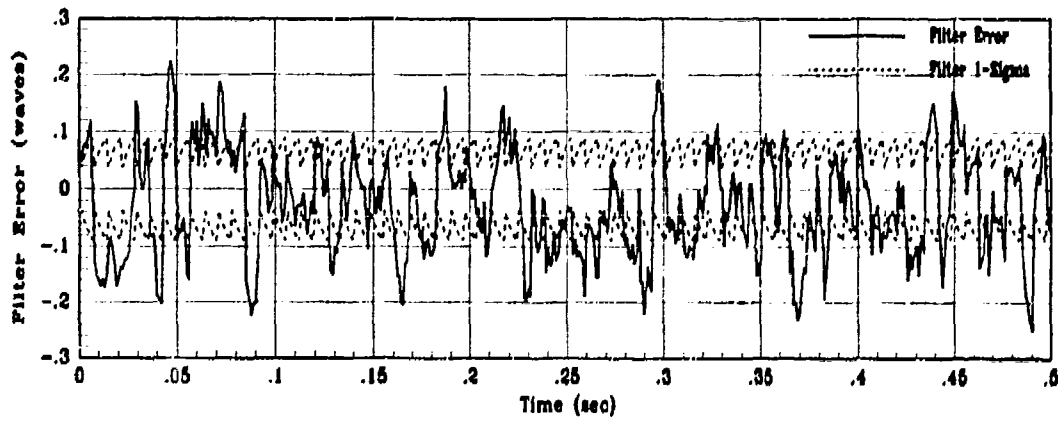
(b) X14 Filter Error for 1 MC Run
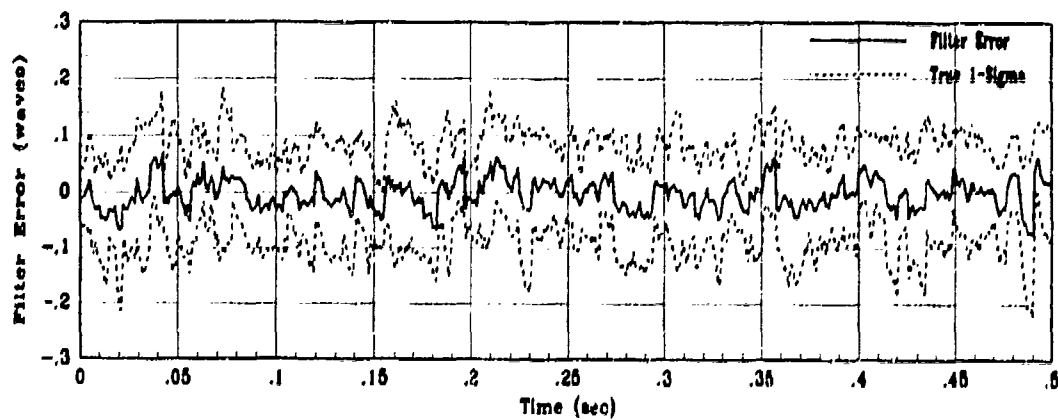
(c) X14 True Filter Error for 10 MC runs

Figure F.38. Baseline State 14 Filter Estimation Error for Study 7
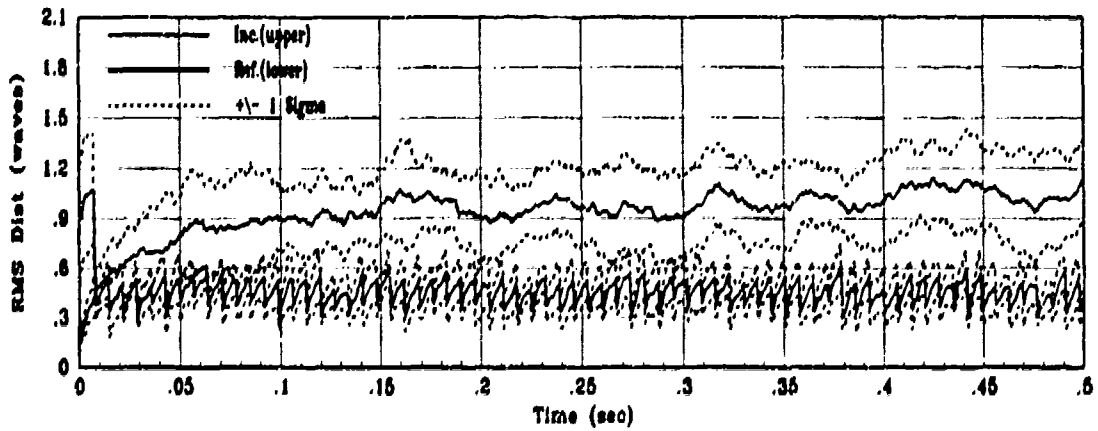
(a) Incident and Reflected RMS Phase Distortion for 10 MC Runs
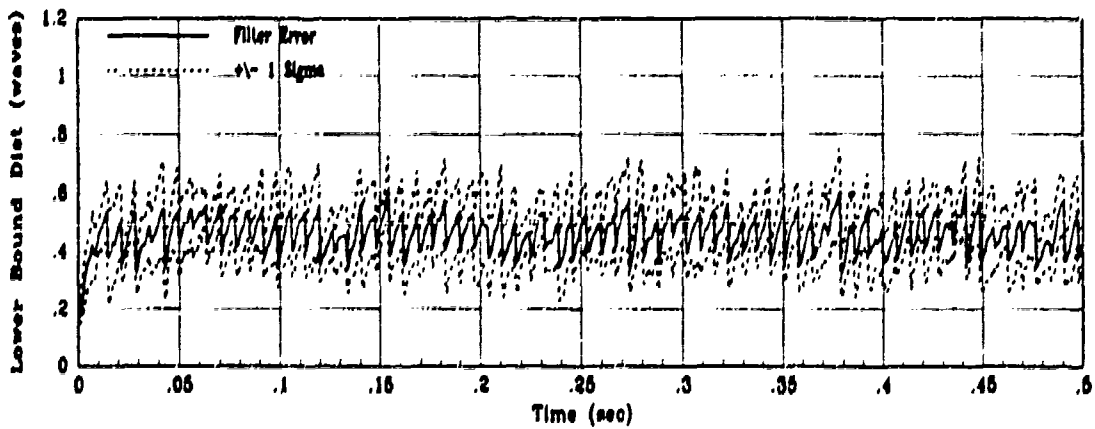
(b) RMS Filter Error for 10 MC Runs
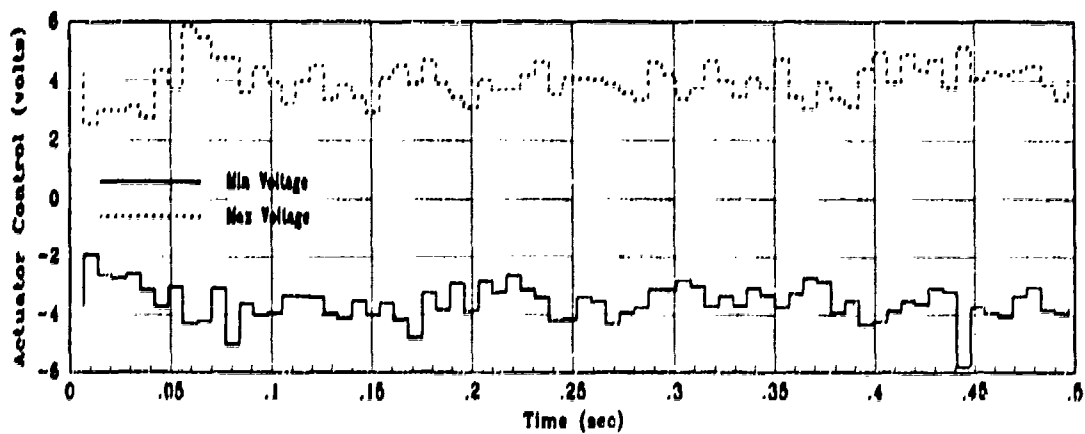
(c) Actuator Control Voltage Envelope

Figure F.39. Baseline Control System Performance for Study 7
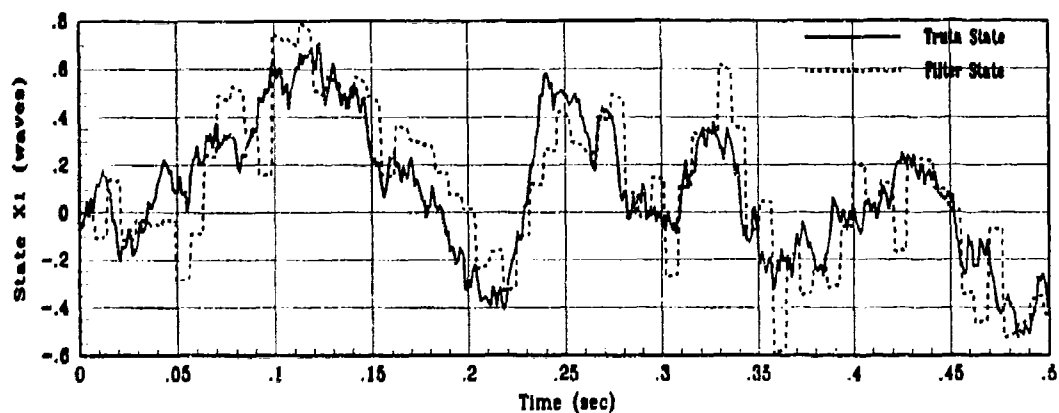
(a) Truth and Filter States: XS1, XF1
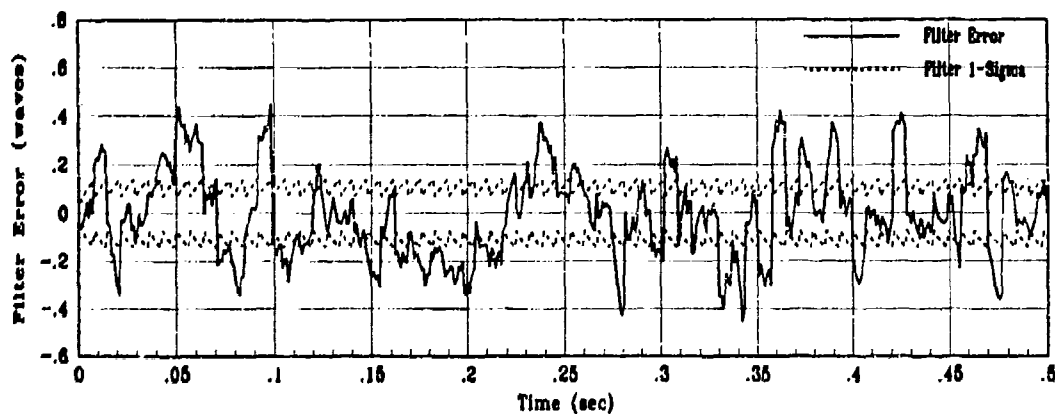
(b) X1 Filter Error for 1 MC Run
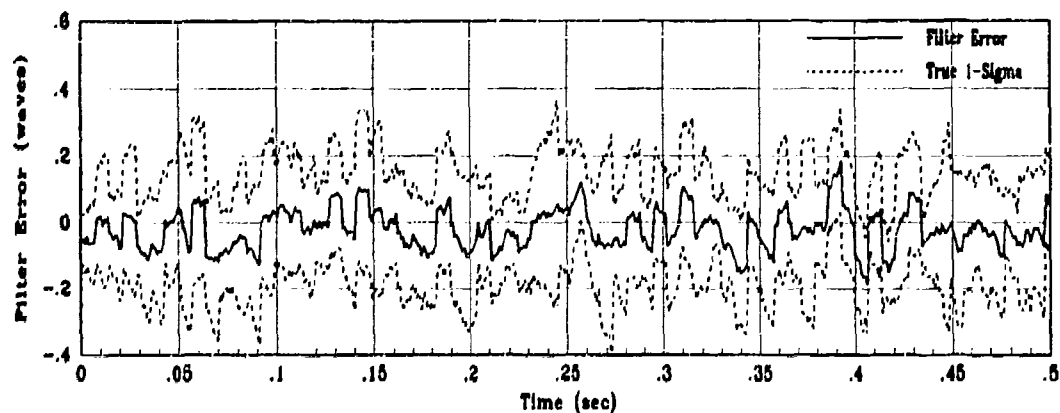
(c) X1 True Filter Error for 10 MC Runs

Figure F.40. Baseline State 1 Filter Estimation Error for Study 8
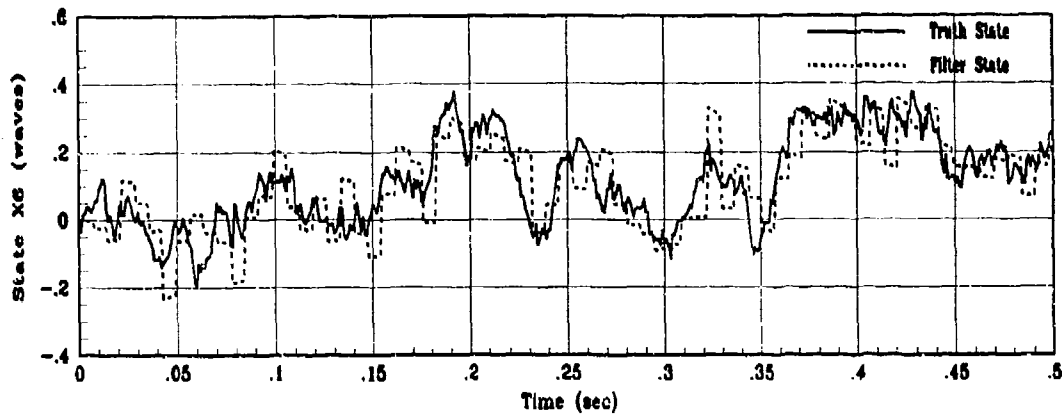
(a) Truth and Filter States: XS6, XF6
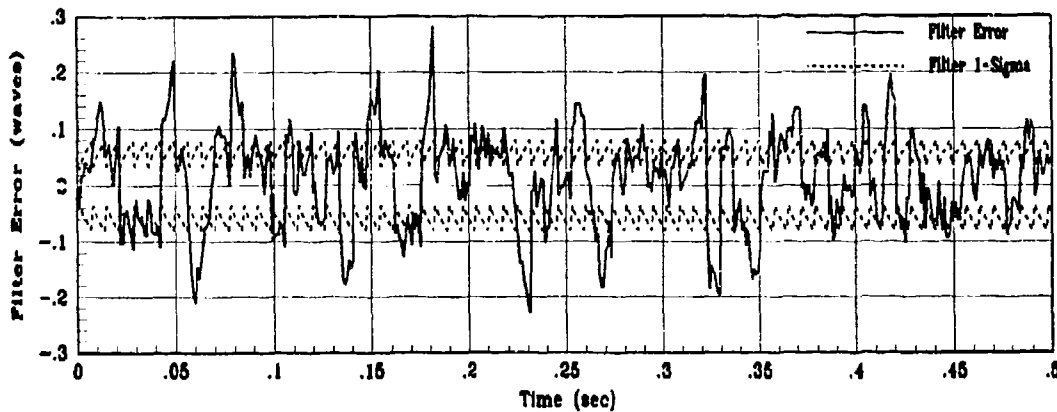
(b) X6 Filter Error for 1 MC Run
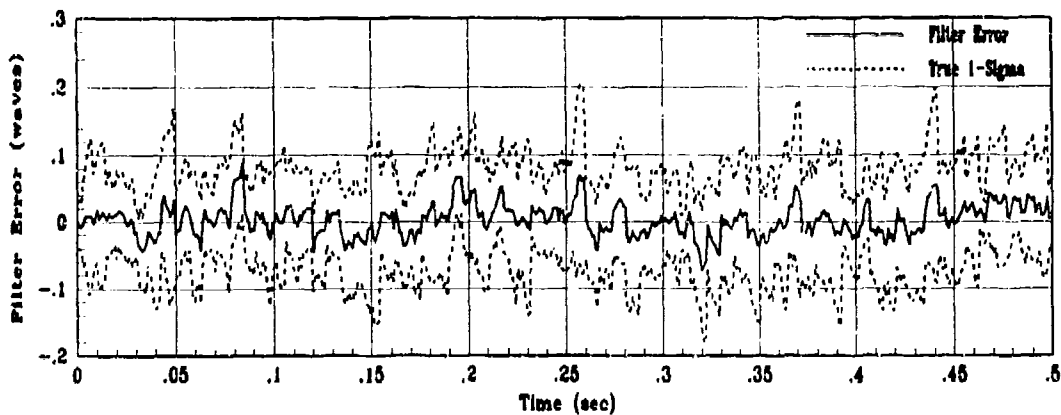
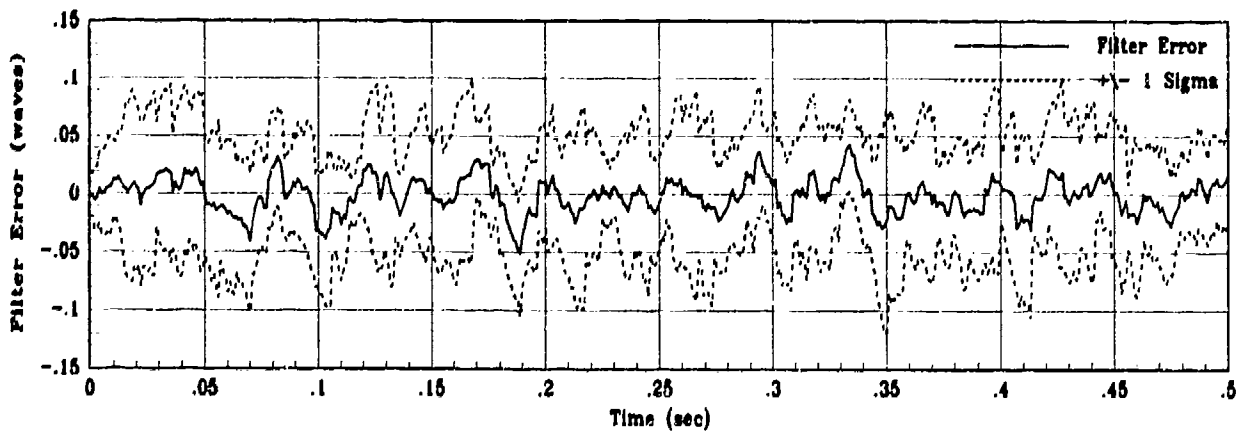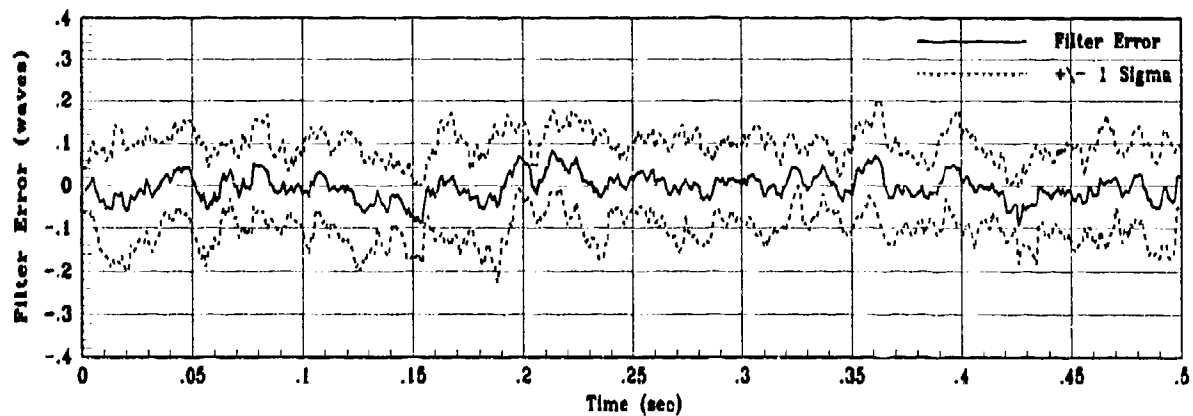(c) X6 True Filter Error for 10 MC runs

Figure F.41. Baseline State 6 Filter Estimation Error for Study 8
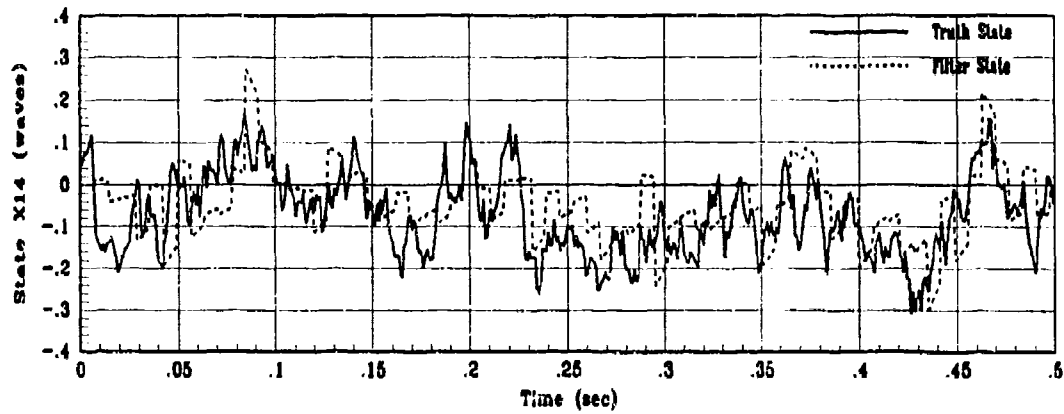
(a) Truth and Filter States: XS14, XF14
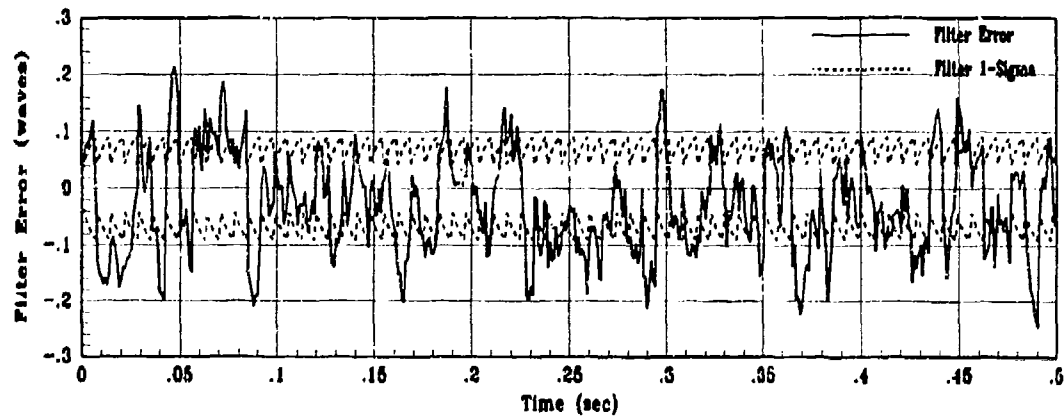
(b) X14 Filter Error for 1 MC Run
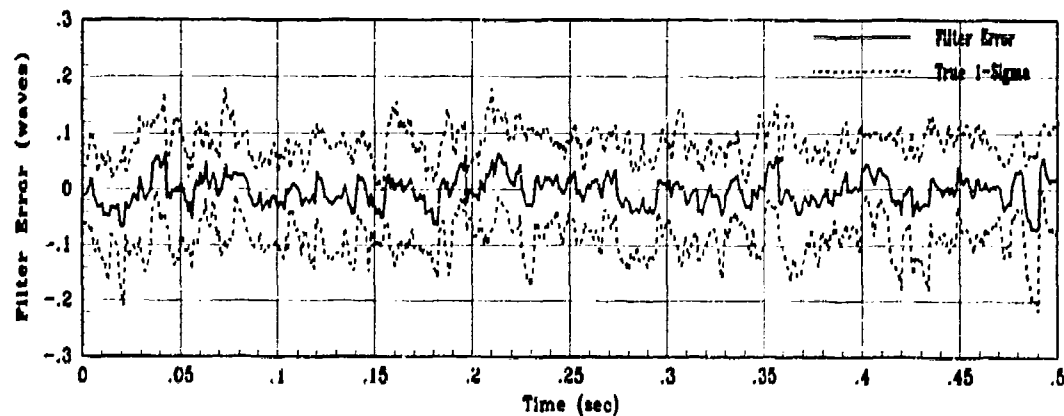
(c) X14 True Filter Error for 10 MC runs

Figure F.42. Baseline State 14 Filter Estimation Error for Study 8
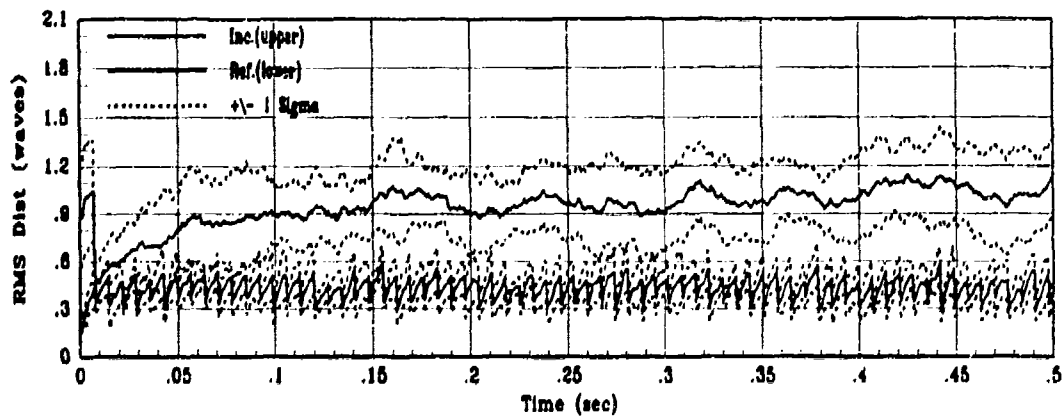
(a) Incident and Reflected RMS Phase Distortion for 10 MC Runs
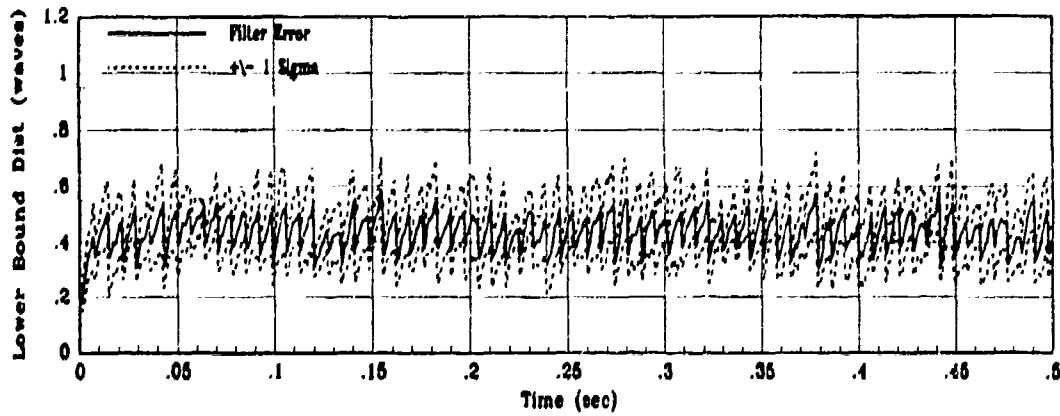
(b) RMS Filter Error for 10 MC Runs
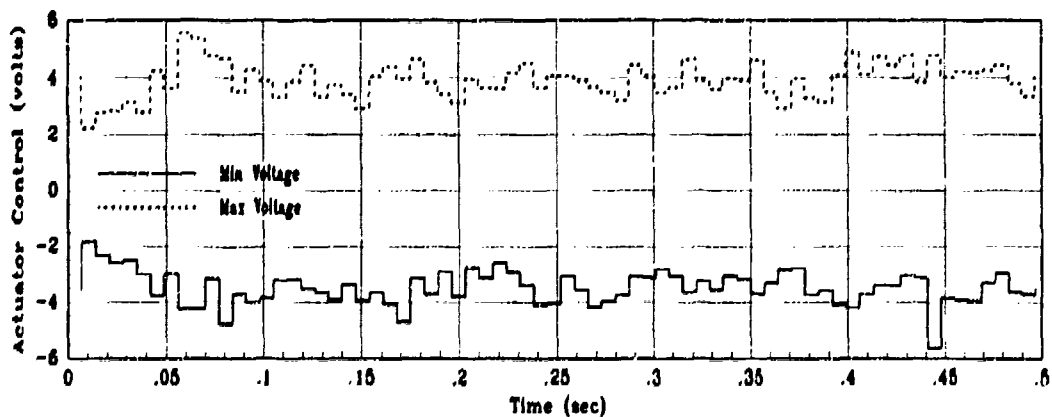
(c) Actuator Control Voltage Envelope

Figure F.43. Baseline Control System Performance for Study 8
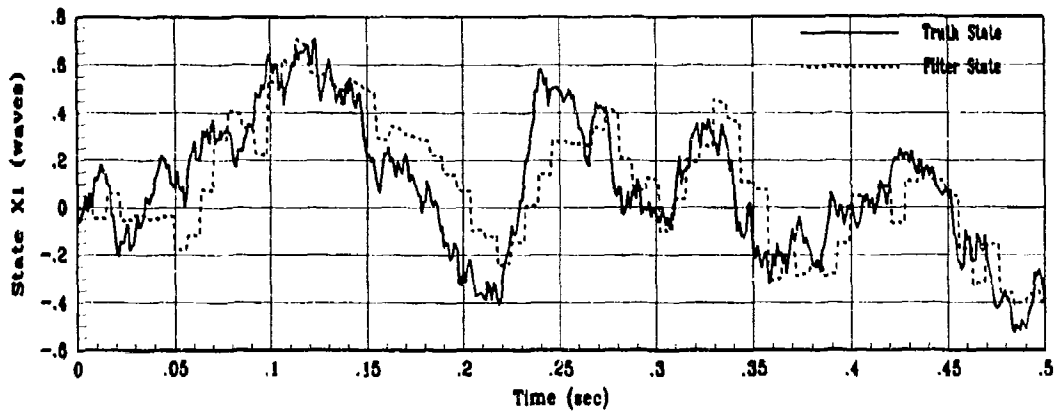
(a) Truth and Filter States: XS1, XF1
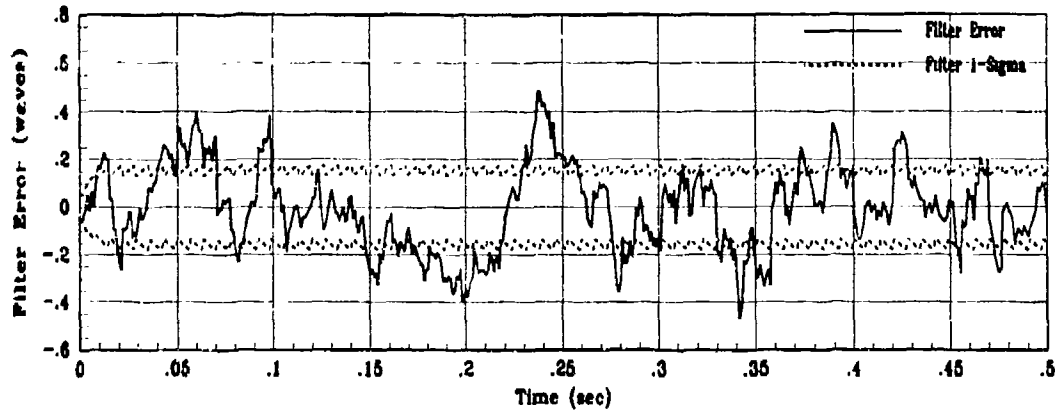
(b) X1 Filter Error for 1 MC Run
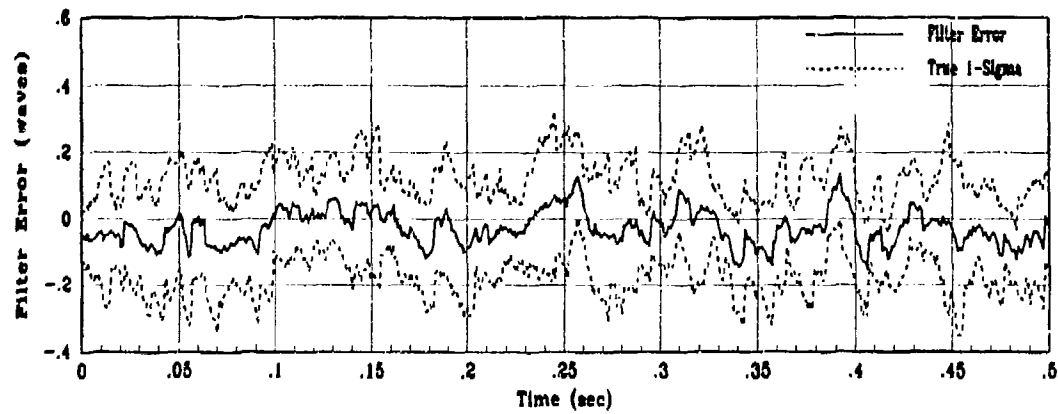
(c) X1 True Filter Error for 10 MC Runs

Figure F.44.   Baseline State 1 Filter Estimation Error for Study 9
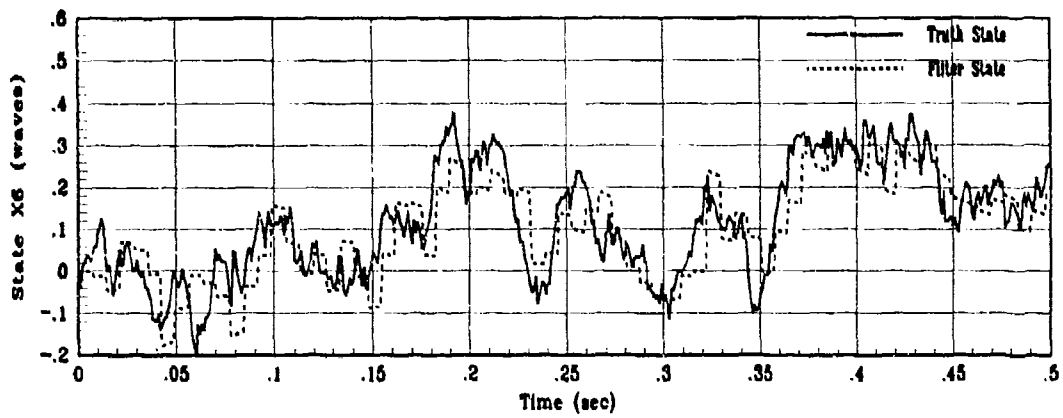
(a) Truth and Filter States: XS6, XF6
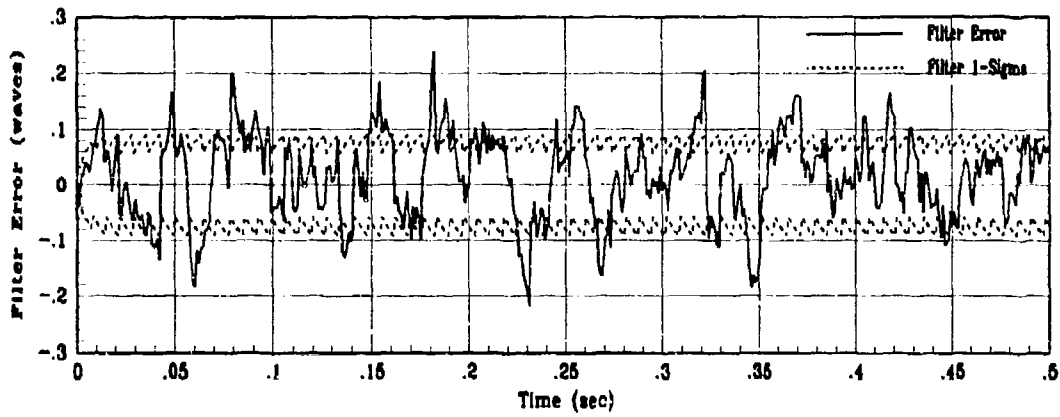
(b) X6 Filter Error for 1 MC Run
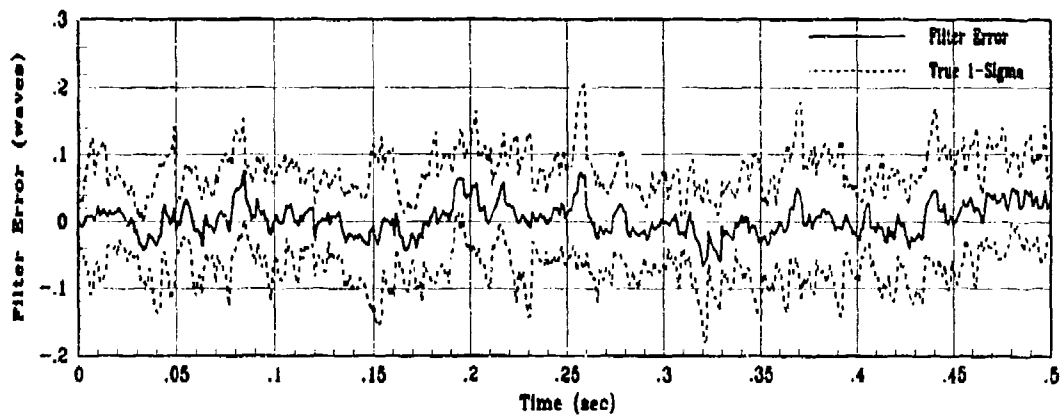
(c) X6 True Filter Error for 10 MC runs

Figure F.45. Baseline State 6 Filter Estimation Error for Study 9
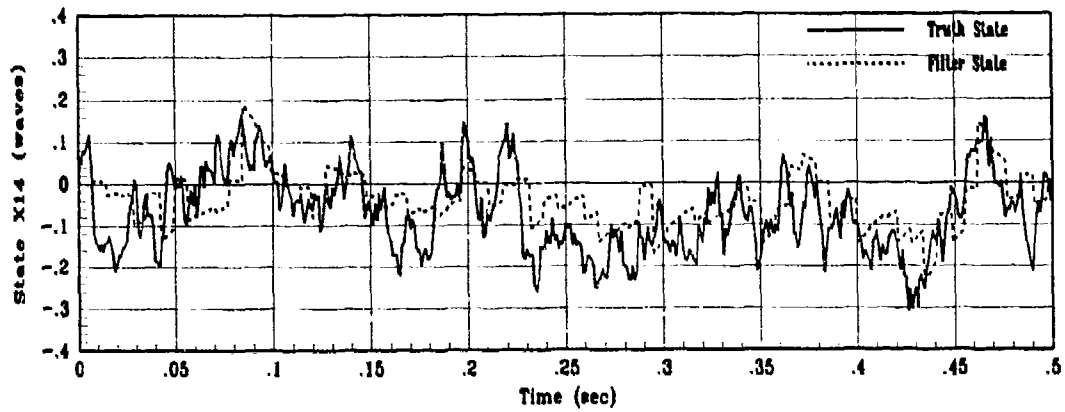
(a) Truth and Filter States: XS14, XF14
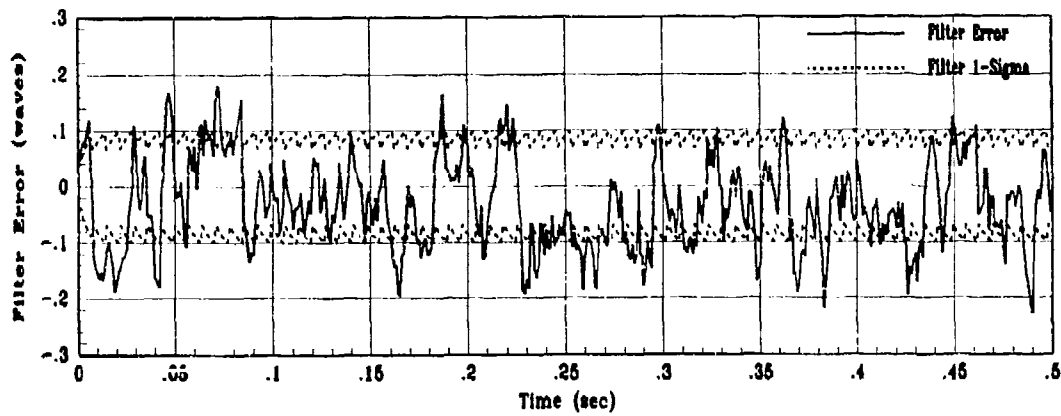
(b) X14 Filter Error for 1 MC Run
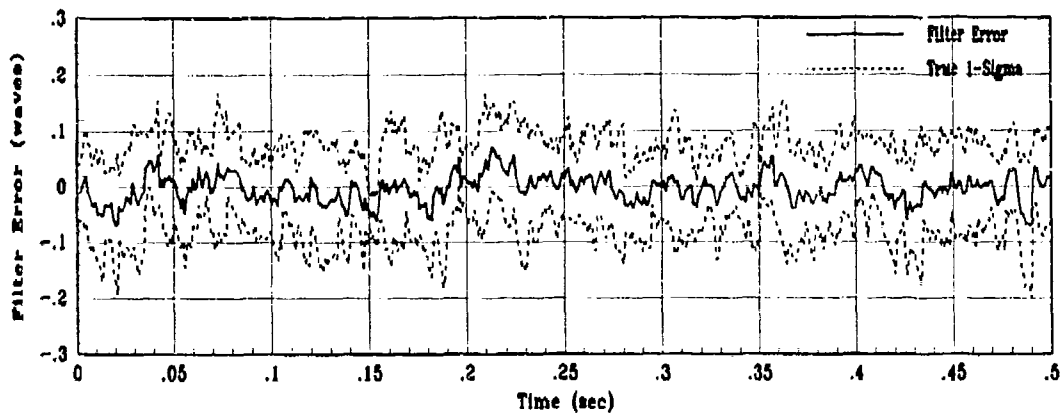
(c) X14 True Filter Error for 10 MC runs

Figure F.46. Baseline State 14 Filter Estimation Error for Study 9
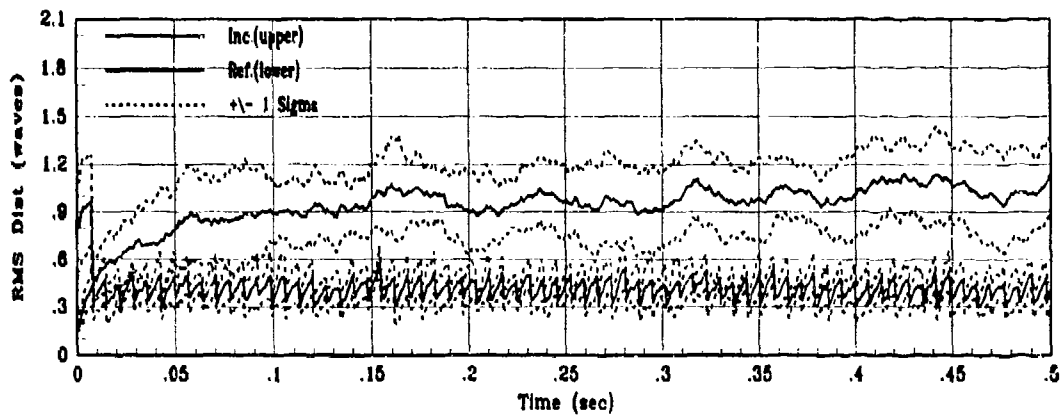
(a) Incident and Reflected RMS Phase Distortion for 10 MC Runs
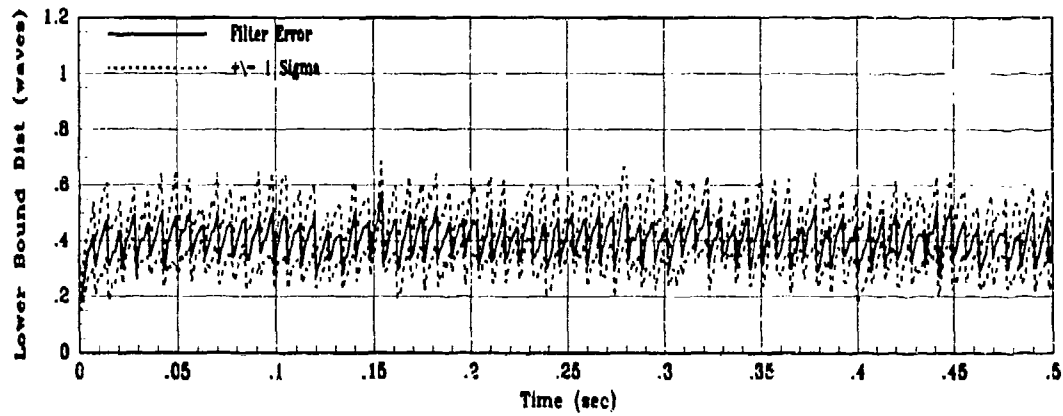
(b) RMS Filter Error for 10 MC Runs
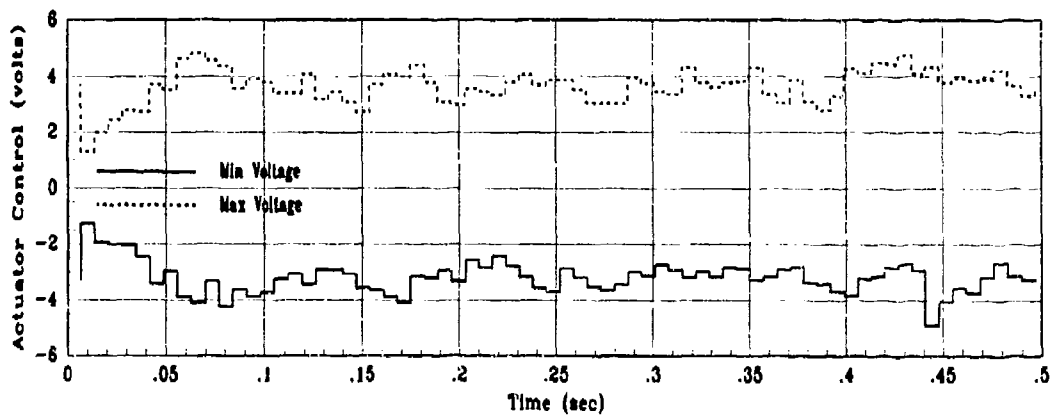
(c) Actuator Control Voltage Envelope

Figure F.47. Baseline Control System Performance for Study 9

Appendix G. Performance Plots for Study 1 with Modified Covariance Controller

This appendix contains the performance plots for the modified baseline controller which includes cross-correlations between the Zernike coefficient states. As in Appendix F, Kalman filter performance plots are arranged in 3-plot sets describing filter tracking of the state, filter-computed estimation error, and true statistics of the estimation error. Overall system performance is also presented as a 3-plot set in terms of the incident vs reflected rms phase distortion, rms filter estimation error, and control voltage envelope over 10 Monte Carlo runs. The plots correspond to the noise study case where low measurement noise is simulated in both the truth and filter models.

Section G.1 shows the performance results when time-varying Kalman filter gains were computed at each sample time. Section G.2 contains filter estimation plots for states 1, 6, and 14 along with overall system performance plots for the case where the steady-state Kalman filter gain was computed once and used for all time, as motivated in Chapters 1, 4, and 5.
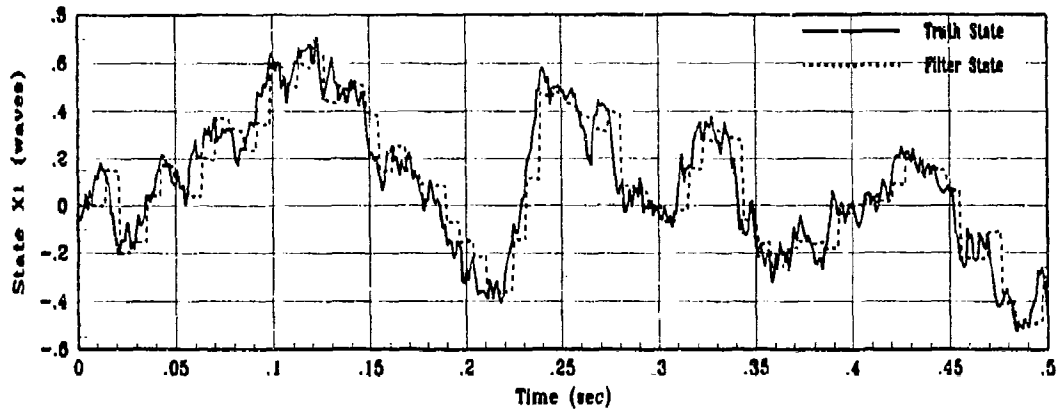
(a) Truth and Filter States: XS1, XF1
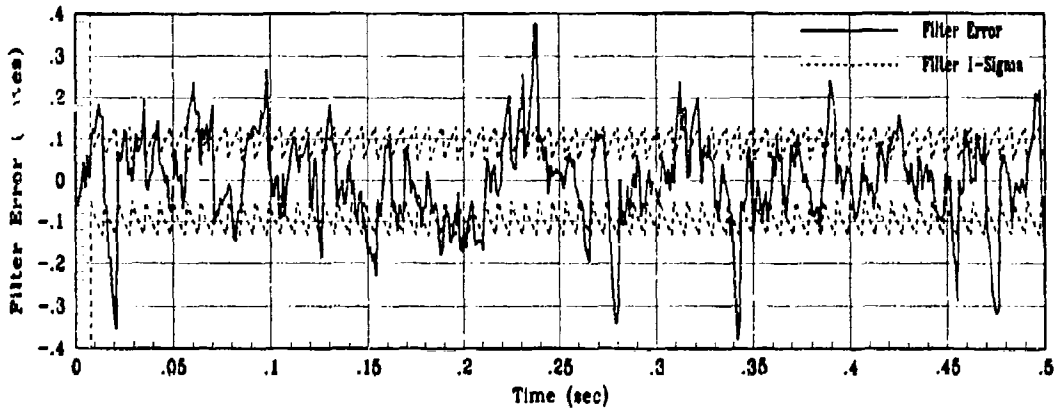
(b) X1 Filter Error for 1 MC Run
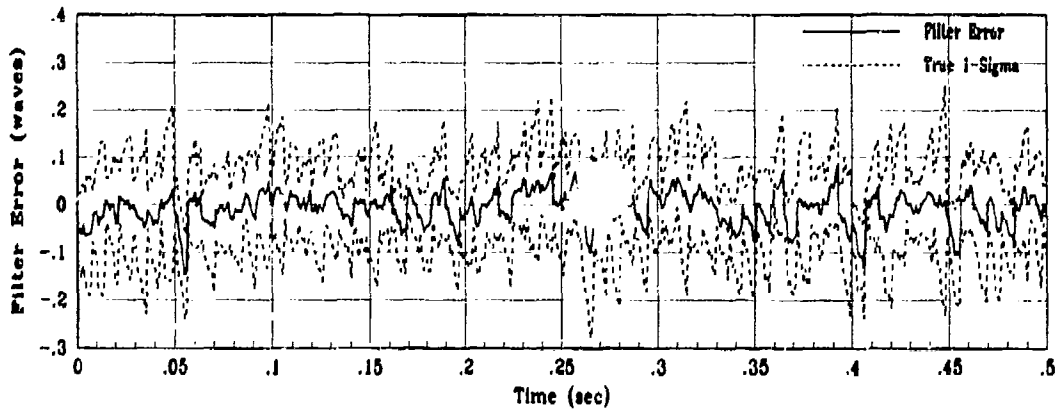
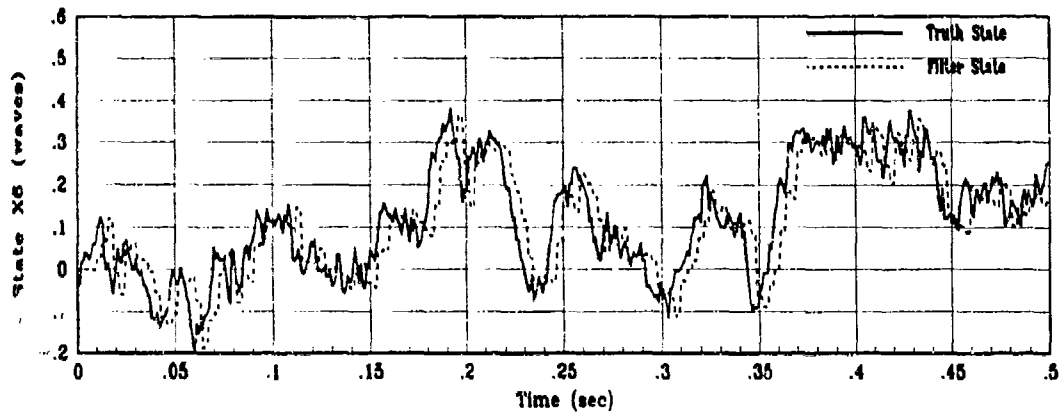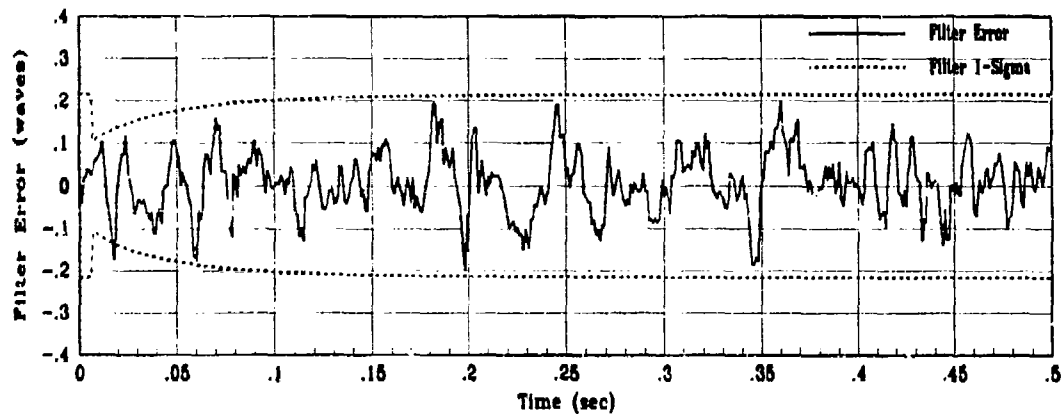
(c) X1 True Filter Error for 10 MC Runs

Figure G.1.   State 1 Filter Estimation Error with Correlated States
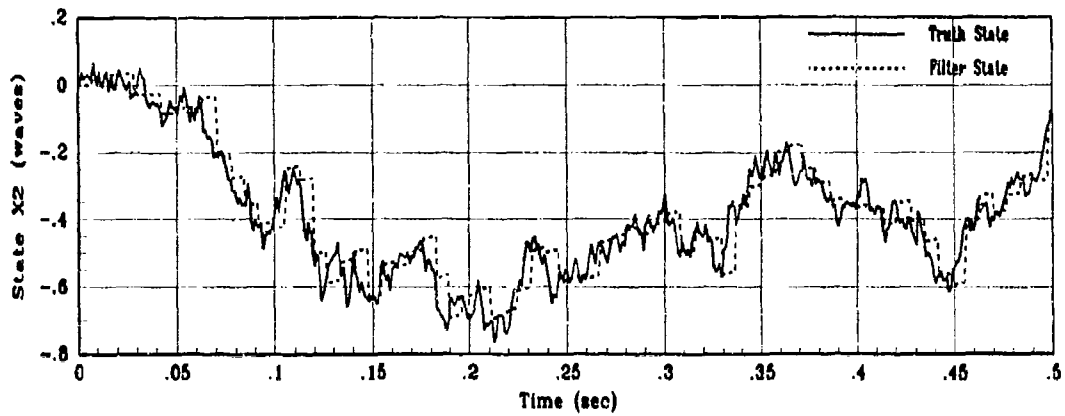
(a) Truth and Filter States: XS2, XF2
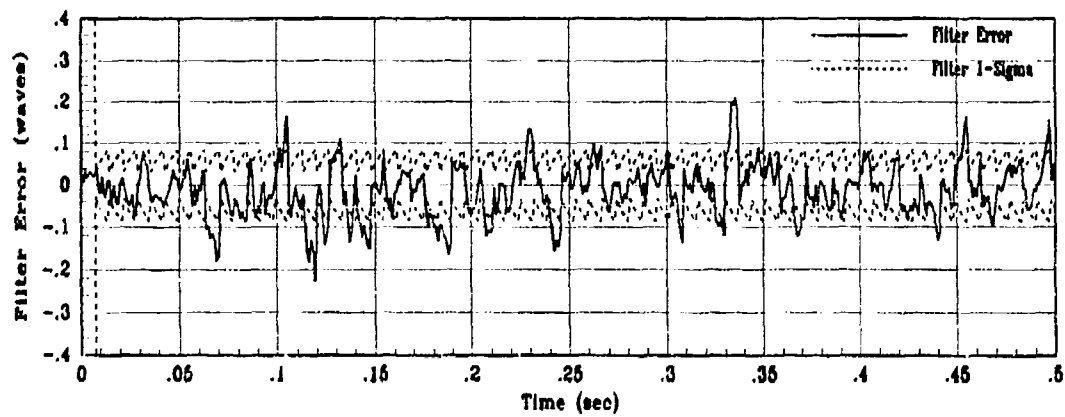
(b) X2 Filter Error for 1 MC Run
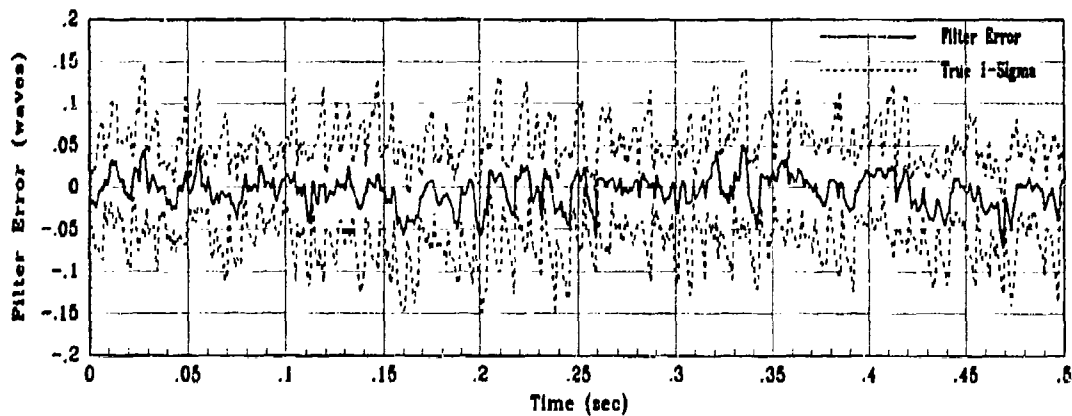
(c) X2 True Filter Error for 10 MC runs

Figure G.2. State 2 Filter Estimation Error with Correlated States
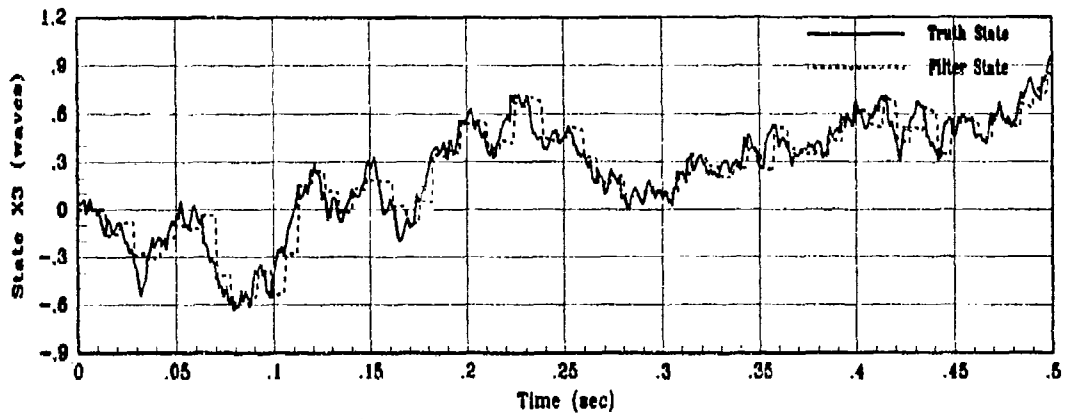
(a) Truth and Filter States: XS3, XF3
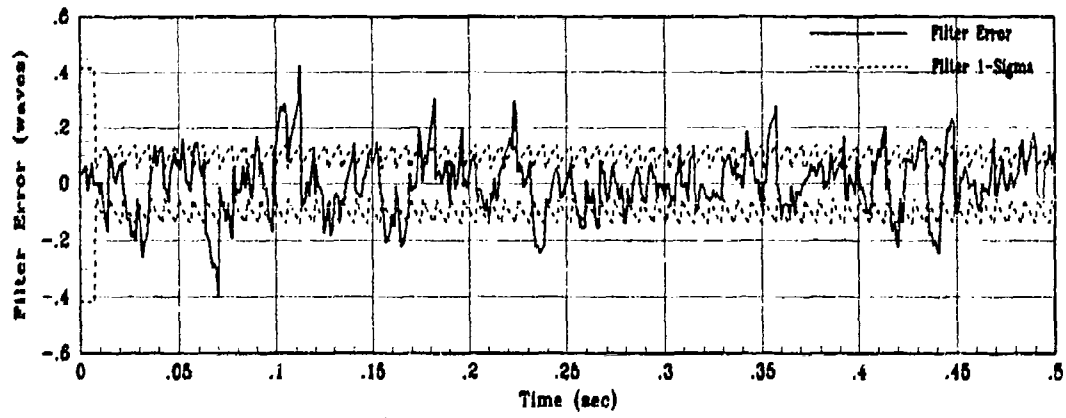
(b) X3 Filter Error for 1 MC Run
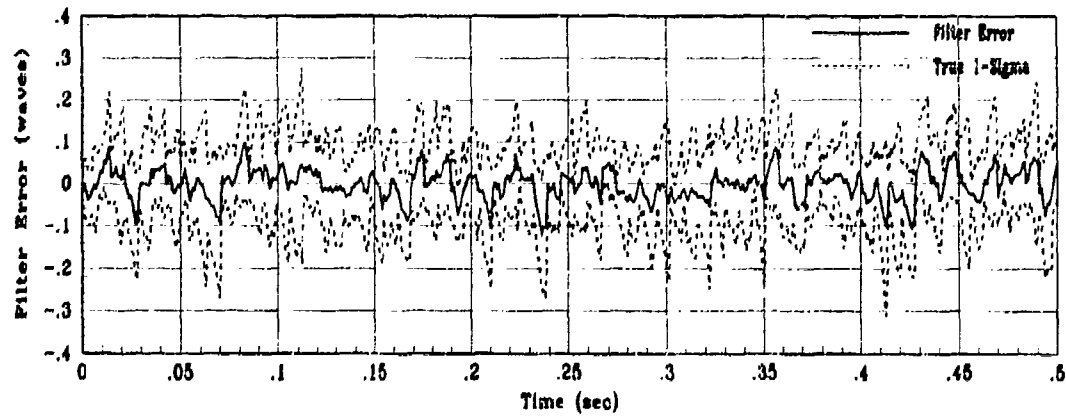
(c) X3 True Filter Error for 10 MC runs

Figure G.3. State 3 Filter Estimation Error with Correlated States
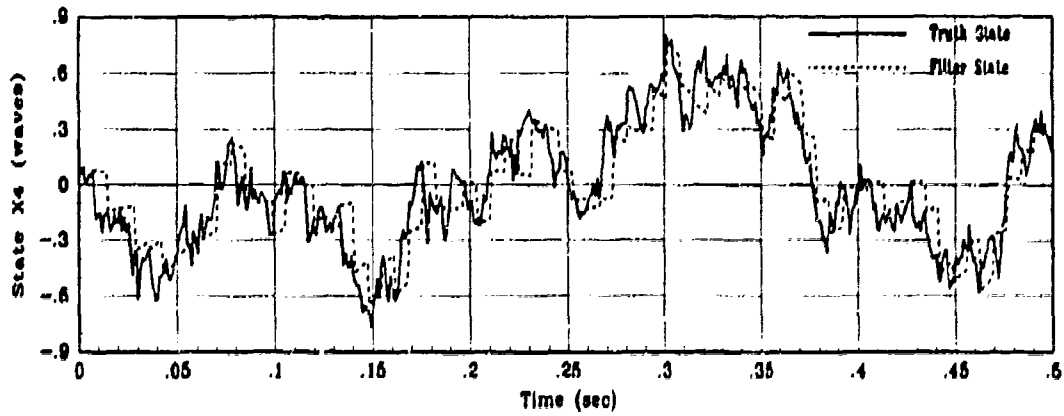
(a) Truth and Filter States: XS4, XF4
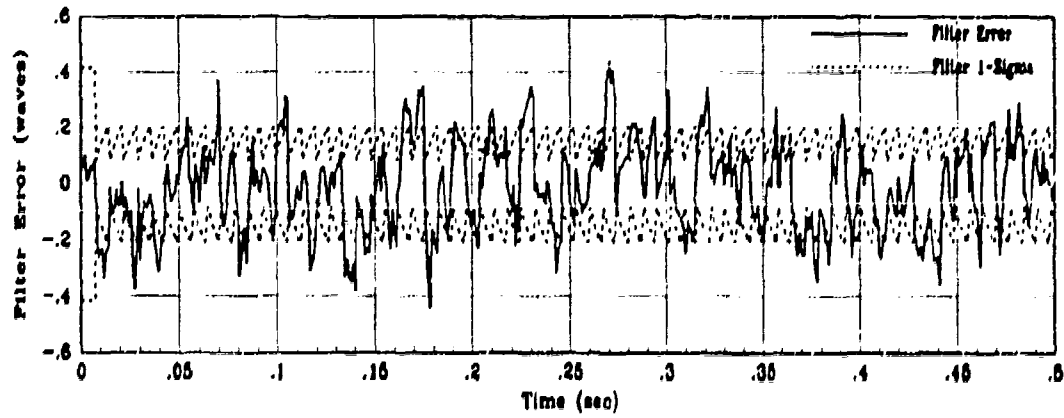
(b) X4 Filter Error for 1 MC Run
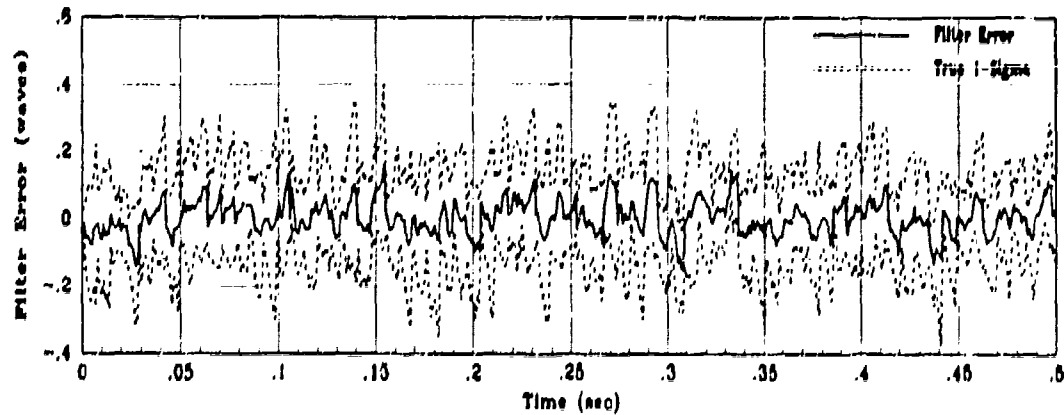
(c) X4 True Filter Error for 10 MC runs

Figure G.4. State 4 Filter Estimation Error with Correlated States
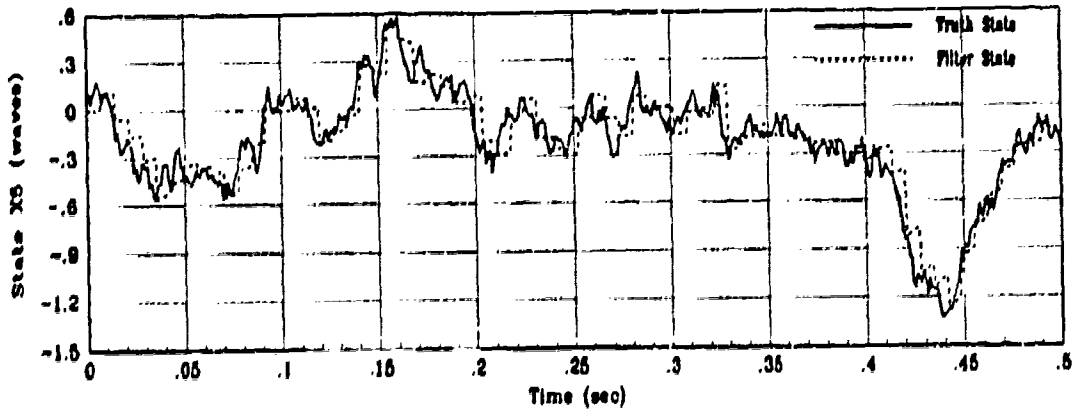
(a) Truth and Filter States: XS5, XF5
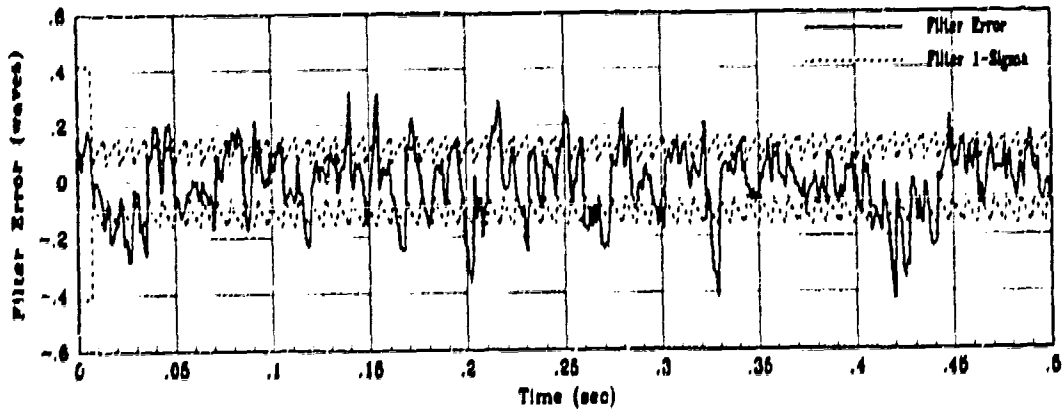
(b) X5 Filter Error for 1 MC Run
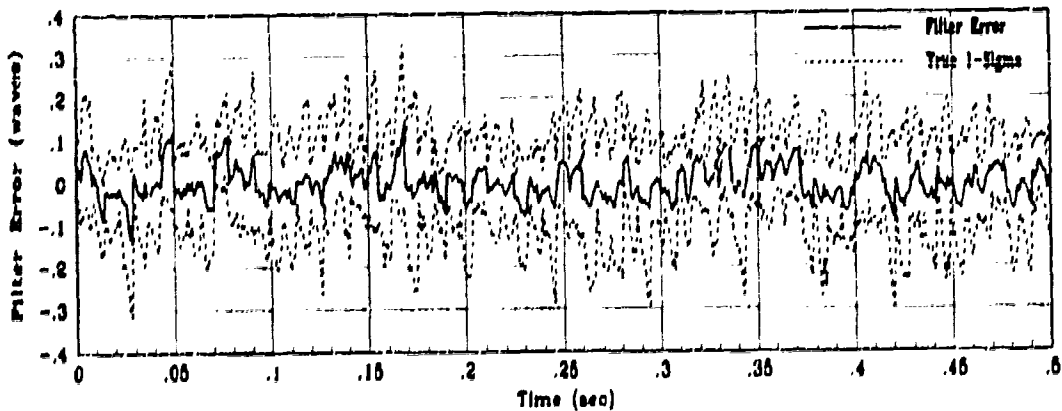
(c) X5 True Filter Error for 10 MC runs

Figure G.5. State 5 Filter Estimation Error with Correlated States
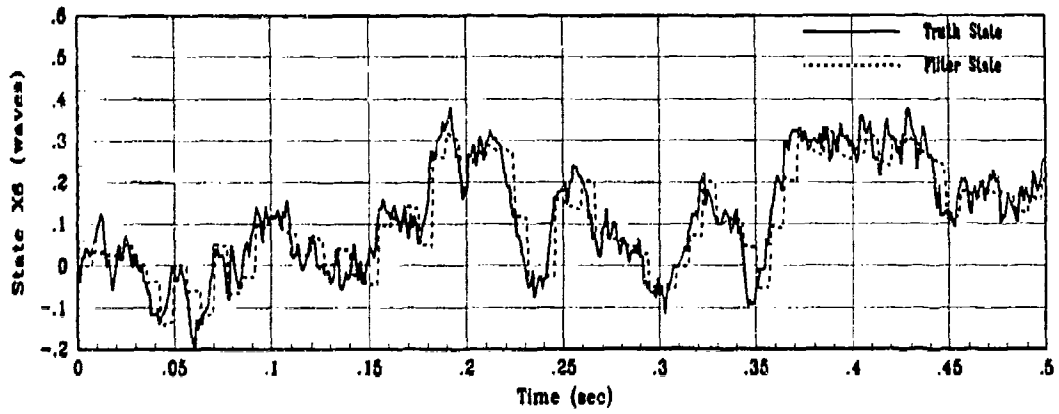
(a) Truth and Filter States: XS6, XF6
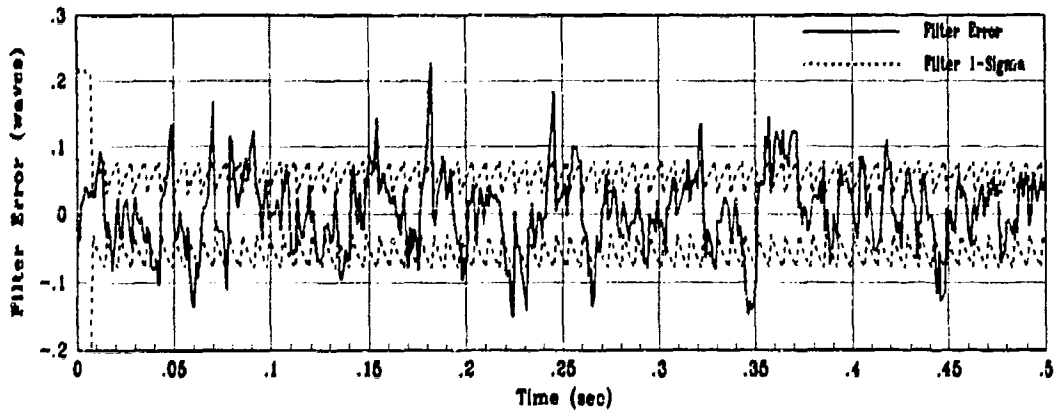
(b) X6 Filter Error for 1 MC Run
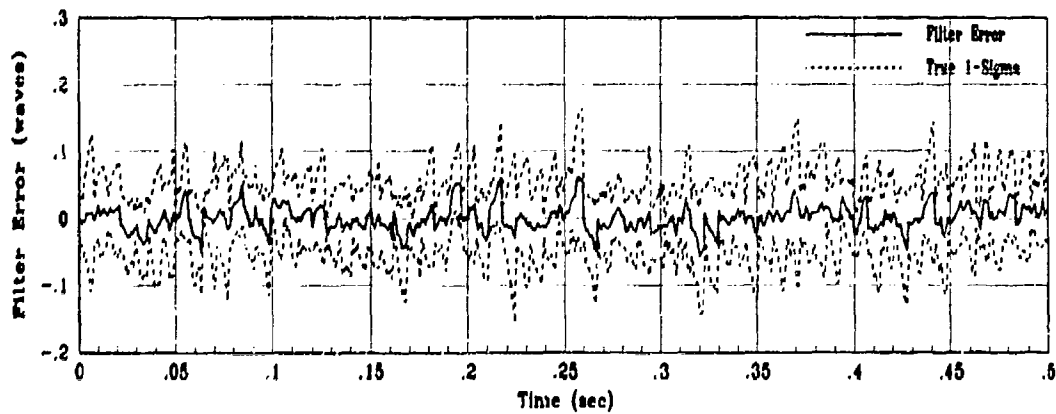
(c) X6 True Filter Error for 10 MC runs

Figure G.6. State 6 Filter Estimation Error with Correlated States
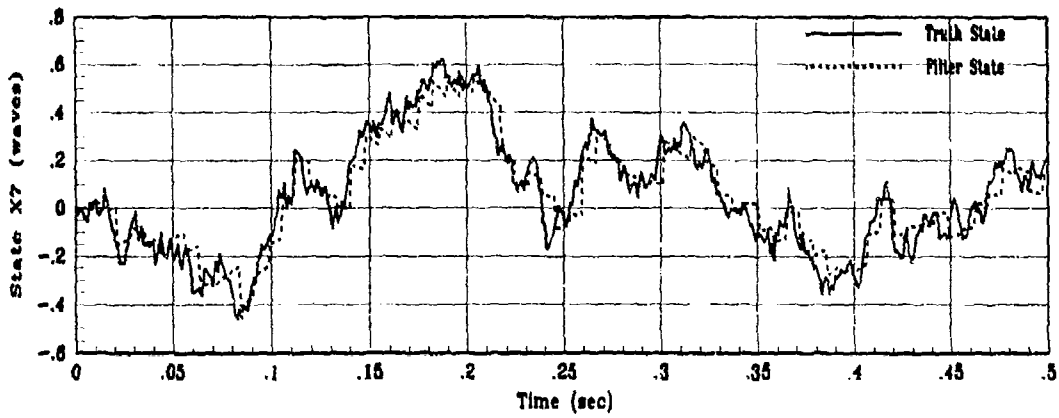
(a) Truth and Filter States: XS7, XF7
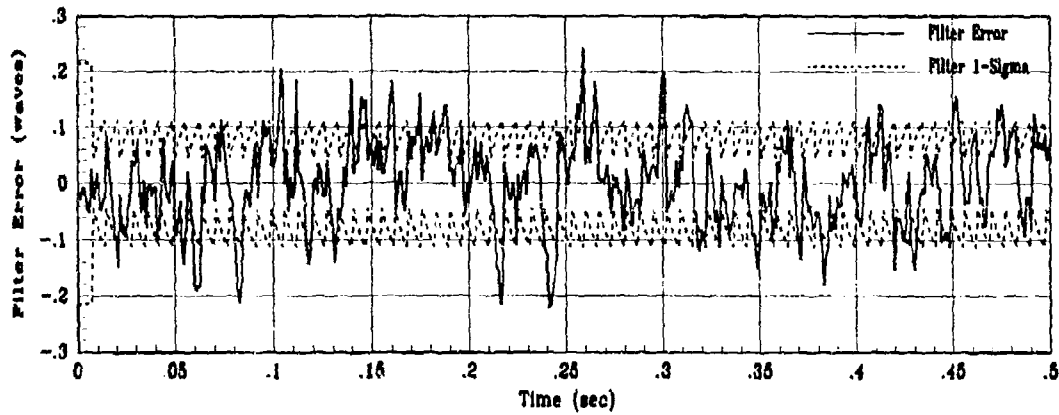
(b) X7 Filter Error for 1 MC Run
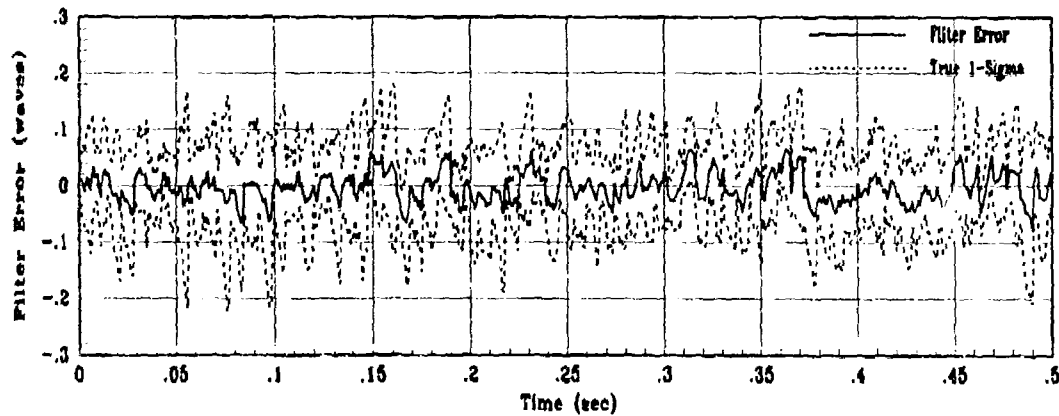
(c) X7 True Filter Error for 10 MC runs

Figure G.7. State 7 Filter Estimation Error with Correlated States
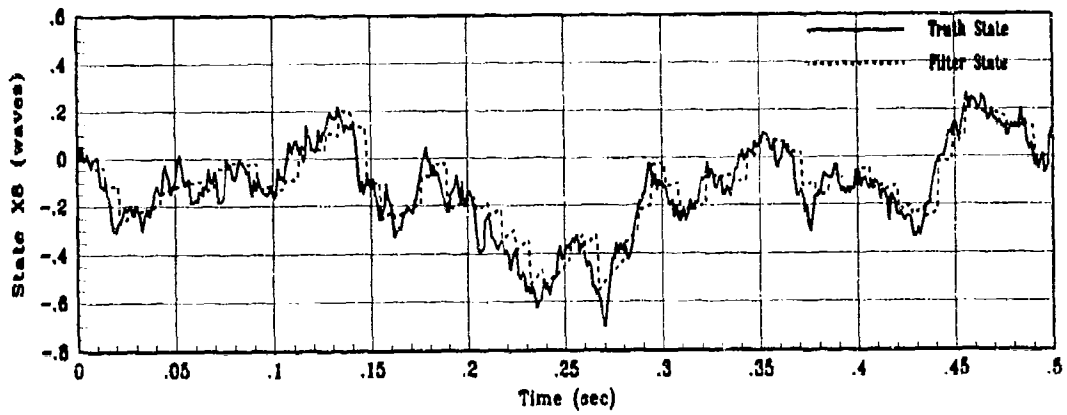
(a) Truth and Filter States: XS8, XF8
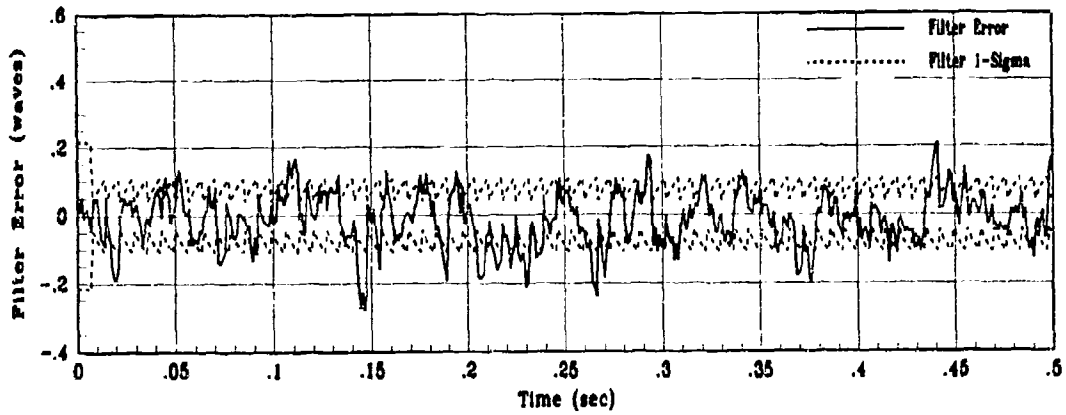
(b) X8 Filter Error for 1 MC Run
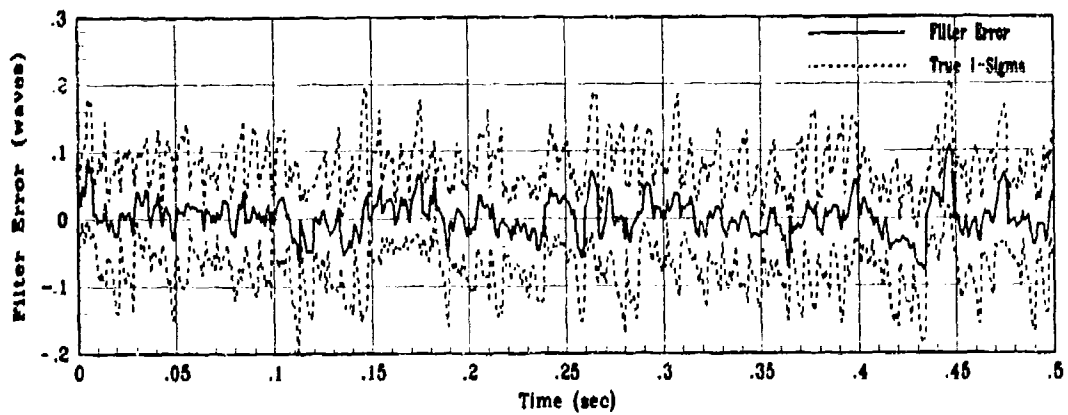
(c) X8 True Filter Error for 10 MC runs

Figure G.8. State 8 Filter Estimation Error with Correlated States
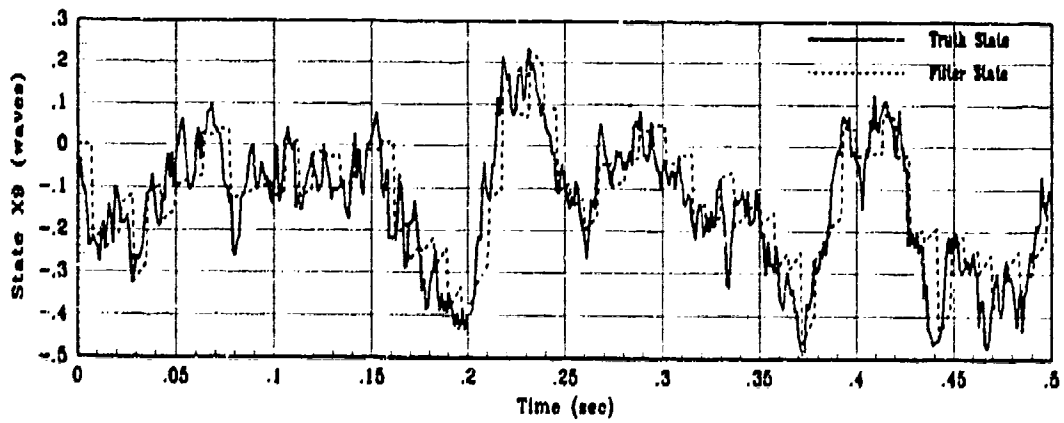
(a) Truth and Filter States: XS9, XF9
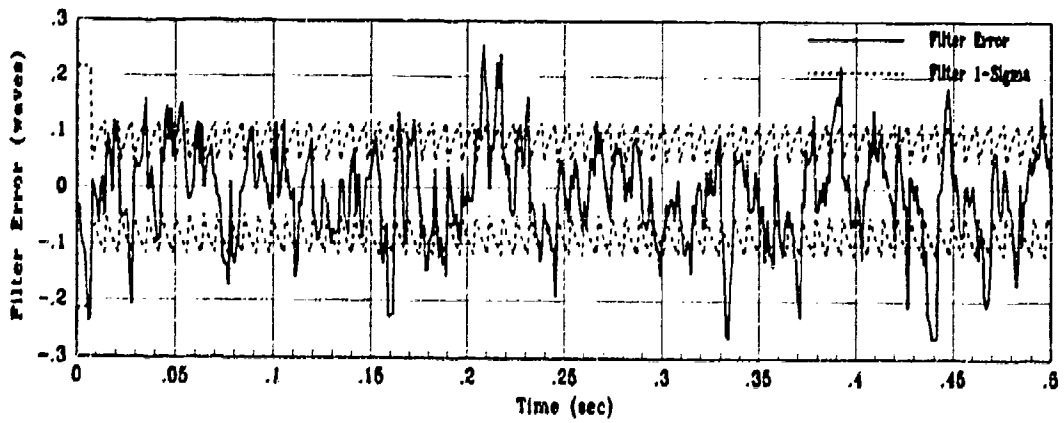
(b) X9 Filter Error for 1 MC Run
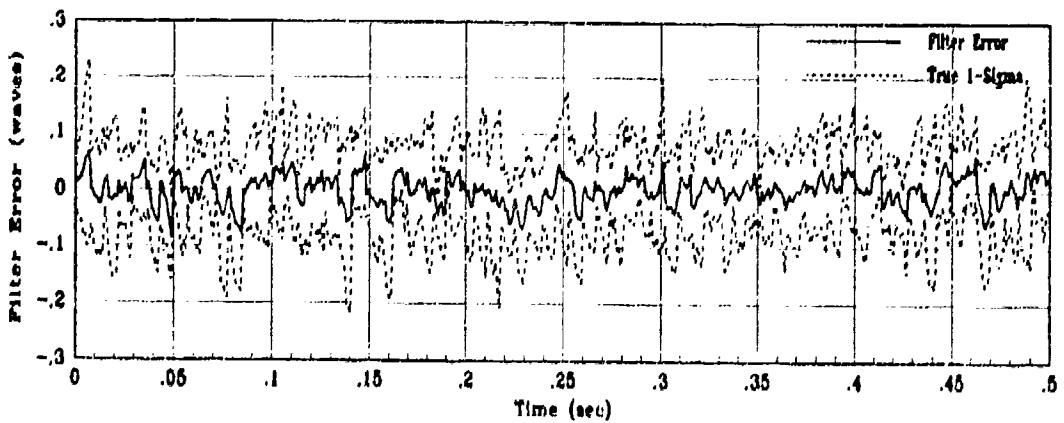
(c) X9 True Filter Error for 10 MC runs

Figure G.9. State 9 Filter Estimation Error with Correlated States.
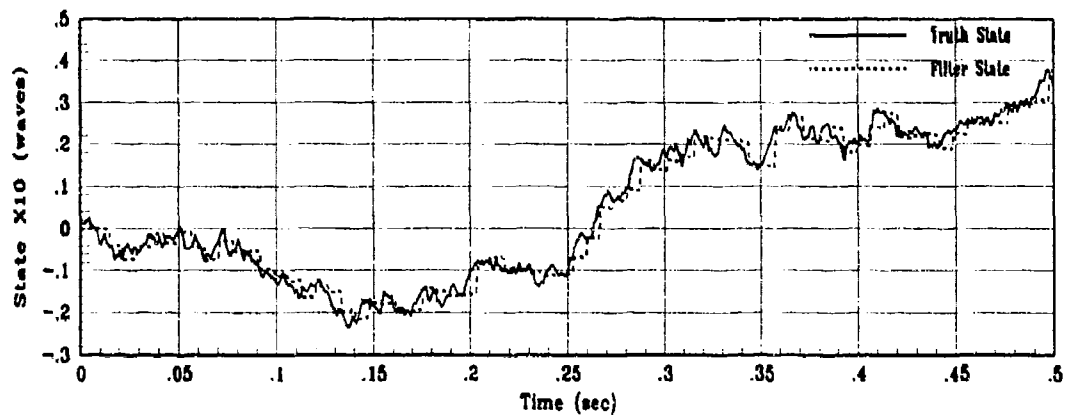
(a) Truth and Filter States: XS10, XF10
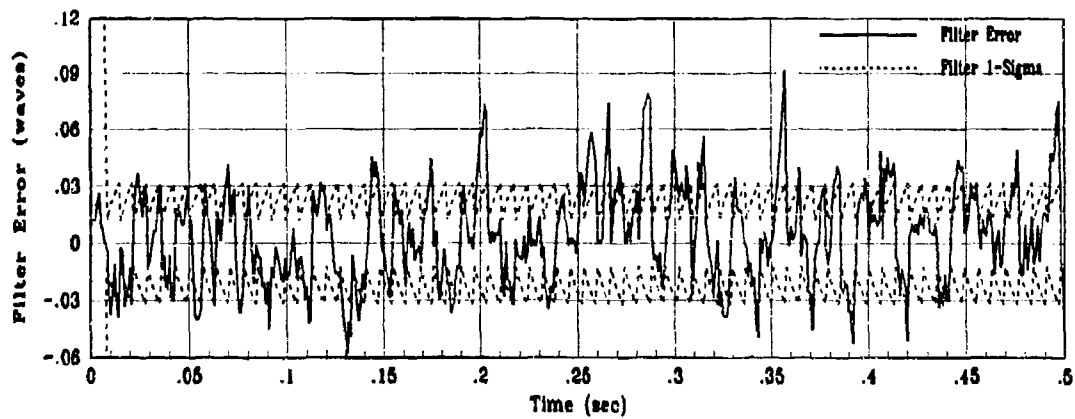
(b) X10 Filter Error for 1 MC Run
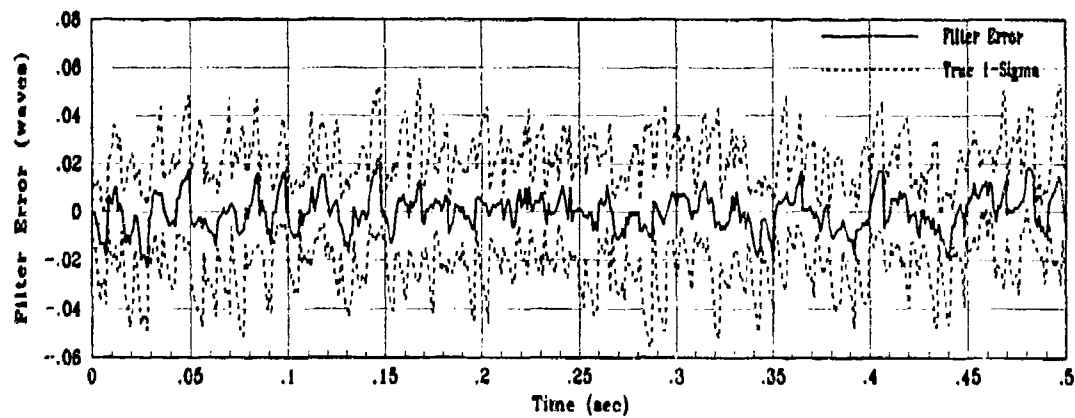
(c) X10 True Filter Error for 10 MC runs

Figure G.10. State 10 Filter Estimation Error with Correlated States
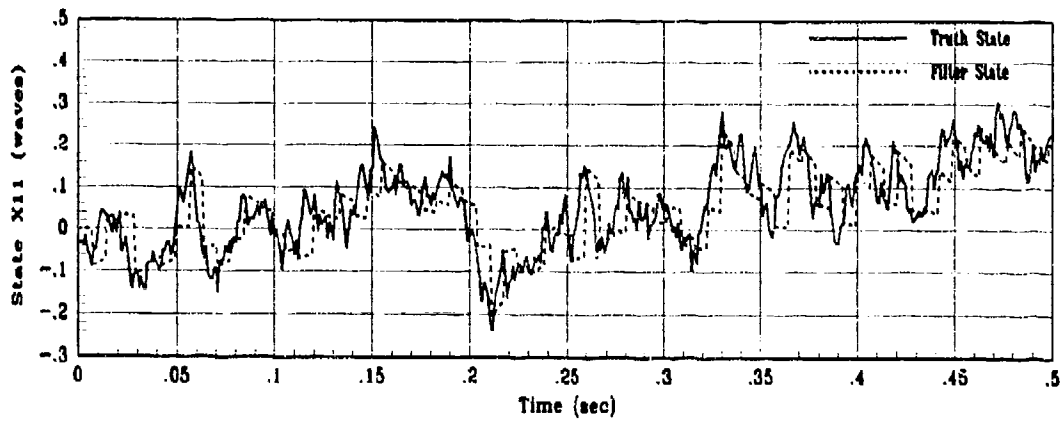
(a) Truth and Filter States: XS11, XF11
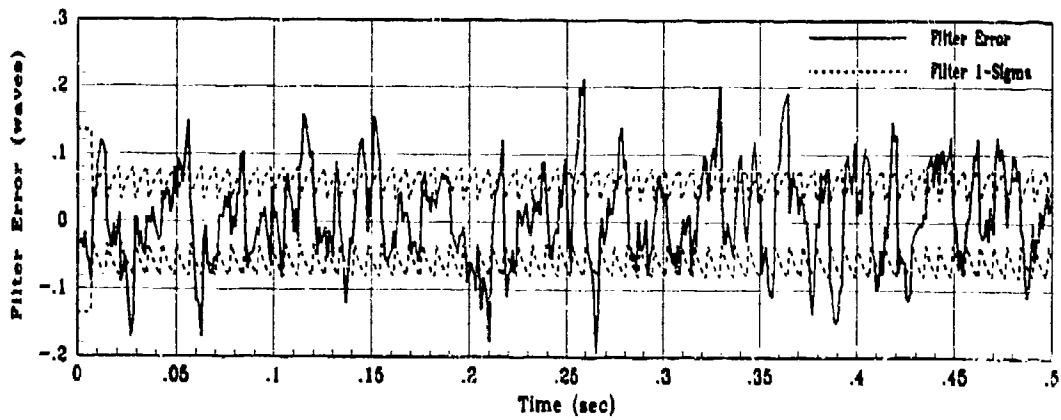
(b) X11 Filter Error for 1 MC Run
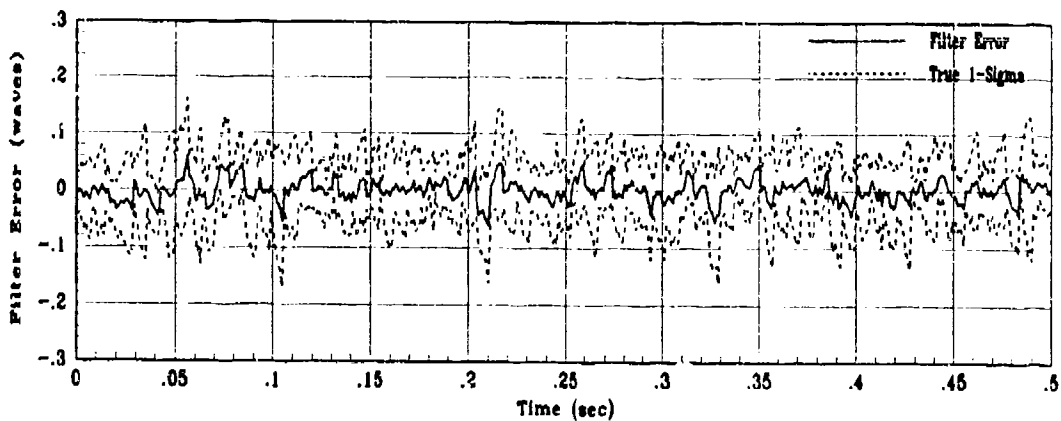
(c) X11 True Filter Error for 10 MC runs

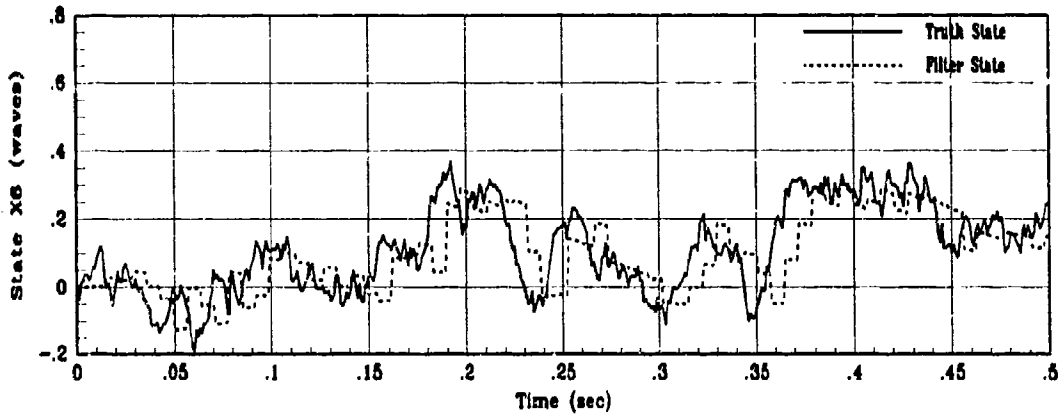Figure G.11. State 11 Filter Estimation Error with Correlated States
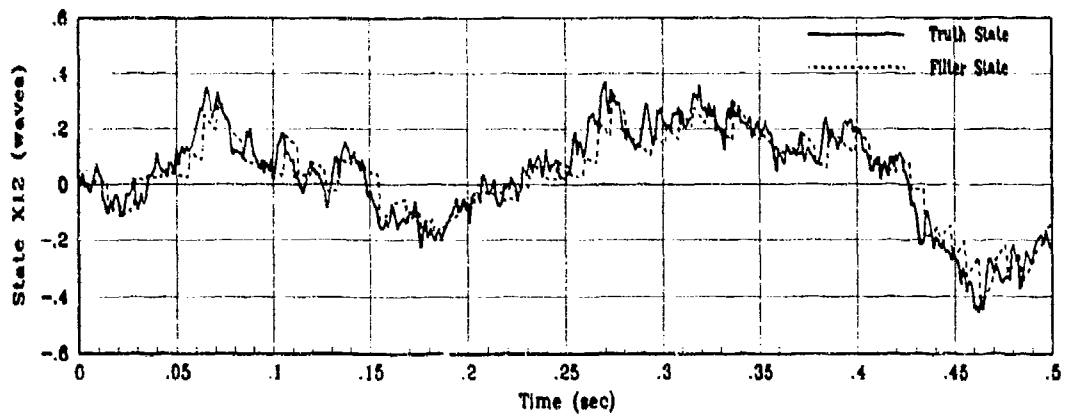
(a) Truth and Filter States: XS12, XF12
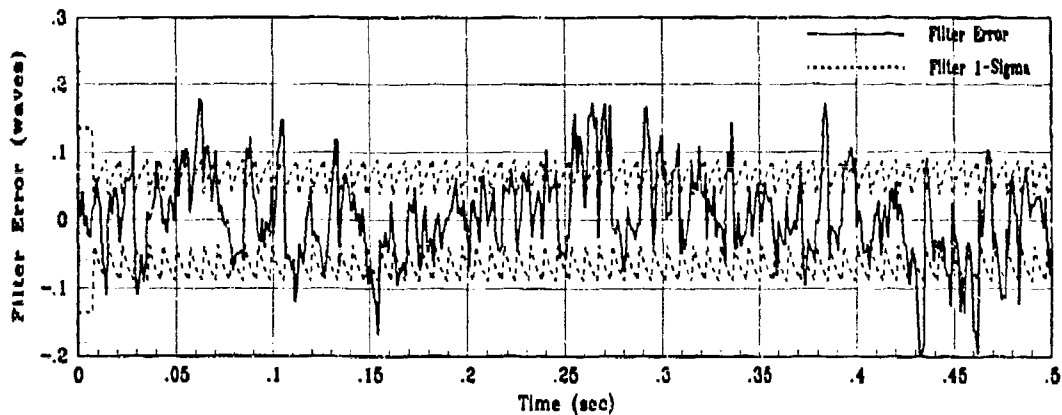
(b) X12 Filter Error for 1 MC Run
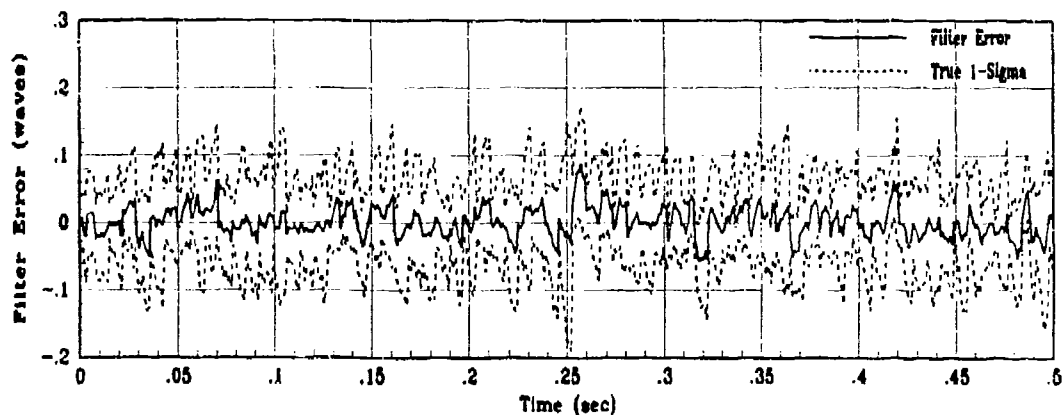
(c) X12 True Filter Error for 10 MC runs

Figure G.12. State 12 Filter Estimation Error with Correlated States
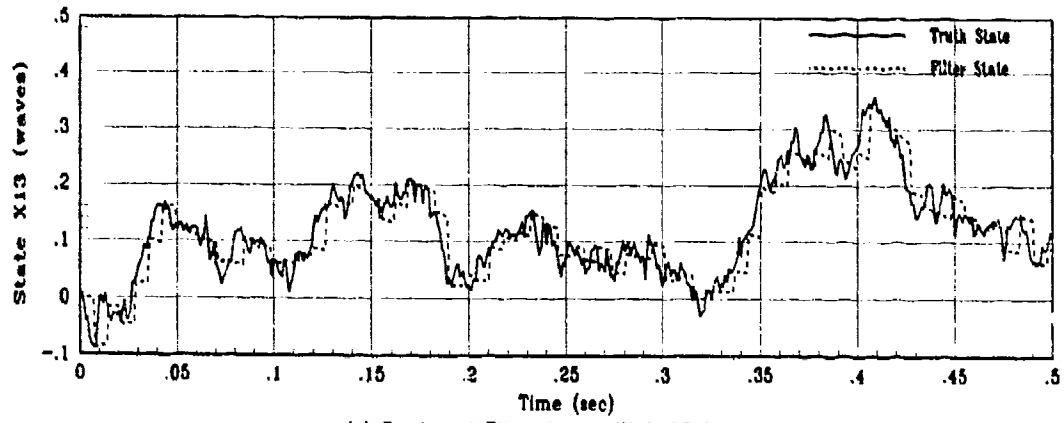
G-13

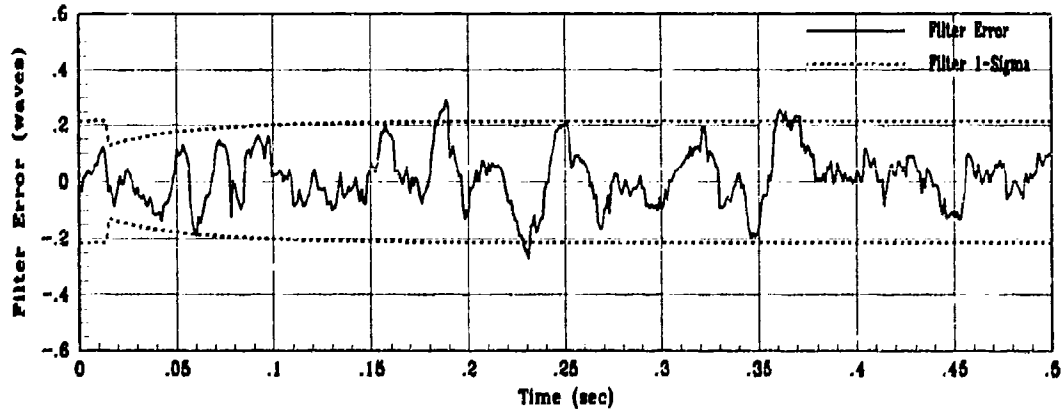(a) Truth and Filter States: XS13, XF13
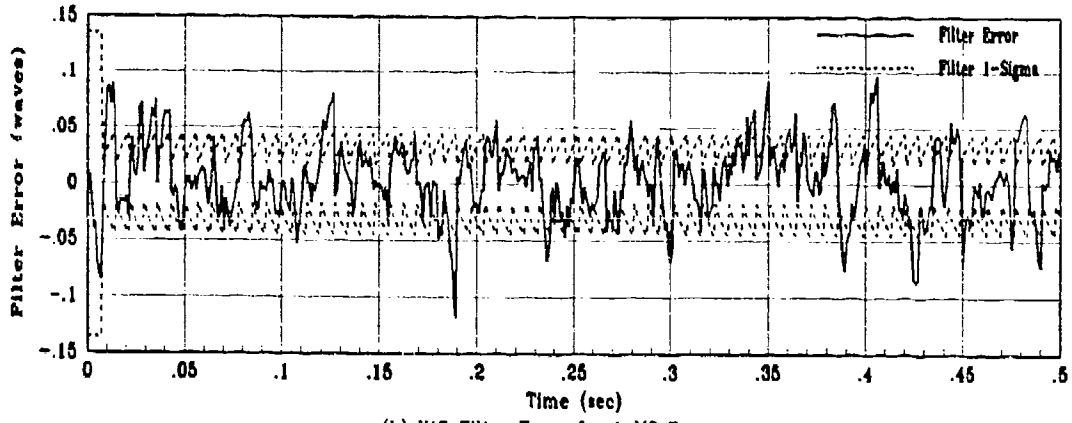
(b) X13 Filter Error for 1 MC Run
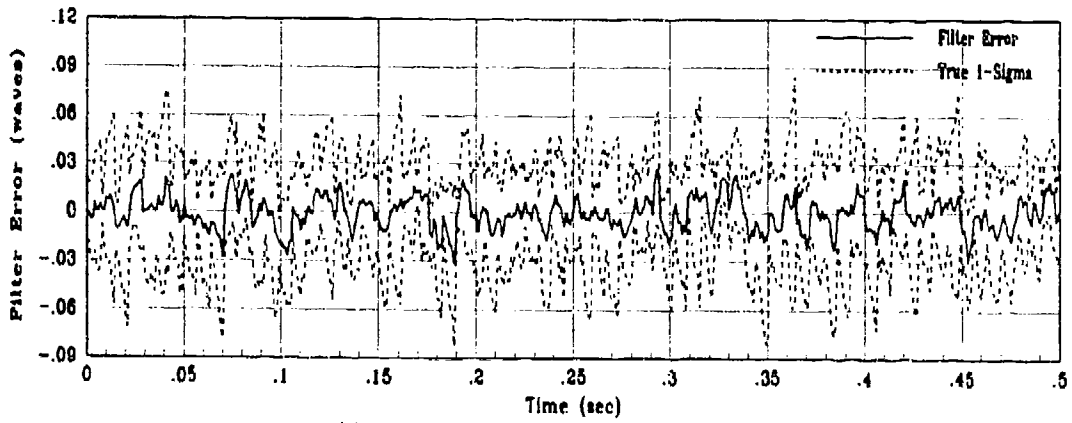
(c) X13 True Filter Error for 10 MC runs

Figure G.13. State 13 Filter Estimation Error with Correlated States
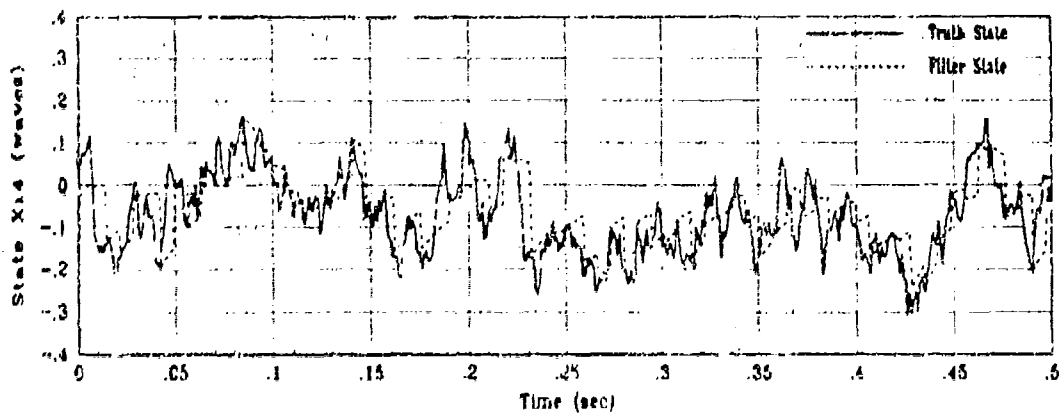
(a) Truth and Filter States: XS14, XF14
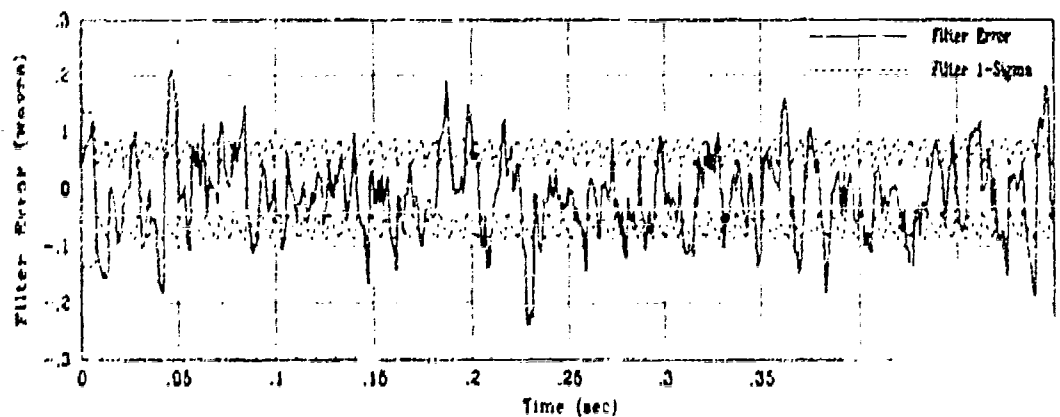
(b) X14 Filter Error for 1 MC Run
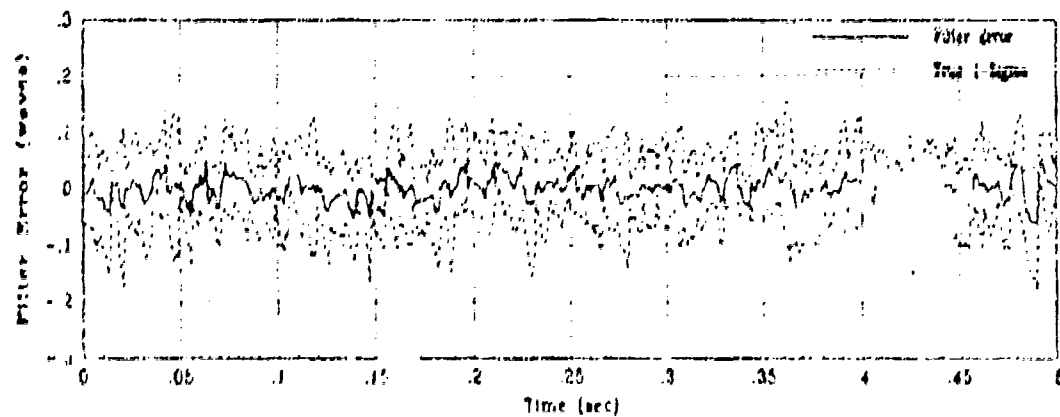
(c) X14 True Filter Error for 10 MC runs

Figure G-14. State 14 Filter Estimation Error With Correlated States
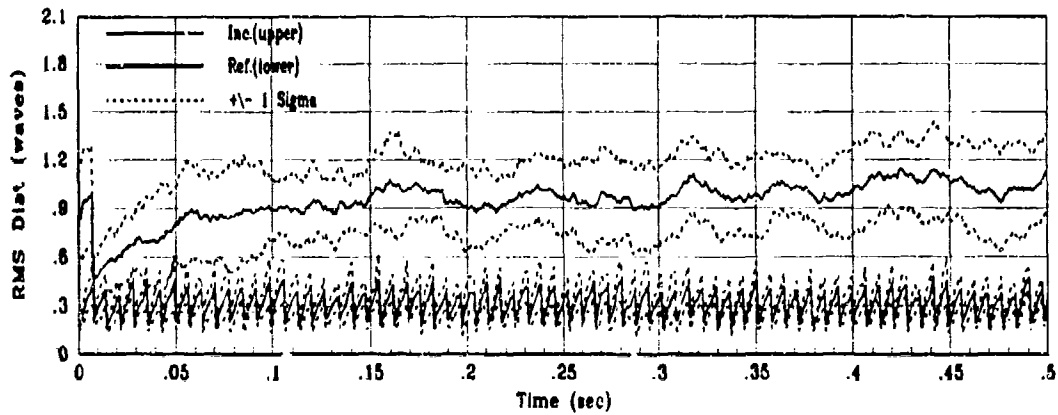
(a) Incident and Reflected RMS Phase Distortion for 10 MC Runs
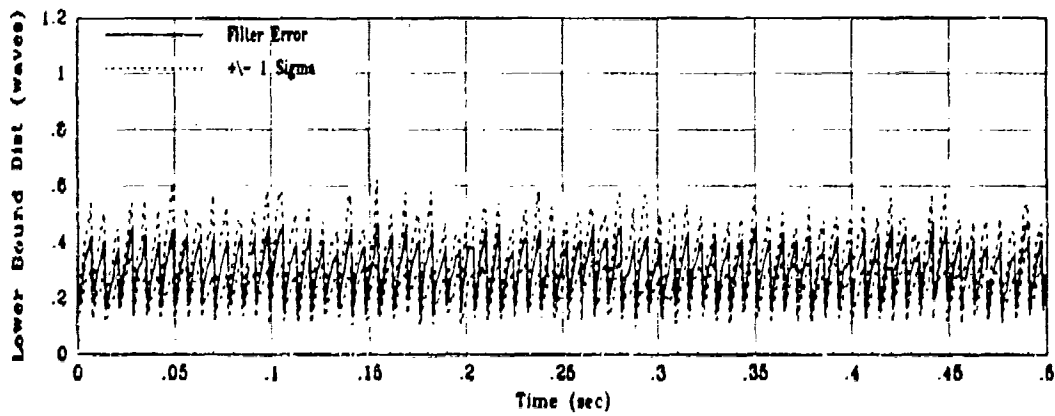
(b) RMS Filter Error for 10 MC Runs
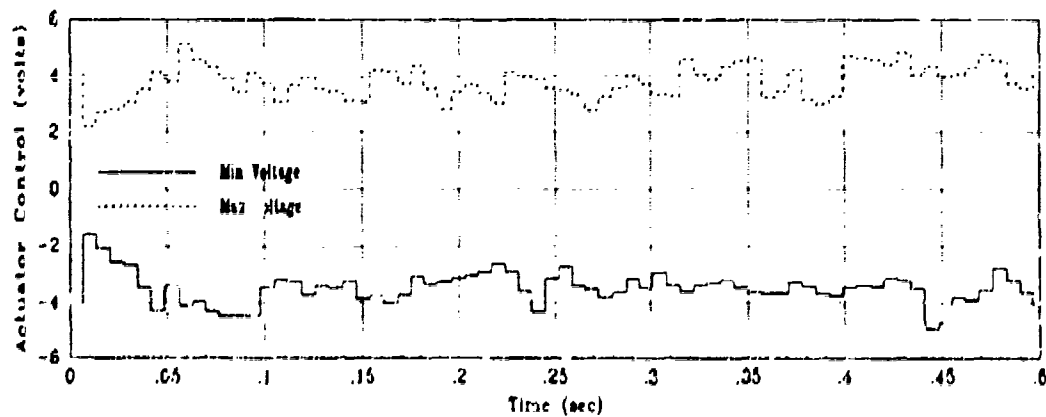
(c) Actuator Control Voltage Envelope

Figure G.15. Control System Performance with Correlated States
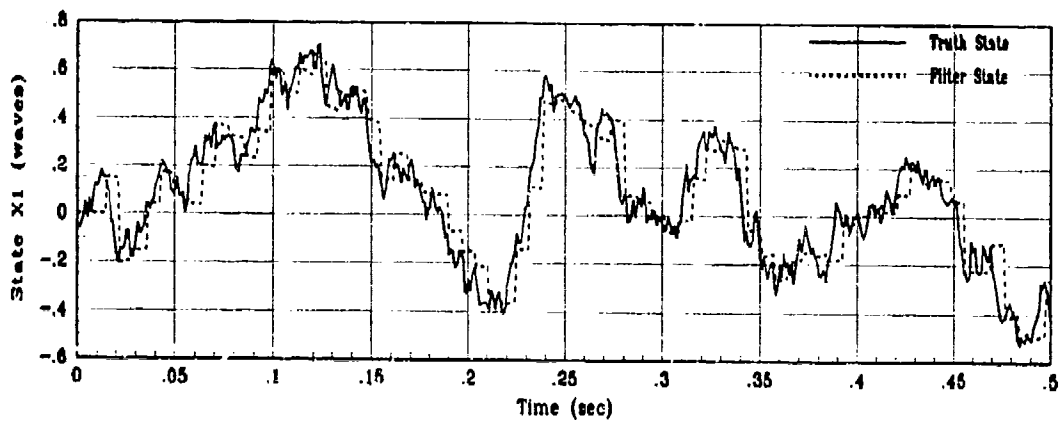
(a) Truth and Filter States: XS1, XF1
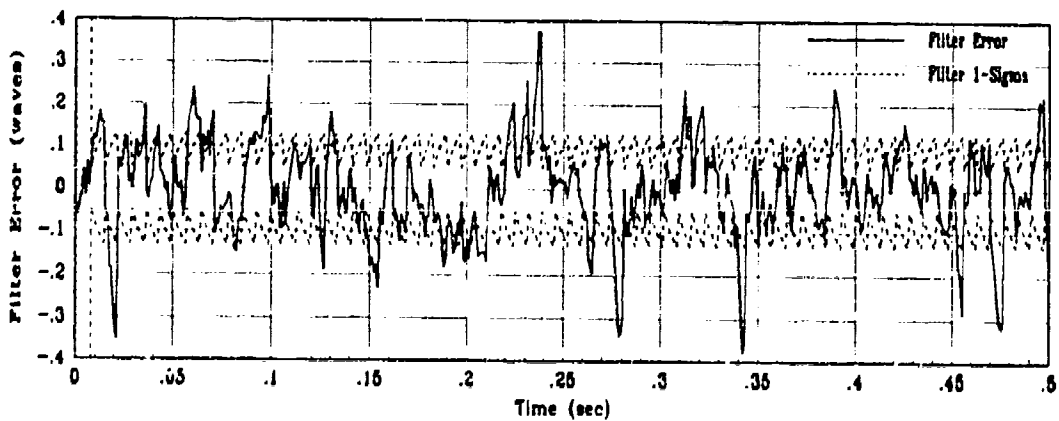
(b) X1 Filter Error for 1 MC Run
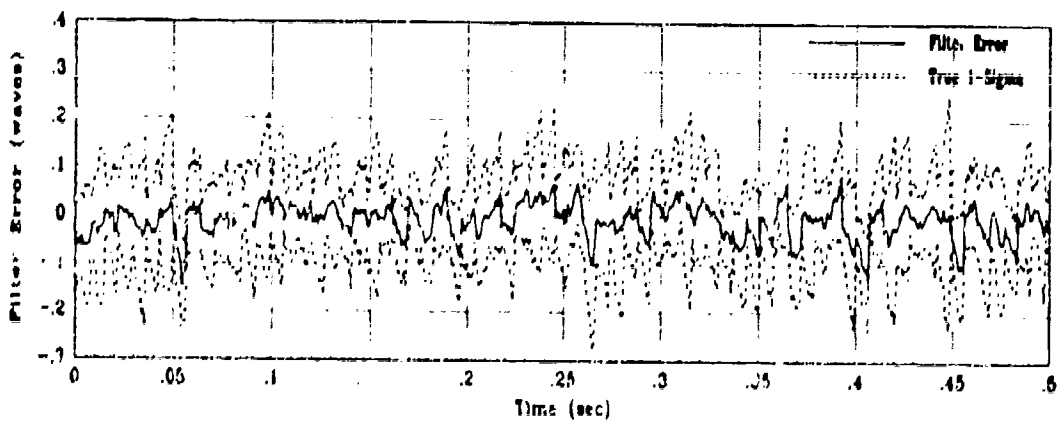
(c) X1 True Filter Error for 10 MC Runs

Figure G.16. State 1 Filter Estimation Error with Correlated States
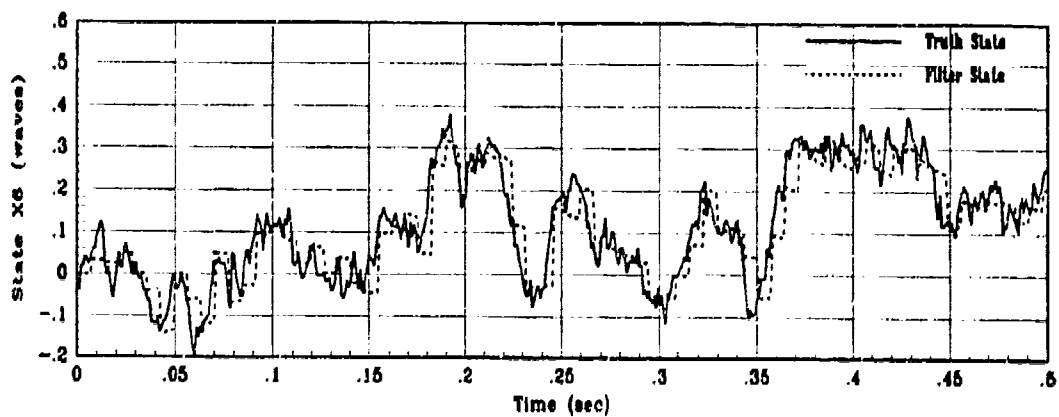
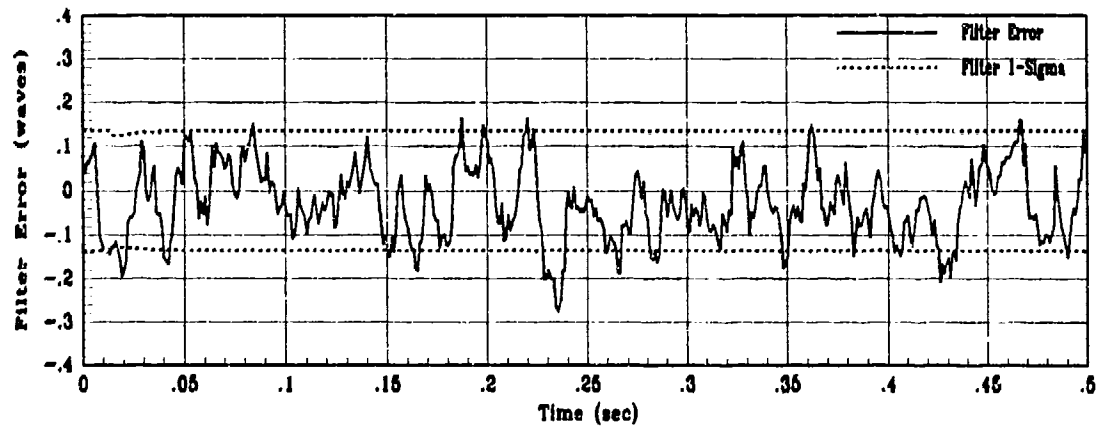(a) Truth and Filter States: XS6, XF6
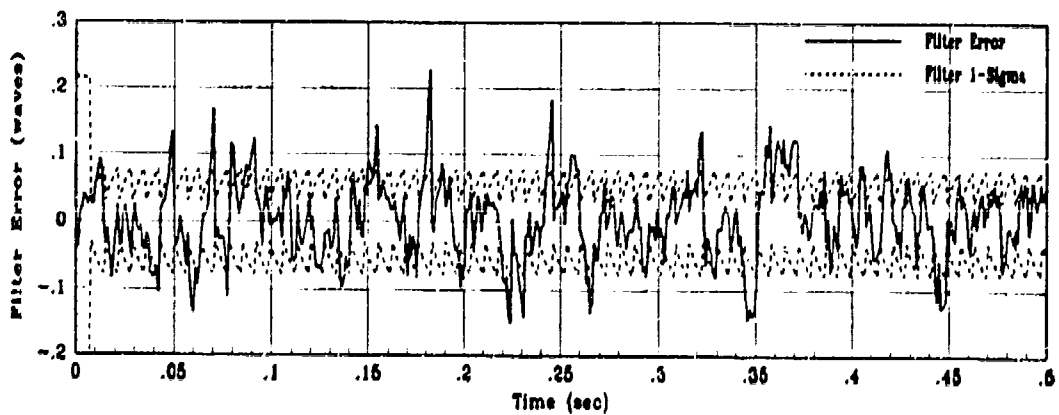
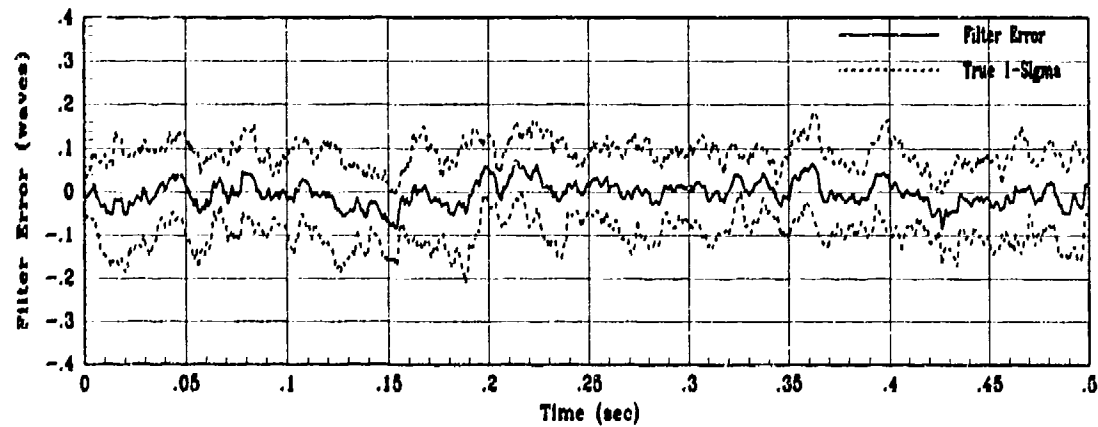(b) X6 Filter Error for 1 MC Run
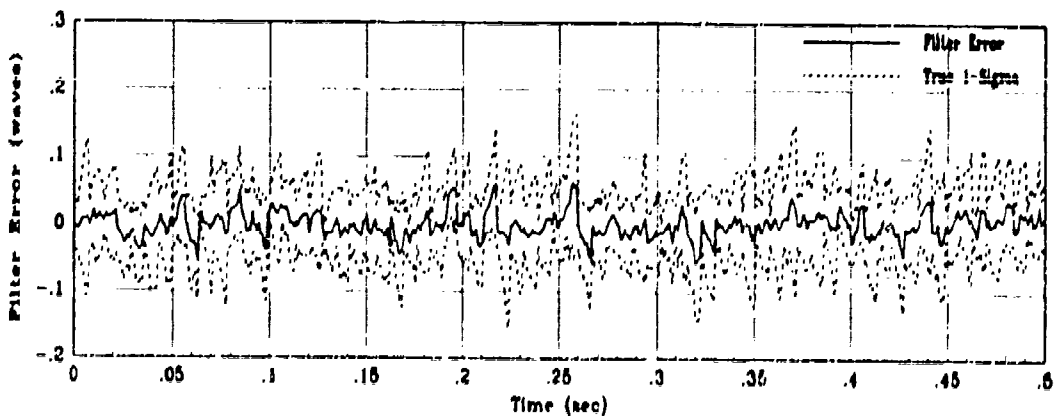
(c) X6 True Filter Error for 10 MC runs

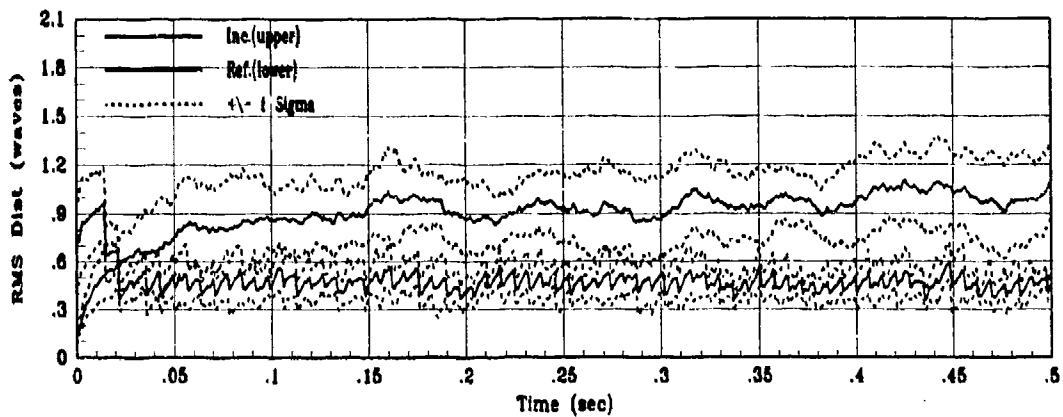Figure G.17. State 6 Filter Estimation Error with Correlated States
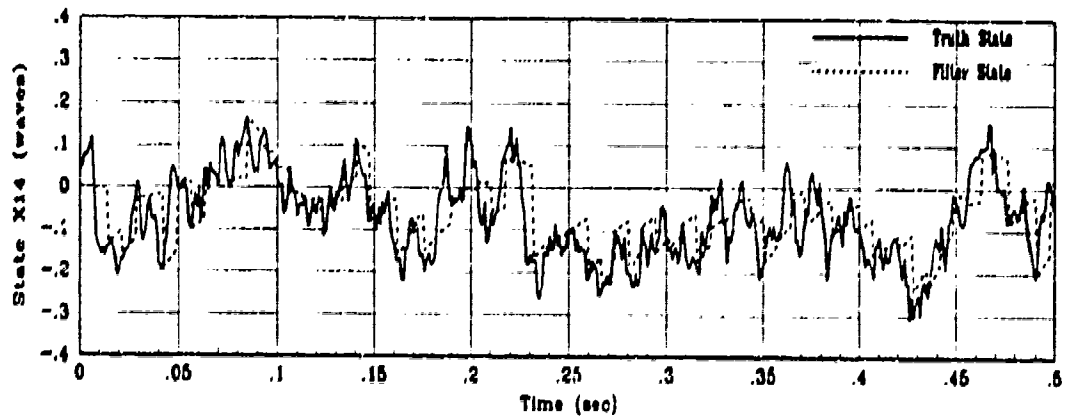
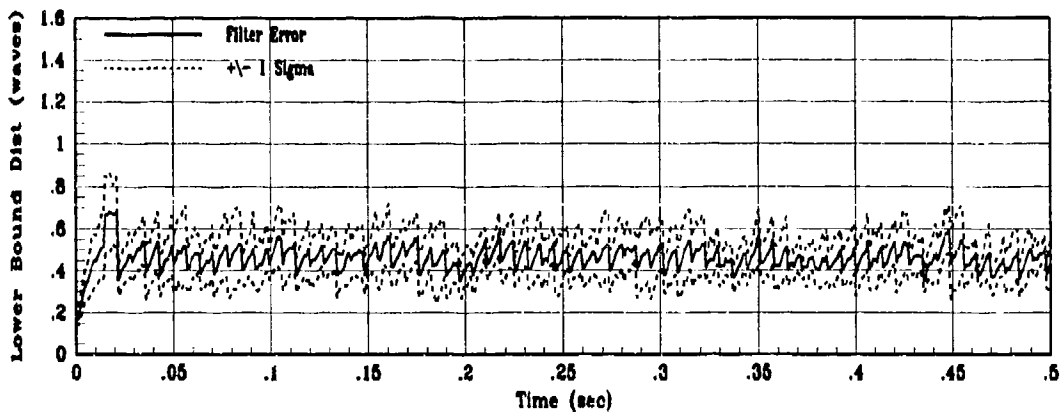(a) Truth and Filter States: XS14, XF14
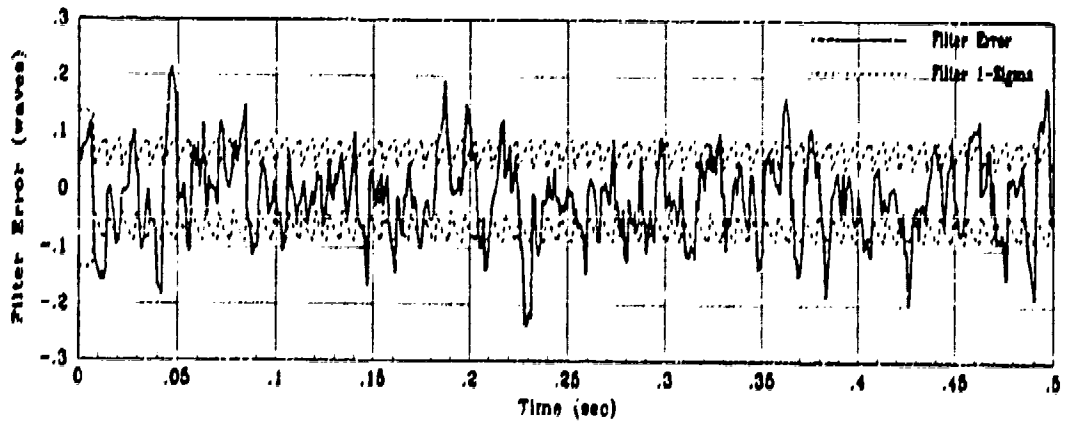
(b) X14 Filter Error for 1 MC Run
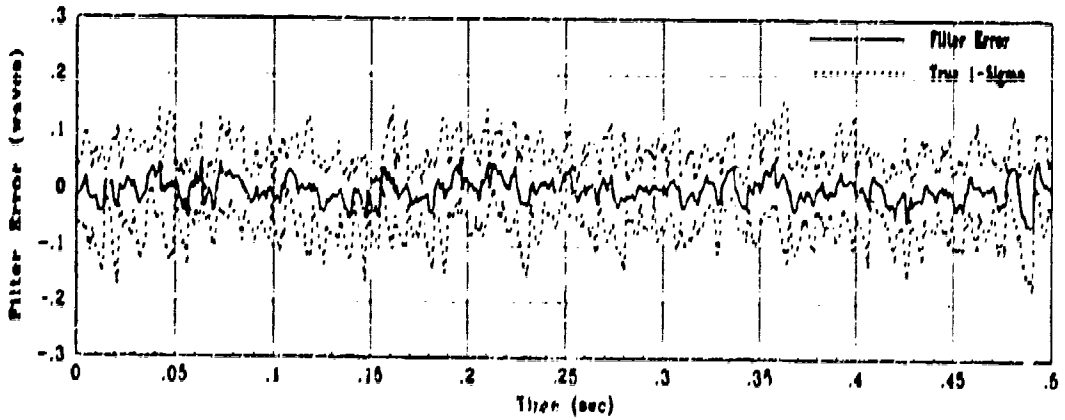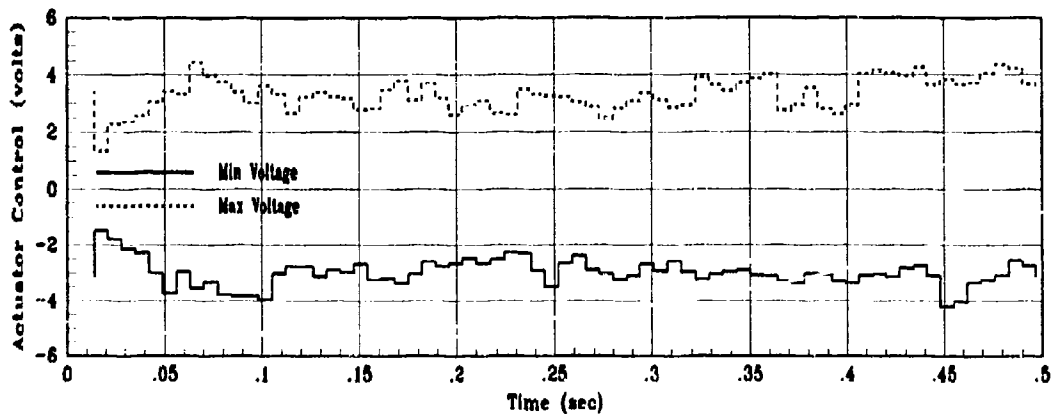
(c) X14 True Filter Error for 10 MC runs

Figure G.18. State 14 Filter Estimation Error with Correlated States
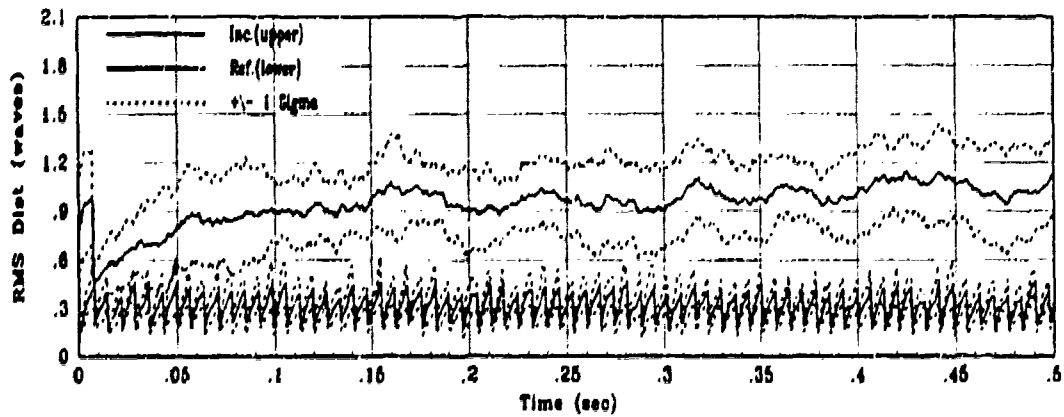
(a) Incident and Reflected RMS Phase Distortion for 10 MC Runs
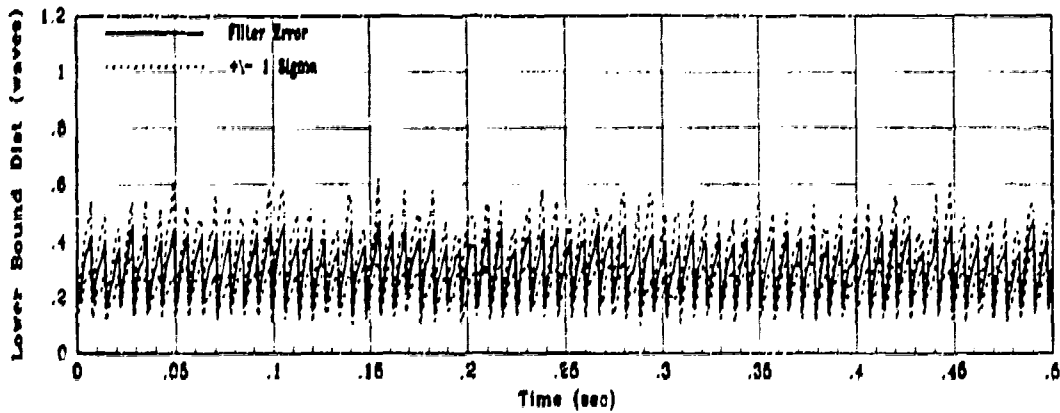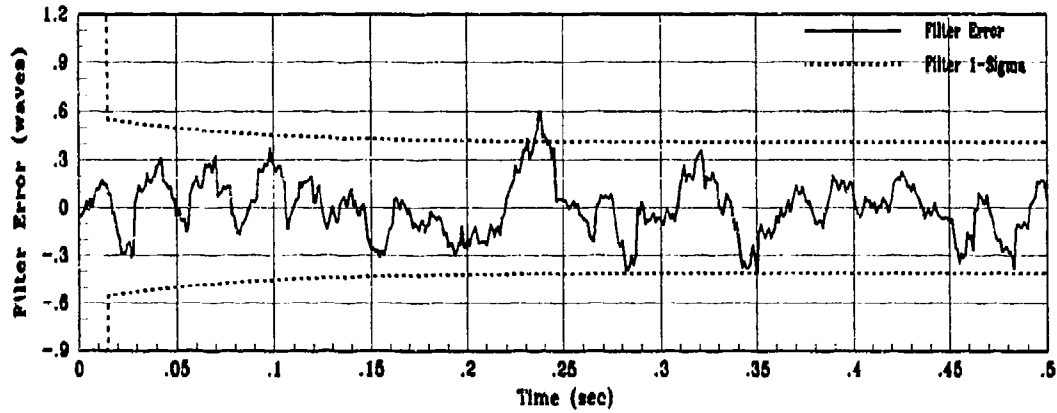

(b) RMS Filter Error for 10 MC Runs
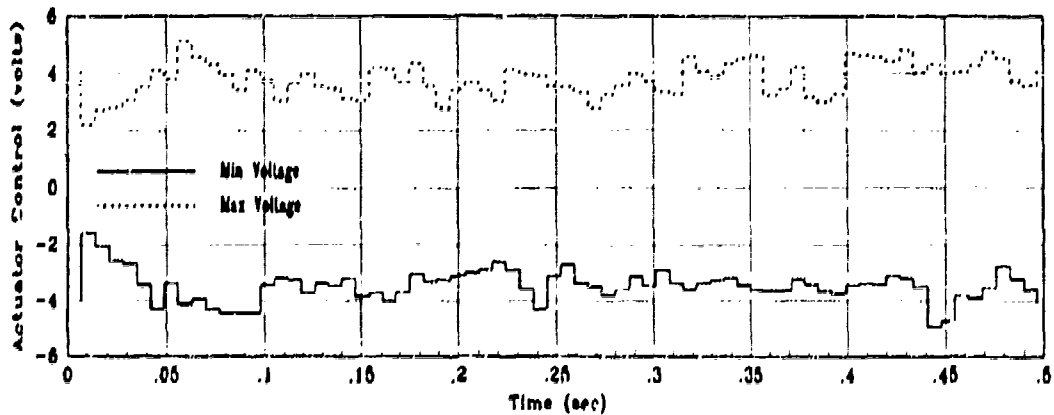
(c) Actuator Control Voltage Envelope

Figure G.19. Control System Performance with Correlated States

Appendix H.   Performance Plots for Study 1 with Delayed Measurements

This appendix contains the plots which describe the modified baseline control system performance in the presence of time-delayed measurements. The time delay in the measurements is 7 msecs, one full sample period, corresponding to the maximum sampling rate of the reticon detector in the wavefront sensor. This simulation was conducted for the measurement noise condition of low noise in both the truth and filter models using time-varying Kalman filter gains. Plots showing filter estimation performance and overall control system performance are presented as described in the previous appendices. The analysis in Section 5.4 discusses the important characteristics associated with these plots.
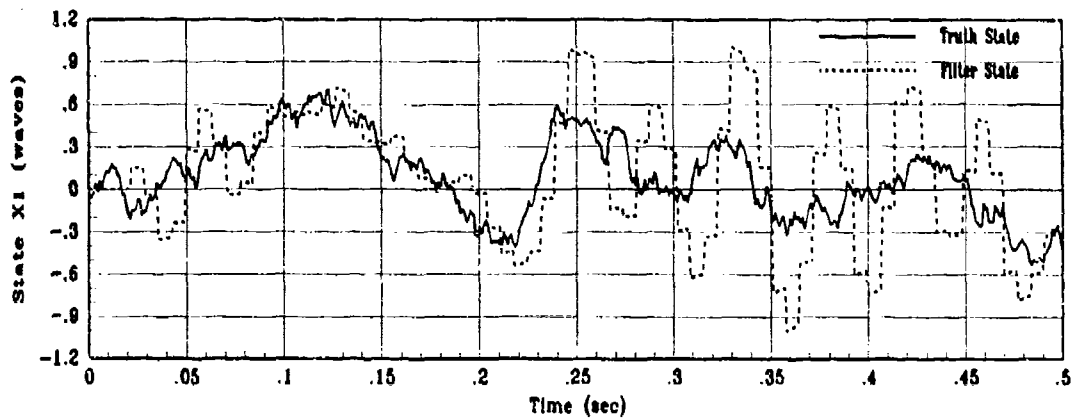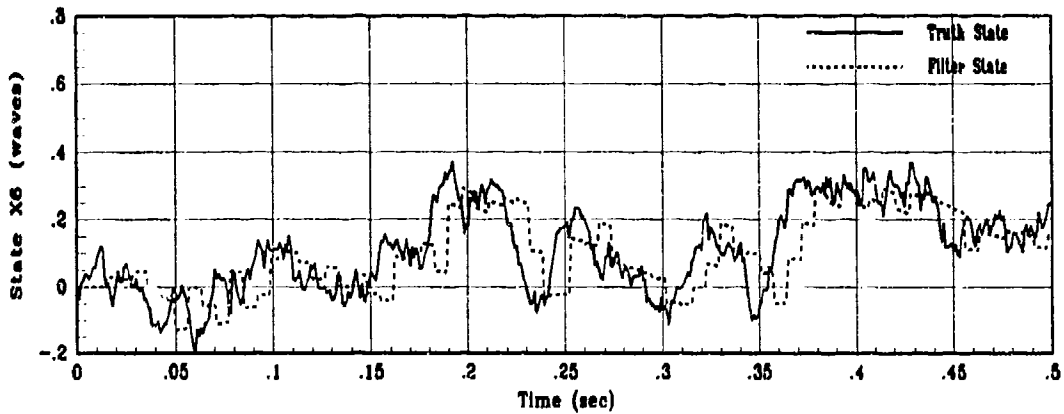
(a) Truth and Filter States: XS1, XF1
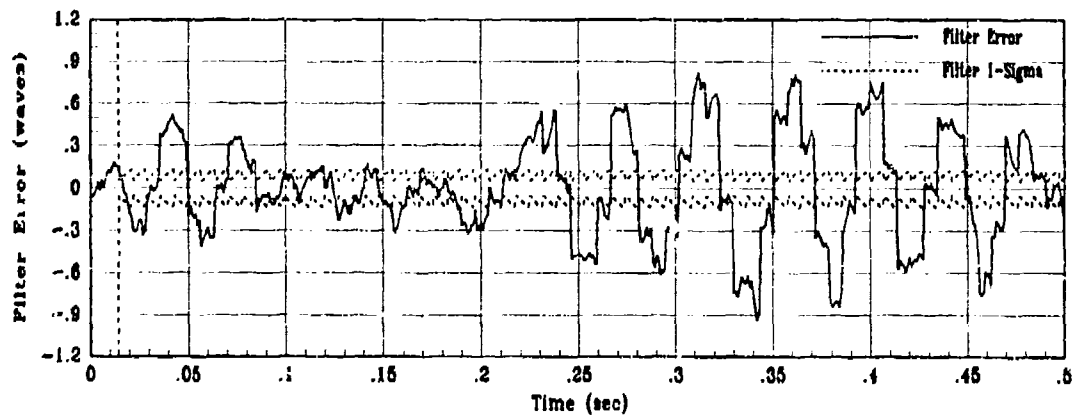
(b) X1 Filter Error for 1 MC Run
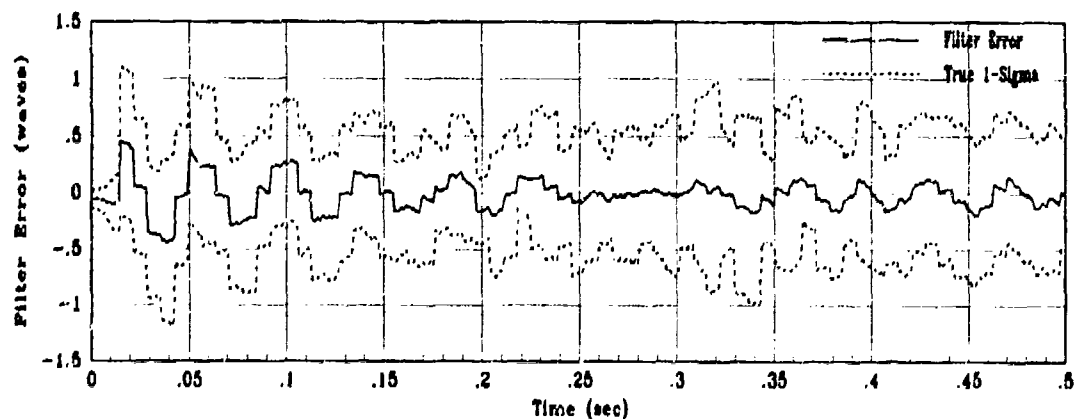
(c) X1 True Filter Error for 10 MC Runs

Figure H.1. State 1 Filter Estimation Error Using Delayed Measurements
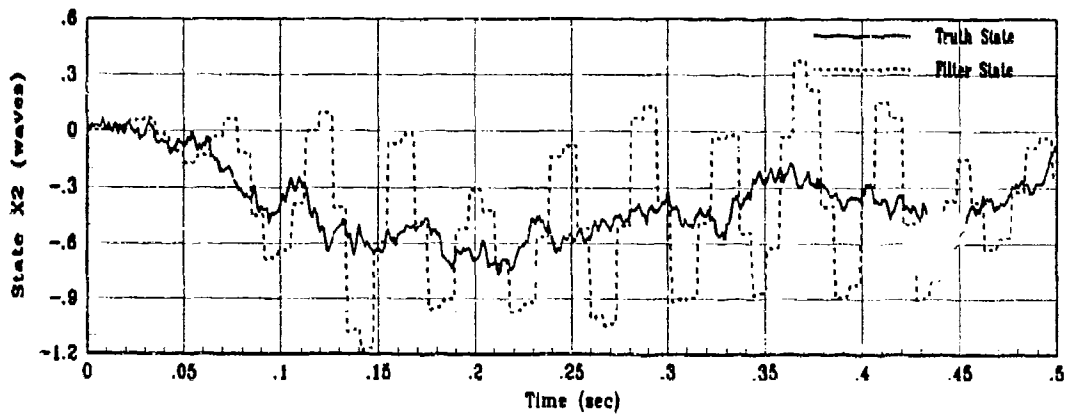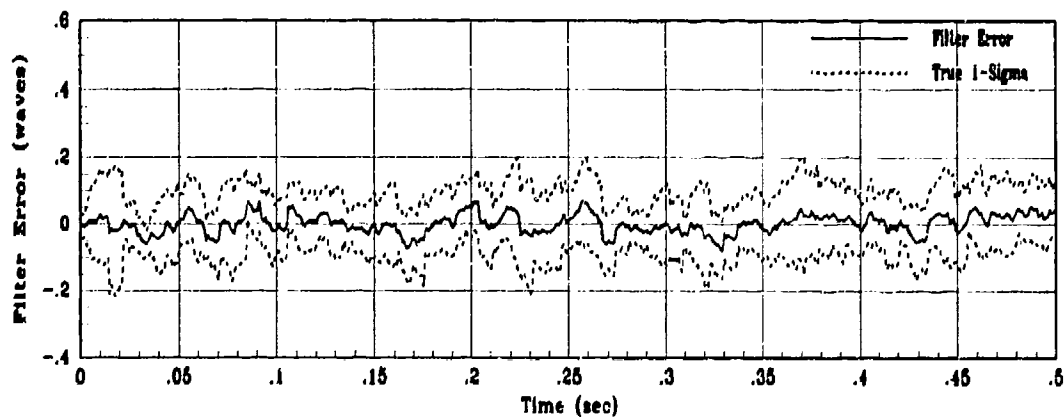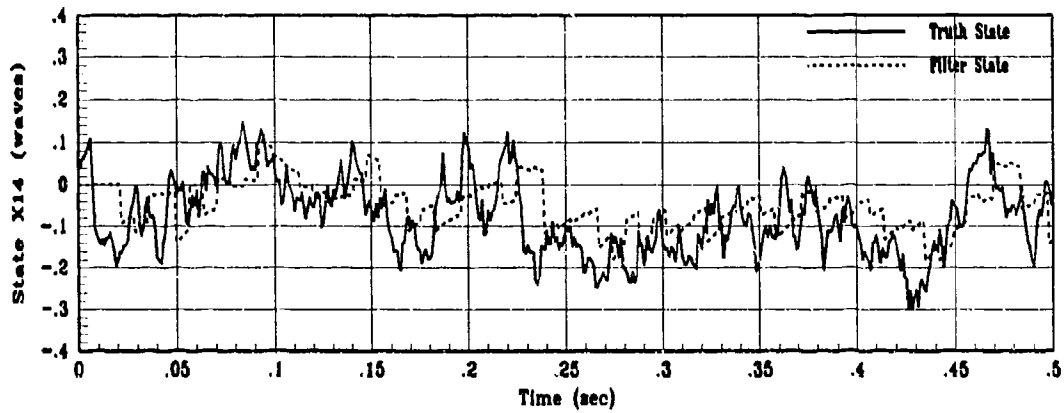
H-2

(a) Truth and Filter States: XS2, XF2
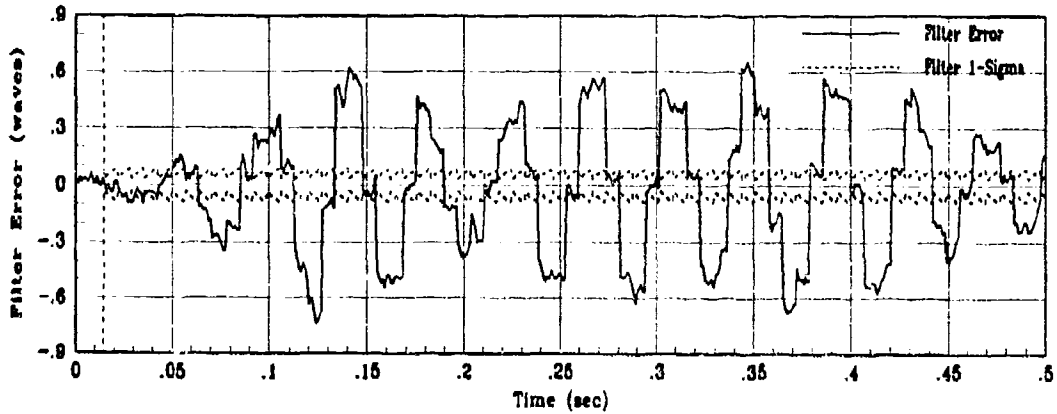
(b) X2 Filter Error for 1 MC Run
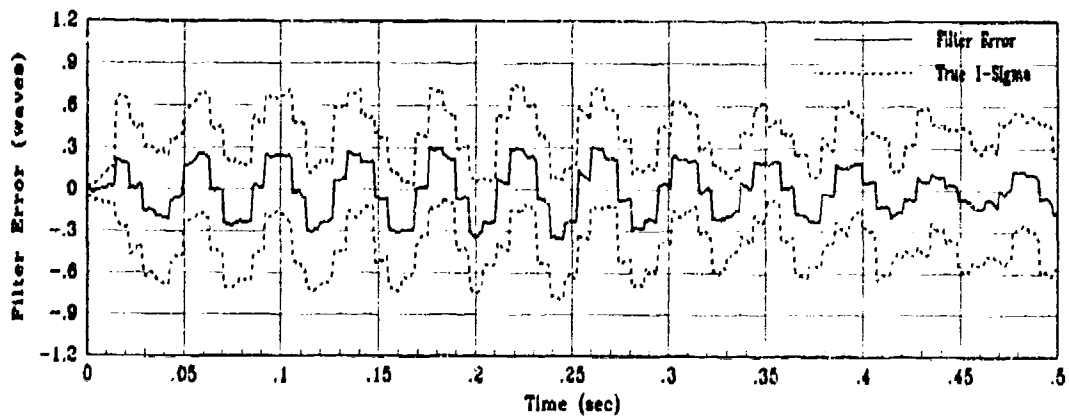
(c) X2 True Filter Error for 10 MC runs

Figure H.2. State 2 Filter Estimation Error Using Delayed Measurements
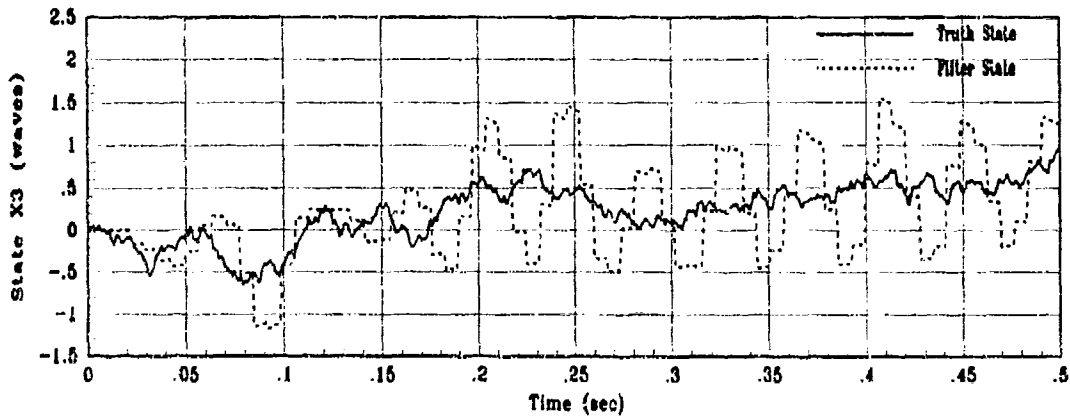
(a) Truth and Filter States: XS3, XF3
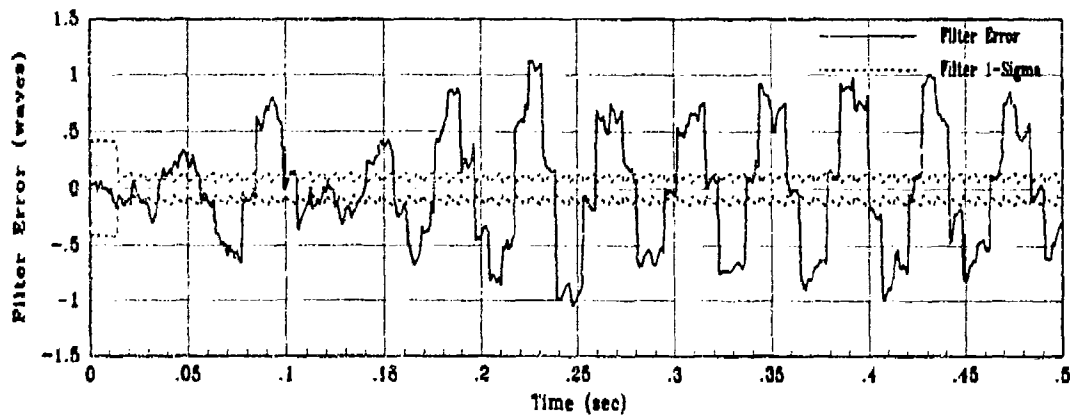
(b) X3 Filter Error for 1 MC Run
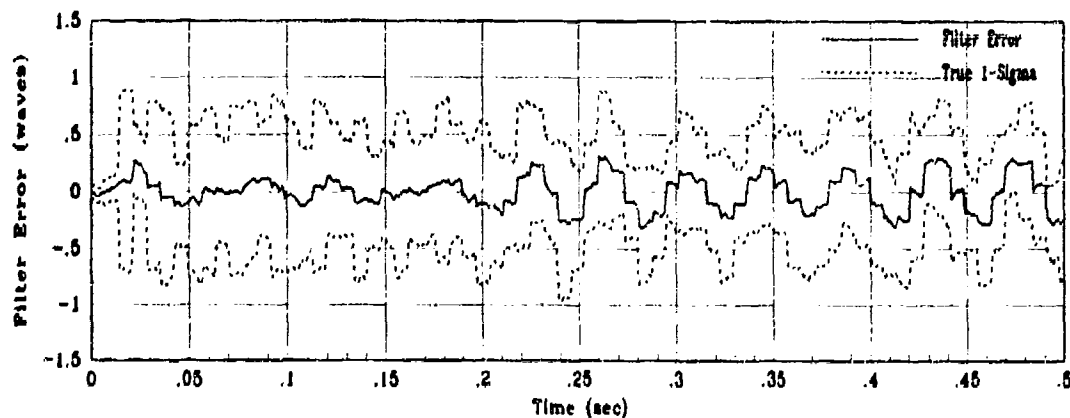
(c) X3 True Filter Error for 10 MC runs

Figure H.3. State 3 Filter Estimation Error Using Delayed Measurements
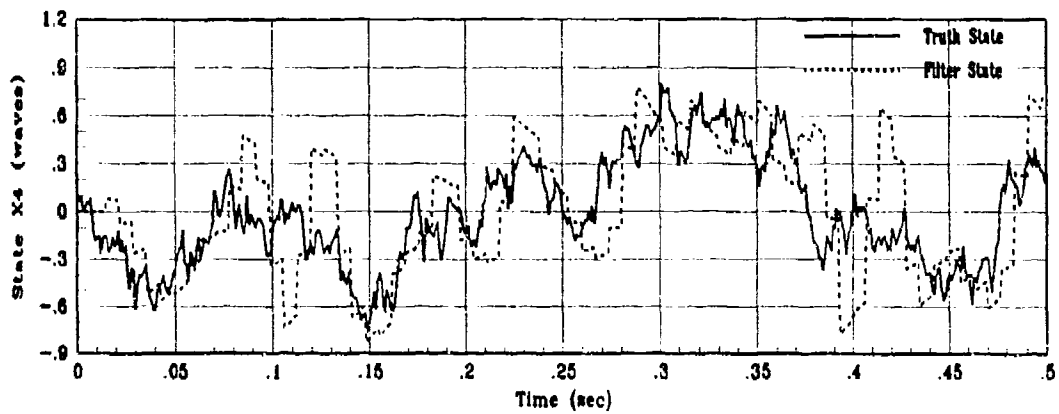
H-4

(a) Truth and Filter States: XS4, XF4
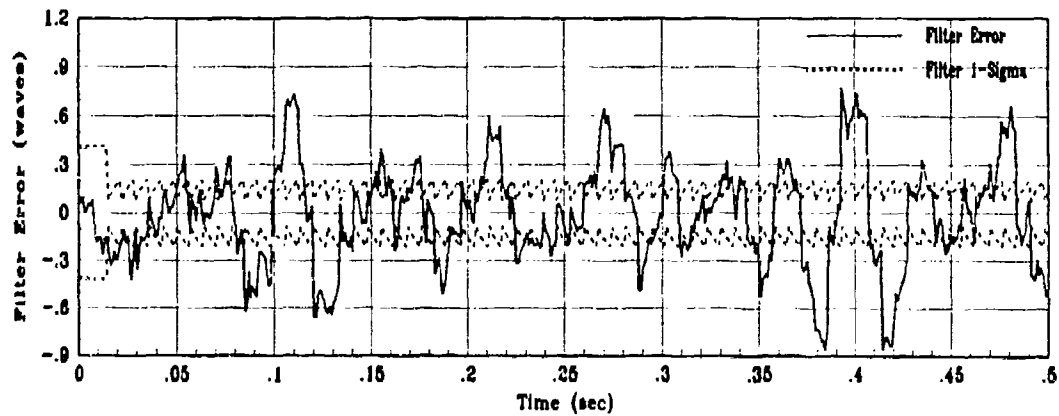
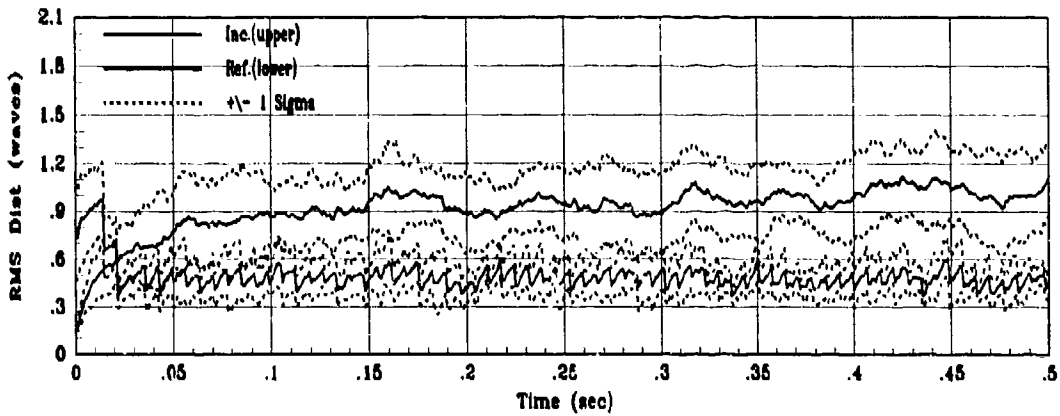(b) X4 Filter Error for 1 MC Run
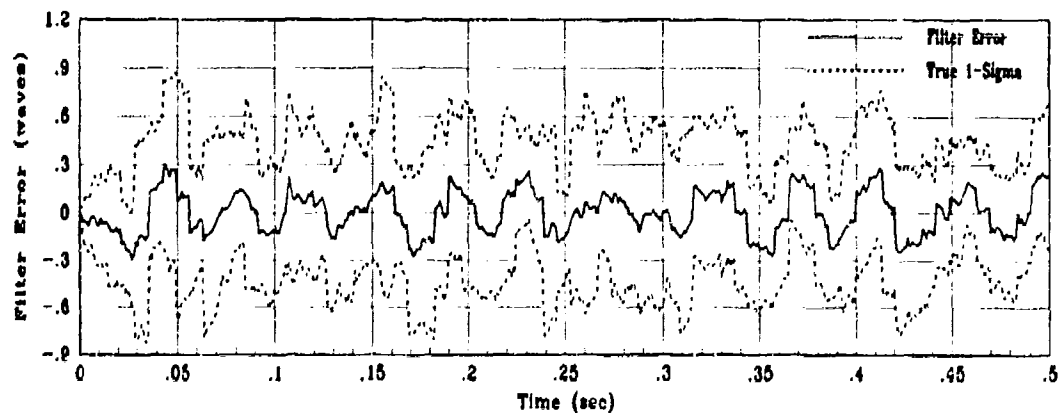
(c) X4 True Filter Error for 10 MC runs

Figure H.4. State 4 Filter Estimation Error Using Delayed Measurements
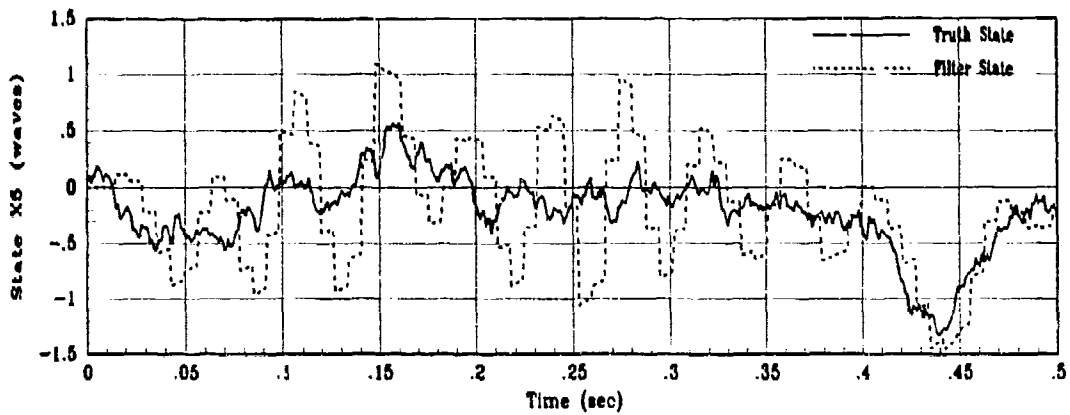
(a) Truth and Filter States: XS5, XF5
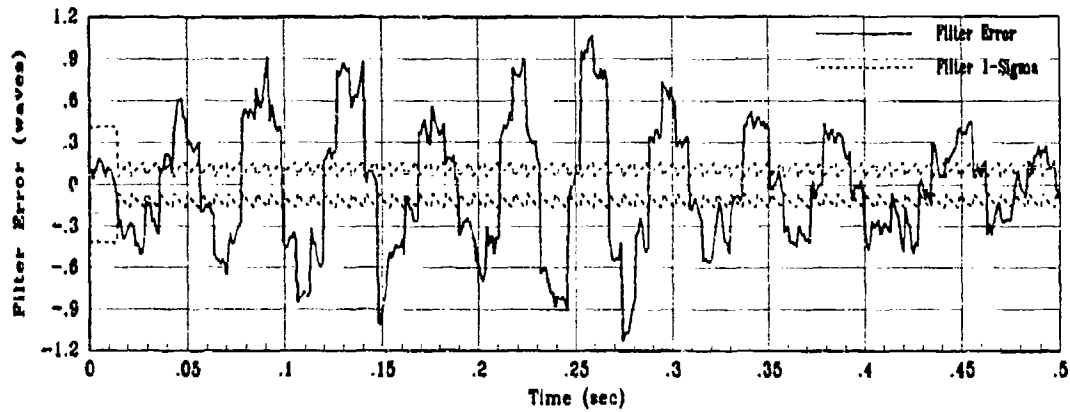
(b) X5 Filter Error for 1 MC Run
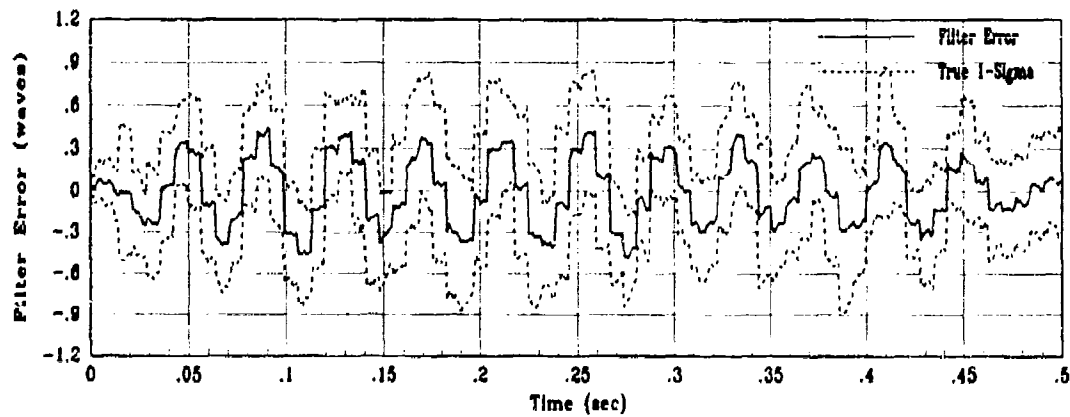
(c) X5 True Filter Error for 10 MC runs

Figure H.5. State 5 Filter Estimation Error Using Delayed Measurements
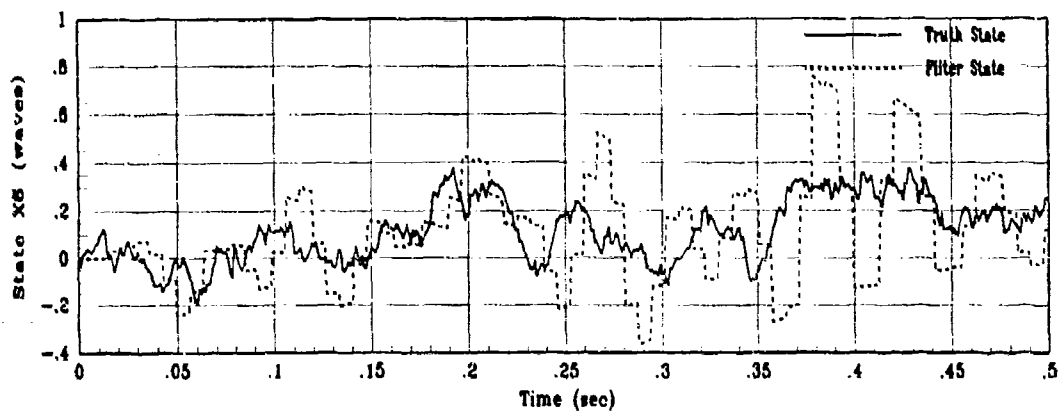
(a) Truth and Filter States: XS6, XF6
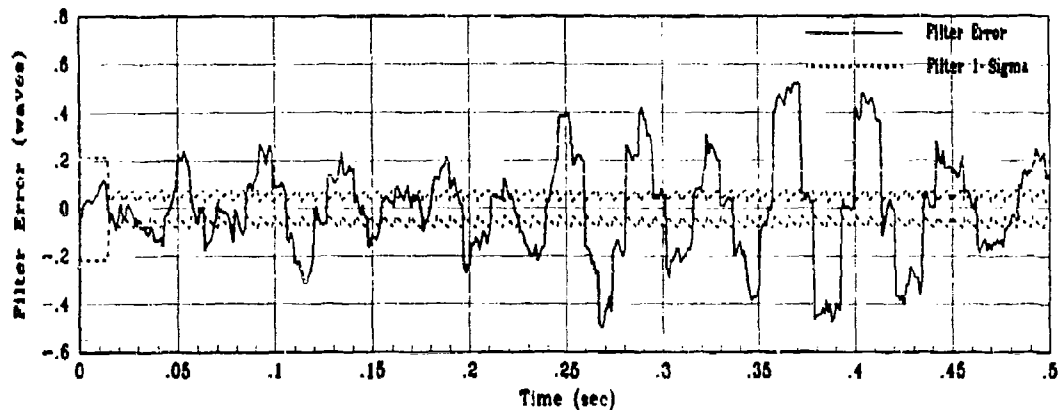
(b) X6 Filter Error for 1 MC Run
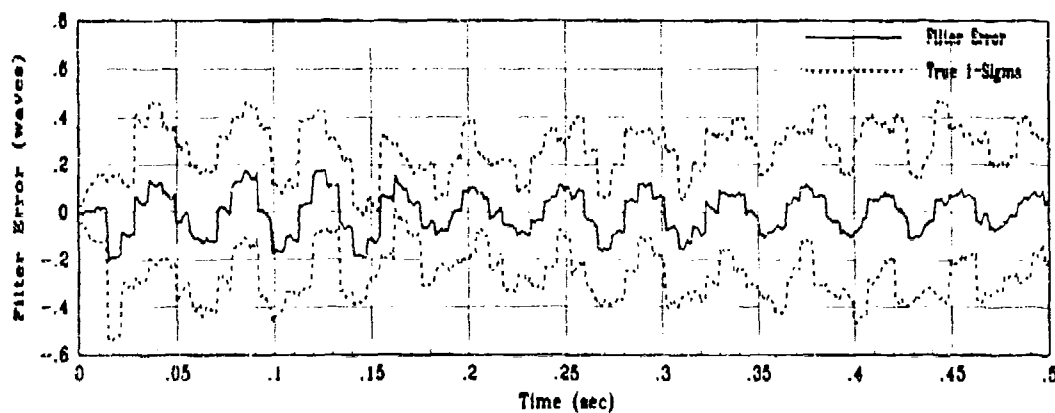
(c) X6 True Filter Error for 10 MC runs

Figure H.6. State 6 Filter Estimation Error Using Delayed Measurements
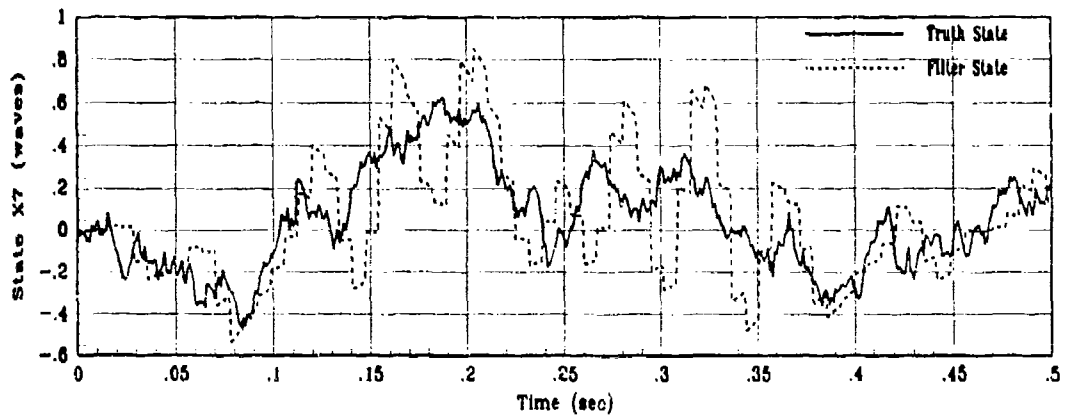
(a) Truth and Filter States: XS7, XF7
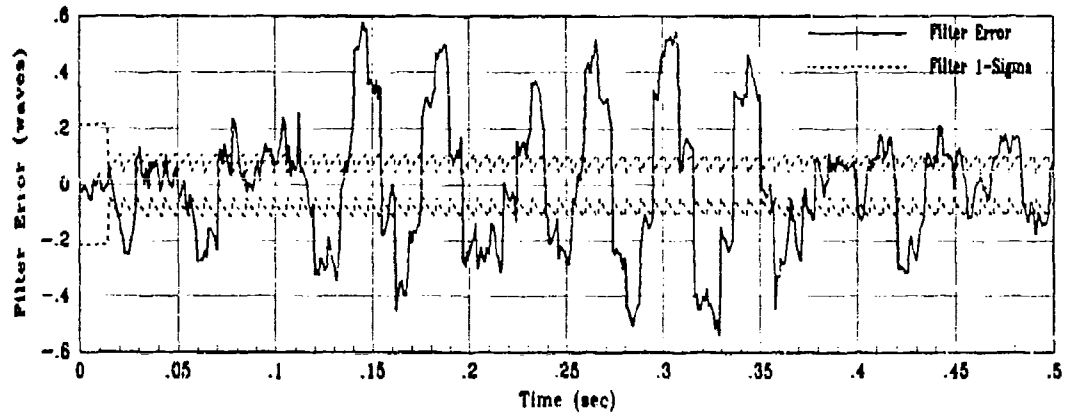
(b) X7 Filter Error for 1 MC Run
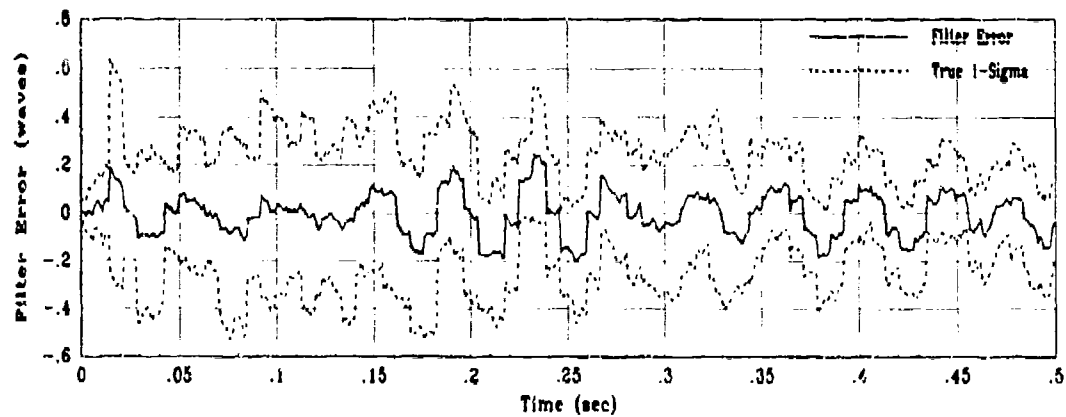
(c) X7 True Filter Error for 10 MC runs

Figure H.7. State 7 Filter Estimation Error Using Delayed Measurements
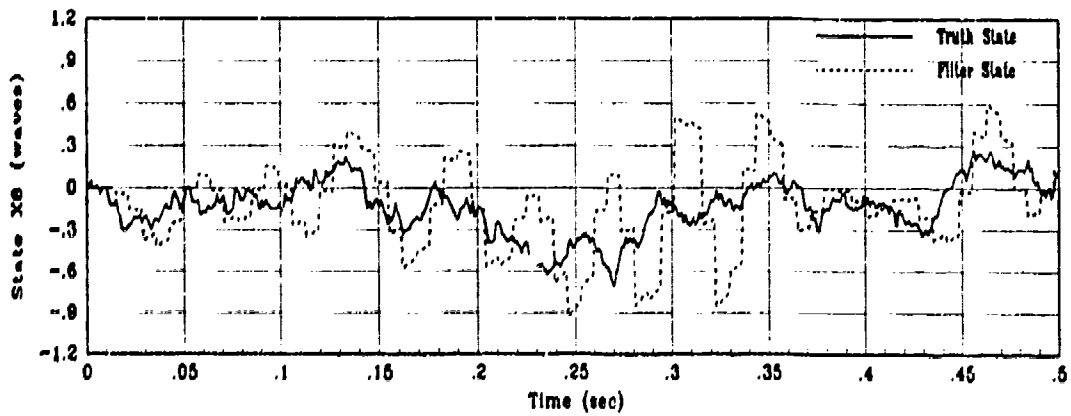
(a) Truth and Filter States: XS8, XF8
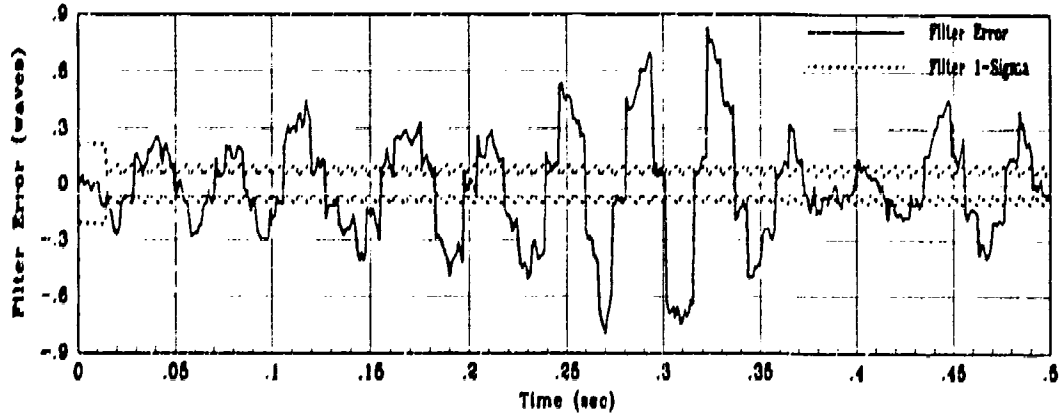
(b) X8 Filter Error for 1 MC Run
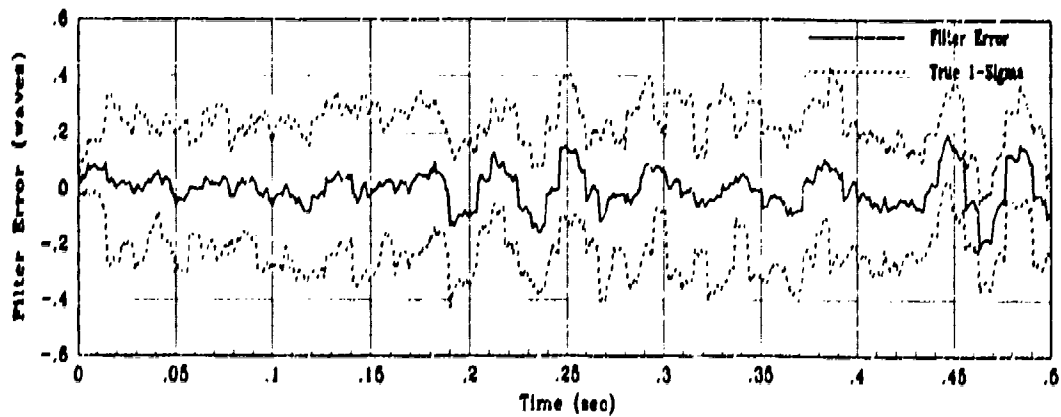
(c) X8 True Filter Error for 10 MC runs

Figure II.8. State 8 Filter Estimation Error Using Delayed Measurements
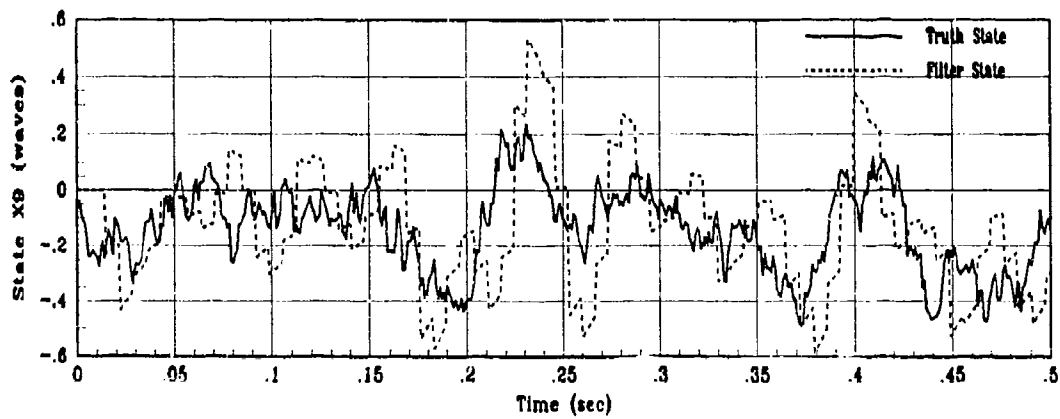
(a) Truth and Filter States: XS9, XF9
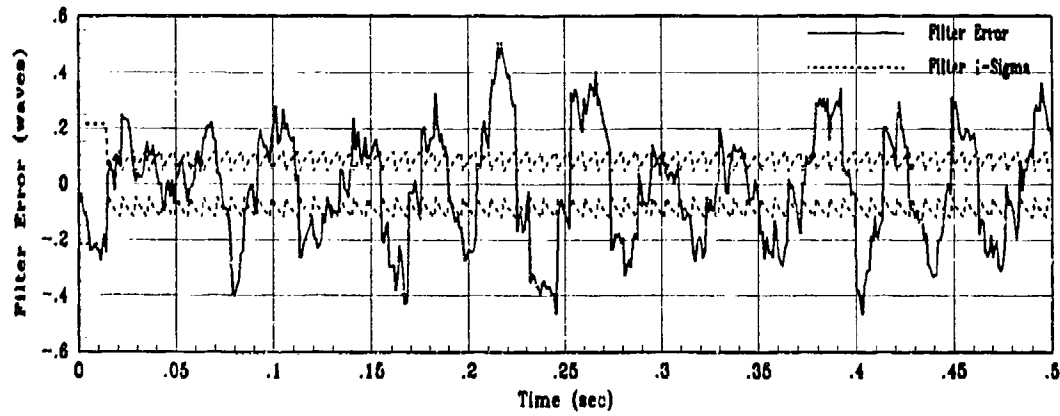
(b) X9 Filter Error for 1 MC Run
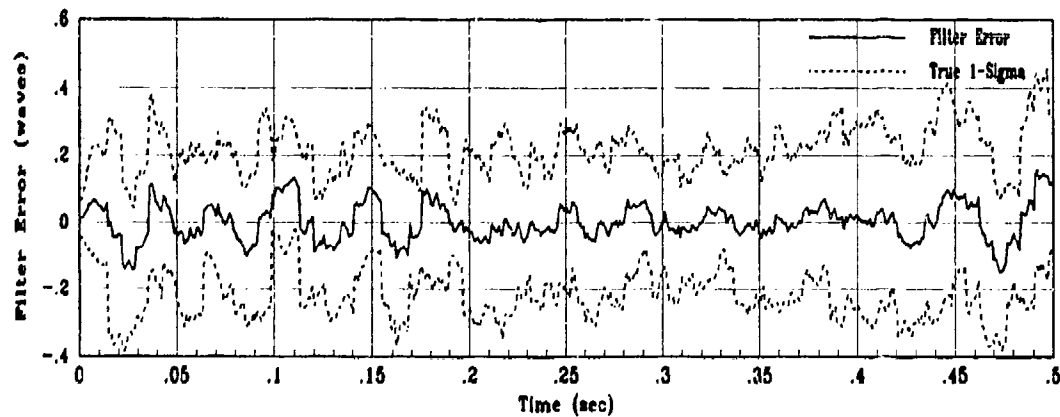
(c) X9 True Filter Error for 10 MC runs

Figure H.9. State 9 Filter Estimation Error Using Delayed Measurements
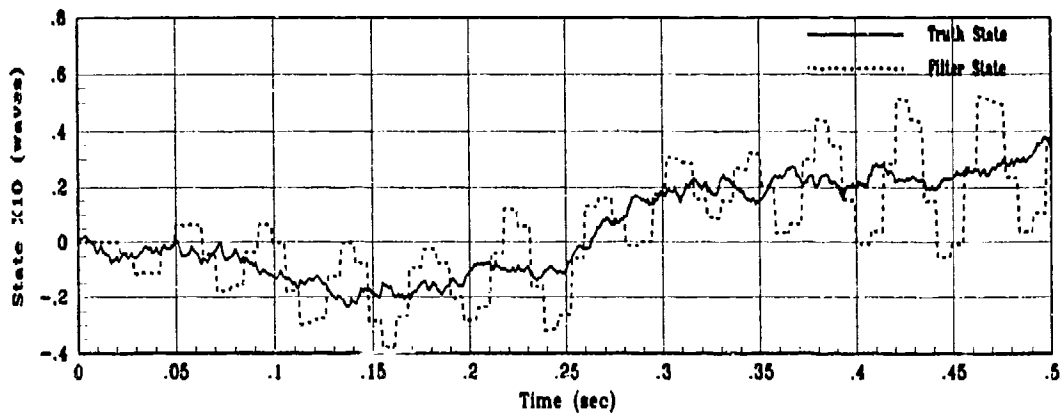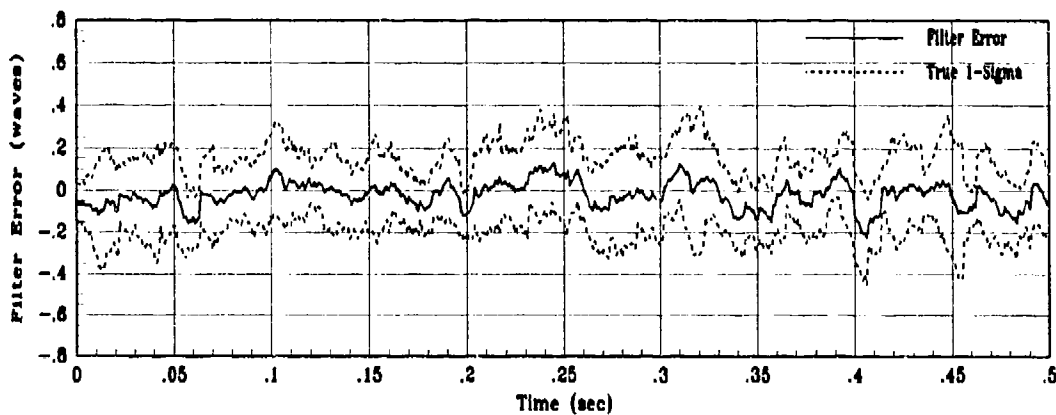
(a) Truth and Filter States: XS10, XF10
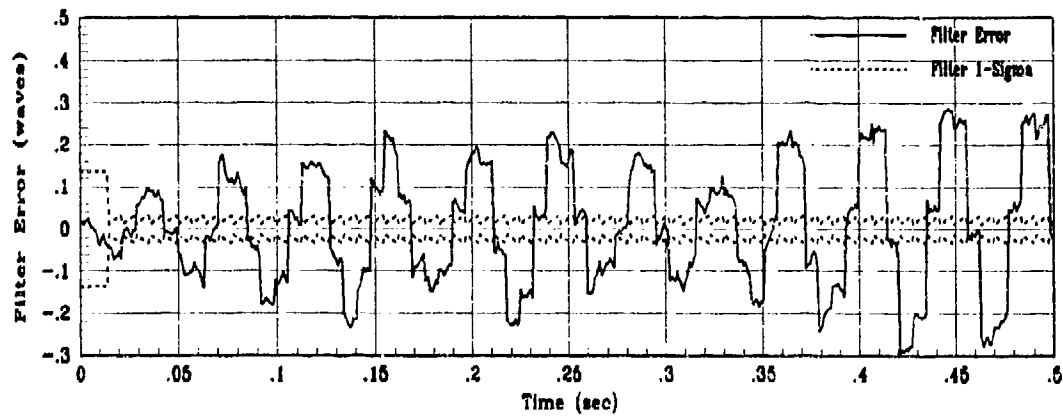
(b) X10 Filter Error for 1 MC Run
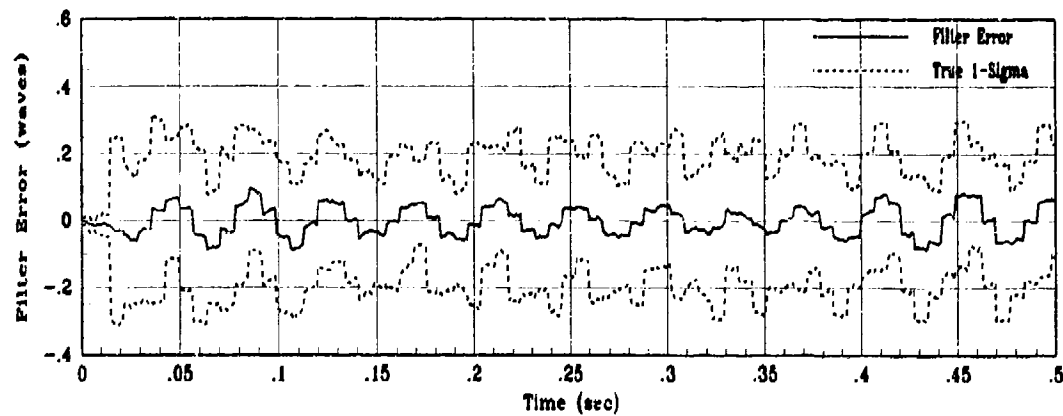
(c) X10 True Filter Error for 10 MC runs

Figure H.10. State 10 Filter Estimation Error Using Delayed Measurements
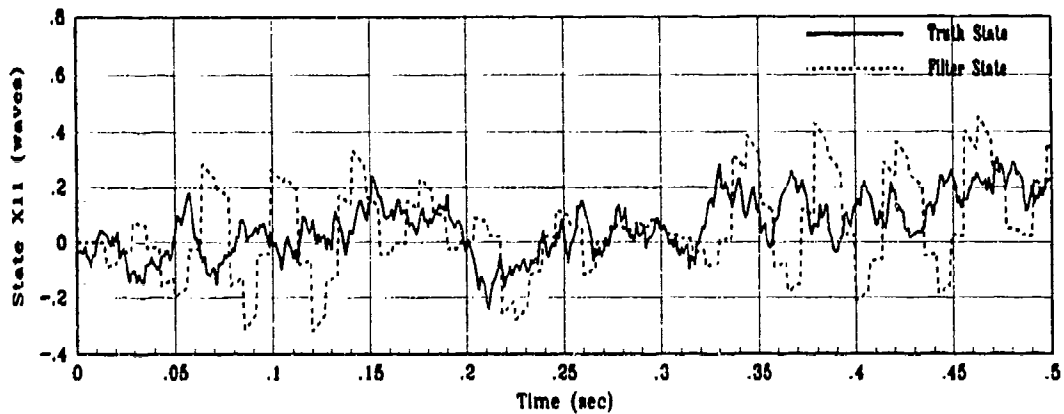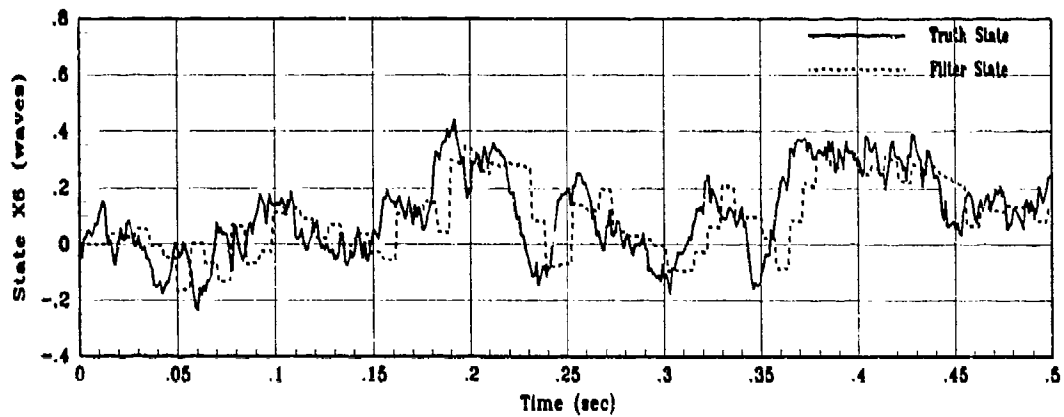
(a) Truth and Filter States: XS11, XF11
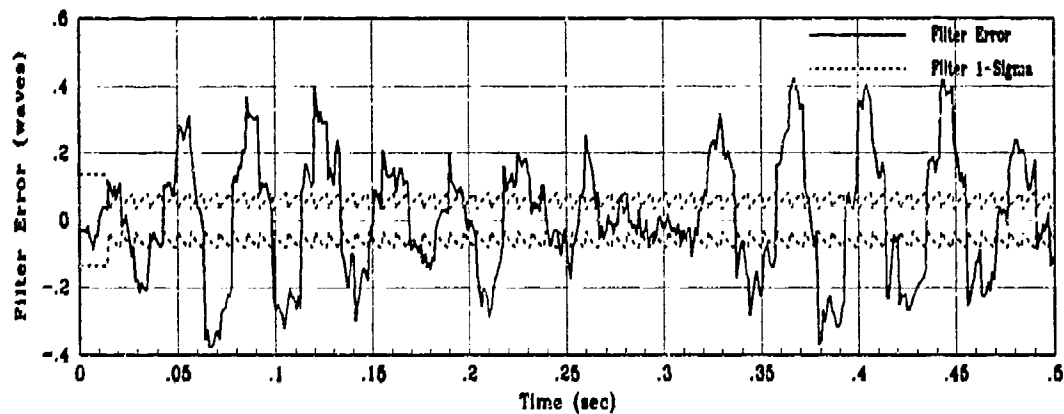
(b) X11 Filter Error for 1 MC Run
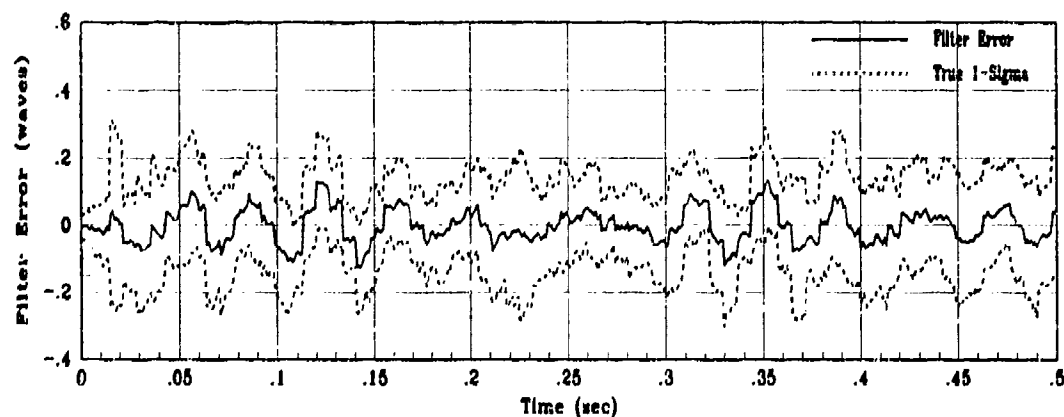
(c) X11 True Filter Error for 10 MC runs

Figure II.11. State 11 Filter Estimation Error Using Delayed Measurements
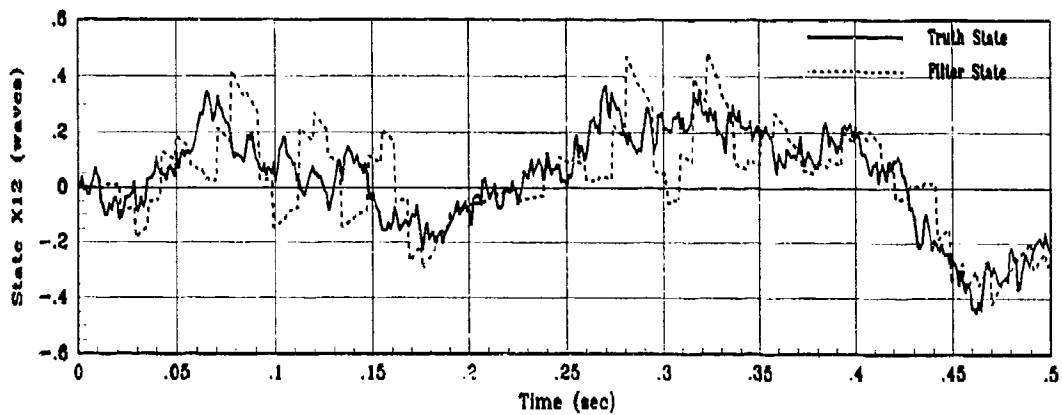
(a) Truth and Filter States: XS12, XF12
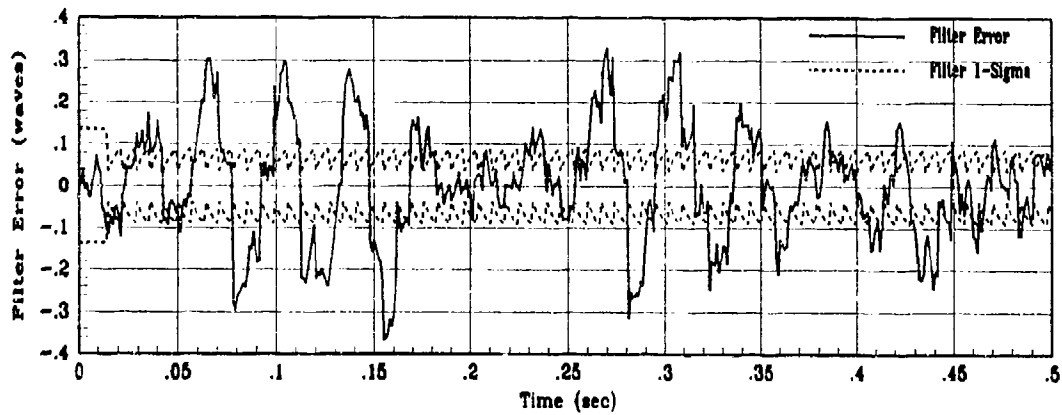
(b) X12 Filter Error for 1 MC Run
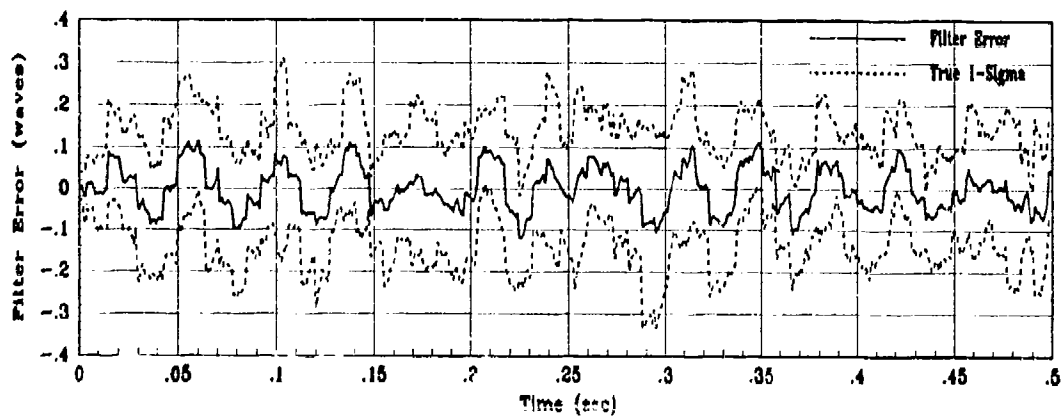
(c) X12 True · · Error for 10 MC runs

Figure H.12. State 12 Filter Estimation Error Using Delayed Measurements
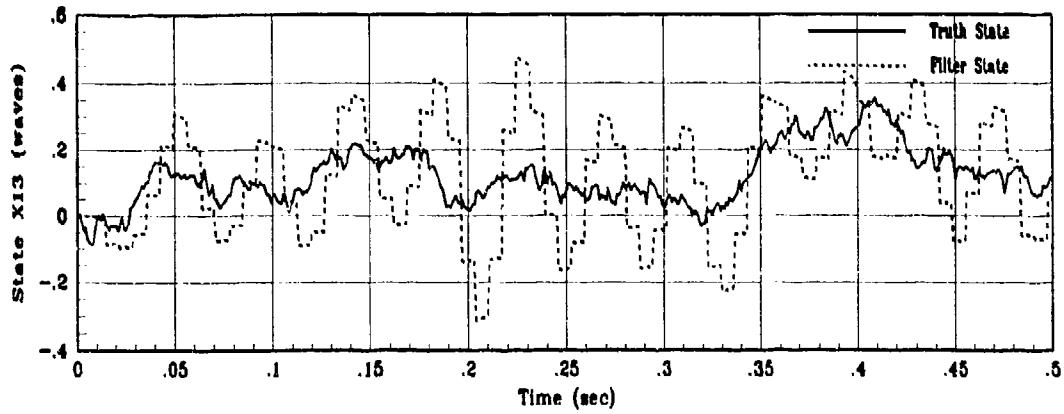
H-13

(a) Truth and Filter States: XS13, XF13
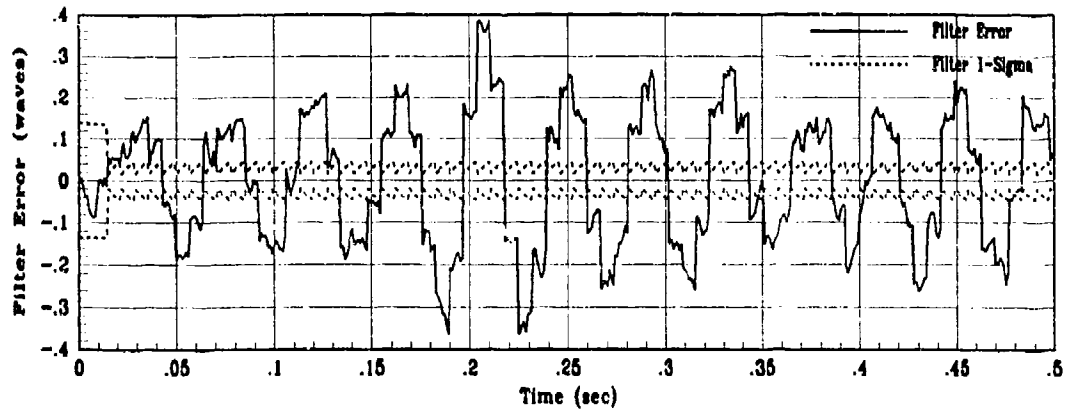
(b) Xi3 Filter Error for 1 MC Run

(c) X13 True Filter Error for 10 MC runs

Figure H.13. State 13 Filter Estimation Error Using Delayed Measurements
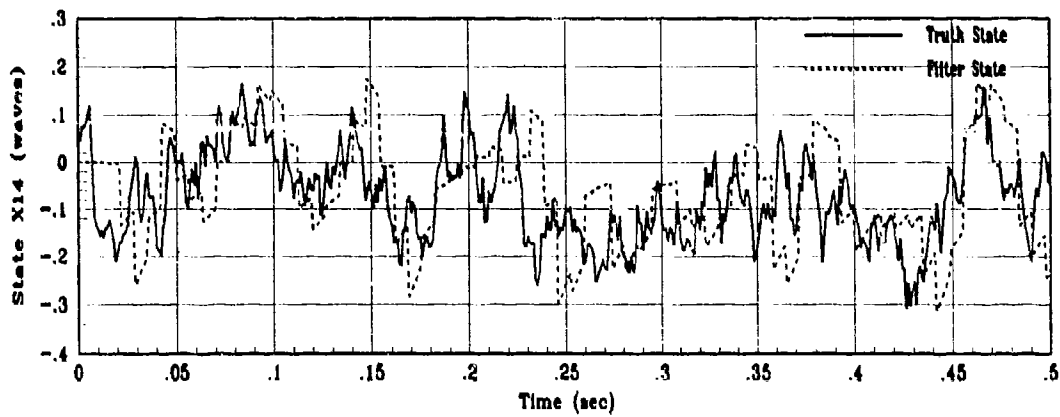
H-14

(a) Truth and Filter States: XS14, XF14
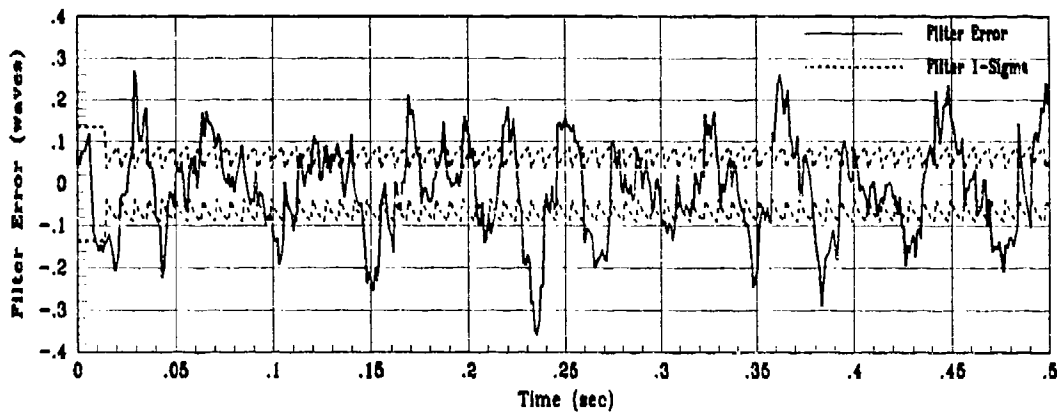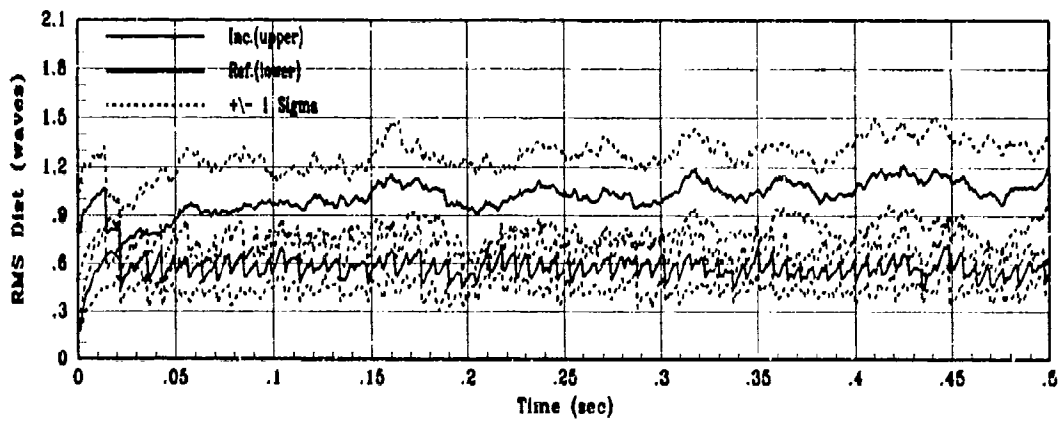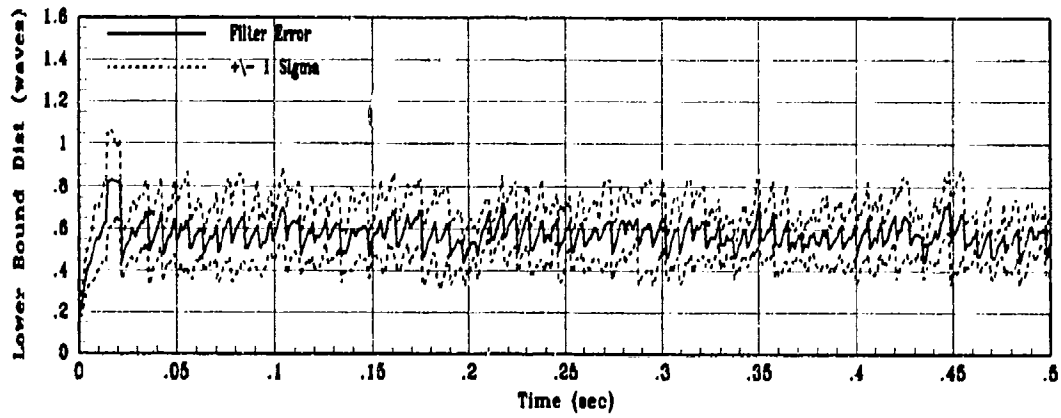

(b) X14 Filter Error for 1 MC Run
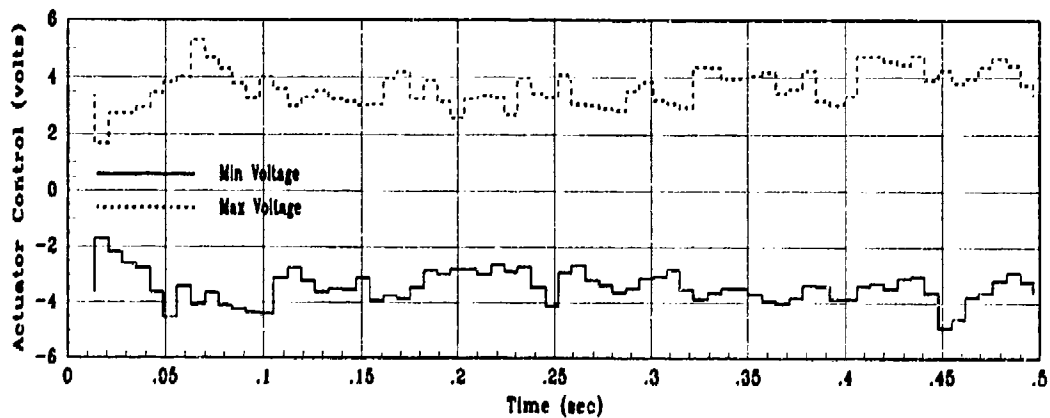

(c) X14 True Filter Error for 10 MC runs

Figure H.14. State 14 Filter Estimation Error Using Delayed Measurements
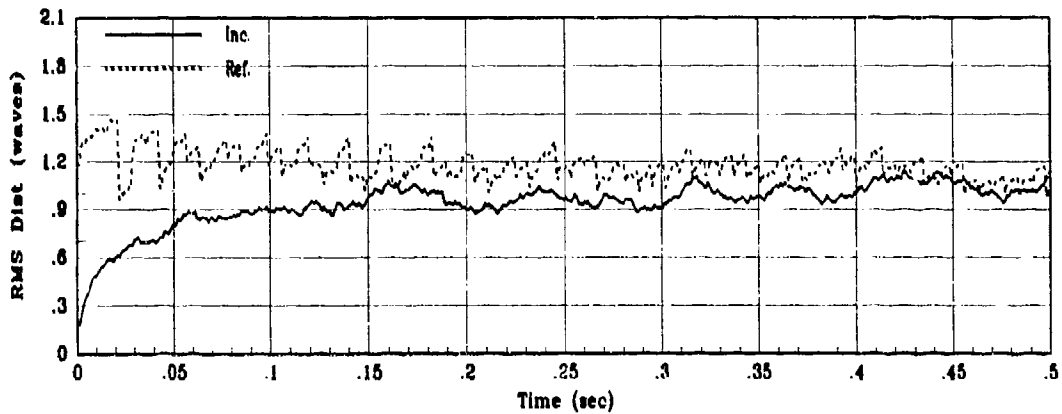
(a) Incident and Reflected RMS Phase Distortion for 10 MC Runs
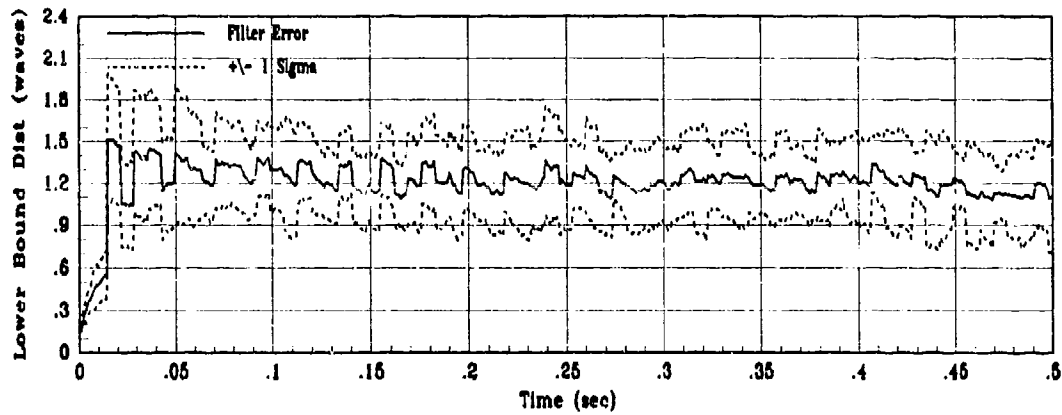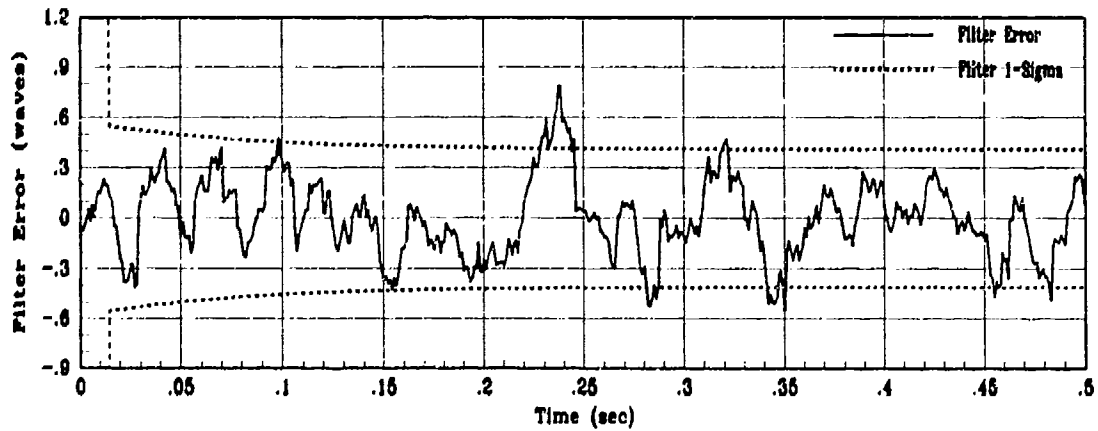

(b) RMS Filter Error for 10 MC Runs
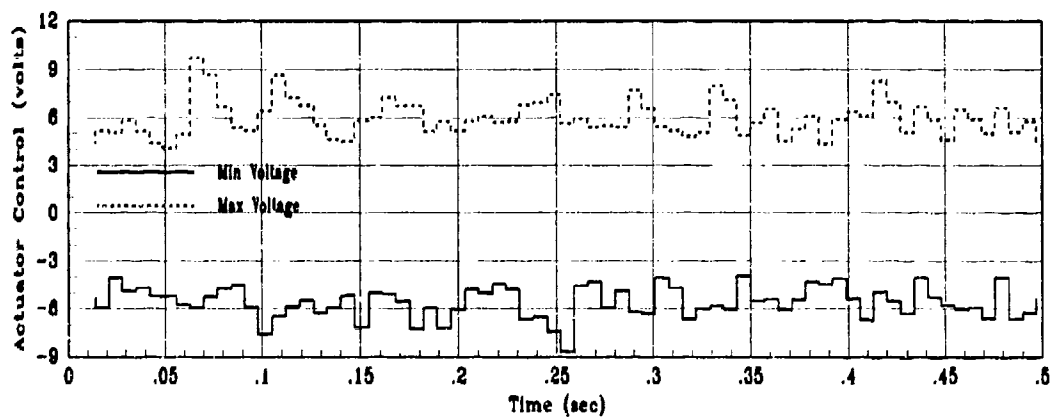
(c) Actuator Control Voltage Envelope

Figure H.15. Control System Performance Using Delayed Measurements

Appendix I. Performance Plots for Study 1 with Filter-Predictor Controller

The plots in this appendix illustrate the controller performance when the predictor is augmented to the system as compensation for the wavefront sensor measurement processing delay. Plots are presented for all 14 states of the Kalman filter and the overall control system performance in the same manner described for previous appendices. Detailed analysis of the data is presented in Section 5.5.

Section I.1 contains the plots of the filter estimation error and control system performance for the filter-predictor model using the 7 msec wavefront sensor sampling period. Section I.2 show the overall control system performance of the suboptimal controller assuming no measurement delays. Filter estimation performance plots are not provided here as the results are identical to the plots shown in Appendix G. This occurs due to the fact that the filter performs identically for both the optimal and suboptimal control laws; the difference lies in the time at which control is applied to the system (t_i^- vs t_i^+), thereby affecting overall system performance. Lastly, Section I.3 shows performance achievable assuming a wavefront sensor with a 3 msec sampling period were available. Plots of both filter and overall control system performance are provⁱ d.
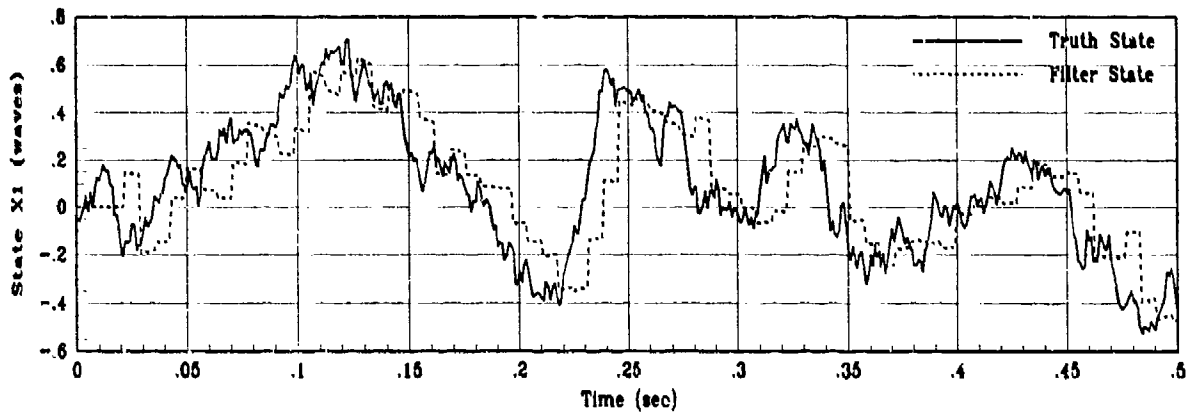
(a) Truth and Filter States: XS1, XF1
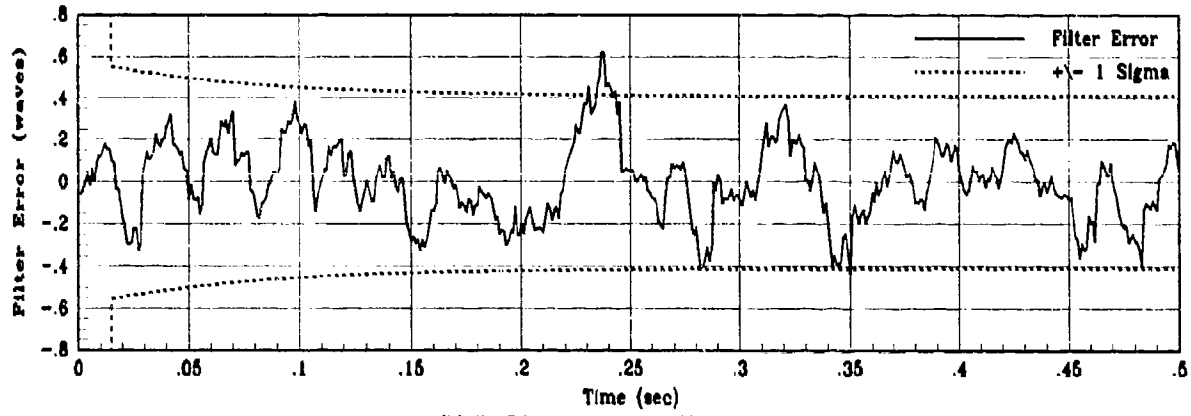
(b) X1 Filter Error for 1 MC Run
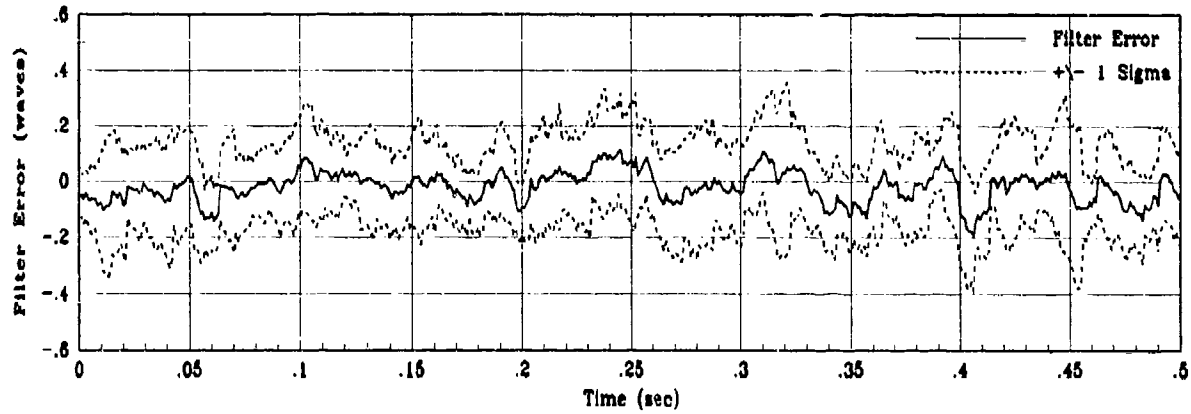
(c) X1 Filter Error for 10 MC Runs

Figure 1.1. State 1 Filter-Predictor Estimation Error
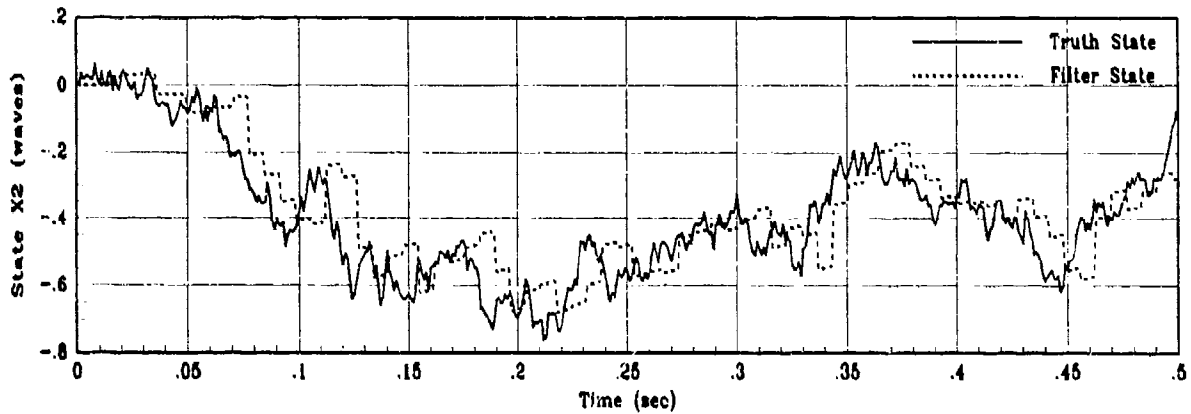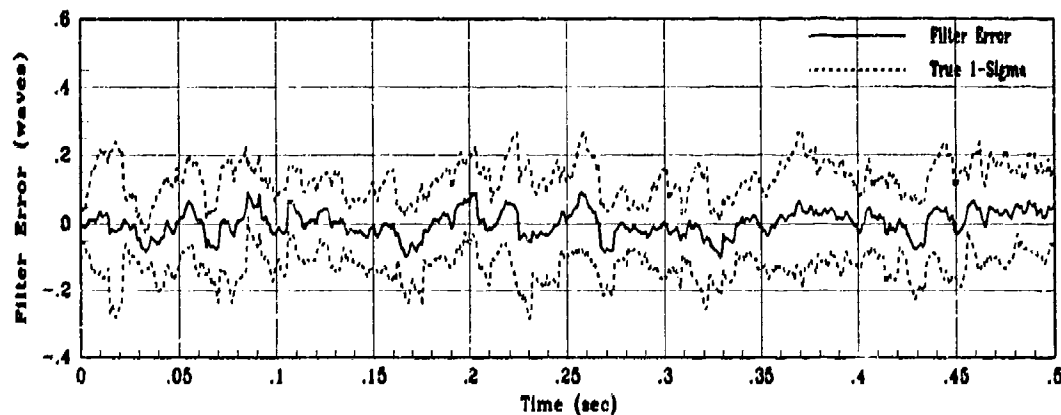
(a) Truth and Filter states: XS2, XF2
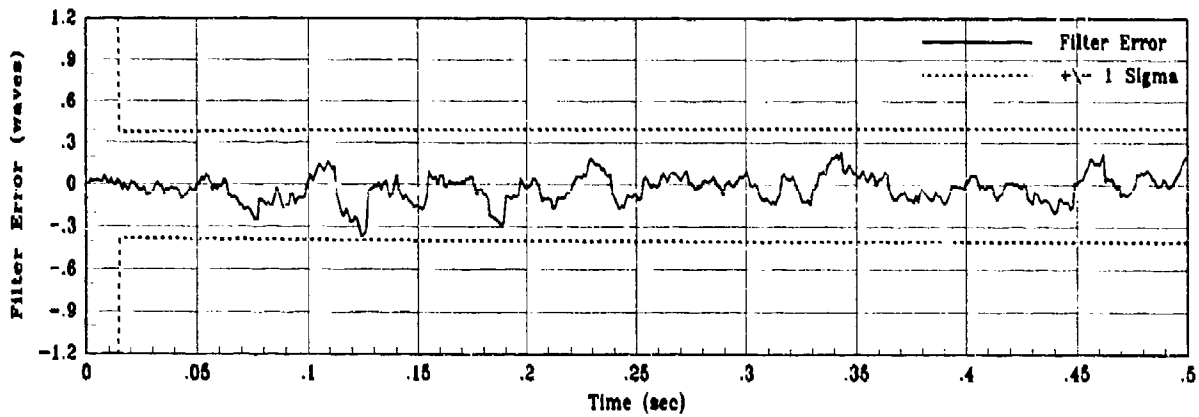
(b) X2 Filter Error for 1 MC Run
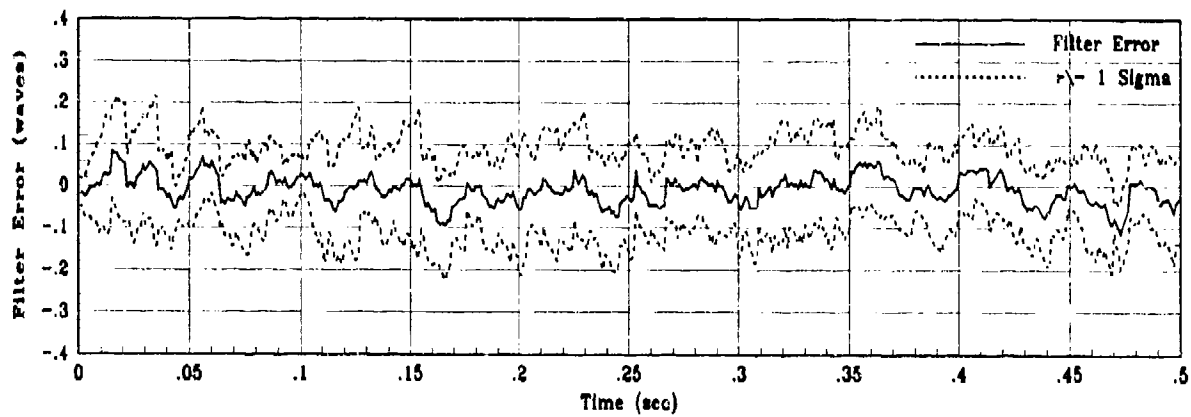
(c) X2 Filter Error for 10 MC runs

Figure I.2. State 2 Filter-Predictor Estimation Error
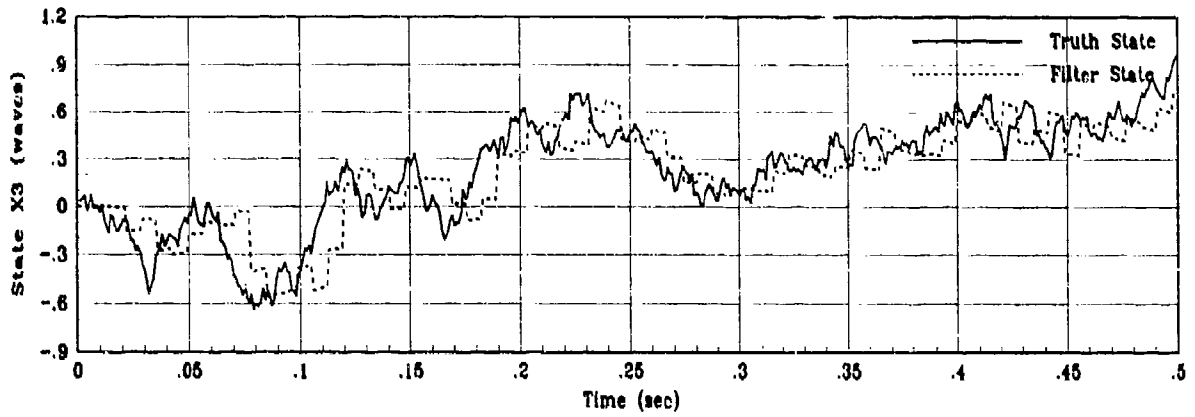
(a) Truth and Filter States: XS3, XF3
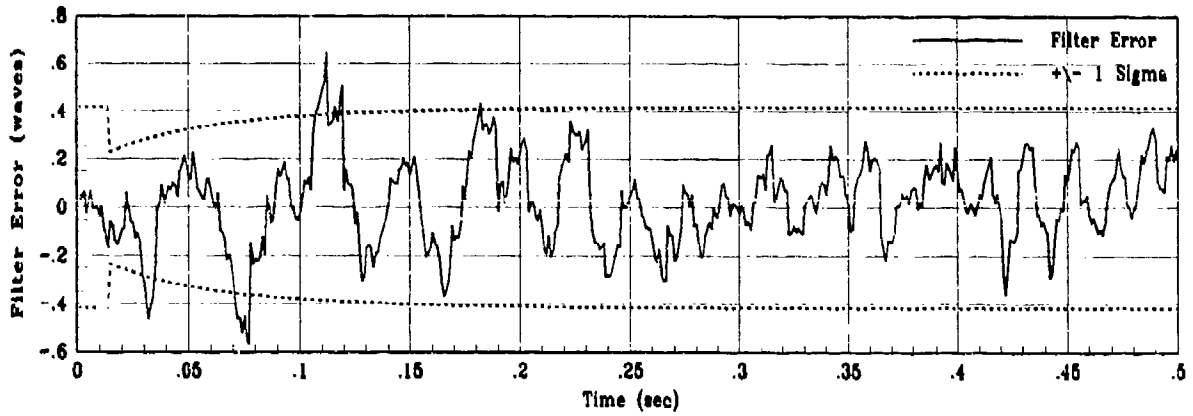
(b) X3 Filter Error for 1 MC Run

(c) X3 Filter Error for 10 MC runs

Figure 1.3. State 3 Filter-Predictor Estimation Error
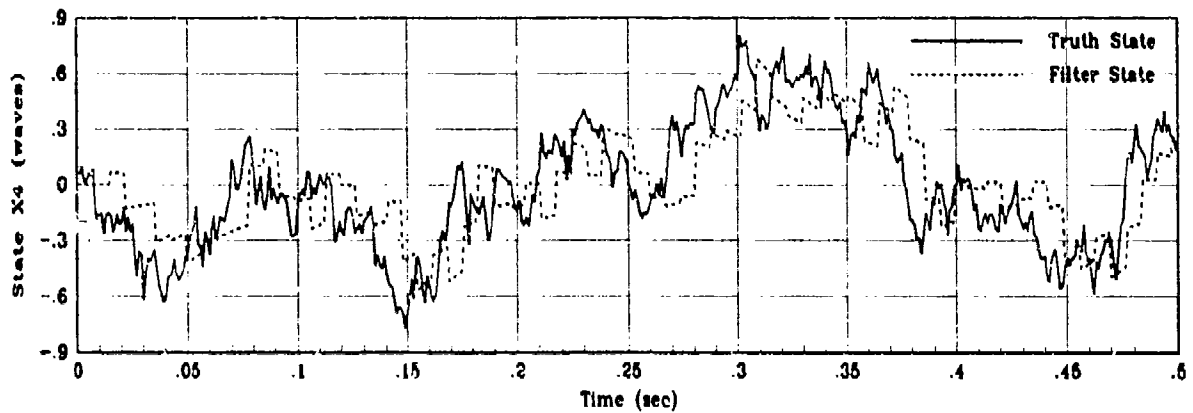
(a) Truth and Filter States: XS4, XF4
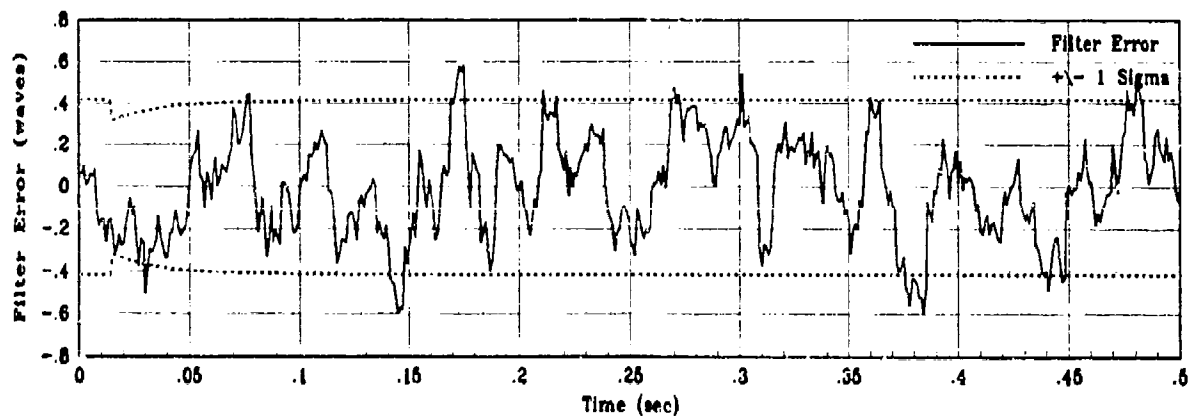
(b) X4 Filter Error for 1 MC Run
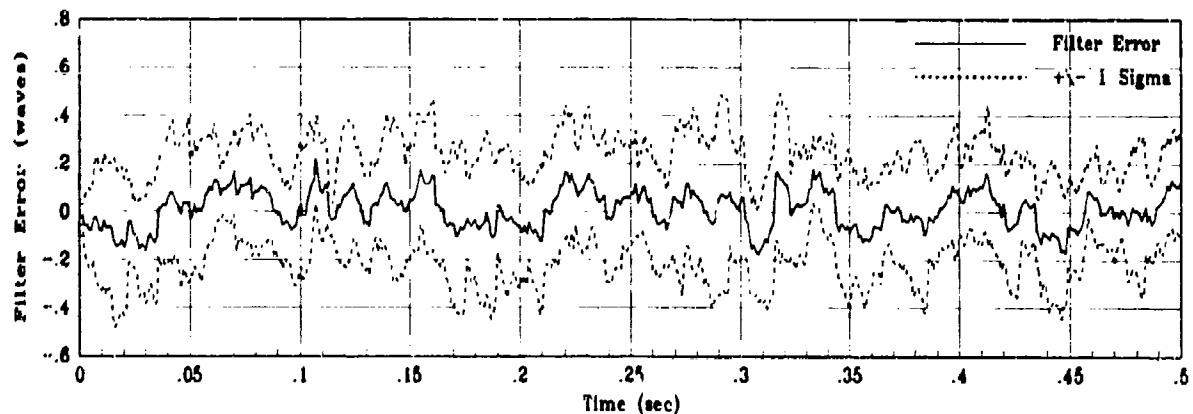
(c) X4 Filter Error for 10 MC runs

Figure 1.4. State 4 Filter-Predictor Estimation Error
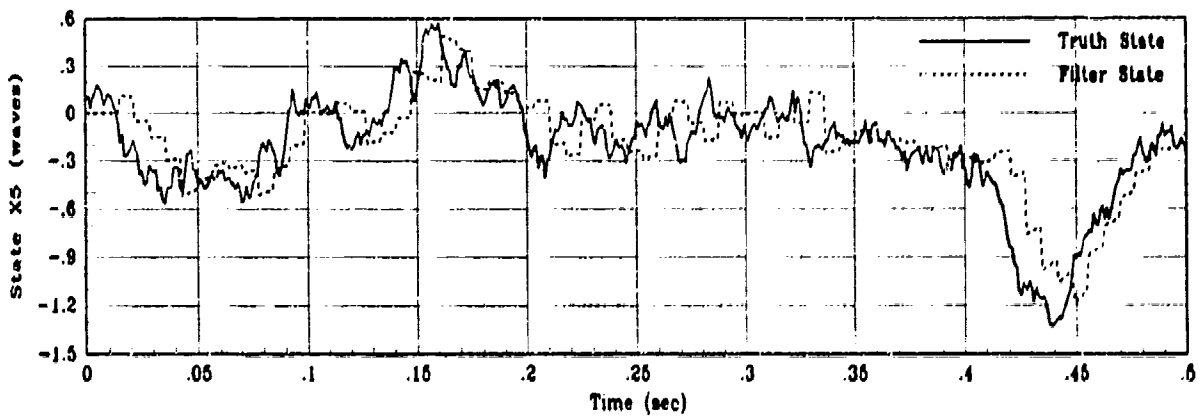
(a) Truth and Filter States: XS5, XF5
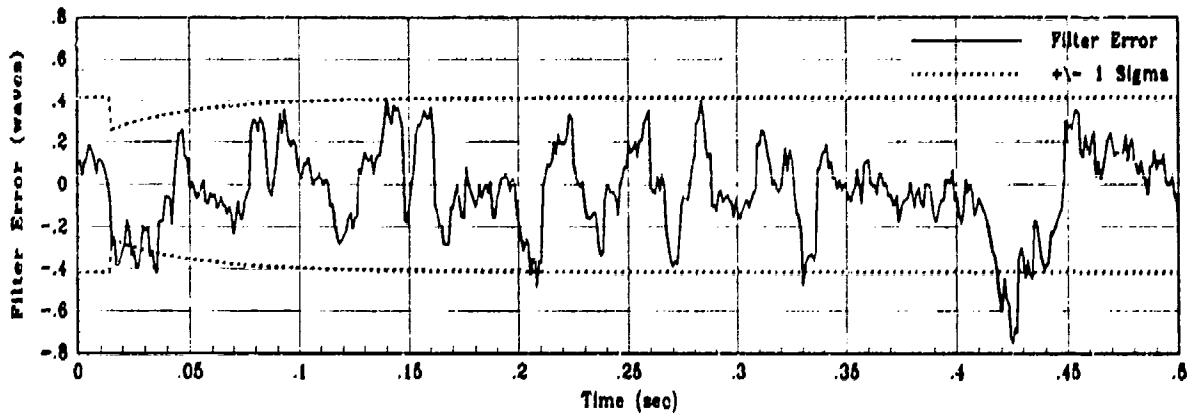
(b) X5 Filter Error for 1 MC Run

(c) X5 Filter Error for 10 MC runs

Figure 1.5. State 5 Filter-Predictor Estimation Error
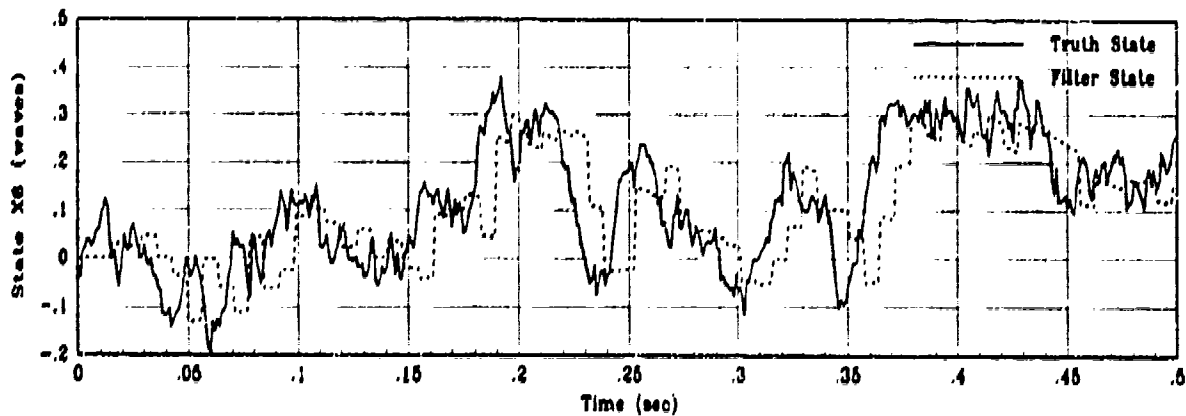
(a) Truth and Filter States: XS6, XF6
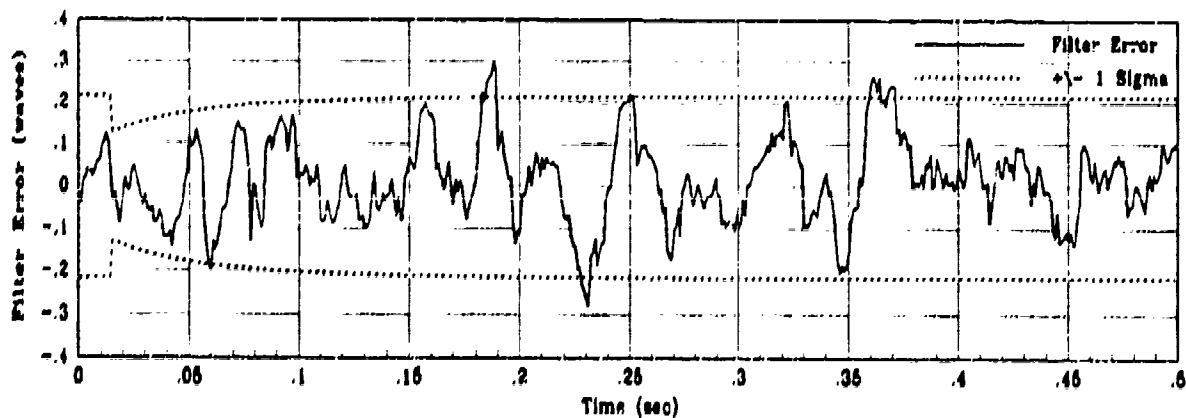
(b) X6 Filter Error for 1 MC Run

(c) X6 Filter Error for 10 MC runs

Figure 1.6. State 6 Filter Predictor Estimation Error
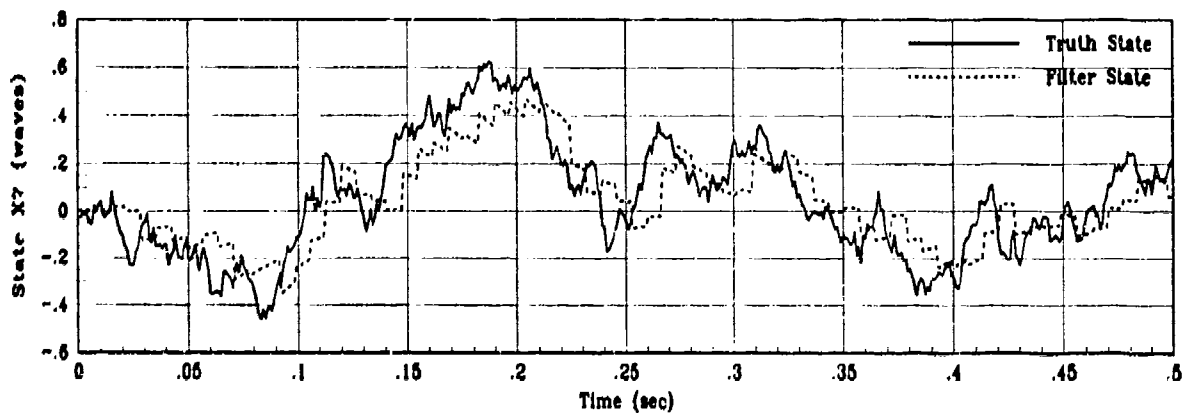
(a) Truth and Filter States: XS7, XF7
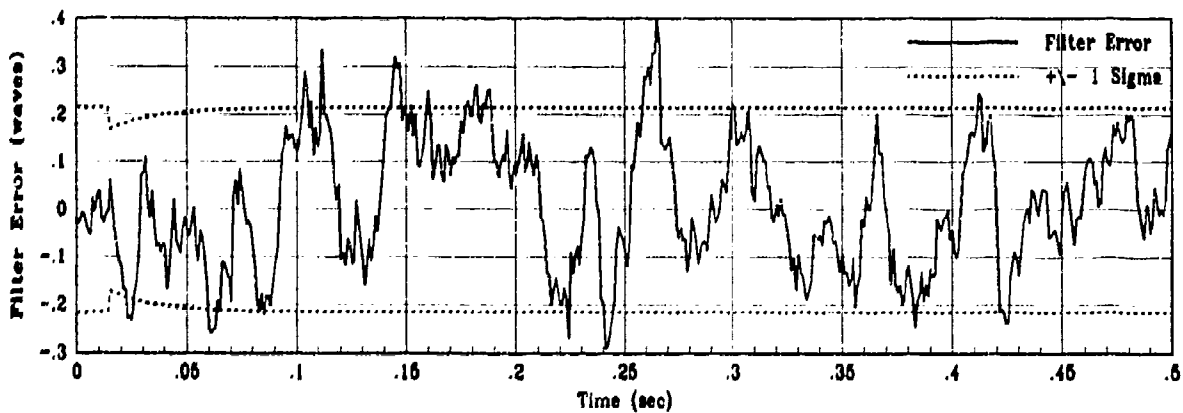
(b) X7 Filter Error for 1 MC Run
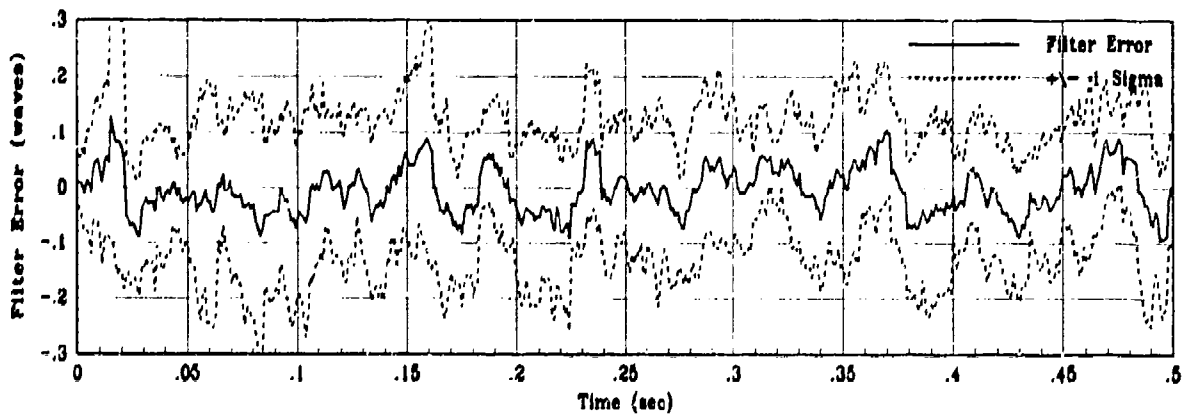
(c) X7 Filter Error for 10 MC runs

Figure I.7. State 7 Filter-Predictor Estimation Error
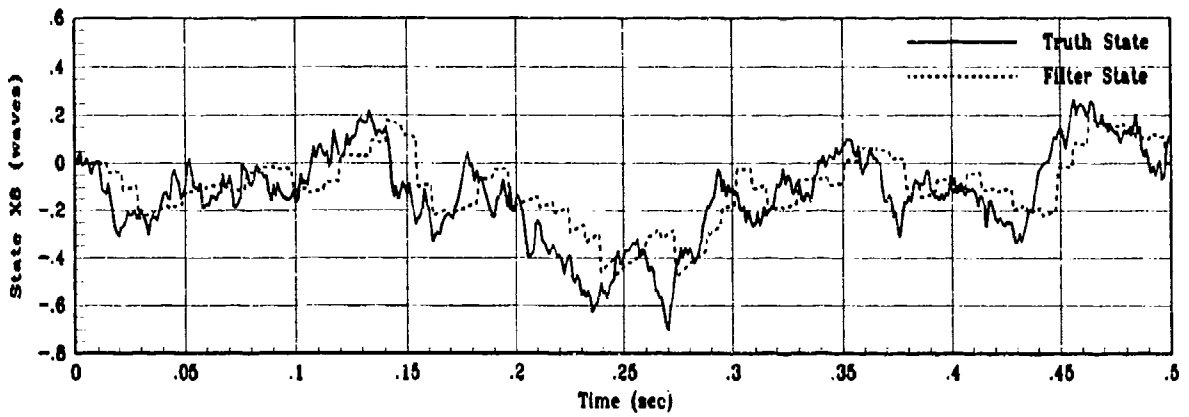
(a) Truth and Filter States: XS8, XF8
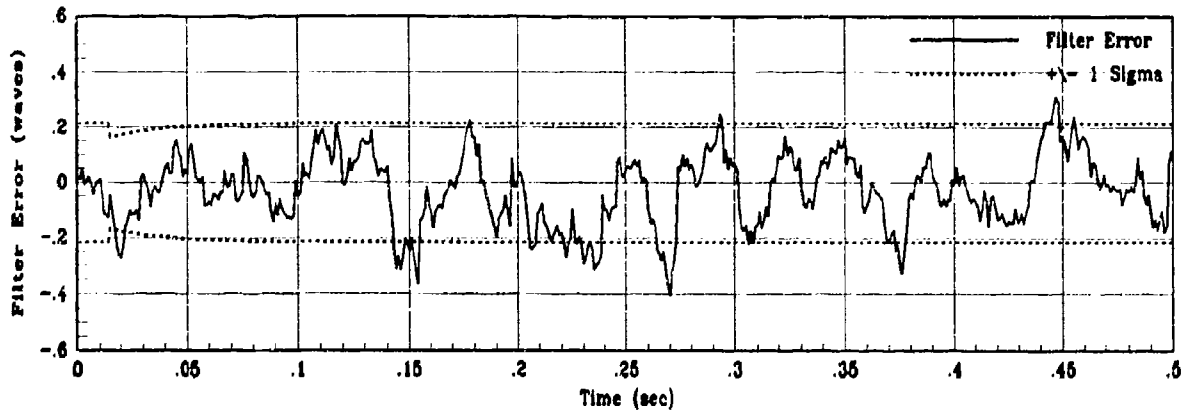
(b) X8 Filter Error for 1 MC Run
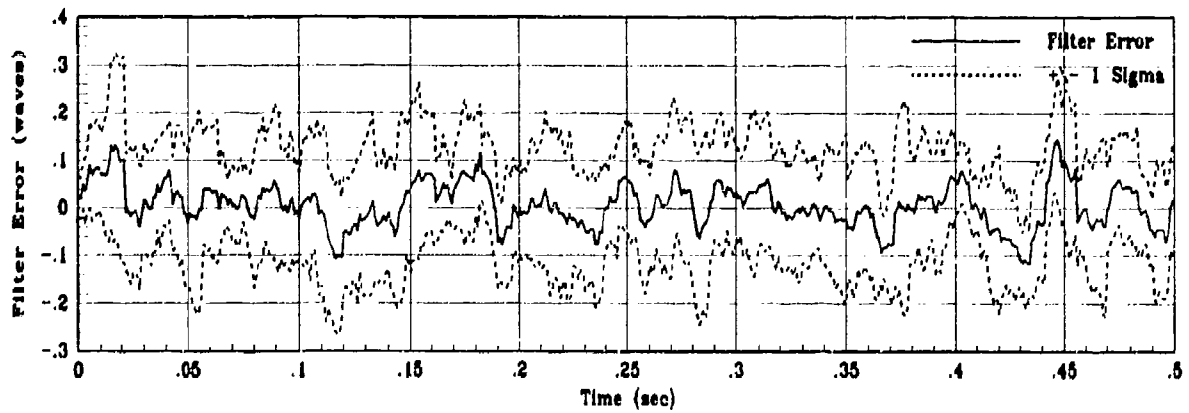
(c) X8 Filter Error for 10 MC runs

Figure I.8. State 8 Filter-Predictor Estimation Error
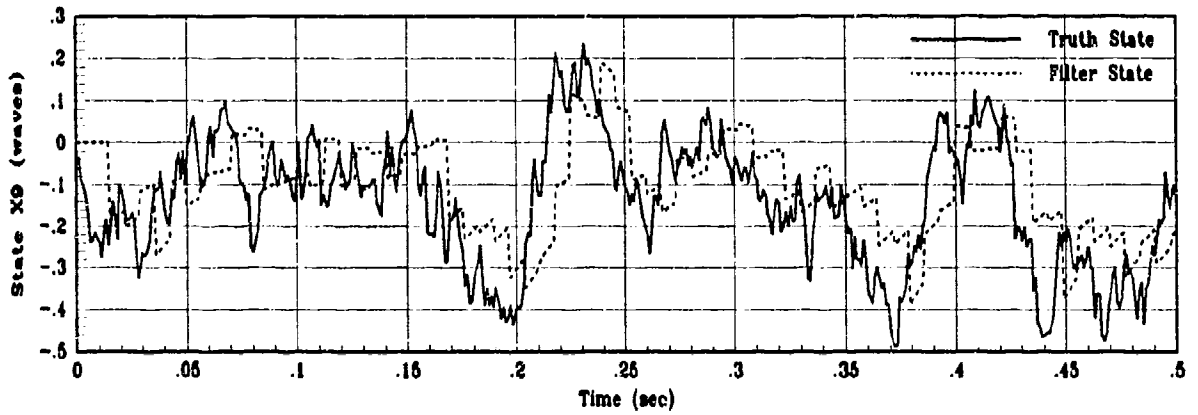
(a) Truth and Filter States: XS9, XF9
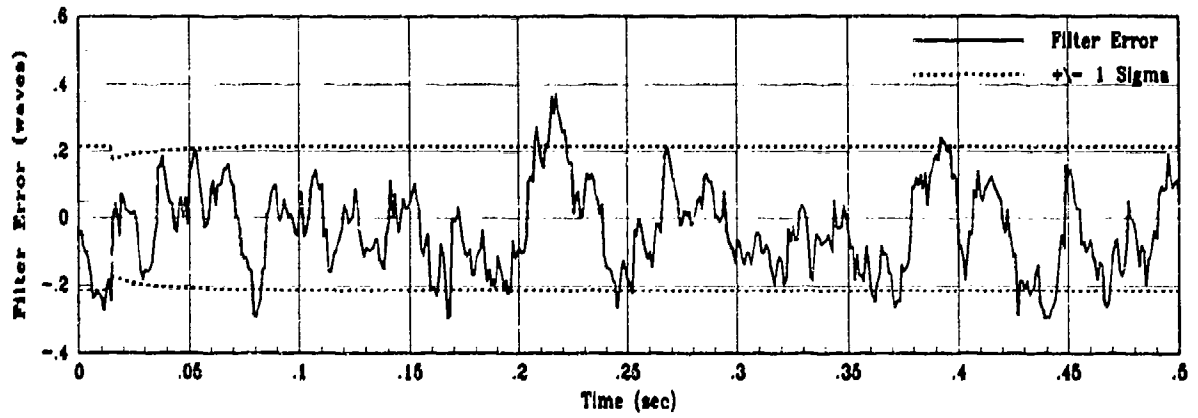
(b) X9 Filter Error for 1 MC Run
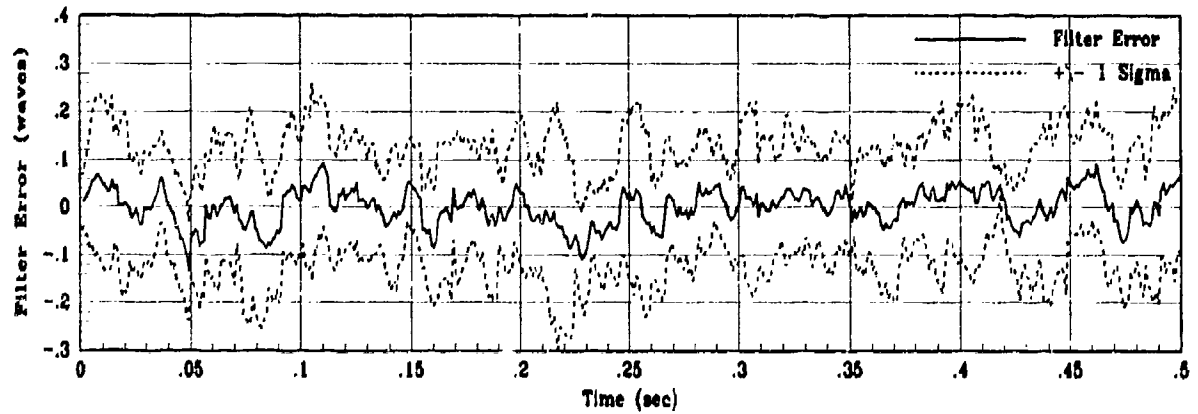
(c) X9 Filter Error for 10 MC runs

Figure 1.9. State 9 Filter-Predictor Estimation Error
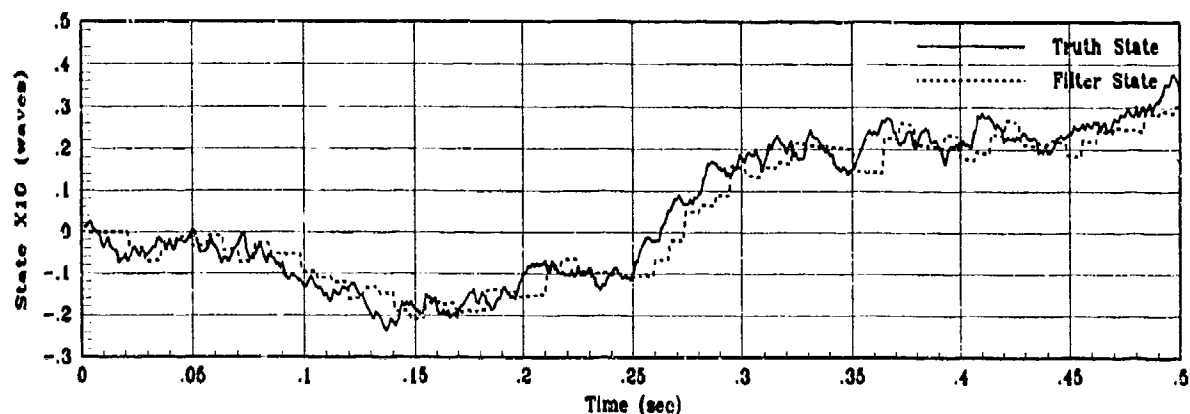
(a) Truth and Filter States: XS10, XF10
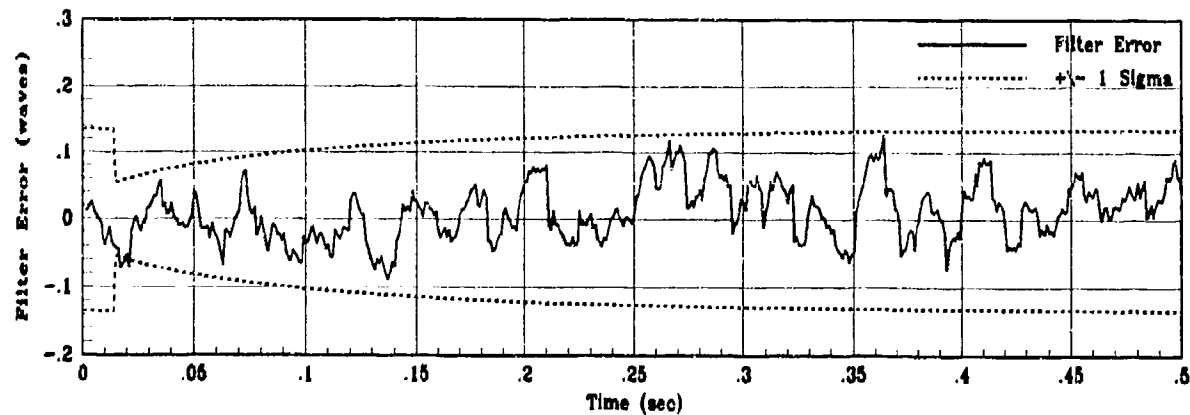
(b) X10 Filter Error for 1 MC Run

(c) X10 Filter Error for 10 MC runs

Figure I.10. State 10 Filter-Predictor Estimation Error
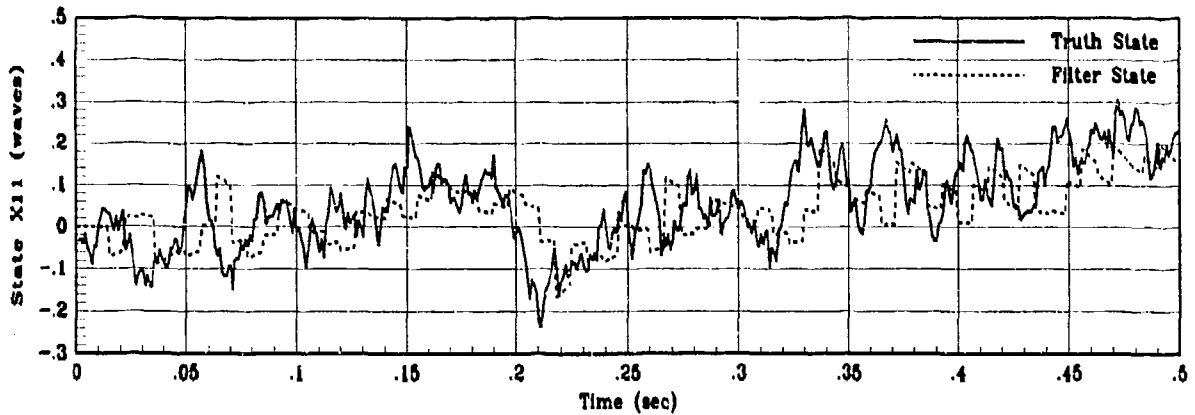
(a) Truth and Filter States: XS11, XF11
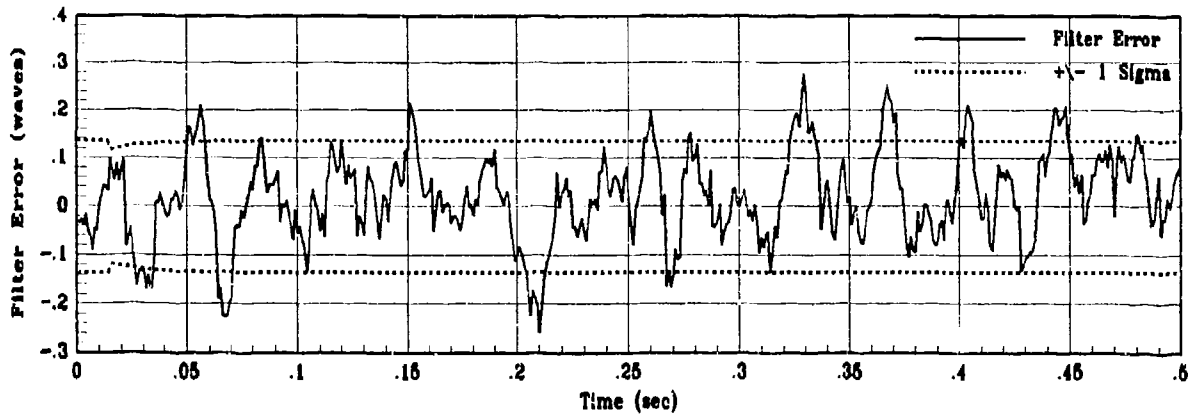
(b) X11 Filter Error for 1 MC Run

(c) X11 Filter Error for 10 MC runs

Figure I.11. State 11 Filter-Predictor Estimation Error

I-12
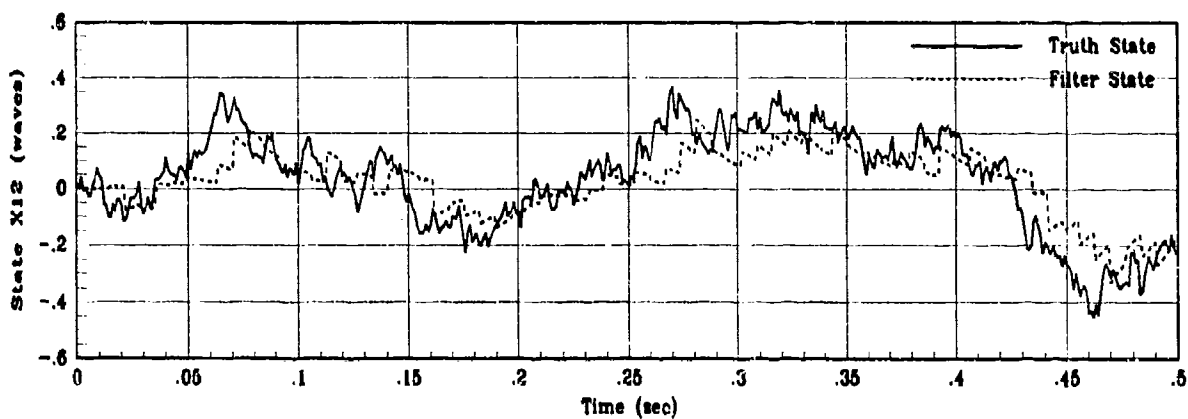
(a) Truth and Filter States: XS12, XF12
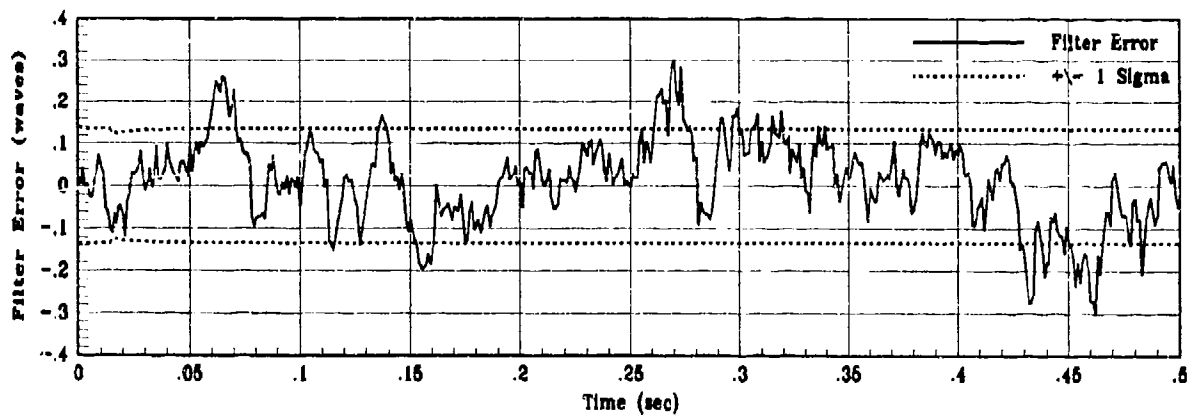
(b) X12 Filter Error for 1 MC Run
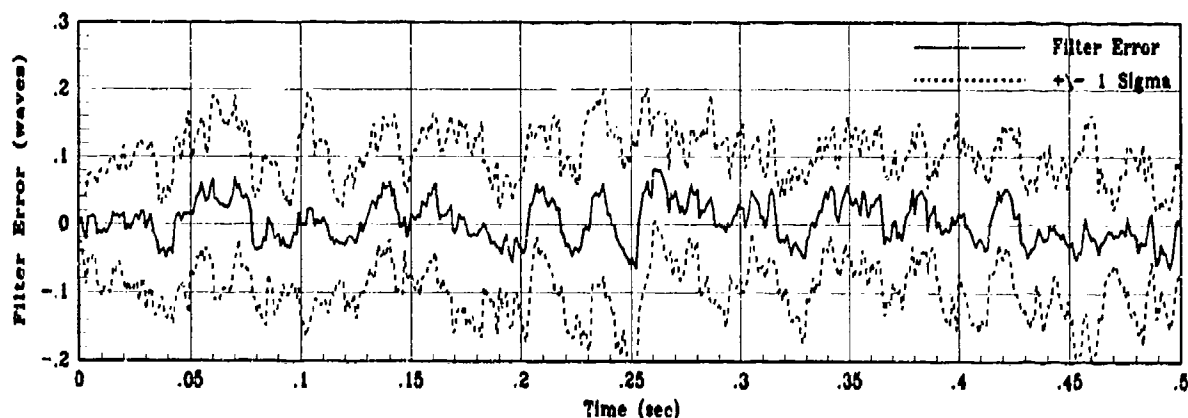
(c) X12 Filter Error for 10 MC runs

Figure 1.12. State 12 Filter-Predictor Estimation Error
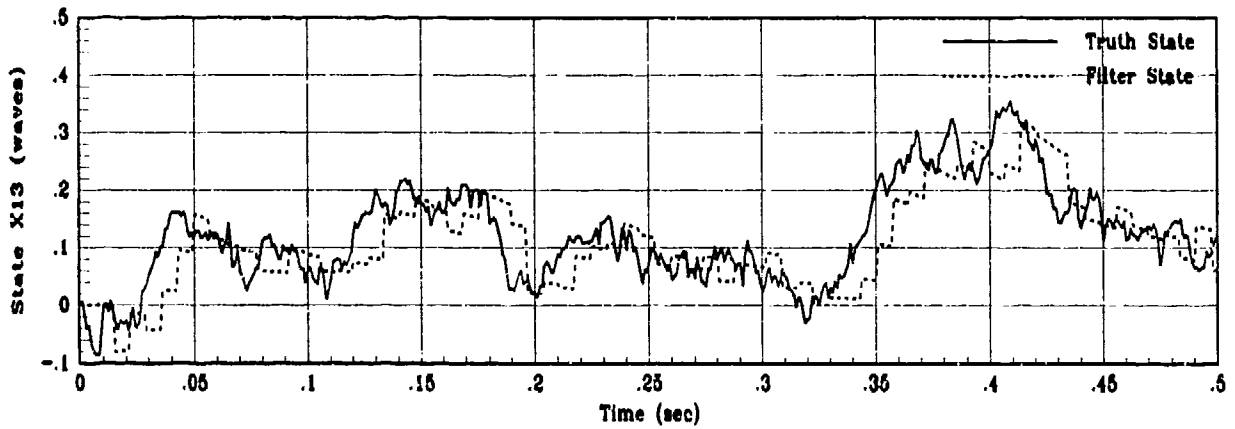
(a) Truth and Filter States: XS13, XF13
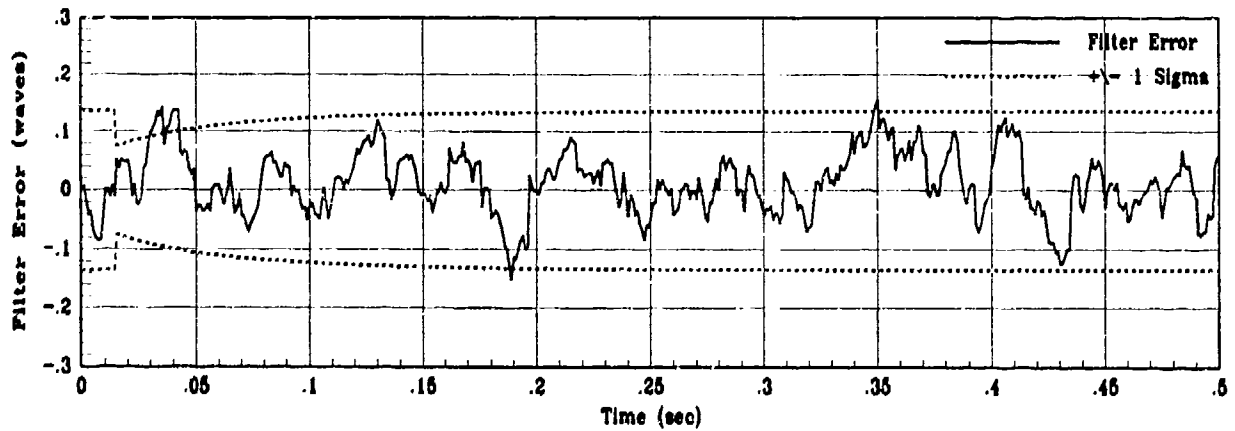
(b) X13 Filter Error for 1 MC Run

(c) X13 Filter Error for 10 MC runs

Figure 1.13. State 13 Filter-Predictor Estimation Error
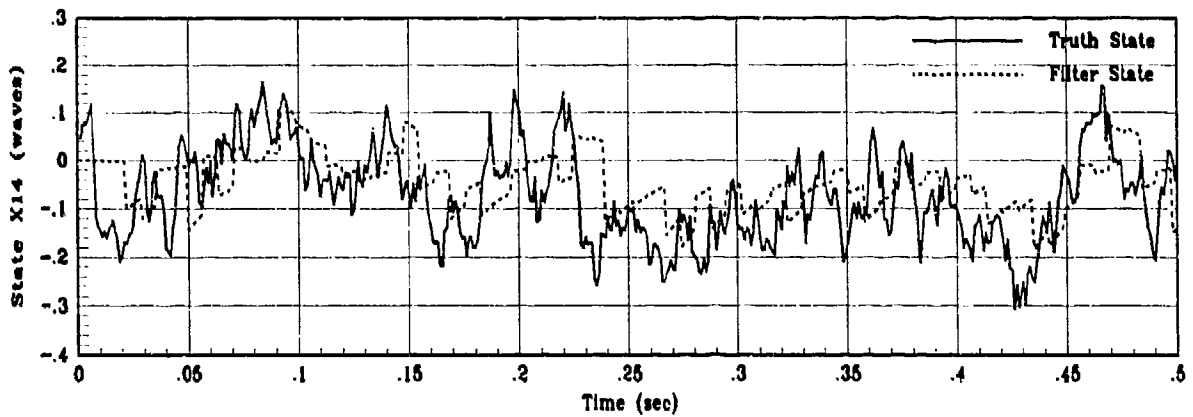
(a) Truth and Filter States: XS14, XF14
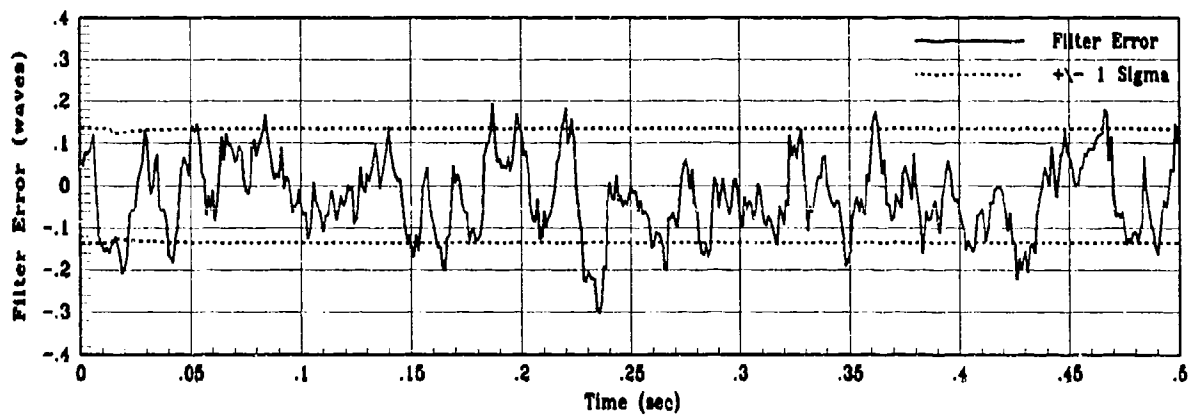
(b) X14 Filter Error for 1 MC Run

(c) X14 Filter Error for 10 MC runs

Figure I.14. State 14 Filter Predictor Estimation Error
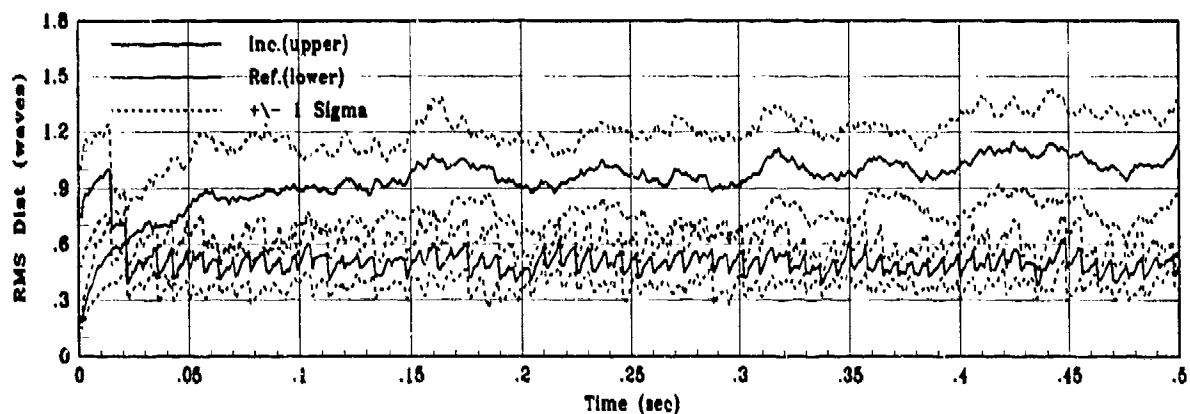
I-15

(a) Incident and Reflected RMS Phase Distortion for 10 MC Runs
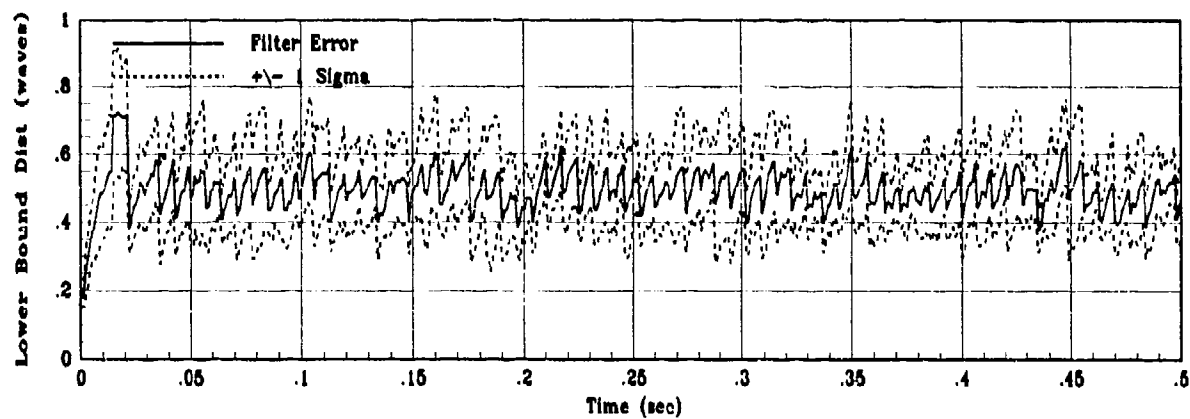
(b) RMS Filter Error for 10 MC Runs
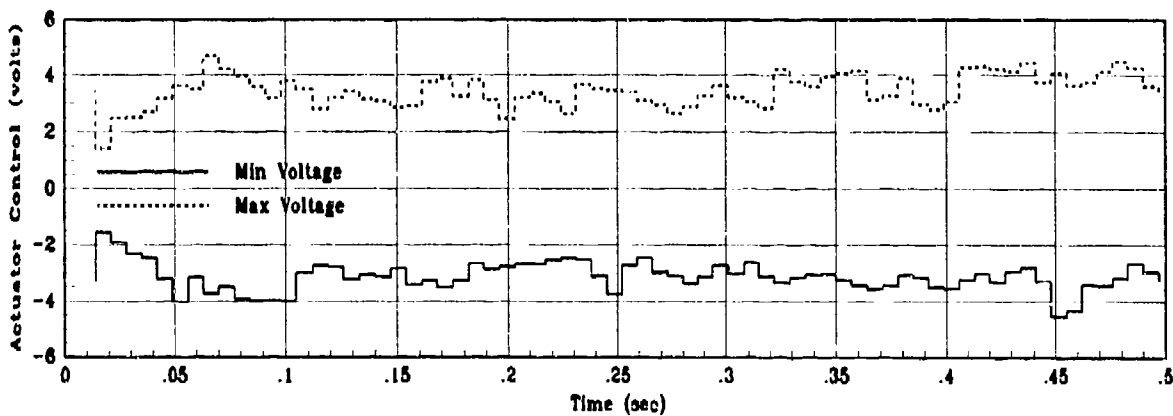
(c) Actuator Control Voltage Envelope

Figure I.15. Control System Performance for Filter-Predictor Model

(a) Incident and Reflected RMS Phase Distortion for 10 MC Runs

(b) RMS Filter Error for 10 MC Runs

(c) Actuator Control Voltage Envelope
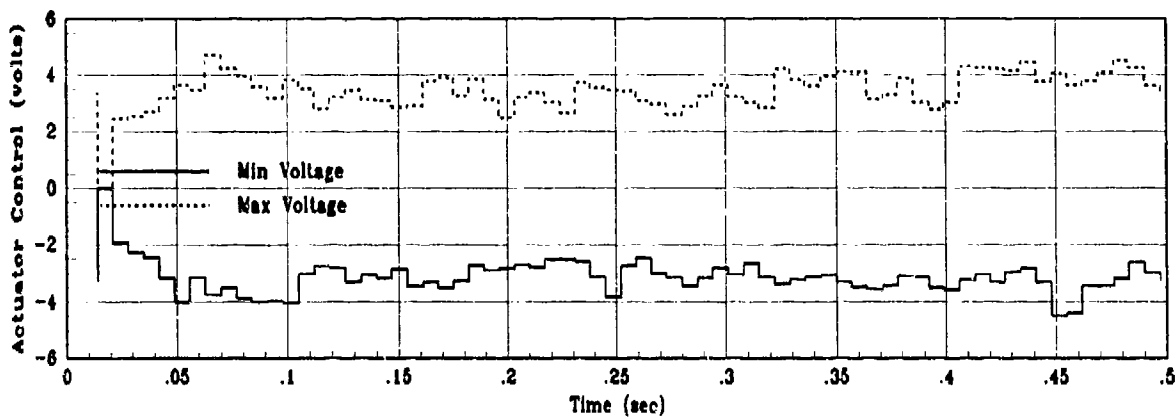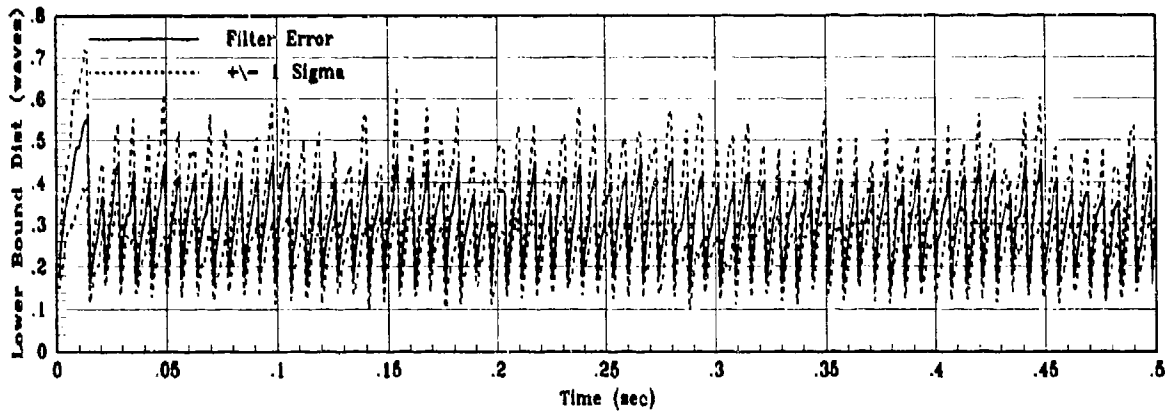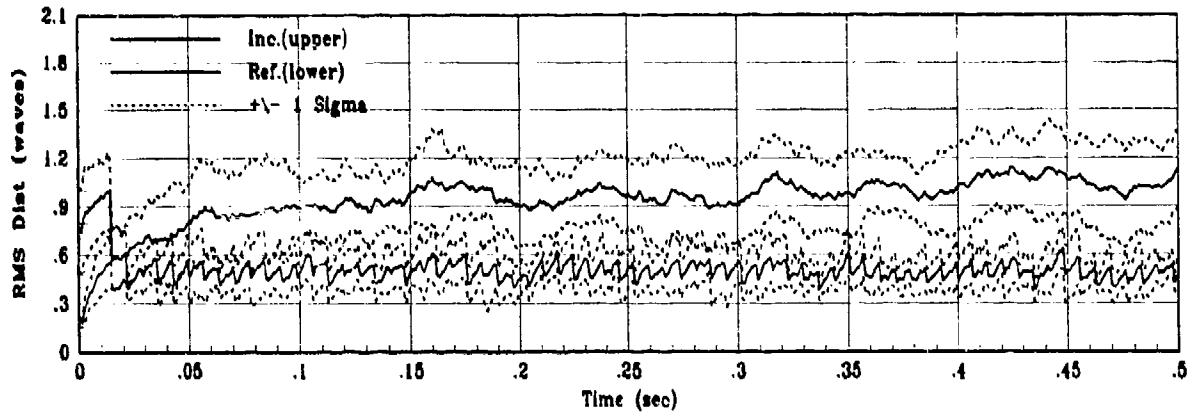
Figure I.16. Suboptimal Control System Performance
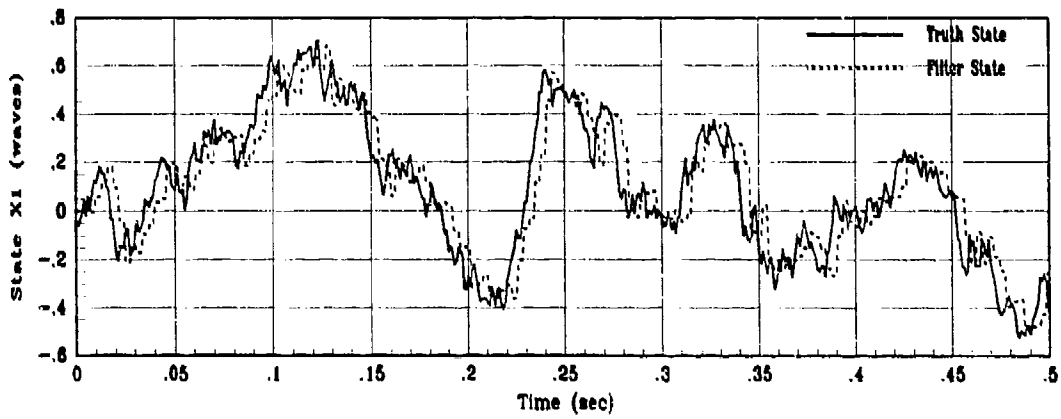
(a) Truth and Filter States: XS1, XF1
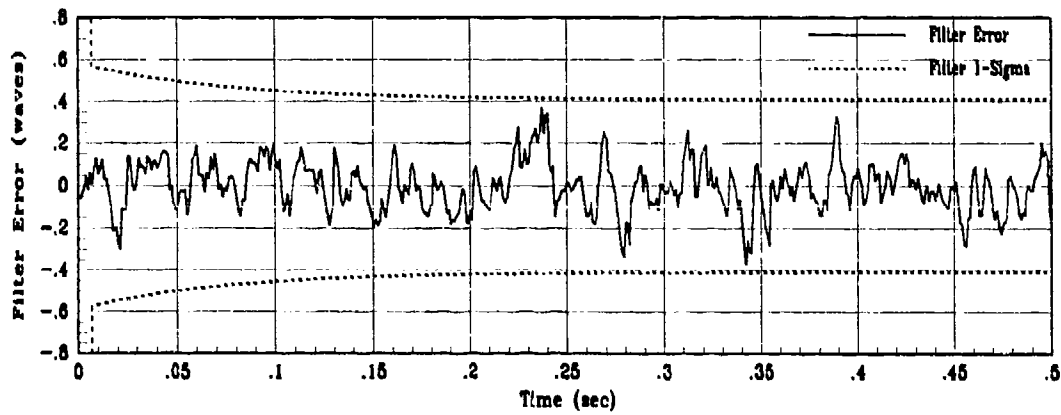
(b) X1 Filter Error for 1 MC Run
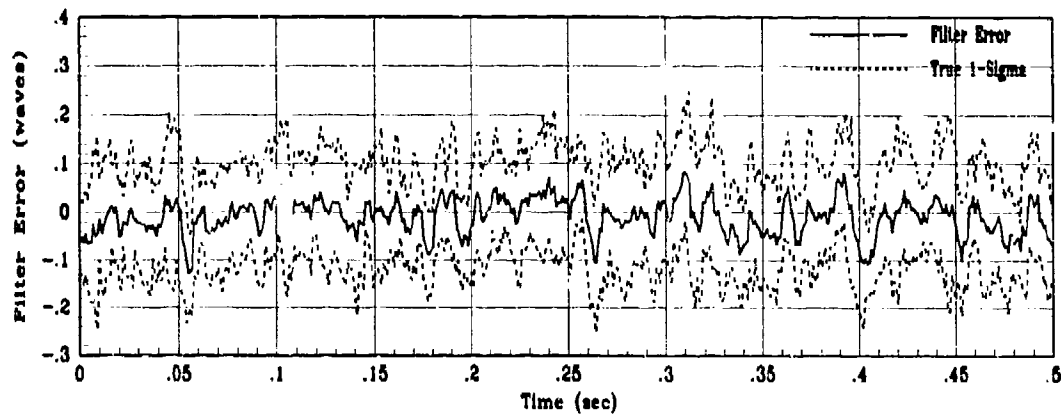
(c) X1 True Filter Error for 10 MC Runs

Figure 1.17. State 1 Filter Predictor Estimation Error for 3 msec Sample Time

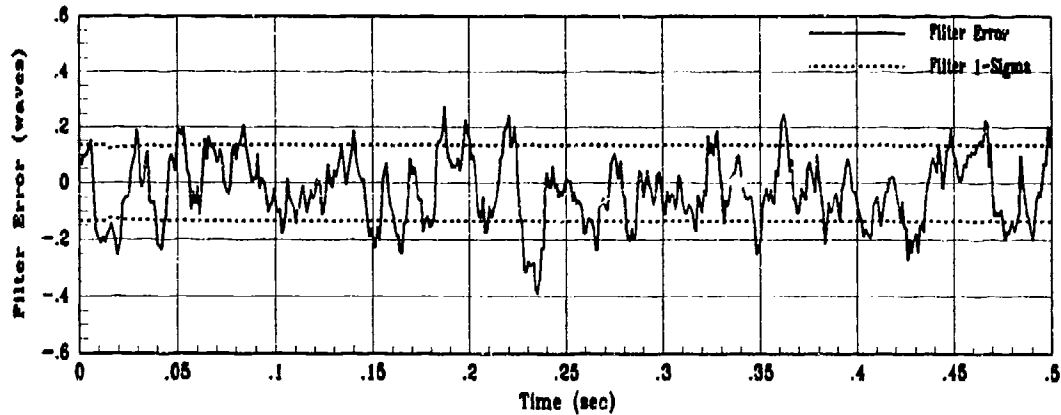(a) Truth and Filter States: XS6, XF6

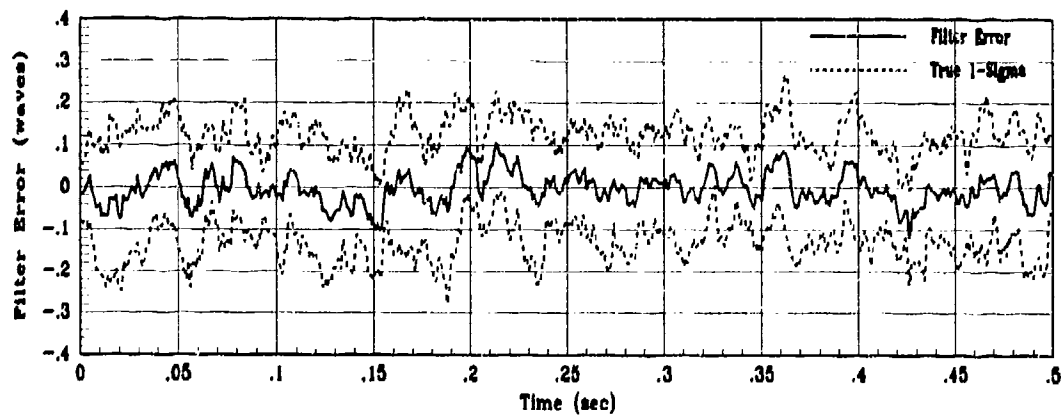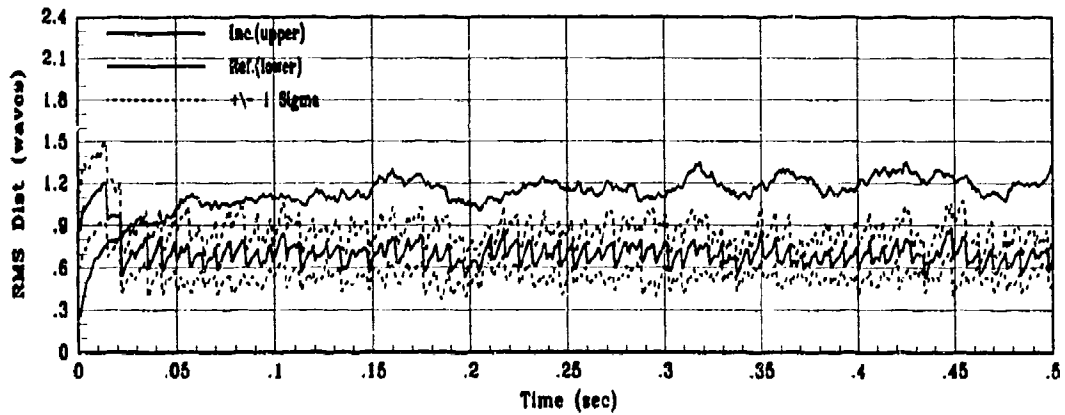(b) X6 Filter Error for 1 MC Run
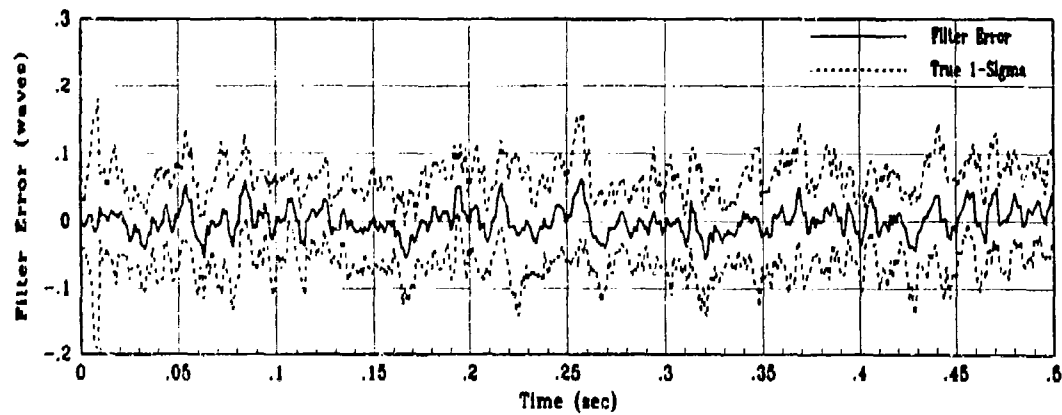
(c) X6 True Filter Error for 10 MC runs

Figure 1.18. State 6 Filter-Predictor Estimation Error for 3 msec Sample Time
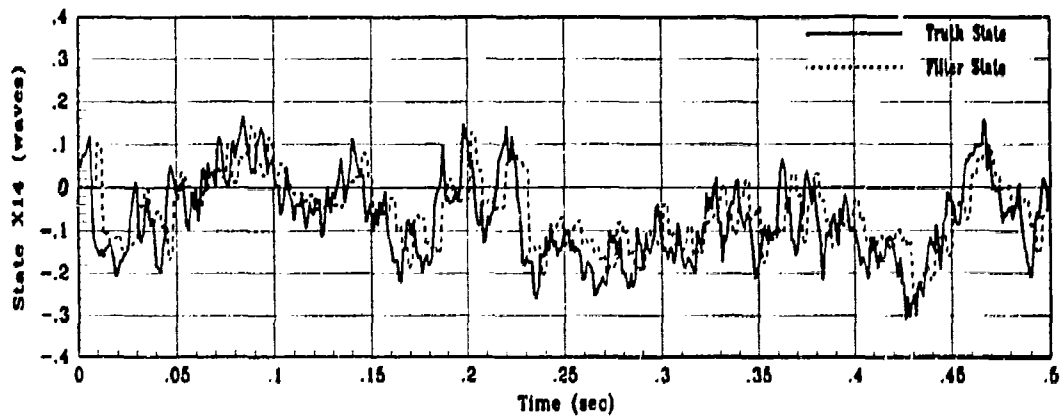
(a) Truth and Filter States: XS14, XF14
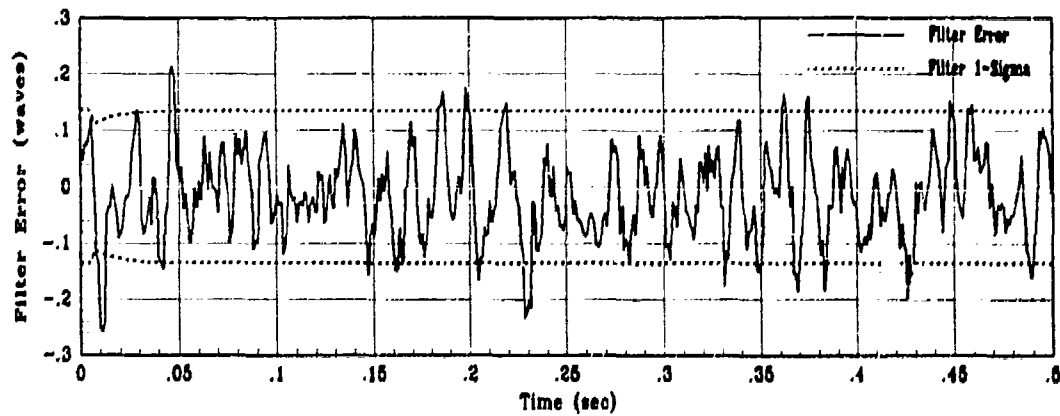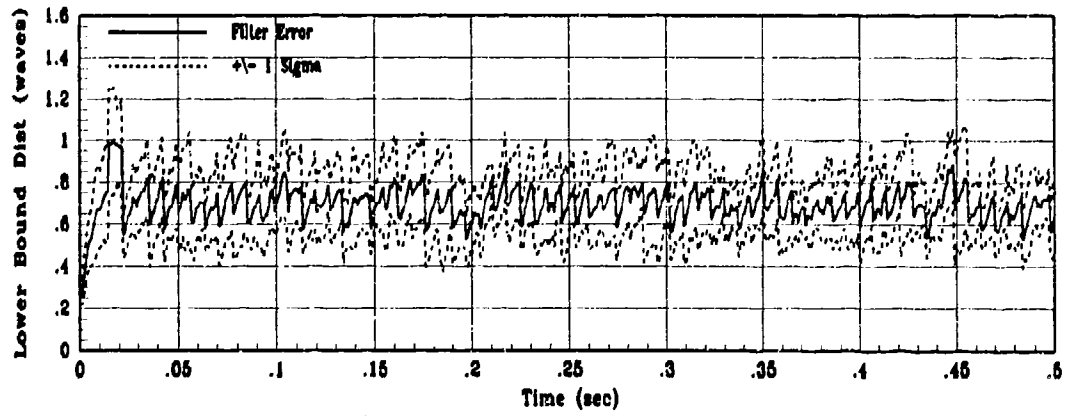
(b) X14 Filter Error for 1 MC Run
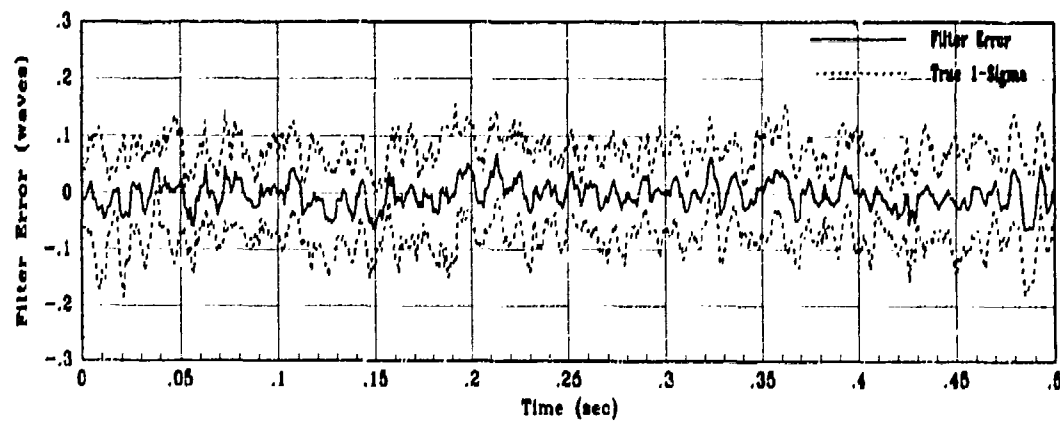
(c) X14 True Filter Error for 10 MC runs

Figure 1.19. State 14 Filter-Predictor Estimation Error for 3 msec Sample Time
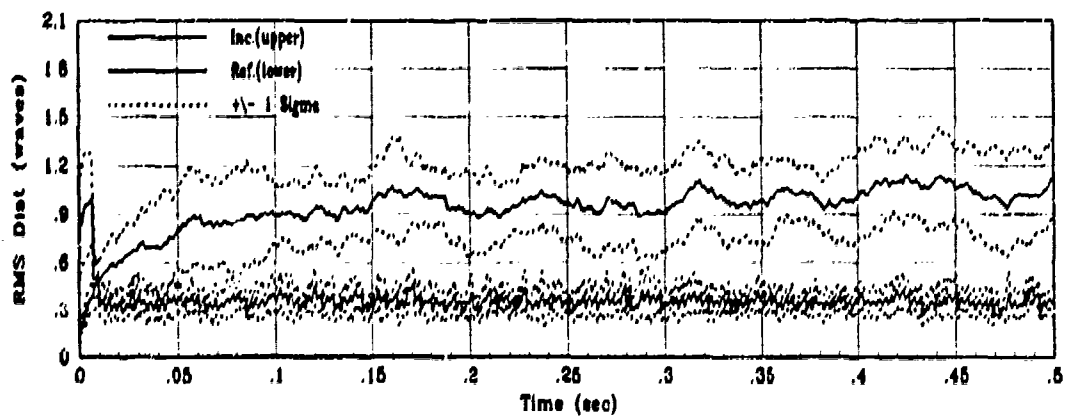
1-20

(a) Incident and Reflected RMS Phase Distortion for 10 MC Runs
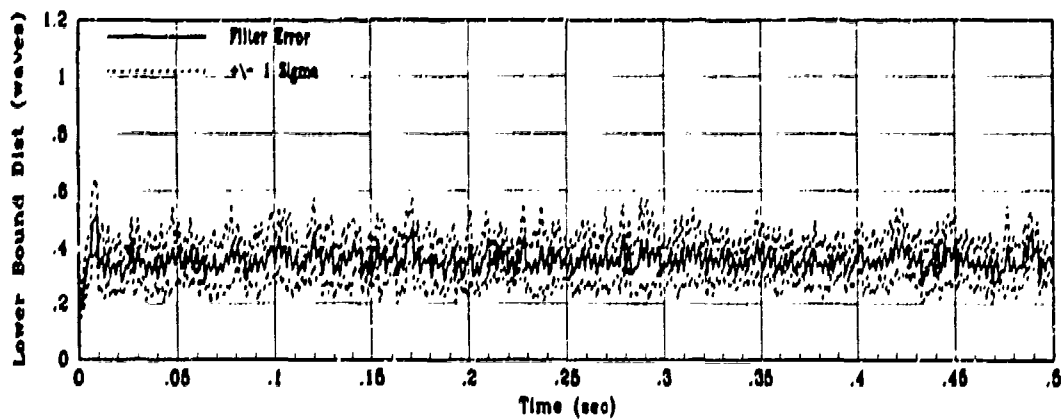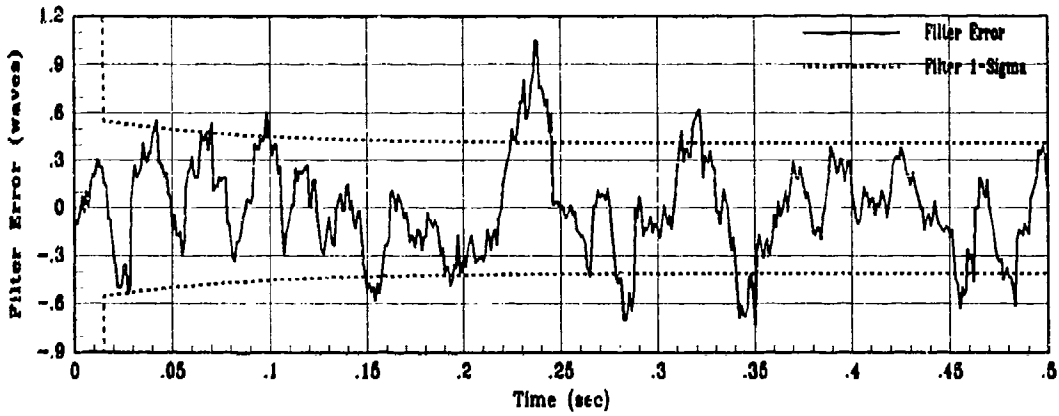

(b) RMS Filter Error for 10 MC Runs

Figure 1.20. Control System Performance of Filter-Predictor with 3 msec Sample Time

Appendix J. Performance Plots for Sensitivity Study

The appendix contains performance plots for the augmented filter-predictor controller when the the nominal controller is evaluated in the presence of changes in the true dynamics of the atmosphere. Results from 10 separate sensitivity studies are provided. The first six studies simulated average wind velocities along the propagation path of 5, 15, 35, 45, 55, and 65 m/sec. The remaining four studies investigated actual zenith angles to the source of 15, 30, 45, and 60 degrees with the controller assuming 0 degrees of zenith angle. Filter performance plots for states 1, 6, and 14 along with control system performance plots are shown for each study. Detailed analysis of the data is presented in Section 5.6.
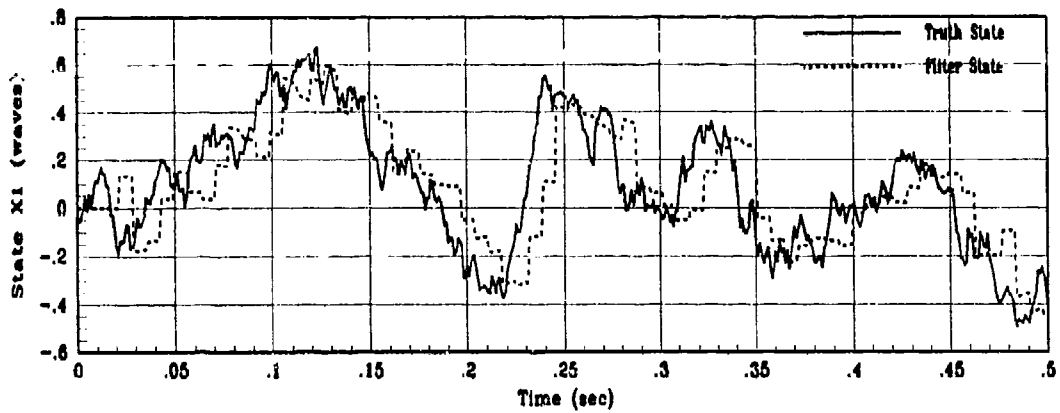
(a) Truth and Filter States: XS1, XF1
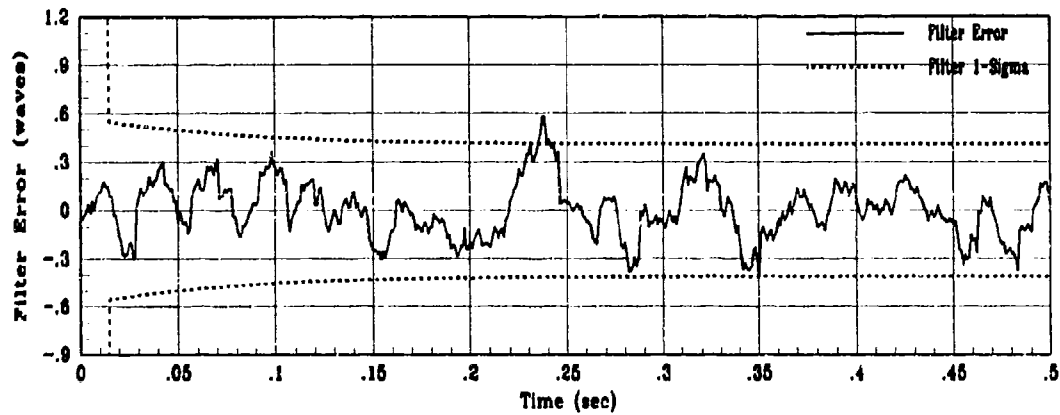
(b) X1 Filter Error for 1 MC Run
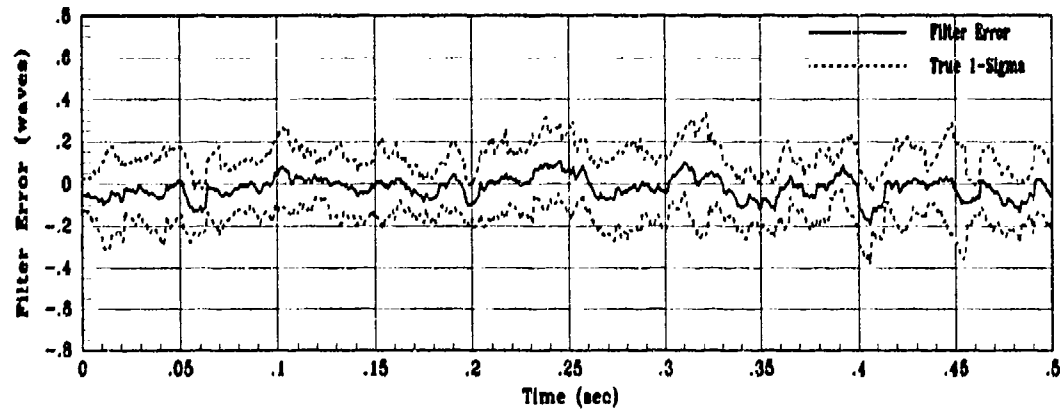
(c) X1 True Filter Error for 10 MC Runs

Figure J.1. State 1 Filter Estimation Error for Average Winds of 5 m/sec
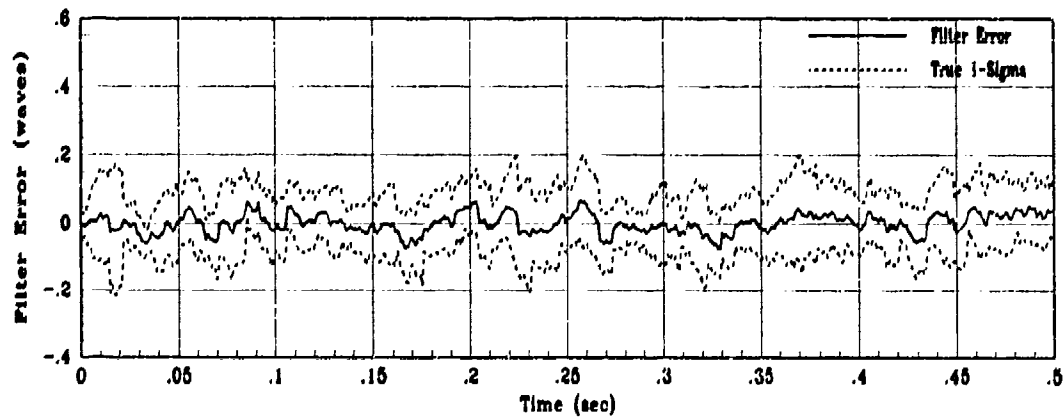
Figure J.2. State 6 Filter Estimation Error for Average Winds of 5 m/sec
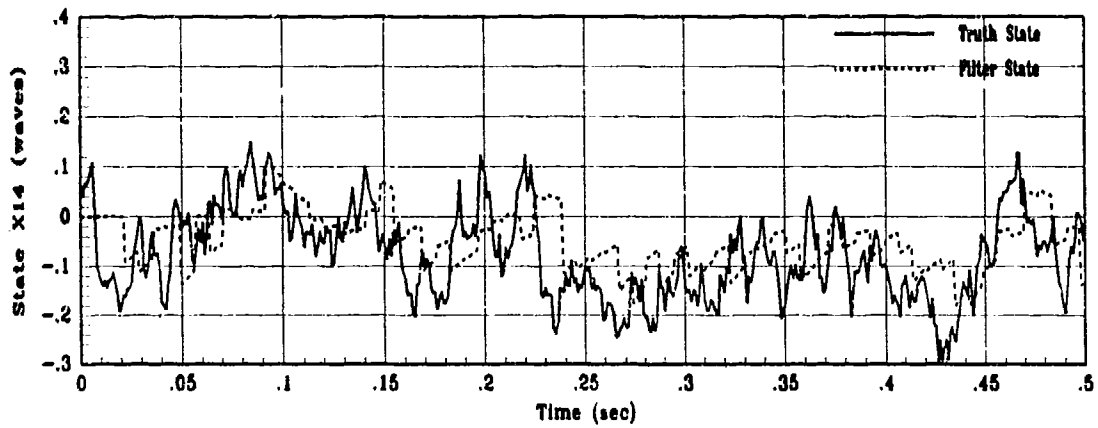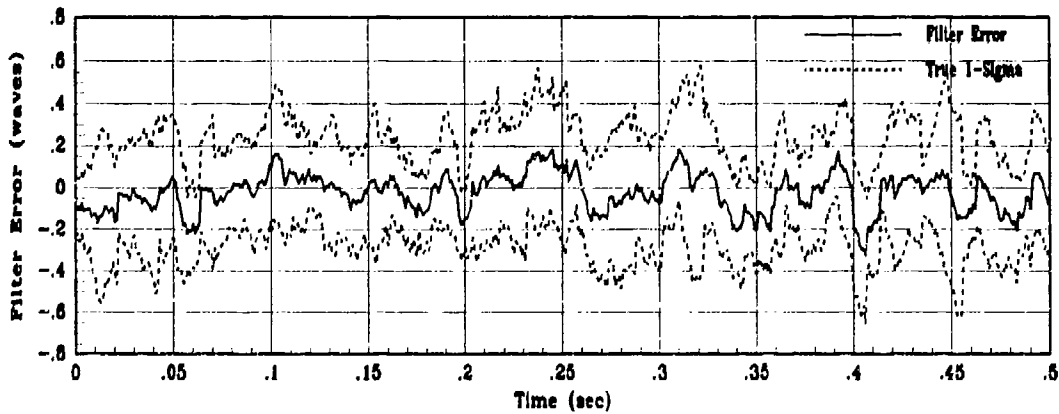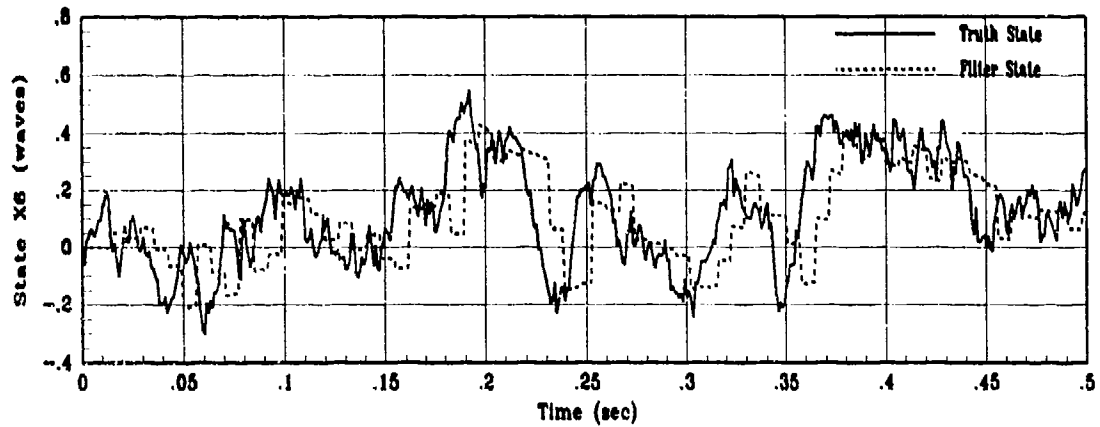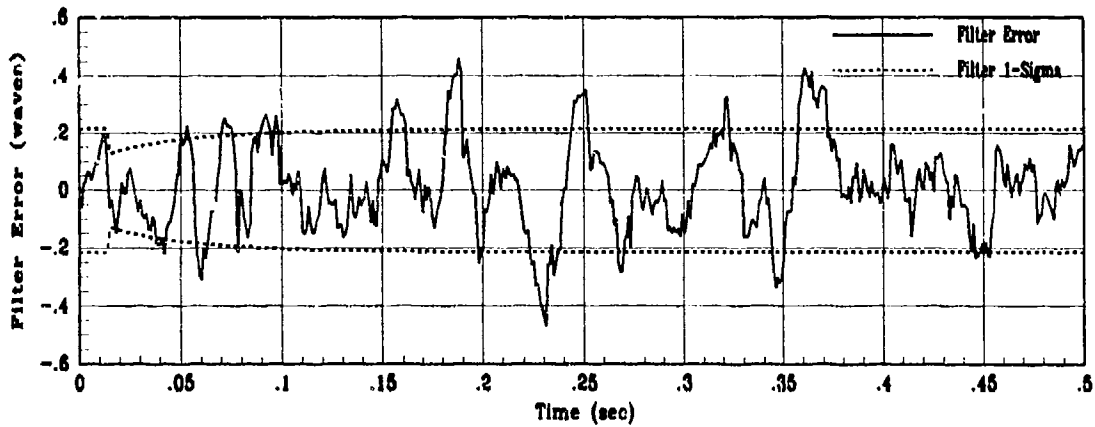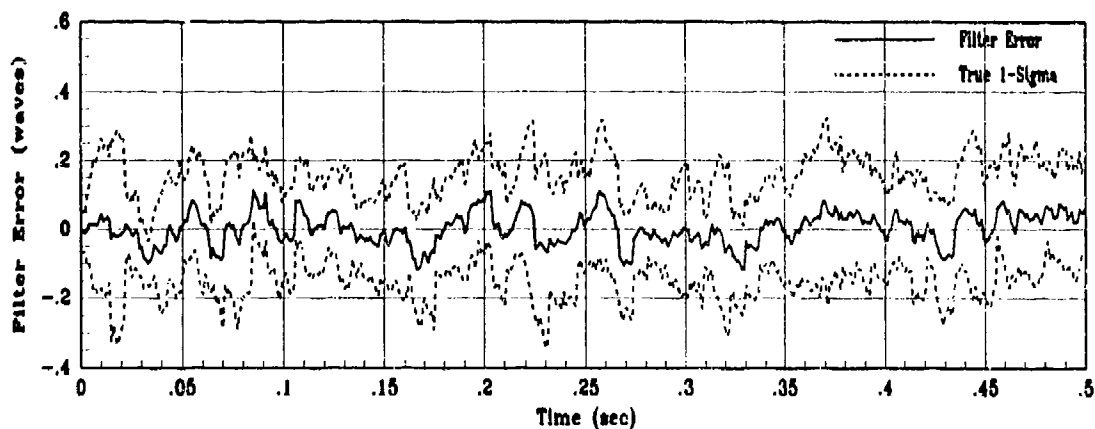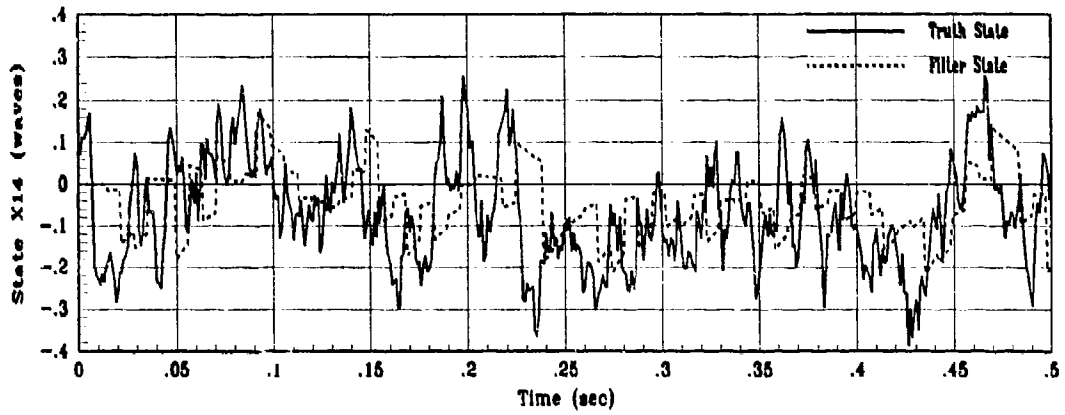
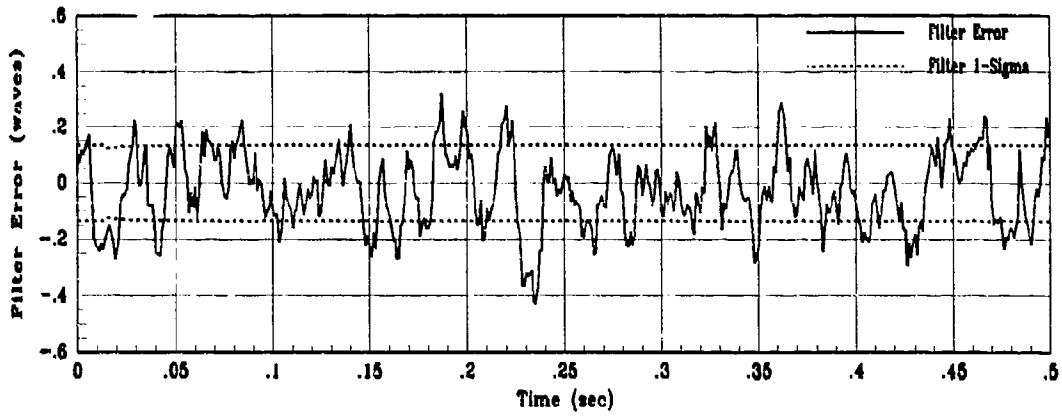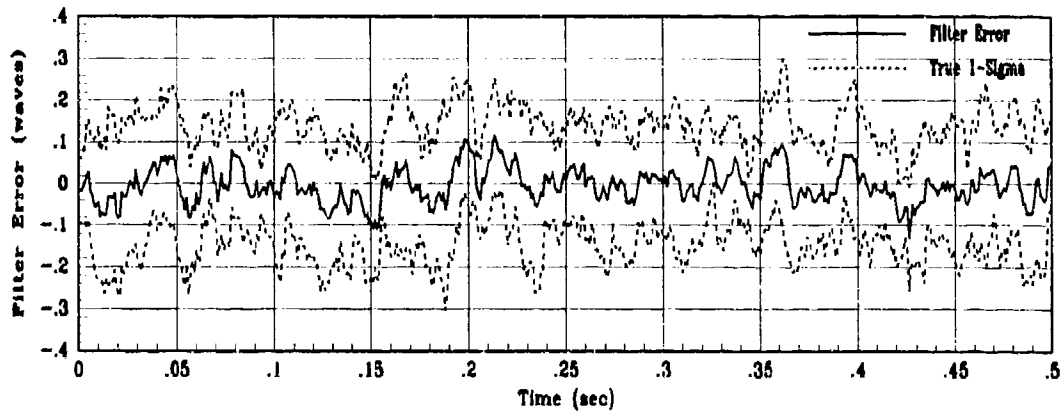(a) Truth and Filter States: XS14, XF14

(b) X14 Filter Error for 1 MC Run

(c) X14 True Filter Error for 10 MC runs

Figure J.3. State 14 Filter Estimation Error for Average Winds of 5 m/sec

(a) Incident and Reflected RMS Phase Distortion for 10 MC Runs

(b) RMS Filter Error for 10 MC Runs

(c) Actuator Control Voltage Envelope

Figure J.4. Control System Performance for Average Winds of 5 m/sec
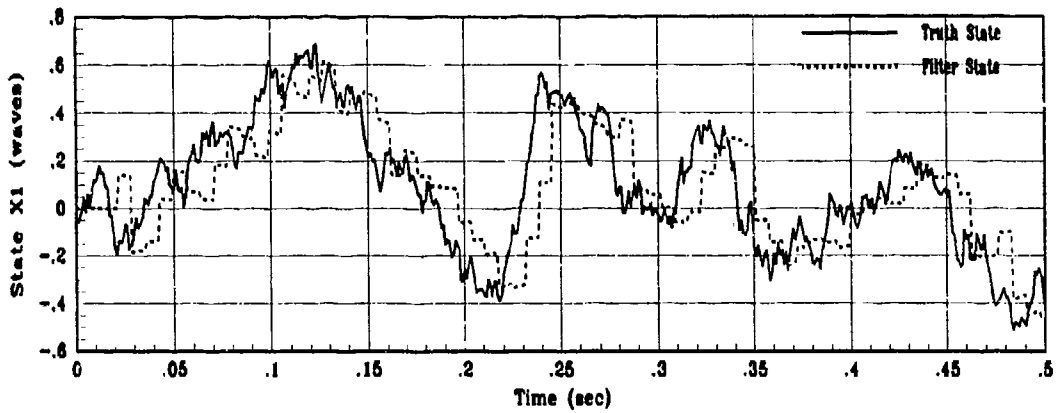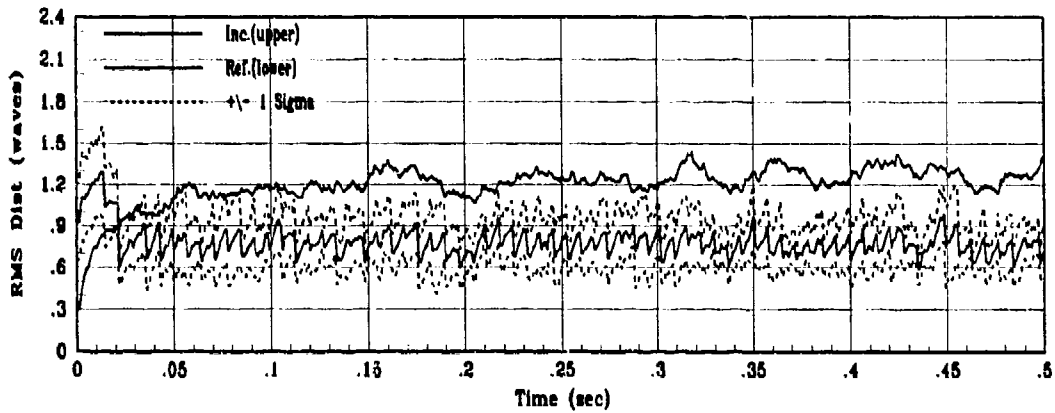
(a) Truth and Filter States: XS1, XF1

(b) X1 Filter Error for 1 MC Run
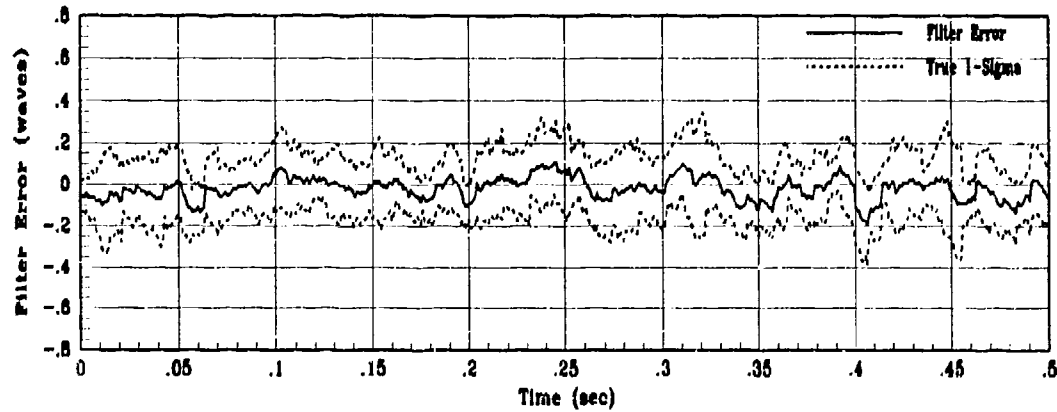
(c) X1 True Filter Error for 10 MC Runs

Figure J.5.   State 1 Filter Estimation Error for Average Winds of 15 m/sec

(a) Truth and Filter States: XS6, XF6
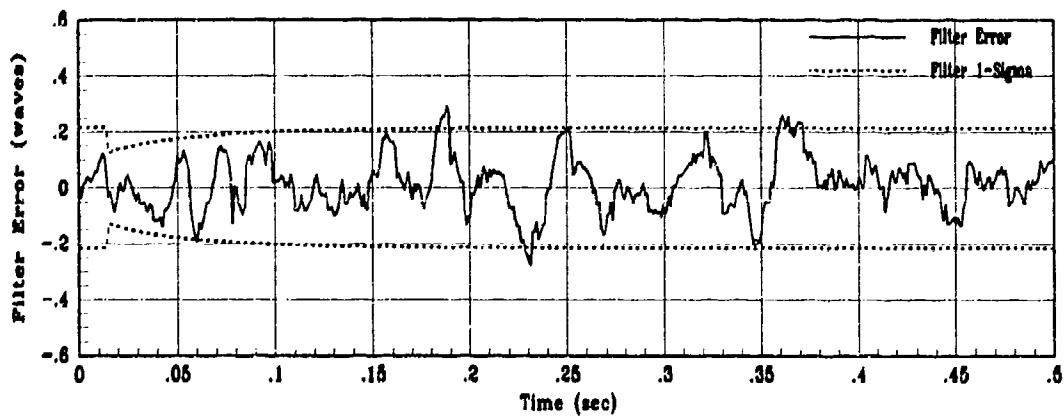
(b) X6 Filter Error for 1 MC Run

(c) X6 True Filter Error for 10 MC runs

Figure J.6. State 6 Filter Estimation Error for Average Winds of 15 m/sec

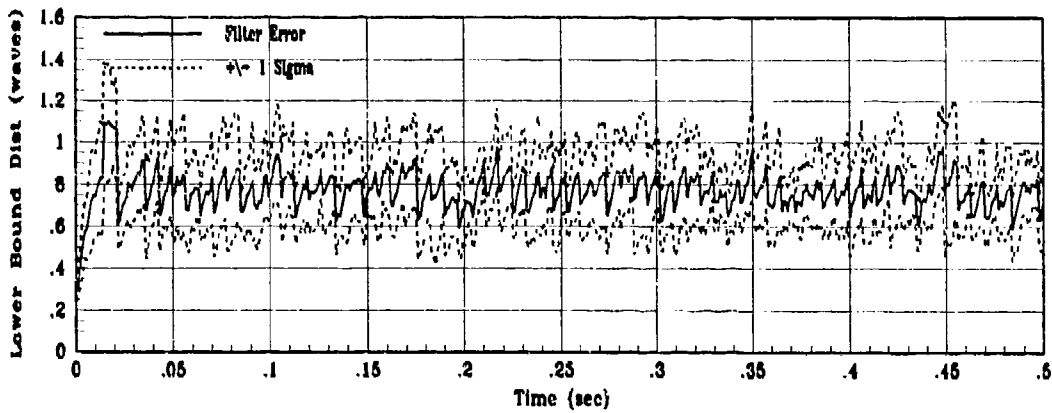(a) Truth and Filter States: XS14, XF14
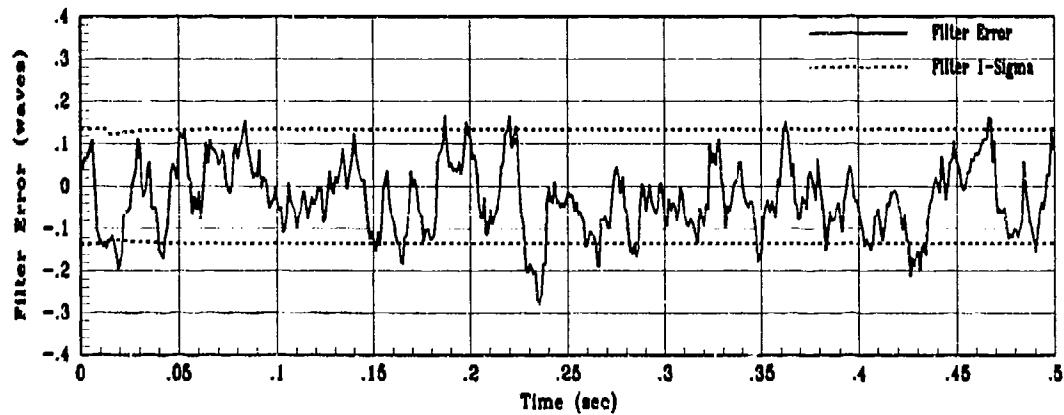
(b) X14 Filter Error for 1 MC Run
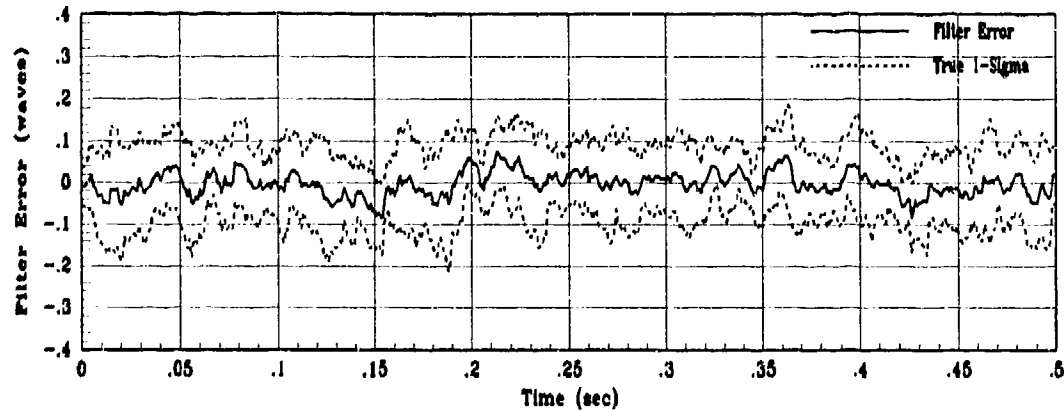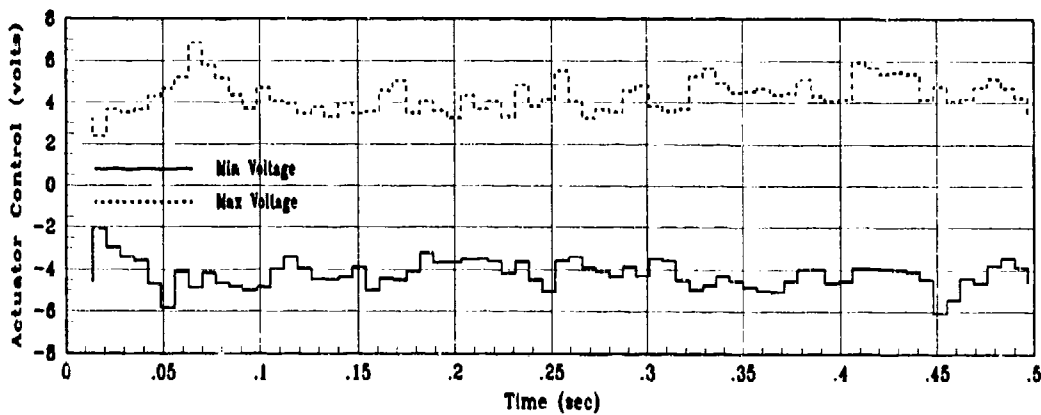

(c) X14 True Filter Error for 10 MC runs

Figure J.7. State 14 Filter Estimation Error for Average Winds of 15 m/sec

J-8

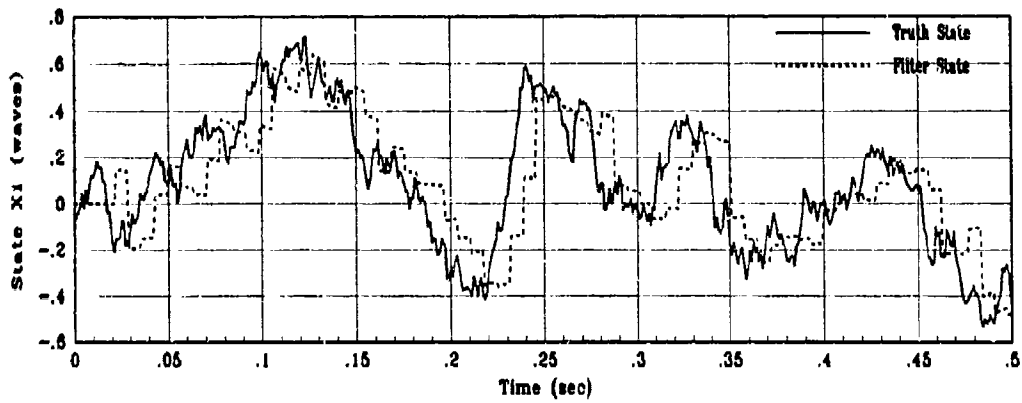(a) Incident and Reflected RMS Phase Distortion for 10 MC Runs
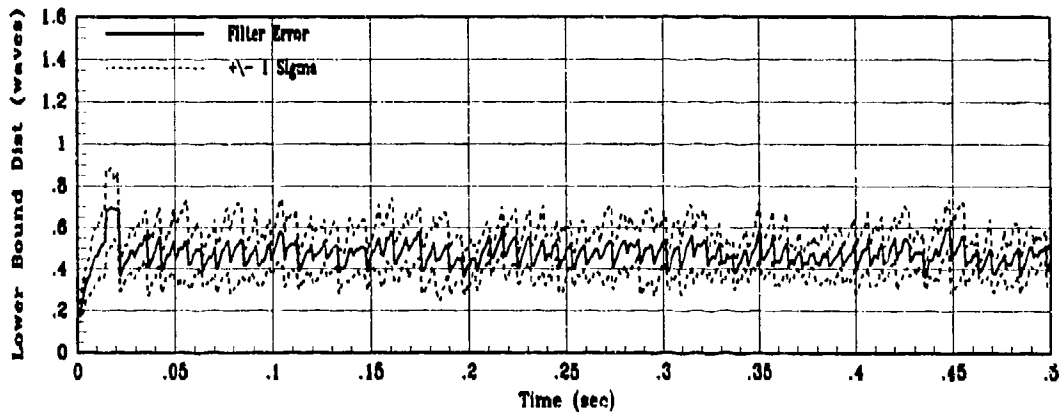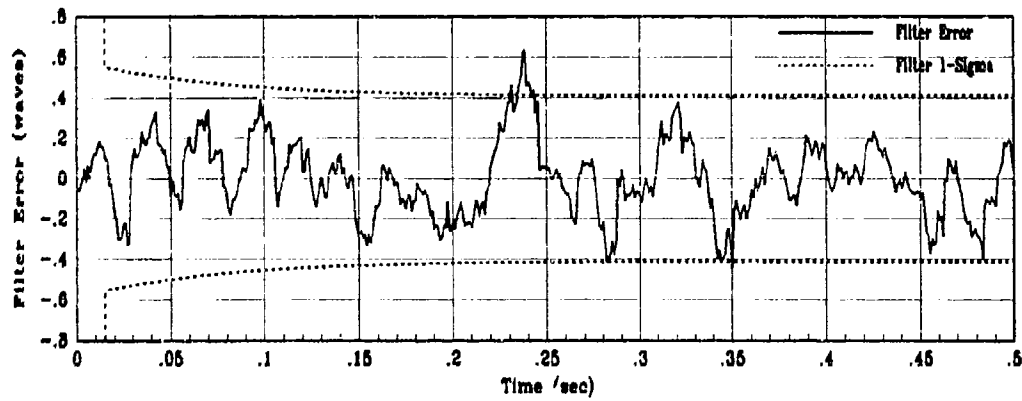

(b) RMS Filter Error for 10 MC Runs
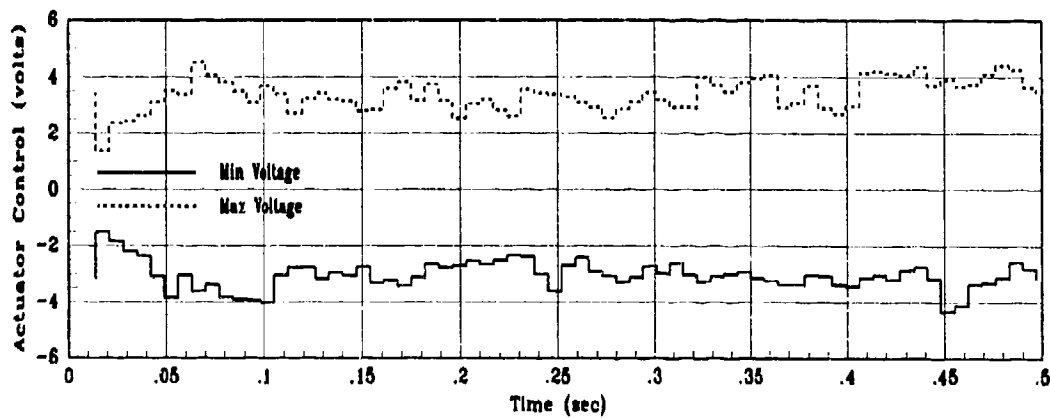
(c) Actuator Control Voltage Envelope

Figure J.8. Control System Performance for Average Winds of 15 m/sec
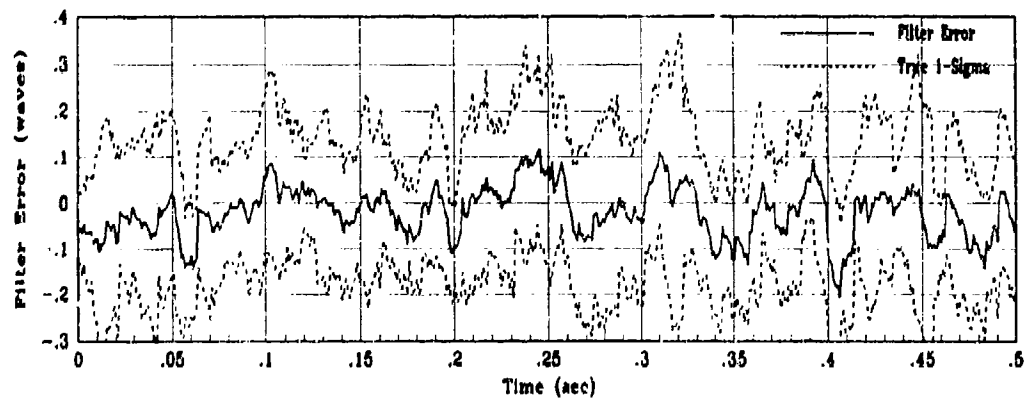
J-9
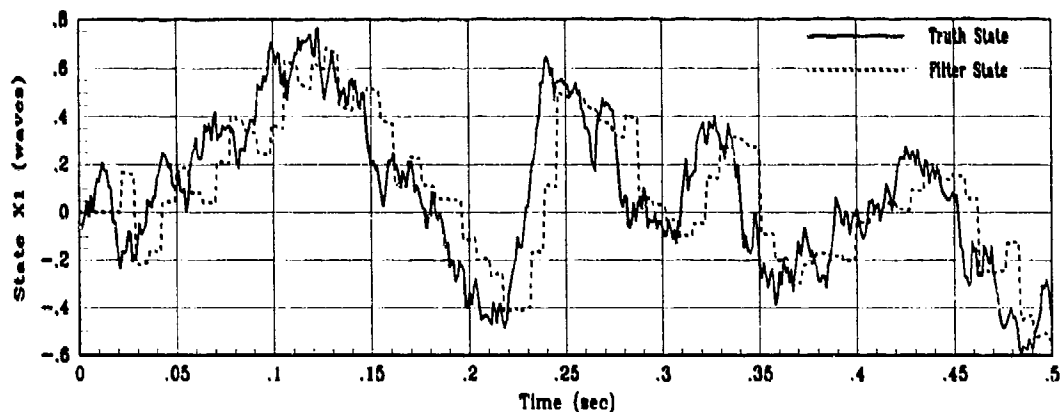
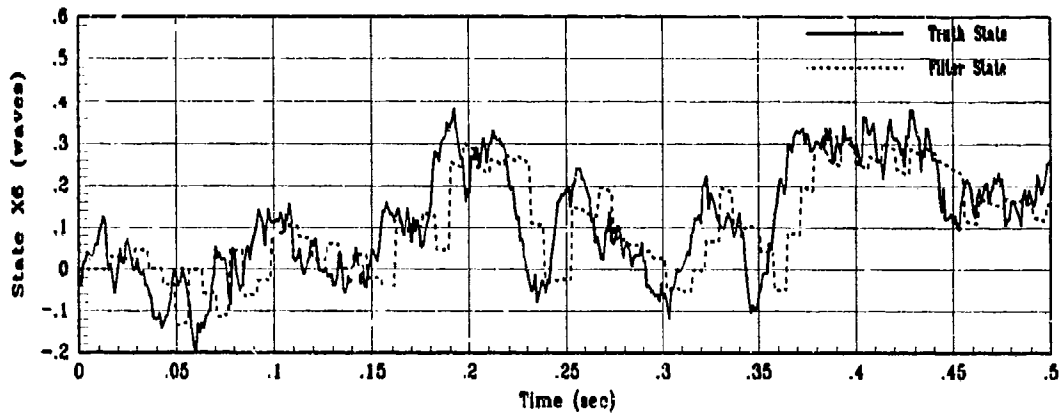(a) Truth and Filter States: XS1, XF1
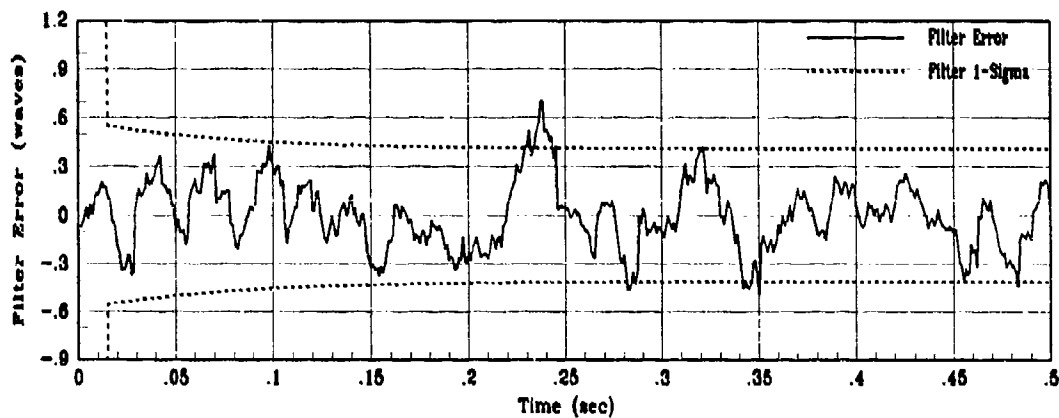
(b) X1 Filter Error for 1 MC Run

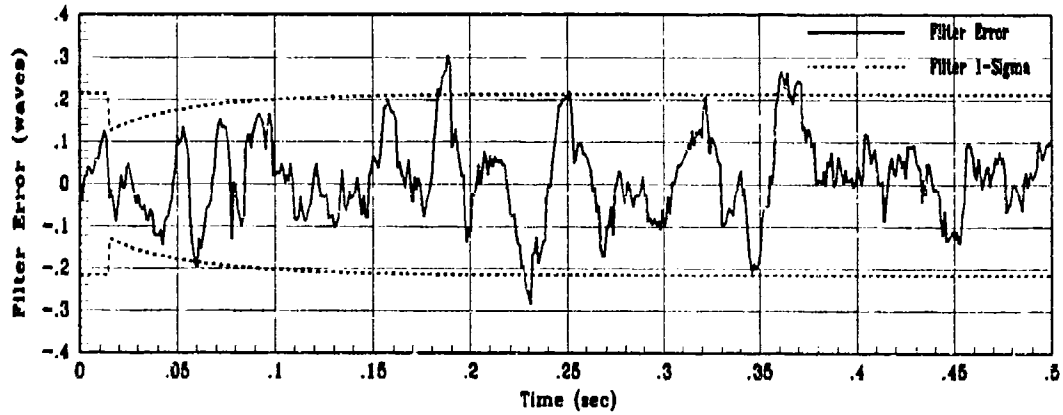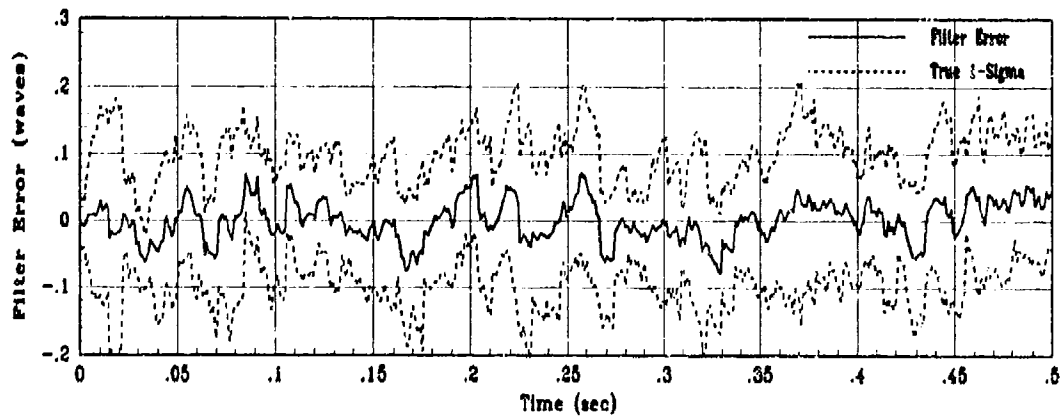(c) X1 True Filter Error for 10 MC Runs

Figure J.9. State 1 Filter Estimation Error for Average Winds of 35 m/sec

(a) Truth and Filter States: XS6, XF6
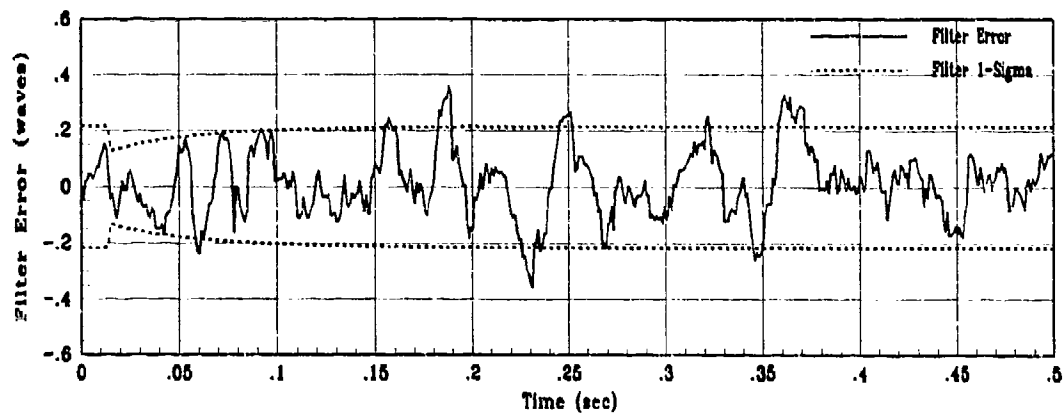
(b) X6 Filter Error for 1 MC Run
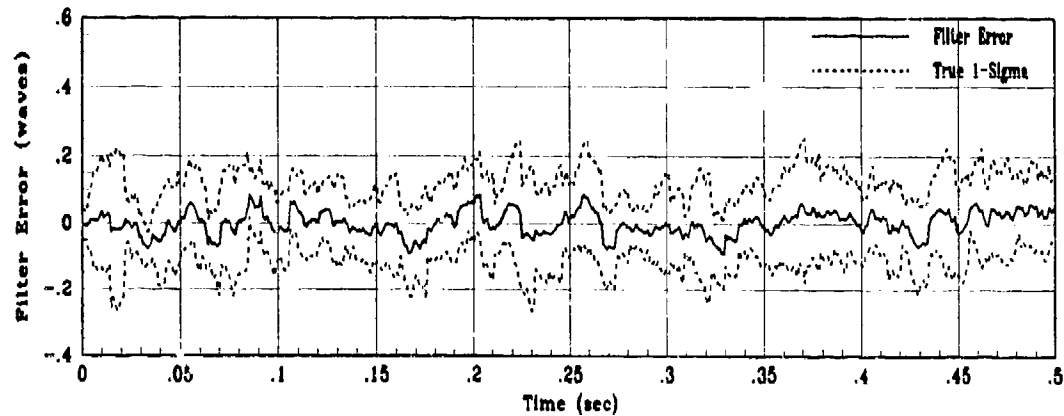
(c) X6 True Filter Error for 10 MC runs

Figure J.10. State 6 Filter Estimation Error for Average Winds of 35 m/sec
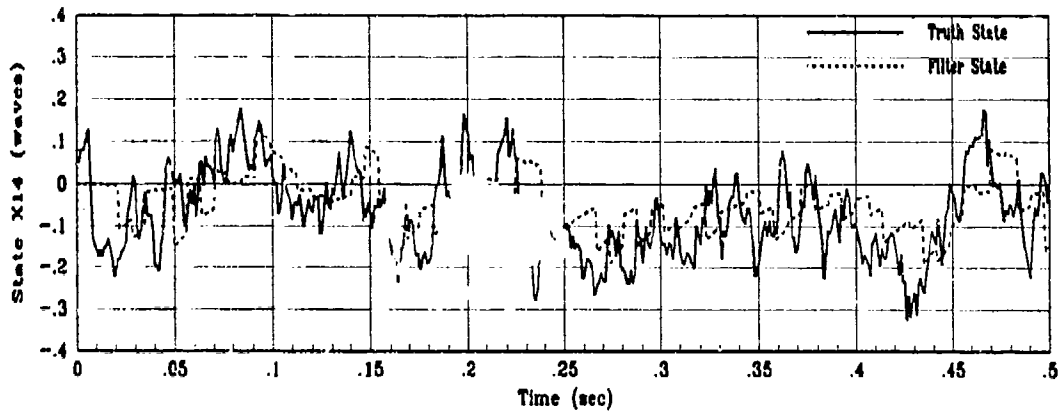
(a) Truth and Filter States: XS14, XF14
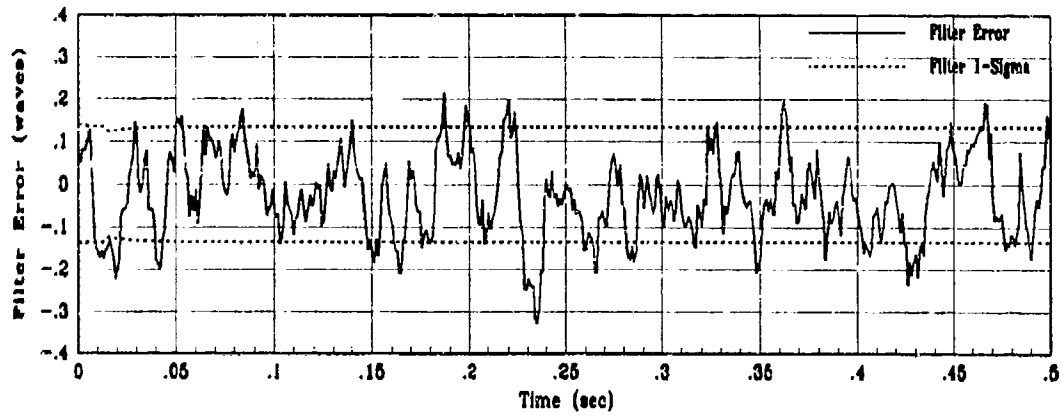
(b) X14 Filter Error for 1 MC Run
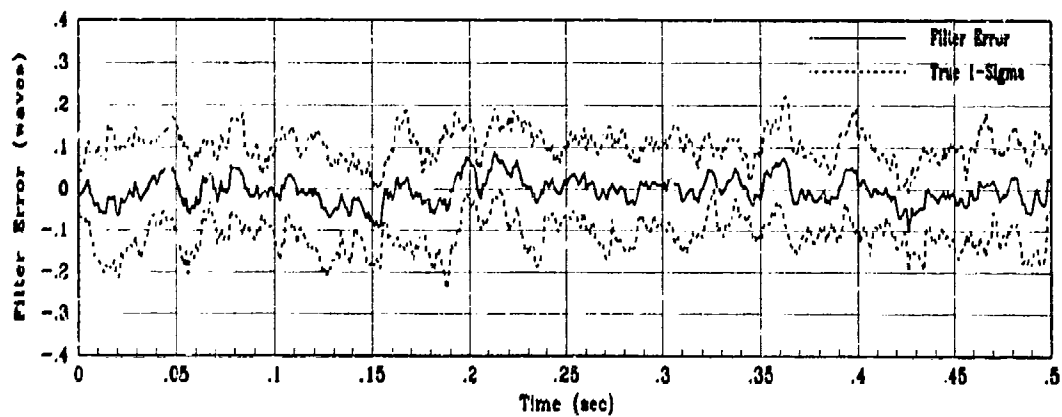
(c) X14 True Filter Error for 10 MC runs

Figure J.11. State 14 Filter Estimation Error for Average Winds of 35 m/sec

(a) Incident and Reflected RMS Phase Distortion for 10 MC Runs

(b) RMS Filter Error for 10 MC Runs

(c) Actuator Control Voltage Envelope

Figure J.12. Control System Performance for Average Winds of 35 m/sec

J-13
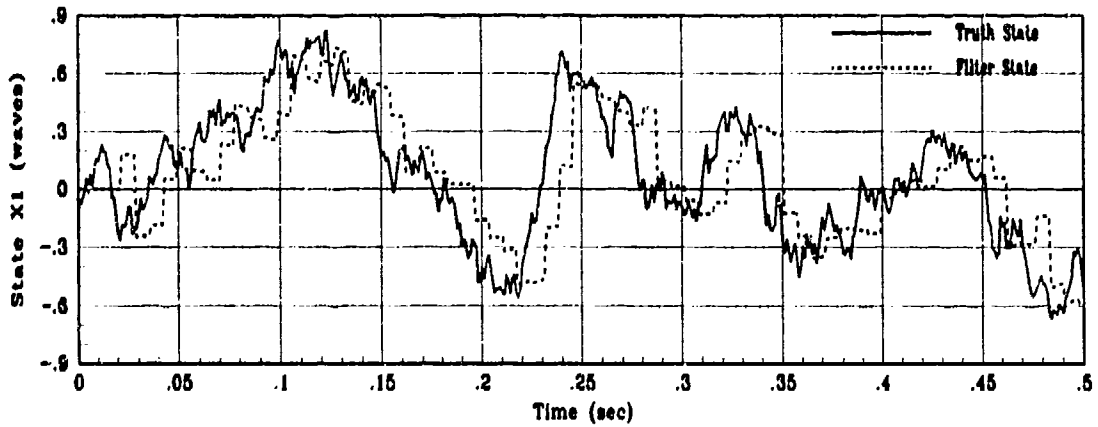
(a) Truth and Filter States: XS1, XF1

(b) X1 Filter Error for 1 MC Run
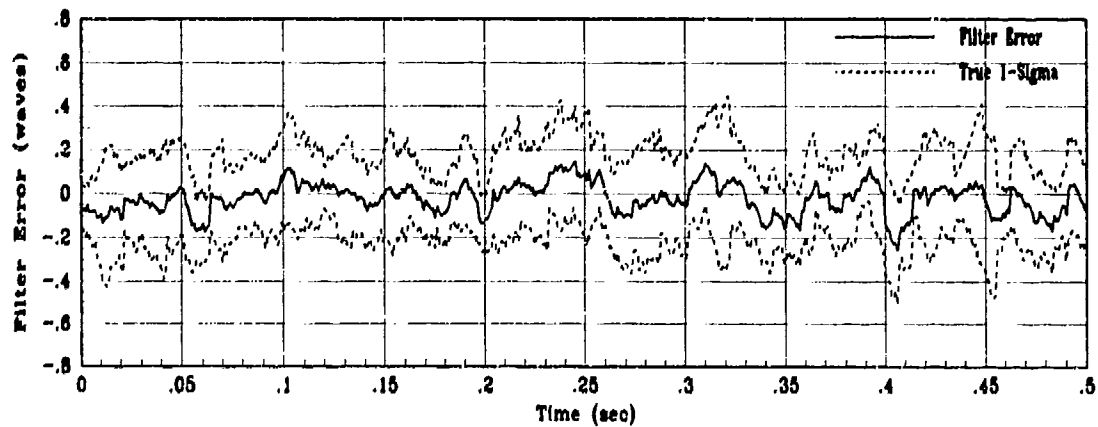
(c) X1 True Filter Error for 10 MC Runs

Figure J.13. State 1 Filter Estimation Error for Average Winds of 45 m/sec
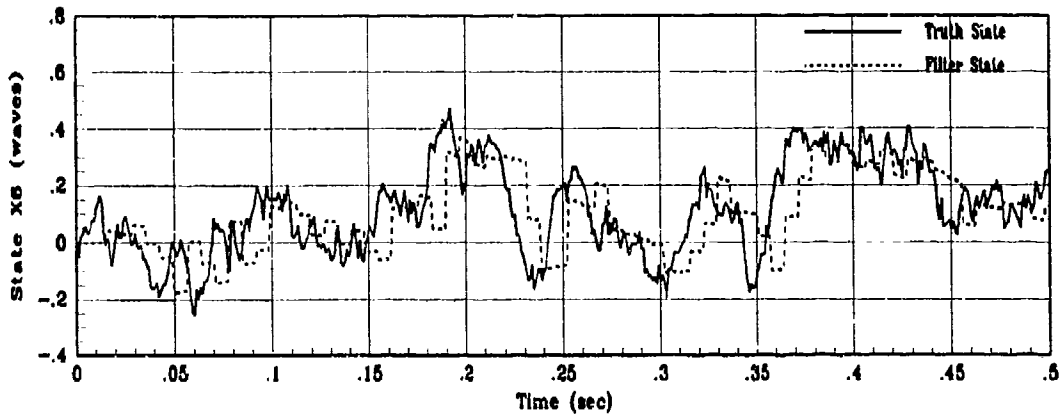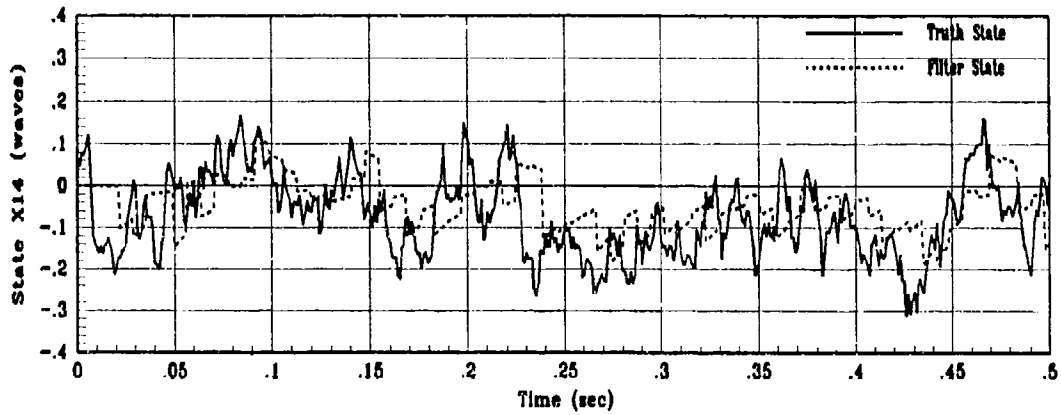
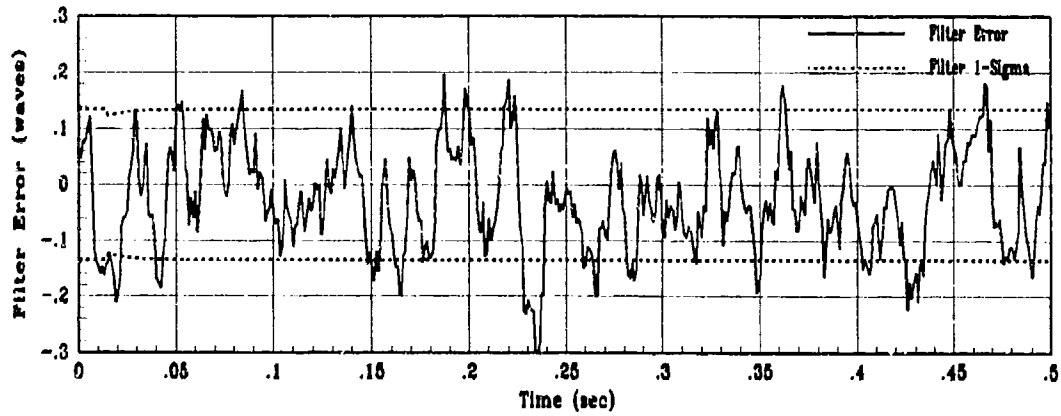(a) Truth and Filter States: XS6, XF6
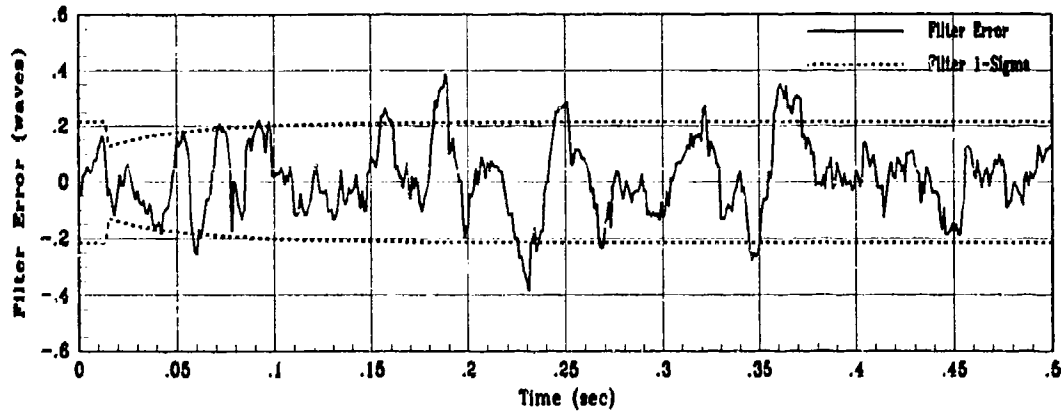
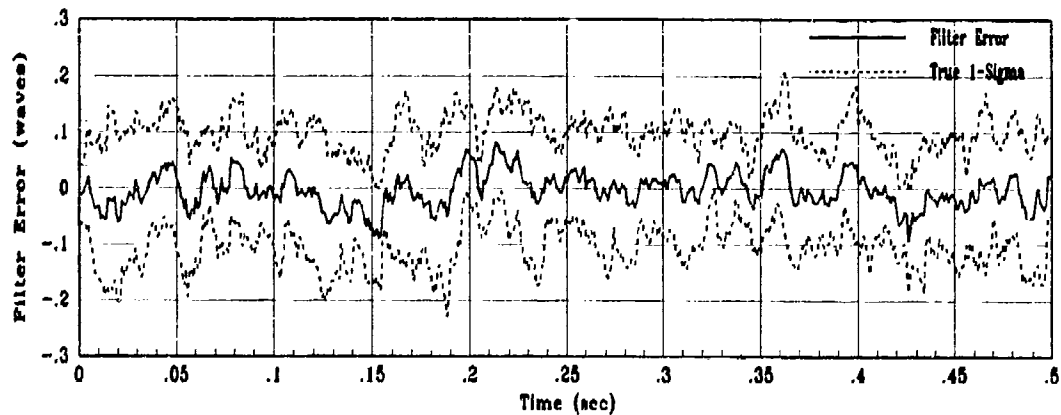(b) X6 Filter Error for 1 MC Run

(c) X6 True Filter Error for 10 MC runs

Figure J.14. State 6 Filter Estimation Error for Average Winds of 45 m/sec
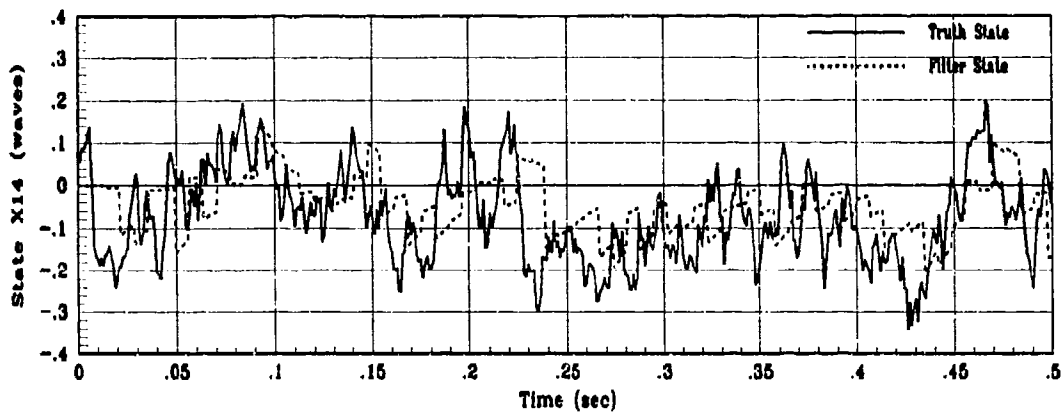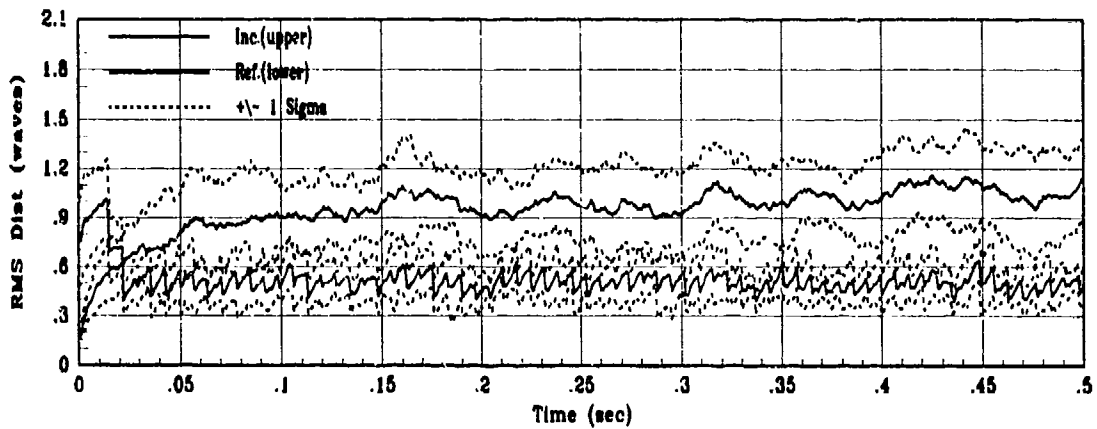
J-15

(a) Truth and Filter States: XS14, XF14
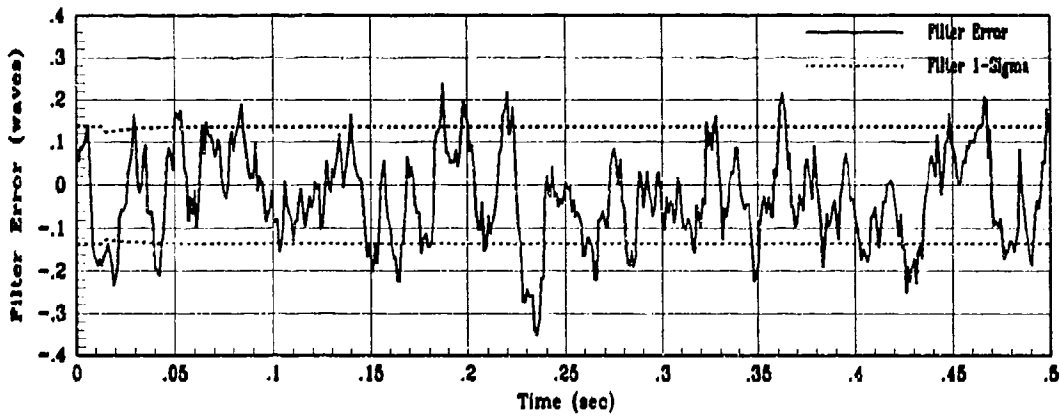
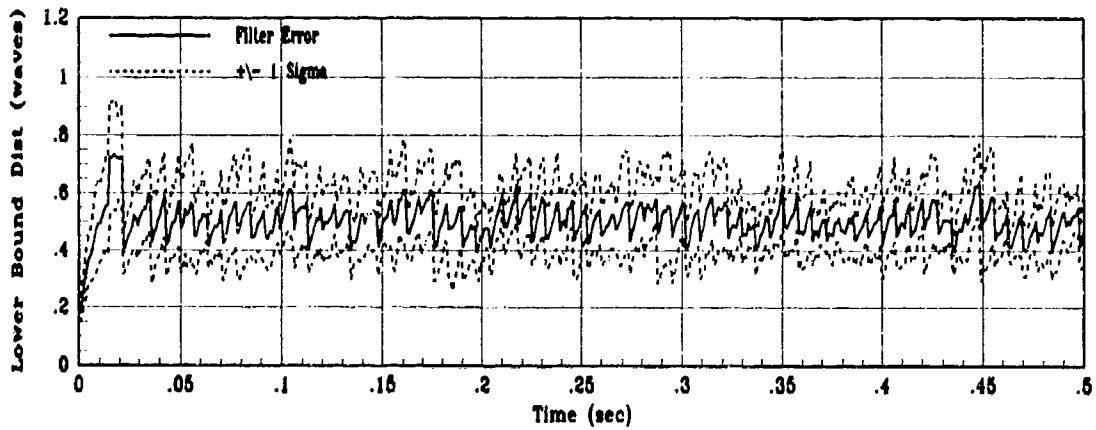(b) X14 Filter Error for 1 MC Run
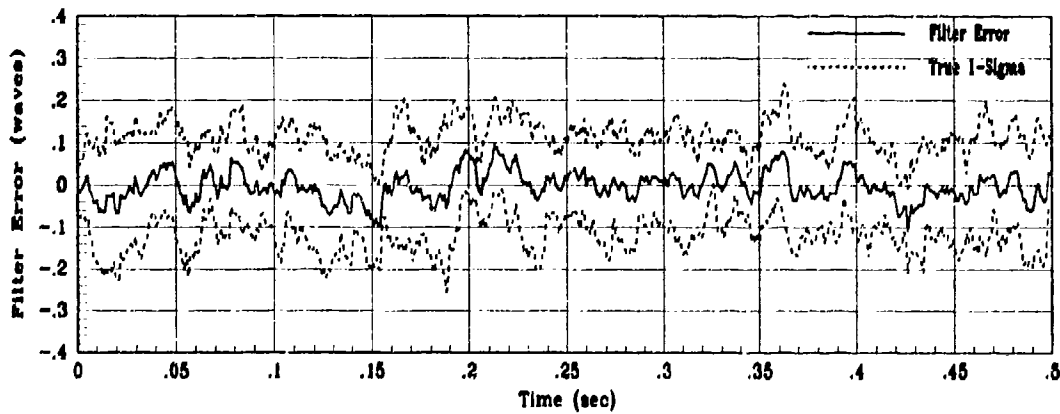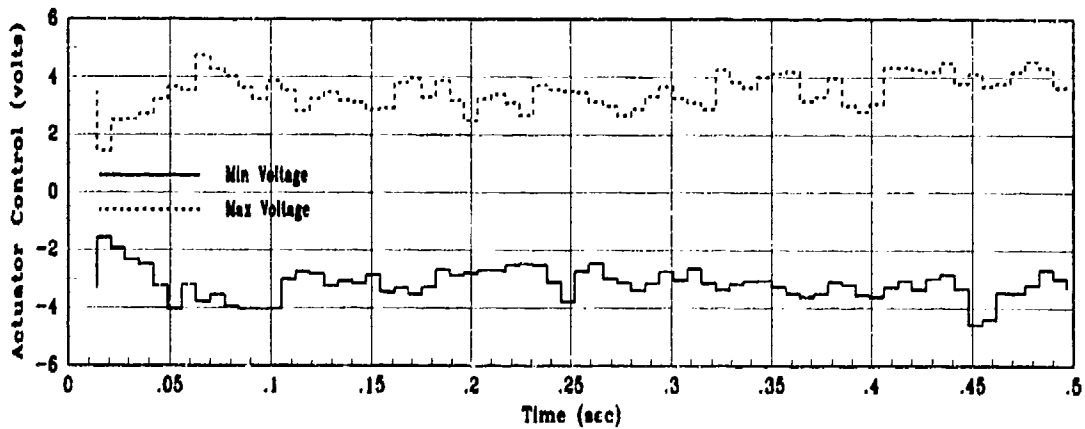

(c) X14 True Filter Error for 10 MC runs

Figure J.15. State 14 Filter Estimation Error for Average Winds of 45 m/sec
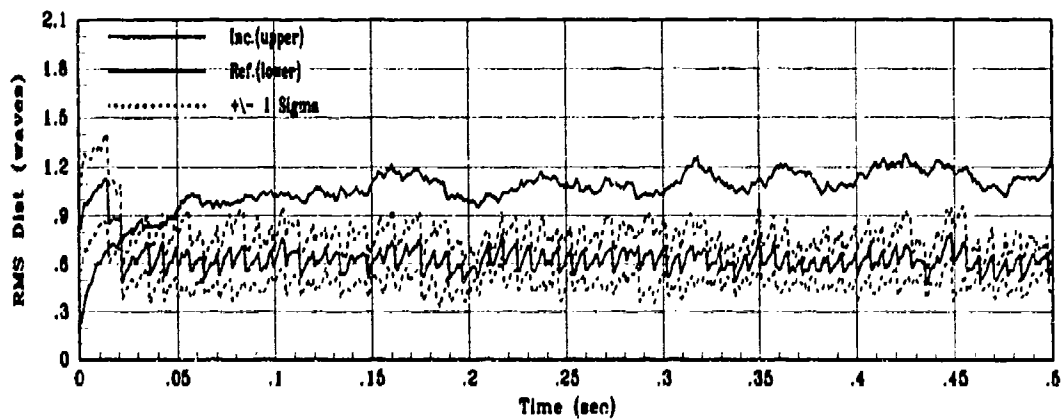
(a) Incident and Reflected RMS Phase Distortion for 10 MC Runs
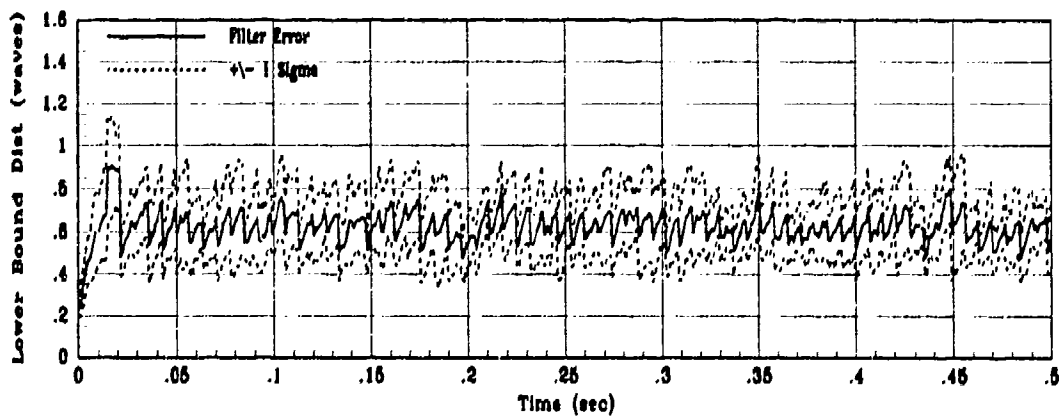
(b) RMS Filter Error for 10 MC Runs
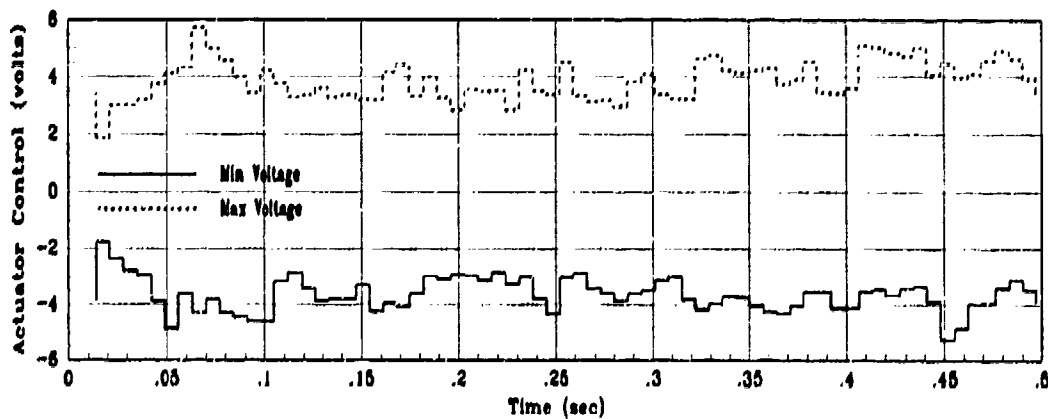
(c) Actuator Control Voltage Envelope

Figure J.16. Control System Performance for Average Winds of 45 m/sec
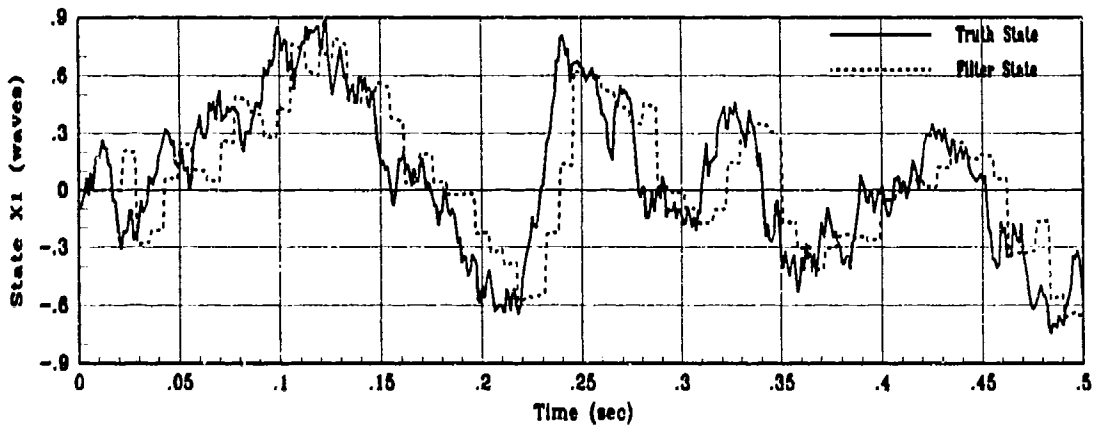
(a) Truth and Filter States: XS1, XF1
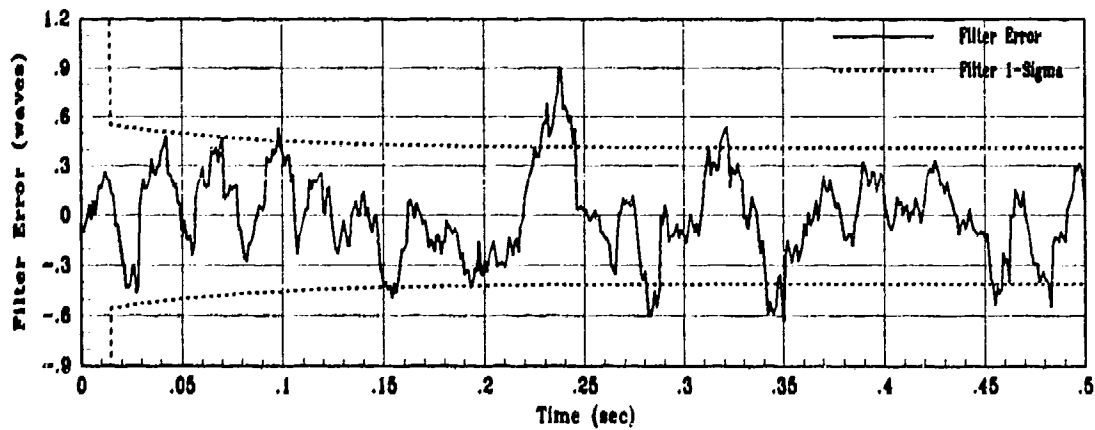
(b) X1 Filter Error for 1 MC Run
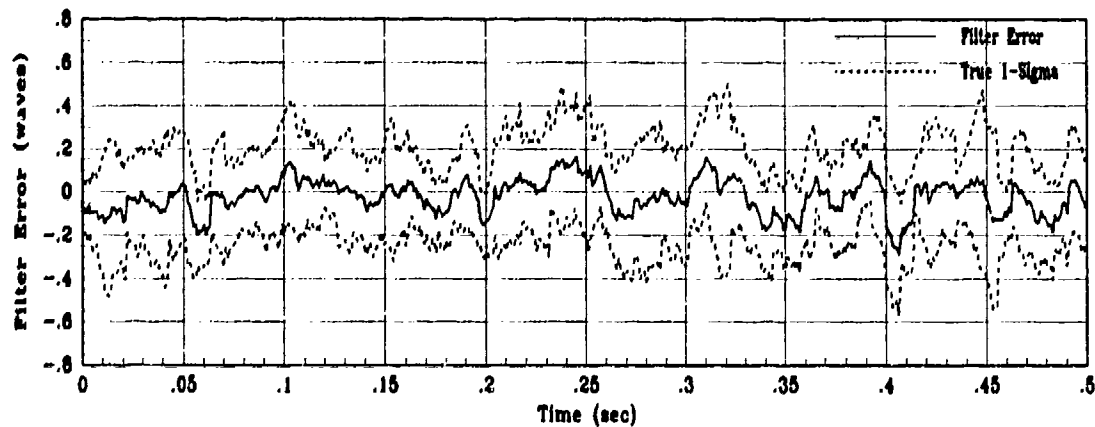
(c) X1 True Filter Error for 10 MC Runs

Figure J.17. State 1 Filter Estimation Error for Average Winds of 55 m/sec
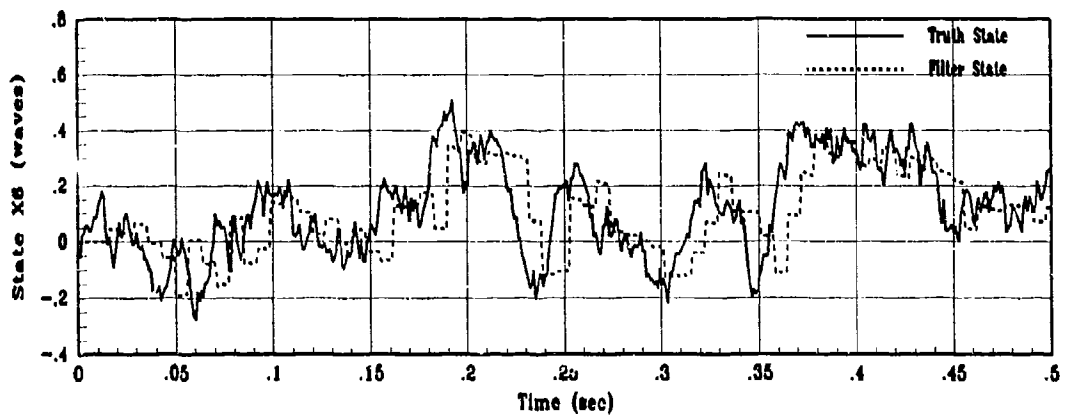
(a) Truth and Filter States: XS6, XF6
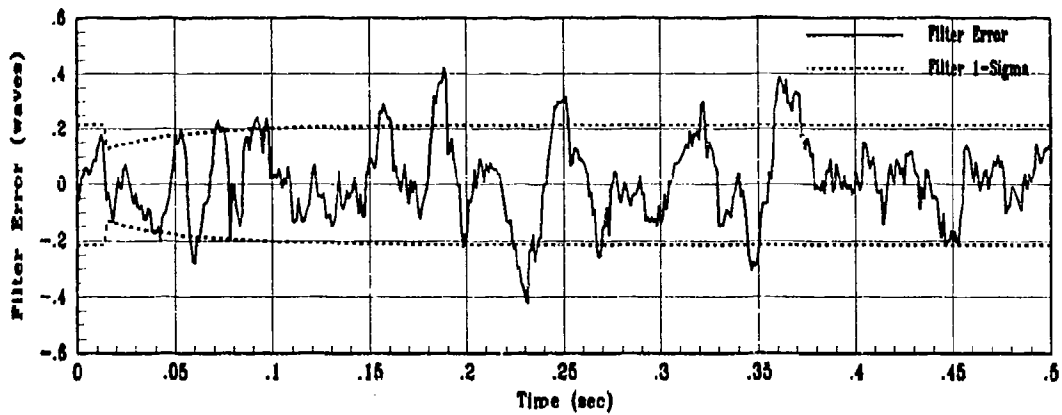
(b) X6 Filter Error for 1 MC Run
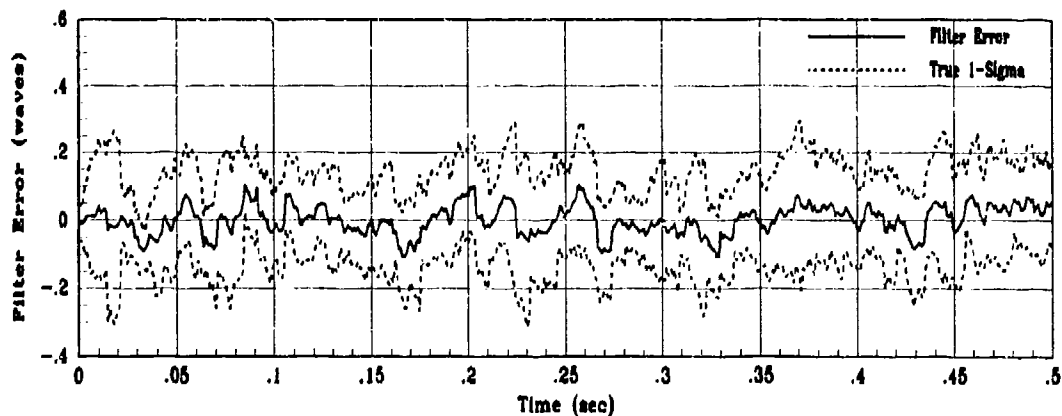
(c) X6 True Filter Error for 10 MC runs

Figure J.18. State 6 Filter Estimation Error for Average Winds of 55 m/sec
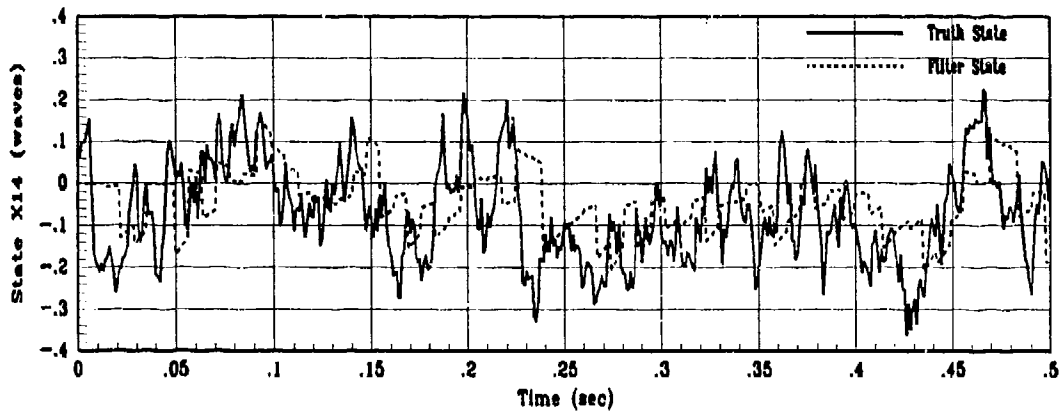
(a) Truth and Filter States: XS14, XF14

(b) X14 Filter Error for 1 MC Run

(c) X14 True Filter Error for 10 MC runs

Figure J.19. State 14 Filter Estimation Error for Average Winds of 55 m/sec

(a) Incident and Reflected RMS Phase Distortion for 10 MC Runs
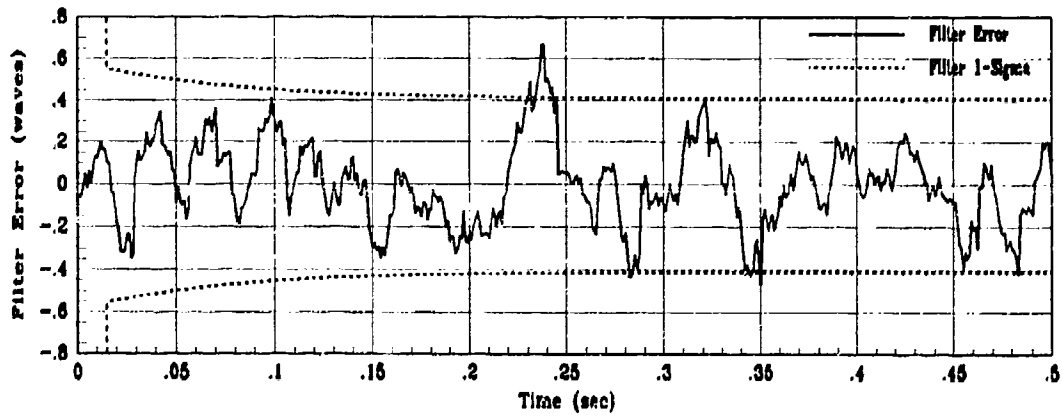

(b) RMS Filter Error for 10 MC Runs
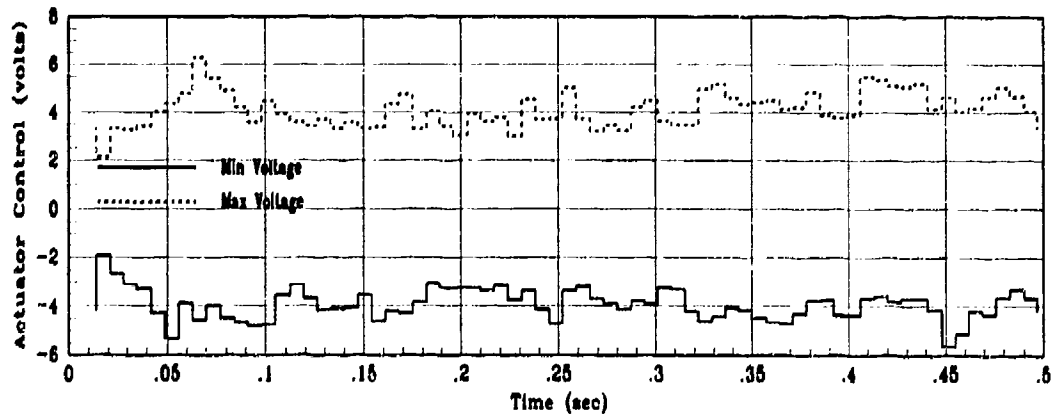
(c) Actuator Control Voltage Envelope
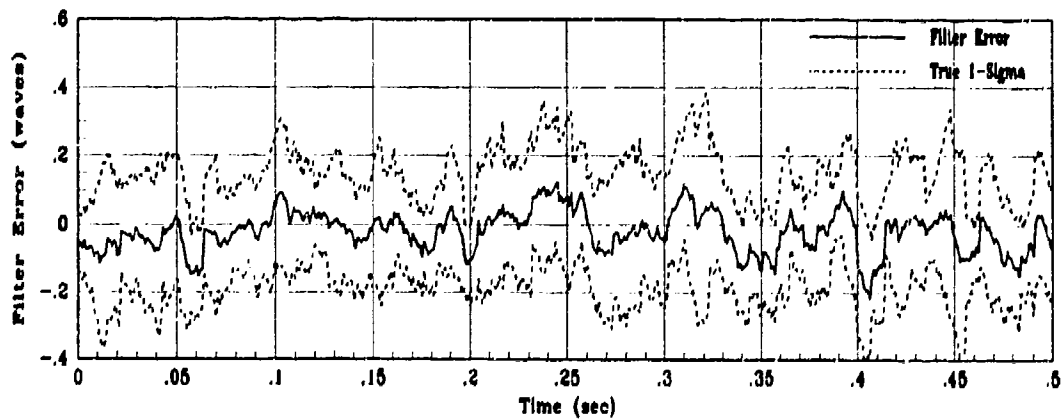
Figure J.20. Control System Performance for Average Winds of 55 m/sec

J-21
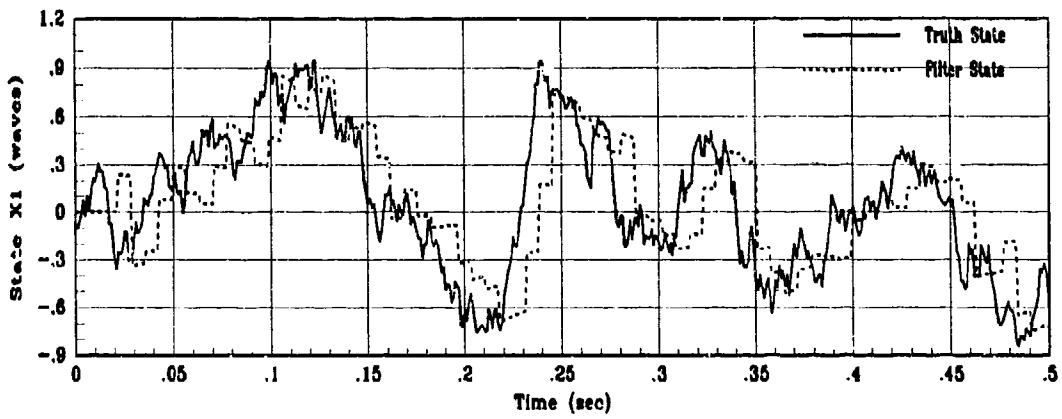
(a) Truth and Filter States: XS1, XF1

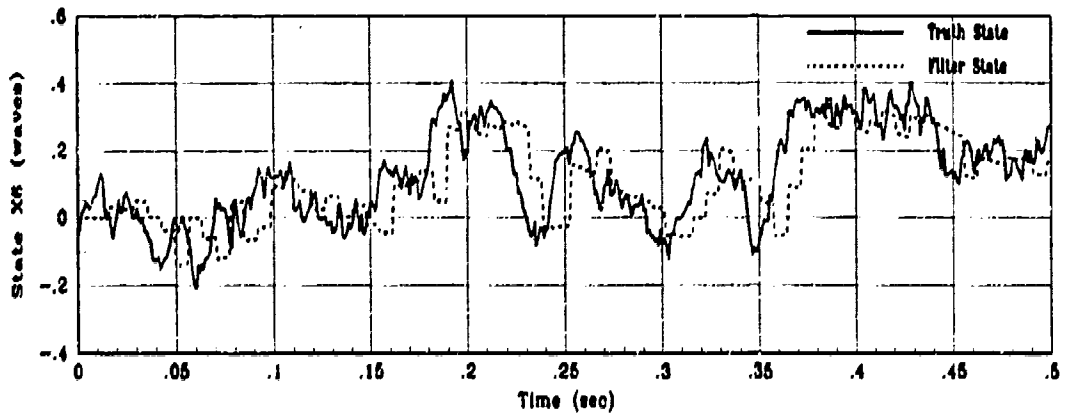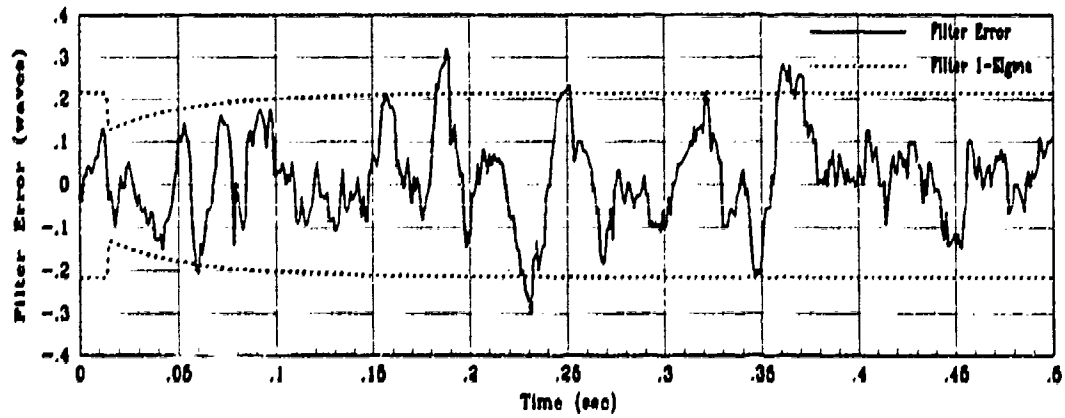(b) X1 Filter Error for 1 MC Run

(c) X1 True Filter Error for 10 MC Runs

Figure J.21. State 1 Filter Estimation Error for Average Winds of 65 m/sec
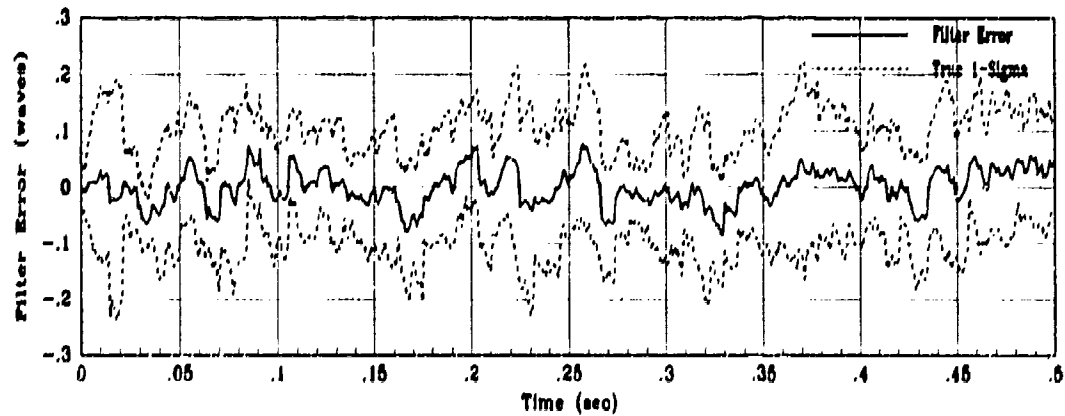
(a) Truth and Filter States: XS6, XF6

(b) X6 Filter Error for 1 MC Run

(c) X6 True Filter Error for 10 MC runs

Figure J.22. State 6 Filter Estimation Error for Average Winds of 65 m/sec

(a) Truth and Filter States: XS14, XF14

(b) X14 Filter Error for 1 MC Run

(c) X14 True Filter Error for 10 MC runs

Figure J.23. State 14 Filter Estimation Error for Average Winds of 65 m/sec

(a) Incident and Reflected RMS Phase Distortion for 10 MC Runs

(b) RMS Filter Error for 10 MC Runs

(c) Actuator Control Voltage Envelope

Figure J.24. Control System Performance for Average Winds of 65 m/sec

(a) Truth and Filter States: XS1, XF1

(b) X1 Filter Error for 1 MC Run

(c) X1 True Filter Error for 10 MC Runs

Figure J.25. State 1 Filter Estimation Error for Zenith Angle of 15 deg
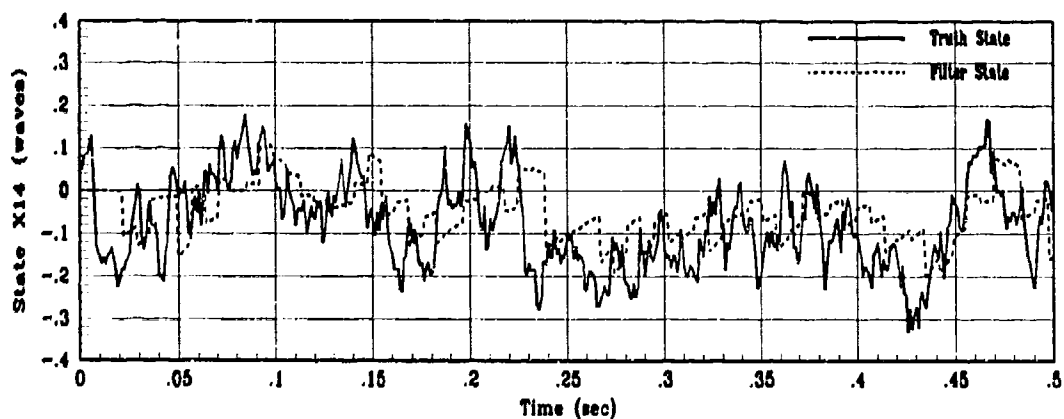
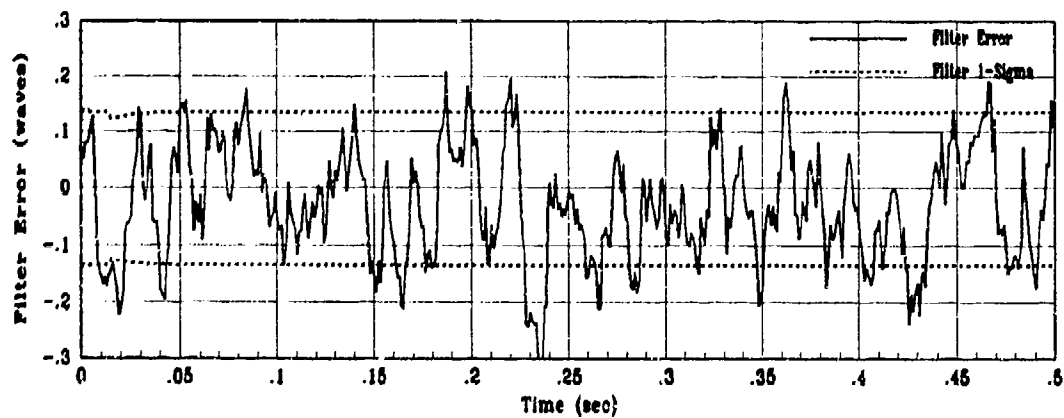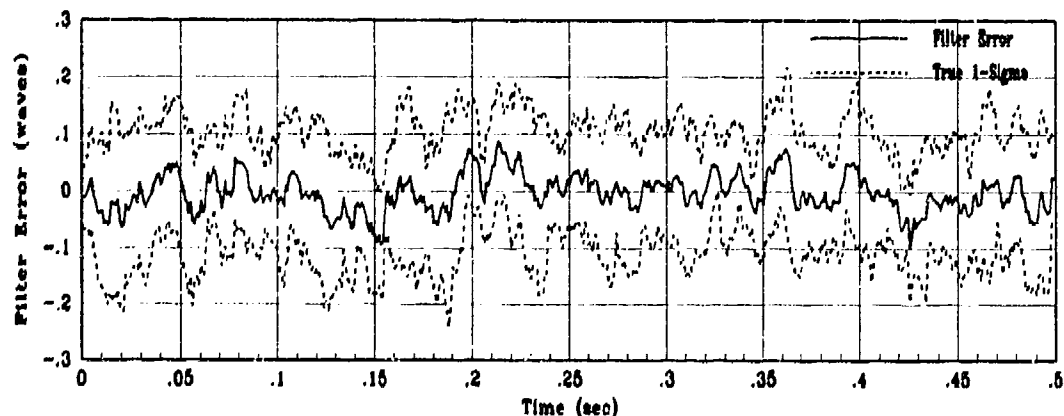(a) Truth and Filter States: XS6, XF6

(b) X6 Filter Error for 1 MC Run

(c) X6 True Filter Error for 10 MC runs

Figure J.26.   State 6 Filter Estimation Error for Zenith Angle of 15 deg

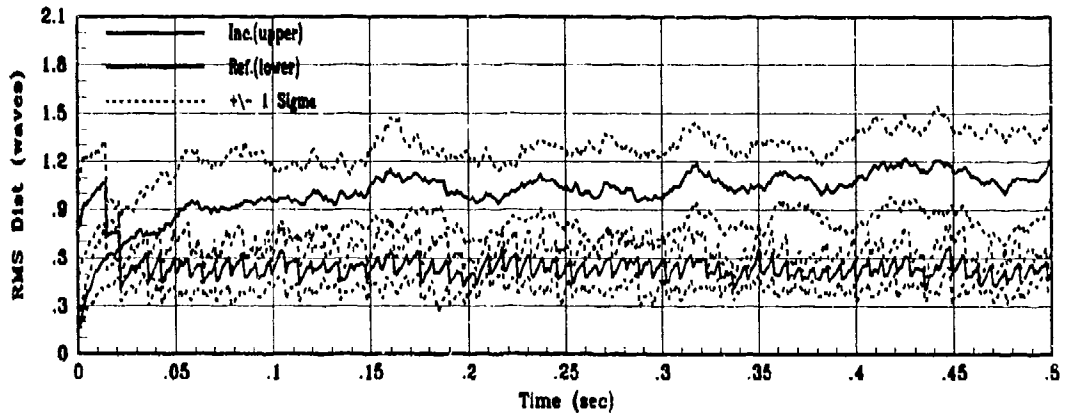(a) Truth and Filter States: XS14, XF14

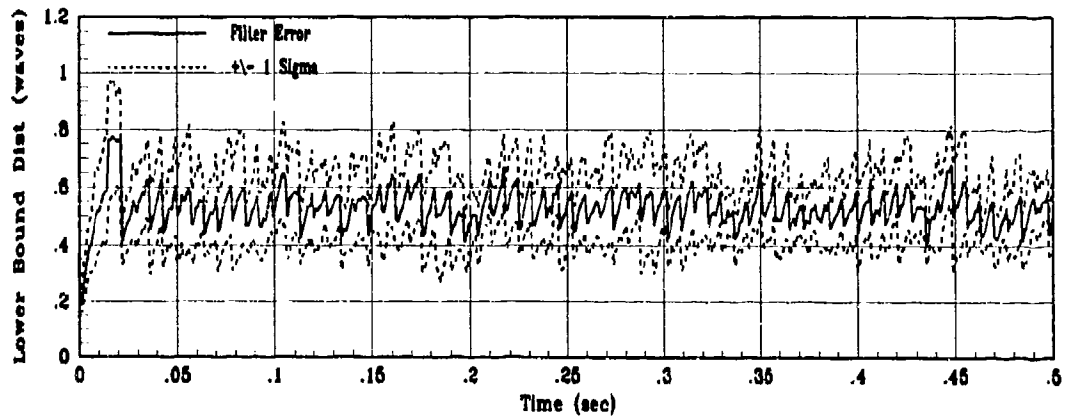(b) X14 Filter Error for 1 MC Run

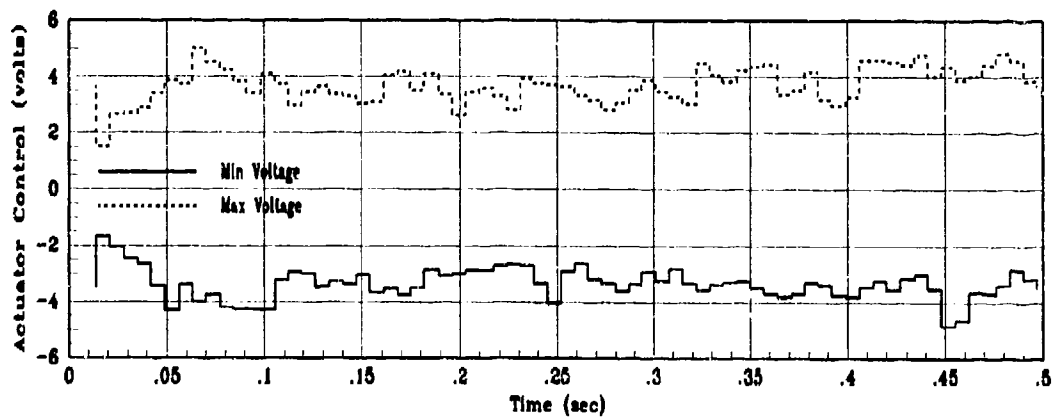(c) X14 True Filter Error for 10 MC runs

Figure J.27. State 14 Filter Estimation Error for Zenith Angle of 15 deg

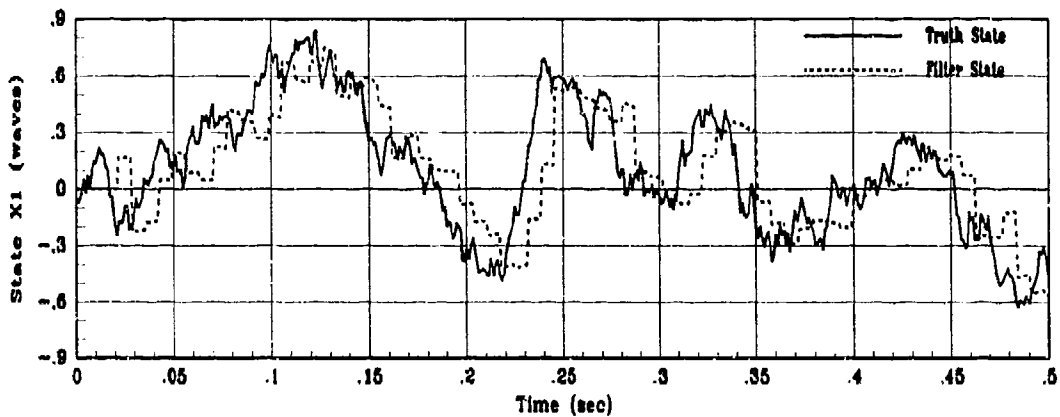(a) Incident and Reflected RMS Phase Distortion for 10 MC Runs
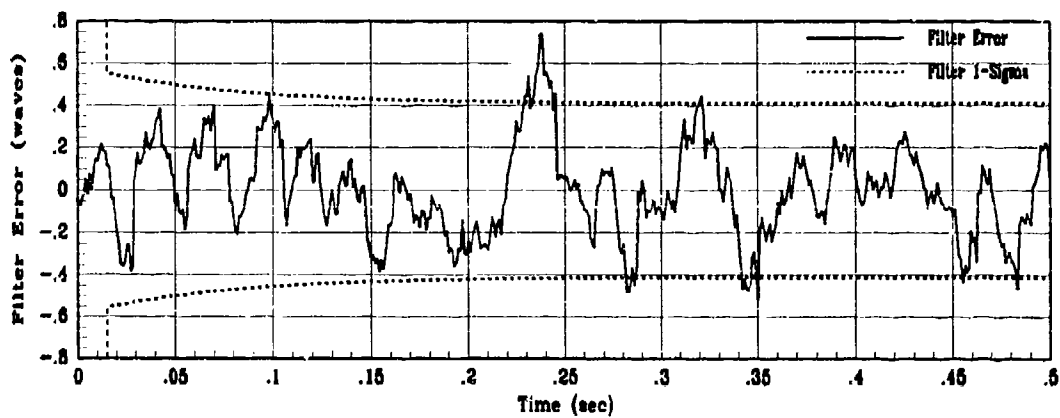
(b) RMS Filter Error for 10 MC Runs

(c) Actuator Control Voltage Envelope

Figure J.28. Control System Performance for Zenith Angle of 15 deg
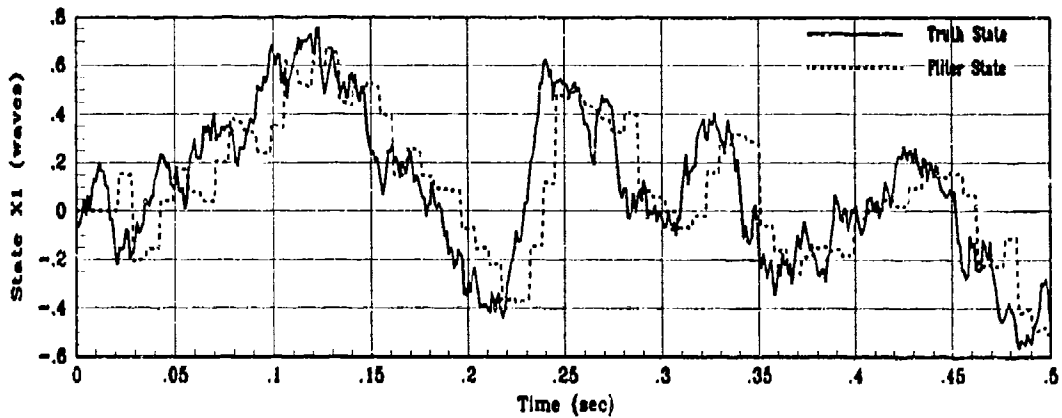
(a) Truth and Filter States: XS1, XF1

(b) X1 Filter Error for 1 MC Run

(c) X1 True Filter Error for 10 MC Runs

Figure J.29. State 1 Filter Estimation Error for Zenith Angle of 30 deg

(a) Truth and Filter States: XS6, XF6

(b) X6 Filter Error for 1 MC Run

(c) X6 True Filter Error for 10 MC runs

Figure J.30. State 6 Filter Estimation Error for Zenith Angle of 30 deg

J-31

(a) Truth and Filter States: XS14, XF14

(b) X14 Filter Error for 1 MC Run

(c) X14 True Filter Error for 10 MC runs

Figure J.31. State 14 Filter Estimation Error for Zenith Angle of 30 deg

(a) Incident and Reflected RMS Phase Distortion for 10 MC Runs

(b) RMS Filter Error for 10 MC Runs

(c) Actuator Control Voltage Envelope

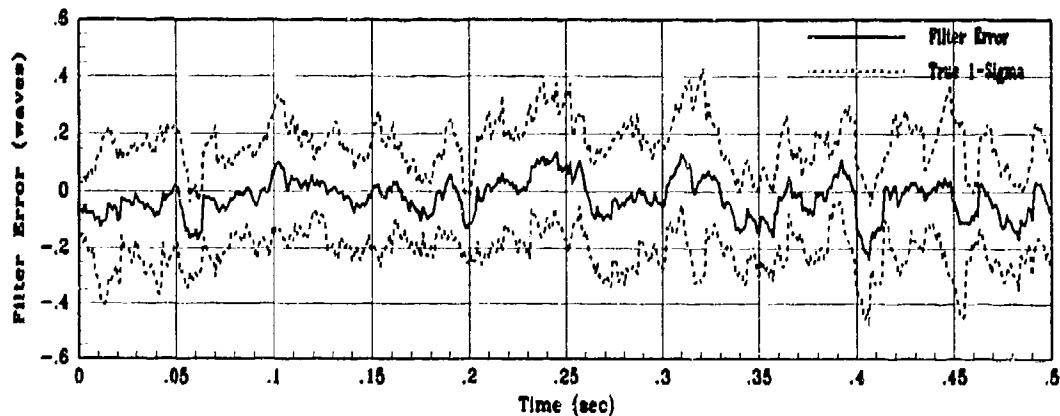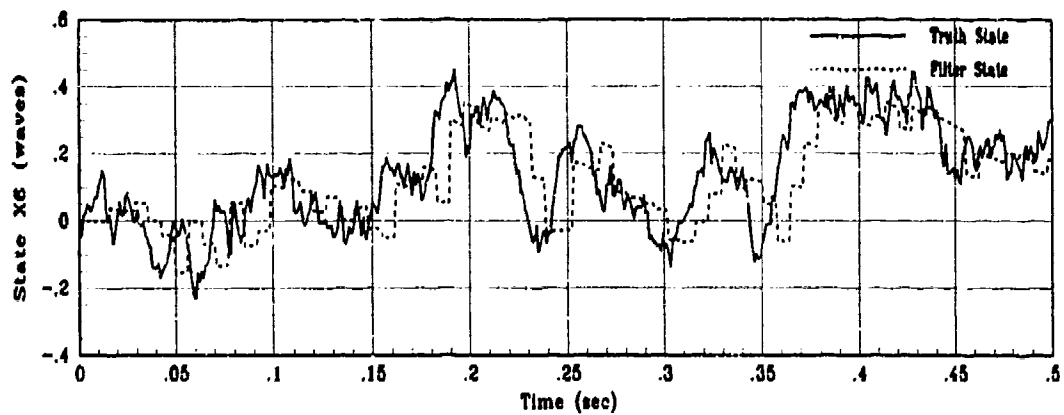Figure J.32. Control System Performance for Zenith Angle of 30 deg

(a) Truth and Filter States: XS1, XF1
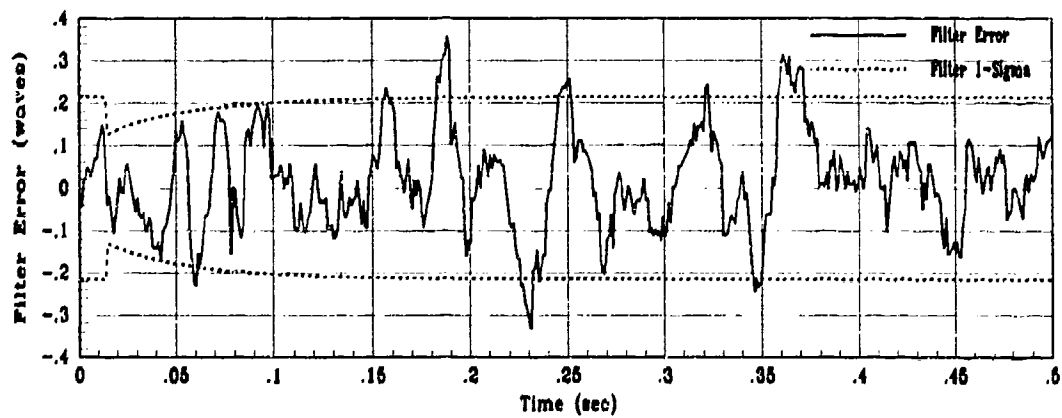

(b) X1 Filter Error for 1 MC Run

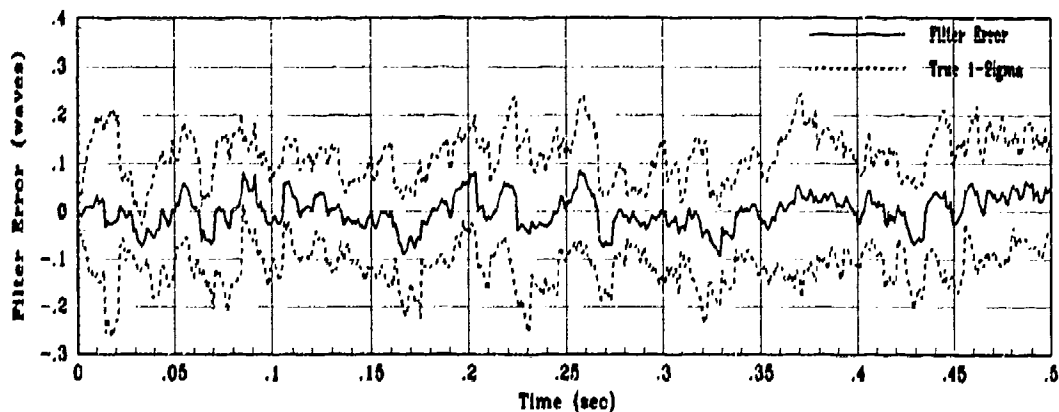(c) X1 True Filter Error for 10 MC Runs

Figure J.33. State 1 Filter Estimation Error for Zenith Angle of 45 deg

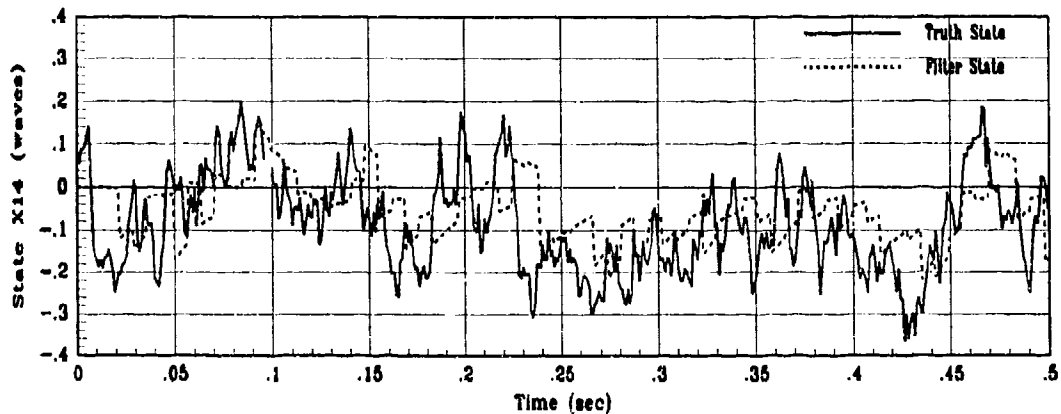(a) Truth and Filter States: XS6, XF6
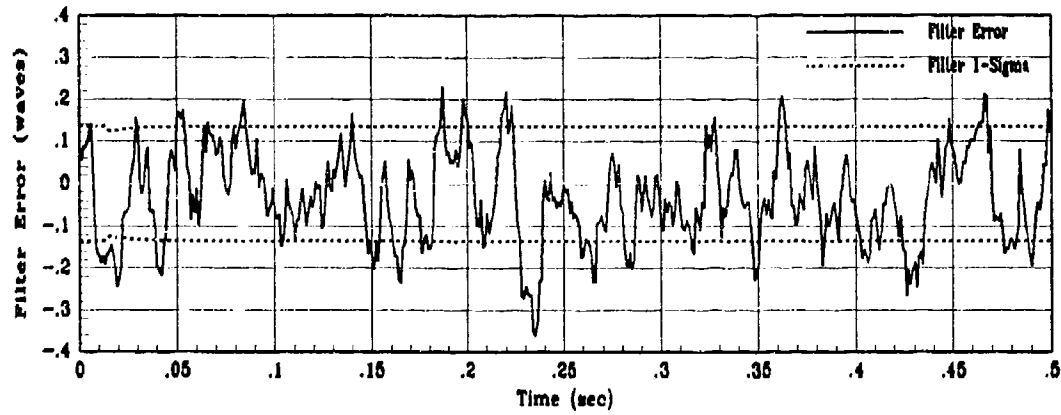
(b) X6 Filter Error for 1 MC Run
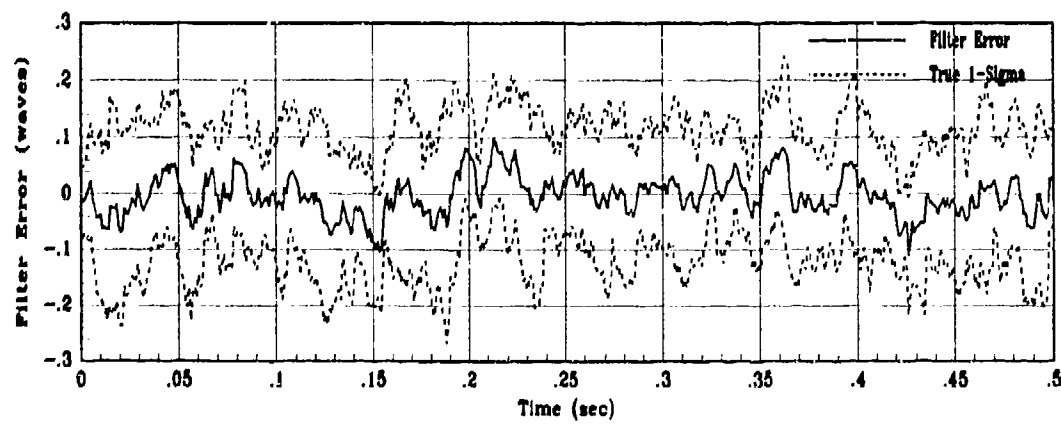
(c) X6 True Filter Error for 10 MC runs

Figure J.34. State 6 Filter Estimation Error for Zenith Angle of 45 deg

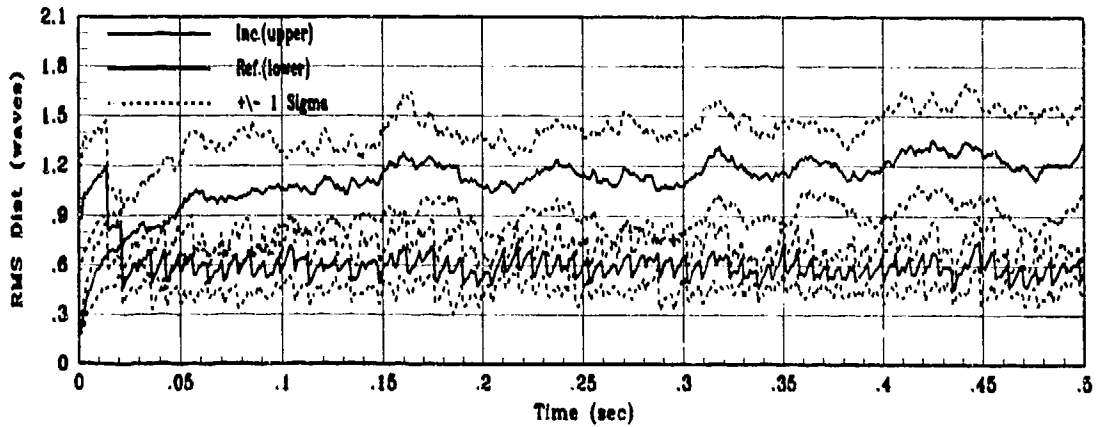(a) Truth and Filter States: XS14, XF14
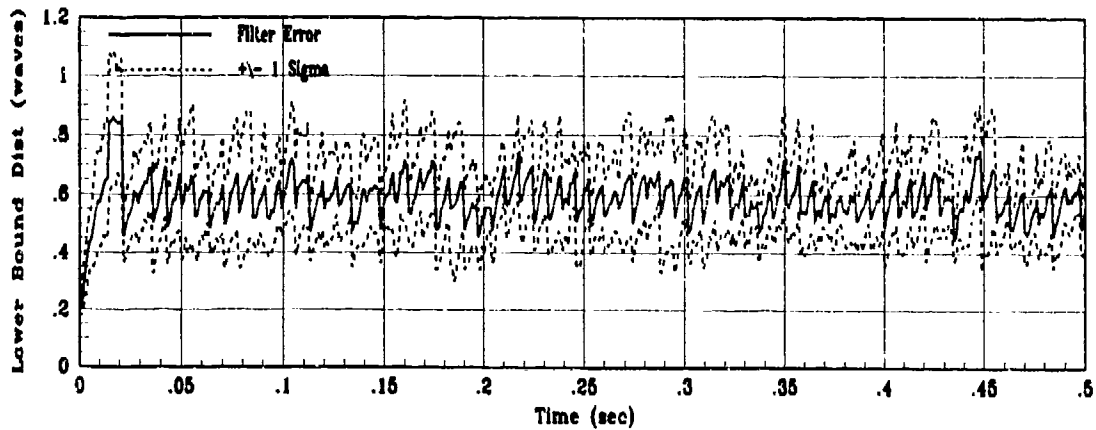
(b) X14 Filter Error for 1 MC Run

(c) X14 True Filter Error for 10 MC runs

Figure J.35. State 14 Filter Estimation Error for Zenith Angle of 45 deg

(a) Incident and Reflected RMS Phase Distortion for 10 MC Runs

(b) RMS Filter Error for 10 MC Runs

(c) Actuator Control Voltage Envelope

Figure J.36. Control System Performance for Zenith Angle of 45 deg

(a) Truth and Filter States: XS1, XF1

(b) X1 Filter Error for 1 MC Run
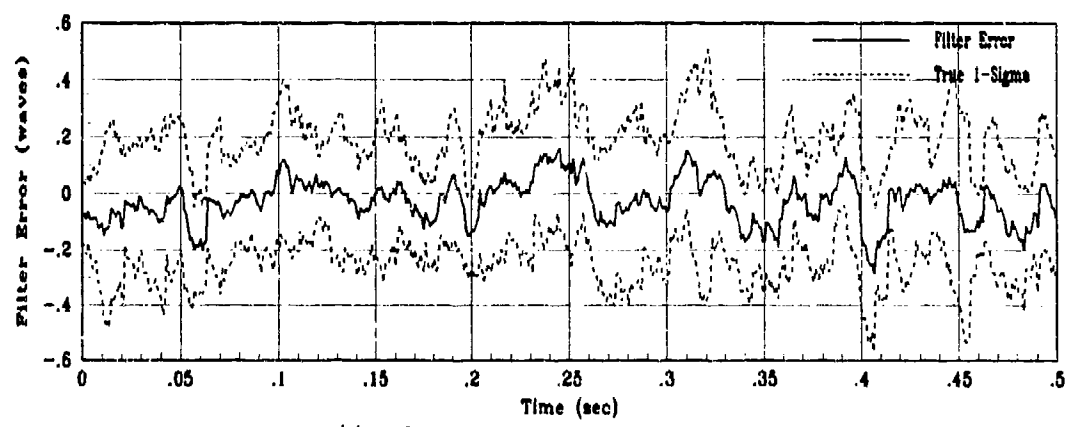
(c) X1 True Filter Error for 10 MC Runs

Figure J.37. State 1 Filter Estimation Error for Zenith Angle of 60 deg

(a) Truth and Filter States: XS6, XF6

(b) X6 Filter Error for 1 MC Run

(c) X6 True Filter Error for 10 MC runs

Figure J.38. State 6 Filter Estimation Error for Zenith Angle of 60 deg

(a) Truth and Filter States: XS14, XF14

(b) X14 Filter Error for 1 MC Run
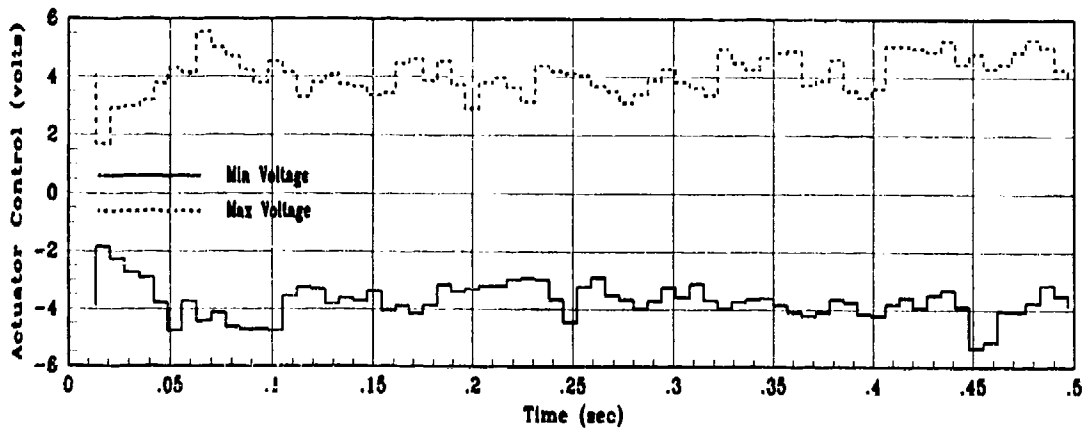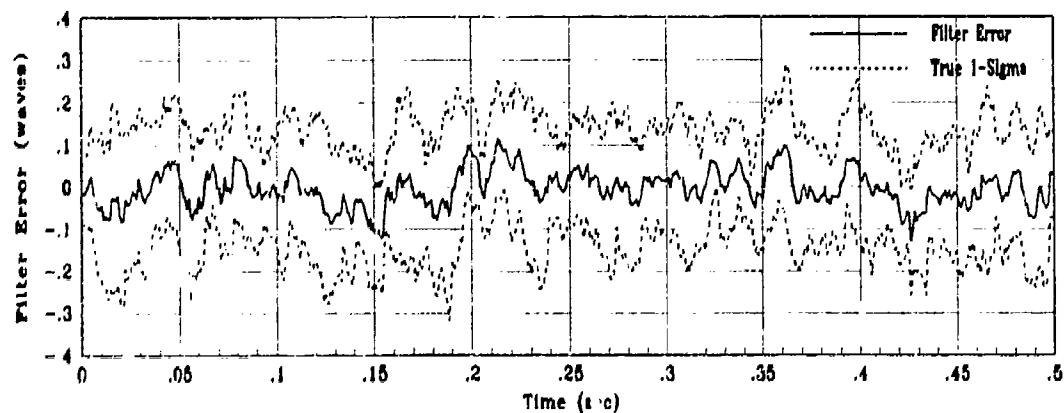
(c) X14 True Filter Error for 10 MC runs

Figure J.39. State 14 Filter Estimation Error for Zenith Angle of 60 deg

(a) Incident and Reflected RMS Phase Distortion for 10 MC Runs
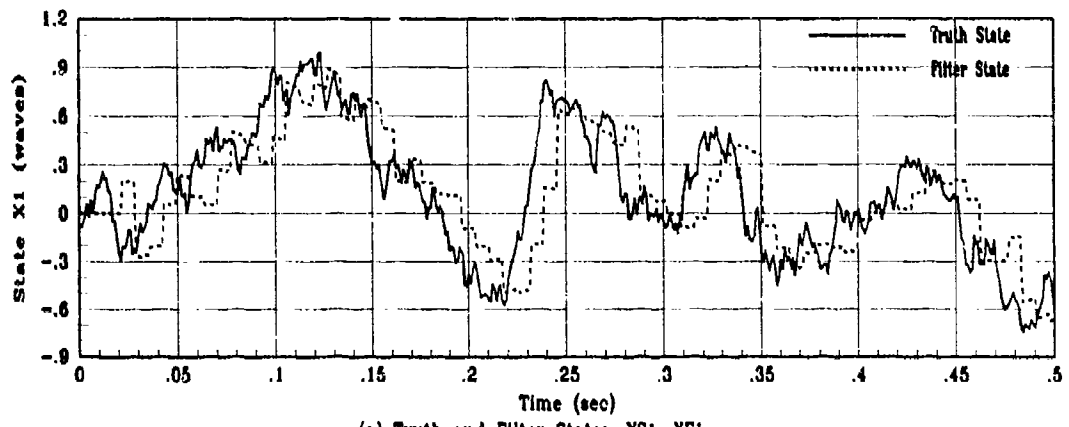
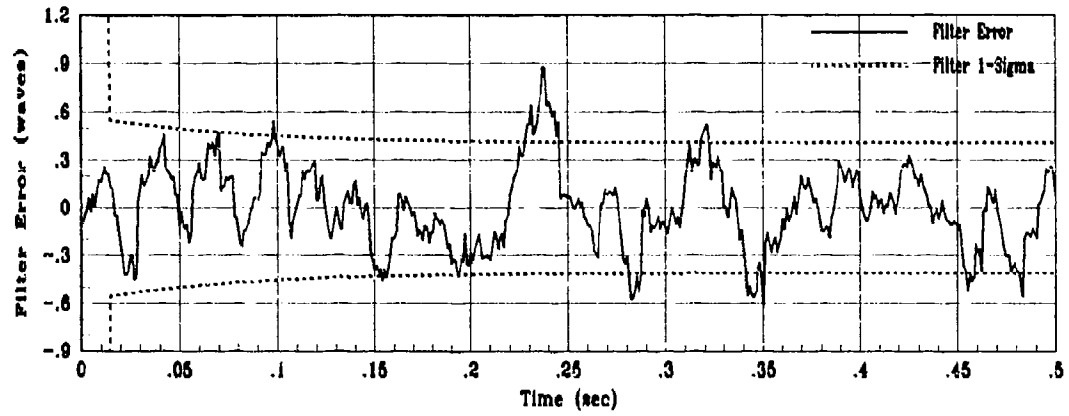(b) RMS Filter Error for 10 MC Runs

(c) Actuator Control Voltage Envelope

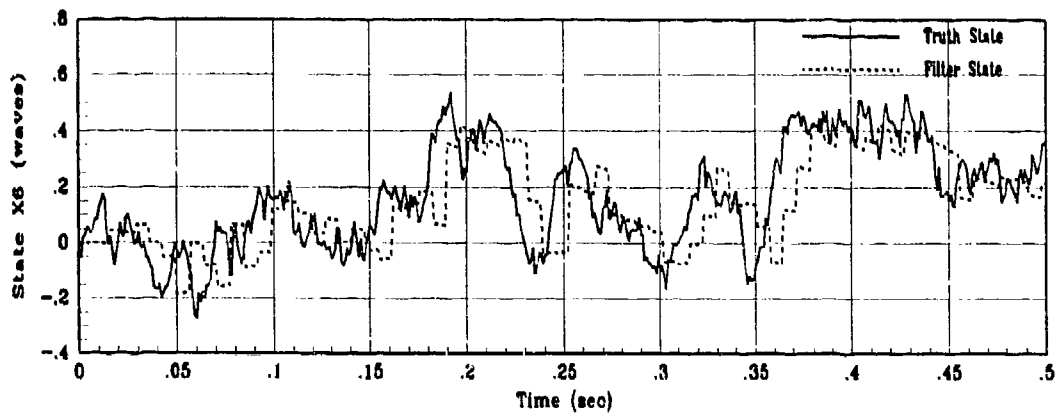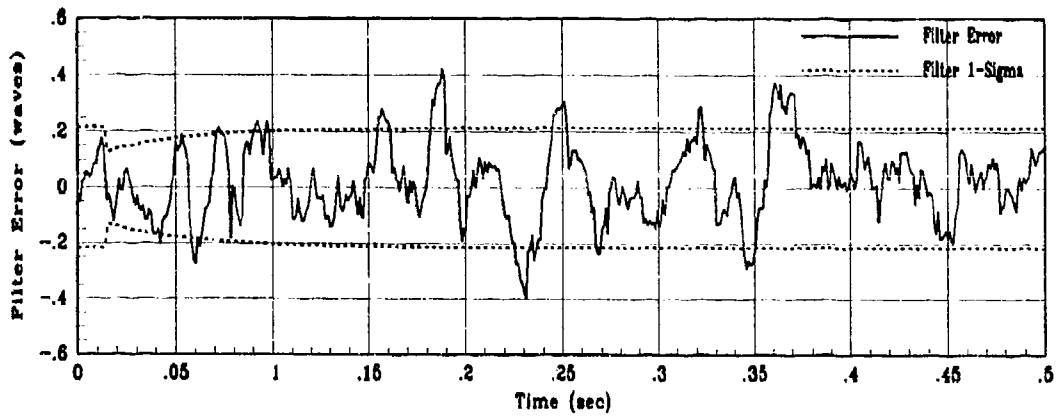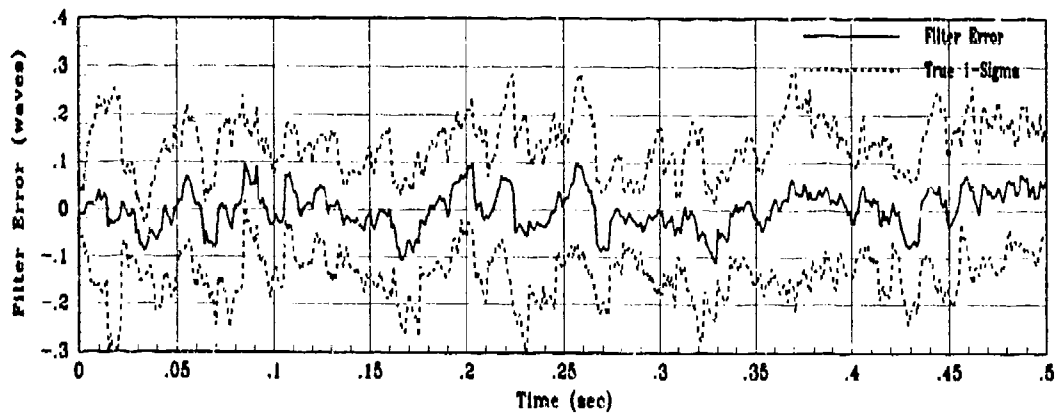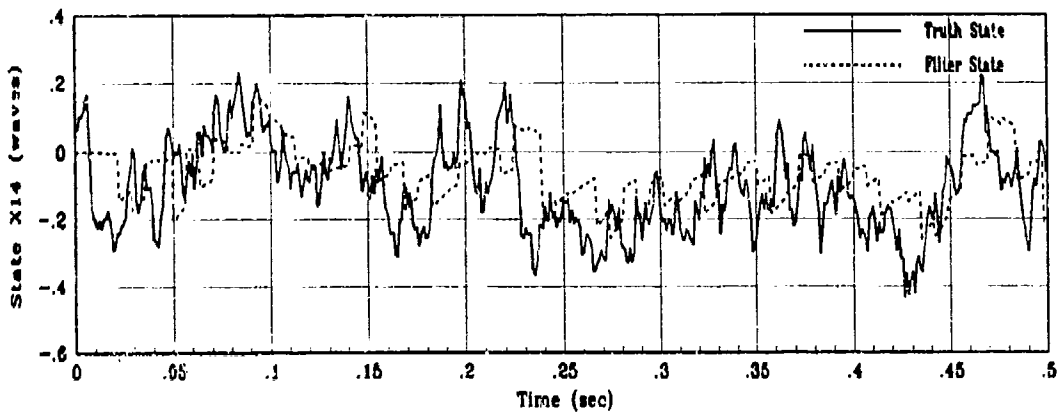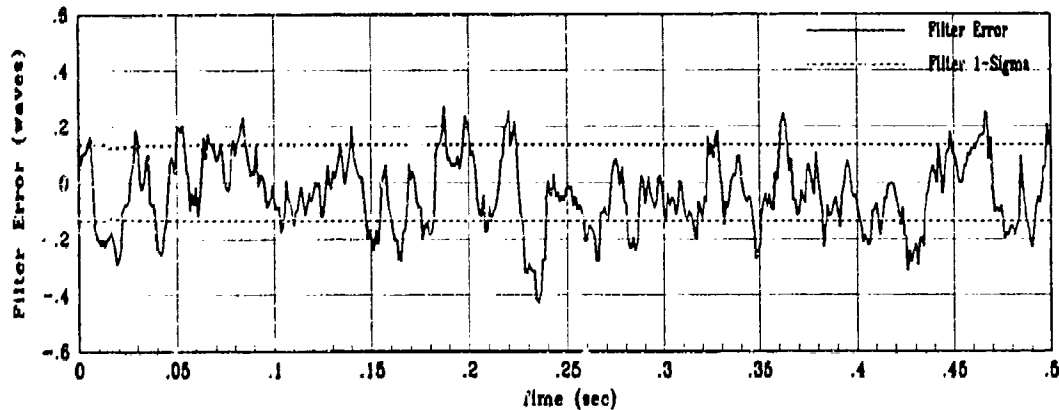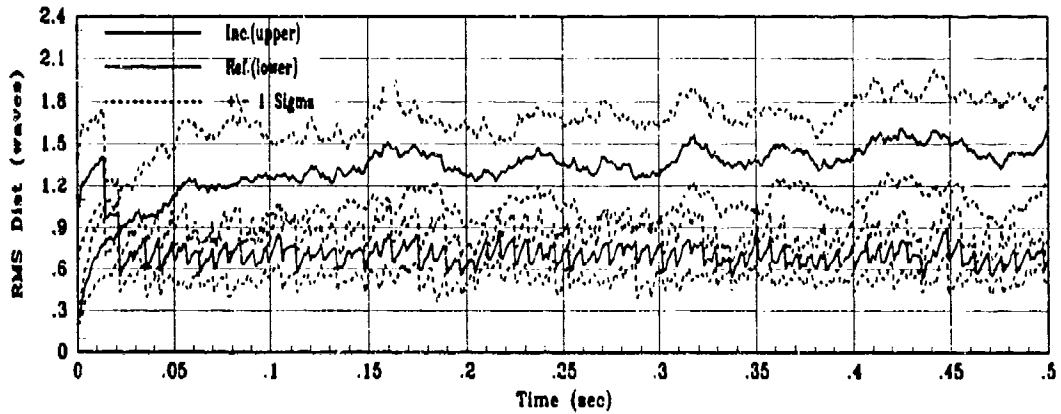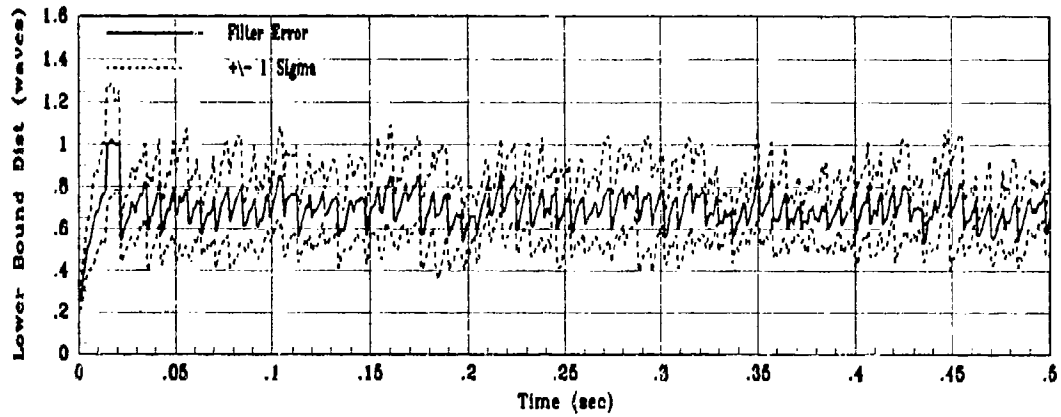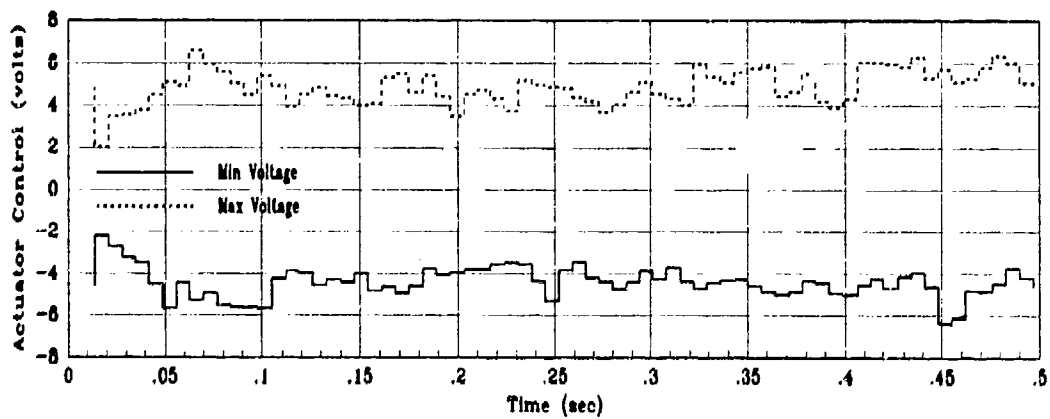Figure J 40. Control System Performance for Zenith Angle of 60 deg

Bibliography

1.   Athans, M. and P. Falb. *Optimal Control*. New York: McGraw-Hill, 1966.

2.   Baron, S. and others. *An Optimal Control Model Approach to the Design of Compensators for Simulator Delay*. NASA-CR-3604. Technical Report, Mountain View, California: Ames Research Center, October 1982.

3.   Bertsekas, D. P. *Dynamic Programming and Stochastic Control*. New York: Academic Press, 1976.

4.   Browne, John T. *Design and Man-in-the-Loop Evaluation of a Robust Lateral-Directional Control Law for a STOL F-15 Using LQG/LTR Design Methodology*. MS thesis, AFIT/GE/ENG/91M-05, School of Engineering, Air Force Institute of Technology (AU), Wright-Patterson AFB OH, March 1991.

5.   Clifford, S.F. "The classical Theory of Wave Propagation in a Turbulent Medium," *Laser Beam Propagation in the Atmosphere*, Volume 25, New York: Springer-Verlag, 1978.

6.   Cubalchini, Ronald. "Modal Wave-Front Estimation from Phase Derivative Measurements," *Journal of the Optical Society of America*, 69:972-977 (July 1979).

7.   Fried, D. L. "Anisoplanatism in Adaptive Optics," *Journal of the Optical Society of America*, 72:52-61 (January 1982).

8.   Fried, D. L. "Statistics of Geometric Representation of Wavefront Distortion," *Journal of the Optical Society of America*, 55:1427-1435 (November 1965).

9.   Halliday, David and Robert Resnick. *Fundamentals of Physics*. New York: Wiley, 1974.

10. Hardy, J. W. and others. "Real-Time Atmospheric Compensation," *Journal of the Optical Society of America*, 67:360-369 (March 1977).

11. Herrmann, Jan. "Cross Coupling and Aliasing in Modal Wave-Front Estimation," *Journal of the Optical Society of America*, 71:989-992 (August 1981).

12. Hogge, C Barry and R. Russell Butts. "Frequency Spectra for the Geometric Representation of Wavefront Distortions Due to Atmospheric Turbulence," *IEEE Transactions on Antennas and Propagation*, AP-24:144-154 (March 1976).

13. Hu, P.H. and others. "Application of Zernike Polynomials to Atmospheric Propagation Problems," *Journal of the Optical Society of America*, 6:1595-1608 (October 1989).

14. Integrated Systems Inc. *Matrixx User's Guide, Engineering Analysis and Control Design*, Version 7.0. Santa Clara, California: Integrated Systems Inc., October 1988.

15. Kleinman, D. L., S. Baron and W. H. Levison. "An Optimal Control Model of Human Response Part I: Theory and Validation," *Automatica*, 6:357-369 (1970).

16. Kleinman, David L. "Optimal Control of Linear Systems with Time-Delay and Observation Noise," *IEEE Transactions on Automatic Control*, AC-14:524-527 (October 1969).

17. Kwakernaak, H. and R. Sivan. *Linear Optimal Control Systems*. New York: Wiley, 1972.

18. Litton. *97-Channel, Low-Voltage, Electrodistortive Mirror: Operation Manual*. Technical Report, Lexington, Massachusetts: Litton Itek Optical Systems, January 1988.

19. Maybeck, Peter S. *Stochastic Models, Estimation, and Control*, Volume 1. New York: Academic Press, 1979.

20. Maybeck, Peter S. *Stochastic Models, Estimation, and Control*, Volume 2. New York: Academic Press, 1982

21. Maybeck, Peter S. *Stochastic Models, Estimation, and Control*, Volume 3. New York: Academic Press, 1982.

22. Miller, Maj Richard G. *Vector Space Approach for Modeling a Hartmann Wavefront Sensor*. MS thesis, AFIT/GE/ENG/89D-33, School of Engineering, Air Force Institute of Technology (AU), Wright-Patterson AFB OH, December 1989.

23. Musick, Stanton H. and Neal A. Carlson. *User's Manual for a Multimode Simulation for Optimal Filter Evaluation (MSOFE)*. Contract F3361586C1047, Winchester, Massachusetts: Integrity Systems Incorporated, April 1990.

24. Noll, Robert J. "Zernike Polynomials and Atmospheric Turbulence," *Journal of the Optical Society of America*, 66:207-211 (March 19˙j).

25. Noll, Robert J. "Phase Estimates from Slope-Type Wave-Front Sensors," *Journal of the Optical Society of America*, 68:139-140 (January 1978).

26. Parenti, Ronald R. "Recent Advances in Adaptive Optics Methods and Technology," *SPII. Vol. 1000--Laser Wavefront Control*, pages 101-109 (1988).

27. Roddier, Nicolas. "Atmospheric Wavefront Simulation using Zernike Polynomials," *Optical Engineering*, 29:1174-1180 (October 1990).

28. Roggemann, Michael and Mark Von Bokern. Telephone interviews. PL/LIII, Kirtland AFB NM, 1991.

29. Tyler, Glenn A., David L. Fried and John F Belsher. *Adaptive Optics Technology and Atmospheric Turbulence Correction, Volume I: Technical Descriptions*. Contract F2960182C0104, Placentia CA: The Optical Sciences Company, March 1988 (AD B121063).

30. Von Bokern, Mark Alan. *Design of a Linear Quadratic Gaussian Control Law for an Adaptive Optics System*. MS thesis, AFIT/GE/ENG/90D-65. School of Engineering, Air Force Institute of Technology (AU), Wright-Patterson AFB OH, December 1990.

31. Wang, J. Y. "Phase-Compensated Optical Beam Propagation Through Atmospheric Turbulence," *Applied Optics*, 17:2580-2590 (August 1978).

32. Wang, J. Y. and J. K. Markey. "Modal Compensation of Atmospheric Turbulence Phase Distortion," *Journal of the Optical Society of America*, 68:78-87 (January 1978).

33. Welsh, B. M. and C. S. Gardner. *Performance Analysis of Adaptive Optics Systems Using Laser Guide stars and Slope Sensors*. Technical Report, Champaign-Urbana, Illinois: University of Illinois, March 1989.

Vita

Captain David J. Anderson was born on 2 October 1962, in Lynn, Massachusetts. Following graduation from Lynn English High School, he enrolled at Northeastern University, Boston, Massachusetts, where he recieved the Bachelor of Science degree in Electrical Engineering. He was commissioned on 14 December 1984 through the ROTC program. Then Second Lieutenant Anderson embarked on a five-year tour with the 4201" and 49th Test Squadrons, Barksdale AFB, Louisiana, Strategic Air Command, as a flight test engineer for operational test and evaluation of the Air-Launched Cruise Missile, Short Range Attack Missile, and Harpoon Anti-ship Missile. In May 1990, he was assigned to the Air Force Institute of Technology, Wright-Patterson AFB, Ohio for a Master of Science degree in Electrical Engineering.